

THESE DE DOCTORAT DE

L'UNIVERSITE DE NANTES
COMUE UNIVERSITE BRETAGNE LOIRE

ÉCOLE DOCTORALE N° 605
Biologie Santé
Spécialité : Immunologie, Cancérologie

Par

Noémie JOALLAND

Immunothérapie anti-tumorale par transfert adoptif de LT V γ 9V δ 2

« Utilisation préclinique de LT V γ 9V δ 2 humains allogéniques en immunothérapie anti-tumorale dans des modèles murins de xénogreffes orthotopiques »

Thèse présentée et soutenue à Nantes, le 16 novembre 2018
Unité de recherche : Equipe 1, CRCINA, Inserm UMR 1232, CNRS ERL 6001
Thèse N° :

Rapporteurs avant soutenance :

Myriam CAPONE
CR – Université de Bordeaux

Jean-Jacques FOURNIE
DR – Université de Toulouse

Composition du Jury :

Président du Jury
Henri VIE DR – Université de Nantes

Jean-Jacques FOURNIE DR – Université de Toulouse
Myriam CAPONE CR – Université de Bordeaux
Virginie LAFONT CR – Université de Montpellier
Claire PECQUEUR CR – Université de Nantes

Directeur de thèse
Emmanuel SCOTET DR – Université de Nantes

Invité(s)
Ulrich JARRY IR – Université de Rennes

Remerciements

Tout d'abord, je tiens à remercier l'ensemble des membres de mon jury : Dr MYRIAM CAPONE et Dr JEAN-JACQUES FOURNIE pour avoir accepté d'être rapporteurs de ce travail ainsi que les Dr VIRGINIE LAFONT, Dr CLAIRE PECQUEUR et Dr HENRI VIE pour l'examen de cette thèse.

Je tiens à remercier tout particulièrement mon directeur de thèse, le Dr EMMANUEL SCOTET, pour m'avoir accueilli dans son équipe, pour l'accompagnement, la confiance et l'autonomie qu'il m'a accordées au cours de ces trois années et qui m'ont permis de m'épanouir. C'est avec grand plaisir que je reste une année supplémentaire afin de poursuivre les nombreuses collaborations, notamment autour des modèles murins, auxquelles j'ai pu participer.

Je souhaite également remercier très sincèrement le Dr ULRICH JARRY pour son encadrement, sa disponibilité, son aide et de m'avoir formée à l'expérimentation animale. Merci pour ta patience et ton soutien aussi bien sur le plan personnel que scientifique, même après ton départ. Ta bonne humeur et tes choix musicaux hétéroclites me manquent lors des longues séances de stéréotaxie à l'animalerie.

J'adresse un remerciement particulier à LAURA LAFRANCE, que j'ai eu la chance d'encadrer en tant que technicienne et de former à l'expérimentation animale. Ta gentillesse, ton esprit d'entraide et ton sourire ont été de précieux compagnons. Un grand merci aussi à LOLA BOUTIN pour ta joie de vivre, tes commandes de gâteaux et les nombreuses citations humoristiques qui rythment nos journées.

Je remercie également tous les stagiaires que j'ai eu l'occasion d'encadrer plus ou moins longtemps : ANDREA, JEAN-BAPTISTE, AUDE, CAMILLE et surtout CHIRINE que j'aurais la chance de continuer de côtoyer pendant le début de sa thèse.

Merci à tous les autres membres de l'Equipe 1, présents ou passés, qui font la vie du laboratoire : CYNTHIA, LUCILE, MARISA, MARIE-CLAUDE, MARIE-CLAIRE, FABIENNE, HENRI, BEATRICE, REGINE, JOCELYN, JEANNE, LAETITA, XAVIER

Merci également à toutes les personnes des équipes 9 et 14 avec qui j'ai eu l'occasion de collaborer grâce à l'expérimentation animale : JULIEN, MARION, CHARLOTTE, MAEVA, NATASHA, LISA, CATHERINE, FANNY. Un grand merci à CLAIRE PECQUEUR pour toutes nos discussions et pour tes conseils, je suis ravie de pouvoir poursuivre notre collaboration.

Merci aussi aux collègues, scientifiques ou non, qu'on ne voit qu'à l'animalerie : SYLVIA, SANDRINE, SEVERINE, THIBAUD, NATHALIE, JULIEN, MARIE ...

Je souhaite ensuite remercier toutes les personnes qui m'entourent dans la vie de tous les jours. Merci à mes amis dont les nombreuses questions me permettent de vulgariser mon travail mais aussi pour tous les bons moments, les fous rires et d'avoir fait de moi une guerrière téméraire lors de nos parties de jeu de rôle.

Merci à ma famille : HUBERT, LOUISE et RENEE, mes grands-parents ; FREDERIQUE et MARC, mes beaux-parents ; ARMELLE et DENIS, mes parents qui m'ont souhaité de devenir chercheur dès mon baptême.

Un immense merci à mes sœurs ELORA et AURELIANE pour m'avoir soutenue toutes ces années et pour tout le bonheur que vous mettez dans ma vie. Depuis peu tata d'un merveilleux petit LOUIS, je lui souhaite autant de bonheur et d'amour qu'on m'en a donné.

Pour finir, je dédie cette thèse à mon mari, SAMUEL. Sans toi rien de tout cela n'aurait été possible, ta présence et ton amour me porte chaque jour. Merci mon inséparable ...

Sommaire

SOMMAIRE	1
LISTE DES ABREVIATIONS	5
TABLE DES FIGURES	8
A. INTRODUCTION	10
I – IMMUNOTHERAPIE ANTI-TUMORALE	11
1 – GENERALITES	11
1.1 – Présentation du système immunitaire	11
1.2 – Rôle du système immunitaire dans le cancer	12
1.3 – Concept d’immuno-édition de la tumeur	13
1.4 – Principe et Classification de l’immunothérapie anti-tumorale	14
2 – IMMUNOTHERAPIE ACTIVE	16
2.1 – Anticorps Immunomodulateurs	16
2.2 – Vaccination anti-tumorale	18
2.3 – Molécules Immunomodulatrices	20
2.4 – Virothérapie	20
3 – IMMUNOTHERAPIE PASSIVE	22
3.1 – Anticorps Thérapeutiques	22
3.2 – Thérapie Cellulaire Adoptive	23
II - LES LYMPHOCYTES T $\gamma\delta$	26
1 - REPERTOIRE DES LT $\gamma\delta$	26
1.1 - Conservation entre les espèces	26
1.2 – Diversité du TCR $\gamma\delta$	26
1.3 – Ontogénèse et sélection thymique	27
2 – MODALITES D’ACTIVATION DES LT $\gamma\delta$	29
2.1 – Diversité des récepteurs exprimés	29
2.2 – Ligands du TCR $\gamma\delta$	30
3 – PLEIOTROPIE FONCTIONNELLE DES LT $\gamma\delta$	32
III – LES LYMPHOCYTES T Vγ9Vδ2	33
1 – GENERALITES	33
2 – MODALITES D’ACTIVATION ANTIGENIQUE DES LT V γ 9V δ 2	35

2.1 – Molécules activatrices directes : les phosphoantigènes	35
2.2 – Molécules modulatrices indirectes : activatrices ou inhibitrices	38
2.3 – Mécanismes de reconnaissance des phosphoantigènes	39
3 – REACTIVITE ET REGULATION DU SIGNAL DES LT V γ 9V δ 2	42
3.1 – Le TCR V γ 9V δ 2	42
3.2 – Les récepteurs NK	43
3.3 – Les Toll-Like Récepteurs	44
3.4 – Les Récepteurs Fc	45
3.5 – Les molécules d'adhésion	45
3.6 – Les cytokines	46
4 – ROLES ET FONCTIONS EFFECTRICES DES LT V γ 9V δ 2	47
4.1 – Cytotoxicité directe	47
4.2 – Interactions avec d'autres cellules de l'immunité	48
4.3 – Plasticité cellulaire	50
IV - IMMUNOTHERAPIE ANTI-TUMORALE ET LT Vγ9Vδ2	52
1 – LT V γ 9V δ 2 ET CANCER	52
1.1 – Surveillance et Fonctions anti-tumorales des LT V γ 9V δ 2	52
1.2 – Intérêt thérapeutique des LT V γ 9V δ 2	53
2 – IMMUNOTHERAPIE ACTIVE	54
3 – IMMUNOTHERAPIE PASSIVE	56
4 – MODELES MURINS PRECLINIQUES ET NOUVELLES STRATEGIES THERAPEUTIQUES	58
V – OBJECTIFS DE MA THESE	59
<u>B. RESULTATS</u>	<u>61</u>
PARTIE 1 : CARACTERISATION DE LT $\gamma\delta$ PRO- OU ANTI-TUMORAUX : INTERET PRONOSTIC ET OPTIMISATION DES IMMUNOTHERAPIES ANTI-TUMORALES	62
1 – OBJECTIFS DU PROJET	62
2 – MATERIELS ET METHODES	63
2.1 – Marquages intra- et extra-cellulaires	63
2.2 – Tri négatif des LT $\gamma\delta$	63
2.3 - Amplification antigénique et non spécifique des LT V γ 9V δ 2	64
2.4 - Dosage de cytokines avec le kit LEGENDplex	65
2.5 - Test de réactivité CD107a	66

3 – ETUDE DU PHENOTYPE DE LT $\gamma\delta$ DIRECTEMENT ISSUS DU SANG DE DONNEURS SAINS	67
4 – DESCRIPTION DES FONCTIONS EFFECTRICES DE LT V γ 9V δ 2 DANS LE CADRE DE LA CREATION D'UNE BANQUE CELLULAIRE ALLOGENIQUE	71
5 – ENCADREMENT DE STAGIAIRES : RESULTATS ANNEXES A LA PARTIE 1	76
5.1 – Avril à Juin 2017 : Stagiaire de Master 1 Biologie Santé (Chirine RAFIA).	76
5.2 - Octobre 2017 - Janvier à Mai 2018 : Stagiaire de Master 2 Biologie Santé (Chirine RAFIA).	77
6 – CONCLUSION	78
PARTIE 2 : APPLICATION AU CANCER EPITHELIAL DE L'OVAIRE	82
1 – LE CANCER EPITHELIAL DE L'OVAIRE	82
1.1 – Classification des cancers de l'ovaire	82
1.2 – Epidémiologie et Etiologie	83
1.3 – Diagnostic et Prise en charge thérapeutique	84
1.4 – Immunothérapie du cancer de l'ovaire	86
2 - ARTICLE 1: COMBINED CHEMOTHERAPY AND ALLOGENEIC HUMAN V γ 9V δ 2 T LYMPHOCYTE-IMMUNOTHERAPY EFFICIENTLY CONTROL THE DEVELOPMENT OF HUMAN EPITHELIAL OVARIAN CANCER CELLS <i>IN VIVO</i>	87
3 – ENCADREMENT DE STAGIAIRES : RESULTATS ANNEXES A LA PARTIE 2	113
3.1 – Avril à Juin 2016 : Stagiaire de Master 1 Biologie Santé (Andréa MUREAU).	113
3.2 – Janvier à Juin 2018 : Stagiaire de Master 2 Biologie Santé Médecine (Camille GORDEEFF).	114
3 - CONCLUSION	115
PARTIE 3 : APPLICATION AU GLIOBLASTOME MULTIFORME	117
1 – LE GLIOBLASTOME MULTIFORME	117
1.1 – Classification des tumeurs cérébrales	117
1.2 – Epidémiologie et Etiologie	118
1.3 – Diagnostic et Prise en charge thérapeutique	118
1.4 – Immunothérapie du GBM	121
2 - ARTICLE 2 : STEREOTAXIC ADMINISTRATIONS OF ALLOGENEIC HUMAN V γ 9V δ 2 T CELLS EFFICIENTLY CONTROL THE DEVELOPMENT OF HUMAN GLIOBLASTOMA BRAIN TUMORS	122
3 – ARTICLE 3 : STEREOTACTIC ADOPTIVE TRANSFER OF CYTOTOXIC IMMUNE CELLS IN MURINE MODELS OF ORTHOTOPIC HUMAN GLIOBLASTOMA MULTIFORME XENOGRAPHS	136
4 – ARTICLE 4 : IL-21 INCREASES THE REACTIVITY OF ALLOGENEIC HUMAN V γ 9V δ 2 T CELLS AGAINST PRIMARY GLIOBLASTOMA TUMORS	144
5 – ARTICLE 5 : ALLOGENEIC HUMAN V γ 9V δ 2 T CELLS NATURALLY RECOGNIZE AND ELIMINATE MESENCHYMAL PRIMARY GLIOBLASTOMA CELLS THROUGH NKG2D AND BTN3 PATHWAYS	154

6 – ETUDE DE LA TOXICITE DU ZOLEDRONATE SUR DES CELLULES CEREBRALES	184
7 - CONCLUSION	187
C. DISCUSSION	190
I – PERTINENCE DES MODELES MURINS PRECLINIQUES	191
II – FAISABILITE D’UNE BANQUE DE LT Vγ9Vδ2 HUMAINS ALLOGENIQUES	195
III – UTILISATION CONCOMITANTE DU ZOLEDRONATE	199
IV – CONCLUSION PERSONNELLE	202
D. BIBLIOGRAPHIE	204
E. ANNEXES	224
LISTES DES PUBLICATIONS	225
ARTICLE 6 : SYNERGISTIC TARGETING OF BREAST CANCER STEM-LIKE CELLS BY HUMAN $\gamma\delta$ T CELLS AND CD8 ⁺ T CELLS	227
ARTICLE 7 : GLUTAMINE UPTAKE AND UTILIZATION OF HUMAN MESENCHYMAL GLIOBLASTOMA IN ORTHOTOPIC MOUSE MODEL	248
ARTICLE 8 : A TRANSIENT POPULATION PRECEDES AND SUPPORTS THE ACQUISITION OF TEMOZOLOMIDE RESISTANCE IN HUMAN GLIOBLASTOMA.	268
ARTICLE 9 : SENESCENT ENDOTHELIAL CELLS INCREASE THE BELLICOSITY OF GBM CELLS SURVIVING FROM RADIATION THERAPY THROUGH SECRETION OF CXCL5/8.	307
LISTES DES COMMUNICATIONS	335

Liste des Abréviations

¹³ C	carbone <u>13</u>
⁵¹ Cr	chrome <u>51</u>
αGalCer :	<u>α</u> -Galactosyl <u>C</u> eramide
ABCA1 :	<u>A</u> TP- <u>b</u> inding <u>c</u> assette transporter <u>A1</u>
ABP :	aminobisphosphonates
ADCC :	antibody <u>d</u> ependant <u>c</u> ell mediated <u>c</u> ytotoxicity
ADN :	acide <u>d</u> ésoxyribo <u>n</u> ucléique
ARN :	acide <u>r</u> ibo <u>n</u> ucléique
B.EBV :	lymphocytes <u>B</u> immortalisés par l' <u>E</u> pstein <u>B</u> arr <u>V</u> irus
BHE :	barrière <u>h</u> émato <u>e</u> ncéphalique
BrHPP :	<u>b</u> romo <u>h</u> ydrique pyrophosphate
BSA :	<u>b</u> ovine <u>s</u> erum <u>a</u> lbumin
BTN :	<u>b</u> utyrophiline
BTN3A1 :	<u>b</u> utyrophiline <u>3</u> isoforme <u>A1</u>
c-HDMAPP :	((2E)-1- <u>h</u> ydroxy-2 <u>m</u> ethylpent-2-enyl-pyrophosphate
CA125 :	cancer <u>a</u> ntigen <u>125</u>
CAMP :	<u>c</u> hanged <u>a</u> ssociated <u>m</u> olecular <u>p</u> attern
CAR :	<u>c</u> himeric <u>a</u> ntigen <u>r</u> eceptor
CDP ME :	4- <u>d</u> iphosphocytidyl <u>m</u> éthyl <u>e</u> rythritol
CDR3 :	<u>c</u> omplementarity <u>d</u> etermining <u>r</u> egion <u>3</u>
CEO :	cancer <u>é</u> pithélial de l' <u>o</u> vaire
CHIP :	<u>c</u> himiothérapie <u>h</u> yperthermique <u>i</u> ntrapéritonéale
CMH :	<u>c</u> omplexe <u>m</u> ajeur d' <u>h</u> istocompatibilité
CMV :	cytomegalovirus
CNP :	<u>c</u> lassique, <u>n</u> eural et <u>p</u> rolifératif
CPA :	<u>c</u> ellule <u>p</u> résentatrice d' <u>a</u> ntigène
CRCINA :	<u>c</u> entre de <u>r</u> echerche en <u>c</u> ancérologie et <u>i</u> mmunologie <u>N</u> antes <u>A</u> ngers
CSC :	<u>c</u> ellule <u>s</u> ouche <u>c</u> ancéreuse
CTLA-4 :	<u>c</u> ytotoxic <u>T</u> lymphocyte <u>a</u> ssociated protein <u>4</u>
CXCL-13 :	<u>C</u> X <u>C</u> -chemokine <u>l</u> igand <u>13</u>
DAMP :	<u>d</u> anger <u>a</u> ssociated <u>m</u> olecular <u>p</u> attern
DC :	<u>d</u> endritic <u>c</u> ell / cellules <u>d</u> endritiques
DD :	<u>d</u> eath <u>d</u> omain
DLI :	<u>d</u> onor lymphocyte <u>i</u> nfusion
DMAPP :	<u>d</u> iméthylallyl pyrophosphate
EC50 :	concentration <u>e</u> fficace <u>m</u> édiane
EGFRvIII :	epithelial growth <u>f</u> actor (EGF) <u>r</u> eceptor <u>v</u> ariant <u>III</u>
FADD :	<u>F</u> as associated protein <u>d</u> eath <u>d</u> omain
Fc :	<u>f</u> ragment <u>c</u> onstant des immunoglobuline (Ig)
FcR :	<u>r</u> écepteur au <u>f</u> ragment <u>c</u> onstant (Fc)
FIGO :	<u>f</u> édération <u>i</u> nternationale de <u>g</u> ynécologie et <u>o</u> bstétrique
FPP :	<u>f</u> arnesyl <u>d</u> iphosphate

FPPS :	farnesyl <u>d</u> iphosphate <u>s</u> ynthase
GBM :	glioblastome <u>m</u> ultiforme
GM-CSF :	granulocyte <u>m</u> acrophage <u>c</u> olony <u>s</u> timulating <u>f</u> actor
GMP :	good <u>m</u> anufacturing <u>p</u> ractices
GVHD :	graft <u>v</u> ersus <u>h</u> ost <u>d</u> isease
Gy :	<u>G</u> rays
HMBPP :	<u>h</u> ydroxymethylbutenyl 4- <u>d</u> iphosphate
HMG-CoA :	<u>h</u> ydroxyméthylglutaryl- <u>C</u> oA
HPV :	<u>h</u> uman papillomavirus
ICAM-1 :	<u>i</u> ntercellular <u>a</u> dhesion <u>m</u> olecule <u>1</u>
IDO :	<u>i</u> ndoleamine-2,3- <u>d</u> ioxygenase
IFN :	<u>i</u> nterféron
Ig :	<u>i</u> mmunoglobuline
IgV/C :	domaine de type <u>i</u> mmunoglobuline <u>v</u> ariable et <u>c</u> onstant
IHC :	<u>i</u> mmunohistochimie
IL- :	<u>i</u> nterleukine
IL-13R α :	<u>i</u> nterleukine <u>13</u> receptor <u>α</u>
ILT-2 :	<u>I</u> g like transcript <u>2</u>
IPP :	<u>i</u> sopentenyl pyrophosphate
IRM :	<u>i</u> magerie par <u>r</u> ésonnance <u>m</u> agnétique
LabEx IGO :	<u>l</u> aboratoire d' <u>e</u> xcellence en <u>i</u> mmunology in graft and <u>o</u> ncology
LAG-3 :	lymphocyte <u>a</u> ctivation gene <u>3</u>
LB :	lymphocytes <u>B</u>
LCR :	<u>l</u> iquide céphalo-rachidien
LFA-1/3 :	lymphocyte <u>f</u> unction associated <u>a</u> ntigen <u>1/3</u>
LILR :	<u>l</u> eukocyte <u>i</u> mmunoglobulin-like receptor
LT :	lymphocytes <u>T</u>
MEcPP :	<u>m</u> éthylerythritol cyclodiphosphate
MEP/DOXP :	<u>m</u> ethylerythritol phosphate / <u>d</u> eoxyxylulose-5-phosphate
MICA/B :	<u>MHC</u> class <u>I</u> polypeptide-related sequence <u>A/B</u>
MS :	<u>m</u> aladie <u>s</u> table
MVA :	<u>m</u> évalonate
MVAP :	5-phosphomévalonate
MVAPP :	<u>m</u> évalonate-5- <u>d</u> iphosphate
NK :	<u>N</u> atural <u>K</u> iller
NKG2D/A :	<u>N</u> atural <u>K</u> iller group <u>2</u> member <u>D/A</u>
NKR :	<u>N</u> atural <u>K</u> iller receptor
NKT :	<u>N</u> atural <u>K</u> iller <u>T</u> cells
NSG :	NOD.Cg-Prkdcscid Il2rgtm1 Wjl/SzJ
OMS :	<u>o</u> rganisation <u>m</u> ondiale de la <u>s</u> anté
PAg :	phosphoantigène
PAMP :	pathogen <u>a</u> ssociated <u>m</u> olecular <u>p</u> attern
PBMC :	peripheral <u>b</u> lood <u>m</u> ononuclear <u>c</u> ells
PBS :	phosphate <u>b</u> uffer <u>s</u> aline
PD1 :	programmed cell <u>d</u> eath <u>1</u>

PDL1/2 :	programmed cell <u>d</u> eath <u>l</u> igand <u>1/2</u>
PDX :	patient <u>d</u> erived <u>x</u> enograft
PFA :	<u>p</u> ara- <u>f</u> orm <u>a</u> ldéhyde
PHA :	phyto <u>h</u> emagglutinine
PMA :	<u>p</u> horbol12- <u>m</u> yrystate13- <u>a</u> cetate
PPP :	polyprenyl <u>d</u> iphosphate
RC :	<u>r</u> émission <u>c</u> omplète
RO :	<u>r</u> éponse <u>o</u> bjective
RP :	<u>r</u> émission partielle
SCID :	<u>s</u> evere <u>c</u> ombined <u>i</u> mmunod <u>e</u> ficiency
SNC :	sys <u>t</u> ème <u>n</u> erveux <u>c</u> entral
SVF :	<u>s</u> érum de <u>y</u> eau <u>f</u> œtal
TCR :	<u>T</u> cell receptor / <u>r</u> écepteur de cellule <u>T</u>
Tfh :	<u>LT</u> follicular <u>h</u> elper
TGF-β :	transforming growth factor <u>β</u>
Th :	<u>LT</u> <u>h</u> elper
TIGIT :	<u>T</u> cell immunoreceptor with <u>I</u> g and <u>IT</u> IM domains
TIL :	<u>t</u> umor <u>i</u> nfiltrating lymphocytes / lymphocytes <u>i</u> nfiltrant les <u>t</u> umeurs
Tim-3 :	<u>T</u> cell <u>m</u> embrane protein <u>3</u>
TLR :	<u>T</u> oll <u>l</u> ike <u>r</u> eceptor
TMZ :	<u>t</u> emozomide
TNF-α :	<u>t</u> umor <u>n</u> ecrosis <u>f</u> actor <u>α</u>
Treg :	<u>LT</u> <u>r</u> égulateur
ULBP :	<u>UL</u> 16 <u>b</u> inding protein
VEGF :	<u>v</u> ascular <u>e</u> ndothelial growth <u>f</u> actor
VIH :	<u>v</u> irus de l' <u>i</u> mmunodéficienc <u>e</u> <u>h</u> umaine

Table des Figures

Figure 1 :	Présentation des différents acteurs cellulaires et moléculaires du système immunitaire.	12
Figure 2 :	L'immuno-édition selon la règle des 3E.	14
Figure 3 :	Classification des différentes stratégies immunothérapeutiques.	15
Figure 4 :	Corécepteurs impliqués dans la régulation de la réponse des LT.	17
Figure 5 :	Différentes stratégies de vaccination anti-tumorale.	19
Figure 6 :	Différentes stratégies de thérapie cellulaire adoptive.	25
Figure 7 :	Les sous-populations de LT $\gamma\delta$ chez l'Homme.	27
Figure 8 :	Modèle présentant les grandes étapes de la sélection thymique et extra-thymique à l'origine du répertoire des LT $\gamma\delta$ en périphérie chez l'adulte.	28
Figure 9 :	Structure tridimensionnelle d'un TCR $\gamma\delta$, d'un TCR $\alpha\beta$ et du Fab d'une Ig.	29
Figure 10 :	Récepteurs modulant l'activation des LT $\gamma\delta$.	30
Figure 11 :	Différentes classes de ligands proposés et/ou confirmés des LT $\gamma\delta$.	31
Figure 12 :	Structure du locus de la chaîne γ humaine et étapes de l'assemblage de la chaîne V γ 9-JP-C1.	34
Figure 13 :	Exemples de PAg (phosphoantigènes) caractérisés pour induire l'activation des LT V γ 9V δ 2.	36
Figure 14 :	Biosynthèse des précurseurs isoprénoïdes chez les vertébrés et les micro-organismes.	37
Figure 15 :	Représentation schématique des différents isoformes de BTN3A/CD277.	40
Figure 16 :	Trois hypothèses sur le mode d'activation des LT V γ 9V δ 2 par les PAg.	41
Figure 17 :	Représentation schématique de la synapse immunologique formée par un LT V γ 9V δ 2.	43
Figure 18 :	Principales fonctions effectrices des LT V γ 9V δ 2.	47
Figure 19 :	Principaux essais cliniques en immunothérapie active basés sur l'utilisation de LT V γ 9V δ 2.	55
Figure 20 :	Principaux essais cliniques en immunothérapie passive basés sur l'utilisation de LT V γ 9V δ 2.	57
Figure 21 :	Présentation du kit de dosage de cytokines LEGENDplex.	66
Figure 22 :	Tri négatif des LT $\gamma\delta$ présents dans le sang périphérique de donneurs sains.	67
Figure 23 :	Etude du sécrétome des LT $\gamma\delta$ présents dans le sang périphérique de donneurs sains.	69

Figure 24 :	Etude de la réactivité naturelle de LT $\gamma\delta$ face à différentes lignées de cellules tumorales.	70
Figure 25 :	Description du protocole d'amplification des LT V γ 9V δ 2	71
Figure 26 :	Analyse de la pureté en LT V γ 9V δ 2 après amplification antigénique.	72
Figure 27 :	Etude du sécrétome des LT V γ 9V δ 2 à différents stades d'amplification.	73
Figure 28 :	Etude de la réactivité naturelle ou induite des LT V γ 9V δ 2 face à des cellules tumorales.	74
Figure 29 :	Analyse de la capacité d'amplification des LT V γ 9V δ 2.	75
Figure 30 :	Impact de cytokines immunomodulatrices sur les fonctions effectrices des LT V γ 9V δ 2.	76
Figure 31 :	Impact de cytokines immunomodulatrices sur la polarisation des LT V γ 9V δ 2.	77
Figure 32 :	Schéma représentatif de la dissémination des cellules tumorales de CEO dans le péritoine.	82
Figure 33 :	Index de Carcinose Péritonéale ou score de Sugarbaker.	85
Figure 34 :	Impact de la chimiothérapie sur la lignée humaine de CEO SHIN-3 <i>in vitro</i> et <i>in vivo</i> .	113
Figure 35 :	Impact de la CHIP sur la réactivité des LT V γ 9V δ 2 face à des cellules tumorales de CEO de la lignée cellulaire SKOV-3.	114
Figure 36 :	Images cérébrales de suivi de patients atteints de GBM.	119
Figure 37 :	Thérapie conventionnelle des patients atteints de GBM : le protocole de Stupp.	120
Figure 38 :	Reconnaissance de cellules cérébrales sensibilisées au zolédronate par les LT V γ 9V δ 2.	185
Figure 39 :	Protocole hypothétique de production d'une banque de LT V γ 9V δ 2 allogéniques au grade GMP.	197

A. INTRODUCTION

I – Immunothérapie anti-tumorale

1 – Généralités

1.1 – Présentation du système immunitaire

Le système immunitaire est composé d'un ensemble d'effecteurs cellulaires et moléculaires capables de reconnaître et d'éliminer aussi bien des agents pathogènes étrangers que des cellules du Soi altérées. On distingue deux composantes majeures au sein du système immunitaire : l'immunité innée et l'immunité adaptative (Figure 1).

L'immunité innée constitue la première ligne de défense de l'organisme. Elle regroupe des acteurs moléculaires tels que le complément et des acteurs cellulaires tels que les granulocytes (basophiles, éosinophiles et neutrophiles), les monocytes, les macrophages, les cellules dendritiques (DC) ou encore les cellules NK (Natural Killer). Ces différents composants permettent une reconnaissance rapide (quelques heures), mais peu spécifique des pathogènes.

L'immunité adaptative est plus longue à se développer (quelques jours) mais est hautement spécifique du pathogène ciblé. Elle est composée de deux effecteurs cellulaires majoritaires : les LT (lymphocytes T) et les LB (lymphocytes B). Ces cellules sont capables de cibler des antigènes spécifiques du pathogène cible et de mettre en place une mémoire afin de réagir plus rapidement en cas de nouvelle infection.

Cependant d'autres types cellulaires présentent des profils hybrides et ne peuvent appartenir qu'à l'une ou l'autre de ces immunités. Une catégorie intermédiaire permet de regrouper ces cellules, nommée l'immunité transitionnelle car elle se situe à l'interface entre l'immunité innée et adaptative. Les NKT (Natural Killer T cells) et les LT $\gamma\delta$ en font partie (Dranoff, 2004) (Figure 1). Leur vitesse de réaction contre les pathogènes se rapprochent de celle de l'immunité innée alors que leurs fonctions effectrices se rapproche plutôt de celles de l'immunité adaptative.

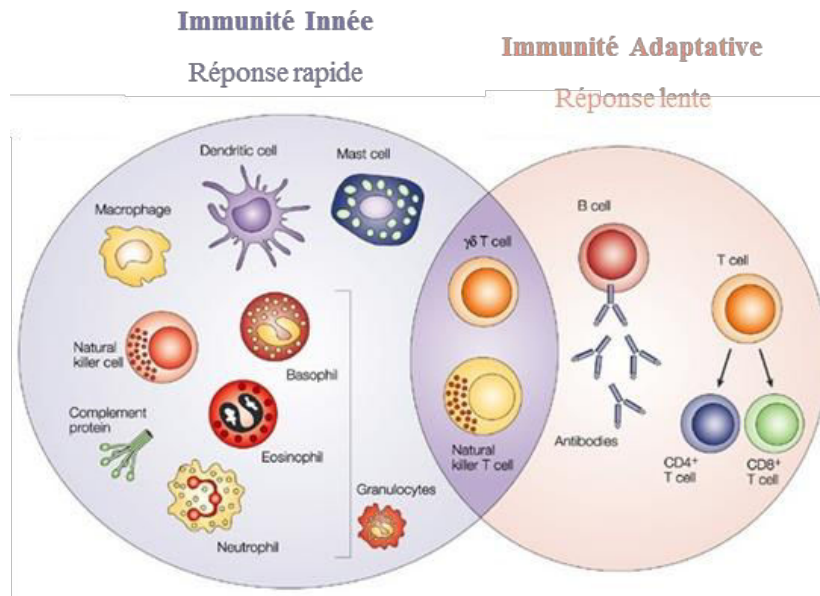


Figure 1 : Présentation des différents acteurs cellulaires et moléculaires du système immunitaire. L'immunité innée regroupe des facteurs solubles (le complément) et des acteurs cellulaires (monocytes, macrophages, DC, cellules NK ...). La réponse immunitaire adaptative est plus spécifique que celle de l'immunité innée et repose sur les LB et les LT $\alpha\beta$. Les cellules telles que les NKT et les LT $\gamma\delta$ se trouvent à l'interface entre ces deux immunités. *Adapté de Dranoff, 2004.*

1.2 – Rôle du système immunitaire dans le cancer

La fonction principale du système immunitaire est de défendre l'organisme contre l'intrusion de pathogènes, via le recrutement des nombreux acteurs complémentaires issus de l'immunité innée et de l'immunité adaptative. Cependant dans certain cas, le système immunitaire peut réagir contre l'hôte notamment lors de maladies auto-immunes. Dans le cas du cancer, le système immunitaire doit réagir contre des cellules de l'organisme devenues anormales et les éliminer pour éviter qu'elles n'altèrent les fonctions du tissu/organe dont elles dérivent.

L'existence d'une immuno-surveillance, phénomène de surveillance de l'apparition de cellules transformées/tumorales par le système immunitaire, a été mise en évidence dans différentes situations physiopathologiques. Les patients présentant une immunodépression, par exemple dans le cas de la prise d'immunosuppresseurs suite à une transplantation d'organe, ou une immunodéficience, comme dans le cas d'une infection par le VIH (virus de l'immunodéficience humaine), ont une incidence accrue de développement de cancers (Dunn et al., 2004).

De plus, la présence de TIL (tumor infiltrating Lymphocytes) chez des patients atteints de cancer peut conduire au développement d'une réponse immunitaire anti-tumorale spontanée et peut également servir d'indicateur pronostic à la survie des patients dans de nombreux cas de cancer (mélanome, cancer de l'ovaire ...) (Burton et al., 2011; Dunn et al., 2004; Sato et al., 2005).

Le système immunitaire est impliqué dans différents processus au cours de la prévention et du développement du cancer. Avant même la croissance d'une tumeur, il protège l'organisme contre les pathogènes, notamment les virus qui peuvent présenter un facteur de risque de transformation cellulaire et conduire au développement de tumeurs viro-induites (Schreiber et al., 2011). Si une tumeur commence à se développer, il élimine les cellules tumorales présentes et participe également à la réduction de l'inflammation qui peut conduire à la mise en place d'un microenvironnement favorisant la croissance tumorale (Schreiber et al., 2011).

1.3 – Concept d'immuno-édition de la tumeur

Des études menées dans des modèles murins ont révélé que les tumeurs se développant chez des souris immunodéficientes sont plus immunogènes que les tumeurs issues de souris immunocompétentes (Shankaran et al., 2001). Suite à ces observations, le concept d'immunosurveillance a été révisé et la notion d'édition de la tumeur a été introduite. En effet, le système immunitaire en réagissant contre des cellules tumorales modifie alors leur immunogénicité (Dunn et al., 2002). Le concept d'immuno-édition de la tumeur, aussi appelé « règle des 3 E », se décompose en 3 étapes (Figure 2) (Schreiber et al., 2011):

- L'Élimination : au cours de cette phase, l'ensemble du système immunitaire (inné et adaptatif) détecte et détruit des cellules tumorales avant la formation d'une tumeur cliniquement détectable.
- L'Équilibre : à ce stade, très peu de cellules tumorales ont survécu à la phase d'élimination. Le système immunitaire adaptatif maintient les cellules tumorales dans un état quiescent en contrôlant leur prolifération. C'est au cours de cette phase, qui peut durer plusieurs années, que l'immunogénicité de la tumeur est la plus impactée.
- L'Échappement : au bout d'un certain temps de pression sélective par le système immunitaire, certaines cellules tumorales vont être capables de contourner leur reconnaissance par celui-ci. Elles vont alors proliférer jusqu'à former une tumeur cliniquement détectable.

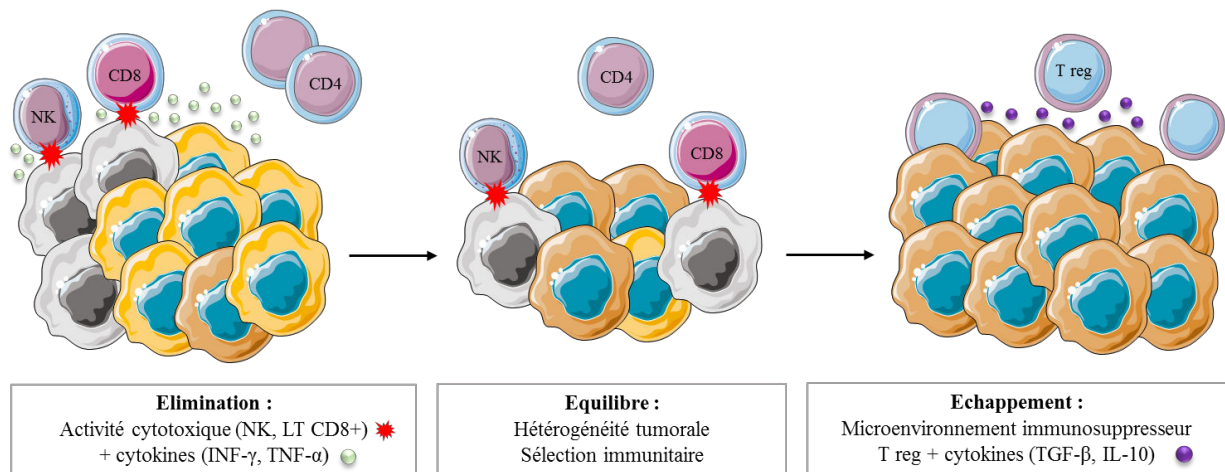


Figure 2 : L'immuno-édition selon la règle des 3E.

Le système immunitaire contrôle le développement des cellules tumorales au cours de la phase d'Elimination, jusqu'à atteindre un stade d'Equilibre, puis des variants tumoraux capables de contourner la réponse immunitaire vont apparaître conduisant à l'Echappement.

Adapté de van der Burg et al., 2016.

La transition entre la phase d'équilibre et la phase d'échappement peut être provoquée par une modification de l'immunogénicité des cellules tumorales liée à la pression de sélection exercée par le système immunitaire ou bien par une altération du système immunitaire liée à la mise en place d'un microenvironnement immunosuppresseur par la tumeur (van der Burg et al., 2016). En effet, les cellules tumorales peuvent modifier le phénotype et les fonctions des cellules qui les entourent pour les rendre immunosuppressives ou pro-tumorales (ex. Treg (LT régulateurs)), via la sécrétion de cytokines immunosuppressives (ex. IL-10 (interleukine 10), TGF- β (transforming growth factor β)). Il est également possible que des facteurs externes permettent aux cellules tumorales d'entrer directement en phase d'équilibre voire d'échappement sans suivre les premières étapes, notamment lors d'un fort stress environnemental ou dans certains cas d'immunodéficience.

1.4 – Principe et Classification de l'immunothérapie anti-tumorale

L'immunothérapie est un traitement qui repose sur la manipulation du système immunitaire afin d'éliminer un pathogène ou une cellule transformée. L'immunothérapie anti-cancéreuse est donc une biothérapie qui utilise le système immunitaire afin d'éliminer spécifiquement les cellules tumorales tout en tentant de limiter les dommages aux cellules saines environnantes.

De nombreux protocoles d'immunothérapie ont été développés au cours des dernières années et sont de plus en plus utilisés en complément des autres traitements (chirurgie, chimiothérapie, radiothérapie ...) dans de nombreux types de cancers tels que le mélanome (Margolin, 2016), le carcinome rénal (Curtis et al., 2016) ou le glioblastome (Tivnan et al., 2017).

Les stratégies d'immunothérapie actuelles reposent sur deux grands principes. L'immunothérapie active qui consiste à stimuler le système immunitaire du patient afin qu'il réagisse à nouveau contre les cellules tumorales (Figure 3). L'immunothérapie passive, quant à elle, est liée au transfert de composants du système immunitaire aux patients afin qu'ils détruisent directement les cellules tumorales ciblées (Figure 3). Plusieurs degrés de complexité sont ajoutés à ces différentes approches d'immunothérapie selon qu'elles utilisent le système immunitaire du patient (autologue) ou celui d'un autre individu (allogénique) et en fonction du/des antigène(s) ciblé(s).

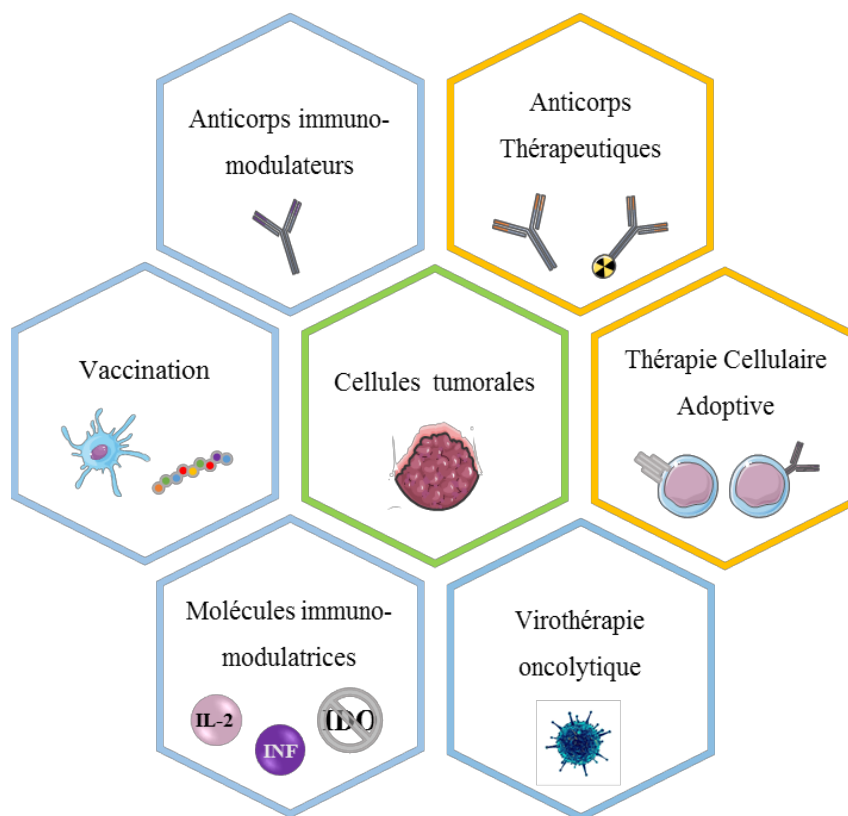


Figure 3 : Classification des différentes stratégies immunothérapeutiques.

L'immunothérapie repose sur deux grands principes : l'activation endogène du système immunitaire du patient ou immunothérapie active (bleu) ; et le transfert de composant(s) du système immunitaire ou immunothérapie passive (jaune). Ces stratégies peuvent être spécifiques d'un antigène de tumeur, comme la vaccination ou les anticorps thérapeutiques, ou non spécifiques, telles que les anticorps ou molécules immunomodulatrices. *Adapté de Velcheti et Schalper, 2016.*

2 – Immunothérapie active

Comme évoqué ci-dessus, l'objectif de l'immunothérapie active est de stimuler le système immunitaire du patient afin de favoriser une réponse dirigée contre les cellules tumorales. Plusieurs méthodes, spécifiques ou non, ont été développées et sont présentées ci-dessous.

2.1 – Anticorps Immunomodulateurs

L'immunothérapie la plus développée actuellement repose sur l'utilisation d'anticorps dirigés contre les points de contrôle inhibiteurs du système immunitaire ou « checkpoint inhibitor ». Ces points de contrôle sont essentiels à la régulation de la réponse immunitaire. Ils jouent un rôle clé dans le maintien de la tolérance face aux cellules de l'organisme et dans l'inhibition des effecteurs cellulaires afin de contrôler la durée et l'intensité de la réaction inflammatoire (Keir et al., 2008). Ainsi dans de nombreux cancers, les cellules tumorales surexpriment les ligands de ces molécules inhibitrices afin d'empêcher l'activation du système immunitaire contre elles (Pardoll, 2012).

Plusieurs couples ligands/molécules inhibitrices sont impliqués dans l'immunosuppression par les cellules tumorales (Figure 4). Parmi eux, CTLA-4 (cytotoxic T lymphocyte associated protein 4) et PD1 (programmed cell death 1) sont deux molécules inhibitrices particulièrement ciblées (Pardoll, 2012). CTLA-4 est un inhibiteur compétitif du récepteur activateur CD28, exprimés par les LT. Ils ont tous les deux pour ligands les molécules CD80/CD86 exprimées par les CPA (cellule présentatrice d'antigène) ou les cellules cibles, mais CTLA-4 présente une meilleure affinité que le CD28 pour ces ligands (Chambers et al., 2001). CTLA-4 est exprimé lors de l'activation du LT et sa haute affinité pour ses ligands va favoriser leur interaction, conduisant alors à l'arrêt de la prolifération et de la différenciation des LT (Chambers et al., 2001). PD1 est également exprimé à la surface des LT activés et possède deux ligands : PDL1 et PDL2 (programmed cell death ligand 1 et 2), qui sont exprimés par les CPA et souvent surexprimés par les cellules tumorales (Freeman et al., 2000). Tout comme pour CTLA-4, l'interaction de PD1 avec ses ligands conduit à l'inhibition de la prolifération et de la production de cytokines pro-inflammatoires par les LT. Elle induit également l'apoptose des LT effecteurs tout en diminuant celle des LT régulateurs, ce qui favorise l'immunosuppression du microenvironnement tumoral (Freeman et al., 2000). Les cellules tumorales, via l'expression des ligands de ces molécules inhibitrices, peuvent donc limiter l'activation et les fonctions effectrices des LT.

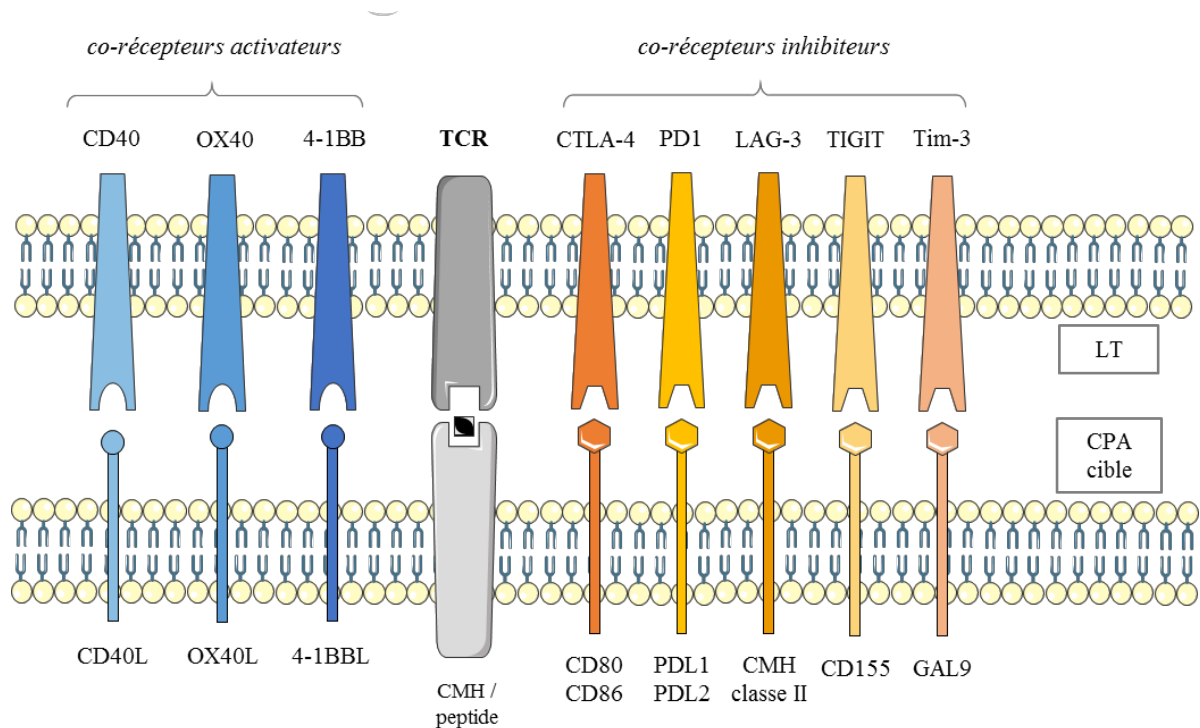


Figure 4 : Corécepteurs impliqués dans la régulation de la réponse des LT.

Plusieurs couples récepteurs/ligands sont impliqués dans la régulation de la réponse des LT face à un antigène. Ces récepteurs peuvent être soit activateurs soit inhibiteurs et possèdent un ou plusieurs ligands qui peuvent être partagés, comme c'est le cas pour CTLA-4 et CD28 qui ont tous les deux pour ligands CD80/CD86. Ces couples sont la cible d'anticorps thérapeutiques visant à moduler la réponse immunitaire dans le cadre d'immunothérapie anti-tumorale. *Adapté de Pradoll, 2012.*

Différents anticorps ont donc été développés pour empêcher les interactions de ces couples récepteurs/ligands, permettant l'activation des LT effecteurs et la destruction des cellules tumorales (Pradoll, 2012). Ainsi, des anticorps inhibiteurs de ces points de contrôle tel que l'ipilimumab, un anticorps anti CTLA-4 ou le nivolumab, un anticorps anti-PD1, ont prouvé leur efficacité dans différents cancers, dont le mélanome (Hodi et al., 2010) et le cancer du poumon (Rizvi et al., 2015).

Bien que leur efficacité ait été démontrée dans différents types de cancers, certains patients restent réfractaires à ce type d'immunothérapie. C'est pourquoi de nouveaux anticorps inhibant d'autres points de contrôle comme LAG-3 (lymphocyte activation gene 3), TIGIT (T cell immunoreceptor with Ig and ITIM domains) ou Tim-3 (T cell membrane protein 3) ont été développés et sont en cours d'évaluation (Velcheti and Schalper, 2016) (Figure 4).

De nombreuses études portent également sur le développement d'anticorps activateurs en ciblant les molécules de costimulation des LT, tels que 4-1BB, OX40 ou encore CD40 (Velcheti and Schalper, 2016) (Figure 4). Cependant, ces stratégies présentent comme inconvénient principal, le développement d'une toxicité auto-immune (ex. colites, atteintes neurologiques) pouvant nécessiter l'arrêt du traitement (Juszczak et al., 2012; Zimmer et al., 2016).

2.2 – Vaccination anti-tumorale

La vaccination thérapeutique dans le cadre de l'immunothérapie anti-tumorale permet d'induire une réponse immunitaire endogène ciblant spécifiquement les cellules tumorales. Tout d'abord, dans le cadre de la prévention des cancers viro-induits, certains vaccins qui n'ont pas été développés pour le traitement de cancers peuvent être utilisés, comme le vaccin contre l'HPV (human papillomavirus) pour le cancer du col de l'utérus (Schiller and Müller, 2015).

Ensuite, différentes stratégies ont été envisagées pour activer le système immunitaire des patients grâce à différentes sources d'antigènes tumoraux, afin de spécifier cette réponse : des peptides ou des protéines exprimés par les cellules tumorales peuvent être utilisés après purification ou synthèse ; des mélanges cellulaires (cellules saines et/ou tumorales) ou lysats obtenus à partir de cellules pouvant provenir d'échantillons frais ou congelés, issus de tumeurs ou de lignées tumorales, autologues ou allogéniques (Butterfield, 2015) (Figure 5).

La stratégie de vaccination anti-tumorale la plus utilisée repose sur l'administration de DC. En effet, les DC sont les cellules immunitaires les plus efficaces pour présenter des antigènes et activer les LT $\alpha\beta$ CD4⁺, CD8⁺ et les cellules NK (Gustafsson et al., 2011). Le plus souvent, les DC sont différenciées, *ex vivo*, à partir des monocytes présents dans les PBMC (peripheral blood mononuclear cells) cultivés en présence d'IL-4 et de GM-CSF (granulocyte macrophage colony stimulating factor) (Figure 5).

Avant d'être injectées aux patients, les DC peuvent être chargées avec des antigènes tumoraux sous différentes formes (peptides synthétisés, lysats cellulaires) ou transfectées avec des ARN (acide ribonucléique) messager issus de cellules tumorales (Butterfield, 2015) (Figure 5). Une fois leur maturation achevée, les DC peuvent être directement administrées aux patients ou bien cryo-préservées avant utilisation.

Plutôt que d'injecter des DC, il est aussi possible d'inoculer directement des peptides antigéniques aux patients (Figure 5). Cette stratégie présente l'avantage de ne pas nécessiter d'étapes de génération et de maturation des cellules *ex vivo*. Cependant, les peptides ne peuvent être utilisés sous leur forme originelle car ils sont faiblement immunogènes. Il est donc nécessaire de les coupler via leur extrémité C-terminale à des protéines porteuses (ex. une toxine) ou de les inclure dans des complexes vaccinaux (ex. protéine chaperonne) qui serviront d'adjuvant (Bröker, 2016; Velcheti and Schalper, 2016). Ainsi modifiés, les peptides pourront être captés par des CPA afin d'induire une réponse immunitaire.

Une fois le vaccin prêt, différentes voies d'inoculations peuvent être utilisées telles que les voies sous-cutanée, intradermique, intramusculaire, intraveineuse ou intralymphatique (Butterfield, 2015). Le choix de la voie d'administration du vaccin dépend du type de cancer, de sa localisation et/ou de l'effet thérapeutique recherché.

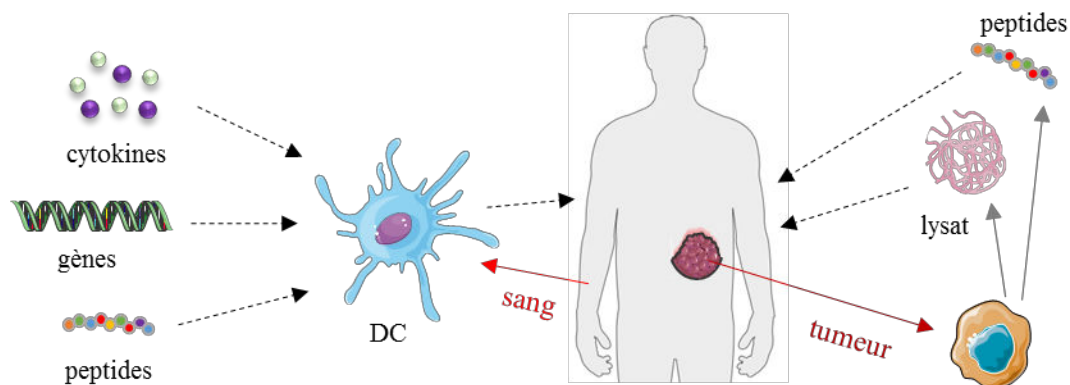


Figure 5 : Différentes stratégies de vaccination anti-tumorale.

La vaccination anti-tumorale est basée soit sur l'injection de DC, après maturation et/ou modifications *ex vivo*, ou sur l'injection de peptides ou lysats issus de cellules tumorales. Ces vaccins peuvent également être combinés à un adjuvant afin de les rendre plus immunogènes.

Adapté de Butterfield, 2015.

Ainsi la vaccination anti-tumorale regroupe de nombreuses stratégies qui ont pour but de promouvoir une réponse immunitaire spécifique de la tumeur. D'autres stratégies thérapeutiques, telles que l'ablation chirurgicale par radiofréquence, la chimio- et la radiothérapie, peuvent être considérées comme des « vaccins » car elles induisent une mort immunogène des cellules tumorales conduisant également à l'activation du système immunitaire spécifiquement contre des antigènes de tumeurs.

2.3 – Molécules Immunomodulatrices

Une approche également utilisée pour stimuler de façon globale et directe la réponse immunitaire est l'utilisation de cytokines, telles que les IFN (interféron) de type I qui permettent la maturation des DC et l'activation d'effecteurs immunitaires (LT, NK) ou bien l'IL-2 pour amplifier les LT (Velcheti and Schalper, 2016). Cependant l'utilisation de ces cytokines reste très délicate du fait de leur manque de spécificité et des nombreux effets secondaires qu'elles déclenchent.

Par exemple, suite à des injections systémiques d'IL-2, l'activation non spécifique du système immunitaire, principalement des LT, conduit à une libération massive de cytokines pro-inflammatoires nommée « tempête cytokinique ». Les effets indésirables les plus courants sont de la fièvre, des malaises, des troubles digestifs et dans certains cas les conséquences peuvent être fatales aux patients (Dhupkar and Gordon, 2017).

Toujours dans le but de restaurer une réponse immunitaire dirigée contre les cellules tumorales, d'autres stratégies, moins directes, ont été développées. C'est le cas des inhibiteurs du métabolisme qui ont pour cible le microenvironnement immunosuppresseur mis en place par la tumeur. Par exemple, des inhibiteurs de l'enzyme IDO (indoleamine-2,3-dioxygénase) ont été développés dans le but de diminuer l'immunosuppression qu'elle engendre (Amobi et al., 2017). En effet, IDO est impliquée dans la dégradation du tryptophane, un acide aminé essentiel, et est surexprimée dans de nombreux types de cancers. Il en découle un dérèglement métabolique caractérisé par une déplétion locale en tryptophane et une accumulation de ses dérivés, favorisant l'immunosuppression (Amobi et al., 2017).

2.4 – Virothérapie

La virothérapie est une autre stratégie en cours de développement qui, en plus de pouvoir détruire directement les cellules tumorales, a l'avantage de provoquer, comme effet secondaire, une réponse immunitaire antivirale. Les virus oncolytiques présentent un tropisme naturel pour les cellules en prolifération, dans lesquelles ils se répliquent (Fountzilias et al., 2017). Ils peuvent donc infecter préférentiellement les cellules tumorales et les détruire sans affecter les cellules saines voisines.

Les virus oncolytiques sont classés en deux grandes catégories en fonction du matériel génétique qu'ils portent : les virus à ADN (acide désoxyribonucléique) et les virus à ARN. Parmi les virus à ADN on retrouve les herpes virus et les adénovirus, alors que les reovirus et le virus de la rougeole appartiennent à la famille des virus à ARN (Fountzilias et al., 2017). Ces virus infectent les cellules cibles via la liaison de récepteurs exprimés à leur surface et/ou par fusion avec la membrane plasmique. Ils profitent ensuite de la machinerie cellulaire très active des cellules tumorales pour se répliquer tout en altérant le fonctionnement de la cellule hôte par des modifications génétiques ou en modifiant des voies de signalisation (ex. voie RAS) (Fountzilias et al., 2017).

De nombreuses équipes ont amélioré cet outil en modifiant le récepteur impliqué dans la liaison à la cellule cible pour qu'il soit spécifique d'un antigène exprimé par la tumeur et/ou en modifiant son matériel génétique pour modifier la régulation de gènes exprimés par la cellule tumorale (Fountzilias et al., 2017).

Bien que les résultats obtenus *in vitro* et *in vivo* soient très encourageants, les effets cliniques observés sont plutôt limités. Néanmoins, T-VEC, un herpes virus génétiquement modifié, est le premier virus oncolytique approuvé pour le traitement des mélanomes localement non-résécables (Hu et al., 2006).

L'effet anti-tumoral induit par les virus oncolytiques peut aussi être lié à la mise en place d'une réponse immunitaire. Il peut s'agir d'une activation en réponse à la mort immunogène des cellules tumorales ou bien d'une réponse antivirale contre les cellules tumorales infectées par le virus mais toujours vivantes. Cette dernière réponse a l'avantage de lyser les cellules tumorales qui n'auraient pas été détruites par le virus et l'inconvénient d'éradiquer le virus de l'organisme (Fountzilias et al., 2017).

3 – Immunothérapie passive

Contrairement à l'immunothérapie active, l'immunothérapie passive est basée sur le transfert de composant(s) du système immunitaire pour détruire directement les cellules tumorales.

3.1 – Anticorps Thérapeutiques

Dans le cadre d'une immunothérapie passive, l'utilisation d'anticorps a pour but la mort des cellules tumorales par différents mécanismes immuns (ADCC (antibody dependant cell mediated cytotoxicity), complément) et non-immuns (lyse directe) (Buss et al., 2012). La subtilité de ce type de traitement repose sur la spécificité de l'antigène ciblé par les anticorps. Ainsi, deux catégories d'antigènes se distinguent : les antigènes spécifiques de tumeur, exprimés exclusivement par les cellules tumorales, et les antigènes associés aux tumeurs, qui eux sont exprimés aussi bien par les cellules tumorales que par le tissu sain mais de façons différentes (surexpression, mutation ...). L'idéal est de pouvoir cibler un antigène spécifique de tumeur pour éviter l'attaque du tissu sain mais l'identification de ce type d'antigène reste rare car ils sont souvent exprimés de façon hétérogène au sein de la tumeur et peu conservés du fait de la pression sélective induite.

Le Rituximab est le premier anticorps thérapeutique développé et validé pour le traitement des lymphomes non-hodgkiniens (Leget and Czuczman, 1998). Cet anticorps monoclonal cible le CD20, un canal calcique préférentiellement exprimé par les LB. A l'origine, il s'agit d'un anticorps chimérique (souris-humain) mais depuis sa première mise sur le marché, en 1997, plusieurs dérivés humanisés, comme l'Ofatumumab ou l'Obinutuzumab, ont été conçus pour être plus spécifiques de la cible et/ou présenter une meilleure activité biologique (Pierpont et al., 2018). Cet anticorps a fourni une preuve de l'efficacité de cette stratégie thérapeutique, ouvrant la voie au développement de nombreux anticorps monoclonaux, aussi bien pour le traitement des tumeurs liquides que solides, tel que le Trastuzumab, dirigé contre le récepteur HER2 et prescrit dans le cancer du sein (Buss et al., 2012).

Grâce à ces anticorps, il est également possible de cibler le microenvironnement tumoral comme c'est le cas pour la thérapie anti-angiogénique. En effet, pour répondre à leurs besoins énergétiques importants les cellules tumorales induisent l'angiogénèse via une forte expression de VEGF (vascular endothelial growth factor) (Falk et al., 2015). Les tumeurs solides sont donc généralement caractérisées par une prolifération excessive et anarchique de micro-vaisseaux.

Le but de la thérapie anti-angiogénique, en ciblant le VEGF, est de ralentir la croissance tumorale et de favoriser une normalisation des vaisseaux pour permettre une meilleure diffusion des autres traitements (chimiothérapie ou immunothérapie). Le Bevacizumab est l'anticorps anti-VEGF le plus utilisé, il est actuellement prescrit dans le cancer du sein ou le cancer colorectal et fait l'objet d'essais cliniques dans d'autres cancers (Falk et al., 2015).

Afin d'améliorer l'efficacité de ces thérapies, de nouvelles stratégies se développent comme le couplage des anticorps à un radioélément ou à une toxine et le développement d'anticorps bispécifiques ayant une double spécificité pour un antigène tumoral et une molécule activatrice exprimée par un effecteur immunitaire (Buss et al., 2012).

3.2 – *Thérapie Cellulaire Adoptive*

La thérapie cellulaire adoptive est basée sur l'administration d'effecteurs immunitaires cytotoxiques aux patients, pour détruire de façon directe la tumeur, sans chercher à induire de réponse immunitaire endogène. Différentes populations lymphocytaires (ex. LT $\alpha\beta$, LT $\gamma\delta$, NK) peuvent être utilisées mais elles doivent partager des caractéristiques communes : une spécificité pour un antigène tumoral, des fonctions effectrices robustes et une bonne capacité d'amplification (Rosenberg and Restifo, 2015).

Généralement, cette stratégie nécessite la manipulation de ces effecteurs *ex vivo* afin de les sélectionner selon leur spécificité antigénique et/ou de les amplifier (Figure 6). Ces cellules peuvent donc provenir directement de l'infiltrat intra-tumoral, des ganglions lymphatiques drainant la tumeur ou bien du sang périphérique (Rosenberg and Restifo, 2015).

La première thérapie cellulaire adoptive a été mise en place par Rosenberg et ses collaborateurs, chez des patients atteints de mélanome (Rosenberg et al., 1988). Une régression tumorale a pu être observée chez plusieurs patients grâce à l'injection de TIL autologues, après amplification *ex vivo* en présence d'IL-2.

Afin d'améliorer le potentiel thérapeutique de cette thérapie, il est possible de trier les LT des patients pour leur spécificité antigénique et/ou de les amplifier *ex vivo* en présence d'un antigène d'intérêt (Rosenberg and Restifo, 2015).

Il est également possible, par génie génétique, de faire exprimer un TCR (T cell receptor) de haute affinité pour un antigène d'intérêt par des effecteurs cytotoxiques (Figure 6). Plusieurs études ont été menées en ce sens, au cours desquelles des LT autologues, collectés dans le sang périphérique, ont été transfectés avec un rétrovirus pour exprimer un TCR spécifique d'un antigène de mélanome (MART-1 ou NY-ESO-1) avant de les réinjecter aux patients (Johnson et al., 2009; Morgan et al., 2006).

En plus de l'effet thérapeutique observé, ces études ont permis de mettre en évidence une longue persistance des cellules dans l'organisme (jusqu'à 1 an) mais aussi des réponses auto-immunes chez les patients ayant reçu des effecteurs modifiés pour exprimer un TCR dirigé contre un antigène associé à la tumeur, donc également exprimé par les cellules saines (Johnson et al., 2009; Morgan et al., 2006).

Cependant ces stratégies présentent des inconvénients qui limitent les possibilités d'applications. En effet, le tri et l'amplification de cellules autologues spécifiques d'un antigène tumoral sont souvent difficiles car elles sont présentes en faibles proportions chez les patients. De plus, leur activation étant restreinte par le CMH (complexe majeur d'histocompatibilité), la meilleure stratégie reste d'utiliser des effecteurs autologues bien qu'ils puissent devenir anergique du fait de l'immunosuppression mise en place par le microenvironnement tumoral du patient. L'une des solutions en réponse à ce problème est une cure de chimiothérapie immunosuppressive (cyclophosphamide et fludarabine) en amont du transfert cellulaire afin d'induire une lymphodépletion, éliminant notamment les Treg, afin d'augmenter l'efficacité du traitement et la persistance des effecteurs chez les patients (Rosenberg and Restifo, 2015).

Grâce au génie génétique une nouvelle famille de récepteurs a été créée : les CAR (chimeric antigen receptor) (Figure 6). Il s'agit d'une molécule hybride composée du domaine variable d'une Ig, qui lui confère sa spécificité antigénique, et la partie constante d'un TCR, assurant la transduction du signal (Gross et al., 1989). Cette combinaison confère aux effecteurs lymphocytaires qui l'expriment la capacité de reconnaître de façon très spécifique un antigène de façon indépendante du CMH et les fonctions effectrices de la cellule qui l'exprime (cytotoxicité, migration, mémoire ...). La preuve de l'efficacité clinique de cette nouvelle famille de récepteurs a été donnée chez des patients atteints de lymphomes qui ont reçu une injection de LT autologues transfectés grâce à un rétrovirus pour exprimer un CAR dirigé contre le CD19 (Kochenderfer et al., 2010).

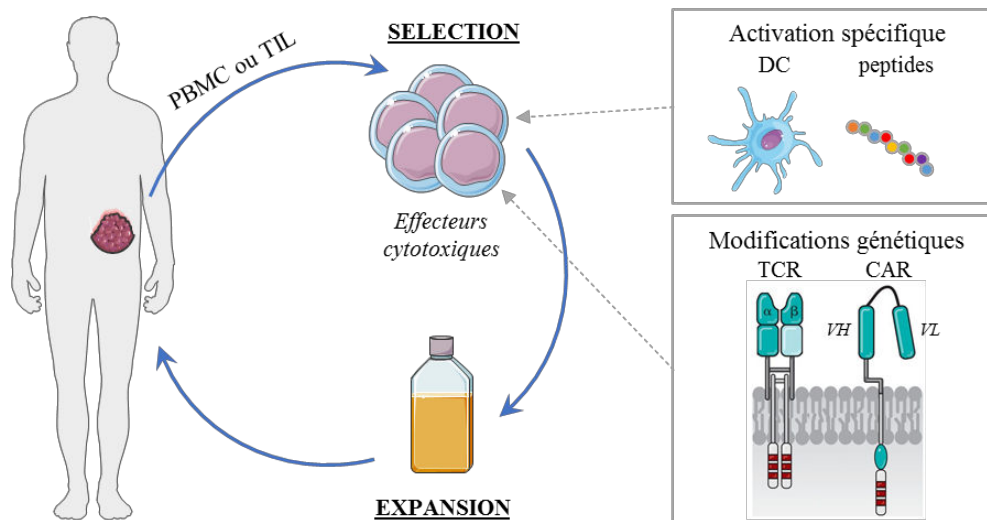


Figure 6 : Différentes stratégies de thérapie cellulaire adoptive.

Les effecteurs cytotoxiques peuvent être issus du sang périphérique (PBMC) ou de l'infiltrat immunitaire de la tumeur (TIL). Au cours du processus de sélection et d'expansion *ex vivo*, il est possible de les activer spécifiquement contre un antigène de tumeur (DC, peptides) et/ou de les modifier génétiquement pour qu'ils expriment un TCR ou un CAR spécifique d'antigènes tumoraux. Les effecteurs cytotoxiques ainsi obtenus sont ensuite administrés aux patients.

Adapté de Rosenberg et Restifo, 2015.

Cette stratégie présente de nombreux avantages mais également plusieurs inconvénients, partagés avec les autres stratégies. La modification de cellules autologues est longue et l'amplification parfois difficile pour obtenir des quantités suffisantes de cellules pour le traitement. De plus, la spécificité de l'antigène cible conditionne l'apparition d'effets secondaires sur les tissus sains qui s'additionnent aux tempêtes cytokiniques fréquemment observées chez les patients (Kalaitidou et al., 2015; Neelapu et al., 2018).

Les stratégies d'immunothérapie dans leur ensemble permettent donc d'améliorer la prise en charge et la survie des patients atteints de cancers. Ces biothérapies restaurent une réponse immunitaire anti-tumorale qui permet l'élimination partielle ou totale des cellules tumorales. Cependant, la pression immunitaire induite peut conduire à l'émergence de nouvelles cellules tumorales résistantes et à la rechute de la maladie. De plus, la réponse immunitaire déclenchée par ces différentes stratégies d'immunothérapie est souvent impactée par le microenvironnement immunosuppresseur mis en place par la tumeur. L'immunothérapie doit donc continuer d'évoluer pour s'adapter à ces problématiques.

II - Les lymphocytes T $\gamma\delta$

Comme évoqué précédemment les LT $\gamma\delta$ font partie de l'immunité transitionnelle. Ils présentent un profil hybride entre des cellules de l'immunité adaptative (ex. LT $\alpha\beta$) et de l'immunité innée (ex. cellules NK).

1 - Répertoire des LT $\gamma\delta$

1.1 - Conservation entre les espèces

Il est important de préciser que bien que des LT $\gamma\delta$ soient retrouvés chez tous les vertébrés étudiés à ce jour, il existe peu de conservation des chaînes γ et δ entre les espèces. Des études génétiques ont révélé une grande hétérogénéité entre les gènes murins et ceux des primates (Sturm et al., 1992). Une autre étude a mis en avant qu'il existe également des différences géniques entre les primates et l'Homme (Kazen and Adams, 2011). Ces données génétiques sont corrélées à l'observation de sous-populations similaires, bien que différentes, entre l'Homme et les primates mais n'ayant pas d'équivalent chez la souris. Dans ce contexte et de façon volontaire, cette introduction est focalisée sur les LT $\gamma\delta$ humains.

1.2 – Diversité du TCR $\gamma\delta$

Les LT $\gamma\delta$ expriment un TCR composé de deux chaînes : une chaîne δ et une chaîne γ , découvertes dans les années 1980 (Brenner et al., 1986; Saito et al., 1984). Tout comme pour le TCR $\alpha\beta$, les chaînes γ et δ vont subir des mécanismes de recombinaisons somatiques. Ces recombinaisons conduisent à l'association d'un segment variable (V) avec un segment de jonction (J) et dans certains cas à un segment de diversité (D), avec pour but la production de milliards de récepteurs spécifiques d'antigènes les plus divers possible. Les LT $\gamma\delta$ possèdent moins de gènes V que les LT $\alpha\beta$ et les possibilités de combinaisons des gènes V sont encore réduites du fait des conditions d'appariement entre les chaînes γ et δ (Pereira and Boucontet, 2004), ce qui laisse supposer une plus faible diversité de répertoire $\gamma\delta$. Néanmoins, cela est compensé par une diversité jonctionnelle élevée liée à une grande variabilité de la boucle CDR3 (complementarity determining region 3) de la chaîne δ (Chien et al., 2014) conduisant à un nombre théorique de TCR 100 fois plus élevé que pour les LT $\alpha\beta$ (Chien and Konigshofer, 2007; Harly et al., 2014).

Les segments variables alors obtenus ($V\gamma$ et $V\delta$) servent de base à la classification des différentes sous-populations. Chez l'Homme, les LT $\gamma\delta$ sont divisés en 4 sous-populations principales en fonction de l'expression de leur chaîne δ : les $V\delta 1$, $V\delta 2$, $V\delta 3$ et $V\delta 5$ (Zhao et al., 2018). En fonction de la chaîne γ qui leur est associée certaines sous-populations de LT $\gamma\delta$ vont avoir des localisations préférentielles dans certains tissus (Figure 7). De plus, certaines combinaisons $V\gamma$ et $V\delta$ ayant des séquences jonctionnelles identiques vont mener à des TCR invariants tel que l'hétérodimère $V\gamma 9V\delta 2$ (sous-population majeure dans le sang périphérique chez l'adulte).

Sous-population	Chaîne $V\gamma$ associée	Localisation
$V\delta 1$	$V\gamma 2, V\gamma 3, V\gamma 4, V\gamma 5, V\gamma 8, V\gamma 9$	Sang périphérique, peau, intestin, rate, foie
$V\delta 2$	$V\gamma 9$	Sang périphérique
$V\delta 3$	$V\gamma 2, V\gamma 3$	Sang périphérique, foie
$V\delta 5$	$V\gamma 4$	Sang périphérique

Figure 7 : Les sous-populations de LT $\gamma\delta$ chez l'Homme.

Les LT $\gamma\delta$ humains peuvent être divisés en 4 sous-populations principales, sur la base de l'expression de la chaîne δ de leur TCR. *Adapté de Zhao et al., 2018.*

1.3 – Ontogénèse et sélection thymique

La plupart des études portant sur le développement thymique des LT $\gamma\delta$ ayant été réalisées chez la souris, qui partage peu d'équivalents structuraux ou fonctionnels avec l'Homme, des incertitudes demeurent sur les mécanismes qui régulent le développement et la sélection de ces lymphocytes. Néanmoins, certaines données obtenues dans ces modèles murins semblent être généralisables à d'autres espèces puisqu'un certain nombre de ces mécanismes ont pu être observés chez l'Homme.

Il a été montré que les LT $\alpha\beta$ et les LT $\gamma\delta$ apparaissent de façon concomitante au cours du développement thymique et ont pour origine un précurseur commun (Dudley et al., 1995; Vantourout and Hayday, 2013) (Figure 8). Ainsi, les LT $\gamma\delta$ peuvent être détectés dès 8 semaines de développement fœtal (McVay and Carding, 1996). S'ensuit une première migration de LT $\gamma\delta$ vers le sang et le foie, participant notamment à la mise en place du répertoire $V\gamma 9V\delta 2$ du sang périphérique.

Après la naissance, les réarrangements des gènes δ impliquent principalement le segment V δ 1, les segments V δ 3 et V δ 5 apparaissent plus rarement (Kragel et al., 1990). Les étapes de maturation qui suivent impliquent de multiples mécanismes de sélection thymique puis extra-thymique qui restent encore à élucider (Parker et al., 1990; Pauza and Cairo, 2015).

A l'âge adulte, les LT $\gamma\delta$ sont répartis dans l'organisme de manière non aléatoire. Ils sont très répandus dans les épithéliums où ils peuvent représenter jusqu'à 50 % des lymphocytes. Ils sont également présents dans le sang périphérique mais en plus faible proportions (1 à 5 % des LT) (Silva-Santos et al., 2015).

Bien que la population de LT $\gamma\delta$ directement issue du thymus soit hétérogène, après passage dans la circulation générale, la sous-population exprimant un TCR V γ 9V δ 2 s'amplifie et s'accumule en périphérie, devenant la sous-population majoritaire de LT $\gamma\delta$ (~80 %) (Figure 8) (Pauza and Cairo, 2015; Vantourout and Hayday, 2013).

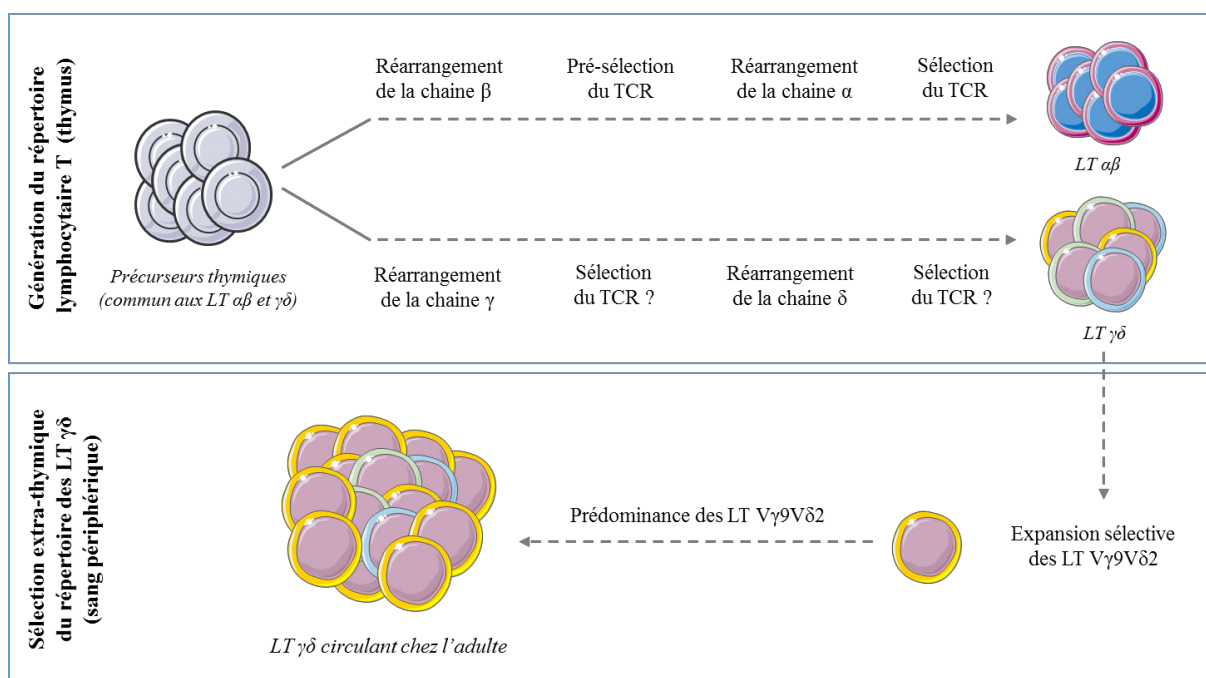


Figure 8 : Modèle présentant les grandes étapes de la sélection thymique et extra-thymique à l'origine du répertoire des LT $\gamma\delta$ en périphérie chez l'adulte.

Les LT $\gamma\delta$ sont issus d'un précurseur commun avec les LT $\alpha\beta$, cependant leur développement thymique n'est pas encore clairement décrit. Les réarrangements des chaînes du TCR $\gamma\delta$, dans le thymus, conduisent à une population hétérogène, sans prédominance d'une sous-population plutôt qu'une autre. Après passage dans la circulation générale, une amplification sélective des LT exprimant un TCR V γ 9V δ 2 est observée (jaune), conduisant à un répertoire majoritairement V γ 9V δ 2 dans le sang périphérique chez l'adulte. *Adapté de Pauza et Cairo, 2015.*

2 – Modalités d’activation des LT $\gamma\delta$

2.1 – Diversité des récepteurs exprimés

Les LT $\gamma\delta$ sont activés via leur TCR, spécifique d’un antigène, et avec l’aide de molécules de costimulation. Cependant cette activation antigénique n’est pas régie par les mêmes lois que celles du TCR $\alpha\beta$. En effet, la reconnaissance d’une cellule cible par un LT $\gamma\delta$ n’est pas restreinte par un complexe CMH/peptide.

Des analyses structurales ont comparé un TCR $\gamma\delta$, un TCR $\alpha\beta$ et la partie Fab d’une immunoglobuline (Ig). Il apparaît alors que la structure du TCR $\gamma\delta$ est différente de celle du TCR $\alpha\beta$, se rapprochant d’avantage du Fab d’une Ig (Figure 9) (Allison et al., 2001). Des études suggèrent également que le mode de reconnaissance des antigènes par le TCR $\gamma\delta$ serait plus proche de celui des Ig que de celui du TCR $\alpha\beta$ (Chien and Konigshofer, 2007; Kazen and Adams, 2011). De plus, les boucles CDR3 (zone d’interaction entre le récepteur et l’antigène) des différents TCR et des Ig ont également été étudiées. Il en ressort que les CDR3 de la chaîne γ sont courts (~ 7 acides aminés) et les CDR3 de la chaîne δ peuvent être de longueur variable (entre 10 et 20 acides aminés) tout comme chez les Ig où la chaîne légère possède des CDR3 plus courts que ceux de la chaîne lourde (Chien et al., 2014; Rock et al., 1994).

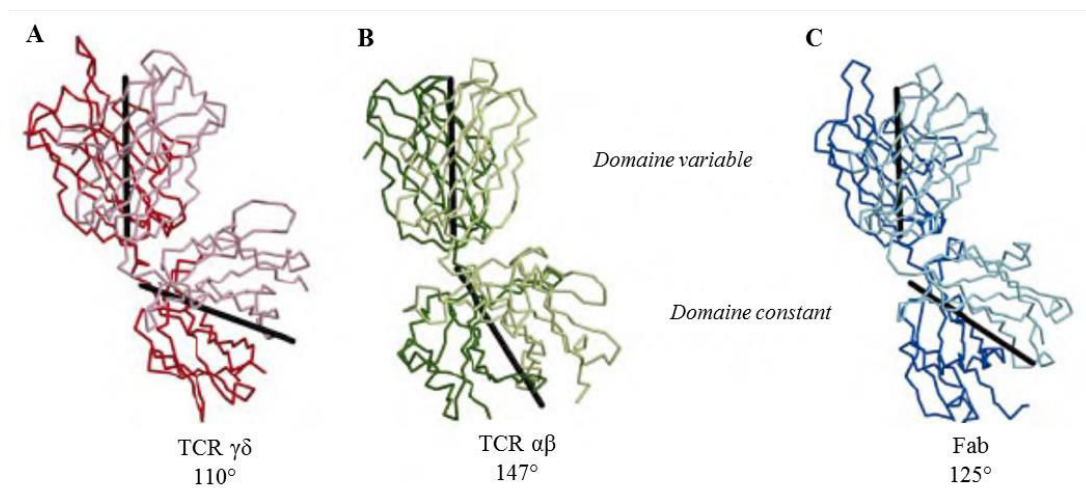


Figure 9 : Structure tridimensionnelle d’un TCR $\gamma\delta$, d’un TCR $\alpha\beta$ et du Fab d’une Ig.

Présentation de la structure (A) d’un TCR $V\gamma 9V\delta 2$, (B) d’un TCR $\alpha\beta$ et (C) d’un fragment Fab d’une Ig. Les chaînes γ , β et lourdes sont en couleurs claires tandis que les chaînes δ , α et légères sont en couleurs foncées. *Adapté d’Allison et al., 2001.*

A l'instar des autres populations de LT, l'activation des LT $\gamma\delta$ est régulée par d'autres récepteurs. Très peu de LT $\gamma\delta$ expriment les corécepteurs CD4 et CD8, largement exprimés par les LT $\alpha\beta$. A la place, ils expriment des récepteurs non-clonaux tels que des récepteurs activateurs et inhibiteurs de type NKR (Natural Killer receptor) ou encore des récepteurs de la famille des TLR (Toll like receptor) (Bonneville et al., 2010) (Figure 10). Ces récepteurs agissent généralement en tant que costimulateurs et non de façon indépendante du TCR.

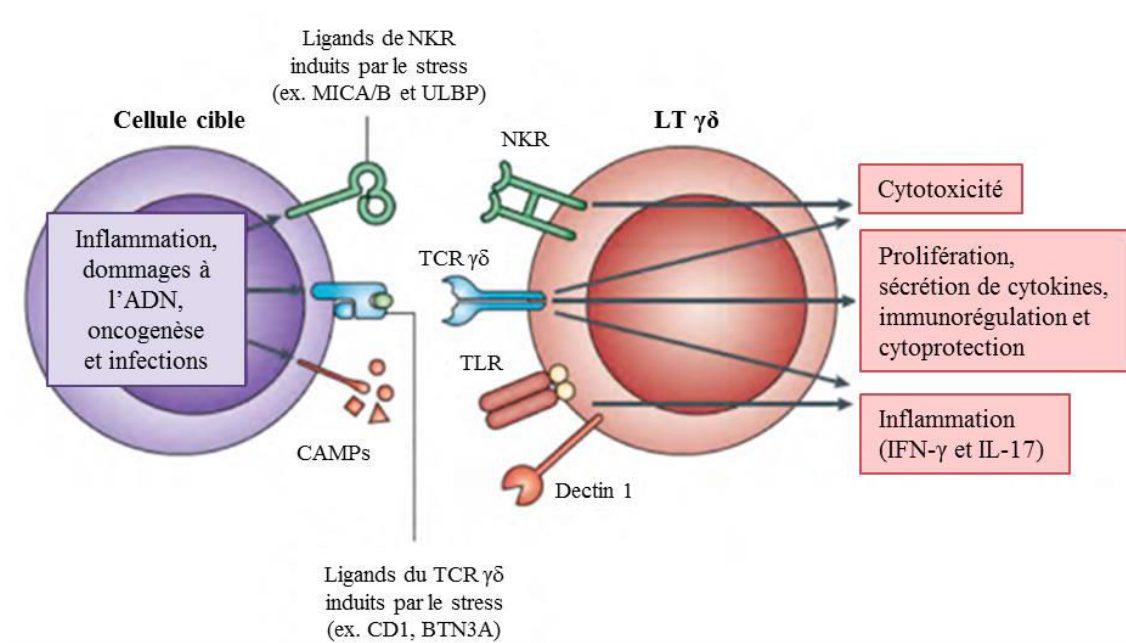


Figure 10 : Récepteurs modulant l'activation des LT $\gamma\delta$.

Les LT $\gamma\delta$ sont capables de reconnaître des cellules stressées (infectées ou transformées) grâce à leur TCR et/ou leurs corécepteurs de type NKR ou TLR. Ces récepteurs fonctionnent de façon indépendante, additionnelle ou synergique afin de déclencher différents types de réponses effectrices par les LT $\gamma\delta$.
Adapté de Bonneville et al., 2010.

2.2 – Ligands du TCR $\gamma\delta$

Théoriquement, la diversité combinatoire du TCR $\gamma\delta$ pourrait permettre d'atteindre 10^{16} TCR différents, mais en réalité la diversité des TCR $\gamma\delta$ observée en périphérie est restreinte. Il est donc logique d'imaginer que les ligands reconnus sont peu diversifiés. Cependant, ils peuvent être de nature très variée : protéique ou lipidique, endogène ou exogène (Vermijlen et al., 2018) (Figure 11), ce qui corrèle avec l'idée que la reconnaissance antigénique des LT $\gamma\delta$ soit proche de celle des Ig.

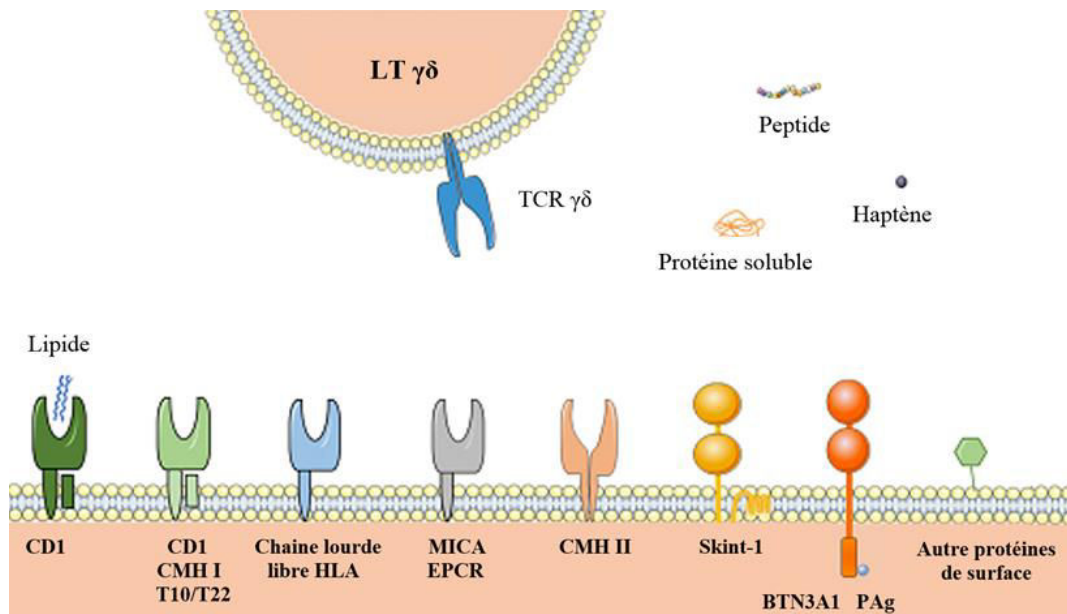


Figure 11 : Différentes classes de ligands proposés et/ou confirmés des LT $\gamma\delta$.
Adapté de Vermijlen et al., 2018.

A ce jour, de nombreuses molécules ont été identifiées pour interagir avec le TCR $\gamma\delta$, bien que leur nature ou leur structure soient très différentes, comme des membres de la famille CD1 qui présentent, ou non, des antigènes lipidiques comme la cardiolipin ou l' α GalCer (α -Galactosyl Ceramide) (Uldrich et al., 2013). Les molécules MICA et MICB (MHC class I polypeptide-related sequence A et B) sont des molécules apparentées aux CMH de classe I, initialement identifiées comme des ligands des NKR, elles peuvent également être reconnues par le TCR $\gamma\delta$ (Xu et al., 2011). D'autres protéines de surfaces viennent s'ajouter à la liste (BTN3A, EphA2, annexin A2), qui s'allonge encore avec des molécules solubles d'origine peptidique (peptide viraux, haptènes, insuline B:9-23 ...) ou non (haptènes, phosphoantigènes ...) (Figure 11). Il est difficile d'arriver à une vision claire de la nature des ligands des TCR $\gamma\delta$. Il ressort tout de même que ces ligands sont liés à un stress cellulaire (infection, transformation) et nombre d'entre eux sont des molécules du Soi (Vermijlen et al., 2018).

L'expression de ces molécules du Soi est régulée par différents mécanismes générant un seuil à dépasser pour permettre l'activation des LT $\gamma\delta$. Ces mécanismes de reconnaissance peuvent inclure une augmentation d'expression à la surface de la cible, l'acquisition de nouveaux composants par association avec une molécule issue du pathogène, le recrutement d'un partenaire du Soi ou encore le relargage du ligand notamment lors de l'apoptose (Chien et al., 2014). Certains de ces mécanismes sont encore mal décrits compliquant la compréhension des mécanismes d'activation des LT $\gamma\delta$.

3 – Pléiotropie fonctionnelle des LT $\gamma\delta$

L'ensemble des LT $\gamma\delta$ est capable de s'activer rapidement afin de défendre l'hôte contre les infections, les transformations cellulaires et les dommages tissulaires. Six mécanismes d'action principaux, qui peuvent varier en fonction de la localisation tissulaire des LT $\gamma\delta$, sont actuellement décrits (Vantourout and Hayday, 2013). Ainsi, les LT $\gamma\delta$ ont la capacité de :

- lyser de façon directe des cellules stressées (infectées ou transformées) notamment par la libération de granules cytotoxiques contenant de la perforine et des granzymes,
- produire un large panel de facteurs solubles tels que des cytokines pro-inflammatoires et des chimiokines permettant la régulation d'autres cellules immunitaires,
- favoriser la production d'anticorps (IgE) par les LB,
- présenter des antigènes aux LT $\alpha\beta$ permettant leur activation,
- collaborer avec des cellules dendritiques afin d'induire leur maturation,
- réguler l'homéostasie des cellules stromales via la production de facteurs de croissance.

Grâce à ces différents mécanismes d'action les LT $\gamma\delta$ joueraient un rôle central dans les défenses immunitaires de l'hôte. Ils sont capables de reconnaître un large panel de pathogènes intra- et extra-cellulaires (bactéries, virus et parasites). Les LT $\gamma\delta$ présents dans les épithéliums et les muqueuses sont particulièrement impliqués dans l'immunité anti-infectieuse du fait de leur localisation préférentielle et permettent le déclenchement rapide de la réponse. Ces LT $\gamma\delta$ expriment principalement les chaînes V δ 1 et V δ 3 et sont capables de détecter la présence aussi bien des bactéries intracellulaires (ex : *Mycobacteria*, *Listeria*, ...) que de virus (ex : CMV (cytomegalovirus), VIH, ...) (Bonneville and Scotet, 2006; Déchanet et al., 1999; Poccia et al., 2005).

Les LT $\gamma\delta$ auraient également un rôle non négligeable dans la surveillance des tumeurs. Cette surveillance est assurée aussi bien par les LT $\gamma\delta$ présents dans les tissus que par ceux circulant dans le sang (Hayday, 2009). Ainsi la présence de LT $\gamma\delta$ infiltrant les tumeurs a pu être observée dans de nombreux cancers, qu'ils soient solides ou liquides, renforçant l'idée de leur implication naturelle dans l'immunité anti-tumorale (Gentles et al., 2015). Toutefois, l'affinité du TCR qu'ils expriment, toutes les autres molécules impliquées dans la reconnaissance de la tumeur ciblée et les fonctions effectrices qui en découlent font varier la capacité anti-tumorale des LT $\gamma\delta$, pouvant également mener à l'apparition de sous-population de LT $\gamma\delta$ pro-tumoraux (Scheper et al., 2014).

III – Les Lymphocytes T $V\gamma 9V\delta 2$

Comme décrit précédemment, les LT $\gamma\delta$ humains sont classés en différentes sous-populations en fonction du segment $V\delta$ qu'ils expriment. Deux grandes catégories sont distinguées : les $V\delta 2$ positifs et les $V\delta 2$ négatifs. Dans le cas des LT $V\delta 2$ positifs, ils expriment majoritairement la chaîne $V\gamma 9$ formant le TCR hétérodimérique $V\gamma 9V\delta 2$ mais cette association n'est pas exclusive, il existe aussi des LT $V\delta 2^+V\gamma 9^-$ (Davey et al., 2018). A l'inverse, les LT $V\delta 2$ négatifs expriment aussi bien les chaînes $V\delta 1$ que $V\delta 3$ associées à diverses chaînes $V\gamma$. Ce travail de thèse portant principalement sur les LT $V\gamma 9V\delta 2$, ils sont décrits plus en détails ci-dessous.

1 – Généralités

Les LT $V\gamma 9V\delta 2$ sont présents quasiment exclusivement chez l'Homme et les primates supérieurs (pas d'homologues murins) et sont parfois nommés $V\gamma 2V\delta 2$ dans la littérature (nomenclature de Seidman). Ils représentent 1 à 5 % des cellules $CD3^+$ et jusqu'à 80 % des LT $\gamma\delta$ dans le sang périphérique, ce qui en fait la sous-population la plus abondante, en périphérie, chez l'adulte sain. Tout comme les autres LT $\gamma\delta$ ils apparaissent dès le stade fœtal, ils sont prédominants à 23 semaines de gestation puis diminuent avant la naissance (Dimova et al., 2015). Les LT $V\gamma 9V\delta 2$ augmentent à la fois en nombre absolu et en proportion de LT $CD3^+$ jusqu'à l'âge de 8 ans.

Le réarrangement de leur TCR se fait par recombinaisons somatiques des segments variables γ et δ puis par épissage de l'ARN messager ainsi généré. Malgré une diversité jonctionnelle importante, la chaîne $V\gamma 9$ présente une recombinaison spécifique avec le segment de jonction JP puis un épissage avec le segment C1 formant ainsi la chaîne $V\gamma 9$ -JP-C1 (Casorati et al., 1989; Pauza and Cairo, 2015) (Figure 12).

Deux hypothèses ont été émises quant à l'association préférentielle de cette chaîne $V\gamma 9$ -JP-C1 avec la chaîne $V\delta 2$. La première met en avant l'orientation des chaînes $V\gamma$ avec les segments J (Tribel et al., 1988). La seconde suggère une sélection positive de ce TCR dans le sang périphérique du fait de sa spécificité antigénique (Band et al., 1989; Borst et al., 1989). Néanmoins, le TCR $V\gamma 9V\delta 2$ va tout de même présenter une certaine diversité du fait de l'ajout aléatoire de nucléotides lors de la recombinaison VJ et du réarrangement supplémentaire du segment de diversité D sur la chaîne $V\delta 2$ (Pauza and Cairo, 2015).

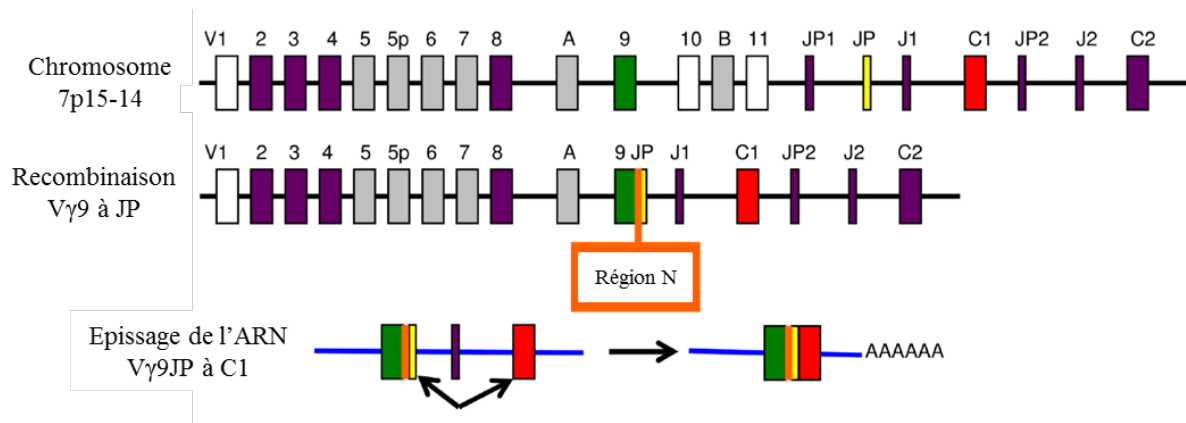


Figure 12 : Structure du locus de la chaîne γ humaine et étapes de l'assemblage de la chaîne $V\gamma 9$ -JP-C1.

Cette figure décrit une portion du chromosome 7 (p15-p14) humain et n'est pas dessinée à l'échelle. Dans la lignée germinale sont présents 14 gènes ou pseudogènes de la chaîne variable (V) γ , 5 segments jonctionnels (J) et 2 régions constantes (C). Les régions violettes, vertes, jaunes et rouges représentent des séquences fonctionnelles. Les régions grises sont des pseudogènes. Les régions blanches sont des cadres de lecture ouverts non fonctionnels. La région N (orange) indique la zone de N-addition de nucléotides et identifie la diversité jonctionnelle introduite durant la recombinaison V-J. Les séquences ne possédant pas de région N sont considérées comme germinales.

Adapté de Pauza et Cairo, 2015.

A la sortie du thymus, les LT $V\gamma 9V\delta 2$ sont peu nombreux alors qu'ils représentent la sous-population majoritaire de LT $\gamma\delta$ circulants chez l'adulte. En effet, lors de leur passage dans la circulation générale, ils vont rencontrer leur antigène spécifique, s'amplifier et s'accumuler en périphérie (Pauza and Cairo, 2015; Vantourout and Hayday, 2013). Ainsi, en vieillissant, la proportion de LT $V\gamma 9V\delta 2$ ayant déjà rencontré leur antigène et exprimant des marqueurs mémoire (ex. CD45RO) devient alors de plus en plus importante (Bonneville and Scotet, 2006; Parker et al., 1990). De sorte que plus d'un LT mémoire circulant sur 40 serait un LT $V\gamma 9V\delta 2$ mémoire, ce qui constituerait la plus vaste mémoire immunitaire chez l'homme (Pauza and Cairo, 2015).

2 – Modalités d'activation antigénique des LT V γ 9V δ 2

2.1 – Molécules activatrices directes : les phosphoantigènes

Les LT V γ 9V δ 2 sont considérés comme des senseurs du stress cellulaire et sont capables de s'activer dans de nombreux contextes (ex. infections, transformations). Leur activation antigénique est dépendante de la reconnaissance et de l'engagement du TCR vis-à-vis d'un antigène présenté à la surface des cellules cibles.

Historiquement la découverte d'antigènes spécifiques des LT V γ 9V δ 2 s'est faite dans les années 1990 lors de l'étude d'extraits de *Mycobacterium tuberculosis* qui s'avéraient capables d'activer des LT V γ 9V δ 2 *in vitro*. Il a alors été mis en évidence des carbohydrates de faibles poids moléculaires contenant un groupement pyrophosphate indispensable à leur fonction activatrice (Constant et al., 1994; Pfeffer et al., 1992). Ces petites molécules non peptidiques phosphorylées ont alors été nommées phosphoantigènes (Morita et al., 1995).

Un de ces PAg (phosphoantigène) a par la suite été identifié comme étant de l'IPP (isopentenyl pyrophosphate) (Figure 13), un des métabolites issu de la voie de synthèse des isoprénoïdes (Tanaka et al., 1995). Cette voie est très conservée, elle est présente à la fois chez les vertébrés et chez les micro-organismes (Figure 14). En effet, les isoprénoïdes sont essentiels au métabolisme cellulaire, ils sont notamment à l'origine de la synthèse du cholestérol, de vitamines, de nombreux autres lipides et de modifications post-traductionnelles des protéines (Coppens, 2013; Thurnher et al., 2012; Wiemer and Wiemer, 2014). Les PAg sont donc naturellement produits chez tous les êtres vivants, ce qui explique en partie la réactivité des LT V γ 9V δ 2 contre un large panel de pathogènes (ex. bactéries, parasites).

Parmi les PAg naturels, l'IPP est produit aussi bien par des eucaryotes que par des procaryotes, et peut être synthétisé selon deux voies différentes en fonction de la nature de l'organisme. Chez les vertébrés, l'IPP est synthétisé à partir de la voie du MVA (mévalonate), tandis que chez les micro-organismes, il dérive de la voie MEP/DOXP (methylerythritol phosphate / deoxyxylulose-5-phosphate) qui conduit également à la synthèse d'un autre PAg reconnu par les LT V γ 9V δ 2, le HMBPP (hydroxymethylbutenyl 4-diphosphate) (Figure 13 et 14).

Il s'avère que le HMBPP, métabolite exclusivement bactérien, présente une bioactivité très largement supérieure à celle de l'IPP (Figure 13), ce qui permet aux LT V γ 9V δ 2 de discriminer plus facilement les cellules infectées des cellules saines (Harly et al., 2014). Bien que l'IPP soit un antigène ubiquitaire, il est impliqué dans la reconnaissance des cellules du Soi stressées ou transformées par les LT V γ 9V δ 2. En effet, les cellules tumorales peuvent présenter une dérégulation de la voie du MVA conduisant à une augmentation d'IPP intracellulaire permettant alors aux LT V γ 9V δ 2 de différencier les cellules stressées/tumorales des cellules saines (Gober et al., 2003; Silva-Santos et al., 2015).

En plus de ces PAg naturels, différents analogues synthétiques ont été développés et sont commercialisés. Les plus connus et plus utilisés sont le c-HDMAPP ((2E)-1-hydroxy-2-méthylpent-2-enyl-pyrophosphate) qui dérive du HMBPP présent chez les micro-organismes, et le BrHPP (bromohydrine pyrophosphate) qui dérive de l'IPP (Figure 13). Ces PAg synthétiques possèdent une bioactivité supérieure à celles des PAg naturels et sont utilisés pour activer et/ou amplifier spécifiquement les LT V γ 9V δ 2 (Espinosa et al., 2001).

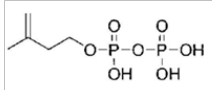
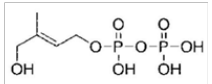
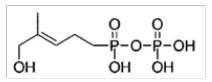
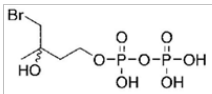
Phosphoantigènes	Type	EC50	Molécule
IPP (Isopentenyl PyroPhosphate)	Naturel (Vertébrés et micro-organismes)	50 - 500 μ M	
HMBPP (HydroxyMethylButenyl 4-diPhosphate)	Naturel (micro-organismes)	39 - 70 pM	
c-HDMAPP ((2E)-1-hydroxy-2-méthylpent-2-enyl-pyrophosphate)	Synthétique	91 pM	
BrHPP (BromoHydrine PyroPhosphate)	Synthétique	20 - 50 nM	

Figure 13 : Exemples de PAg (phosphoantigènes) caractérisés pour induire l'activation des LT V γ 9V δ 2.

Ces PAg sont soit d'origine naturelle (vertébrés et/ou micro-organismes), soit d'origine synthétique. Ils peuvent induire des degrés d'activation variables des LT V γ 9V δ 2, avec des valeurs d'EC50 (concentration efficace médiane) pouvant varier d'un donneur à l'autre.

Adapté de Harly et al., 2014.

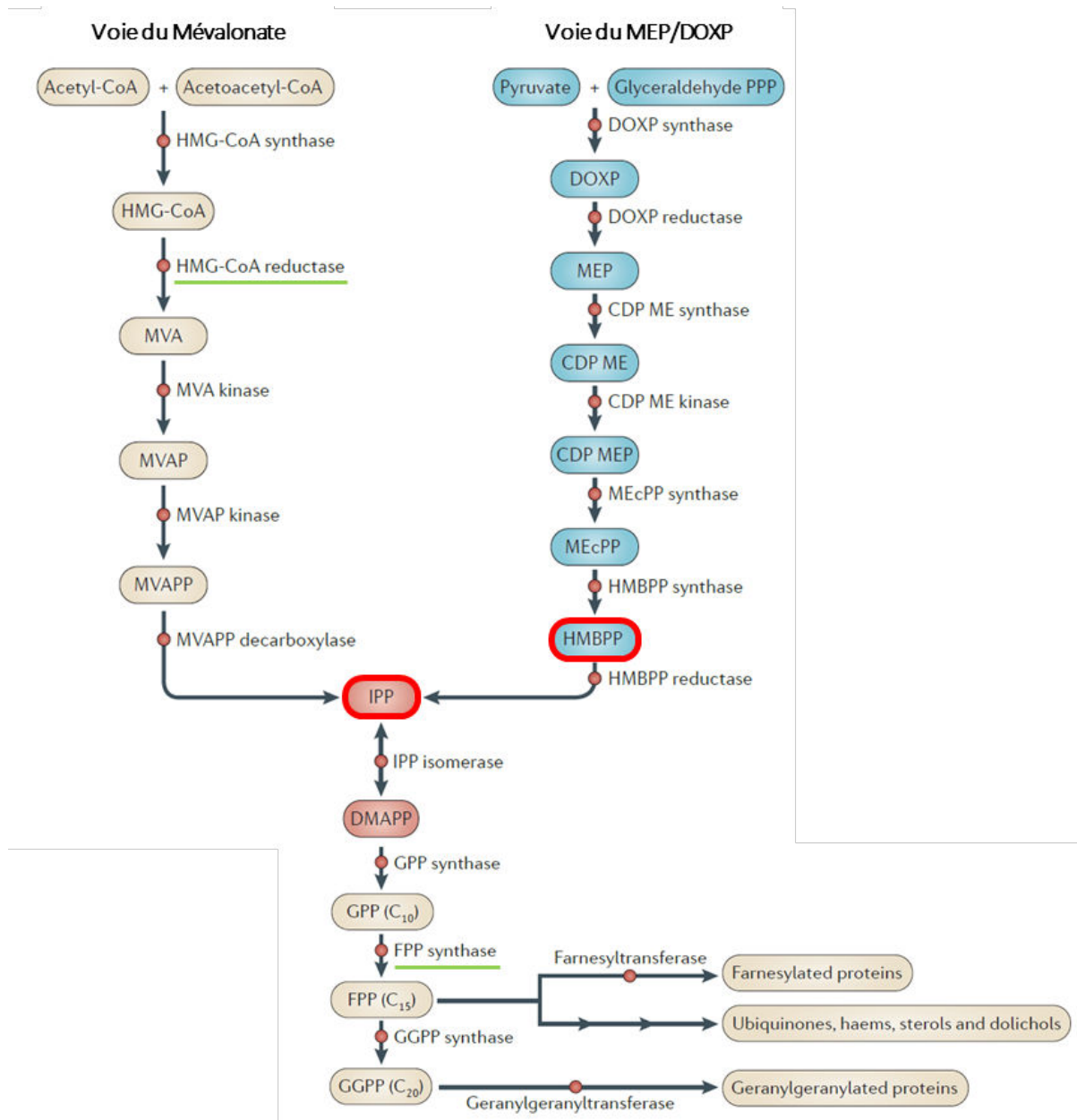


Figure 14 : Biosynthèse des précurseurs isoprénoides chez les vertébrés et les micro-organismes. Représentation schématique de la voie du MVA chez les vertébrés et de la voie du MEP/DOXP chez les micro-organismes. Ces voies conduisent à la synthèse de deux phosphoantigènes (rouge), l'IPP et le HMBPP.

HMG-CoA : hydroxméthylglutaryl-CoA ; MVAP : 5-phosphomévalonate ; MVAPP : mévalonate-5-diphosphate ; DMAPP : diméthyllalyl pyrophosphate ; PPP : polyprényl diphosphate ; CDP ME : 4-diphosphocytidyl méthylerythritol ; MEcPP : méthylerythritol cycloddiphosphate.

Adapté de Coppens, 2013.

2.2 – Molécules modulatrices indirectes : activatrices ou inhibitrices

D'autres molécules, naturelles ou synthétiques, que les PAg sont capables de moduler l'activation des LT V γ 9V δ 2 en inhibant spécifiquement certaines enzymes de la voie des isoprenoïdes, modifiant la concentration intracellulaire en PAg. Ainsi l'accumulation d'IPP dans les cellules peut être induite par des molécules telles que les ABP (aminobisphosphonates). Ce sont des composés pharmacologiques utilisés contre les troubles de la résorption osseuse, généralement administrés aux patients atteints d'ostéoporose ou de métastases osseuses (Dhillon and Lyseng-Williamson, 2008; Thurnher et al., 2012).

Bien qu'il est été proposé que les ABP soit des ligands naturels du TCR, leur mécanisme d'action est indirect et repose sur l'inhibition de la FPPS (farnesyl diphosphate synthase), enzyme qui transforme l'IPP en FPP (farnesyl diphosphate) dans la voie des isoprénoides (Coppens, 2013; Thompson and Rogers, 2004) (Figure 14). Cette inhibition de la FPPS bloque la synthèse de FPP ce qui mène à une accumulation d'IPP endogène pouvant induire de manière indirecte l'activation des LT V γ 9V δ 2. Par la suite, plusieurs études ont confirmé cette observation et démontré l'existence d'une corrélation positive entre l'accumulation d'IPP induite par l'inhibition de la FPPS dans les cellules traitées et l'activation des LT V γ 9V δ 2 (Das et al., 2001a; Gober et al., 2003; Sanders et al., 2004). Le zolédronate et le pamidronate sont les ABP les plus utilisés, aussi bien en recherche qu'en clinique.

Une autre famille de molécules induit une inhibition de la FPPS et donc une accumulation d'IPP endogène, il s'agit des alkylamines (Bukowski et al., 1999; Thompson et al., 2006). Ces molécules sont naturellement sécrétées par des bactéries commensales ou pathogènes et sont donc communément retrouvées dans les fluides humains (Morita et al., 2007). Elles sont également présentes dans de nombreux végétaux comestibles tels que le thé, le vin, les pommes ou certains champignons (Kamath et al., 2003; Morita et al., 2007). Néanmoins de plus forte concentration d'alkylamines, que d'ABP, sont nécessaires pour déclencher l'activation indirecte des LT V γ 9V δ 2.

Il est également possible d'inhiber la production d'IPP en bloquant la voie du MVA plus en amont. La Mévastatine est un composé pharmacologique, de la famille des statines qui inhibe l'HMG-CoA réductase (Figure 14). C'est l'équipe de Genaro DeLibero qui a montré en premier que l'activation des LT V γ 9V δ 2 induite par le Zolédronate pouvait être bloquée par la Mévastatine (Gober et al., 2003).

L'accumulation d'IPP endogène, qu'elle soit induite par un aminobisphosphonate ou par une alkylamine, peut être bloquée par les statines et ainsi inhiber l'activation des LT V γ 9V δ 2 (Thompson and Rogers, 2004).

2.3 – Mécanismes de reconnaissance des phosphoantigènes

Il a clairement été établi que l'activation des LT V γ 9V δ 2 par les PAg est dépendante de son TCR. Le blocage du TCR ou du CD3 permet d'inhiber la réactivité des LT V γ 9V δ 2 (Constant et al., 1994; Gober et al., 2003; Tanaka et al., 1995) tandis que la transfection d'un TCR V γ 9V δ 2 dans la lignée Jurkat (LT $\alpha\beta$ leucémique n'exprimant pas de TCR) la rend capable de reconnaître aussi bien des PAg que des cellules sensibilisées par des ABP (Marcu-Malina et al., 2011).

Cependant les mécanismes moléculaires de l'interaction entre le TCR des LT V γ 9V δ 2 et les PAg, dans des contextes infectieux ou tumoraux, n'ont pas encore été clairement identifiés et beaucoup d'études se penchent sur le sujet (Riganti et al., 2012). Tout d'abord, l'hypothèse d'une interaction directe, sans intervention d'un partenaire moléculaire entre les PAg et le TCR, a rapidement été réfutée par la nécessité de contacts cellulaires pour activer les LT V γ 9V δ 2 (Lang et al., 1995; Morita et al., 1995).

Par la suite, de nombreuses études ont porté sur l'identification des partenaires potentiels qui seraient impliqués dans la présentation des PAg aux LT V γ 9V δ 2. Parmi les candidats étudiés, l'Ecto-F1-ATP synthase pourrait s'associer à l'apolipoprotéine A1 pour former un complexe de présentation des PAg à la surface des cellules cibles (Scotet et al., 2005).

Plusieurs études se sont également concentrées sur une autre famille de protéine, les BTN (butyrophilines). Ces protéines sont des glycoprotéines de type I et font partie de la super famille des Ig au même titre que les molécules de la famille B7. A l'origine, les BTN ont été identifiées comme étant des molécules B7-like car elles présentent une forte homologie structurelle au niveau des domaines extracellulaires IgV et IgC (domaine de type immunoglobuline variable et constant), suggérant une fonction immunologique de cette famille de protéines (Arnett and Viney, 2014).

Il existe plusieurs sous-familles de BTN, notamment BTN3A (ou CD277) qui comprend 3 isoformes : BTN3A1, BTN3A2 et BTN3A3, et qui sont exprimés de façon ubiquitaire chez l'Homme (Harly et al., 2014). Tout comme les autres BTN, BTN3A1 est composée de 2 domaines extracellulaires de type IgV et IgC ainsi qu'un domaine intracellulaire de type B30.2 (Figure 15). Bien qu'il existe une très forte homologie (> 95 %) entre les domaines extracellulaires des trois isoformes de BTN3A, leur domaine transmembranaire et intracellulaire présente une grande diversité (Gu et al., 2014). Seuls les isoformes A1 et A3 possèdent un domaine intracellulaire de type B30.2, l'isoforme A2 est tronquée et ne comporte pas de domaine intracellulaire (Figure 15).

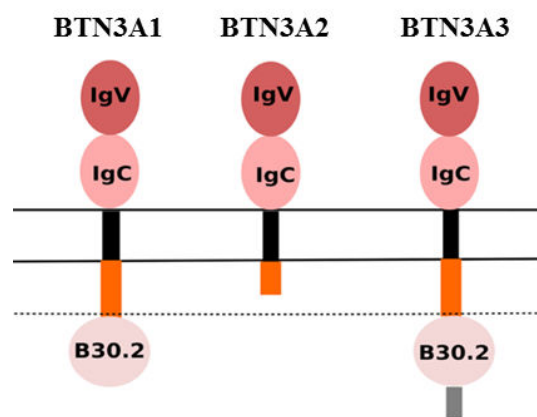


Figure 15 : Représentation schématique des différents isoformes de BTN3A/CD277.

Les protéines de la famille BTN3 présentent une forte homologie structurelle de leurs domaines extracellulaire. La région transmembranaire (noir) ainsi que la partie intracellulaire sont peu conservées. Le domaine juxtamembranaire se trouve juste sous la membrane (orange). BTN3A1 et BTN3A3 possèdent un domaine B30.2 mais pas BTN3A2. L'isoforme BTN3A3 est également composée d'une petite extension en C-terminal (gris). *D'après Boutin et Scotet, 2018.*

Au cours des dernières années, l'implication de BTN3A1 dans la réactivité des LT V γ 9V δ 2 a pu être clairement démontrée (Harly et al., 2012; Vavassori et al., 2013). Les mécanismes moléculaires impliqués dans l'activation des LT V γ 9V δ 2 via l'interaction entre BTN3A1 et les PAg n'étant pas encore élucidés, deux modèles principaux sont proposés (Figure 16) :

- Le premier est un modèle « allostérique » basé sur l'interaction des PAg (endogènes ou internalisés) avec le domaine intracellulaire B30.2 de BTN3A1, qui induirait des modifications alors perçues par les LT V γ 9V δ 2 et permettrait leur activation. Ces modifications allostériques peuvent être des modifications conformationnelles, des variations de la topographie membranaire et/ou le recrutement/exclusion de partenaires moléculaires (Harly et al., 2012).

- Le second est un modèle de « présentation antigénique » basé sur l'interaction des pAg (extrudés ou exogènes) avec le domaine extracellulaire IgV de BTN3A1 formant ainsi un complexe antigénique reconnu par les LT $V\gamma9V\delta2$ et menant à leur activation (Vavassori et al., 2013). Dans le cas de pAg endogènes, ce modèle nécessite l'implication d'un transporteur membranaire permettant l'extrusion de ces pAg vers le milieu extracellulaire car ils ne traversent par naturellement la membrane plasmique. Le transporteur ABCA1 (ATP-binding cassette transporter A1), impliqué dans la voie du cholestérol, a récemment été identifié pour jouer un rôle dans l'export d'IPP endogène, en association avec l'apolipoprotéine A1 et BTN3A1 (Castella et al., 2017).

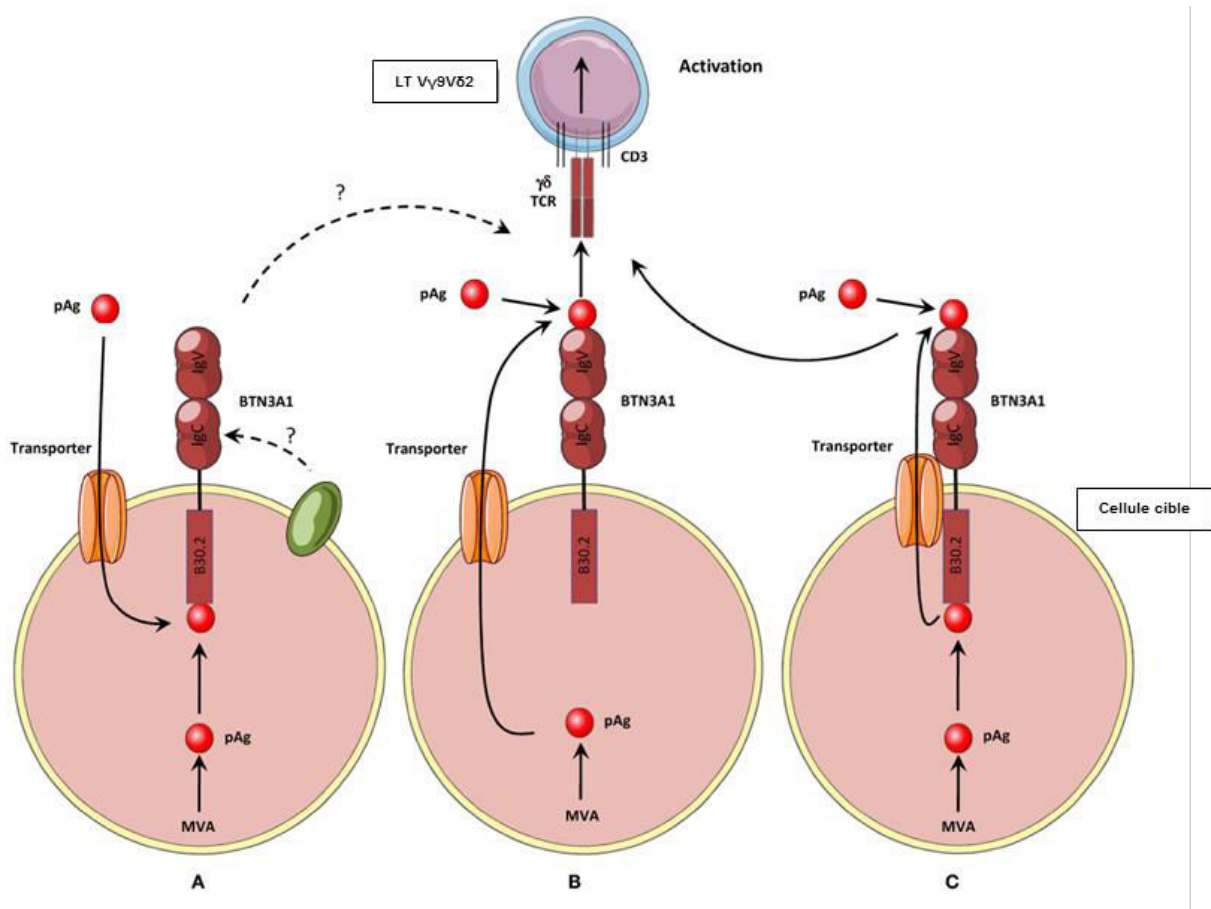


Figure 16 : Trois hypothèses sur le mode d'activation des LT $V\gamma9V\delta2$ par les pAg.

(A) Modèle allostérique : Les pAg (intracellulaires ou internalisés) interagissent avec le domaine B30.2 induisant des modifications de la topologie membranaire de BTN3A1 ou le recrutement de partenaires moléculaires. (B) Modèle de présentation directe : Les pAg (extrudés ou extracellulaires) interagissent avec le domaine IgV de BTN3A1 pour être présentés comme un complexe antigénique. (C) Modèle commun : ce modèle partage les mécanismes des deux premiers modèles.

D'après Harly et al., 2014.

Cependant, la protéine BTN3A1 est nécessaire à l'activation des LT V γ 9V δ 2 mais pas suffisante lorsqu'elle est transfectée dans des cellules murines en présence de PAg (Riaño et al., 2014). Ainsi la quête de partenaires protéiques, conservés chez les primates, est toujours en cours. De récentes études proposent des molécules telles que : RhoB, une petite protéine G impliquée dans l'organisation des filaments d'actine et le transport vésiculaire (Sebestyen et al., 2016); Periplakin, un membre de la famille des protéines adaptatrices du cytosquelette (Rhodes et al., 2015) ; ou encore les autres isoformes de la famille BTN3 (Gu et al., 2017).

En effet, l'existence de multimères de BTN3 a récemment été confirmée mais l'hypothèse selon laquelle les autres isoformes de BTN3 pourraient jouer le rôle de régulateurs activateur (BTN3A3) ou inhibiteur (BTN3A2) n'a pu être démontrée. Il est donc nécessaire de mener des études plus approfondies des changements de conformations de ces multimères et de leur impact sur l'activation ou l'inhibition des LT V γ 9V δ 2 (Boutin and Scotet, 2018).

En fin de compte et malgré la persévérance des spécialistes de l'immunobiologie des LT V γ 9V δ 2, les nombreuses avancées de ces dernières années et la proposition de plusieurs hypothèses aussi diverses que variées, la compréhension des mécanismes d'activation par les PAg des LT V γ 9V δ 2 reste imprécis à ce jour.

3 – Réactivité et régulation du signal des LT V γ 9V δ 2

3.1 – Le TCR V γ 9V δ 2

Comme décrit ci-dessus, l'activation des LT V γ 9V δ 2 par leur TCR est spécifique des PAg bien que les mécanismes de reconnaissance de ces PAg comprennent encore de nombreuses zones d'ombres. Il est tout de même important de noter que cette reconnaissance n'est pas restreinte par les molécules du CMH classique, ainsi les LT V γ 9V δ 2 ne sont pas alloréactifs.

De plus, bien que la chaîne V δ 2 s'associe majoritairement à la chaîne V γ 9, le TCR V γ 9V δ 2 possède tout de même une diversité qui affecte la capacité de prolifération de cette population après une activation antigénique (Hebbeler et al., 2007). Ainsi, au sein d'une population de LT V γ 9V δ 2 issue d'un même donneur sain adulte, chaque clone cellulaire peut proliférer plus ou moins rapidement après stimulation (Pauza and Cairo, 2015).

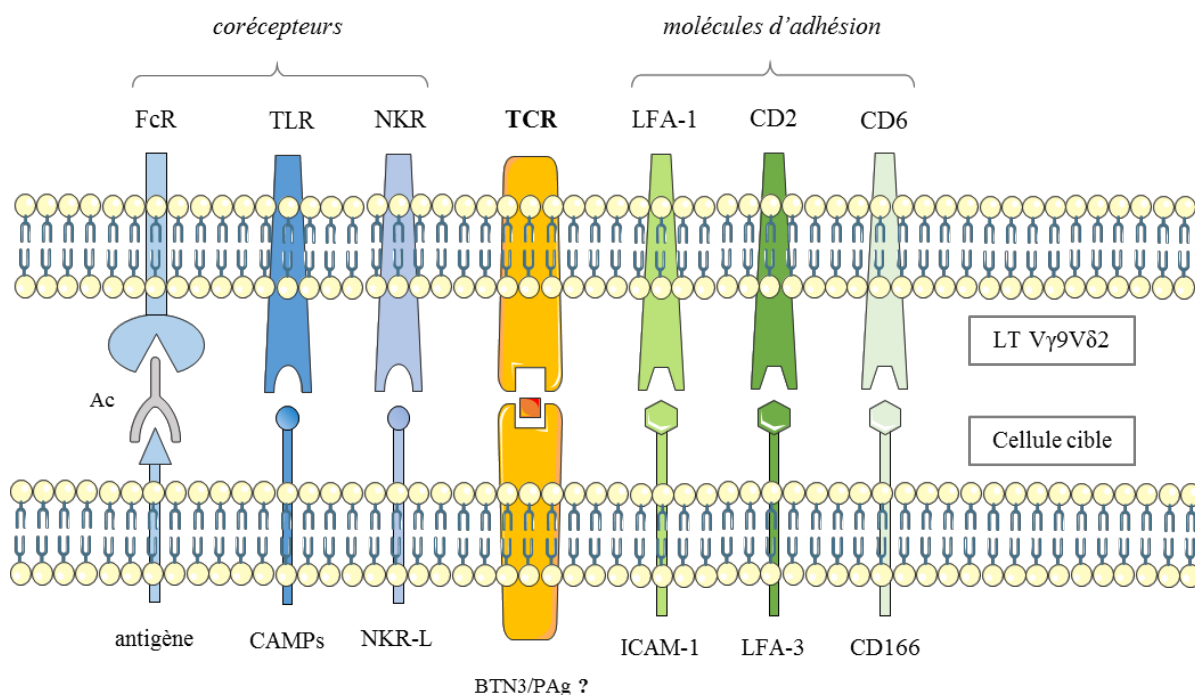


Figure 17 : Représentation schématique de la synapse immunologique formée par un LT V γ 9V δ 2. L'activation des LT V γ 9V δ 2 est dépendante de son TCR mais est également modulée par différents corécepteurs tels que les NKR, les TLR ou les FcR. Elle dépend également de la stabilisation de cette synapse par des molécules d'adhésion comme LFA-1, le CD2 et le CD6.

Adapté de Wiemer et Wiemer, 2014 et Bonneville et al., 2010.

3.2 – Les récepteurs NK

Les LT V γ 9V δ 2, comme tous les LT $\gamma\delta$, présentent un profil hybride entre les LT $\alpha\beta$ et les cellules NK, ils expriment donc naturellement de nombreux NKR (Pont et al., 2012) (Figure 17). Ces NKR peuvent être inhibiteurs ou activateurs et contribuent de façon importante à la réactivité des LT V γ 9V δ 2 (Bonneville et al., 2010; Raullet and Guerra, 2009).

NKG2D (Natural Killer group 2 member D) est un NKR activateur de la famille des lectines de type II. Il possède beaucoup de ligands qui sont généralement surexprimés à la surface des cellules suite à un stress cellulaire (infection ou transformation), tels que les molécules du CMH de classe I non classiques MIC A/B et les molécules de type ULBP (UL16 binding protein) (Raullet and Guerra, 2009). Au cours de la formation de la synapse immunologique entre un LT V γ 9V δ 2 et une cellule cible, NKG2D est recruté et joue un rôle important dans la costimulation des LT V γ 9V δ 2. Ainsi, il s'associe au niveau intracellulaire et de façon non covalente à la protéine adaptatrice DAP10 permettant ainsi la transduction d'un signal activateur.

Le récepteur activateur NKG2D amplifie alors l'activation des LT V γ 9V δ 2 via leur TCR (Bonneville et al., 2010; Das et al., 2001b). Dans certains cas, l'engagement du NKG2D peut conduire à une cytotoxicité directe, en l'absence de signal TCR, contre des cellules infectées par des virus (Qin et al., 2009).

Parmi les NKR inhibiteurs, NKG2A (Natural Killer group 2 member A) et ILT-2 (Ig like transcript 2) sont souvent exprimés par les LT V γ 9V δ 2. NKG2A est également une protéine de la famille des lectines de type II et forme un complexe avec le CD94 permettant la reconnaissance de molécules du CMH non classiques HLA-E (Poccia et al., 1997). ILT-2 quant à lui appartient à la famille des LILR (leukocyte immunoglobulin-like receptor) et interagit avec la molécule du CMH non classique HLA-G (Lesport et al., 2011). A l'instar des cellules NK, ces différents récepteurs inhibiteurs vont induire des signaux inhibiteurs qui entrent en compétition avec les signaux activateurs et permettent une régulation très fine de la réponse des LT V γ 9V δ 2 (Trichet et al., 2006).

3.3 – Les Toll-Like Récepteurs

Tout comme de nombreuses cellules de l'immunité innée, les LT V γ 9V δ 2 expriment des TLR (Figure 17). Ces récepteurs reconnaissent des PAMP (pathogen associated molecular pattern) et/ou des DAMP (danger associated molecular pattern) qui peuvent être regroupés sous le terme de CAMP (changed associated molecular pattern) (Pradeu and Vivier, 2016). Ces ligands des TLR sont des molécules non-peptidiques hautement conservées présentes chez certains microorganismes et généralement surexprimées en cas de stress cellulaire (infection ou transformation) (Devilder et al., 2009). La détection de CAMPs issus de pathogènes, tels que les glycolipides ou les lipopolysaccharides, passe par la formation d'hétérodimères entre le TLR2 et un autre TLR (ex. TLR1/6/10) ou une dectine (Wesch et al., 2011). Cependant, et contrairement aux NKR, il n'a pas encore été démontré, chez les primates, que les TLR sont capables d'induire une activation indépendante du TCR, ils agissent uniquement en tant que costimulateurs (Wesch et al., 2011).

Dans le cas des LT V γ 9V δ 2, l'association des TLR, des NKR et du TCR induit des signaux séparés, synergiques ou additifs déclenchant les fonctions effectrices de ces LT V γ 9V δ 2 (Bonneville et al., 2010).

3.4 – Les Récepteurs Fc

Les LT V γ 9V δ 2 peuvent également exprimer des FcR (récepteurs aux fragments constants (Fc) des Ig). Il existe de nombreux membres dans cette famille des FcR qui sont capables de reconnaître différents isotypes d'Ig avec différents niveaux d'affinité. Le Fc γ RIIIA ou CD16 est un FcR qui est constitutivement exprimé par les cellules NK et exprimé par certains LT V γ 9V δ 2 (Figure 17). Bien qu'il possède une faible affinité pour les anticorps, la fixation spécifique d'un Fc à ce récepteur permet la transduction d'un signal activateur menant à l'ADCC et donc à la lyse des cellules reconnues par l'anticorps (Tokuyama et al., 2008). Chez les LT V γ 9V δ 2, le CD16 joue un rôle de costimulateur pendant l'activation via le TCR, tout comme les autres récepteurs décrits ci-dessus. Cette activation conduit à une augmentation de la capacité cytotoxique des LT V γ 9V δ 2, de la production de TNF- α (tumor necrosis factor α) et également à une maturation en LT effecteurs (Angelini et al., 2004; Lafont et al., 2001).

3.5 – Les molécules d'adhésion

Au cours de l'interaction entre un LT et sa cible, il y a formation de la synapse immunologique et recrutement de plusieurs molécules qui vont participer à l'activation du LT. Les molécules d'adhésion jouent un rôle important dans la stabilisation de cette synapse immunologique mais ne sont pas suffisantes à activer les LT V γ 9V δ 2. Les molécules d'adhésion fonctionnent également en couple avec un ligand et les trois complexes suivants ont été identifiés pour jouer un rôle important dans l'activation des LT V γ 9V δ 2 : LFA-1/ICAM-1 ; CD2/LFA-3 et CD6/CD166 (Nedellec et al., 2010; Wiemer and Wiemer, 2014) (Figure 17).

LFA-1 (lymphocyte function associated antigen 1) est fortement exprimé par les LT V γ 9V δ 2, il appartient à la famille des intégrines et a pour ligand ICAM-1 (intercellular adhesion molecule 1). L'engagement de ce couple LFA-1/ICAM-1 est nécessaire à l'activation des LT V γ 9V δ 2 et est impliqué dans leurs fonctions cytotoxiques mais n'a pas d'effet sur leur prolifération ni sur leur production de cytokines (Kato et al., 2003; Wang and Malkovsky, 2000).

Le CD2, quant à lui, est exprimé par tous les LT et les cellules NK, il appartient à la superfamille des Ig et a pour ligand LFA-3 (lymphocyte function associated antigen 3). A l'inverse du couple précédent, l'interaction entre le CD2 et LFA-3 n'impacte pas les fonctions cytotoxiques des LT V γ 9V δ 2 mais influence leur prolifération et leur production de cytokines telles que le TNF- α (Wang and Malkovsky, 2000).

Enfin le CD6 est exprimé par tous les lymphocytes et appartient à la famille des récepteurs scavengers. L'association avec son ligand, le CD166, semble jouer un rôle activateur pour les LT V γ 9V δ 2. De plus une corrélation entre le niveau d'expression du CD166 sur les cellules cibles et sa capacité à activer des LT V γ 9V δ 2 a été démontrée (Kato et al., 2003, 2006).

Ces molécules d'adhésion jouent donc un rôle important dans la formation, la stabilisation de la synapse immunologique et également dans la mise en place des fonctions effectrices des LT V γ 9V δ 2.

3.6 – Les cytokines

Comme pour beaucoup de LT, les cytokines présentes dans l'environnement des LT V γ 9V δ 2 modulent leur activation et leur fonction. L'IL-2 est une des cytokines les plus importantes. Elle agit comme un facteur de croissance qui régule la prolifération des LT et augmente la cytotoxicité des cellules NK (Rochman et al., 2009). Lorsqu'elle est utilisée sur des PBMC en combinaison avec un PAg ou un ABP pour activer spécifiquement les LT V γ 9V δ 2, elle induit leur prolifération et leur maturation en cellules effectrices (Espinosa et al., 2001).

Un nombre extrêmement important de cytokines fournit des signaux variés et joue un rôle important dans l'immunomodulation des LT V γ 9V δ 2. De plus, en fonction du temps d'exposition, de la concentration, de la présence d'autres cytokines ..., une cytokine peut induire des effets divers et variés sur l'activité des LT V γ 9V δ 2.

Par exemple, l'IL-21 qui lorsqu'elle est combinée à l'IL-2, lors de l'amplification des LT V γ 9V δ 2, peut :

- A la fois favoriser un phénotype pro-inflammatoire, leur prolifération et leurs fonctions cytotoxiques, via la production de perforine et de granzymes (Thedreuz et al., 2009).
- Et aussi conduire à l'émergence de LT V γ 9V δ 2 avec un profil régulateur via la surexpression du CD73 (Barjon et al., 2017).

En conclusion, beaucoup d'acteurs sont impliqués et/ou peuvent moduler l'activation et les fonctions des LT V γ 9V δ 2. De plus, la contribution de ces différents acteurs, seuls ou associés les uns avec les autres, induit des conséquences très variées et dépendantes du contexte physiopathologique.

4 – Rôles et Fonctions effectrices des LT V γ 9V δ 2

Comme tous les LT $\gamma\delta$, les LT V γ 9V δ 2 ont de nombreuses fonctions effectrices. Les principales fonctions citées dans le paragraphe II-3 seront détaillées ici, appliquées au LT V γ 9V δ 2 (Vantourout and Hayday, 2013) (Figure 18).

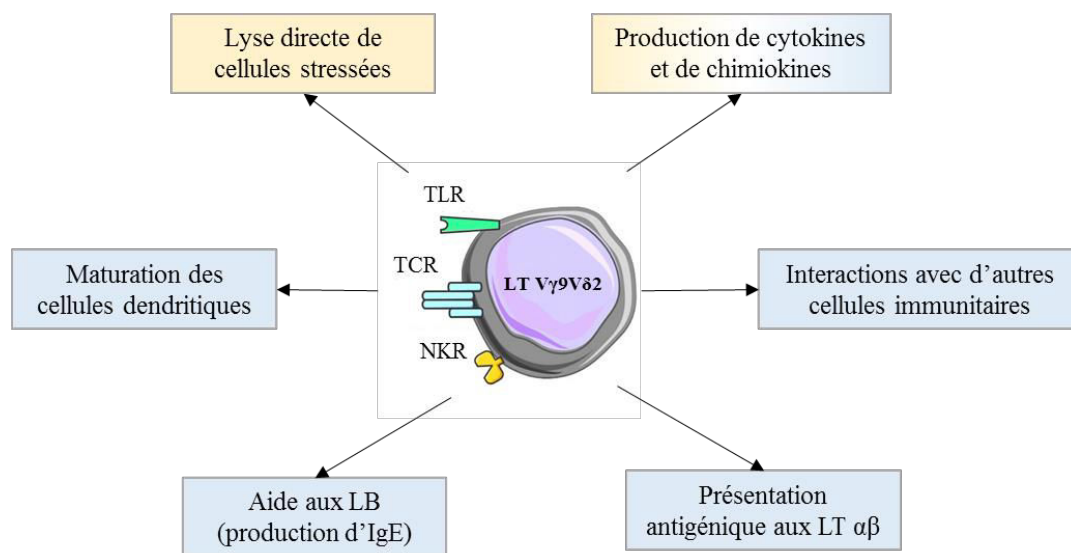


Figure 18 : Principales fonctions effectrices des LT V γ 9V δ 2.

Afin de défendre l'organisme contre les pathogènes, les LT V γ 9V δ 2 sont capable de mettre en place différents mécanismes d'action. Ils peuvent réagir de façon directe (jaune) via la libération de granules cytotoxiques et la production de cytokines ou de chimiokines. Ils peuvent également interagir avec d'autres effecteurs de l'immunité (bleu) pour induire une réponse des LB, des LT $\alpha\beta$ ou induire la maturation de cellules présentatrices d'antigènes. *Adapté de Vantourout et Hayday, 2013.*

4.1 – Cytotoxicité directe

Après activation, les LT V γ 9V δ 2 mettent en place une réponse de type Th1 (LT helper de type 1), impliquant une forte activité cytotoxique (Dunne et al., 2010; García et al., 1997; Thedrez et al., 2007). En effet, les LT V γ 9V δ 2 sont capables de détruire de façon directe des cellules infectées ou transformées via deux mécanismes principaux, détaillés ci-dessous :

Le premier mécanisme va leur permettre d'induire la lyse de cellules cibles via la libération de granules lytiques stockées dans leur cytoplasme. Ces granules contiennent deux types de molécules qui agissent de concert afin d'induire la mort de la cellule cible.

Dans un premier temps, plusieurs molécules de perforine vont s'insérer dans la membrane plasmique de la cellule cible et y former un pore. Dans un second temps, des enzymes lytiques telles que les granzymes A/B et la granulysine vont pouvoir entrer dans la cellule cible par ce pore et déclencher son apoptose (Dieli et al., 2001; Spencer et al., 2013).

Le second mécanisme est basé sur l'interaction entre des récepteurs de mort présents à la surface des cellules cibles et de leurs ligands, exprimés par les LT V γ 9V δ 2 activés, afin de déclencher l'apoptose de ces cellules cibles. Les deux grands couples activant cette fonction sont les récepteurs de mort FAS/CD95 et TRAIL-R ainsi que leurs ligands respectifs : FAS-L/CD95-L et TRAIL (TNF related apoptosis induced ligand) (Lo Presti et al., 2014; Walczak and Krammer, 2000). Ces deux récepteurs ont le même mode d'action. Ils possèdent tous deux un domaine intracellulaire de type DD (death domain) qui, après interaction avec son ligand, va recruter la FADD (Fas associated protein death domain). Cette protéine cytoplasmique va alors activer la voie des caspases et conduire à l'apoptose de la cellule.

Grâce à ces différents mécanismes et les nombreuses molécules qui les composent, les LT V γ 9V δ 2 sont capables de lyser de façon directe un large spectre de pathogènes de diverses origines (bactéries, champignons, parasites) (Vantourout and Hayday, 2013).

4.2 – Interactions avec d'autres cellules de l'immunité

Suite à une activation antigénique, les LT V γ 9V δ 2 mettent en place une réponse pro-inflammatoire, via la production de cytokines, les principales étant l'IFN- γ et le TNF- α , mais également de chimiokines (Dunne et al., 2010). Chacun de ces facteurs solubles va avoir un rôle différent et va permettre aux LT V γ 9V δ 2 de communiquer avec de nombreuses cellules de l'immunité et donc de moduler leurs réponses/fonctions.

Les neutrophiles, du fait de leur localisation tissulaire, font partie des premiers effecteurs à être recrutés, notamment lors d'infections bactériennes. Après activation, leur phénotype va évoluer afin de faciliter la différenciation des monocytes, la maturation des DC et l'interaction avec les lymphocytes (Mantovani et al., 2011; Mócsai, 2013; Scapini and Cassatella, 2014). Les LT V γ 9V δ 2 sont généralement corecrutés avec les neutrophiles sur les sites infectieux et ils vont interagir ensemble.

En effet, les LT V γ 9V δ 2 activés vont favoriser la chimiotaxie et la phagocytose par les neutrophiles (Agrati et al., 2009; Müller et al., 2009). Après activation rapide par des composés microbiens relargués par les neutrophiles, les LT V γ 9V δ 2 produisent de l'IFN- γ , du TNF- α et du GM-CSF qui facilitent la différenciation des neutrophiles en CPA (Davey et al., 2011). Cette différenciation conduit à une augmentation de l'expression des molécules du CMH de classe I et II, les rendant capables d'activer des LT $\alpha\beta$ CD4⁺ ou CD8⁺ par la présentation d'antigènes.

Les monocytes sont également de se différencier en DC capables de jouer le rôle de CPA (Sallusto and Lanzavecchia, 1994). Après activation, les LT V γ 9V δ 2 vont sécréter de l'IFN- γ , du TNF- α , du GM-CSF et de l'IL-4 qui vont participer à cette différenciation des monocytes en DC (Eberl et al., 2009; Wesch et al., 2001). Les monocytes vont alors subir des modifications morphologiques et phénotypiques, notamment l'expression de marqueurs de CPA tels que CD40, CD86 et HLA-DR. Les monocytes différenciés en DC sont alors capables d'induire l'activation de LT $\alpha\beta$ CD4⁺ par la présentation d'antigènes bactériens (Eberl et al., 2009).

Les DC sont les CPA de référence et afin d'activer des LT elles doivent maturer. Cette maturation peut être déclenchée par les signaux de danger qu'elles reçoivent de l'environnement mais également par la présence d'IFN- γ et de TNF- α (Deauvieu et al., 2015; Kaiko et al., 2008). Après activation, les LT V γ 9V δ 2 produisent de grandes quantités de ces deux cytokines, ce qui influence probablement ce processus. En effet, la coculture de LT V γ 9V δ 2 et de DC immatures, en absence d'autres stimuli, conduit à l'augmentation de l'expression de marqueurs de CPA, de molécules de costimulation et à l'acquisition d'un phénotype de DC matures permettant l'activation de LT $\alpha\beta$ CD4⁺ (Ismaili et al., 2002). En retour, les DC vont produire des IFN de type I afin de favoriser la prolifération, la production de molécules lytiques (perforine) et de cytokines pro-inflammatoires (IFN- γ et TNF- α) par les LT V γ 9V δ 2 (Conti et al., 2005; Devilder et al., 2006, 2009; Fiore et al., 2007; Kunzmann et al., 2004). Ce système d'entraide entre les DC et les LT V γ 9V δ 2 fait toujours l'objet de nombreuses études notamment sur la polarisation des LT CD4⁺ naïfs, après activation, vers différents phénotypes (Th1, Th2, Treg ...).

Les LT V γ 9V δ 2 ne sont pas seulement capables d'induire des fonctions de CPA par les autres cellules de l'immunité (DC, monocytes, neutrophiles, LB ...), ils sont également capables de remplir eux-mêmes cette fonction (Brandes et al., 2005). Après endocytose ou phagocytose de composés exogènes, les LT V γ 9V δ 2 vont exprimer des molécules de costimulation (CD80/86) et présenter ces antigènes sur leurs molécules du CMH de classe I ou II afin d'activer respectivement des LT $\alpha\beta$ CD8⁺ et CD4⁺ naïfs (Brandes et al., 2005, 2009; Meuter et al., 2010; Wu et al., 2009).

Les LT V γ 9V δ 2 sont également capables d'influencer la réponse humorale. Les LB sont la clé de cette réponse et lors d'une infection, ils vont muter afin de produire des anticorps spécifiques des pathogènes ciblés. Ce processus nécessite l'aide d'autres cellules de l'immunité au niveau des centres germinatifs, il s'agit des Tfh (LT follicular helper) (Tangye et al., 2013; Vinuesa et al., 2005). Bien que ce rôle soit généralement tenu par des LT $\alpha\beta$ CD4⁺, les LT $\gamma\delta$ peuvent également y participer (Ehl et al., 2005). Plusieurs études *in vitro* ont montré que les LT V γ 9V δ 2 activés pouvaient interagir avec les LB notamment en participant à leur organisation et au maintien des centres germinatifs via la production de cytokines telles que de l'IL-4 et de l'IL-10, ou de chimiokines telles que CXCL13 (CXC-chemokine ligand 13), favorisant ainsi la production d'anticorps (Brandes et al., 2003; Caccamo et al., 2006). Ces LT V γ 9V δ 2 peuvent également induire l'expression de marqueurs de CPA, notamment CD40, CD86 et HLA-DR. (Bansal et al., 2012; Caccamo et al., 2006).

4.3 – Plasticité cellulaire

Bien que la réponse principale des LT V γ 9V δ 2 soit une réponse Th1 incluant la production de cytokines pro-inflammatoires et une forte activité cytotoxique, ils sont également capables de s'adapter aux différents signaux qu'ils perçoivent dans leur environnement (Vermijlen et al., 2007). Ainsi, ils peuvent se polariser en fonction du signal TCR et des différents stimuli présents dans l'environnement, présentant une plasticité fonctionnelle à la fois innée et acquise (Bonneville et al., 2010). La plasticité innée fait référence aux fonctions effectrices mises en place de façon immédiate et transitoire. La plasticité acquise, quant à elle, fait référence à la mise en place de fonction corégulatrices qui apparaissent à plus long terme.

Les LT V γ 9V δ 2 peuvent donc avoir différents phénotypes en plus du profil Th1 initial (Lafont et al., 2014; Morita et al., 1991) :

- Th2 : les LT de type Th2 sont caractérisés par la production d'IL-4 et sont impliqués dans le développement de la réponse humorale et/ou la lutte contre les parasites (Wesch et al., 2001).
- Th17 : les LT de type Th17, comme leur nom l'indique, sécrètent de l'IL-17 qui est liée à une réponse pro-inflammatoire par de nombreuses cellules immunitaires et à l'activation des neutrophiles, le tout dans un contexte d'infection bactérienne (Caccamo et al., 2011).
- Treg : les LT régulateurs quant à eux sont plutôt impliqués dans une réponse anti-inflammatoire via la sécrétion de cytokines telles que le TGF- β et l'IL-10. Ils jouent un rôle important dans la mise en place du microenvironnement immunosuppresseur en inhibant l'activation et la prolifération des effecteurs anti-tumoraux (Casetti et al., 2009).

Dans le contexte physiopathologique qu'est le cancer, des sous-populations de LT V γ 9V δ 2 présentant un profil Treg voir Th17 ont été décrite pour exercer des fonctions pro-tumorales et immunosuppressives, notamment via l'inhibition des fonctions anti-tumorales des LT CD8⁺ ou des NK par la production d'IL-10 et de TGF- β (Kühl et al., 2009), ou en recrutant des cellules myéloïdes suppressives par la sécrétion d'IL-17 (Wu et al., 2014), entretenant ainsi l'immunosuppression caractéristique du microenvironnement tumoral. A ce jour, la description de ces sous-population de LT $\gamma\delta$ pro-tumoraux fait l'objet de nombreuses études qui portent aussi bien sur les mécanismes aboutissant à l'apparition de ces sous-population que sur les fonctions effectrices régulatrices et/ou immunosuppressives qu'ils mettent en place (Lafont et al., 2014).

IV - Immunothérapie anti-tumorale et LT V γ 9V δ 2

Comme décrit précédemment les LT V γ 9V δ 2 possèdent de nombreuses fonctions effectrices qui peuvent varier en fonction de la cible reconnue et de l'environnement dans lequel ils se trouvent (facteurs solubles, interactions avec d'autres cellules de l'immunité ...). Nous allons maintenant nous intéresser à un contexte physiopathologique particulier : le cancer.

1 – LT V γ 9V δ 2 et Cancer

1.1 – Surveillance et Fonctions anti-tumorales des LT V γ 9V δ 2

Les LT V γ 9V δ 2 se trouvent en périphérie, dans le sang circulant, ils peuvent donc atteindre un site inflammatoire rapidement afin de participer à la lutte contre le stress cellulaire. Leur pléiotropie fonctionnelle leur permet à la fois de reconnaître et détruire directement les cellules cancéreuses et également de stimuler la réponse cytotoxique d'autres effecteurs de l'immunité innée ou adaptative contre cette cible (Vantourout and Hayday, 2013). Les capacités anti-tumorales des LT V γ 9V δ 2 ont été étudiées et confirmées aussi bien *in vitro* qu'*in vivo*.

Dans un premier temps, *in vitro*, leur activité anti-tumorale a été démontrée contre des tumeurs d'origine hématopoïétique, telles que le myélome multiple ou des lymphomes (Kunzmann et al., 2000; Sturm et al., 1990). Par la suite, elle a été confirmée contre plusieurs tumeurs solides d'origines tissulaires différentes : mammaire (Bank et al., 1993), rénale (Kobayashi et al., 2001; Viey et al., 2005), du colon (Corvaisier et al., 2005), prostatique (Liu et al., 2005) ou encore pulmonaire (Ferrarini et al., 1996). De plus, chez les patients atteints de cancer, les LT V γ 9V δ 2 peuvent s'amplifier en périphérie et infiltrer un grand nombre de tumeurs dont le cancer du sein (Ma et al., 2012) et le mélanome (Cordova et al., 2012).

Dans un second temps, le potentiel anti-tumoral des LT V γ 9V δ 2 a été démontré *in vivo* dans des modèles de souris immunodéprimées ou SCID (severe combined immunodeficiency). Plusieurs stratégies ont été développées en ce sens, dont la reconstitution d'un « système immunitaire humain » par injection de PBMC chez ces souris SCID. Différentes tumeurs ont ensuite été greffées (ex. pancréas, vessie, sein, mélanome) et une infiltration de LT V γ 9V δ 2 dans ces tumeurs a pu être observée (Kabelitz et al., 2004; Zheng et al., 2001). Cette infiltration est généralement accompagnée d'une diminution de la croissance tumorale et une augmentation de la survie des souris traitées.

1.2 – Intérêt thérapeutique des LT V γ 9V δ 2

L'implication naturelle des LT V γ 9V δ 2 dans l'immunothérapie anti-tumorale est fortement appuyée par le fait que des LT V γ 9V δ 2 infiltrant les tumeurs sont retrouvés chez les patients atteints de nombreux types de cancers. Cependant leur rôle et leur valeur pronostique peuvent varier à cause du microenvironnement tumoral qui peut moduler les LT V γ 9V δ 2 du fait de leur plasticité fonctionnelle. En effet, lorsque l'on s'intéresse aux TIL issus de différentes tumeurs, la signature des LT $\gamma\delta$ est associée à un pronostic favorable dans la majorité des cas mais la corrélation avec la réponse clinique n'est pas toujours vraie (Gentles et al., 2015; Lo Presti et al., 2014).

Néanmoins, les LT V γ 9V δ 2 présentent un intérêt thérapeutique pour beaucoup de raisons :

- Leur activité cytotoxique directe ou indirecte envers les cellules tumorales, notamment par la sécrétion de molécules lytiques et de cytokines pro-inflammatoires,
- L'expression d'un FcR leur confère une activité d'ADCC qui peut être exploitée par l'injection concomitante d'anticorps,
- Leur abondance dans le sang périphérique qui facilite leur manipulation,
- Leur spécificité antigénique dirigée contre des molécules associées au stress cellulaire qui sont souvent surexprimées par les cellules cancéreuses,
- L'existence de molécules pharmacologiques, telles que les ABP, permettant une activation/ expansion spécifique et/ou la sensibilisation des cellules tumorales,
- L'absence de restriction aux molécules du CMH classiques pour la présentation de leur(s) antigène(s).

La documentation de ce potentiel anti-tumoral des LT V γ 9V δ 2 a conduit à la réalisation de plusieurs essais cliniques chez l'Homme, décrits dans la suite de cette introduction, afin de tester l'efficacité mais aussi la toxicité de diverses stratégies centrées sur les LT V γ 9V δ 2.

2 – Immunothérapie active

Parmi les différentes stratégies d'immunothérapies actives décrites précédemment, plusieurs ont été envisagées sur la base de l'utilisation de LT V γ 9V δ 2. Le modèle selon lequel ils sont capables de lyser des cellules stressées, récupérer des protéines relarguées et les présenter comme antigènes aux LT $\alpha\beta$ ouvre des possibilités de protocoles de vaccination (Khan et al., 2014; Werter et al., 2014). Cependant seules des preuves indirectes de ce phénomène ont pu être collectées chez des patients infectés qui présentaient alors une augmentation d'expression d'HLA-DR sur des LT V γ 9V δ 2 activés (Jouen-Beades et al., 1997). L'utilisation de cytokines, telles que l'IL-2, présente les mêmes avantages (amélioration de l'amplification) et inconvénients (toxicité) que pour les autres LT.

La stratégie la plus intéressante et la plus développée avec pour objectif l'activation *in vivo* des LT V γ 9V δ 2 repose sur l'administration aux patients de molécules activatrices spécifiques telles que des PAg ou des ABP (Fournié et al., 2013; Zou et al., 2017). Tout a commencé avec l'observation d'une réponse immunitaire caractérisée par l'augmentation du nombre de LT V γ 9V δ 2 circulants chez des patients traités au pamidronate (Kunzmann et al., 1999).

Cette stratégie a ensuite été développée dans un but thérapeutique. La première étude à prouver le potentiel thérapeutique des LT V γ 9V δ 2 a été menée par Wilhelm et al., chez des patients atteints de lymphome non-Hodgkinien ou de myélome multiple (Wilhelm et al., 2003). Les patients ont reçu une injection de pamidronate par voie intraveineuse suivie de doses croissantes d'IL-2. L'association du pamidronate et de faibles doses d'IL-2 a été bien tolérée par les patients et a conduit à une prolifération des LT V γ 9V δ 2 *in vivo*, voire à une rémission partielle du cancer chez certains patients (Wilhelm et al., 2003). Par la suite, il a été confirmé que l'activation des LT V γ 9V δ 2 *in vivo* était associée au développement d'une réponse pro-inflammatoire (IFN- γ) (Dieli et al., 2003).

Suite à ces résultats encourageants, plusieurs essais cliniques ont été conduits chez des patients atteints de carcinome rénal ou de métastases osseuses dérivant de cancer du sein ou de la prostate (Fournié et al., 2013; Zou et al., 2017) (Figure 19). Ces patients ont été traités par injection intraveineuse de Zolédronate associée ou non à des injections de faibles doses d'IL-2.

De façon générale, ces études ont mis en évidence une réponse thérapeutique sous la forme de stabilisation de la maladie et même de rémission partielle chez certains patients (Dieli et al., 2007; Lang et al., 2011; Meraviglia et al., 2010) (Figure 19). De plus, la majorité des patients n'ont présenté que des effets secondaires de faible intensité (syndrome grippal). Une autre étude a également prouvé l'efficacité de cette stratégie chez des patients atteints d'hémopathies malignes et ayant reçu une DLI (donor lymphocyte infusion) haploidentique, permettant d'obtenir des rémissions complètes chez 3 patients (Wilhelm et al., 2014).

Afin d'augmenter la spécificité de cette stratégie thérapeutique, des PAg de synthèse produit au grade GMP (good manufacturing practices), tel que le BrHPP (Phosphostim, Innate Pharma), ont été testé. Ainsi, des patients atteints de différentes tumeurs solides ont reçu par injection intraveineuse des doses croissantes de BrHPP, seules ou associées à des faibles doses d'IL-2 (Bennouna et al., 2010) (Figure 19). Comme attendu, ce traitement a induit une activation importante et spécifique des LT V γ 9V δ 2 *in vivo*, associé à des effets secondaires modérés principalement dus à l'injection d'IL-2. Cette étude a surtout permis de déterminer la dose maximale tolérable de BrHPP injectable aux patients tout en démontrant l'efficacité thérapeutique de ce protocole.

Traitements	Pathologies	Nombre de patients traités	Réponses Clinique	Références
<i>Traitement par injection d'ABP</i>				
Pam + IL-2	Hémopathies Malignes	19	3 RO	Wilhelm et al. 2003
Zol + IL-2	Cancers avec métastases osseuses	9	-	Dieli et al. 2003
Zol + IL-2	Carcinome Rénal	18	5 MS et 3 RP	Dieli et al. 2007
Zol + IL-2	Cancer du sein	10	2 MS et 1 RP	Meraviglia et al. 2010
Zol + IL-2	Carcinome Rénal	12	5 MS	Lang et al. 2011
Zol + IL-2 après DLI haploidentique	Hémopathies Malignes	4	3 CR	Wilhelm et al. 2014
<i>Traitement par injection de PAg</i>				
BrHPP + IL-2	Diverses Tumeurs Solides	28	12 MS	Bennouna et al. 2010

Figure 19 : Principaux essais cliniques en immunothérapie active basés sur l'utilisation de LT V γ 9V δ 2.

Plusieurs essais cliniques ont été réalisés chez des patients atteints de cancers solides ou liquides et qui ont été traités par injection de PAg (BrHPP) ou d'ABP (Pam : pamidronate ; Zol : Zolédronate) dans le but d'activer *in vivo* leurs LT V γ 9V δ 2. RO = réponse objective ; MS = maladie stable ; RP = rémission partielle ; RC = rémission complète ; DLI = donor lymphocyte infusion.

Adapté de Fournié, 2013 et Zhou, 2017.

Ces stratégies thérapeutiques présentent l'avantage d'utiliser des molécules produites et commercialisées au grade GMP et même déjà prescrites dans le traitement de certains cancers comme le Zolédronate pour le traitement des métastases osseuses (Dhillon and Lyseng-Williamson, 2008; Green and Lipton, 2010). Bien qu'elles permettent une activation spécifique des LT V γ 9V δ 2, l'association à l'IL-2 et l'activation de ces effecteurs cytotoxiques *in vivo* induit des effets secondaires pouvant aller jusqu'à la tempête cytokinique (Fournié et al., 2013; Zou et al., 2017).

3 – Immunothérapie passive

Dans le cas de l'immunothérapie passive, Kobayashi et ses collaborateurs, ont été les premiers à traiter des patients atteints de carcinome rénal par transfert adoptif autologue (Kobayashi et al., 2007). Après une étape de pré-activation, *ex vivo*, grâce à un PAg, de multiples injections de LT V γ 9V δ 2 autologues ont été réalisées, combinées à de faibles doses d'IL-2. Bien qu'une amplification des LT V γ 9V δ 2 puissent être enregistrée *in vivo*, l'efficacité thérapeutique observée reste faible avec un ralentissement de la croissance tumorale mais aucune rémission (Kobayashi et al., 2007).

Au cours d'un autre essai clinique, l'utilisation de LT V γ 9V δ 2 radio-marqués à l'indium 111 a permis d'observer la dissémination de ces effecteurs après injection systémique (Nicol et al., 2011). Ils sont principalement retrouvés dans les poumons, le foie, la rate et chez certains patients atteints de diverses tumeurs solides, ils ont aussi été retrouvés au niveau des métastases. Cette étude a également mis en évidence l'absence de toxicité liée à la quantité de cellules injectées. Par la suite de nombreux essais cliniques ont été réalisés chez des patients atteints de cancers hématologiques ou de tumeurs solides, qui ont été traités par transfert adoptif de LT V γ 9V δ 2 autologues, amplifiés *ex vivo*, associés à de l'IL-2 et du Zolédronate (Fournié et al., 2013; Zou et al., 2017).

Ces études ont documenté une bonne efficacité thérapeutique de cette thérapie avec plusieurs cas de rémission partielle et quelques cas de rémission complète (Figure 20). Une étude récente réalisée chez des patients atteints de cancer gastrique a même testé cette stratégie par injection intra-péritonéale afin de cibler au mieux les cellules tumorales infiltrantes (Wada et al., 2014).

Traitements	Pathologies	Nombre de patients traités	Réponses Clinique	Références
Autologue	Carcinome Rénal	7	3 RO	Kobayashi et al. 2007
Autologue	Carcinome Rénal	10	6 MS	Bennouna et al. 2008
Autologue	Myélome Multiple	6	4 MS	Abe et al. 2009
Autologue	Cancer du poumon	10	6 SM	Nakajima et al. 2010
Autologue	Carcinome Rénal	1	RC	Kobayashi et al. 2010
Autologue	Diverses Tumeurs Solides	25	4 RO, 3 MS et 3 RP	Noguchi et al. 2011
Autologue	Cancer Métastatique	18	3 MS, 2 RP et 1 RC	Nicol et al. 2011
Autologue + Zol	Carcinome Rénal	11	1 RC et 5 MS	Kobayashi et al. 2011
Autologue + Zol	Cancer gastrique	7	2 RO	Wada et al. 2014

Figure 20 : Principaux essais cliniques en immunothérapie passive basés sur l'utilisation de LT V γ 9V δ 2.

Plusieurs essais cliniques ont été réalisés chez des patients atteints de cancers solides ou liquides qui ont été traités par injections de LT V γ 9V δ 2 autologues amplifiés *ex vivo* de façon spécifique (PAg ou ABP) seuls ou combinés à l'administration de Zolédronate (Zol). RO = réponse objective ; MS = maladie stable ; RP = rémission partielle ; RC = rémission complète.

Adapté de Fournié, 2013 et Zhou, 2017.

De nouvelles stratégies sont également en cours de développement. Grâce au génie génétique, il est possible de transférer un TCR $\gamma\delta$ dans un LT $\alpha\beta$ avant de les réinjecter aux patients. Cette stratégie présente l'avantage d'utiliser un TCR $\gamma\delta$ dont la reconnaissance est indépendante des molécules du CMH, tout comme les CAR, mais avec une spécificité non restreinte à un antigène tumoral qui est souvent également exprimé par les cellules saines (Straetemans et al., 2018). La production au grade GMP de cette nouvelle famille d'effecteurs a récemment été validée et sera prochainement testée chez des patients atteints de leucémie ou de myélome multiple (Straetemans et al., 2018).

4 – Modèles murins précliniques et nouvelles stratégies thérapeutiques

Pour finir, beaucoup d'études précliniques sont en cours afin d'évaluer le potentiel thérapeutique de nouvelles stratégies d'immunothérapie basées sur l'utilisation de LT V γ 9V δ 2. Actuellement, de nombreuses équipes tentent de proposer des stratégies thérapeutiques permettant d'augmenter le potentiel cytotoxique des LT V γ 9V δ 2 et/ou leur reconnaissance des cellules tumorales (Hoeres et al., 2018). Pour cela, des modèles précliniques de tumeurs liquides ou solides, implantées en orthotopique ou non, ont été mis en place dans des souris immunodéficientes supportant la greffe de cellules tumorales et immunitaires humaines.

Voici quelques exemples de stratégies évaluées dans ces modèles précliniques et fournissant des preuves de concept *in vivo* pour la combinaison des LT V γ 9V δ 2 à :

- L'utilisation d'ABP, afin d'augmenter la reconnaissance des cellules tumorales et d'induire une forte activation des LT V γ 9V δ 2 (Santolaria et al., 2013).
- La chimiothérapie, traitement standard dans la majorité des cancers, qui induit un stress cellulaire pouvant favoriser la reconnaissance naturelle des cellules tumorales par les LT V γ 9V δ 2 (Chitadze et al., 2016; Todaro et al., 2013).
- Des Ac thérapeutiques mettant ainsi à profit l'activité d'ADCC des LT V γ 9V δ 2 exprimant le CD16 et permettant de cibler spécifiquement les cellules tumorales pour un antigène de tumeur (Capietto et al., 2011; Gertner-Dardenne et al., 2009).
- Des Ac bispécifiques qui, comme leur nom l'indique, présentent une double spécificité pour un antigène de tumeur et ici pour le TCR V γ 9V δ 2, forçant le contact et l'activation d'un effecteur face à sa cible (de Bruin et al., 2017).
- Des Ac ciblant la partie extracellulaire de BTN3A afin d'induire une reconnaissance TCR-spécifique par les LT V γ 9V δ 2 mais indépendamment de la perturbation de la voie du MVA dans les cellules tumorales (Benyamine et al., 2016).

Il est tout de même important de noter que ces études précliniques sont réalisées dans des modèles de xénogreffes chez des souris immunodéficientes, du fait de l'absence d'équivalent des LT V γ 9V δ 2 chez la souris. Bien que ces modèles murins fournissent des preuves de l'efficacité de ces stratégies, ils sont peu ou pas représentatifs du microenvironnement tumoral et de l'immunosuppression qu'il induit. Les mécanismes d'échappement au système immunitaire restant, à ce jour, la principale cause d'échec des stratégies d'immunothérapies.

V – Objectifs de ma thèse

Le cancer de façon générale représente l'une des premières causes de mortalité dans le monde. On distingue deux types de tumeurs : les tumeurs bénignes qui restent localisées au tissu d'origine, et les tumeurs malignes qui se caractérisent par leur profil fortement prolifératif et invasif. Les récentes avancées technologiques dans les domaines de l'imagerie médicale et de la chirurgie ont permis d'améliorer à la fois le diagnostic et la prise en charge des patients atteints de cancer. Bien que le développement des traitements par chimiothérapie et radiothérapie ait permis d'augmenter la survie des patients, des effets secondaires importants découlent de leur faible spécificité d'action et des cellules tumorales résistantes apparaissent. Ainsi, le cancer est une maladie présentant une forte variabilité inter- et intra-individu, qui représente donc un défi thérapeutique encore de nos jours.

Le développement des immunothérapies a permis d'améliorer encore la prise en charge et la survie des patients et certains de ces bio-médicaments font maintenant partie des lignes de traitement standard dans différents types de cancers. Actuellement, ce sont les anticorps thérapeutiques les plus développés mais de nombreuses autres stratégies d'immunothérapies sont également en cours de développement, comme le transfert adoptif d'effecteurs immunitaires.

L'objectif de ce travail de thèse a été d'optimiser l'utilisation de LT V γ 9V δ 2 humains allogéniques par transfert adoptif dans des modèles murins précliniques. En effet, les LT V γ 9V δ 2 présentent de nombreux avantages pour ce type de stratégie d'immunothérapie anti-tumorale. Ils représentent environ 5 % des cellules CD3⁺ dans le sang périphérique ce qui facilite leur manipulation. Leur spécificité antigénique en lien avec le stress cellulaire permet à la fois une reconnaissance naturelle des cellules tumorales ou une reconnaissance induite par des molécules pharmacologiques telles que les ABP. De plus, cette reconnaissance n'étant pas restreinte par les molécules du CMH, il est envisageable de créer des banques de cellules allogéniques issues de donneurs sains. Cette stratégie assure aux patients un traitement constamment disponible et sans risque de réaction GVHD (graft versus host disease).

Les précédents travaux de l'équipe ont permis de valider la faisabilité d'un traitement par transfert adoptif de LT V γ 9V δ 2 associé au Zolédronate pour sensibiliser les cellules tumorales dans un modèle sous-cutané de tumeur de la prostate (Santolaria et al., 2013). Ces résultats encourageants nous ont poussé à améliorer à la fois les modalités d'administration du traitement et la pertinence des modèles murins utilisés afin de tester l'efficacité de ces traitements.

Dans un premier temps, une étude *in vitro* a porté sur l'analyse des fonctions effectrices des LT $\gamma\delta$ directement issus du sang périphérique puis des LT V γ 9V δ 2 après amplification (spécifique ou non). En effet, le maintien de ces fonctions est un point critique dans le développement d'immunothérapies par transfert adoptif d'effecteurs cytotoxiques. Ils doivent être capables de survivre, patrouiller et proliférer *in vivo* chez les patients pour assurer une bonne efficacité thérapeutique.

Dans un second temps, différents protocoles d'immunothérapies basés sur le transfert adoptif de LT V γ 9V δ 2 humains allogéniques ont été testés dans deux pathologies :

- Un modèle de cancer de l'ovaire avec xélogreffe orthotopique des cellules tumorales suivi du traitement standard des patientes, chirurgie et chimiothérapie, a été mis en place. Ce modèle nous a permis d'étudier l'impact de la chimiothérapie sur la réactivité des LT V γ 9V δ 2 *in vitro* avant de combiner ces deux traitements *in vivo* de façon efficace dans notre modèle murin.
- Plusieurs modèles de glioblastome multiforme, également basés sur une xélogreffe orthotopique de cellules tumorales humaines, ont été mis en place avec injection locale du traitement, dans la zone péri-tumorale. Ces modèles nous ont permis d'évaluer différentes stratégies autour du transfert adoptif de LT V γ 9V δ 2, telles que la combinaison au Zolédronate pour sensibiliser les cellules tumorales, l'augmentation de la cytotoxicité des LT V γ 9V δ 2 *ex vivo* par un pré-conditionnement à l'IL-21 mais également la reconnaissance spontanée de primocultures de glioblastome multiforme.

Une présentation de chacune de ces pathologies précèdera les résultats correspondant et une conclusion ciblée clôturera ces différents exemples d'applications.

B. RESULTATS

PARTIE 1 : Caractérisation de LT $\gamma\delta$ pro- ou anti-tumoraux : Intérêt pronostic et optimisation des immunothérapies anti-tumorales

1 – Objectifs du projet

Les LT $\gamma\delta$ font partie des cellules pouvant jouer un rôle dans la réponse immunitaire anti-tumorale, cependant leur contribution réelle est encore mal comprise. Malgré la variété et la puissance de leur fonction effectrice, leur présence dans le microenvironnement tumoral a pu être associée à un mauvais pronostic dans plusieurs types de cancers (Castiglione et al., 2008; Ma et al., 2012). Cela suggère l'existence de sous-populations de LT $\gamma\delta$ dotées de fonctions suppressives, voir pro-tumorales. Cette étude vise donc à identifier de nouvelles sous-populations de LT $\gamma\delta$ exerçant des fonctions régulatrices. Une fois identifiées, l'étude des mécanismes impliqués dans la mise en place de ces populations permettra d'apporter un nouvel éclairage sur la pertinence physiopathologique des LT $\gamma\delta$ au sein du microenvironnement tumoral. A terme, une meilleure compréhension des mécanismes régulant leur émergence, leur recrutement et leur activité pro-tumorale permettra une optimisation et/ou l'élaboration de nouvelles stratégies immunothérapeutiques.

Dans un premier temps, cette étude a porté sur l'identification de nouvelles populations de LT $\gamma\delta$ présentant des fonctions régulatrices. Deux hypothèses ont été émises quant à l'émergence de ces sous-populations. Tout d'abord, il est possible qu'elles soient présentes de façon constitutive. Leur présence en périphérie résulterait de mécanismes de sélection thymique ou extra-thymique inconnus à ce jour. Leurs fonctions pro-tumorales se révéleraient lors du développement d'un cancer. A l'inverse, il est possible que tous les LT $\gamma\delta$ présents en périphérie présentent un profil commun, de type pro-inflammatoire, associé aux fonctions d'un effecteur cytotoxique. Leur recrutement sur le site de la tumeur, notamment au sein du microenvironnement immunosuppresseur inhiberait leurs fonctions effectrices et pourrait induire leur polarisation en cellules régulatrices.

Afin de tester ces hypothèses, nous avons commencé par étudier les fonctions des LT $\gamma\delta$ présents dans le sang périphérique de donneurs sains. Le but étant de déterminer si les LT $\gamma\delta$ circulants peuvent d'emblée présenter un profil régulateur ou s'ils présentent tous un profil pro-inflammatoire.

2 – Matériels et Méthodes

2.1 – Marquages intra- et extra-cellulaires

Pour les marquages membranaires, 1.10^5 à 2.10^5 cellules sont resuspendues dans du PBS (phosphate buffer saline) contenant 0,5 % de BSA (bovine serum albumin, Sigma Aldrich, Saint-Louis, MO), 0,1 % de PFA (para-formaldéhyde, Electron Microscopy Sciences, Hatfield, PA), et les anticorps d'intérêt. Après incubation, pendant 20 min à l'obscurité et à température ambiante, les cellules sont lavées puis analysées par cytométrie en flux. Parmi les anticorps utilisés, l'anticorps anti-CD3 couplé APC dilué au $1/50^{\text{ème}}$ (UCHT1, Beckman Coulter, Brea, CA), l'anticorps anti-pan $\gamma\delta$ couplé PE-Cy5 dilué au $1/20^{\text{ème}}$ (IMMU510, Beckman Coulter) et l'anticorps anti-V δ 2 couplé FITC dilué au $1/30^{\text{ème}}$ (IMMU389, Beckman Coulter) sont utilisés pour la réalisation des tests de pureté. Pour les marquages permettant de définir le profil effecteur mémoire, l'anticorps anti-CD27 couplé PE (1A4CD27, Beckman Coulter) et l'anticorps anti-CD45RA (HI100, BD Biosciences, Franklin Lakes, NJ) sont utilisés au $1/30^{\text{ème}}$.

Pour les marquages intracellulaires (test IFN- γ), les LT sont tout d'abord activés de façon spécifique par 30 μ M de BrHPP (InnatePharma, Marseille, France) ou non spécifique par un mélange de 500 ng/mL de PMA (phorbol12-myristate13-acetate) et 1 μ M de ionomycine (Sigma), en présence de 10 μ M monensine (Sigma). Après activation, 1.10^5 cellules sont resuspendues dans 100 μ L de PBS-PFA 4 % et incubées pendant 15 min à température ambiante pour fixation. Après lavage, elles sont resuspendues dans un tampon de perméabilisation (eBiosciences, San Diego, CA) et centrifugées deux fois pendant 5 min à 530 g. Le culot de cellules est repris dans le tampon de perméabilisation contenant l'anticorps anti-IFN- γ couplé PE dilué au $1/50^{\text{ème}}$ (4S.B3, eBiosciences). Elles sont alors incubées pendant 20 min à l'obscurité et à température ambiante puis lavées, avant analyse par cytométrie de flux.

L'acquisition des données est réalisée sur un cytomètre de type BD FACS Calibur (BD Biosciences) ou de type Accuri C6Plus (BD Biosciences). L'analyse sera ensuite effectuée à l'aide du logiciel FlowJo (TreeStar, Ashland, OR) ou sur l'Accuri C6Plus (BD Biosciences).

2.2 – Tri négatif des LT $\gamma\delta$

Le tri négatif des LT $\gamma\delta$ est réalisé à partir de PBMC à l'aide du kit Human Gamma/Delta T Cell Isolation de chez StemCell (Vancouver, Canada).

Les PBMC sont tout d'abord collectés par un gradient de densité (Ficoll) à partir de sang périphérique prélevé chez des donneurs sains et fourni sous forme de concentré leucoplaquettaire par l'Etablissement Français du Sang (EFS, Nantes). Le sang est dilué (1/4) dans du PBS, 0,02 % EDTA (éthylènediaminetetraacetic acid, Gibco, Carlsbad, CA) ou du RPMI (Roswell Park Memorial Institute medium 1640) (Gibco). Puis 35 mL de sang sont déposés délicatement sur 15 mL de milieu de séparation lymphocytaire (Eurobio, Courtaboeuf, France). Le tout est ensuite centrifugé pendant 20 min à 1500 g, avec faible accélération et sans frein. Les PBMC, qui se situent alors à l'interphase entre le milieu de séparation lymphocytaire et le plasma, sont prélevés. Les traces de milieu de séparation lymphocytaire sont éliminées par centrifugation pendant 10 min à 530 g. Afin d'éliminer les plaquettes résiduelles, 2 lavages supplémentaires sont effectués par centrifugation 10 min à 240 g. Si nécessaire, il est également possible de réaliser une lyse des globules rouges (BD PharmLyse ; BD Biosciences).

Après récupération, et afin de réaliser le tri négatif des LT $\gamma\delta$, les PBMC sont repris à raison de $50 \cdot 10^6$ cellules/mL dans du PBS, 1 mM EDTA, 2 % SVF (sérum de veau fœtal) avant d'ajouter 50 μ L de Human Gamma/Delta T Cell Isolation Cocktail par mL de cellules. Après 15 minutes d'incubation à température ambiante, 50 μ L de billes magnétiques sont ajoutés pour chaque mL de cellules, avant d'incuber à nouveau 10 min à température ambiante. Le volume du tube est alors complété à 40 mL avec du PBS, 1 mM EDTA, 2 % SVF puis placé sur un aimant adapté. Après 10 minutes d'incubation le surnageant est récupéré et cette opération est répétée afin de s'assurer que toutes les billes sont bien éliminées. Les cellules récupérées sont alors transférées dans du milieu de culture et utilisées, après vérification de la pureté en LT $\gamma\delta$ (cf section 2.1).

2.3 - Amplification antigénique et non spécifique des LT $V\gamma 9V\delta 2$

Les LT $V\gamma 9V\delta 2$ peuvent être amplifiés de façon antigénique, directement à partir de PBMC, par stimulation avec du BrHPP (InnatePharma) utilisé à 3 μ M ou avec du Zolédronate (Sigma) utilisé à 5 μ M. Les PBMC sont incubés à 37°C à raison de $1 \cdot 10^6$ cellules/puits dans du RPMI supplémenté avec 10 % de SVF, 2 mM de L-Glutamine, 10 mg/mL de streptomycine, 100 UI/mL de pénicilline (tous de chez Gibco, appelé RPMI complet), contenant également 100 UI/mL d'IL-2 (Novartis, Bale, Suisse) et la molécule activatrice. Lorsque des agrégats cellulaires sont visibles à l'œil nu (4 à 5 jours), du RPMI complet enrichi en IL-2 est alors rajouté dans les puits afin d'obtenir une concentration finale en IL-2 de 300 UI/mL.

Les cellules sont ensuite transférées en flasque en RPMI complet contenant 300 UI/mL d'IL-2 et conservées à 1.10^6 cellules/mL jusqu'à revenir à un état de repos (environ 3 semaines).

L'expansion des LT peut également se faire par stimulation non-spécifique induite par la PHA (phytohemagglutinine, Sigma). Des cellules nourricières irradiées à 35 Gy (Grays) (PBMC et B.EBV (lymphocytes B immortalisés par l'Epstein Barr Virus) issus de trois donneurs différents) fournissent un environnement idéal à leur prolifération. Les LT au repos (entre 2 et 4.10^5 cellules au total) sont incubés à 37°C en plaque 96 puits à fond rond ou en flasque de 75 cm² debout dans du RPMI complet contenant 300 UI/mL d'IL-2, 1 µg/mL de PHA et en présence de 1.10^7 PBMC et 1.10^6 B.EBV irradiés jusqu'à ce que des agrégats soit visibles à l'œil nu (6 à 7 jours). Les cellules sont ensuite regroupées en flasques dans du RPMI complet contenant 300 UI/mL d'IL-2 et conservées à 1.10^6 cellules/mL jusqu'à revenir à un état de repos (environ 3 semaines). Avant utilisation des LT, un test de pureté est réalisé (cf section 2.1).

2.4 - Dosage de cytokines avec le kit LEGENDplex

Le dosage des cytokines secrétées par les LT $\gamma\delta$ a été réalisé à l'aide du kit de dosage LEGENDplex Human Th Cytokine Panel (Biolegend, San Diego, CA). Le principe de ce kit repose sur un test ELISA sandwich et sur l'utilisation de billes. Deux types d'anticorps sont donc utilisés : des anticorps de détection couplés à des billes qui permettront de les différencier par leurs tailles au cytomètre, et des anticorps de dosage biotinylés. Le dosage des différentes cytokines se fait par mesure de l'intensité de fluorescence grâce à l'ajout de streptavidine couplée à la phycoérythrine (SA-PE) (Figure 21). Une gamme étalon est donc réalisée afin de corrélérer l'intensité de fluorescence à la concentration des différentes cytokines. Pour cela, un mélange des 13 cytokines, dosable à 10 000 pg/mL, est prévu dans le kit. La gamme est ensuite réalisée en 8 points : chaque point correspondant à une dilution au quart du précédent. Le seuil de détection du kit étant de 2 pg/mL pour toutes les cytokines.

Après activation, ou non, de 1.10^5 cellules dans 100 µL de RPMI complet, les surnageants sont récupérés à différents temps d'incubation et le dosage des cytokines peut être réalisé immédiatement ou en différé (conservation des surnageants à -80°C). Sur les recommandations du fournisseur, 25 µL de surnageant à tester ou 25 µL d'un point de la gamme sont mélangés à 25 µL de tampon, 25 µL d'un mélange des billes et 25 µL d'anticorps de détection. Le tout est alors mis sous agitation (500 rpm) à l'obscurité et à température ambiante pendant 2 heures.

Ensuite 25 µL de SA-PE sont ajoutés dans chaque puits avant de remettre sous agitation pendant 30 minutes. Deux lavages successifs sont réalisés à l'aide d'un tampon de lavage, fourni dans le kit, avant de resuspendre les culots dans ce même tampon pour l'analyse par cytométrie en flux. Pour finir, la quantification des différentes cytokines est faite à l'aide du logiciel LEGENDplex 7 fourni avec le kit.

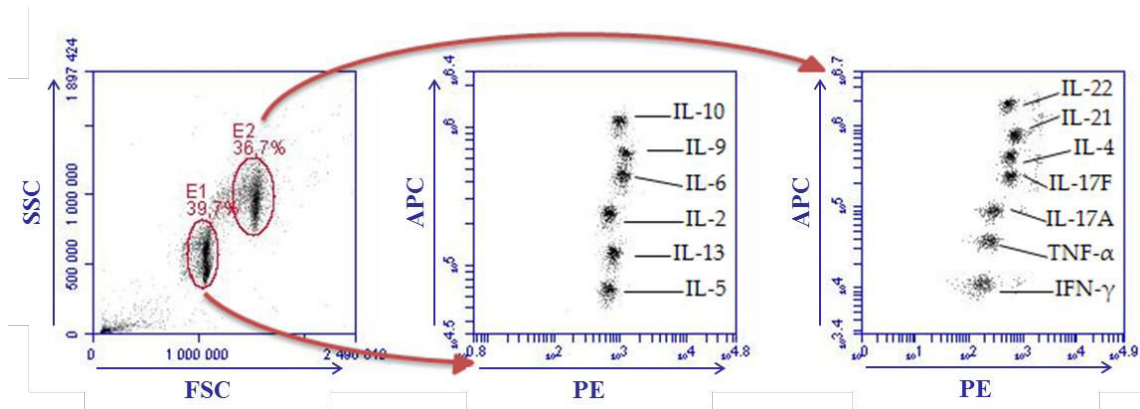


Figure 21 : Présentation du kit de dosage de cytokines LEGENDplex.

Afin de pouvoir doser 13 cytokines différentes, des billes de deux tailles différentes sont utilisées et se différencient en fonction de leur taille et de leur granulosité (*gauche*). Ensuite, les anticorps de détection de chaque cytokine sont discriminés grâce à leur intensité de fluorescence en APC (*milieu et droite*). Enfin, la concentration en cytokine est corrélée à l'intensité de fluorescence en PE (*milieu et droite*) et peut être calculée grâce à la réalisation d'une gamme étalon.

2.5 - Test de réactivité CD107a

Ce test fonctionnel a pour but d'étudier, de façon quantitative et qualitative, la réactivité des lymphocytes contre des cellules cibles afin d'analyser et de comparer leur capacité d'activation. Les cellules cibles peuvent être préalablement sensibilisées, pendant la nuit avec différentes concentrations de Zolédronate (Sigma). Elles sont ensuite cocultivées avec les LT pendant 4 heures à un ratio effecteurs : cibles de 1:1. La coculture est réalisée en présence de monensine (5 µM, Sigma), et d'un anticorps dirigé contre le CD107a (dilué au 1/80^{ème}, H4A3, BD Biosciences ou Biolegend). Après incubation pour la coculture, un marquage du TCR (pan γδ et/ou Vδ2) est réalisé (cf section 2.1), puis les cellules marquées sont analysées par cytométrie de flux afin de déterminer le pourcentage de cellules activées (cellules CD107a positives).

3 – Etude du phénotype de LT $\gamma\delta$ directement issus du sang de donneurs sains

Afin de réaliser cette étude sur les LT $\gamma\delta$ circulants dans le sang périphérique, nous avons décidé de les trier avec le kit de tri négatif $\gamma\delta$ de chez StemCell (Matériels et Méthodes section 2.2). Les LT $\gamma\delta$ représentent entre 1 et 10 % des cellules CD3⁺ dans le sang périphérique selon les donneurs (Figure 22 A et C) et grâce à ce kit il est possible d'extraire ces LT $\gamma\delta$ afin de travailler sur une préparation cellulaire pure à environ 90 % en LT $\gamma\delta$ (Figure 22 B et C). Nous avons également analysé les proportions en sous-populations de LT $\gamma\delta$ présentes à l'issue de ce tri. Comme attendu, la majorité des LT $\gamma\delta$ récupérés sont des LT V γ 9V δ 2 (V δ 2⁺) mais des LT V δ 2⁻ sont également retrouvés (Figure 22 B et C).

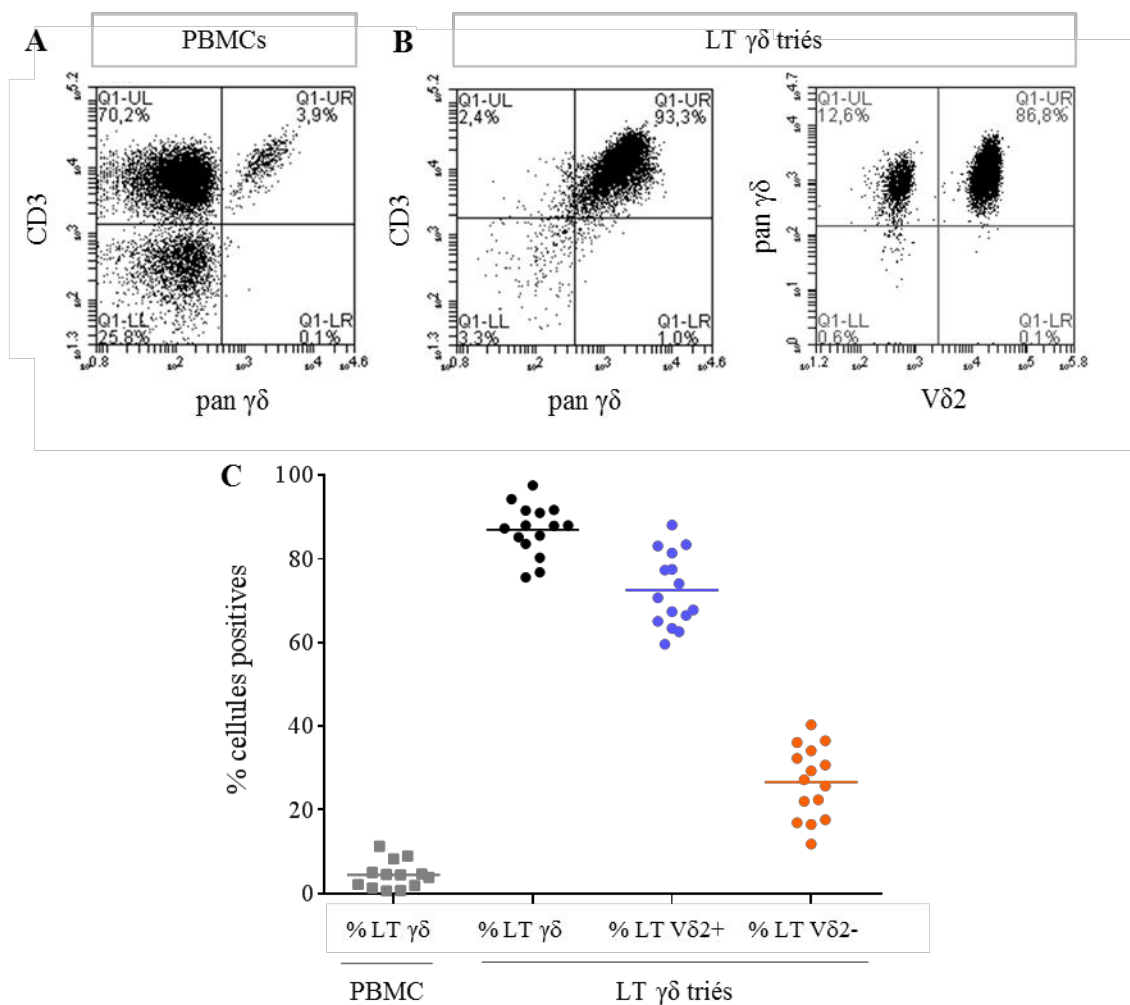


Figure 22 : Tri négatif des LT $\gamma\delta$ présents dans le sang périphérique de donneurs sains.

Après récupération des PBMC par Ficoll, un tri négatif des LT $\gamma\delta$ est réalisé. La pureté en LT $\gamma\delta$ est contrôlée sur les PBMC avant tri (A) et sur les LT $\gamma\delta$ après tri négatif (B, gauche) avec une analyse de la proportion en LT V δ 2⁺ et V δ 2⁻ (B, droite). (C) Compilation des résultats pour 15 donneurs de PBMC.

A l'issue de ce tri il est possible d'étudier le phénotype de ces LT $\gamma\delta$ circulants. Les fonctions effectrices des LT $\gamma\delta$, notamment les interactions avec les cellules de l'environnement, passent principalement par la sécrétion de cytokines ou de chimiokines. En effet, les LT $\gamma\delta$ présentant un profil pro-inflammatoire secrètent des cytokines telles que l'IFN- γ ou le TNF- α , mais certains LT $\gamma\delta$ sont également capables de sécréter des cytokines immunomodulatrices telles que l'IL-10, le TGF- β ou l'IL-17. C'est pourquoi nous avons décidé de réaliser une étude du profil sécrétoire de ces LT $\gamma\delta$ circulants.

Pour cela, les LT $\gamma\delta$, issus du tri, ont été stimulés, ou non, de façon non spécifique grâce à un mélange de PMA et ionomycine afin d'induire le relargage de toutes les cytokines produites par ces LT $\gamma\delta$. A différents temps après cette activation (6 et 24 heures), le surnageant de culture a été récupéré et un dosage de cytokines a été réalisé. Afin de pouvoir étudier le maximum de cytokines, nous avons choisi d'utiliser un kit de dosage par billes qui permet de doser 13 cytokines différentes en même temps (Matériels et Méthodes section 2.4). Ces 13 cytokines sont l'IL-5, l'IL-13, l'IL-2, l'IL-6, l'IL-9, l'IL-10, l'IL-17A, l'IL-17F, l'IL-4, l'IL-21, l'IL-22, l'IFN- γ et le TNF- α .

A l'issue de ce dosage, seulement trois cytokines sont détectées : l'IL-2, l'IFN- γ et le TNF- α (Figure 23). Tout d'abord, l'IL-2 est naturellement sécrétée, en absence d'activation, dans de faible proportion et l'activation des LT $\gamma\delta$ conduit à une augmentation de la libération de cette cytokine, notamment à 24 heures (Figure 23A). L'IFN- γ et le TNF- α , quant à eux présentent un profil de sécrétion similaire. En absence d'activation, aussi bien à 6 heures qu'à 24 heures, il n'y a que très peu ou pas de cytokines de secrétées (Figure 23 B et C). Après activation, une forte libération de ces cytokines est observable à 6 heures et à 24 heures (Figure 23 B et C).

Cependant cette analyse de la sécrétion de cytokines ne nous permet pas de savoir quelle sous-population de LT $\gamma\delta$ les sécrète. Ainsi des marquages intracellulaires de l'IFN- γ ont été réalisés 6 heures après activation (Matériels et Méthodes section 2.1). Grâce à un marquage pan $\gamma\delta$ et V δ 2 il est possible de discriminer efficacement les LT V γ 9V δ 2, des LT $\gamma\delta$ V δ 2 négatif. Les résultats obtenus concordent avec le dosage de cytokines. En absence d'activation le niveau d'expression d'IFN- γ est faible aussi bien chez les LT V δ 2⁺ que chez les LT V δ 2⁻ (Figure 23D). Par contre, après activation, une forte augmentation du niveau d'IFN- γ intracellulaire est observée. Il est également intéressant de noter que le niveau intracellulaire d'IFN- γ est plus élevé chez les LT V δ 2⁺ que chez les LT V δ 2⁻ (Figure 23D).

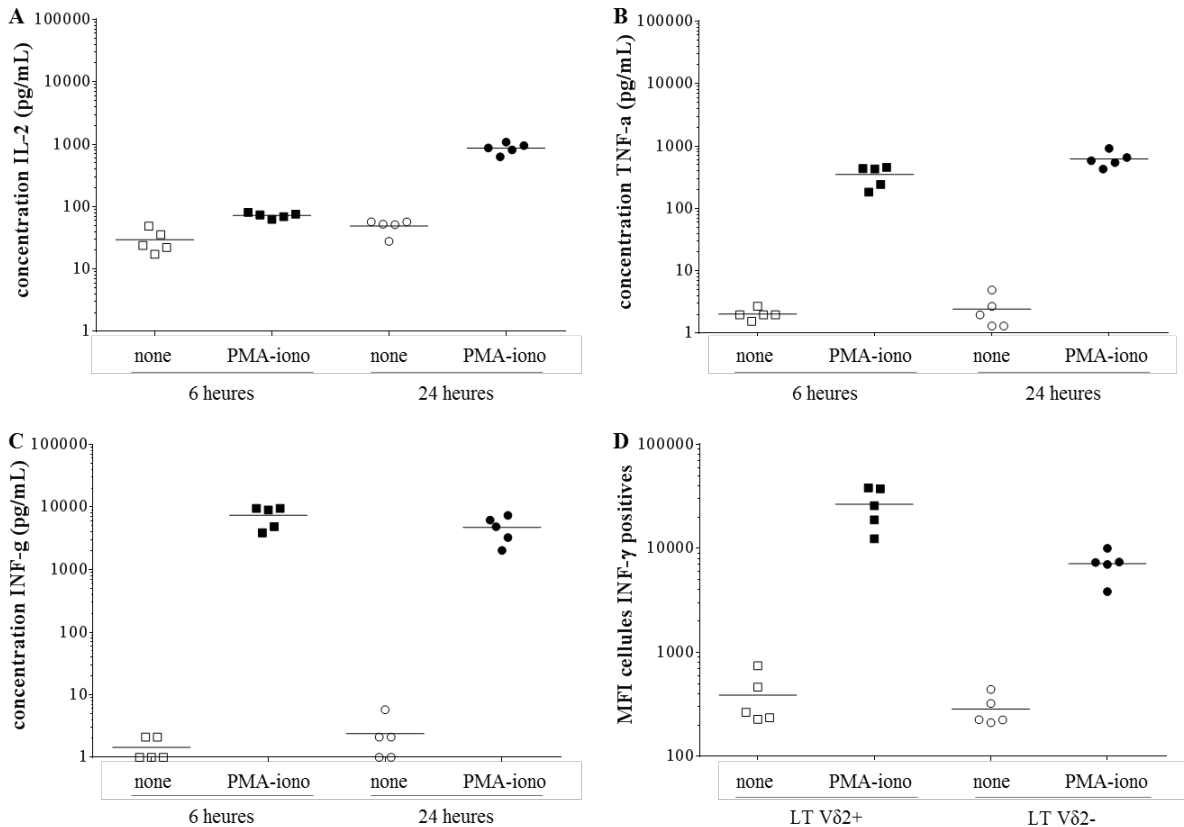


Figure 23 : Etude du sécrétome des LT $\gamma\delta$ présents dans le sang périphérique de donneurs sains. Après un tri négatif, les LT $\gamma\delta$ isolés sont activés, ou non, de façon non spécifique (PMA ionomycine). Un dosage des cytokines qu'ils sécrètent est réalisé sur les surnageants récupérés à 6 et 24 heures après activation (kit LEGENDplex Human Th Cytokine). Seules les cytokines détectées sont présentées : l'IL-2 (A), le TNF- α (B) et l'IFN- γ (C). Des marquages intracellulaires de l'IFN- γ ont également été réalisés 6 heures après activation (D).

Ces résultats semblent favoriser la seconde hypothèse émise précédemment : tous les LT $\gamma\delta$ circulants présentent un profil pro-inflammatoire et la présence de LT $\gamma\delta$ pro-tumoraux ou régulateurs au sein des tumeurs serait alors liée au microenvironnement immunosuppresseur qu'elles génèrent.

Nous nous sommes également intéressés à la réactivité de ces effecteurs contre des cellules tumorales. Pour cela, des tests de réactivité, par marquage du CD107a, ont été réalisés face à 6 lignées commerciales de cellules tumorales de diverses origines tissulaires (Matériels et Méthodes section 2.5). La coculture a été réalisée avec les populations de LT $\gamma\delta$ triées puis amplifiées de façon non spécifique par PHA-feeders afin d'obtenir un nombre de cellules suffisant pour les expériences (Matériels et Méthodes section 2.3). A l'issue de ces amplifications, la pureté en LT $\gamma\delta$, notamment la proportion en LT V δ 2⁺ et en LT V δ 2⁻, a été vérifiée et elle ne varie pas (résultats non montrés).

A l'issue de la coculture entre ces populations de LT $\gamma\delta$ et les différentes lignées de cellules tumorales, un marquage extracellulaire pan $\gamma\delta$ et V δ 2 a été réalisé afin de discriminer les deux sous-populations de LT $\gamma\delta$. L'analyse du CD107a sur les LT V γ 9V δ 2 révèle une reconnaissance hétérogène des différentes lignées de cellules tumorales. En effet, certaines sont très faiblement reconnues (< 5 % de cellules CD107a positives) alors que d'autres sont naturellement reconnues (entre 5 et 15 % de cellules CD107a positives) (Figure 24). Concernant les LT V δ 2⁻, l'analyse du CD107a montre une absence complète de réactivité contre toutes les cibles (< 1 % de cellules CD107a positives) (Figure 24).

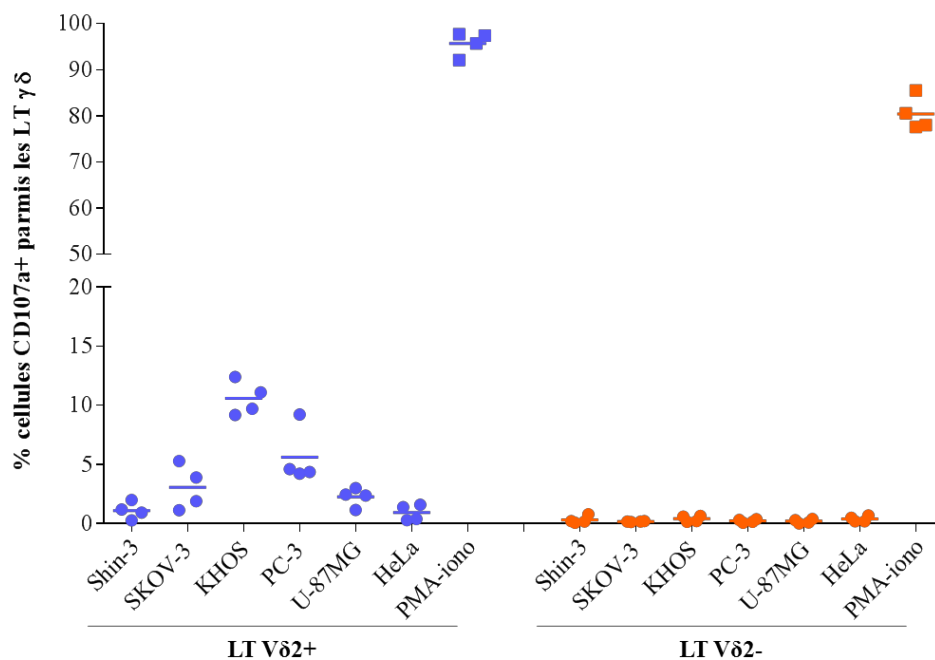


Figure 24 : Etude de la réactivité naturelle de LT $\gamma\delta$ face à différentes lignées de cellules tumorales. Les LT $\gamma\delta$ triés négativement ont été amplifiés de façon non spécifique (PHA-feeders) avant de réaliser des tests de réactivité face à des lignées cellulaires tumorales commerciales. Les LT $\gamma\delta$ ont été cocultivés à un ratio E:T de 1:1 en présence d'un anticorps anti-CD107a. A l'issue des 4 heures de coculture, un marquage du TCR $\gamma\delta$ est réalisé et le pourcentage de cellules CD107a⁺ est analysé sur les sous-populations de LT V δ 2⁺ et V δ 2⁻.

Suite à ces résultats, nous avons décidé de poursuivre ces travaux uniquement par l'analyse des LT V γ 9V δ 2. Bien que les mécanismes d'activation des LT V γ 9V δ 2 soit encore mal compris, nous avons à notre disposition plusieurs molécules pharmacologiques (ex. BrHPP, Zolédronate) nous permettant de les activer/amplifier spécifiquement, ce qui n'est pas le cas pour les LT V δ 2. La suite de cette étude a également été divisée en deux axes : l'étude de l'impact de cytokines immunomodulatrices sur des LT V γ 9V δ 2 et la description des fonctions effectrices de LT V γ 9V δ 2 dans le cadre de la création d'une banque cellulaire allogénique à visée thérapeutique.

4 – Description des fonctions effectrices de LT V γ 9V δ 2 dans le cadre de la création d'une banque cellulaire allogénique

Il existe beaucoup d'intérêts à utiliser des LT V γ 9V δ 2 allogéniques dans le cadre d'un transfert adoptif. Non seulement ils présentent de nombreuses fonctions effectrices anti-tumorales, mais la reconnaissance des cellules tumorales n'étant pas restreinte par les molécules du CMH classique, le risque de réactions allogéniques contre l'hôte est pratiquement nul. De plus, grâce au développement de molécules pharmacologiques activant spécifiquement cette population, il est possible de les amplifier de façon antigénique *ex vivo*. Ainsi la création d'une banque de LT V γ 9V δ 2 humains allogéniques permettrait de disposer d'un traitement prêt à l'emploi pour soigner des patients. Néanmoins, cela implique de pouvoir amplifier des quantités très importantes de cellules au préalable. Pouvoir réaliser plusieurs amplifications sur les LT V γ 9V δ 2 d'un même donneur sain pour obtenir de très grandes quantités de cellules présente donc un intérêt tout particulier. Nous avons donc focalisé l'étude sur le maintien des fonctions effectrices des LT V γ 9V δ 2 au cours de ces multiples amplifications.

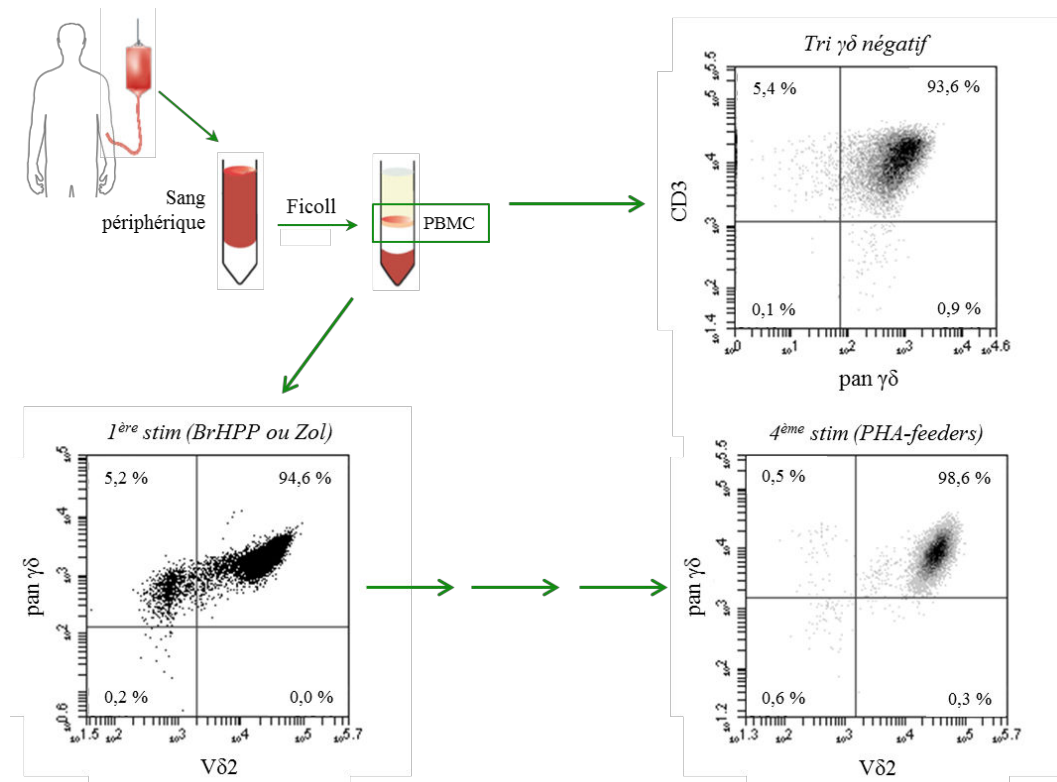


Figure 25 : Description du protocole d'amplification des LT V γ 9V δ 2

Les PBMC sont soit triés afin d'isoler les LT $\gamma\delta$ de manière négative (*en haut à droite*), soit incubés en présence d'une molécule activant spécifiquement les LT V γ 9V δ 2 (*en bas à gauche*). Ces derniers, une fois revenus à un état de repos, sont ré-amplifiés, 3 fois, de façon non spécifique (*en bas à droite*). A chaque étape, la pureté de la population récupérée est vérifiée par un marquage CD3, pan $\gamma\delta$ et V δ 2.

Différentes analyses ont donc été réalisées sur (Figure 25) :

- des LT V γ 9V δ 2 issus du sang périphérique, récupérés grâce au protocole de tri négatif décrit précédemment (Matériel et Méthodes section 2.2).
- des LT V γ 9V δ 2 après un cycle d'amplification antigénique, réalisé sur PBMC, grâce au BrHPP ou au Zolédronate (Matériel et Méthodes section 2.3).
- des LT V γ 9V δ 2 ayant subi trois cycles d'amplification non spécifique, par PHA-feeders, après l'étape d'amplification antigénique décrite ci-dessus (Matériel et Méthodes section 2.3).

Tout d'abord, concernant l'étape d'amplification antigénique, deux molécules activatrices ont été utilisées : un PAg de synthèse, le BrHPP, ou un ABP, le Zolédronate. Les deux techniques sont efficaces pour stimuler spécifiquement les LT V γ 9V δ 2 présents dans le sang circulant d'un même donneur, menant à une population cellulaire presque pure en LT V γ 9V δ 2 (Figure 26A). Apparaît également une variabilité de la pureté en LT V γ 9V δ 2 de la population cellulaire récupérée à l'issue de cette étape d'amplification en fonction des donneurs (entre 70 et 100 % de LT V γ 9V δ 2 ; Figure 26B). Pour la suite des expériences nous avons donc choisi de ne travailler qu'avec les populations pures à plus de 90 % en LT V γ 9V δ 2, quelle que soit la molécule activatrice utilisée.

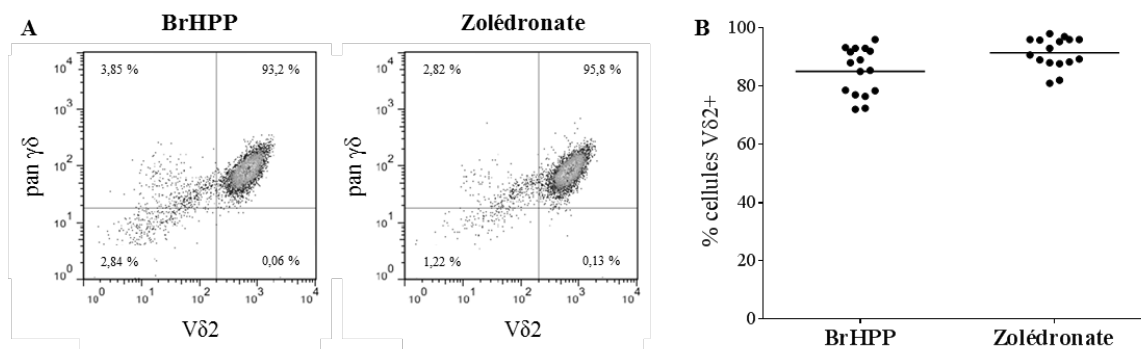


Figure 26 : Analyse de la pureté en LT V γ 9V δ 2 après amplification antigénique.

Afin d'amplifier spécifiquement les LT V γ 9V δ 2, des PBMC ont été incubés soit avec un PAg de synthèse, le BrHPP, soit avec un ABP, le Zolédronate. Après 3 semaines d'amplification, la pureté en LT V γ 9V δ 2 est vérifiée par un marquage pan $\gamma\delta$ et V δ 2. (A) Résultats représentatifs sur un donneur de PBMC après amplification soit BrHPP (*gauche*), soit Zolédronate (*droite*). (B) Compilation des résultats des tests de pureté réalisés sur 16 donneurs de PBMC.

Tout d'abord, nous avons effectué une étude du sécrétome, grâce au kit de dosage LEGENDplex (Matériel et Méthodes section 2.4), et comme précédemment, seulement trois cytokines sont détectées par le kit : l'IL-2, le TNF- α et l'IFN- γ (Figure 27). Après activation spécifique par du BrHPP, les LT V γ 9V δ 2 issus du tri négatif sécrètent de l'IL-2 (Figure 27A), du TNF- α (Figure 27B) et de l'IFN- γ (Figure 27C), ce qui concorde avec l'étude précédente, menée sur les LT $\gamma\delta$ en général (Figure 23). Il est tout de même intéressant de noter que les quantités d'IL-2 sécrétées varient peu au fur et à mesure des cycles d'amplifications (Figure 27A), alors que les quantités de TNF- α et d'IFN- γ vont plutôt en augmentant (Figure 27 B et C). Ces résultats ont été confirmés grâce à des marquages intracellulaires de l'IFN- γ , réalisés 6 heures après activation antigénique (Figure 27D).

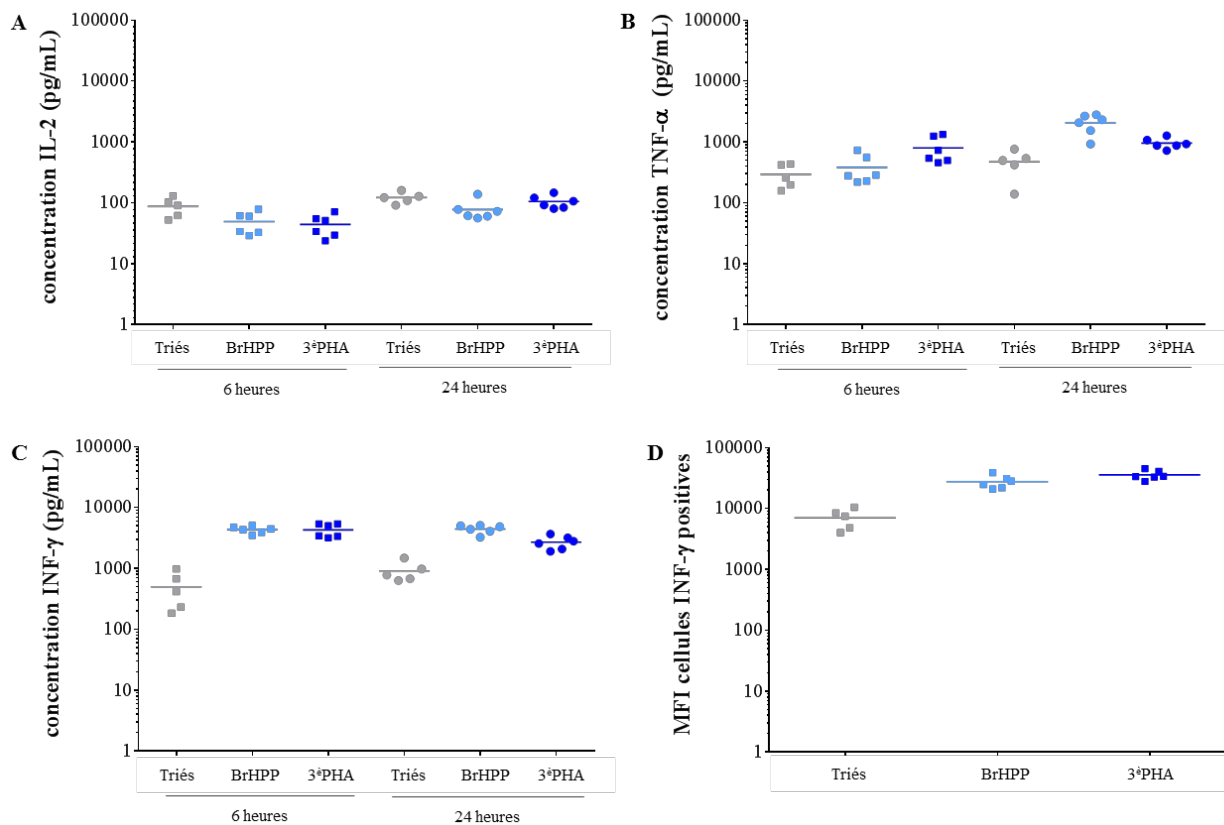


Figure 27 : Étude du sécrétome des LT V γ 9V δ 2 à différents stades d'amplification.

Un dosage de cytokines a été réalisé grâce au kit LEGENDplex Human Th Cytokine après activation spécifique (BrHPP) des LT V γ 9V δ 2 issus soit du tri négatif des LT $\gamma\delta$ (Triés), soit après amplification spécifique sur PBMC (BrHPP), soit après 3 cycles d'amplification non spécifique par PHA-feeders (3 $^{\circ}$ PHA). Seules les cytokines détectées par le kit sont présentées soit l'IL-2 (A), le TNF- α (B) et l'IFN- γ (C). (D) Des marquages intracellulaires de l'IFN- γ ont également été réalisés 6 heures après activation.

Ensuite, nous nous sommes intéressés à la réactivité de ces LT V γ 9V δ 2 face à des cellules tumorales. L'analyse de cette réactivité a été effectuée sur des cellules tumorales sensibilisées, ou non, par du Zolédronate, afin d'induire une forte réactivité des LT V γ 9V δ 2 contre elles. Comme évoqué précédemment, la réactivité naturelle des LT V γ 9V δ 2 est hétérogène face aux lignées cellulaires commerciales, mais également face à différentes primocultures (Figure 28A). Ainsi, certaines d'entre elles sont naturellement reconnues avec une réactivité des LT V γ 9V δ 2 pouvant atteindre 15 % de cellules CD107a positives. Il est également intéressant de noter que pour toutes les cellules tumorales utilisées, la sensibilisation au Zolédronate est efficace et permet d'atteindre au moins 70 % de LT V γ 9V δ 2 activés (Figure 28A). Ces conditions nous assurant une bonne réactivité de nos effecteurs, nous avons comparé la réactivité de LT V γ 9V δ 2 à différents stades d'amplification face à une lignée de cellules tumorales bien caractérisée, les RAJI (Figure 28B). Comme attendu, quel que soit le nombre de cycles d'amplification subis par les LT V γ 9V δ 2 d'un même donneur, leur réactivité face à des cellules tumorales, sensibilisées au Zolédronate, est très élevée et ne diminue légèrement qu'après 6 cycles d'amplification.

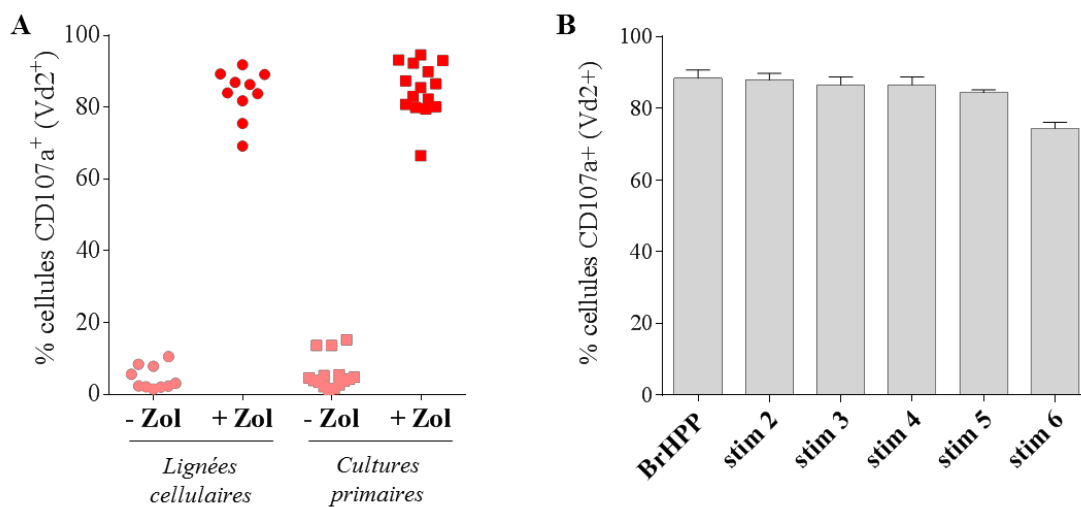


Figure 28 : Etude de la réactivité naturelle ou induite des LT V γ 9V δ 2 face à des cellules tumorales. Les LT V γ 9V δ 2 ont été cocultivés à un ratio E:T de 1:1, en présence d'un anticorps anti-CD107a, face à des cellules tumorales primaires (n=15) ou provenant de lignées commerciales (n=10). A l'issue des 4 heures de coculture, un marquage du TCR V δ 2 est réalisé et le pourcentage de cellules CD107a positives est analysé. **(A)** Analyse de la réactivité en fonction de l'origine des cellules tumorales (primaires ou lignées) et de la sensibilisation, ou non, au Zolédronate (chaque point correspond à la moyenne en cellules CD107a⁺ de 4 donneurs de LT V γ 9V δ 2). **(B)** Analyse de la réactivité en fonction du nombre de stimulations des populations de LT V γ 9V δ 2 face à la lignée tumorale RAJI (n=2-5).

Enfin, nous nous sommes intéressés à la capacité de prolifération des LT V γ 9V δ 2 au cours de ces multiples amplifications non spécifiques. Pour cela, à chaque cycle d'amplification, nous avons relevé le nombre de cellules obtenues 21 jours après stimulation PHA-feeders et calculé le nombre de divisions effectuées en fonction du nombre de cellules stimulées au départ : $\ln(\text{nombre de cellules à J0}/\text{nombre de cellules à J21})/\ln(2)$. Bien que le nombre de divisions varie en fonction des donneurs, à chaque stimulation, chaque LT V γ 9V δ 2 se divise environ 9 fois et ce jusqu'à 6 stimulations (Figure 29A). A partir et au-delà de la 7^{ème} stimulation, leur capacité de prolifération diminue fortement, associée à une augmentation de la mortalité cellulaire. Les LT V γ 9V δ 2 utilisés sont donc capables de réaliser au moins 60 divisions, la moyenne du nombre de mitoses pour un LT étant estimée entre 30 et 100 (McCarron et al., 1987; Pawelec et al., 2002). Nous avons également contrôlé la pureté en LT V γ 9V δ 2 à chaque étape de stimulation et il s'avère qu'elle ne diminue pas au fur et à mesure des cycles d'amplification (>90 % en LT V γ 9V δ 2 ; Figure 29B). Pour finir, nous avons également analysé leur profil mémoire (Figure 29C). La majorité des LT V γ 9V δ 2 présents dans le sang périphérique présente ce profil effecteur mémoire (~90 %) et après amplification, spécifique puis non spécifique, tous les LT V γ 9V δ 2 sont des effecteurs mémoire (> 95 %).

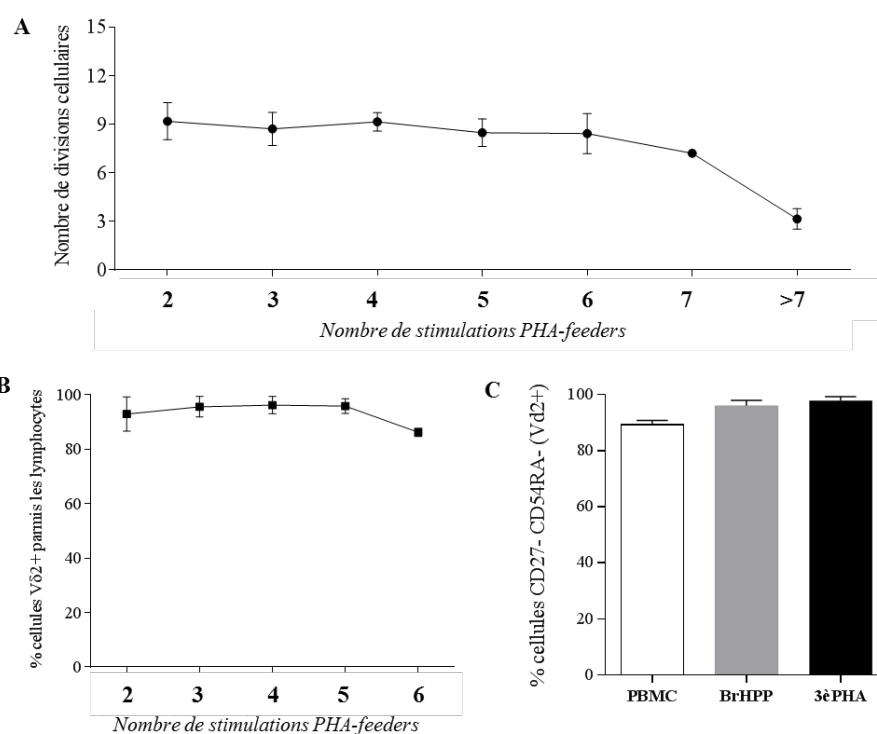


Figure 29 : Analyse de la capacité d'amplification des LT V γ 9V δ 2.

Les LT V γ 9V δ 2 ont été amplifiés de façon spécifique à partir de PBMC puis amplifiés plusieurs fois de façon non spécifique par PHA-feeders afin de déterminer le nombre de divisions qu'ils peuvent réaliser (A ; n=2-5) et de vérifier la pureté en LT V γ 9V δ 2 à chaque cycle d'amplification (B ; n=2-5) ainsi que le maintien de leur profil effecteur mémoire (C ; n=4).

5 – Encadrement de stagiaires : Résultats Annexes à la Partie 1

5.1 – Avril à Juin 2017 : Stagiaire de Master 1 Biologie Santé (Chirine RAFIA).

Les LT $\gamma\delta$ font partie des cellules jouant un rôle dans la réponse anti-tumorale mais leur présence dans le microenvironnement tumoral peut être associée à un mauvais pronostic, suggérant l'existence de sous-populations pro-tumorales ou régulatrices. Cette étude porte sur la plasticité des LT $V\gamma9V\delta2$, sous-population majoritaire dans le sang périphérique. Pour cela différentes cytokines immuno-modulatrices ont été utilisées : l'IL-10, le TGF- β , l'IL-6 et l'IL-1 β , seules ou en combinaison. Les résultats obtenus montrent de faibles modifications du profil cytokinique, l'IL-2, l'IFN- γ et le TNF- α restent les cytokines majoritaires bien que de faibles quantités d'IL-9 et d'IL-22 ait été détectées. De façon intéressante, une augmentation de la réactivité des LT $V\gamma9V\delta2$ face à des cellules tumorales a été observée.

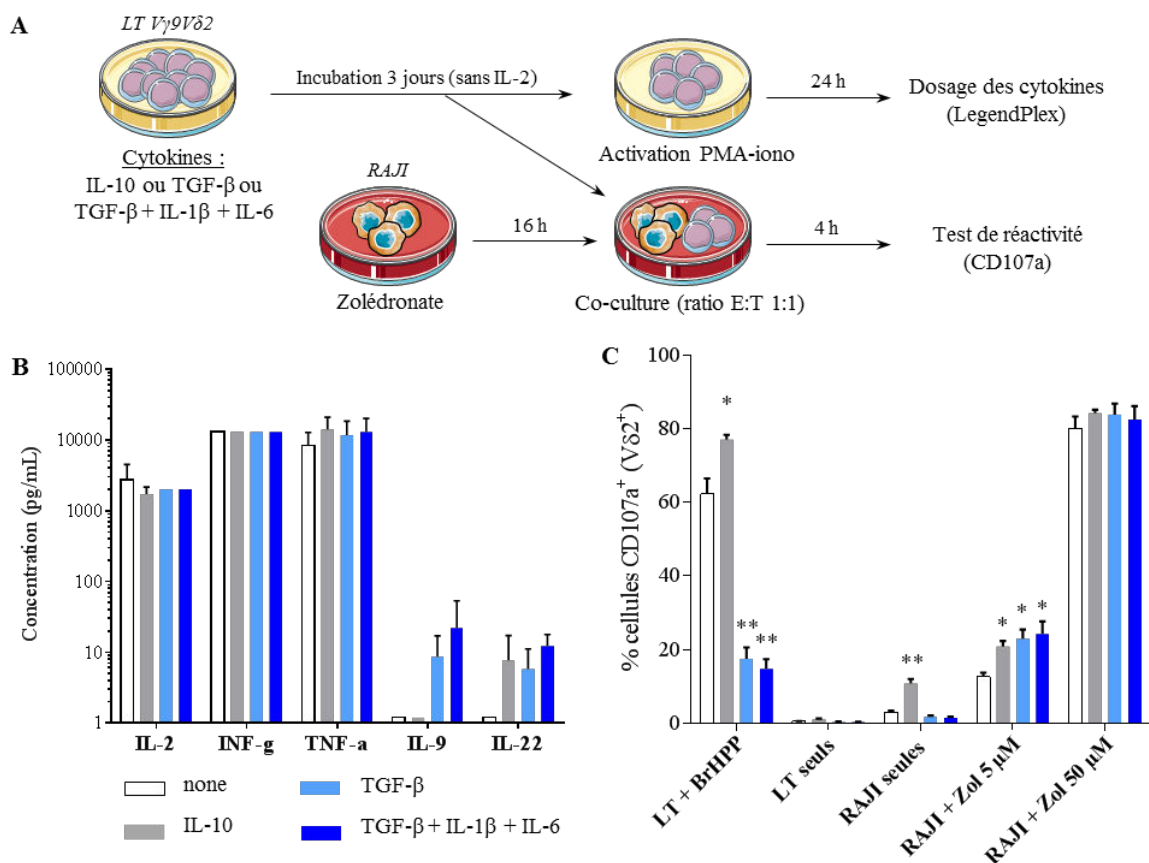


Figure 30 : Impact de cytokines immunomodulatrices sur les fonctions effectrices des LT $V\gamma9V\delta2$. (A) Description de la procédure de conditionnement et des différents test fonctionnels réalisés. Après 3 jours de conditionnement avec les différents cocktails de cytokines (et en absence d'IL-2), les LT $V\gamma9V\delta2$ sont soit (B) activés par PMA-ionomycine et un dosage des cytokines est réalisé sur les surnageants récupérés à 24 heures (moyenne \pm SD ; n=4), soit (C) cocultivés en présence de cellules tumorales de la lignée RAJI, sensibilisées ou non au Zolédrionate, afin d'évaluer leur réactivité (cellules CD107a⁺ parmi les V δ 2⁺ ; moyenne \pm SD ; n=5).

Les LT V γ 9V δ 2 présentent de puissantes fonctions effectrices et ont la capacité de reconnaître des signaux de stress émis notamment par les cellules transformées. Ainsi, la présence de LT $\gamma\delta$ au sein des tumeurs a pu être corrélée de façon tant positive que négative à une réponse clinique chez les patients. Cette dichotomie est en partie due à leur plasticité qui dépend de l'environnement cytokinique dans lequel ils se trouvent. Le but de cette étude est donc d'analyser l'impact de cytokines immunomodulatrices sur les fonctions effectrices de LT V γ 9V δ 2. Nos précédents résultats montrent que des cytokines comme l'IL-10 et le TGF- β ont un effet bénéfique sur la réactivité anti-tumorale des LT V γ 9V δ 2. De façon intéressante, nous avons remarqué que cette augmentation de la réactivité n'est pas forcément liée à une augmentation de leur cytotoxicité. De plus, ces cytokines induisent une modulation de l'expression des corécepteurs de type NKR exprimés par les LT V γ 9V δ 2.

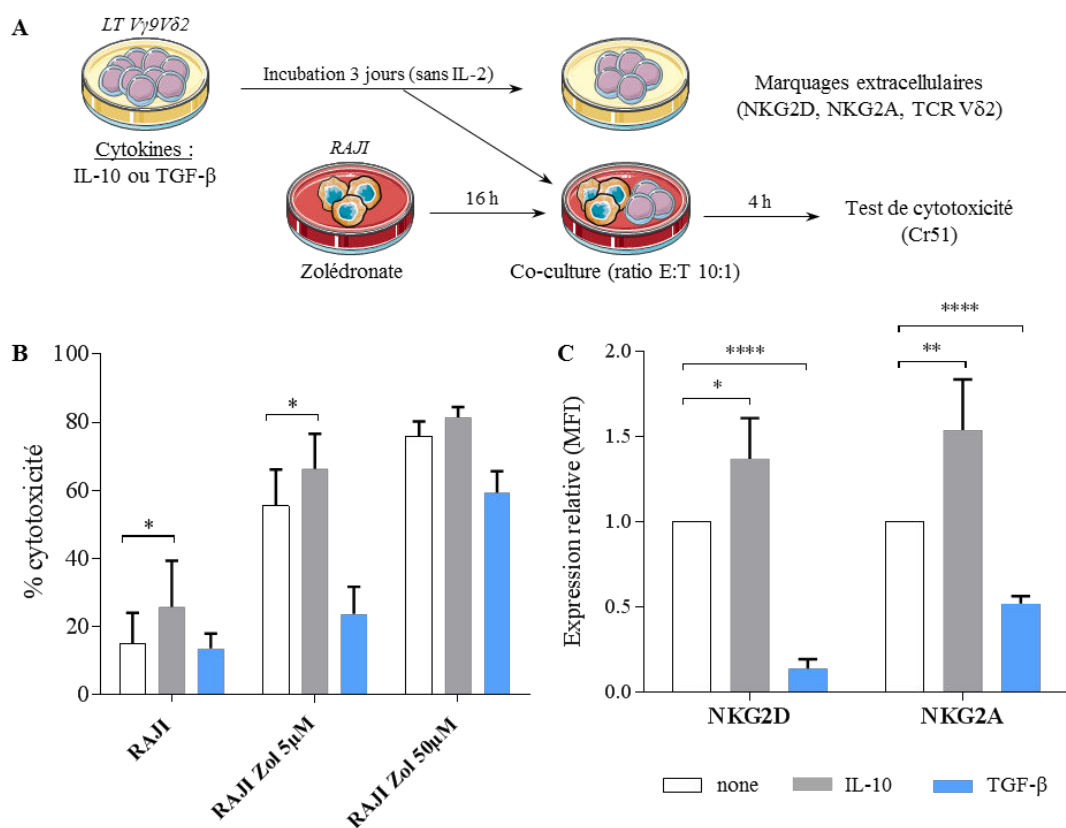


Figure 31 : Impact de cytokines immunomodulatrices sur la polarisation des LT V γ 9V δ 2.

(A) Description de la procédure de conditionnement et des différentes expériences réalisées. Après 3 jours de conditionnement avec les différentes cytokines (en absence d'IL-2), les LT V γ 9V δ 2 sont soit (B) cocultivés en présence de cellules tumorales de la lignée RAJI, sensibilisées ou non au Zolédronate, afin d'évaluer leur potentiel cytotoxique (% de cellules cibles lysées ; moyenne \pm SD ; n=4), soit (C) des marquages extracellulaires (NKG2D, NKG2A, TCR V δ 2) sont réalisés (MFI \pm SD ; n=5).

6 – Conclusion

Ce projet, financé par l'Institut National du Cancer, a fait l'objet d'une collaboration avec l'Inserm U1100 à Tours et l'Inserm U896 de Montpellier. Cette étude a porté sur l'analyse des modalités d'activation et de recrutement des LT $\gamma\delta$ au cours du développement tumoral, la caractérisation phénotypique de sous-populations de LT $\gamma\delta$ humains régulatrices/immunosuppressives au sein du microenvironnement tumoral et l'optimisation de stratégies d'immunothérapies utilisant des LT $\gamma\delta$.

Notre premier objectif a été de déterminer quelle est l'origine de sous-populations pro-tumorales ou régulatrices. Deux hypothèses ont été émises : soit il s'agit de processus de sélection thymique et/ou extra-thymique encore inconnus, soit c'est l'influence du microenvironnement immunosuppresseur qui conduit à la polarisation de ces cellules du fait de leur plasticité fonctionnelle. Pour départager ces deux hypothèses, nous avons choisi d'étudier le sécrétome des LT V γ 9V δ 2 circulants afin de déterminer si des cellules présentant un profil immunosuppresseur, via la sécrétion de cytokines, étaient présentes d'emblée dans le sang de donneurs sains. Les résultats obtenus ne donnent pas de signe évident de la présence de LT $\gamma\delta$ déjà polarisés dans le sang périphérique. Les LT V γ 9V δ 2 circulant présentent donc un profil pro-inflammatoire, ce qui est en accord avec la littérature (Dunne et al., 2010). Ces populations pro-tumorales ou régulatrices auraient donc plutôt pour origine l'influence du microenvironnement tumoral, connu pour polariser les LT effecteurs en LT régulateurs, du fait de la plasticité fonctionnelle des LT V γ 9V δ 2 (Lafont et al., 2014).

Nous avons donc poursuivi ce projet par une étude de l'impact de cytokines immunomodulatrices sur les fonctions effectrices des LT V γ 9V δ 2 au cours des stages de Master 1 puis de Master 2 de Chirine RAFIA (pages 76 et 77). Tout d'abord, nous avons sélectionné plusieurs cytokines et un cocktail cytokinique sur la base de la littérature : l'IL-10 ou le TGF- β qui sont connus pour induire une immunosuppression et/ou un profil régulateur (Li et al., 2011; Yi et al., 2013), et une combinaison de TGF- β , d'IL-1 β et d'IL-6 qui polarise les LT V γ 9V δ 2 vers un profil Th17 (Caccamo et al., 2011).

Dans un premier temps, nous avons cherché à savoir si le conditionnement de LT V γ 9V δ 2 au repos, par ces cytokines, peut modifier leur sécrétome. Bien que de faibles quantités d'IL-9 ou d'IL-22 ait été retrouvées, aucune trace d'IL-10 ou d'IL17 n'a été détectée, l'IFN- γ et de le TNF- α restant les cytokines les plus fortement produites (page 76 ; Figure 30B).

Nous avons donc cherché à savoir si ces conditionnements pouvaient affecter la réactivité des LT V γ 9V δ 2. Pour cela, nous avons utilisé la lignée cellulaire RAJI, sensibilisée ou non avec une dose maximale ou sous-optimale de Zolédronate (page 76 ; Figure 30C). Il est connu dans la littérature que l'IL-10 peut conduire à une augmentation de la réactivité des LT $\alpha\beta$ (Li et al., 2017), phénomène également observé ici sur la réactivité et la cytotoxicité des LT V γ 9V δ 2 (pages 76 et 77 ; Figure 30C et 31B).

De façon intéressante, un conditionnement des cellules au TGF- β ou avec le cocktail TGF- β , IL-1 β et IL-6, conduit également à une augmentation de la réactivité des LT V γ 9V δ 2 face aux cellules tumorales, mais induit une perte de réactivité lors de l'induction d'une lyse fratricide induite par l'ajout de BrHPP sur des LT V γ 9V δ 2 seuls. Après avoir démontré que l'effet obtenu avec le cocktail de cytokines était dû exclusivement à la présence de TGF- β , nous avons mis de côté cette condition de culture. Nous avons alors mis en évidence que l'augmentation de la réactivité observée après conditionnement au TGF- β n'était pas associée à une augmentation de la cytotoxicité (page 77 ; Figure 31B). Il s'avère que le TGF- β , contrairement à l'IL-10, induit une forte diminution des NKR exprimés par les LT V γ 9V δ 2 (page 77 ; Figure 31C), corécepteurs fortement impliqués dans la modulation de l'activation des LT V γ 9V δ 2 (Bonneville et al., 2010).

L'impact de cytokines immunomodulatrices sur la polarisation des LT $\gamma\delta$ et notamment sur celle des LT V γ 9V δ 2 fait déjà l'objet de nombreuses études (Lafont et al., 2014; Wesch et al., 2014). Bien que plusieurs équipes aient réussi à démontrer qu'il est possible de générer, *in vitro*, des LT V γ 9V δ 2 régulateurs ou pro-tumoraux, il est difficile de corrélérer ces données et les mécanismes décrits avec la réalité physiopathologique du microenvironnement tumoral. Par exemple, l'existence de LT V γ 9V δ 2 ayant un profil Th17 est fortement remise en cause car bien que l'existence de population de LT $\gamma\delta$ produisant de l'IL-17 soit bien décrite chez la souris (Patin et al., 2018), et que l'existence de LT $\gamma\delta$ produisant de l'IL-17 ait été démontrée *in vitro* (Lo Presti et al., 2016), chez l'Homme aucune preuve directe de la sécrétion de cette cytokine, par les LT V γ 9V δ 2, chez des patients atteints de cancer, n'a été fournie. La description et l'étude des mécanismes aboutissant à l'apparition de LT V γ 9V δ 2 pro-tumoraux ou régulateurs, dans le contexte physiopathologique qu'est le cancer, restent encore vastes. Ainsi, une meilleure compréhension de ces mécanismes nous permettrait non seulement de mieux appréhender le rôle des LT $\gamma\delta$ dans le microenvironnement tumoral, mais également d'anticiper les effets néfastes de cette immunosuppression sur la capacité anti-tumorale des LT V γ 9V δ 2 dans le cadre d'une immunothérapie par transfert adoptif.

Le deuxième objectif de ce projet porte sur l'optimisation des immunothérapies anti-tumorales basées sur l'utilisation de LT V γ 9V δ 2. Dans notre cas, nous nous sommes focalisés sur l'étude des fonctions effectrices des LT V γ 9V δ 2 au cours de multiples amplifications non spécifiques, atout indéniable pour la création d'une banque cellulaire de LT V γ 9V δ 2 humains allogéniques. Pour cela, nous avons mis en place un protocole permettant de réaliser de nombreuses stimulations des LT V γ 9V δ 2 d'un même donneur.

Dans un premier temps, ils sont amplifiés spécifiquement, grâce au BrHPP ou au Zolédronate, directement sur les PBMC de donneurs sains. A l'issue de cette étape, il n'est pas possible de reproduire ce protocole car il induit une lyse fratricide des LT V γ 9V δ 2. Bien qu'il soit possible d'utiliser des feeders (PBMC et B.EBV irradiés) combinés à du Zolédronate pour induire une stimulation spécifique, ce protocole n'est pas aussi efficace que la stimulation PHA-feeders, en terme de force du signal et de la quantité de cellules récupérées (résultats non montrés). Ainsi, après une première amplification antigénique, nous avons donc réalisé plusieurs amplifications non spécifiques et étudier les fonctions effectrices des LT V γ 9V δ 2 à différents moments de ce processus.

Les résultats obtenus confirment ceux obtenus précédemment quant au profil naturellement pro-inflammatoire des LT V γ 9V δ 2 et mettent également en avant le maintien de ces puissantes fonctions effectrices à long terme (Dunne et al., 2010; Vantourout and Hayday, 2013). Le nombre de divisions que les LT V γ 9V δ 2 d'un donneur sont capables de faire est un atout majeur dans le cadre de la création d'une banque cellulaire allogénique. En effet, l'objectif étant de pouvoir traiter beaucoup de patients avec des LT V γ 9V δ 2 allogéniques, la production de plusieurs milliards de cellules est donc indispensable. Non seulement cela ne posera pas de problème au vu de ces résultats, mais les LT V γ 9V δ 2 injectés seront encore capables de se diviser *in vivo*, condition indispensable pour l'obtention d'une bonne efficacité thérapeutique.

Cet aspect est d'autant plus important que lors du traitement des patients, les LT sont injectés immédiatement après décongélation. Chez les LT V γ 9V δ 2, cela a pour conséquence une diminution de leur cytotoxicité, pouvant réduire le bénéfice thérapeutique du traitement (résultats non montrés). Il est donc très important que les LT survivants soient encore capables de proliférer afin de compenser cette perte.

Le renforcement des fonctions effectrices lié aux multiples amplifications sera également un atout afin d'assurer une bonne réactivité des LT V γ 9V δ 2 *in vivo*. De plus, la forte production d'IFN- γ peut également jouer un rôle non négligeable dans la réponse thérapeutique. En effet, l'IFN- γ produit par les LT V γ 9V δ 2 leur permet de communiquer et de recruter avec d'autres effecteurs immunitaires mais peut également agir directement sur les cellules tumorales. Ainsi, en collaboration avec l'équipe de Matthias EBERL (Cardiff, Royaume-Uni), nous avons démontré que l'IFN- γ sécrété par les LT V γ 9V δ 2 après activation conduit à une augmentation de l'expression des molécules du CMH de classe I par des cellules tumorales de cancer du sein, augmentant de ce fait la réactivité et la cytotoxicité de LT CD8⁺ cytotoxiques (Chen et al., 2017) (Annexes pages 228 à 248).

Ces résultats encourageants fournissent donc de nouvelles preuves en faveur de la création et de l'utilisation d'une banque de LT V γ 9V δ 2 humains allogéniques dans le cadre d'immunothérapies anti-tumorales passives.

PARTIE 2 : Application au Cancer Epithélial de l'Ovaire

1 – Le Cancer Epithélial de l'Ovaire

1.1 – Classification des cancers de l'ovaire

Le CEO (cancer épithélial de l'ovaire) est un cancer gynécologique qui se développe aussi bien au niveau de l'ovaire que dans la cavité intra-péritonéale sous forme de nodules de carcinose (Figure 32). Le CEO est également caractérisé par la production d'un liquide inflammatoire, appelé liquide d'ascite, qui peut être très abondant dans la cavité intra-péritonéale.

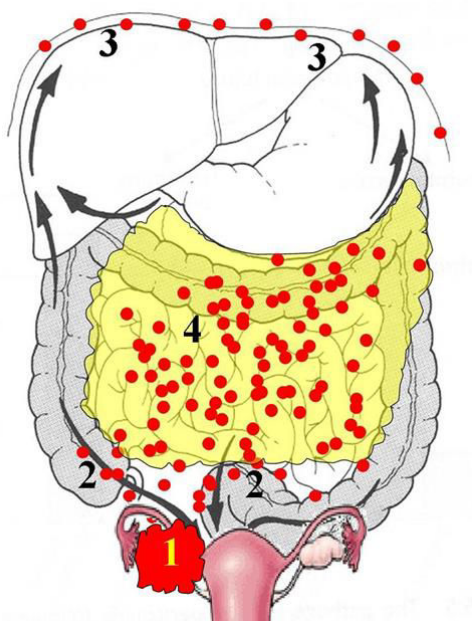


Figure 32 : Schéma représentatif de la dissémination des cellules tumorales de CEO dans le péritoine.

L'initiation du cancer se fait au niveau de l'ovaire (1) puis des cellules tumorales vont se décrocher et disséminer dans la cavité intra-péritonéale. Des métastases péritonéales peuvent être retrouvées sur les intestins (2), contre le diaphragme (3) ou couvrir la graisse abdominale liée à l'épiploon (4).

D'après <http://www.drmulier.com/2%20fr%20pat%20info%20ovarium.html>

Ainsi, plusieurs classifications ont été établies selon le stade de dissémination, par la FIGO (fédération internationale de gynécologie et obstétrique). La classification FIGO actualisée en 2014 compte 4 stades de dissémination (Prat and FIGO Committee on Gynecologic Oncology, 2015) :

- Stade I : tumeur limitée aux ovaires et aux trompes de Fallope
- Stade II : Présence de cellules tumorales dans le liquide d'ascite
- Stade III : Tumeur primaire avec extension péritonéale et/ou adénopathies métastatiques
- Stade IV : Présence de métastases hors de la cavité péritonéale

La définition du stade des CEO est également associée à une analyse histologique, réalisée sur une biopsie ou une pièce chirurgicale, qui permet de définir l'agressivité de la tumeur. Les critères histopathologiques permettent de différencier 5 sous-types de CEO : les séreux de haut grade (70 %), les séreux de bas grade (5 %), les endométrioïdes (10 %), les carcinomes à cellules claires (10 %) et les mucineux (3 %) (Prat and FIGO Committee on Gynecologic Oncology, 2015).

Un autre modèle de classification proposé permet de regrouper les CEO de bas grade sous le nom de type I (séreux de bas grade, carcinomes endométrioïdes, mucineux et à cellules claires). A l'inverse, les CEO de haut grade sont dits de type II (séreux de haut grade, carcinomes endométrioïdes de haut grade et les carcinomes indifférenciés) (Kurman and Shih, 2016).

1.2 – Epidémiologie et Etiologie

Le CEO représente aujourd'hui la 5^{ème} cause de décès par cancer chez les femmes alors qu'il ne représente que 5 % de leurs cancers (Siegel et al., 2016). Le taux de mortalité associé au CEO est bien plus élevé que celui d'autres cancers ayant une incidence plus élevée, comme le cancer du sein. En effet, il représente 23 % des cancers gynécologiques mais est responsable de la moitié des décès dans cette catégorie (Torre et al., 2018). Le mauvais pronostic associé à ce cancer est lié à son caractère asymptomatique, à son évolution indolente et à sa forte dissémination.

L'âge influence positivement l'incidence du CEO, avec un âge médian au diagnostic de 63 ans (Torre et al., 2018). Plusieurs autres facteurs peuvent également influencer positivement, ou négativement, le développement du CEO. Les principaux facteurs de risques associés à une augmentation de l'incidence du CEO sont les antécédents familiaux, l'obésité et la nulliparité. A l'inverse les facteurs de risque associés à une incidence diminuée sont la contraception orale, l'hystérectomie et/ou l'oophorectomie (Matulonis et al., 2016). L'influence de ces facteurs de risque peut varier en fonction du sous-type histologique de CEO.

1.3 – Diagnostic et Prise en charge thérapeutique

Près de 75 % des patientes sont diagnostiquées tardivement, avec un âge médian au diagnostic de 63 ans, du fait de la non spécificité des symptômes et de l'indolence du développement du CEO (Bhoola and Hoskins, 2006; Torre et al., 2018). En effet, la majorité des patientes présentent des symptômes similaires à ceux de la ménopause, tels que ballonnement, douleurs pelviennes ou abdominales et fatigue prolongée.

Actuellement, il existe un marqueur tumoral mesurable dans le sang, le CA125 (cancer antigen 125, glycoprotéine de haut poids moléculaire), qui est élevé chez les patientes atteints de CEO (Su et al., 2013). Cependant, il ne s'agit pas d'un marqueur spécifique, il est donc nécessaire d'y associer des techniques d'imagerie afin de valider le diagnostic. Dans un premier temps, un examen gynécologique et/ou une échographie peut permettre de mettre en évidence une masse tumorale. Dans tous les cas, une IRM (imagerie par résonance magnétique) sera nécessaire afin d'établir la malignité et l'étendue de la tumeur (Matulonis et al., 2016). Par la suite, une cœlioscopie permettra de confirmer l'étendue et la résecabilité de la tumeur en plus de permettre le prélèvement d'une biopsie afin de déterminer le sous-type histologique.

Dans le cas des CEO de type I, le diagnostic se fait généralement à un stade précoce du fait de leur progression lente. La tumeur est donc encore limitée à l'ovaire et la chirurgie représente le traitement de référence. Ce type de cancer est associé à un bon pronostic et suite à une résection chirurgicale complète la survie à 5 ans est supérieure à 80 % (Kurman and Shih, 2016). Cependant ils ne représentent que 10 % des CEO.

En effet, 90 % des CEO sont des cancers de type II, diagnostiqués tardivement et associés à une progression rapide et invasive (Kurman and Shih, 2016). La chirurgie reste l'élément clé de la prise en charge des patientes. Elle peut être initiale ou précédée de cures de chimiothérapies néo-adjuvantes dans le cas des tumeurs non résécables au moment du diagnostic. Dans tous les cas, une corrélation a pu être établie entre le résidu tumoral après chirurgie et la survie des patientes (du Bois et al., 2009). La chirurgie représente encore aujourd'hui un challenge thérapeutique du fait de la multiplicité des organes pouvant être atteints par la carcinose péritonéale. Afin d'augmenter la qualité de cette chirurgie un index de carcinose péritonéale a également été mis en place afin d'aider les chirurgiens à obtenir la résection la plus complète possible (Sugarbaker, 1995) (Figure 33).

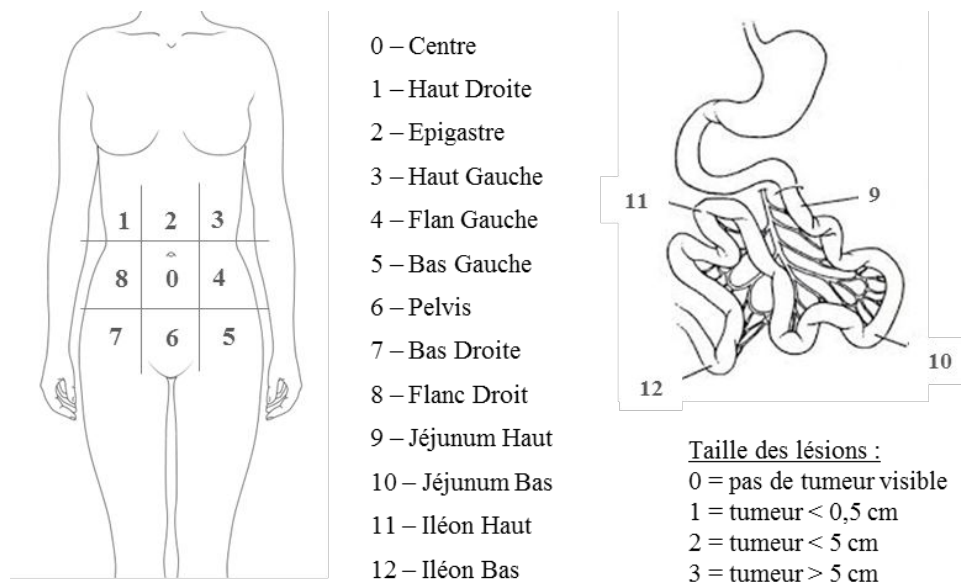


Figure 33 : Index de Carcinose Péritonéale ou score de Sugarbaker.

L'abdomen et le pelvis sont divisées en 13 zones : un cadran de 9 régions sur la cavité abdominale et 4 régions plus précises le long de l'intestin. Les chirurgiens peuvent alors indiquer pour chaque zone la taille des lésions résiduelles à la fin de l'intervention. *Adapté de Sugarbaker, 1995.*

Le traitement se poursuit par des cures de chimiothérapie administrées par voie intraveineuse et combinant deux agents chimiothérapeutiques : la Carboplatine et le Paclitaxel (Colombo et al., 2014). La Carboplatine est un sel de platine qui appartient au groupe des agents alkylant de l'ADN. Le Paclitaxel quant à lui est un alcaloïde de la famille des taxanes, agissant comme un poison du fuseau. Bien qu'environ 80 % des patientes répondent à cette chimiothérapie, 10 % sont d'emblée résistantes aux sels de platine et 30 % des patientes répondeuses acquièrent cette résistance dans les 6 mois (Colombo et al., 2014). De plus, la majorité des patientes rechutent dans les 18 mois, avec développement d'une carcinose péritonéale importante. Ainsi, et malgré l'amélioration des techniques de chirurgie et de chimiothérapie, la survie à 5 ans des patientes atteints de CEO reste d'environ 35 % (Torre et al., 2018).

La nécessité d'améliorer la prise en charge thérapeutique des patientes et notamment le besoin de traitements plus efficaces pour lutter contre la dissémination péritonéale des cellules tumorales a poussé les médecins à mettre en place de nouveaux protocoles de chimiothérapie, notamment par injection intrapéritonéale. En effet, l'administration localisée de la chimiothérapie permet à la fois de cibler de façon plus efficace les cellules tumorales et d'augmenter les concentrations de chimiothérapies (Jaaback et al., 2016). Grâce à l'existence de la barrière naturelle qu'est le péritoine, isolant la cavité abdominale de la circulation systémique, il est possible de multiplier les doses de chimiothérapie par 100.

De nombreux essais cliniques ont été menés en ce sens et ont démontré une amélioration d'environ un an de la médiane de survie et une diminution du risque de rechute d'au moins 20 % (Elit et al., 2007; Jaaback et al., 2016). Malgré ces résultats très encourageants, la chimiothérapie intrapéritonéale n'est pas encore devenue un traitement de référence en France, bien que plusieurs pays anglo-saxons l'utilisent en routine.

1.4 – Immunothérapie du cancer de l'ovaire

De nombreuses stratégies thérapeutiques, dont l'immunothérapie, ont été étudiées dans le CEO du fait de la nécessité d'une amélioration de la prise en charge des patientes. Comme beaucoup de cancers, le CEO présente un niveau élevé de VEGF qui est corrélé à la formation d'ascite. C'est donc tout naturellement que le Bevacizumab a été testé en clinique. Malheureusement, les essais de phase II réalisés n'ont pas permis d'améliorer la survie des patientes de plus de 5 mois (Colombo et al., 2016). Les checkpoint inhibitors quant à eux ont montré de meilleurs résultats. L'ipilimumab (anti-CTLA-4) et le pembrolizumab (anti-PD1) présentent des résultats similaires, avec environ 20 % de rémission partielle supérieure à 36 mois (Krishnan et al., 2017). Cependant, chez la majorité des patientes, ces traitements restent peu ou pas efficaces.

Plusieurs essais cliniques basés sur le transfert adoptif d'effecteurs cytotoxiques ont également été réalisés. Notamment, deux études basées sur l'injection intra-péritonéale de LT CD8⁺ autologues afin de cibler au mieux les cellules tumorales disséminées dans la cavité péritonéale (Aoki et al., 1991; Fujita et al., 1995). Ces deux études ont été menées chez des patientes ayant eu une résection chirurgicale sans tumeur résiduelle visible macroscopiquement. Après chimiothérapie, des TIL récupérés au moment de la chirurgie et amplifiés *ex vivo* en présence d'IL-2 ont été réinjectés. Bien que réalisés sur un nombre restreint de patientes (une dizaine), ces deux essais cliniques ont mis en évidence une survie sans maladie à trois ans de 56 % et 82 %, respectivement (Aoki et al., 1991; Fujita et al., 1995).

2 - Article 1: Combined chemotherapy and allogeneic human V γ 9V δ 2 T lymphocyte-immunotherapy efficiently control the development of human epithelial ovarian cancer cells *in vivo*

Noémie Joalland^{1,2}, Laura Lafrance^{1,2}, Thibault Oullier³, Séverine Marionneau-Lambot³, Delphine Loussouarn⁴, Ulrich Jarry^{1,2,†} and Emmanuel Scotet^{1,2,†}

¹ CRCINA, INSERM, CNRS, Université d'Angers, Université de Nantes, Nantes, France

² LabEx IGO “Immunotherapy, Graft, Oncology”, Nantes, F-44000, France

³ Cancéropôle du Grand Ouest, Plateforme In Vivo, 44000 Nantes, France

⁴ Centre Hospitalier-Universitaire (CHU) de Nantes, Nantes, France

† co-senior authors

Le but de cette étude a été de mettre en place un modèle préclinique de CEO le plus représentatif possible de la pathologie humaine afin d’y évaluer l’efficacité d’un traitement basé sur le transfert adoptif de LT V γ 9V δ 2 humains allogéniques. Dans un premier temps, nous avons tenté de mettre en place un modèle reposant sur l’implantation en orthotopique de primocultures de CEO (fournies par le Centre de Ressources Biologique de Rennes, sous la direction de Véronique CATROS). Malheureusement, la croissance de ces cellules tumorales primaires s’est avérée beaucoup trop lente. Nous avons donc mis en place un modèle murin par xélogreffe orthotopique de cellules tumorales, issues d’une lignée cellulaire (SKOV-3), transformées pour exprimer la luciférase, nous permettant de réaliser de manière non invasive un suivi de la croissance et de la dissémination des cellules tumorales *in vivo*. Afin d’être le plus représentatif de la pathologie humaine, ce modèle comprend également une étape de résection chirurgicale incluant une ovariectomie et un traitement par chimiothérapie (Carboplatine et Paclitaxel). Ainsi ce modèle récapitule à la fois le traitement standard des patientes et la rechute liée au développement d’une carcinose péritonéale. Au travers une série d’expérience *in vitro* et *in vivo* nous avons également déterminé les meilleures conditions d’association de la chimiothérapie (Carboplatine et Paclitaxel) et de l’immunothérapie (LT V γ 9V δ 2 et Zolédronate) permettant d’obtenir une efficacité thérapeutique dans notre modèle préclinique. Les résultats obtenus *in vivo* sont très encourageants et fournissent une preuve de concept de l’efficacité thérapeutique de cette nouvelle ligne d’immunothérapie, basée sur l’injection locale de LT V γ 9V δ 2 allogéniques, combinée aux traitements standards.

Soumis

Combined chemotherapy and allogeneic human V γ 9V δ 2 T lymphocyte-immunotherapies efficiently control the development of human epithelial ovarian cancer cells *in vivo*

Noémie Joalland^{1,2}, Laura Lafrance^{1,2}, Thibault Oullier³, Séverine Marionneau-Lambot³, Delphine Loussouarn^{1,4}, Ulrich Jarry^{1,2,†} and Emmanuel Scotet^{1,2,†}

¹ CRCINA, INSERM, CNRS, Université d'Angers, Université de Nantes, Nantes, France

² LabEx IGO “Immunotherapy, Graft, Oncology”, Nantes, F-44000, France

³ Cancéropôle du Grand Ouest, Plateforme In Vivo, 44000 Nantes, France

⁴ Centre Hospitalier-Universitaire (CHU) de Nantes, Nantes, France

† co-senior authors

Running title: Chemo-Immunotherapies control human epithelial ovarian tumors

Correspondence: E. Scotet, INSERM UMR1232, Centre de Recherche en Cancérologie et Immunologie Nantes-Angers, IRS_UN, 8 quai Moncousu, 44007 Nantes cedex 1, France. Emmanuel.Scotet@inserm.fr

Keywords: Human V γ 9V δ 2 T lymphocytes, Zoledronate, Chemotherapy, Immunotherapy, Epithelial Ovarian Cancer, Orthotopic Xenograft Mouse Model

Funding: *This work was supported by INSERM, CNRS, Université de Nantes, Association pour la Recherche contre le Cancer (R10139NN), Institut National du Cancer (INCa, PLBio2013-201, PLBio2014-155), Ligue Nationale contre le Cancer (AO InterRegional 2012). This work was realized in the context of the LabEX IGO and the IHU-Cesti programs, supported by the National Research Agency Investissements d'Avenir via the programs ANR-11-LABX-0016-01 and ANR-10-IBHU-005, respectively. The IHU-Cesti project is also supported by Nantes Metropole and the Pays de la Loire Region.*

Conflicts of Interest: The authors disclose no potential conflicts of interest

Abbreviations: EOC, epithelial ovarian cancer; $\gamma\delta$ T cells, gamma delta T cells; PAg, phosphoantigen; NBP, aminobisphosphonate; NSG, *NOD.Cg-Prkdcscid Il2rgtm1Wjl/SzJ*.

Abstract

Epithelial ovarian cancer (EOC), which represents 5% of human gynecologic cancers in the world, is heterogeneous and highly invasive, with a dismal prognosis (5 year-survival rate <35%). Diagnosis of EOC is frequently made at advanced stages and, despite aggressive treatments combining surgery and chemotherapy, fatal relapse rapidly occurs and is accompanied by a peritoneal carcinosis. In this context, novel therapeutical advances are urgently required. Adoptive transfer(s) of immune effector cells, including allogeneic human V γ 9V δ 2 T lymphocytes, represent attractive targets for efficiently and safely tracking tissue-invasive tumor cells and controlling tumor dissemination in the organism. Our study describes the establishment of robust and physiological orthotopic model of human EOC in mouse, that includes surgical resection (ovariectomy) and chemotherapy, which are ineluctably accompanied by a fatal peritoneal carcinosis recurrence. Through a complementary set of *in vitro* and *in vivo* experiments, we provide here a preclinical proof of interest for the antitumor efficiency of adoptive transfers of allogeneic human V γ 9V δ 2 T lymphocytes against EOC, in association with surgical debulking and standard chemotherapies (ie, taxanes and platinum salts). Moreover, our results indicate that chemo- and immunotherapies can be combined to improve the antitumor efficiency of immunotherapeutic lines. Altogether, these results further pave the way for next-generation antitumor immunotherapies, based on local administrations of human allogeneic human V γ 9V δ 2 T lymphocytes, in association with standard treatments.

Introduction

Ovarian cancer represents the seventh most common cancer in women worldwide. Epithelial ovarian cancer (EOC) accounts for >95% of the ovarian malignancies and is the leading cause of gynecologic cancer deaths with a 5-year survival of 35% (Siegel et al., 2016; Torre et al., 2018). The absence of symptoms at early stages is a major problem implying that most patients are diagnosed with an advanced-stage disease. Despite surgical debulking and initial response to chemotherapy mostly based on platinum salts (eg., Carboplatin) and antimetabolic agents (eg., Paclitaxel), the majority of EOC recurs. This fatal evolution is principally accompanied by the development of chemoresistance and peritoneal carcinosis (Colombo et al., 2014). As this first indicates that more efficient and less toxic therapeutic approaches are urgently required, this also evidences the main location of resistant tumor EOC cells within the peritoneal cavity therefore representing a unique opportunity for targeting and eliminating them by local administrations of selected immune effectors (Ventriglia et al., 2017). This unique therapeutic opportunity is further supported by the results of studies that reported the feasibility and the clinical benefits of intraperitoneal adoptive transfers of lymphocytes (eg, tumor-infiltrative T and Natural Killer (NK) lymphocytes) (see Mittica et al., 2016 for a review). Importantly, they suggested that their clinical efficacy could be enhanced by optimizing associations and positioning with standard therapeutic lines (eg, maintenance).

Non-conventional V γ 9V δ 2 T lymphocytes are almost exclusively present in primates and represent the most frequent peripheral $\gamma\delta$ T lymphocyte subset in adults (80% of $\gamma\delta$ T lymphocytes). They express a TCR composed of V δ 2 chains which are predominantly paired to V γ 9 chains (Hayday, 2000). Importantly, the antigenic activation of V γ 9V δ 2 T lymphocytes is both species-specific and contact-dependent, but is not restricted by MHC molecules, which limits the emergence of deleterious alloreactivities (Chien et al., 2014). The strong and specific antigenic activation of V γ 9V δ 2 T lymphocytes is induced by low molecular weight phosphorylated non-peptidic molecules, hereafter called phosphoantigens (PAg), that are metabolic intermediates of the endogenous mevalonate pathway (eg, IPP, isopentenyl pyrophosphate). Interestingly, cells with elevated pinocytic activity (ie, tumor cells), following sensitization with aminobiphosphonate (NBP) compounds (eg, zoledronate), which are pharmacologic inhibitors blocking the mevalonate pathway downstream of the PAg synthesis, activate V γ 9V δ 2 T lymphocytes through upregulated levels of endogenous PAg. This antigenic activation process is tightly regulated by adhesion molecules and NK receptors

axes (Thedrez et al., 2007) and controlled by target cell-expressed butyrophilins BTN3A molecules (Harly et al., 2012, 2014). Several studies have now reported that allogeneic human V γ 9V δ 2 T lymphocytes detect and kill a broad range of transformed target cells, with a dysregulated mevalonate pathway, from various tissular origins *in vitro*, including cells from human ovarian tumors (Lai et al., 2012; Lavoué et al., 2012). We have recently shown that locally administrated allogeneic human V γ 9V δ 2 T lymphocytes patrol for several days and efficiently eliminate human glioblastoma tumor cells infiltrated within the brain *in vivo* (Jarry et al., 2016).

Although passive and active human $\gamma\delta$ T lymphocyte-immunotherapies has yielded promising safety and antitumor efficiency results (Fournié et al., 2013), the preclinical analysis of some of these parameters in EOC, in association with standard therapies, represents a necessary stage. This study first aimed at establishing an orthotopic xenograft model of human EOC with the injection of ovarian tumor cells, followed by a tumor resection by surgery and intraperitoneal chemotherapy, in order to recapitulate human EOC disease and standard treatments *in vivo*. Using this model and *ex vivo* analysis, we next showed the antitumor efficiency of intraperitoneal transfers of allogeneic human $\gamma\delta$ T lymphocytes, in combination, before or after, with standard chemotherapy. Together, our observations further pave the way for next-generation antitumor immunotherapies, based on local administrations of human allogeneic human V γ 9V δ 2 T lymphocytes, in association with standard treatments.

Materials and Methods

Human tumor cells and V γ 9V δ 2 T lymphocytes

Human EOC cells from SKOV-3 (SKOV-3-luc-D3, Perkin Elmer, Waltham, MA, USA) and SHIN-3-luc cell lines (kindly provided by M. Cherel, CRCINA Nantes France) were cultured in Dulbecco's Modified Eagle's Medium (DMEM, Gibco, Carlsbad, CA, USA) supplemented with 10% heat-inactivated fetal calf serum (Gibco), 2 mM L-glutamine (Gibco), 10 mg/mL streptomycin (Gibco), 100 IU/mL penicillin (Gibco). Human primary cells were derived from EOC patients (CRB Santé, CHU de Rennes, France) and originated from either primary solid tumor (CKT), carcinomatosis (CKC), or ascites (CASC). These cells were cultured in Roswell Park Memorial Institute medium (RPMI, Gibco) supplemented with 10% heat-inactivated fetal calf serum, 2 mM L-glutamine, 10 mg/mL streptomycin, 100 IU/mL penicillin, 1 mM Sodium Pyruvate (all from Gibco) and 10 mM HEPES Buffer (Sigma Aldrich, Saint-Louis, MO, USA).

Allogeneic human V γ 9V δ 2 T lymphocytes were amplified from peripheral blood mononuclear cells (PBMC) obtained from healthy donor blood samples provided by the Etablissement Français du Sang (EFS, Nantes, France) and after Ficoll density centrifugation (Eurobio, Les Ulis, France). For specific expansions of peripheral allogeneic human V γ 9V δ 2 T lymphocytes, PBMC were incubated with 3 μ M of bromohydrin pyrophosphate (BrHPP), kindly provided by Innate Pharma (Marseille, France) in RPMI medium supplemented with 10% heat-inactivated fetal calf serum, 2 mM L-glutamine, 10 mg/mL streptomycin, 100 IU/mL penicillin, and 100 IU/mL human recombinant IL-2 (Proleukin, Novartis, Basel, Switzerland). After 4 days, cell cultures were supplemented with 300 IU/mL IL-2. At day 21, the purity of cultures was checked by flow cytometry. These pure (purity > 90%) human V γ 9V δ 2 T lymphocyte preparations were non-specifically expanded using mixed feeder cells, composed of 35 Gy-irradiated Epstein-Barr Virus-transformed human B lymphocytes and PBMC, and PHA-L in RPMI medium supplemented with 10% heat-inactivated fetal calf serum, 2 mM L-glutamine, 10 mg/mL streptomycin, 100 IU/mL penicillin, and 300 IU/mL recombinant human IL-2. After three weeks of culture, resting *ex vivo* expanded-V γ 9V δ 2 T lymphocytes were used for *in vitro* and *in vivo* assays. Tumor cells and $\gamma\delta$ T lymphocytes were cultured at 37°C in humidified atmosphere with 5% CO₂.

Flow cytometry

Human V γ 9V δ 2 T lymphocytes were stained with FITC-labelled anti-human TCR V δ 2 mAb (#IMMU389, Beckman Coulter, Brea, CA, USA) and APC-labelled anti-human CD3 ϵ mAb (#UCHT1, Beckman Coulter), to assess for the purity of the populations. SKOV-3 cells were incubated with FcR blocking reagent (Miltenyi, Bergisch Gladbach, Germany) and surface stained with either APC-labelled anti-human CD54 mAb (#HA58, BD Biosciences, Franklin Lakes, NJ, USA), PE-labelled anti-human CD44 mAb (#BJ18, Biolegend, San Diego, CA, USA) or anti-human CD166 (#3A6, BD Biosciences) followed by secondary staining with AlexaFluor 647-labelled anti-mouse IgG Ab (A21235, Life Technologies, Carlsbad, CA, USA). Acquisition was performed using an Accuri C6 PLUS flow cytometer (BD Biosciences) and the collected events were analyzed using the FlowJo software (Treestar, Ashland, OR, USA).

***in vitro* functional assays**

For CD107a surface mobilization assay, primary EOC cells or cell lines were sensitized, or not, with 50 μ M of zoledronic acid (Sigma Aldrich) overnight before incubation with allogeneic human V γ 9V δ 2 T lymphocytes (effector to target ratio 1:1). The coculture was performed in RPMI medium containing 5 μ M monensine (Sigma) and AlexaFluor 647-labelled anti-human CD107a mAb (#H4A3, Biolegend). After 4 hours, human V γ 9V δ 2 T lymphocytes were collected and stained with a FITC-labelled anti-human TCR V δ 2 mAb (#IMMU389, Beckman Coulter) and analyzed by flow cytometry.

For cytolytic assays, EOC tumor cells, previously treated with zoledronate overnight, were incubated with ^{51}Cr (75 $\mu\text{Ci}/10^6$ cells) for 1 hour. After washes, cells were cocultured with human V γ 9V δ 2 T lymphocytes (10:1) for 4 hours. ^{51}Cr release activity was measured in supernatants using a MicroBeta counter (Perkin Elmer). Percentage of target cell lysis = (experimental release – spontaneous release)/(maximum release – spontaneous release) x 100. Spontaneous release and maximum release were determined by adding, respectively, medium or 1% Triton X-100 to ^{51}Cr -labelled target cells in absence of human V γ 9V δ 2 T lymphocytes.

Tumor cell- $\gamma\delta$ T lymphocyte conjugates

Tumor SKOV-3 cells were stained with Zombie GreenTM Fixable Viability kit (Biolegend), diluted at 1:100 in phosphate buffer saline (PBS). Human V γ 9V δ 2 T lymphocytes were stained with an APC-labelled anti-human TCR V δ 2 mAb (#B6, Biolegend) for 20 minutes. After washes, SKOV-3 cells and V γ 9V δ 2 T lymphocytes were cocultured (1:1) in PBS in round-bottom polystyrene tubes at 37°C for 30 minutes. Cells were gently resuspended before analysis by flow cytometry.

Immunodeficient mice

Immunodeficient NSG (*NOD.Cg-Prkdcscid Il2rgtm1Wjl/SzJ*) female mice were obtained from Charles River Laboratories (Wilmington, MA, USA), bred in the animal facility of the Université de Nantes (UTE, SFR F. Bonamy Nantes, France) under SPF status and used at 8-12 weeks of age. This study was carried out in accordance with the recommendations of the French Regional Ethics Committee of the Pays de la Loire, France (*Approvements #2168 and #10746*).

Orthotopic xenograft model of EOC

For human EOC cells orthotopic implantation, NSG mice received 0,15 μ g/g buprenorphine by subcutaneous injection 15 minutes before being anesthetized with isoflurane 2%. Skin was disinfected using povidone-iodine 5% (eg, Vetidine) and a 5 mm incision was made, on the left flank, parallel to the spine, between the last rib and the iliac crest. Muscle and peritoneum were also incised before exteriorizing the left ovary by carefully pulling the fat attached to this organ using atraumatic forceps. Tumor cells suspended in PBS were injected directly into the ovary, using a NanoFil syringe (WPI, Sarasota, FL). After repositioning the ovary, muscles and skin were closed with Vicryl 4-0 (Ethicon, Somerville, NJ). Local analgesia was enhanced by application of lidocaine gel 2 % (Xylocaine, Astrazeneca, Cambridge, UK) on the scar. Mice stayed in a warm environment until full recovery and received 0,15 μ g/g buprenorphine twice a day for 48 hours after surgery. For ovariectomy and tumor resection, anesthesia and analgesia were carried out in the same manner as described above. Skin, muscles and peritoneum were incised on the scar. Next the left ovary and uterine horn were exposed and clamped close to the bottom of the uterine horn. A single ligature was placed around the uterine horn and blood vessels before being cut just above the clamp and the ligature.

Any visible tumor cells were also removed from the peritoneum or the adipose tissue. Peritoneum, muscles and skin were closed using Vicryl 4-0 before apply analgesia as previously described. Surgery was performed under sterile conditions and mice were placed on heating pad to maintain body temperature.

***in vivo* activation assays**

$5 \cdot 10^5$ SKOV-3 cells were intraperitoneally injected in NSG mice and five days later, $1 \cdot 10^7$ of human V γ 9V δ 2 T lymphocytes were injected, with or without 20 μ g zoledronate (Zometa, Novartis), following the same route. The next day, mice were euthanized and a peritoneal wash was performed using 5 mL PBS. Collected cells were stained with AlexaFluor 647-labelled anti-human CD69 mAb (#FN50, Biolegend) and FITC-labelled anti-human TCR V δ 2 mAb and analyzed by flow cytometry.

Bioluminescence imaging

Following orthotopic implantation of SKOV-3 luc cells, the development of ovarian tumors and peritoneal carcinosis were monitored by bioluminescence assays once a week. Mice were intraperitoneally injected with 1.5 mg of D-luciferin (Interchim, San Diego, CA), 8 minutes before anesthesia with isoflurane 2% and optical imaging with Biospace Imager (Biospace Lab, Nesles-la-Vallée, France). In some case, after euthanasia, imaging of whole body, opened peritoneum and separated organs was performed.

Chemotherapy and immunotherapy

Paclitaxel (6 mg/mL, Fresenius Kabi, Bad Homburg vor der Höhe, Germany) and Carboplatin (10 mg/mL, Fresenius Kabi) as pharmacological chemotherapeutic drugs. Chemotherapies were intraperitoneally injected and used at the maximum tolerable dosage (MTD) concentrations for NSG mice: 15 mg/kg Paclitaxel and 12 mg/kg Carboplatin after tumor resection (Helland et al., 2014). For *in vitro* experiments, Paclitaxel was used at 300 μ g/mL and Carboplatin was used at 375 μ g/mL, which corresponds to the chemotherapy concentration used *in vivo*. In this study, the immunotherapy tested is based on intraperitoneal injections of $2 \cdot 10^7$ human allogeneic V γ 9V δ 2 T cells and 20 μ g zoledronate (Zometa).

Immunohistochemistry analysis

Resected ovaries or carcinosis tumors were collected from xenografted mice, fixed with 4% paraformaldehyde (PFA)-PBS, embedded in paraffin wax and serially sectioned. Sections were incubated with 2% bovine serum albumin (BSA) and then with polyclonal rabbit anti-human MHC class I Ab (clone EPR1394Y, Abcam, Cambridge, UK). Revelation was performed by using polymer histofine rabbit to mouse coupled to HRP (Microm Microtech France, Francheville, France) and a DAB detection system (Leica, Wetzlar, Germany). Slides were scanned using the NanoZoomer 2.0 HT (Hamamatsu Photonics K.K., Hamamatsu, Japan).

Statistical Analysis

Data are expressed as mean \pm SD and were analyzed using GraphPad Prism 6.0 software (GraphPad Software, Inc., San Diego, CA). Two-way ANOVA and Mann & Withney or log rank tests (see indicated *p* value) were used to reveal significant differences.

Results

Establishment of a preclinical orthotopic human EOC model in mouse

Owing to the species-restricted reactivity of V γ 9V δ 2 T lymphocytes and the lack of natural counterparts in rodents, our study first aimed at designing a preclinical model of human EOC xenografts *in vivo* allowing assessment of combined conventional therapies and adoptive transfers of allogeneic human V γ 9V δ 2 T lymphocytes. By lacking a large range of immune cells, including lymphocytes and NK cells, NSG mice represented a relevant recipient mouse strain that support a better engraftment of cells of human origin as compared to other immunocompromised mice. To select the most relevant model, EOC tumor cells should be recognized by allogeneic human V γ 9V δ 2 T lymphocytes (naturally or after NBP treatment) and their orthotopic implantation should lead to a discernible solid tumor by bioluminescence. Moreover, after primary tumor resection a fatal recurrence of the disease should take place through a typical peritoneal carcinosis.

First, the reactivity of allogeneic V γ 9V δ 2 T lymphocytes against EOC cells from ovarian cancer patients (pEOC; n=10 patients) and commercial cell lines (cEOC; SKOV-3, SHIN-3), sensitized or not with zoledronate, was analyzed. While V γ 9V δ 2 T lymphocytes poorly naturally react against tumor cells from pEOC and cEOC, zoledronate sensitization induced a strong reactivity of V γ 9V δ 2 T lymphocytes, whatever the tumor origin (CKT, CKC, CASC) (**Figure 1A**). Next, pEOC and cEOC tumor cells were injected in the ovary of immunodeficient NSG mice (**Figure 1B**). In the pEOC conditions, no disease symptoms (eg, weight loss, production of ascite) were detected up to six months after implantation. Immunohistochemistry and necropsy analysis, by showing weak tumors, confirmed these biological observations and did not reveal any sign of peritoneal carcinosis formation (**Figure 1C**).

In contrast, three weeks after orthotopic injection of cEOC (20.10³ SKOV-3 cells injected in the ovary of female mice), discernable tumor developed around the injected ovary (**Figure 2A**; *picture 1*). At this timepoint, tumor resection, with ovariectomy, was performed to mimic surgery of patients (**Figure 2A**; *picture 2*). One week after ovariectomy, residual tumor cells were detected only on surgical site (**Figure 2A**; *picture 3*). Importantly, an extended peritoneal carcinosis was detected 45 days after ovariectomy (**Figure 2A**; *pictures 4&5*) accompanied by invasion of lungs and all peritoneal organs, which recapitulates human

disease recurrence (**Figure 2A**; pictures 6-10). Chemotherapies (Carboplatin and Paclitaxel) were intraperitoneally delivered, at recommended MTD for NSG mice (15 mg/kg Paclitaxel and 12 mg/kg Carboplatin) (Helland et al., 2014). Bioluminescence monitoring analysis showed a significant decrease of peritoneal carcinosis, 45 days after tumor resection (**Figure 2B**). Compared analysis of survival rates between treated and untreated mice confirmed this observation (66 vs 50 days, respectively) (**Figure 2C**). Of note, similar results were obtained using tumor cells from either SKOV-3 or SHIN-3 lines (data not shown). Moreover, anatomopathology analysis (p53 and WT1 staining) performed on resected ovary and peritoneal carcinosis tumors indicated the presence of high grade serous carcinoma tumors (**Supp Figure S1**).

Collectively, these results show the establishment of a relevant preclinical physiological model of human EOC in mouse. They evidence that: (i) human EOC tumor cells, originating from patients and cell lines, activate allogeneic human V γ 9V δ 2 T lymphocytes only upon NBP sensitization, (ii) EOC cells from lines (ie, SKOV-3), but not from patients, display growth kinetics and peritoneal tumor cell dissemination criteria that are compatible with establishment of preclinical orthotopic EOC xenograft models in mouse, (iii) as it is the case for patients, the combination of resection surgery and chemotherapy lines improves survival of EOC mice.

Zoledronate sensitizes EOC tumor cells in vivo

Following establishment of a physiological preclinical human EOC model, our study focused on *in vivo* reactivity of allogeneic V γ 9V δ 2 T lymphocytes against tumor cells, which is a key prerequisite for the efficiency of immunotherapeutic approaches. In line with our last results, allogeneic human V γ 9V δ 2 T lymphocytes not only recognized (CD107a) but also killed (^{51}Cr release) SKOV-3 tumor cells, in a NBP dose-dependent manner (**Figure 3A**). One day following intraperitoneal injection (lymphocytes +/- NBP) in SKOV-3 tumor bearing mice, expression levels of CD69, an activation marker, were analyzed and compared on allogeneic V γ 9V δ 2 T lymphocytes. As shown in **Figures 3B and 3C**, independent experiments (n=5) showed that NBP represent key pharmacological compounds to efficiently and in a dose-dependent manner, sensitize EOC tumor cells to recognition by allogeneic human V γ 9V δ 2 T lymphocytes *in vivo*.

The reactivity of V γ 9V δ 2 T lymphocytes against EOC cells can be affected by chemotherapy

Our study next aimed at defining ideal time windows for V γ 9V δ 2 immunotherapies, related to standard platinum salts- and taxanes-based chemotherapies and their relationships. SKOV-3 tumor cells treated with chemotherapeutic agents, alone or in combination, and sensitized with zoledronate were co-cultured with V γ 9V δ 2 T lymphocytes. EOC tumor cells are only recognized upon NBP sensitization and chemotherapies did not induce any cell stress-related reactivity (**Figure 4A**). Interestingly, NBP-induced reactivity was significantly reduced in the presence of Paclitaxel, but not Carboplatin, and only under suboptimal NBP-sensitization (**Figure 4B**), as maximal NBP-sensitization reverse side effects of Paclitaxel on V γ 9V δ 2 T lymphocytes reactivity (**Figure 4C**). Previous studies indicated that some antimitotic agents, such as paclitaxel, reduce the expression of adhesion molecules and consequently can affect the overall anti-tumor reactivity of effector immune cells (Loubani and Hoskin, 2005). Conjugate formation assays confirmed that Paclitaxel, alone or in combination with Carboplatin, decreased cellular interactions between allogeneic human V γ 9V δ 2 T cells and EOC tumor cells (**Figure 4D ; Supp Figure S2A**). CD54 is important adhesion molecule expressed by the SKOV-3 cells but his low expression was not affected by chemotherapeutic agents (**Figure 4E**, left). Interestingly, expression of CD166 and CD44, other important cell adhesion molecules (**Supp Figure S2B**) (Kato et al., 2006), are strongly decreased after Paclitaxel treatment, alone or in combination with Carboplatin (**Figure 4E**, middle and right). Together, these results indicate that: (i) standard Paclitaxel-based chemotherapies, alone or in combination, hamper the antitumor reactivity of allogeneic human V γ 9V δ 2 T lymphocyte effectors by reducing cellular interactions, via a decreased expression of some adhesion molecules, such as CD44 or CD166, (ii) V γ 9V δ 2 immunotherapies should not be delivered simultaneously, or immediately after, Paclitaxel-based chemotherapy treatment.

Adoptive transfers of allogeneic human V γ 9V δ 2 T lymphocytes, combined to surgery and chemotherapy, enhance the survival of EOC mice

Finally, based on the results of these complementary experiments, our study aimed at assessing the impact of combined standard therapies and immunotherapies *in vivo*. As above described, our preclinical model relied on development of primary EOC tumors following intra-ovarian injection of tumor cell. After three weeks, tumor resection by surgery

(ovariectomy) was performed and chemotherapy was delivered by intraperitoneal injections of Carboplatin and Paclitaxel (**Figure 5A**). Immunotherapy lines were based on intraperitoneal simultaneous injections of NBP (zoledronate), to sensitize EOC tumor cells, and allogeneic human *ex vivo*-amplified V γ 9V δ 2 T lymphocytes. Due to the interferences of Paclitaxel on the antitumor reactivity of V γ 9V δ 2 T lymphocytes, these therapies could not be simultaneously delivered. V γ 9V δ 2 T lymphocytes and NBP were delivered before chemotherapy (days 1, 3, 5 and 7 after tumor resection) to avoid any inhibiting effect of Paclitaxel and to assess the sole activity of immunotherapy (**Figure 5A**). When performed at day 9 (two days after the last injection of immunotherapy but before the first injection of chemotherapy) bioluminescence imaging showed that mice treated with V γ 9V δ 2 T lymphocytes had reduced bioluminescence signals probably due to an elimination of EOC tumor cells (**Figure 5B**). At day 45, a massive peritoneal carcinosis had developed in untreated mice, while mice treated by chemotherapy alone show a small restricted tumor area (**Figure 5C**). Strikingly, bioluminescence signals were weak, even absent, in mice treated by combined immunotherapy and chemotherapy which is linked to an important elimination of EOC tumor cells (**Figure 5C-D**). The enhanced efficacy of combined immunotherapy and chemotherapy was also significantly evidenced on survival curves showing that EOC mice treated by combined V γ 9V δ 2-immunotherapy and chemotherapy exhibited a higher median survival as compared to mice treated by chemotherapy alone (90 days vs 66 days) (**Figure 5E**). Reverse combination assays, in which immunotherapy was delivered several days after chemotherapy (days 19, 21, 23 and 25 after tumor resection) to avoid inhibiting effects of Paclitaxel, were performed. As for experiments described above, this combined treatment decreased the peritoneal carcinosis and significantly improved the survival of EOC mice (**Figure 5D-E**).

Altogether, these *in vivo* experiments with a murine physiological EOC model, clearly suggested that in EOC patients, following debulking surgery, immunotherapies (adoptive transfer of allogeneic human V γ 9V δ 2 T lymphocytes) could be administrated in complement to standard chemotherapy, before or after, to enhance the elimination of infiltrative EOC tumor cells and to improve their survival.

Discussion

Immunotherapies based on adoptive transfer of tumor-reactive T lymphocytes represent promising approaches to improve therapeutically care and survival of cancer patients. For lately diagnosed EOC, patients rapidly relapse, after debulking surgery and aggressive chemotherapy, with a fatal and massive peritoneal carcinosis. These novel therapies are expected to efficiently eliminate malignant infiltrative peritoneal tumor cells with limited, if any, deleterious effect on healthy surrounding cells. Among safety and efficiency analysis, one important issue associated to the design of these approaches is the selection of efficient immune effectors and the positioning of these approaches with standard therapies (ie, surgery, chemotherapy). Our study demonstrated that purified allogeneic human V γ 9V δ 2 T lymphocytes efficiently recognize and kill human EOC tumor cells. After establishing a physiological orthotopic xenograft model of human EOC from a commercially available line, this work indicated that peritoneal delivery of allogeneic *ex vivo*-amplified human V γ 9V δ 2 T lymphocytes could be combined to debulking surgery and chemotherapy and could significantly control dissemination of tumor cells *in vivo*.

This study first showed that EOC cells, originating from either primary tumors or cell lines, are all targeted by allogeneic human V γ 9V δ 2 T lymphocytes *in vitro*, upon NBP treatment. While yielding promising results, clinical trials revealed issues that should be addressed (eg, reduced reactivity of V γ 9V δ 2 T lymphocytes against fresh tumors). Importantly, the antigenic activation process of V γ 9V δ 2 T lymphocytes is not restricted by MHC molecules, which eliminates any risk of deleterious direct alloreactive reactivities towards non-transformed cells. The constitution of clinical allogeneic human V γ 9V δ 2 T lymphocyte banks, established from PBMC of healthy donors, would represent a unique opportunity for designing adoptive transfer immunotherapies in cancer patients. Once selected, amplified and prepared, administration of peripheral effector $\gamma\delta$ T lymphocytes could be hampered by the physiological status of the ovary and peritoneum.

To assess this, our study aimed at establishing a physiological orthotopic xenograft model of human EOC. As previously observed for s.c. and ip. xenografts (data not shown), elevated numbers of primary EOC cells that were injected in the ovary of immunodeficient NSG mice poorly grewed and survived *in vivo*, making them unusable for kinetics and reliability reasons. As grading number of cells have been tested, this quantity remains limited due to the

size of grafted organ (mouse ovary). Patient Derived Xenograft (PDX) would represent an alternative model as previous studies have shown the preservation of the original structure of ovarian carcinoma (Colombo et al., 2015). However, these attractive but long-growing and non-yet robust EOC models do not induce peritoneal carcinosis. As the elevated infiltrative feature of EOC tumor cells remains a key characteristic and a challenge for novel therapeutically approaches, currently designed PDX models do not meet therapeutically expectations at the moment. Bioluminescent EOC tumor cells from SKOV-3, a commercial human ovary cell line was selected to establish our preclinical model for the following reasons: (i) reduced injected cell quantities ($20 \cdot 10^3$ cells) and growth kinetics (2 months), (ii) reliability and reproducibility, (iii) disease follow-up by non-invasive imaging, (iv) formation of high grade serous tumors and development of a fatal peritoneal carcinosis.

Although recapitulating the peritoneal infiltration features of recurring human EOC tumors, this orthotopic *in vivo* model was established in immunodeficient NSG mice and did not take into account the inflammatory and immunosuppressive tumor microenvironments. Several studies showed that peritoneal inflammation fosters the development of regulatory T lymphocytes and inhibits the maturation of myeloid cells and the cytotoxicity of effector cells (Cubillos-Ruiz et al., 2010). While needing to be further assessed, this issue should be limited by the local delivery of elevated numbers of mature T cell effectors, whose low-sensitivity to inhibitory signals is further enhanced by counteracting activatory NBP treatments of EOC tumors (Lavoué et al., 2012).

As almost human EOC cells are not naturally recognized by V γ 9V δ 2 T lymphocytes, *in vitro* and *in vivo* assays were carried out with dose-dependent zoledronate sensitizations of a EOC cells to trigger strong V γ 9V δ 2 T lymphocyte recognition, as already used for enhancing such reactivities in other oncological contexts. Zoledronate administrations, which were already indicated for other human pathologies, such as osteoporosis and multiple myeloma (Dhillon and Lyseng-Williamson, 2008; Green and Lipton, 2010), have been proposed for V γ 9V δ 2 T cell-based immunotherapies. Recent preclinical approaches have suggested that NBP-sensitizations of tumor cells could be combined with adoptive transfers of V γ 9V δ 2 T cells in order to induce/enhance their antitumor reactivity. In this study, similar effects were targeted in simultaneous direct peritoneal combined injections *in vivo*. As expected from previous studies, combined injections of zoledronate and human allogeneic V γ 9V δ 2 T lymphocytes did not induce any adverse effects in treated mice.

This preclinical model of human EOC was next used to assess the clinical efficacy of immunotherapies and their positioning with standard treatments for EOC (debulking surgery followed by chemotherapy). *In vitro* chemotherapeutic assays showed that they did not enhance V γ 9V δ 2 T lymphocytes reactivity and but rather induced inhibiting effects (eg, Paclitaxel) on the expression of selected adhesion molecules (eg, CD44, CD166) expressed by tumor cells and on their subsequent interactions with V γ 9V δ 2 T lymphocytes. Based on these observations, preclinical combinations of surgery, standard chemotherapy and immunotherapy were designed to limit such effects and immunotherapy was delivered before or some days after chemotherapy. In this preclinical settings, V γ 9V δ 2 T lymphocyte-immunotherapies, when combined to debulking resection surgery and chemotherapy, significantly reduced the spreading of human EOC tumors and improved the survival of treated mice.

In conclusion, this study highlights the feasibility and the antitumor effects of intraperitoneal immunotherapies, based on allogeneic human V γ 9V δ 2 T lymphocytes, using a novel and robust orthotopic human EOC model in mouse. This work also clearly positioned immunotherapies with standard EOC treatments by showing that delivered V γ 9V δ 2 T lymphocytes can act, not as first line antitumor effectors, but rather to track and eliminate residual invasive EOC cells, likely accounting for a fatal recurring peritoneal carcinosis. Therefore, these results evidenced that adoptive allogeneic immunotherapies could represent promising and effective approaches for the treatment of human EOC which remains one of the deadliest cancers.

Acknowledgements

We thank the staff of University Hospital animal facility of Nantes for animal husbandry and care, the cellular and tissular imaging core facility of Nantes university (MicroPICell) for imaging, and the Cytometry Facility Cytocell from Nantes for their expert technical assistance. We also thank Veronique Catros and technical staff of the CRB Rennes for providing primary EOC cells and Jean-Marc Classe for providing chemotherapeutic agents at GMP grade format.

References

- Chien, Y., Meyer, C., and Bonneville, M. (2014). $\gamma\delta$ T cells: first line of defense and beyond. *Annu. Rev. Immunol.* *32*, 121–155.
- Colombo, P.-E., Fabbro, M., Theillet, C., Bibeau, F., Rouanet, P., and Ray-Coquard, I. (2014). Sensitivity and resistance to treatment in the primary management of epithelial ovarian cancer. *Crit. Rev. Oncol. Hematol.* *89*, 207–216.
- Colombo, P.-E., du Manoir, S., Orsett, B., Bras-Gonçalves, R., Lambros, M.B., MacKay, A., Nguyen, T.-T., Boissière, F., Pourquier, D., Bibeau, F., et al. (2015). Ovarian carcinoma patient derived xenografts reproduce their tumor of origin and preserve an oligoclonal structure. *Oncotarget* *6*, 28327–28340.
- Cubillos-Ruiz, J.R., Rutkowski, M., and Conejo-Garcia, J.R. (2010). Blocking ovarian cancer progression by targeting tumor microenvironmental leukocytes. *Cell Cycle Georget. Tex* *9*, 260–268.
- Dhillon, S., and Lyseng-Williamson, K.A. (2008). Zoledronic acid : a review of its use in the management of bone metastases of malignancy. *Drugs* *68*, 507–534.
- Fournié, J.-J., Sicard, H., Poupot, M., Bezombes, C., Blanc, A., Romagné, F., Ysebaert, L., and Laurent, G. (2013). What lessons can be learned from $\gamma\delta$ T cell-based cancer immunotherapy trials? *Cell. Mol. Immunol.* *10*, 35–41.
- Green, J., and Lipton, A. (2010). Anticancer properties of zoledronic acid. *Cancer Invest.* *28*, 944–957.
- Harly, C., Guillaume, Y., Nedellec, S., Peigné, C.-M., Mönkkönen, H., Mönkkönen, J., Li, J., Kuball, J., Adams, E.J., Netzer, S., et al. (2012). Key implication of CD277/butyrophilin-3 (BTN3A) in cellular stress sensing by a major human $\gamma\delta$ T-cell subset. *Blood* *120*, 2269–2279.
- Harly, C., Peigné, C.-M., and Scotet, E. (2014). Molecules and Mechanisms Implicated in the Peculiar Antigenic Activation Process of Human V γ 9V δ 2 T Cells. *Front. Immunol.* *5*, 657.
- Hayday, A.C. (2000). $[\gamma][\delta]$ cells: a right time and a right place for a conserved third way of protection. *Annu. Rev. Immunol.* *18*, 975–1026.
- Helland, O., Popa, M., Vintermyr, O.K., Molven, A., Gjertsen, B.T., Bjørge, L., and McCormack, E. (2014). First in-mouse development and application of a surgically relevant xenograft model of ovarian carcinoma. *PloS One* *9*, e89527.

Jarry, U., Chauvin, C., Joalland, N., Léger, A., Minault, S., Robard, M., Bonneville, M., Oliver, L., Vallette, F.M., Vié, H., et al. (2016). Stereotaxic administrations of allogeneic human V γ 9V δ 2 T cells efficiently control the development of human glioblastoma brain tumors. *Oncoimmunology* 5, e1168554.

Kato, Y., Tanaka, Y., Hayashi, M., Okawa, K., and Minato, N. (2006). Involvement of CD166 in the activation of human gamma delta T cells by tumor cells sensitized with nonpeptide antigens. *J. Immunol. Baltim. Md 1950* 177, 877–884.

Lai, D., Wang, F., Chen, Y., Wang, C., Liu, S., Lu, B., Ge, X., and Guo, L. (2012). Human ovarian cancer stem-like cells can be efficiently killed by $\gamma\delta$ T lymphocytes. *Cancer Immunol. Immunother. CII* 61, 979–989.

Lavoué, V., Cabillic, F., Toutirais, O., Thedrez, A., Dessarthe, B., de La Pintièrre, C.T., Daniel, P., Foucher, F., Bauville, E., Henno, S., et al. (2012). Sensitization of ovarian carcinoma cells with zoledronate restores the cytotoxic capacity of V γ 9V δ 2 T cells impaired by the prostaglandin E2 immunosuppressive factor: implications for immunotherapy. *Int. J. Cancer* 131, E449-462.

Loubani, O., and Hoskin, D.W. (2005). Paclitaxel inhibits natural killer cell binding to target cells by down-regulating adhesion molecule expression. *Anticancer Res.* 25, 735–741.

Siegel, R.L., Miller, K.D., and Jemal, A. (2016). Cancer statistics, 2016. *CA. Cancer J. Clin.* 66, 7–30.

Thedrez, A., Sabourin, C., Gertner, J., Devilder, M.-C., Allain-Maillet, S., Fournié, J.-J., Scotet, E., and Bonneville, M. (2007). Self/non-self discrimination by human gammadelta T cells: simple solutions for a complex issue? *Immunol. Rev.* 215, 123–135.

Torre, L.A., Trabert, B., DeSantis, C.E., Miller, K.D., Samimi, G., Runowicz, C.D., Gaudet, M.M., Jemal, A., and Siegel, R.L. (2018). Ovarian cancer statistics, 2018. *CA. Cancer J. Clin.*

Ventriglia, J., Paciolla, I., Pisano, C., Cecere, S.C., Di Napoli, M., Tambaro, R., Califano, D., Losito, S., Scognamiglio, G., Setola, S.V., et al. (2017). Immunotherapy in ovarian, endometrial and cervical cancer: State of the art and future perspectives. *Cancer Treat. Rev.* 59, 109–116.

Figure 1

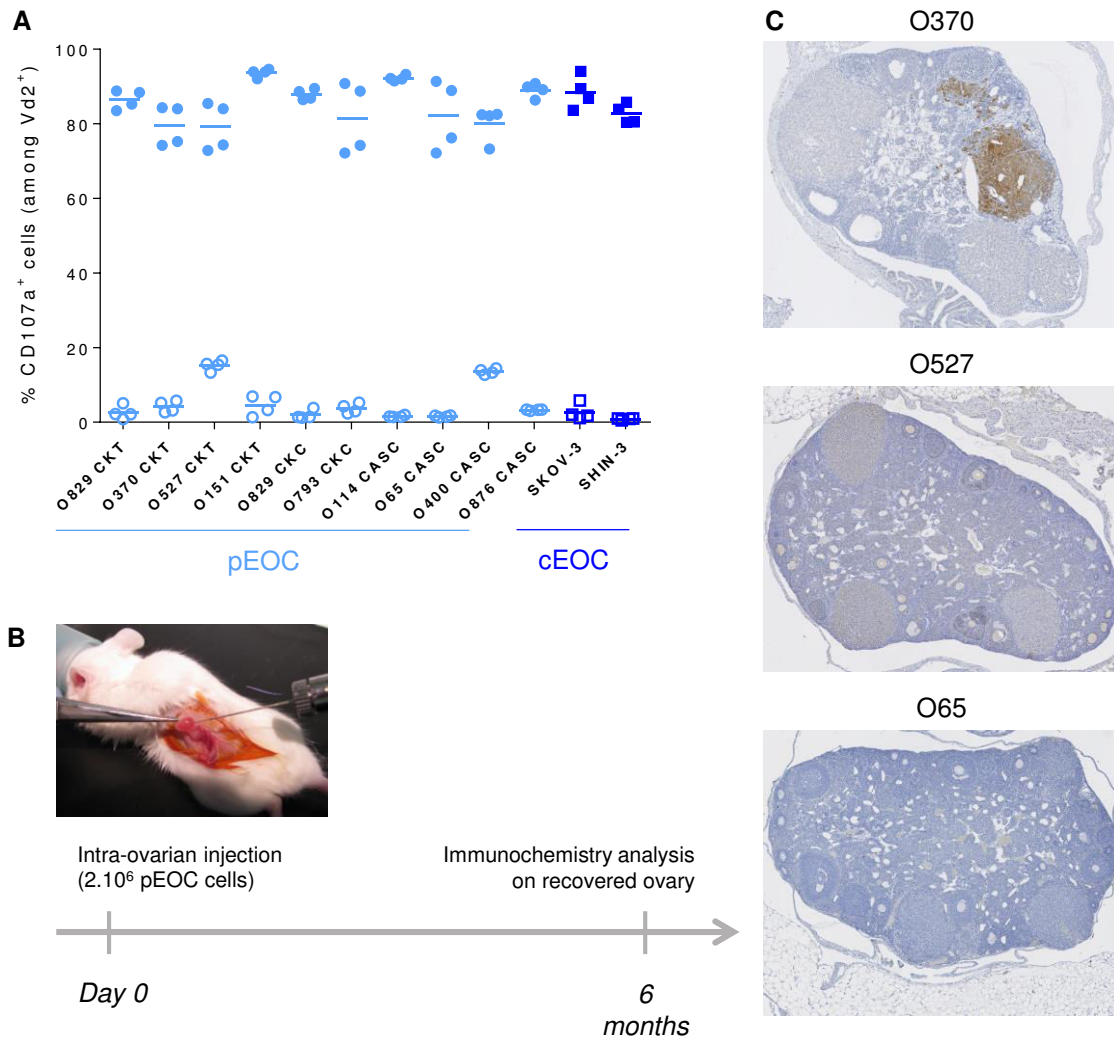


Figure 1. Primary EOC cells as cellular basis for the establishment of physiological EOC mouse model. (A) Primary EOC cells (pEOC; light blue symbols) and cell lines (cEOC; dark blue symbols) were sensitized (filled symbols), or not (empty symbols), with zoledronate overnight before a 4h-coculture with human allogeneic V γ 9V δ 2 T lymphocytes (E:T 1:1). Upregulation of CD107a was analyzed on gd T lymphocytes by flow cytometry. Results are expressed as % of CD107a⁺ cells among V δ 2⁺ T lymphocytes (n=4, each point correspond to different donors of V γ 9V δ 2 T lymphocytes). (B-C) *in vivo* development of primary EOC cells after orthotopic injection in the ovary of NSG mice. 6 months after injection, ovary were collected, fixed, sectioned and stained with anti-human MHC class I mAb. (C) Representative section of three different primary EOC cells from three different patients.

Figure 2

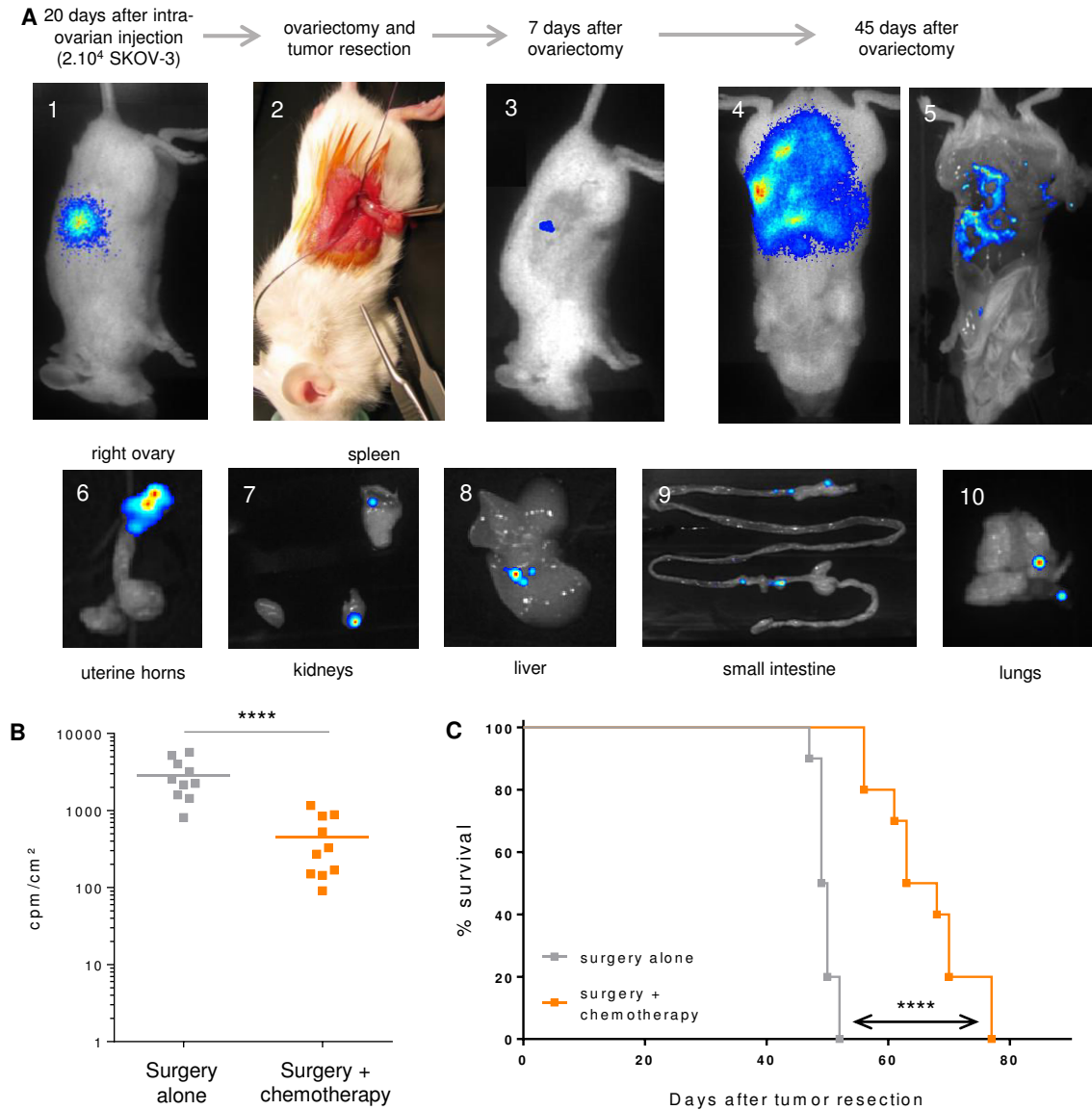


Figure 2. Establishment of a preclinical orthotopic human EOC mice model. (A) Representative optical and bioluminescence pictures showing the chronological development of orthotopic EOC xenografts (pictures 1 to 5) and subsequent peritoneal carcinosis (pictures 6 to 10) in NSG mice. (B) Bioluminescence analysis of mice performed at day 45 after tumor resection in surgery (surgery alone) or surgery combined to chemotherapy (surgery + chemotherapy) (n=10 mice; **** p<0,0001). Results are expressed as cpm/cm². (C) Survival curves of mice treated by surgery alone (-■-) or surgery and chemotherapy (-■-) (n=10 mice per group; **** p<0,0001).

Figure 3

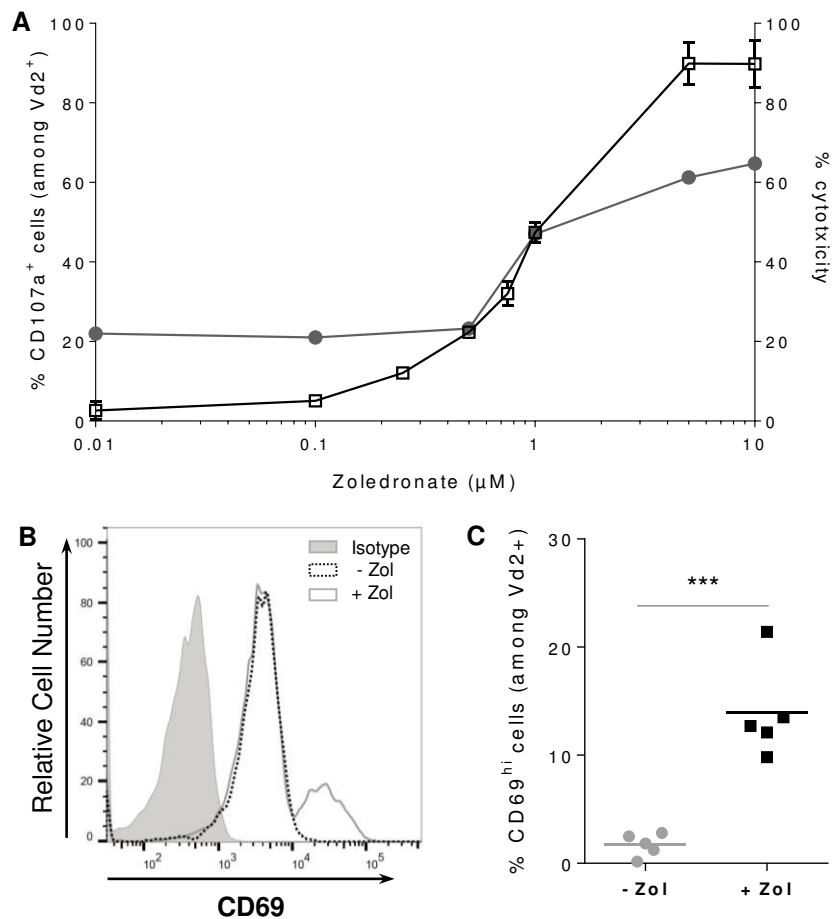


Figure 3. Zoledronate is essential to efficiently sensitize human EOC tumor cells to V γ 9V δ 2 T lymphocyte recognition *in vitro* and *in vivo*. (A) Cytotoxicity of allogeneic human V γ 9V δ 2 T lymphocytes against EOC cells. In these ^{51}Cr release assays, SKOV-3 cells were sensitized at various concentrations of zoledronate overnight before a 4 hour-coculture with human allogeneic V γ 9V δ 2 T lymphocytes performed at E:T ratio 1:1 (-□-) and 10:1 (-●-). Results are respectively expressed as % of CD107a⁺ cells among V δ 2⁺ T lymphocytes and % cytotoxicity (mean \pm SD; n=4). (B-C) V γ 9V δ 2 T lymphocytes were intraperitoneally injected, with or without zoledronate, in SKOV-3 tumor-bearing NSG mice. After peritoneal wash, CD69 expression was analyzed on V δ 2⁺ T lymphocytes. Representative histogram (B) or compiled results (C) of CD69 expression on V γ 9V δ 2 T lymphocytes (n=5; *** p<0,001).

Figure 4

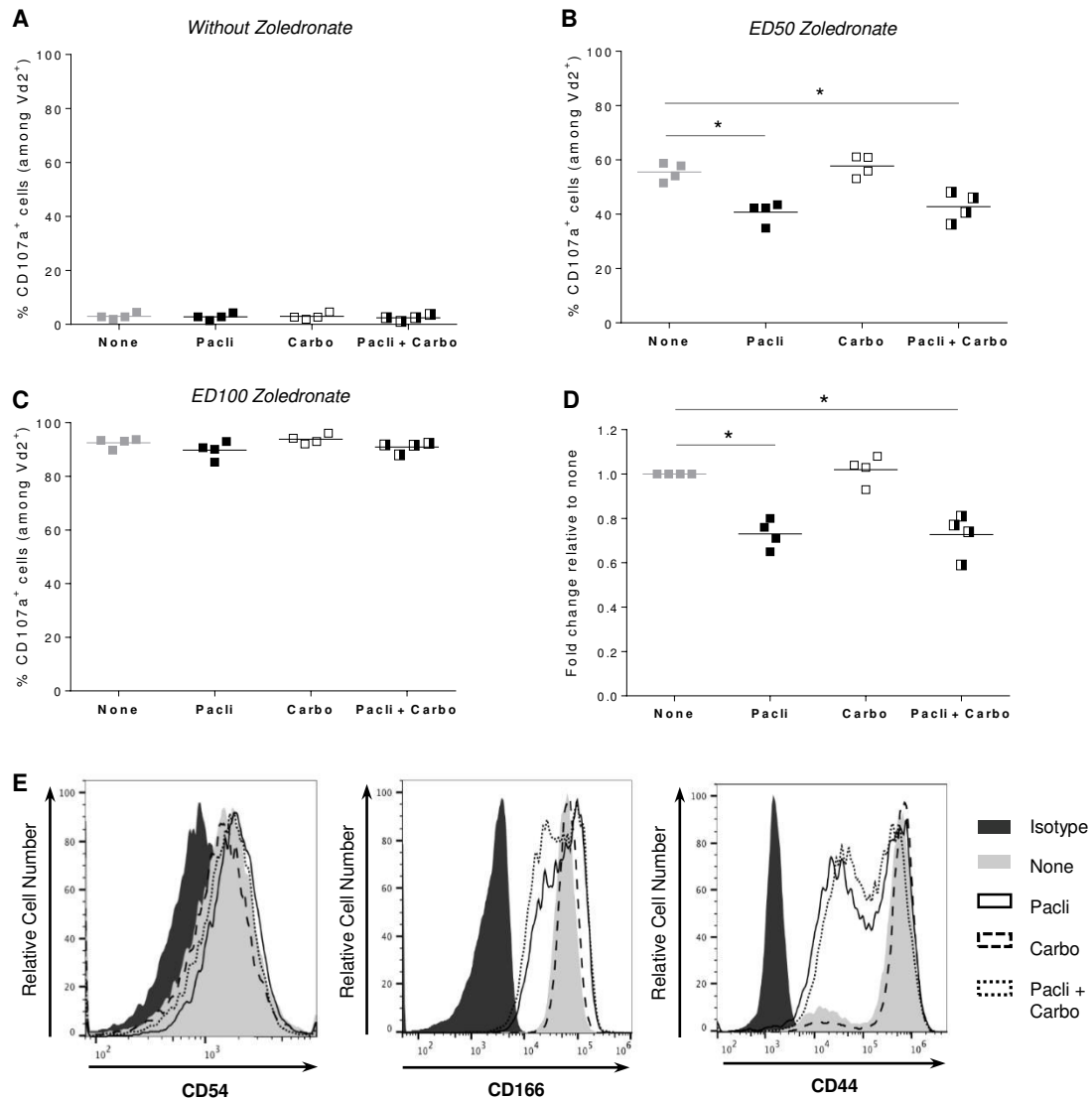


Figure 4. Paclitaxel alters the reactivity of V γ 9V δ 2 T lymphocytes by inducing a decrease of the expression of adhesion molecules on tumor cells. (A-B-C) SKOV-3 cell lines were treated for 1 hour with the following chemotherapies: Paclitaxel alone (Pacli), Carboplatin alone (Carbo), or both (Pacli + Carbo). After zoledronate sensitization performed at different concentrations: without (A), ED₅₀ (B) or ED₁₀₀ (C), tumor cells were co-cultured for 4 hours with V γ 9V δ 2 T lymphocytes (E:T ratio 1:1) which were analyzed for expression of CD107a by flow cytometry. Results are expressed as % of CD107a⁺ cells among V δ 2⁺ T lymphocytes (n=4; * p<0,05). (D) SKOV-3 cells were stained with Zombie Green and V γ 9V δ 2 T lymphocytes were stained with anti-V δ 2 mAb before incubation during 30 minutes and flow cytometry analysis. % double positive events were recovered and results are expressed as fold change relative to the none condition (n=4; * p<0,05). (E) Representative histograms of extracellular staining of CD54 (left) CD166 (middle) and CD44 (right) on SKOV-3 cells after chemotherapies treatment.

Figure 5

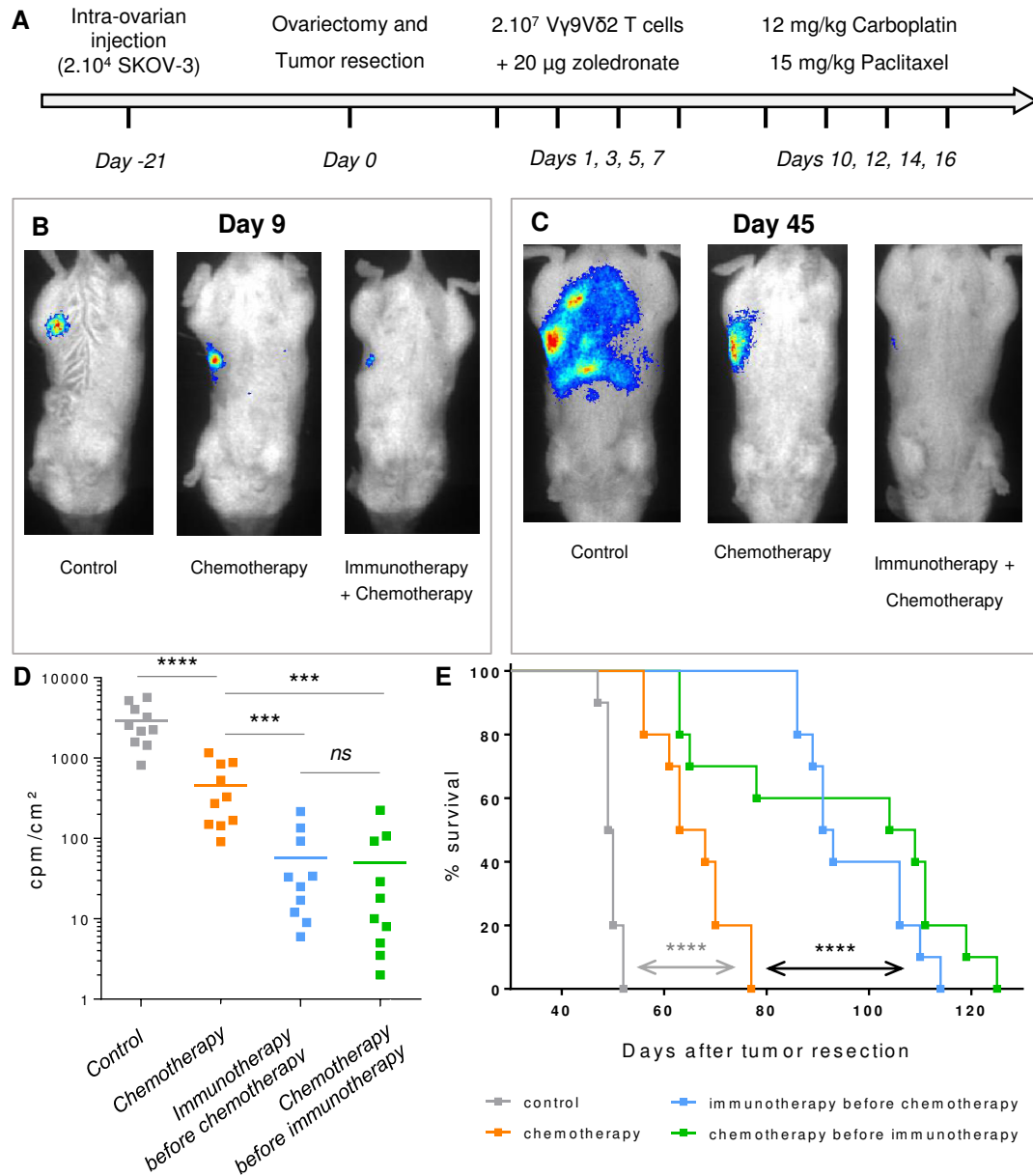
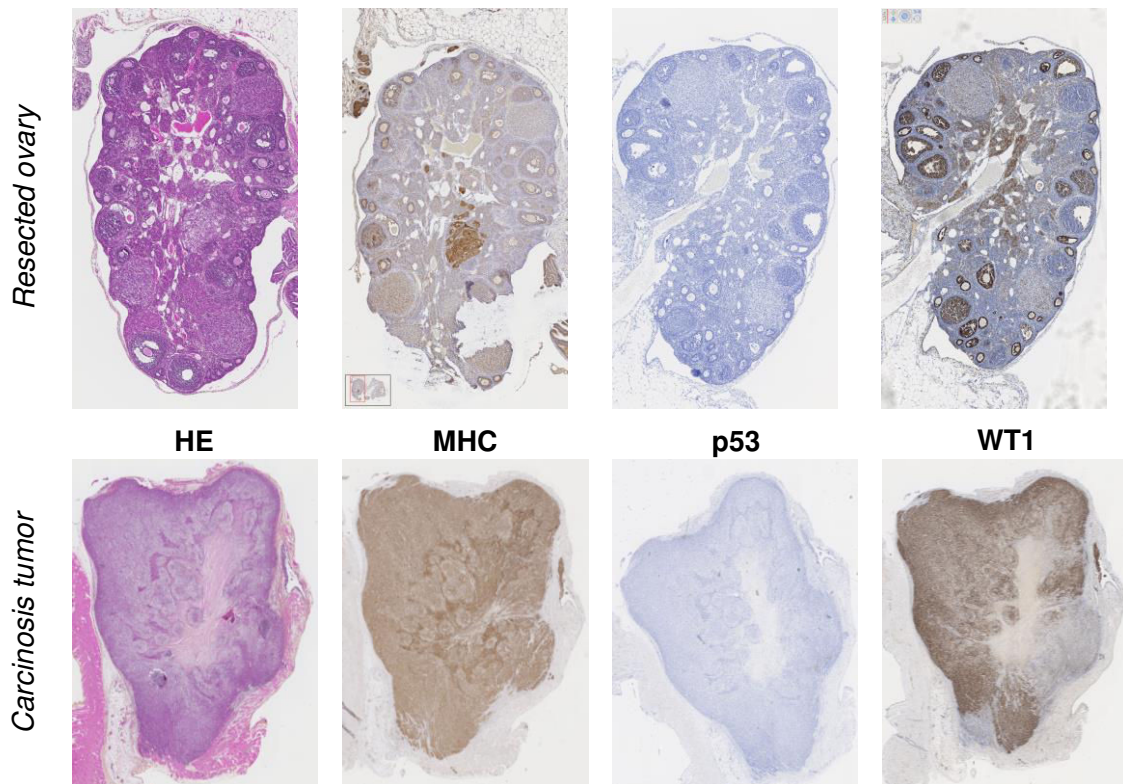


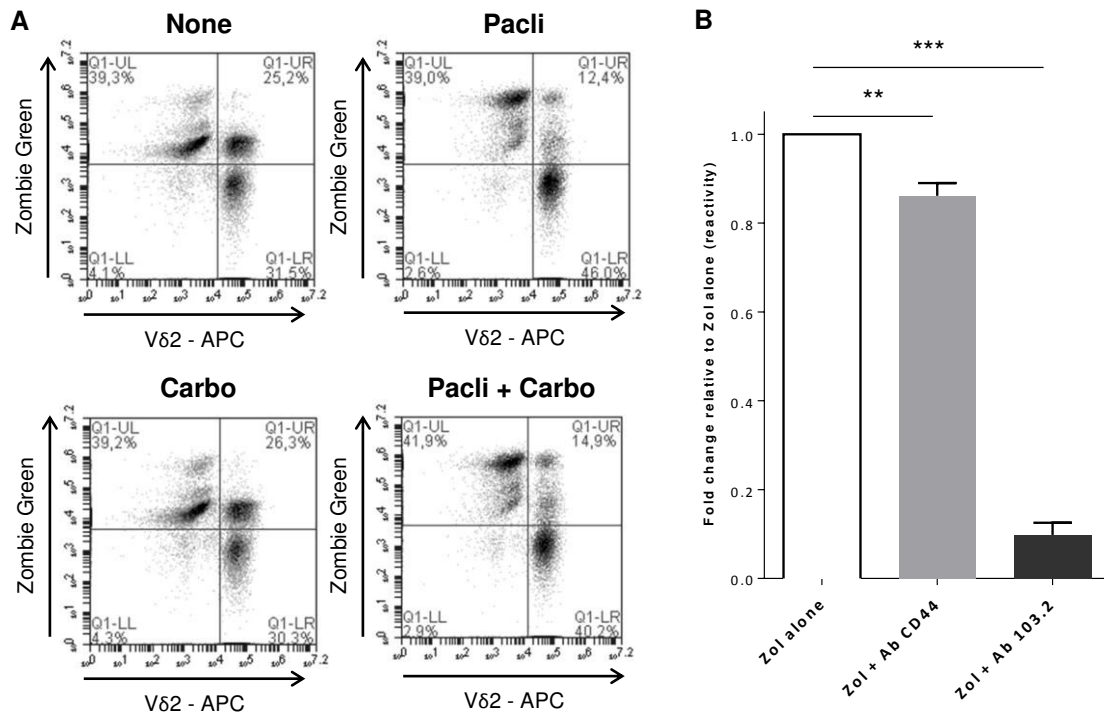
Figure 5. *in vivo* combination of chemotherapy and immunotherapy strongly improves EOC mice survival. (A) Design of the trial. (B-C) Representative bioluminescence pictures of one mice per group at day 9 (B) and day 45 (C) after tumor resection. (D) Compiled results of bioluminescence intensity for each group. (n=10 mice; *** p<0,001). (E) Survival curves of control mice (-■-), mice treated by chemotherapy (-■-), immunotherapy before chemotherapy (-■-) or chemotherapy before immunotherapy (-■-) (n=10 mice per group; **** p<0,0001).

Joalland et al.

Supplemental Figure S1



Supplemental Figure S1. Anatomopathological analysis on resected ovary (upper pictures) and carcinosis tumors (down pictures). Sections were stained with hematoxylin eosine (HE); anti-MHC class I mAb (clone EPR1394Y, Abcam); anti-p53 mAb (clone DO.7, Dako) or an anti-WT1 mAb (clone 6F-H2, Dako).



Supplemental Figure S2. Negative impact of Paclitaxel on adhesion molecule expressed by tumor cells and reactivity of V γ 9V δ 2 T lymphocytes. **(A)** Paclitaxel, alone or combined with Carboplatin, decreases formation of cellular conjugates. SKOV-3 cells and V γ 9V δ 2 T lymphocytes were stained and flow cytometry analysis allowed the identification of double positive events which correspond to cellular conjugates. Representative dot plots for each conditions (control, Paclitaxel alone, Carboplatin alone, Paclitaxel + Carboplatin). **(B)** CD44 blockade decreases the reactivity of V γ 9V δ 2 T lymphocytes against SKOV-3 cells. After zoledronate sensitization (ED₅₀), SKOV-3 cells were incubated for 15 minutes with an anti-CD44 (10 μ g/mL, IM7, Biologend) or anti-BTN3 (10 μ g/mL, 103.2, ImCheck Therapeutics, Marseille, France) mAbs. V γ 9V δ 2 T lymphocytes were added and CD107a upregulation was measured on T lymphocytes by flow cytometry. Results are expressed as fold change compared to control condition (Zoledronate alone) (mean \pm SD ; n=4 ; ** p<0,01 ; *** p<0,001).

3 – Encadrement de stagiaires : Résultats Annexes à la Partie 2

3.1 – Avril à Juin 2016 : Stagiaire de Master 1 Biologie Santé (Andréa MUREAU).

Malgré les stratégies mises en place dans le traitement du CEO, une rechute de type carcinose péritonéale est fréquemment observée chez les patientes (survie à 5 ans < 45 %). Parmi les nouvelles voies thérapeutiques, l'immunothérapie par transfert adoptif de LT V γ 9V δ 2 associés au traitement chimiothérapeutique de référence, semble être une stratégie intéressante à envisager. Après avoir déterminé l'effet du Paclitaxel et de la Carboplatine sur la viabilité des cellules tumorales, nous avons mis en évidence un impact négatif de la chimiothérapie (Paclitaxel) sur la réactivité des LT V γ 9V δ 2 vis à vis d'une lignée humaine de CEO. Une stratégie thérapeutique, combinant chimiothérapie et immunothérapie, a ensuite été mise en place *in vivo* dans un modèle murin orthotopique de CEO avec carcinose péritonéale.

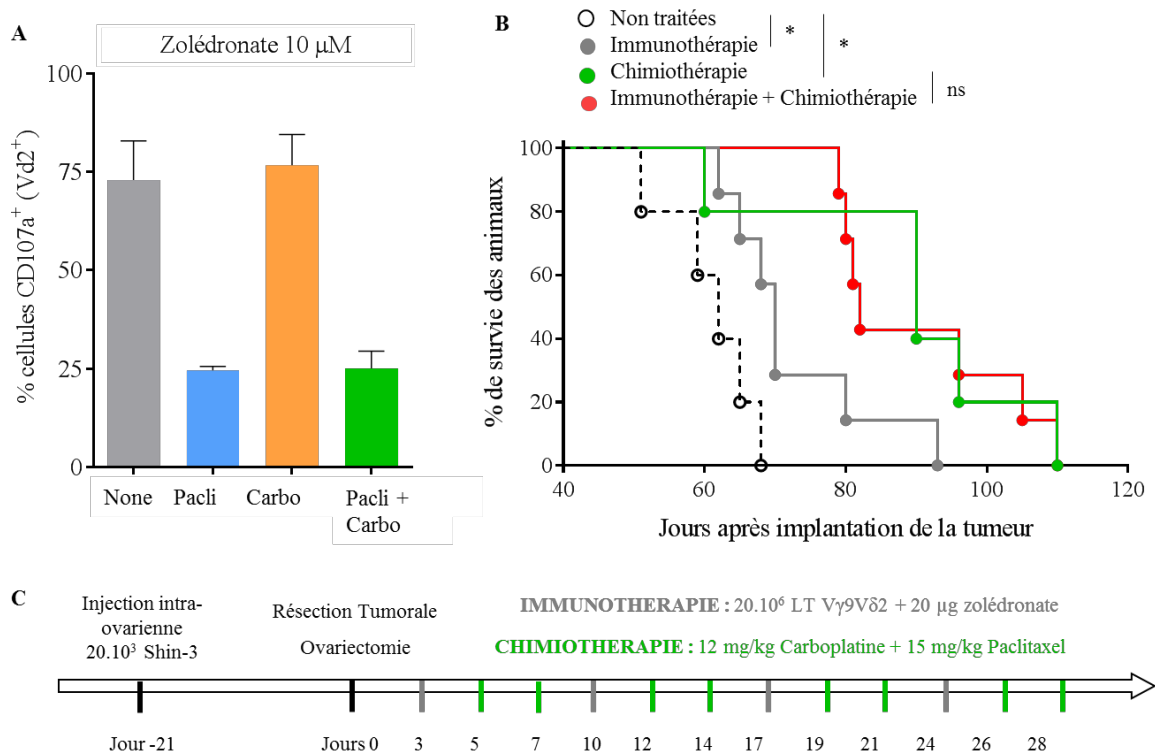


Figure 34 : Impact de la chimiothérapie sur la lignée humaine de CEO SHIN-3 *in vitro* et *in vivo*. (A) Réactivité des LT V γ 9V δ 2 face à des cellules tumorales de la lignée SHIN-3 sensibilisées au Zolédronate et traitées, ou non (none), avec de la chimiothérapie : Paclitaxel seul (Pacli), Carboplatine seule (Carbo), ou les deux combinées (Pacli + Carbo) (moyenne \pm SD ; n=3). (B) Courbe de survie des souris non traitées (n=7), traitées par injection intrapéritonéale de LT V γ 9V δ 2 allogéniques et de Zolédronate (immunothérapie ; n=7), traitées par injection intrapéritonéale de Paclitaxel et de Carboplatine (Chimiothérapie ; n=5) ou traitées par la combinaison des deux (Immunothérapie + Chimiothérapie ; n=7). (C) Protocole de traitement des animaux.

3.2 – Janvier à Juin 2018 : Stagiaire de Master 2 Biologie Santé Médecine
(Camille GORDEEFF).

La chirurgie de réduction tumorale associée à la chimiothérapie par voie systémique est le traitement de référence des patientes atteintes de CEO. Du fait des récives liées à la formation de carcinose péritonéale, la Chimiothérapie Hyperthermique IntraPéritonéale (CHIP) représente une alternative thérapeutique prometteuse. Sa réalisation en per opératoire permet une meilleure diffusion péritonéale ainsi qu'une potentialisation de l'effet de la chimiothérapie grâce à l'hyperthermie. Cependant, à long terme, l'éradication tumorale reste incomplète. Dans ce contexte, l'immunothérapie, et plus particulièrement le transfert adoptif de LT V γ 9V δ 2 humains allogéniques, permettrait de cibler spécifiquement les cellules tumorales infiltrantes, résistantes aux traitements standards et potentiellement stressées par la CHIP. L'objectif de ce projet a donc été d'évaluer l'impact de la CHIP sur la réactivité anti-tumorale des LT V γ 9V δ 2 humains. Après avoir validé l'approche thérapeutique CHIP, *in vitro*, la réactivité des LT V γ 9V δ 2 a été étudiée face à des cellules tumorales d'une lignée cellulaire humaine. A terme, cette stratégie pourrait être adaptée, *in vivo*, dans un modèle murin de xénogreffe orthotopique.

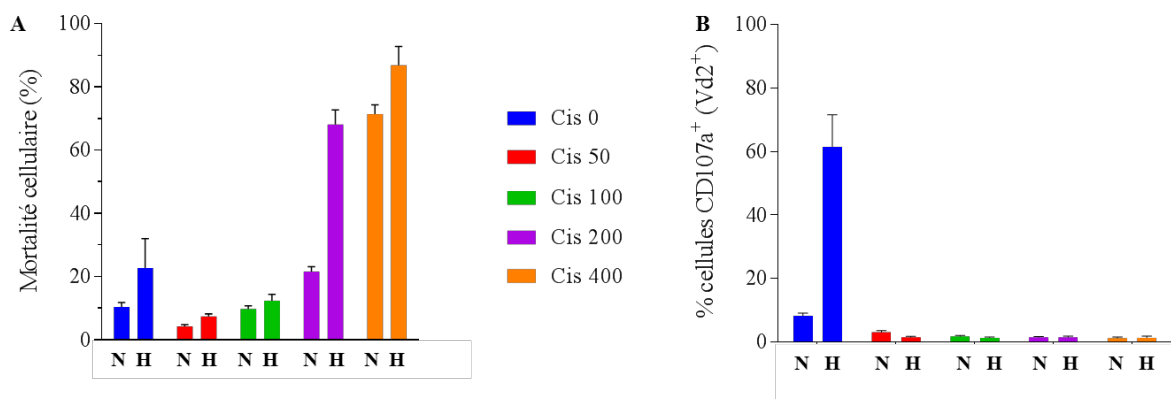


Figure 35 : Impact de la CHIP sur la réactivité des LT V γ 9V δ 2 face à des cellules tumorales de CEO de la lignée cellulaire SKOV-3.

Après traitement, de cellules tumorales de CEO, de la lignée SKOV-3, avec différentes doses de cisplatine (Cis ; μ g/mL) et incubation soit 1 heure en normothermie (N, 37°C) soit 1 heure 20 minutes en hyperthermie (H, 42°C) : (A) un test de mortalité par marquage 7-AAD est réalisé (moyenne \pm SD ; n=3) ou (B) les cellules tumorales sont cocultivées 4 heures en présence de LT V γ 9V δ 2, après sensibilisation au Zolédronate (0,1 μ M), afin d'évaluer leur réactivité (cellules CD107a+ parmi les V δ 2+ ; moyenne \pm SD ; n=4).

3 - Conclusion

Cette étude est incluse dans un programme collaboratif financé par le Canceropole Grand Ouest et reposant sur le partage d'échantillons, issus de patientes, récoltés par le Centre de Ressources Biologiques de Rennes. Bien que l'utilisation de ces primocultures n'ait pas abouti, nous avons tout de même pu mettre en place un modèle préclinique de CEO représentatif de la pathologie humaine et incluant le traitement standard des patientes (chirurgie et chimiothérapie).

Au cours de cette étude, nous avons eu l'occasion de travailler avec deux lignées de CEO : SKOV-3 et SHIN-3. Une partie des résultats présentés dans cet article ont été confirmés avec cette deuxième lignée. Ainsi, l'utilisation de la lignée SHIN-3, *in vivo*, reproduit de façon similaire le modèle mis en place avec la lignée SKOV-3, en termes de vitesse de croissance et de dissémination des cellules tumorales, bien qu'elle soit caractérisée pour être un carcinome de type endométriöide par IHC (immunohistochimie). L'impact négatif induit par le Paclitaxel sur la réactivité des LT V γ 9V δ 2 a également été démontré sur cette lignée au cours du stage de Master 1 d'Andréa MUREAU (page 113 ; Figure 34A), et pourrait expliquer l'échec du premier protocole combinant immunothérapie et chimiothérapie mis en place dans ce modèle. En effet, ce premier protocole reposait sur l'alternance des injections de chimiothérapie (Carboplatine et Paclitaxel) et d'immunothérapie (LT V γ 9V δ 2 et Zolédronate), et bien que les traitements séparés aient démontré leur efficacité, leur combinaison n'améliorait pas la survie des souris en comparaison des animaux traités uniquement par chimiothérapie (page 113 ; Figure 34B et C).

Dans cet article, nous confirmons également l'intérêt de combiner l'injection des LT V γ 9V δ 2 au Zolédronate afin de sensibiliser les cellules tumorales. En effet, l'utilisation du Zolédronate permet d'induire une forte réactivité des LT V γ 9V δ 2 aussi bien face aux primocultures de CEO qu'aux lignées, qu'elles soient résistantes à la chimiothérapie, ou non. Son utilisation permet également d'annuler l'impact négatif des molécules immunomodulatrices présentes dans l'ascite (ex. PGE2) et réduisant la réactivité des LT V γ 9V δ 2 (Lavoué et al., 2012).

Fin 2014, un essai clinique a démarré au Japon, sous la direction de Yuki Abe et Hideo Matsui, intitulé "Intraperitoneal injection of *in vitro* expanded Gamma Delta T cells together with Zoledronate for the treatment of malignant ascites to ovarian cancer ; to evaluate the safety and efficacy (A Phase 1/2a study)".

Cet essai repose sur l'expansion *ex vivo* des LT V γ 9V δ 2 des patientes grâce à un PAg de synthèse, le 2-méthyl-3-butenyl-1-pyrophosphate. Les LT V γ 9V δ 2 sont ensuite réinjectés, via un cathéter, dans la cavité intrapéritonéale, combinés à du Zolédronate. Bien que le suivi des patientes ait été annoncé jusqu'en août 2017, les résultats de cette étude n'ont pas encore été publiés.

De notre côté et afin d'améliorer notre modèle, nous avons eu l'occasion, au cours du stage de Master 2 de Camille GORDEEFF, d'étudier l'impact de la chimiothérapie hyperthermique sur la réactivité des LT V γ 9V δ 2 (page 114). Bien que le traitement par CHIP (chimiothérapie hyperthermique intrapéritonéale) ne fasse pas partie du traitement standard des patientes atteintes de CEO, cette stratégie est de plus en plus utilisée et a démontré son efficacité thérapeutique (van Driel et al., 2018). Contrairement aux autres protocoles de chimiothérapie qui ont lieu à distance de la résection chirurgicale, la CHIP a lieu pendant l'intervention. Cela permet au(x) chirurgien(s) de brasser les anses intestinales afin de faire diffuser la chimiothérapie dans toute la cavité abdominale afin d'atteindre un maximum de cellules tumorales avant qu'elles ne soit séquestrées par les adhérences post-opératoires. Comme son nom l'indique, cette thérapie associe chimiothérapie et hyperthermie. La chimiothérapie la plus couramment utilisée est la cisplatine chauffée à 42°C et utilisée en bain abdominal pendant une heure (Gouy et al., 2016). Ainsi, l'hyperthermie, en plus de son effet cytotoxique direct, potentialise l'effet de la chimiothérapie et augmente son absorption par les tissus (Maymon et al., 1994).

Le but de ce stage était de déterminer si ces conditions (chimiothérapie et hyperthermie) pouvaient provoquer un stress suffisant des cellules tumorales pour augmenter la réactivité des LT V γ 9V δ 2. Dans un premier temps, un modèle de CHIP *in vitro* a été mis en place en incubant, à 42°C pendant une heure, la lignée cellulaire SKOV-3 avec des doses croissantes de cisplatine (page 114 ; Figure 35A). Ensuite la réactivité de LT V γ 9V δ 2 a été évaluée face à ces cibles, à différents temps après la CHIP, et malheureusement il ne nous a pas été possible de mettre en avant des conditions améliorant suffisamment la réactivité des LT V γ 9V δ 2 pour envisager de combiner de façon bénéfique ces deux stratégies dans notre modèle murin (page 114 ; Figure 35B).

PARTIE 3 : Application au Glioblastome Multiforme

1 – Le Glioblastome Multiforme

1.1 – Classification des tumeurs cérébrales

L'ensemble des tumeurs bénignes et malignes se développant dans le parenchyme cérébral sont appelées tumeurs cérébrales, qu'elles soient primaires (dérivant de cellules cérébrales) ou secondaires (métastases issues d'un autre cancer). Parmi les tumeurs cérébrales malignes, les gliomes qui dérivent des cellules gliales (cellules de soutien), sont les plus fréquents (80 %) (Ostrom et al., 2017).

Différentes classifications ont été proposées sur la base du degré de malignité, selon des critères histologiques et plus récemment grâce à des marqueurs génétiques et moléculaires (Louis et al., 2016). Dans un premier temps, l'OMS (organisation mondiale de la santé) décrit 4 grades de malignité allant du gliome bénin au grade I, jusqu'au grade IV pour les gliomes les plus agressifs (Louis et al., 2007). Les gliomes sont également divisés en 4 groupes en fonction du sous-type de cellules gliales à l'origine de la transformation (Louis et al., 2007) :

- Les astrocytomes ayant pour origine les astrocytes, les cellules de soutien du SNC (système nerveux central),
- Les oligodendrogliomes sont issus des oligodendrocytes, les cellules à l'origine de la synthèse de la myéline des neurones,
- Les oligoastrocytomes, présentant des caractéristiques mixtes entre les deux types de tumeurs précédentes,
- Les épendymomes, eux dérivent des cellules épendymaires, qui forment la paroi du SNC et synthétisent du LCR (liquide céphalo-rachidien).

Les glioblastomes sont des astrocytomes de grade IV et sont appelés glioblastome multiforme (GBM) du fait de leurs importantes variabilités morphologiques, cytologiques et moléculaires. De ce fait, une seconde classification a été proposée par l'OMS en 2016 basée sur leur profil transcriptomique (Phillips et al., 2006; Verhaak et al., 2010). Cette classification comprend également 4 sous-types :

- Mésenchymateux, associé à une perte d'expression du gène NF1,
- Classique, avec une importante amplification de l'EGFR,
- Neural, caractérisé par l'expression de marqueurs de neurones tel que NEFL,
- Proneural, présentant des mutations d'IDH et/ou de TP53.

Les sous-types Classique et Neural étant souvent regroupés sous le nom de prolifératif. Le sous-type mésenchymateux, quant à lui a été identifié comme le plus agressif (Phillips et al., 2006; Verhaak et al., 2010). De plus, les patients présentant le même profil moléculaire répondent de façon similaire aux traitements, permettant d'adapter les thérapies pour une meilleure efficacité.

1.2 – Epidémiologie et Etiologie

Le GBM est la tumeur cérébrale maligne la plus fréquente et également la plus agressive. Il représente 15 % des tumeurs malignes du SNC et 56 % des gliomes (Ostrom et al., 2017). Le GBM reste tout de même une pathologie rare, avec une incidence de 4 GBM pour 100 000 adultes de plus de 20 ans (Ostrom et al., 2017). Il est intéressant de noter que cette incidence est corrélée avec l'âge, avec un maximum de survenue entre 75 et 84 ans et un âge médian des patients au diagnostic de 64 ans (Ostrom et al., 2017).

Différents facteurs de risque influencent également sur la survenue du GBM. Tout d'abord des facteurs génétiques, tels que le sexe (1,58 hommes pour 1 femme), l'ethnie (1,93 caucasiens pour 1 afro-américain), certaines maladies génétiques ou les antécédents familiaux (Ostrom et al., 2017; Reni et al., 2017). Les facteurs environnementaux jouent également un rôle important, notamment l'exposition aux irradiations, aux pesticides ou à certains agents pathogènes comme le CMV (Hashida et al., 2015; Reni et al., 2017). Bien que l'utilisation du téléphone portable soit fortement suspectée d'être un facteur risque, aucune étude n'a clairement mis en évidence de corrélation entre son utilisation et la survenue du GBM.

1.3 – Diagnostic et Prise en charge thérapeutique

La majorité des patients sont diagnostiqués tardivement du fait de la multiplicité et de la non-spécificité des symptômes rencontrés (Ostrom et al., 2017). En effet, selon la zone du cerveau atteinte et l'étendue de la tumeur, les symptômes peuvent être très variable.

Ces symptômes vont du déficit neurologique (moteur, visuel et/ou sensitif), au syndrome d'hypertension intracrânienne (compression ou accumulation de LCR), en passant par l'épilepsie. Ils sont généralement accompagnés de céphalées, vomissements voire de paralysie.

A ce jour, aucun facteur sérique n'est utilisé pour le diagnostic, le principal outil étant l'imagerie, qui permet aussi de localiser la tumeur et préciser son étendue. L'IRM est la technique standard utilisée et est généralement associée à un produit de contraste (Reni et al., 2017) (Figure 36).

Cependant la neuro-imagerie n'est pas suffisante pour discriminer le GBM des autres tumeurs cérébrales, il est donc nécessaire de réaliser une analyse histologique. Cette analyse manquant de précision, notamment du fait de l'existence de sous-types moléculaires au sein d'un sous-type histologique, elle est de plus en plus fréquemment couplée à une analyse des biomarqueurs moléculaires. Ces analyses peuvent être réalisées, soit sur une biopsie si la tumeur n'est pas opérable, soit directement sur la résection chirurgicale (Reni et al., 2017).

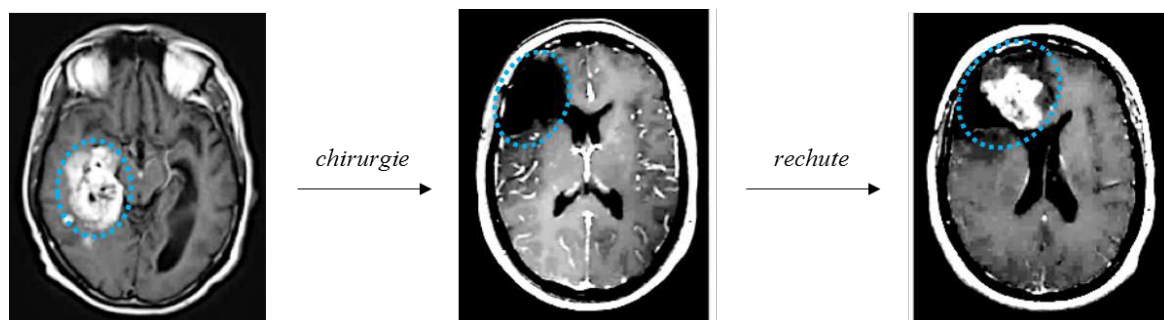


Figure 36 : Images cérébrales de suivi de patients atteints de GBM.

Images obtenues par IRM au moment du diagnostic (*gauche*), après chirurgie (*centre*) et au moment de la rechute (*droite*). La masse tumorale et/ou la cavité de résection sont délimitées en pointillés.

Adapté de (Muldoon et al., 2007).

La chirurgie représente la première étape du traitement des patients. Tous les chirurgiens s'accordent sur le fait que meilleure est la résection, meilleure est la survie. Néanmoins, il n'est pas toujours possible de réaliser une résection totale, l'étendue de l'exérèse et le volume tumoral résiduel sont souvent difficiles à évaluer et à améliorer du fait de l'importance physiologique du tissu sain environnant (Figure 36). Dans ce but, plusieurs stratégies ont été mises au point afin d'améliorer l'identification des bordures de la tumeur, telle que la fluorescence en per opératoire, et d'épargner les zones fonctionnelles, grâce à la cartographie cérébrale éveillée (Schucht et al., 2012).

Le traitement conventionnel des patients atteints de GBM se poursuit par le protocole de Stupp, qui repose sur l'association de radiothérapie et de chimiothérapie (Stupp et al., 2005). Plusieurs semaines après la chirurgie, une première phase de radio- et chimio- thérapie concomitantes débute à raison de 5 irradiations de 2 Gy (Grays) par semaine pendant 6 semaines, et de TMZ (temozolomide) pendant toute la durée de la radiothérapie. La chimiothérapie est ensuite poursuivie à raison de 5 jours par mois pendant 6 mois à une dose plus élevée (Stupp et al., 2005) (Figure 37).

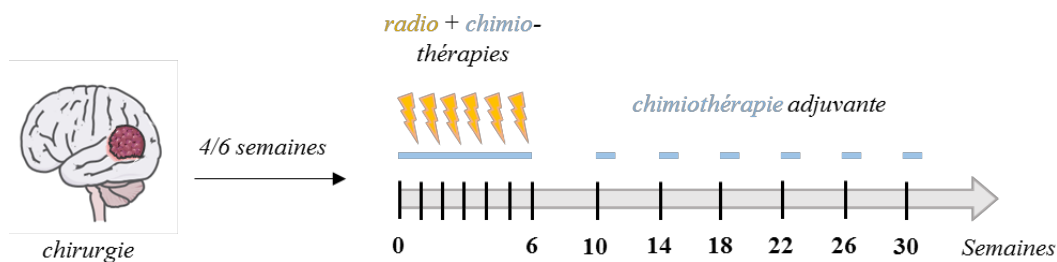


Figure 37 : Thérapie conventionnelle des patients atteints de GBM : le protocole de Stupp.

Après chirurgie, les patients subissent une première phase de radiothérapie (5j/sem pendant 6 sem) concomitante à la chimiothérapie (quotidienne pendant 6 sem), suivie d'une phase de chimiothérapie adjuvante (5j/mois). *Adapté de Stupp et al., 2005.*

Malgré ce traitement considéré comme « maximaliste », la médiane de survie n'excède pas 15 mois et la survie à 5 ans est seulement de 5,5 % (Ostrom et al., 2017; Stupp et al., 2005). Le GBM, comme toutes les tumeurs cérébrales, fait partie des cancers les plus difficiles à prendre en charge du fait de :

- L'infiltration des cellules tumorales et de l'importance d'épargner le tissu environnant, ce qui rend l'exérèse chirurgicale complète impossible,
- L'hétérogénéité intra-tumorale, qui se traduit par la présence de plusieurs sous-types moléculaires de GBM au sein d'une même tumeur,
- La présence de CSC (cellule souche cancéreuse), présentant une forte plasticité cellulaire et généralement résistantes au traitement standard (radio-chimiothérapie),
- Du microenvironnement tumoral, qui en plus d'être immunosuppresseur est souvent hypoxique et nécrotique.

Tous ces facteurs compliquent la prise en charge thérapeutique des patients et les mènent inexorablement vers la rechute (Figure 36). De nouvelles stratégies thérapeutiques sont donc nécessaires, et parmi elles l'immunothérapie fait l'objet de nombreuses études.

1.4 – Immunothérapie du GBM

Bien que plusieurs stratégies d'immunothérapies aient été envisagées et testées dans le GBM (vaccination, virothérapie, anticorps thérapeutiques ...), très peu sont actuellement préconisées pour le traitement des patients (Calinescu et al., 2015). Seul le Bevacizumab est utilisé en 3^{ème} ligne thérapeutique chez les patients en rechute prolongée (Taal et al., 2014).

Parmi les essais cliniques actuellement en cours dans le GBM, plusieurs sont basés sur le transfert adoptif de LT modifiés génétiquement pour exprimer un CAR.

En 2016, Brown et al., présentent le cas d'un patient atteint d'un GBM dans le lobe temporal droit et traité par injection intra-crâniale de CAR anti-IL-13R α (interleukine 13 receptor α) (Brown et al., 2016). Grâce à la pose d'un cathéter, 16 injections de CAR ont pu être réalisées en intra-cavitaire (dans la cavité de résection chirurgicale) et en intra-ventriculaire (dans le ventricule cérébral adjacent). Après 6 cycles d'infusion intra-cavitaire, la tumeur du lobe temporal avait presque totalement régressé. De plus, les injections intra-ventriculaires ont permis une diffusion des CAR hors du SNC conduisant à la régression de masses tumorales présentes le long de la colonne vertébrale. Malheureusement au bout de 7 mois, ce patient a rechuté avec l'apparition de nouvelles tumeurs IL-13R α négatives.

Des résultats similaires (une efficacité thérapeutique et une perte de l'expression de l'antigène cible) ont pu être observés dans une étude clinique réalisée sur une dizaine de patients traités par injection intraveineuse de CAR anti EGFRvIII (epithelial growth factor (EGF) receptor variant III) (O'Rourke et al., 2017).

Ces études ont notamment documenté la faisabilité et la sécurité de l'injection intra-crâniale de CAR chez ces patients. En effet, des quantités de CAR assez importantes ont pu être produites au grade GMP et leur injection n'a pas induit d'effets secondaires de grade 3 ou plus (Brown et al., 2016 ; O'Rourke et al., 2017).

2 - Article 2 : Stereotaxic administrations of allogeneic human V γ 9V δ 2 T cells efficiently control the development of human glioblastoma brain tumors

Ulrich Jarry^{a,b,*}, Cynthia Chauvin^{a,b,*}, Noémie Joalland^{a,b}, Alexandra Leger^{a,b}, Sandrine Minault^a, Myriam Robard^c, Marc Bonneville^{a,b}, Lisa Oliver^{a,b,d}, Francois M. Vallette^{a,b}, Henri Vie^{a,b}, Claire Pecqueur^{a,b}, and Emmanuel Scotet^{a,b}

^a INSERM, U892, Nantes, France, Univ Nantes, Nantes, France, CNRS, UMR 6299, Nantes, France ; ^b LabEx IGO, “Immunotherapy Graft Oncology”, Nantes, France ; ^c Cellular and Tissular Imaging Core Facility of Nantes University (MicroPICell), Structure Fédérative de Recherche François Bonamy, University of Nantes, Nantes, France ; ^d Hôtel Dieu, Hôpital de Nantes, Nantes, F-44000, France.

* These authors contributed equally to this work.

L’objectif de ce premier article est de fournir une justification préclinique pour les immunothérapies du GBM basé sur l’administration stéréotaxique de LT V γ 9V δ 2 humains allogéniques. La faisabilité et l’efficacité anti-tumorale d’injections stéréotaxiques de LT V γ 9V δ 2 ont été étudiées chez des souris porteuses de cellules tumorales humaines de GBM soit de lignée, soit de primocultures, injectées en orthotopique. Dans un premier temps, nous avons mis en évidence que les LT V γ 9V δ 2 humains allogéniques survivent et patrouillent pendant plusieurs jours dans le parenchyme cérébral, condition indispensable si l’on souhaite espérer une efficacité thérapeutique du transfert adoptif. Dans un second temps, nous avons démontré que la croissance, *in vivo*, des cellules tumorales de lignées est rapide et conduit au développement d’une masse tumorale très dense, ce qui est peu représentatif de la pathologie humaine. Cependant, l’utilisation de cellules primaires permet d’obtenir un modèle beaucoup plus proche du développement tumoral des patients, avec une croissance plus lente, une masse tumorale hétérogène et l’infiltration de cellules tumorales dans le parenchyme cérébral. L’efficacité de l’injection stéréotaxique de LT V γ 9V δ 2 humains allogéniques, combinée ou non au Zolédronate, a été évalués dans ces deux modèles. De façon très intéressante, une amélioration de la survie des souris et même l’élimination complète des cellules de GBM chez certains animaux sont observées. Ces données ouvrent la voie aux immunothérapies anti-tumorales optimisées basées sur l’injection stéréotaxique de LT V γ 9V δ 2 humains allogéniques chez les patients atteints de GBM.

Publié dans Oncoimmunology, 2016

ORIGINAL RESEARCH

Stereotaxic administrations of allogeneic human V γ 9V δ 2 T cells efficiently control the development of human glioblastoma brain tumors

Ulrich Jarry^{a,b,*}, Cynthia Chauvin^{a,b,*}, Noémie Joalland^{a,b}, Alexandra Léger^{a,b}, Sandrine Minault^a, Myriam Robard^c, Marc Bonneville^{a,b}, Lisa Oliver^{a,b,d}, François M. Vallette^{a,b}, Henri Vie^{a,b}, Claire Pecqueur^{a,b}, and Emmanuel Scotet^{a,b}

^aINSERM, U892, Nantes, France, Univ Nantes, Nantes, France, CNRS, UMR 6299, Nantes, France; ^bLabEx IGO, "Immunotherapy Graft Oncology", Nantes, France; ^cCellular and Tissular Imaging Core Facility of Nantes University (MicroPICell), Structure Fédérative de Recherche François Bonamy, University of Nantes, Nantes, France; ^dHôtel Dieu, Hôpital de Nantes, Nantes, F-44000, France

ABSTRACT

Glioblastoma multiforme (GBM) represents the most frequent and deadliest primary brain tumor. Aggressive treatment still fails to eliminate deep brain infiltrative and highly resistant tumor cells. Human V γ 9V δ 2 T cells, the major peripheral blood $\gamma\delta$ T cell subset, react against a wide array of tumor cells and represent attractive immune effector T cells for the design of antitumor therapies. This study aims at providing a preclinical rationale for immunotherapies in GBM based on stereotaxic administration of allogeneic human V γ 9V δ 2 T cells. The feasibility and the antitumor efficacy of stereotaxic V γ 9V δ 2 T cell injections have been investigated in orthotopic GBM mice model using selected heterogeneous and invasive primary human GBM cells. Allogeneic human V γ 9V δ 2 T cells survive and patrol for several days within the brain parenchyma following adoptive transfer and can successfully eliminate infiltrative GBM primary cells. These striking observations pave the way for optimized stereotaxic antitumor immunotherapies targeting human allogeneic V γ 9V δ 2 T cells in GBM patients.

Abbreviations: ADCC, antibody-dependent cellular cytotoxicity; BrHPP, bromohydrin pyrophosphate; CSCs, cancer stem cells; E:T, effector-to-target ratio; $\gamma\delta$ T cells, gamma delta T cells; GBM, glioblastoma multiforme; IPP, isopentenyl pyrophosphate; NBP, aminobisphosphonates; PAg, phosphoantigens

ARTICLE HISTORY

Received 6 January 2016
Revised 11 March 2016
Accepted 14 March 2016

KEYWORDS

Aminobisphosphonate; human glioblastoma; immunotherapy; mice model; V γ 9V δ 2 T cells

Introduction

GBM represents the most aggressive glioma (WHO grade IV) with a dismal prognosis (median survival of 9.4 mo and 2 y-mortality > 86%).¹ Surgery followed by radiotherapy and temozolomide-based chemotherapy represents the current standard of care for patients and modestly improves their median survival.² Moreover, rapid tumor relapse often takes place in the vicinity of the resected tumor³ and could be attributed to a high molecular/cellular heterogeneity in GBM combined with a diffuse and deep invasion of highly radio- and chemoresistant cell subsets,^{4,5} called cancer stem cells (CSC), which share phenotypic features with normal stem cells.^{6,7}

Chemotherapies remain associated with important toxicities and their efficiency is strongly reduced due to inadequate target drug delivery. In this context, immunotherapies represent effective therapeutic options with minimal toxicities.⁸ Cellular immunotherapies have been explored⁹ and could allow the elimination of deep brain infiltrative tumor cells. GBM-specific tumor antigens (Ag) recognized by $\alpha\beta$ T cells,¹⁰ stress-induced molecules activating $\gamma\delta$ T cells or specific surface molecules that can trigger ADCC have been identified and proposed for

effective immunotherapies in GBM.¹¹ Clinical trials have been performed by systemic or intracranial infusion of *ex vivo*-amplified T lymphocytes from either the GBM tumor, draining lymph nodes, or HLA-mismatched T cells from healthy donors,¹² but have had limited success. Post-resection administrations of selected GBM-reactive cytotoxic T cells in the vicinity of the primary tumor could represent a unique opportunity to deliver concentrated cellular immunotherapy directly to the site of residual malignancy.

V γ 9V δ 2 T cell, characterized by V δ 2 paired to V γ 9 chains TCR,¹³ represents about 5% of CD3⁺ cells in peripheral blood and more than 80% of the peripheral $\gamma\delta$ T cell population in healthy human.¹⁴ V γ 9V δ 2 T cells are rapidly activated during infection and tumor contexts associated with strong functional responses (e.g., proliferation, cytotoxicity, cytokine release).¹⁵ The antigenic activation of V γ 9V δ 2 T cells is both a species-specific and cell-to-cell contact-dependent process that requires the engagement of the $\gamma\delta$ TCR complex. Most V γ 9V δ 2 T cells are specifically activated by small organic pyrophosphate molecules (phosphoantigens (PAg)) such as isopentenyl pyrophosphate (IPP), which could be produced endogenously as

intermediates of the mammalian mevalonate pathway. PAg can accumulate intracellularly upon cell distress induced by transformation or infection events. Aminobisphosphonate (NBP), a pharmacologic inhibitor of the mevalonate pathway, increases IPP levels in cells with elevated pinocytotic activity and/or deregulated metabolism such as tumor cells. NBP efficiently sensitize tumor cells for V γ 9V δ 2 T cell recognition *in vitro*, a process regulated by both adhesion (e.g., ICAM-1) and NK receptors (e.g., NKG2D) axes. Zoledronate (Zometa[®]; GMP-grade) is a third generation NBP compound used in humans for the treatment of bone disorders (e.g., metastases from solid tumors).¹⁶

The antitumor functions and the physiological roles played by human $\gamma\delta$ T cells *in vivo* have been severely hampered due to: (i) the lack of V γ 9V δ 2 T cell counterparts in non-primate species, (ii) the lack of tumor models in non-human primates, and (iii) the strict species-specificity requirements for antigenic activation.¹⁵ Both passive and active immunotherapies targeting $\gamma\delta$ T cells in cancer patients have yielded encouraging clinical responses.¹⁷ Passive cancer immunotherapies are based on adoptive transfers of PBL-V γ 9V δ 2 T cells previously amplified using both GMP-grade agonist compounds and IL-2, while active immunotherapy aims at directly activating and expanding V γ 9V δ 2 T cells *in vivo* by using administrations of GMP-grade agonist compounds and IL-2. Under these conditions, most side effects are attributed to the toxicity of IL-2, used at high doses to support the peripheral expansion of $\gamma\delta$ T cells.

Our group has recently shown that combined administration of NBP and allogeneic *ex vivo*-amplified human V γ 9V δ 2 T cells efficiently controls the development of *sc* tumors in xenografted mice.¹⁸ Moreover, NBP-treated human glioma tumor cells are efficiently recognized by V γ 9V δ 2 T cells^{19,20} illustrating the practicality of using human $\gamma\delta$ T cells as an attractive tool for immunotherapies of GBM. In this study, we have investigated the feasibility and the antitumor efficacy of local allogeneic V γ 9V δ 2 T cell immunotherapies in murine models of orthotopic human GBM tumors using commercial cell line (U-87MG) and highly infiltrative primary GBM cells (GBM-10).

Materials and methods

Expansions of human V γ 9V δ 2 T cells

Human PBMCs were isolated from informed consented healthy blood donors obtained from the Etablissement Français du Sang (Nantes, France). For specific expansions of V γ 9V δ 2 T cells, PBMCs were incubated with 3 μ M BrHPP (bromohydrin pyrophosphate), kindly provided by Innate Pharma (Marseille, France) in RPMI supplemented with 10% heat inactivated FCS, 2 mM L-glutamine, 10 mg/mL streptomycin, 100 IU/mL penicillin (all from Gibco, Carlsbad, CA) and 100 IU/mL recombinant human IL-2 (rhIL-2) (Chiron, Emeryville, CA). 4 d cultures were supplemented with rhIL-2 (300 IU/mL). Specific amplification of V δ 2⁺ T cells was estimated by flow cytometry (resting V γ 9V δ 2 T cell lines purity > 85–95% (Fig. S1)).

Immunodeficient mice

NSG (*NOD.Cg-Prkdcscid Il2rgtm1Wjl/SzJ*) mice (Charles River Laboratories; Wilmington, MA), were bred in the animal facility of the University of Nantes (UTE, SFR F. Bonamy) under SPF status and used at 6–12 weeks of age, accordingly to institutional guidelines (Agreement # 00186.02; Regional ethics committee of the Pays de la Loire (France)).

Human GBM tumor cells

U-87MG cell line (HTB-14TM, ATCC, Manassas, VA) was cultured in DMEM low glucose (Gibco) supplemented with 10% heat inactivated FCS, 2 mM L-glutamine, 10 mg/mL streptomycin and 100 IU/mL penicillin. GBM-10 primary culture was grown in defined medium (DEF) containing DMEM/Ham-F12 (Gibco) supplemented with 2 mM L-glutamine, N2 and B27 supplements (Gibco), 2 μ g/mL heparin (Sigma-Aldrich, Louis, MO), 20 ng/mL EGF (Peprotech, Rocky Hill, NJ), 25 ng/mL bFGF (Peprotech), 10 mg/mL streptomycin and 100 IU/mL penicillin.

Stereotaxic implantation of human GBM and T cells in mouse

Human GBM cells (10⁴ in 2 μ L PBS) were injected using a stereotaxic frame (Stoelting, Wood Dale, IL) at 2 mm on the right of the medial suture and 0.5 mm in front of the bregma, depth: 2.5 mm. For *in vivo* sensitization assay, 0.4 or 1 μ g of zoledronate were injected into the tumor bed of 14 d tumor bearing mice. For adoptive T cell transfer assays, 2 \times 10⁷ human V γ 9V δ 2 T cells were stereotaxically injected, either in 10 μ L sterile PBS or 40 μ g/mL zoledronate solution (Zometa[®]; Novartis, Basel, Switzerland), into the GBM tumor bed, 7 (1 injection) or 7 and 14 d (2 injections) after tumor implantation.

Flow cytometry

For cell surface staining, human GBM cells were incubated with 10 μ g/mL of APC-labeled anti-human CD44 mAb (clone G44-26; BD Biosciences, Franklin lakes, NJ), PE-Cy5-labeled anti-human CD90 mAb (clone Thy1/310; Beckman Coulter, Fullerton, CA), PE-labeled anti-human CD133 mAb (clone AC133; Myltenyi Biotec, Bergisch-Gladbach, Germany), AF488-labeled anti-human SSEA1 mAb (clone MC480, BD Biosciences) or associated isotype controls. For intracellular staining, human GBM cells were permeabilized, incubated with anti-human Nestin mAb (clone 10C2, Millipore, Billerica, MA), anti-human Olig2 mAb (clone ab81093, Abcam, Cambridge, UK), anti-human Tuj polyclonal Rabbit Ab (Sigma-Aldrich), anti-human GFAP mAb (clone 52, BD Biosciences) or associated isotype controls, followed with secondary staining with AF488-labeled or AF647-labeled antibodies. Acquisition was performed using a FACSCalibur flow cytometer (BD Biosciences) and the events were analyzed using the FlowJo software (Treestar, Ashland, OR).

Limiting dilution assay (LDA)

For LDA analysis, cells were dissociated and seeded at an initial concentration of 2 \times 10³ cells / mL from which serial dilutions

were performed in 96-well plate. Cells were cultured for 15 d, after which the fraction of wells that did not contain neurospheres for each cell-plating density was calculated as described by Das and colleagues.²¹

Immunohistochemistry (IHC) analysis

Brains were fixed with 4% paraformaldehyde-PBS, embedded in paraffin wax and serially sectioned. Sections were incubated with 2% BSA and then with polyclonal Rabbit anti-human CD3 Ab (Dako, Agilent Technologies, Santa Clara, CA) or rabbit anti-human MHC class I Ab (clone EPR1394Y; Abcam). Revelation was performed by using polymer histofine rabbit to mouse coupled to HRP (Microm Microtech France, Francheville, France) and DAB detection system (Leica, Wetzlar, Germany). Slides were scanned using the NanoZoomer 2.0 HT (Hamamatsu Photonics K.K., Hamamatsu, Japan).

Isolation and staining of fresh brain cells

For human T cell detection assays, cells collected from the brains, by using the adult brain dissociation kit (Myltenyi Biotech), were labeled with PE-labeled anti-human CD3 mAb (clone UCHT1; Beckman Coulter) and analyzed by flow cytometry. For GBM cells isolations, cells were collected from the brains by using the human tumor dissociation kit (Myltenyi Biotech) followed by a discontinuous 30/70% isotonic Percoll gradient (Sigma-Aldrich)²² and isolated by using anti-human HLA mAb (clone w6/32; BioXCell, West Lebanon, NH) and the “CELLlection™ Pan Mouse IgG Kit” (Gibco), accordingly to the manufacturer’s instructions. Cell purity was assessed by flow cytometry using APC-labeled mouse anti-human HLA-ABC mAb (clone G46–2.6; BD Biosciences) and routinely rated higher than 85%. Isolated cells were then used for *in vitro* functional assays.

In vitro functional assays

Cultured or mouse brain isolated human GBM cells were pre-treated 16 h with zoledronate (at the indicated concentrations). For CD107a surface mobilization assays, GBM cells were co-cultured 0, 24 or 72 h after zoledronate-sensitization, with V γ 9V δ 2 T cells (E/T ratio: 1/1) in culture medium containing 5 μ M monensin (Sigma) and APC-labeled anti-human CD107a mAb (clone H4A3; BD Biosciences) for 4 h. V γ 9V δ 2 T cells were then labeled with FITC-labeled anti-human V δ 2 TCR mAb (IMMU389; Beckman Coulter) and analyzed by flow cytometry. For cytolytic activity assays, GBM cells were incubated 1 h with ⁵¹Cr (2,77 μ Ci / 10⁶ cells), washed and co-cultured 4 h with V γ 9V δ 2 T cells (E/T ratio: 10/1). ⁵¹Cr release activity was measured in supernatants using a MicroBeta counter (PerkinElmer, Waltham, MA). Percentage of tumor target cell lysis = (experimental release – spontaneous release)/(maximum release – spontaneous release) \times 100. Maximum and spontaneous releases were determined by adding 1% Triton X-100 or medium respectively, to ⁵¹Cr-labeled tumor target cells in the absence of T cells.

Statistical analysis

Data are expressed as mean \pm SEM and were analyzed using GraphPad Prism 6.0 software (GraphPad Software, Inc., San Diego, CA). *In vitro* dose-response experiments were analyzed by calculating log effective concentration 50% (logEC50) using nonlinear regression and variable slope. Student’s *t* (**p* < 0.05; ***p* < 0.005; ****p* < 0.0005) or log rank tests (see indicated *p* value) were used to reveal significant differences.

Results

Adoptively-transferred human PBL V γ 9V δ 2 T cells survive and patrol within the brain

We aimed to evaluate whether V γ 9V δ 2 T cells, amplified from PBLs of healthy donors, survived and moved within the brain parenchyma following a stereotaxic injection. Then, IHC analysis of human CD3 expression was performed on sections prepared from the brains of NSG mice previously injected with resting V γ 9V δ 2 T cells (2 \times 10⁶ cells). As expected, at day 1, CD3⁺ T cells were preferentially localized in the brain tissue surrounding the injection site (Fig. 1A). Interestingly, at day 7 those cells were detected not only in the regions adjacent to the injection site (Fig. 1B, upper panel), but also in the second brain hemisphere that did not receive $\gamma\delta$ T cell injection (Fig. 1B, lower panel). Cytometry analysis, performed on cells isolated from mice stereotaxically injected with V γ 9V δ 2 T cells (10⁷ cells), showed high frequency values of CD3⁺ T cells on day 1 (40 \pm 8% of total isolated brain cells) which progressively decreased to reach 8% at day 7 (32 \pm 3% and 8 \pm 2% on day 3 to day 7, respectively) (Fig. 1C). Moreover, CD3⁺ T cells isolated from the mouse brains could also be activated and expanded, following sorting and antigenic stimulation, indicating that T lymphocytes can survive within the brain (*data not shown*). Similar results were obtained using $\gamma\delta$ T cells prepared from different healthy donor samples but also using human $\alpha\beta$ T cells. These results indicate that resting human V γ 9V δ 2 T cells, amplified from PBLs of healthy donors, can survive and patrol within mouse brain parenchyma for several days following their stereotaxic injection.

Human allogeneic V γ 9V δ 2 T cells react against U-87MG tumor cells

Based on these physiological features and their unique intrinsic characteristics, cytotoxic V γ 9V δ 2 T lymphocytes represent attractive effector candidates for immunotherapies against GBM, especially for the eradication of highly resistant and infiltrative brain tumor cells. The antitumoral reactivity of human allogeneic V γ 9V δ 2 T cells against the prototypical commercially available U-87MG human glioma cell line was analyzed *in vitro* (⁵¹Cr-release assays) (Fig. 2A). As expected, no natural reactivity of allogeneic V γ 9V δ 2 T cells against U-87MG cells was detected and zoledronate pre-treatments of U-87MG induced a significant V γ 9V δ 2 T cells dose-dependent antigenic activation (logEC₅₀ = 0.12 μ M). Similar reactivity patterns were established by measuring CD107a expression and IFN γ production in co-culture assays (Fig. S2A and S2B). Blocking assays performed using the antagonist 103.2 mAb,²³ indicate

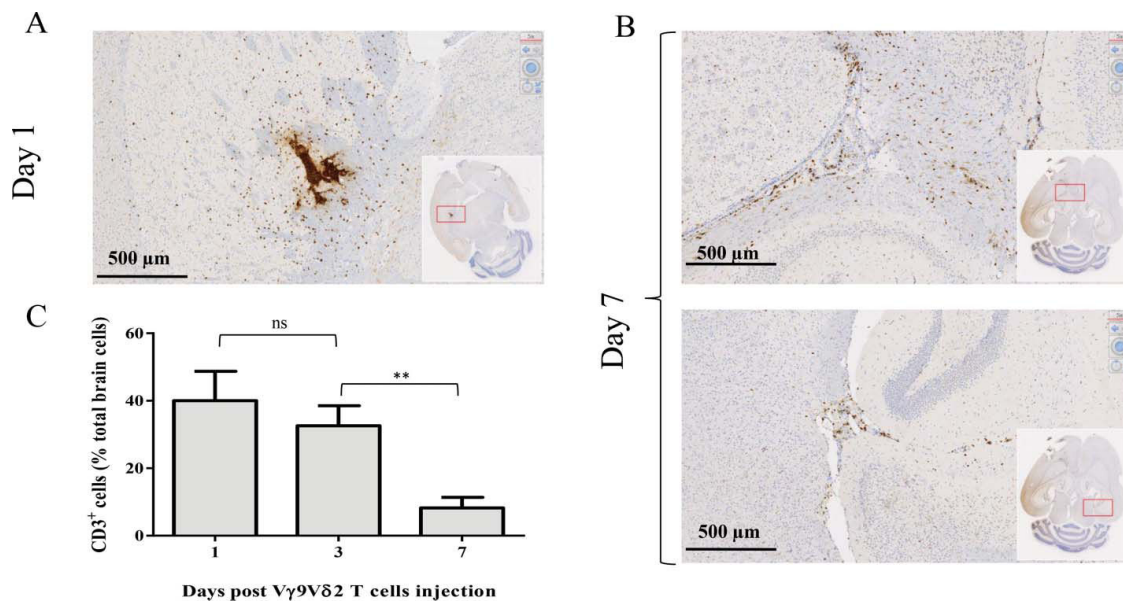


Figure 1. Human V γ 9V δ 2 T cells survive and patrol within the brain of NSG mice. NSG mice underwent intracranial injection of 2×10^6 (A–B) or 10^7 V γ 9V δ 2 T cells (C). Human-CD3 expression was analyzed by IHC on brain sections on days 1 (A) and 7 (B), or by flow cytometry on brain cells on days 1, 3 and 7 (C). Results are expressed as % of CD3⁺ cells among total brain cells (mean \pm SEM, $n = 3$; ns: not significant, ** $p < 0.005$).

that BTN3A/CD277 molecules expressed by these GBM tumor cells mainly contribute to the antigenic reactivity of human V γ 9V δ 2 T cells (Fig. S3). As expected, NK (CD3⁻CD56⁺) and $\alpha\beta$ T cells, which frequently contaminate the amplified peripheral V γ 9V δ 2 T cells preparations (~5–10%), were not activated by untreated or zoledronate treated U-87MG (*data not shown*).

To determine the duration and stability of zoledronate sensitizations, the activation of V γ 9V δ 2 T cells was assessed at increasing time points following U-87MG zoledronate treatments. CD107a expression on V γ 9V δ 2 T cells did not vary during the first 24 h post-treatment, while a marked reduction was measured when GBM tumor cells were sensitized with 0.1, 0.5 or 1 μ M of zoledronate 72 h before co-culture (Fig. 2B). No significant modulation was detected for high doses of zoledronate (5 and 10 μ M). This indicates that the dose-dependent sensitization step, though transient, can last for several days. We further investigated whether zoledronate efficiently sensitizes human GBM cells *in vivo* to V γ 9V δ 2 T cell recognition. Two weeks after brain implantation of U-87MG cells, the mice received stereotaxic injections of zoledronate (0.4 μ g vs. 1 μ g). After 24 h, tumor cells were collected and used in *in vitro* functional assay. Only U-87MG tumor cells isolated from zoledronate-injected mice strongly activated V γ 9V δ 2 T cells (Fig. 2C). As a control, no effect was observed with the MHC class I-specific mAb (clone w6/32), used for human GBM cells sorting. This indicates that human allogeneic V γ 9V δ 2 T cells can strongly react against zoledronate sensitized human GBM cells and that this reactivity can last for several days.

Adoptively-transferred allogeneic V γ 9V δ 2 T cells eradicate U-87MG cells *in vivo*

We next investigated whether allogeneic human V γ 9V δ 2 T cells react against human GBM tumor cells *in vivo*. Following orthotopic implantation of U-87MG cells, mice were treated with either one (day 7) or two cycles (days 7 and 14) of

stereotaxic injections of V γ 9V δ 2 T cells and/or zoledronate (Fig. 2D). Untreated mice died within 40 d after tumor grafting (median survival = 27 d) (Fig. 2E) with no significant delay after injection(s) of either zoledronate or V γ 9V δ 2 T cells alone. However, a single combined co-administration of zoledronate and V γ 9V δ 2 T cells already improved the survival of approximately 50% of the treated mice and most of GBM tumor-bearing mice survived after the successive co-administration of zoledronate and V γ 9V δ 2 T cells. Interestingly, no tumor cell was detected in mice brain by IHC at day 90, indicating a complete tumor rejection (*data not shown*). Then stereotaxic administration(s) of human allogeneic V γ 9V δ 2 T cells efficiently eradicates orthotopic human GBM tumors *in vivo* and also highlights the opportunity to target allogeneic specific cytotoxic human cells for immunotherapies against GBM.

Primary human GBM cells as cellular tools for the establishment of physiological orthotopic GBM mouse models

One of the main limits of *in vivo* models established with cell lines is their relative homogeneity associated with the establishment of a compact and poorly invasive tumor while the main clinical features of human GBM is their cellular heterogeneity associated with a very invasive character. An alternative of human GBM cell lines is to use primary cells isolated from human tumor fragments screened, selected²⁴ and grown under defined media to maintain cellular heterogeneity. Then, primary GBM-10 cells grow as spheres and express high levels of “stemness” markers (e.g., CD133, CD90, CD44) (Fig. 3A). Furthermore, limiting dilution and cell differentiation assays, to determine the presence of CSC, showed that ~25% of this primary GBM cells are able to give rise to new neurospheres (Fig. 3B). Furthermore, the cells lost the expression of “stemness” markers, such as Nestin, CD133 and SSEA1 upon serum-induced differentiation (Fig. 3C), while expression of the

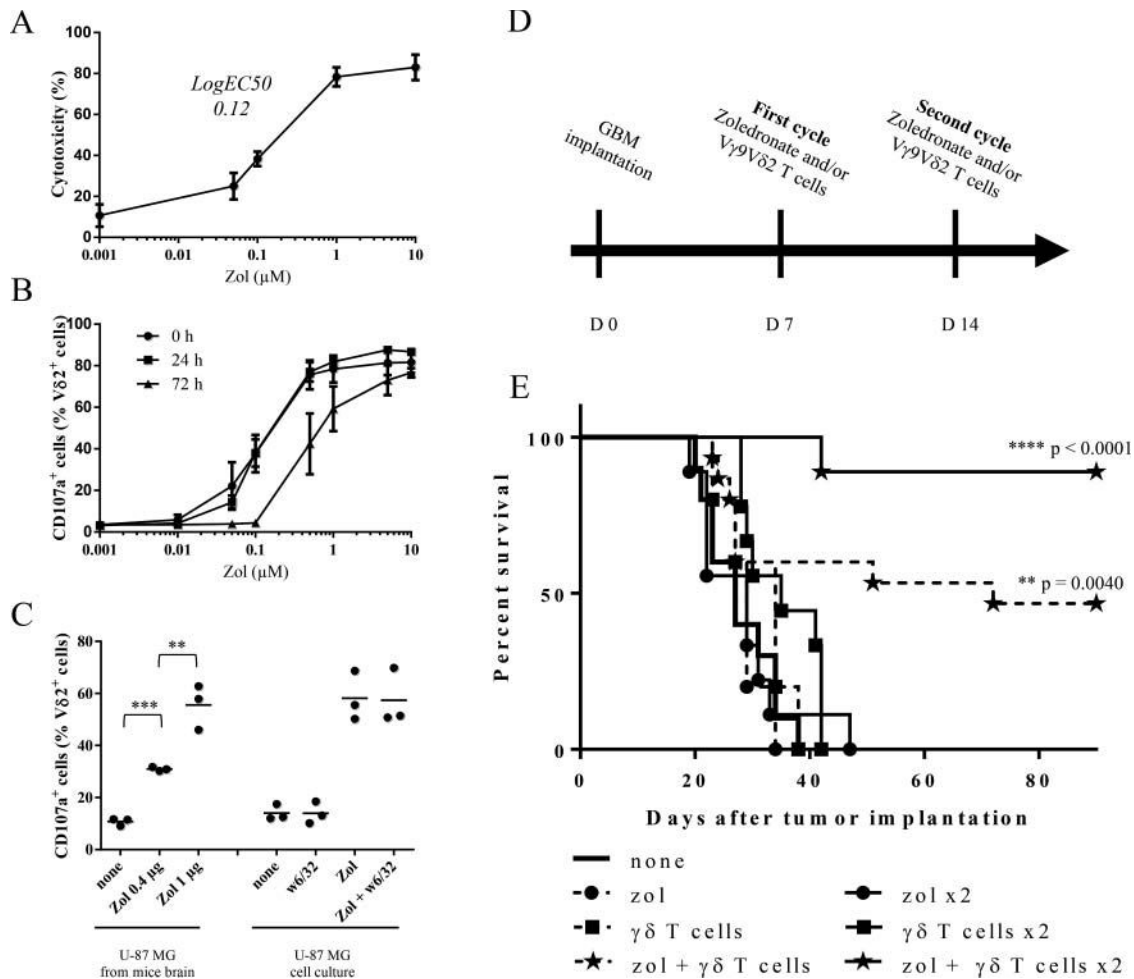


Figure 2. Human allogeneic $V\gamma 9V\delta 2$ T cells react against U-87MG tumor cells *in vitro* and eradicate U-87MG cells *in vivo*. (A–B) U-87MG cells were pretreated overnight with different concentrations of zoledronate. (A) After zoledronate pretreatment, cells were loaded with ^{51}Cr and co-cultured 4 h with $V\gamma 9V\delta 2$ T cells (E/T ratio: 10/1). ^{51}Cr release was measured in culture supernatants. Results are expressed as % cytotoxicity (mean \pm SEM, $n = 3$). (B) 0, 24 or 72 h after zoledronate pretreatment, U-87MG cells were co-cultured 4 h with $V\gamma 9V\delta 2$ T cells (E/T ratio: 1/1). $V\gamma 9V\delta 2$ T cells were analyzed by flow cytometry for CD107a expression. Results are expressed as % of positive cells among $V\delta 2^+$ cells (mean \pm SEM, $n = 3$). (C) U-87MG brain tumor-bearing NSG mice were injected at day 14 with zoledronate (0.4 μg or 1 μg). One day later, tumor cells were magnetically isolated using w6/32 mAb and co-cultured 4 h with $V\gamma 9V\delta 2$ T cells (E/T ratio: 1/1). $V\gamma 9V\delta 2$ T cells were analyzed by flow cytometry for CD107a expression. U-87MG cells cultured *in vitro* and pretreated or not with zoledronate (10 μM), in presence or absence of the w6/32 mAb, were used as control. Results are expressed as % of positive cells among $V\delta 2^+$ cells (mean \pm SEM, $n = 3$; ** $p < 0.005$, *** $p < 0.0005$). (D–E) U-87MG brain tumor-bearing NSG mice were treated, or not (—; $n = 10$), with single injection (day 7) of zoledronate (—●—; $n = 5$), $V\gamma 9V\delta 2$ T cells (—■—; $n = 5$) or both (—★—; $n = 15$), or with double injections (days 7 and 14) of zoledronate (—●—; $n = 9$), $V\gamma 9V\delta 2$ T cells (—■—; $n = 9$) or both (—★—; $n = 9$). Statistical analysis was performed by log rank-test compared with control (see the indicated p value).

differentiation markers GFAP, TUJ and Olig-2 were significantly increased (Fig. 3D). Finally, stereotaxic implantation in NSG mice of GBM-10 cells led to a disseminated (some tumor cells detected in the second non-injected hemisphere) and slow-growing brain tumors (Fig. 4), as opposed to U-87MG cells that rapidly grow to form a compact well-defined tumor mass. These results indicate that heterogeneous human GBM-10 primary cells, containing a fraction of CSC, can reproduce physiological features of human GBM and represent a tool for establishing a robust orthotopic GBM model in mouse.

Adoptively-transferred allogeneic human $V\gamma 9V\delta 2$ T cells efficiently eliminate invasive GBM-10 primary tumor cells

The direct reactivity of allogeneic human $V\gamma 9V\delta 2$ T cells against primary GBM-10 tumor cells was next assessed *in vitro*. As for U-87MG cells, $V\gamma 9V\delta 2$ T cells did not naturally react against

GBM-10 tumor cells, while zoledronate triggered a strong and dose-dependent antigenic activation of these effectors (Fig. 5A). Of note, higher doses of zoledronate were required to sensitize primary GBM-10 cells ($\text{logEC}_{50} = 6.20 \mu\text{M}$ and maximal cytotoxicity at 10 μM), as compared to U-87MG cells. Similar reactivity features were established for CD107a expression and IFN γ production (Figs. S2C, S2D and S3). Next, the ability of $V\gamma 9V\delta 2$ T cells to react against GBM-10 cells was evaluated *in vivo*. GBM-10 bearing-NSG mice were treated with one (day 7) or two cycles (days 7 and 14) of stereotaxic administrations of allogeneic human $V\gamma 9V\delta 2$ T cells and/or zoledronate. Untreated mice died within 60 d (median survival = 54.5 d) and no significant variation was measured after single/double stereotaxic injection(s) of either zoledronate or $V\gamma 9V\delta 2$ T cells alone (Fig. 5B). Importantly, single and also double administrations of zoledronate and $V\gamma 9V\delta 2$ T cells strongly improved the survival of mice (respectively 20 and 70%). As for U-87MG model, no

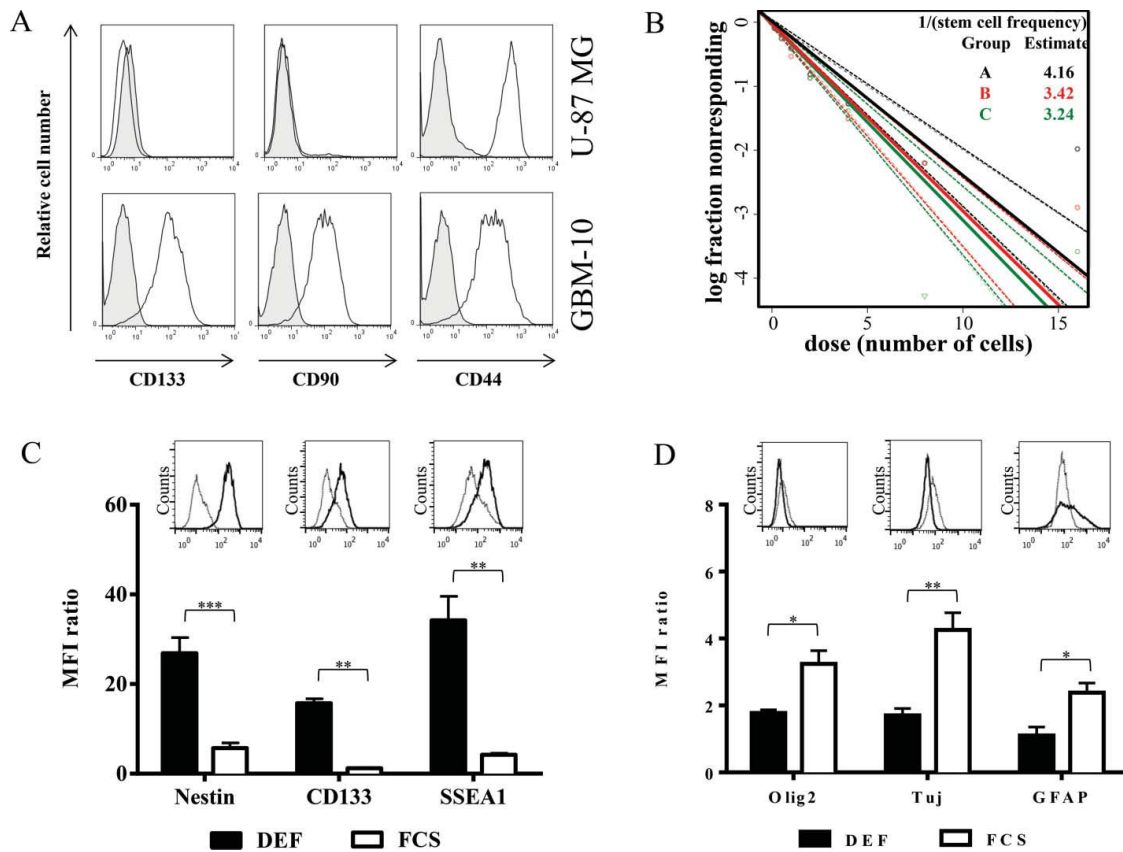


Figure 3. Primary GBM-10 cells as cellular tools for the establishment of a physiological orthotopic human GBM graft model in NSG mice. (A) U-87MG cells and GBM-10 cells were analyzed by flow cytometry for CD133, CD90 and CD44 expression. Gray histograms correspond to isotype control mAbs. (B) GBM-10 cells were seeded with an initial concentration of 2×10^3 cells/mL in 96-well plate. 15 d later the fraction of wells not containing neurospheres for each cell-plating density was calculated. (C–D) GBM-10 primary cells were cultured in DEF or in medium containing FCS and were analyzed by flow cytometry for the Nestin, CD133, SSEA1 (C), Olig2, Tuj and GFAP expression (D). Results are expressed as the median fluorescence intensity (MFI) ratio (MFI test/isotype control) (mean \pm SEM, $n = 3$; * $p < 0.05$, ** $p < 0.005$, *** $p < 0.0005$). Inserts show representative histograms from one experiment of three performed.

tumor cell was detected in brain by IHC at day 200, indicating that tumor rejection seemed complete (*data not shown*). Altogether, these results indicate that stereotaxic administration(s) of allogeneic human $V\gamma 9V\delta 2$ T cells *plus* zoledronate efficiently eliminate heterogeneous primary human GBM tumors characterized by “stemness” and invasive properties.

Discussion

Adoptive transfer of tumor-specific T lymphocytes represent promising approaches to efficiently cure malignant infiltrative brain tumors with limited deleterious effect on healthy cells.⁸ Using orthotopic xenograft mouse models of human GBM cells from either commercially available cell lines or primary GBM cells, our study indicates that stereotaxic administrations of allogeneic *ex vivo*-amplified human $V\gamma 9V\delta 2$ T cell effectors *plus* zoledronate efficiently eradicate brain tumors.

Our results support that cytotoxic human T cells efficiently eliminate most residual tumoral cells which have deeply infiltrated the brain parenchyma, including highly resistant GBM CSC.²⁵ CSC may be involved in tumor recurrence, due to their ability to both infiltrate brain parenchyma and to resist to aggressive chemo- and radiotherapy.²⁶ GBM-10 primary cells, isolated from a fresh biopsy and cultured in defined media maintain the cellular heterogeneity and especially the presence of CSC,²⁴ have been used for establishing new and robust

human GBM xenograft mouse model. In contrary to U-87MG cell line triggering a compact and homogenous tumor mass, primary GBM-10 cells are highly infiltrative and exhibiting typical morphological features of human GBM,²⁷ representing new tools for establishing the next-generation animal models of human GBM tumors.

$V\gamma 9V\delta 2$ T lymphocytes, the most frequent and conserved human peripheral $\gamma\delta$ T cell subset in adults,^{15,28} react against a wide range of tumor cell targets.¹⁵ Both active and passive $V\gamma 9V\delta 2$ T cell immunotherapies have been considered for patients with solid or circulating malignancies.¹⁷ While yielding promising results, these phase 0/I trials revealed some issues that will need to be resolved, such as the reduced reactivity of $V\gamma 9V\delta 2$ T cells against fresh tumors and their possible exhaustion in some patients. Importantly, as for some other non-conventional T cell subsets, the antigenic activation process of $V\gamma 9V\delta 2$ T cells is TCR- and contact-dependent, involving the expression of key molecules (eg., PAg and butyrophilins),²⁹ but not restricted by MHC class I/II molecules, then eliminating any risk of deleterious direct alloreactive responses toward non-transformed cells.^{30,31} Therefore, the constitution of clinical allogeneic human $V\gamma 9V\delta 2$ T cell banks, established from healthy donors, could represent a unique opportunity for designing adoptive transfer antitumor immunotherapies. Administration of effector T cells could be further hampered by the particular immunological status of the central nervous

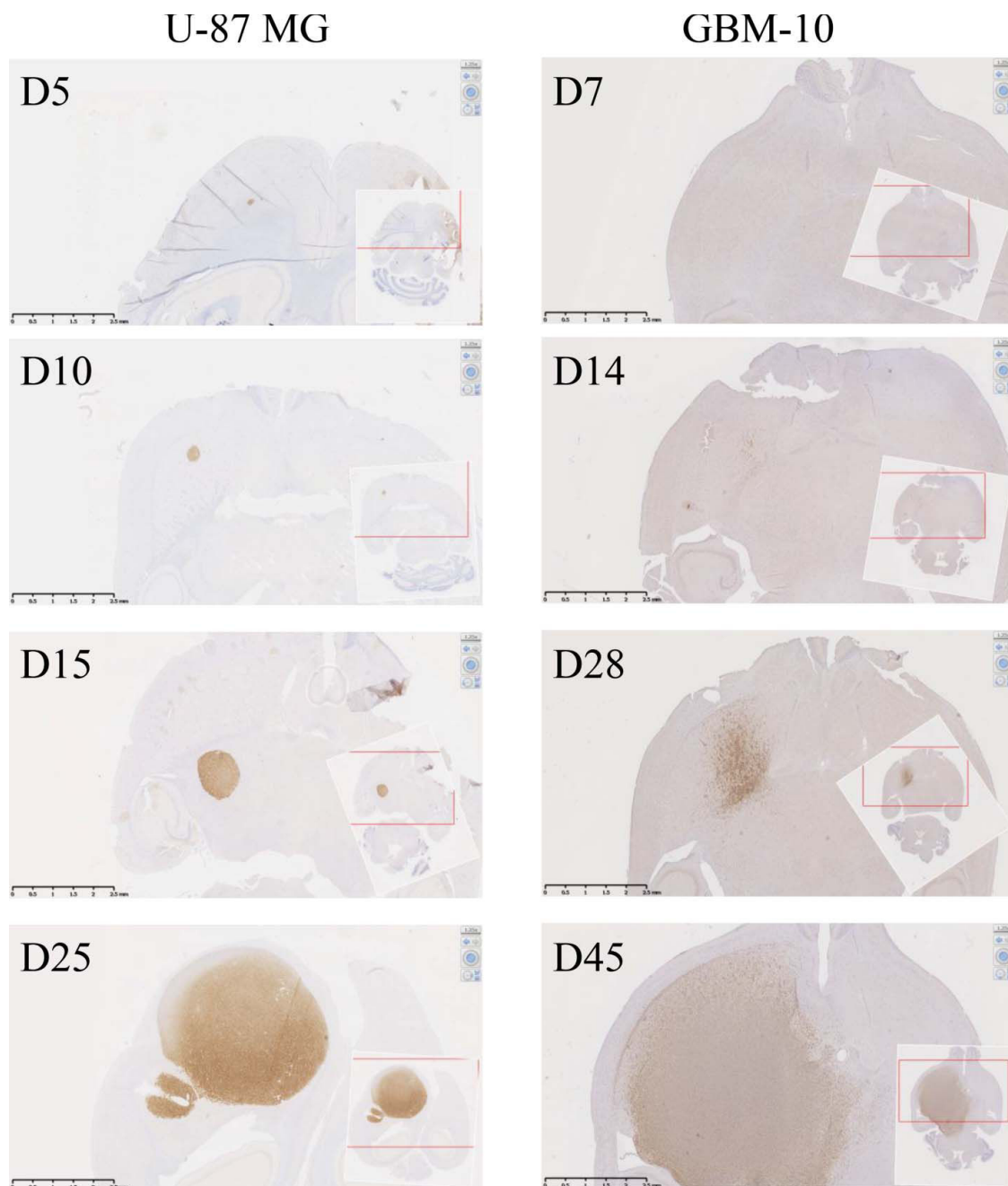


Figure 4. *In vivo* development of orthotopic human-GBM brain model in NSG mice. Human-MHC class I expression was analyzed by IHC on NSG mouse brain sections performed at days 5, 10, 15 and 25 after U-87MG brain implantation (left pictures) or at days 7, 14, 28 and 45 after GBM-10 implantation (right pictures).

system, notably characterized by the presence of the blood-brain barrier (BBB) and the absence of classical lymphatic drainage system,^{32,33} then limiting T cell trafficking within the brain parenchyma and representing an additional obstacle to intravenous injections. Clinical trials of adoptive immunotherapy of GBM with human T lymphocytes were based on either intravascular or intracavitary administrations.³⁴⁻³⁶ However, the survival and activity of T cells within the cerebro-spinal fluid remains unclear as no studies have been performed to describe their behavior or their ability to move and infiltrate the brain parenchyma. Our approach is based on the direct injection of allogeneic amplified $\gamma\delta$ T cells in the parenchyma, all around the resection cavity. Such per-operative administrations are already carried out during surgery delivering local

chemo- or gene-therapies to GBM patients.³⁷ Supporting this possibility, this study unambiguously shows that a significant fraction of $V\gamma 9V\delta 2$ T cells survive for several days following a stereotaxic injection into the mouse brain parenchyma and subsequently deeply infiltrate brain tissue. Both *in vitro* and *in vivo* assays were carried out with dose-dependent zoledronate sensitizations of a GBM cell line and primary human GBM cells in order to trigger strong $V\gamma 9V\delta 2$ T cell recognition, as already used for enhancing such reactivities in other oncological contexts.³⁸ Phase I/II trials³⁹ have shown that zoledronate, indicated for other human pathologies (eg. osteoporosis, multiple myeloma),⁴⁰ leads to significant IL-2-dependent $\gamma\delta$ T cell expansions, correlating to partial or complete clinical responses, thus indicating the feasibility and efficacy of this

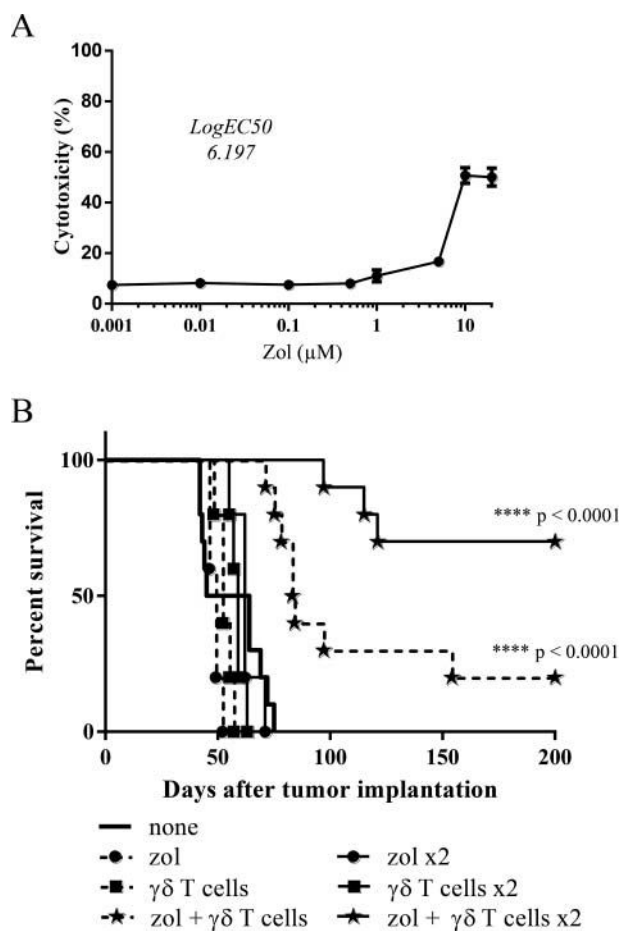


Figure 5. Adoptively-transferred allogeneic $V\gamma 9V\delta 2$ T cells efficiently eliminate invasive GBM-10 primary tumor cells (A) GBM-10 cells were pretreated overnight with different concentrations of zoledronate, loaded with ^{51}Cr and then co-cultured 4 h with $V\gamma 9V\delta 2$ T cells (E/T ratio: 10/1). ^{51}Cr release was measured in culture supernatants and the results are expressed as % cytotoxicity (mean \pm SEM, $n = 3$). (B) Survival curves of GBM-10 brain tumor-bearing NSG mice treated, or not (—; $n = 10$), with single injection (day 7) of zoledronate (---; $n = 7$), $V\gamma 9V\delta 2$ T cells (---■---; $n = 7$) or both (---★---; $n = 10$), or with double injections (days 7 and 14) of zoledronate (—●—; $n = 7$), $V\gamma 9V\delta 2$ T cells (—■—; $n = 7$) or both (—★—; $n = 10$). Statistical analysis was performed by log-rank test compared with control (see the indicated p value).

approach in some cancer patients. Preclinical approaches suggested that NBP-injection could be combined with $V\gamma 9V\delta 2$ T cells administration in order to induce/enhance their antitumor reactivity.¹⁸ As zoledronate does not cross the BBB,⁴¹ administrations for GBM immunotherapies required direct brain injections. As expected, stereotaxic administrations of zoledronate and $V\gamma 9V\delta 2$ T cells did not induced deleterious effects in mice.⁴² The toxicity of such effective antitumor associations cannot be ruled out in GBM patients and will need to be extensively investigated. Some studies have described that zoledronate, like some other bisphosphonate molecules, might induce the depletion of macrophages⁴³ and act on microglia,⁴⁴ the main brain myeloid-immune cells. Then, to avoid the use of zoledronate it might be interesting to select particular $V\gamma 9V\delta 2$ T cells that could naturally and specifically react more efficiently against GBM cells.

In conclusion, this study highlights the feasibility and the antitumor effect of immunotherapies based on local administrations of allogeneic human $V\gamma 9V\delta 2$ T cells using novel and

robust orthotopic human GBM *in vivo* models. Altogether, these results demonstrate that adoptive allogeneic immunotherapies could represent a promising and effective approach for the treatment of human GBM that remains one of the faster spreading and deadliest cancers.

Disclosure of potential conflicts of interest

No potential conflicts of interest were disclosed.

Acknowledgments

We thank the staff of University Hospital animal facility of Nantes for animal husbandry and care, the cellular and tissular imaging core facility of Nantes university (MicroPICell) for imaging, and the Cytometry Facility Cytocell from Nantes for their expert technical assistance. We thank also F. Cadeau and R.N. Hellman for the correction of the manuscript.

Funding

This work has been supported by INSERM, CNRS, Université de Nantes, Association pour la Recherche contre le Cancer (#R10139NN), Institut National du Cancer (#V9V2THER, INCa #PLBio2013-201, #PLBio2014-155), Agence Nationale de la Recherche (ANR, #GDSTRESS), Ligue Nationale contre le Cancer (AO InterRegional 2012). This work was realized in the context of the LabEX IGO and the IHU-Cesti programs, supported by the National Research Agency Investissements d'Avenir via the programs ANR-11-LABX-0016-01 and ANR-10-IBHU-005, respectively. The IHU-Cesti project is also supported by Nantes Metropole and the Pays de la Loire Region. The authors declare no competing financial interests. M.B. is currently vice president of the Institut Mérieux (Institut Mérieux, Lyon, F-69002, France) in charge of scientific and medical affairs.

References

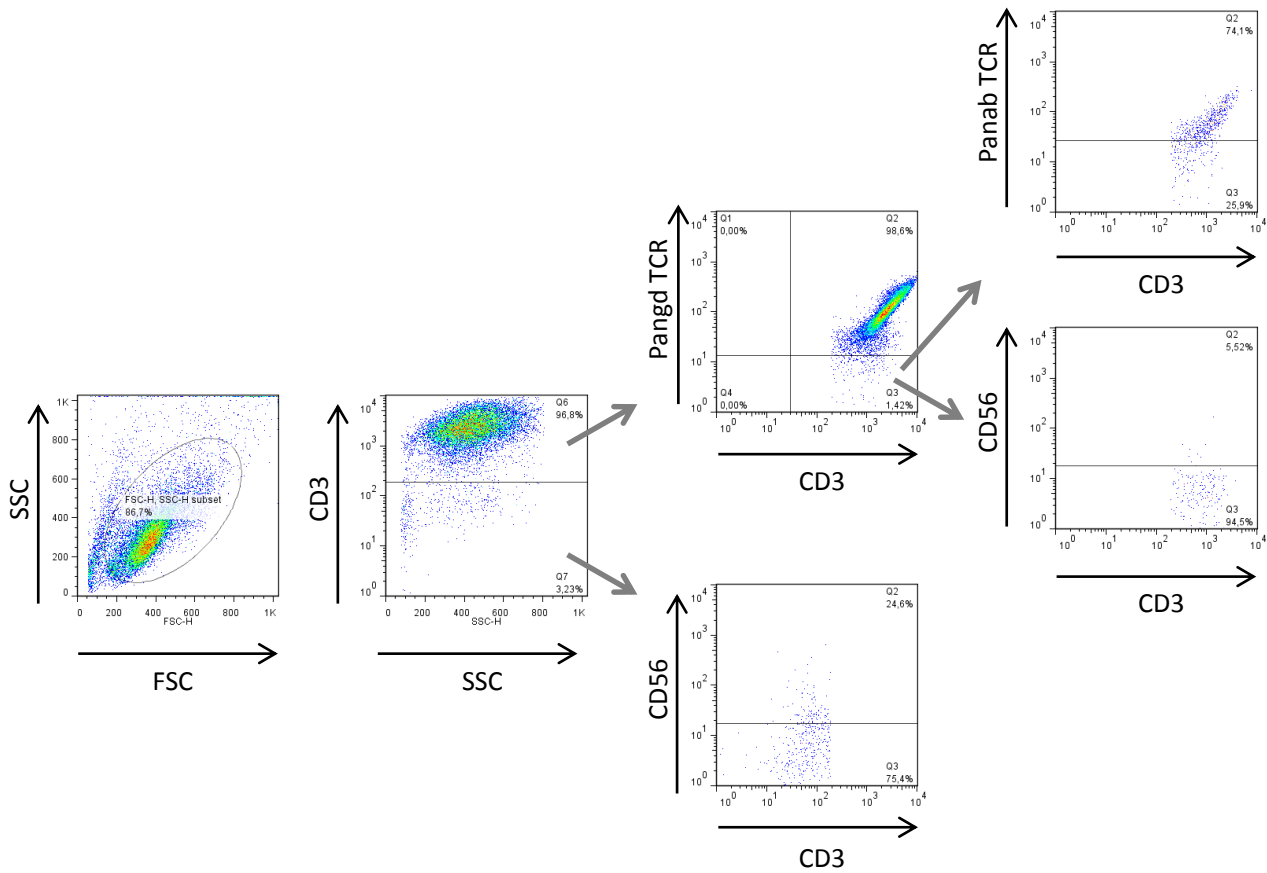
- Ricard D, Idhah A, Ducray F, Lahutte M, Hoang-Xuan K, Delattre JY. Primary brain tumours in adults. *Lancet* 2012; 379(9830):1984-96; PMID:22510398; [http://dx.doi.org/10.1016/S0140-6736\(11\)61346-9](http://dx.doi.org/10.1016/S0140-6736(11)61346-9)
- Stupp R, Hegi ME, Mason WP, van den Bent MJ, Taphoorn MJ, Janzer RC, Ludwin SK, Allgeier A, Fisher B, Belanger K et al. Effects of radiotherapy with concomitant and adjuvant temozolomide versus radiotherapy alone on survival in glioblastoma in a randomised phase III study: 5-year analysis of the EORTC-NCIC trial. *Lancet Oncol* 2009; 10(5):459-66; PMID:19269895; [http://dx.doi.org/10.1016/S1470-2045\(09\)70025-7](http://dx.doi.org/10.1016/S1470-2045(09)70025-7)
- Buckner JC, Brown PD, O'Neill BP, Meyer FB, Wetmore CJ, Uhm JH. Central nervous system tumors. *Mayo. Clin. Proc.* 2007; 82(10):1271-86; PMID:17908533; <http://dx.doi.org/10.4065/82.10.1271>
- Bao S, Wu Q, McLendon RE, Hao Y, Shi Q, Hjelmeland AB, Dewhirst MW, Bigner DD, Rich JN. Glioma stem cells promote radioresistance by preferential activation of the DNA damage response. *Nature* 2006; 444(7120):756-60; PMID:17051156; <http://dx.doi.org/10.1038/nature05236>
- Singh SK, Clarke ID, Terasaki M, Bonn VE, Hawkins C, Squire J, Dirks PB. Identification of a cancer stem cell in human brain tumors. *Cancer Res.* 2003; 63(18):5821-8; PMID:14522905
- Singh SK, Hawkins C, Clarke ID, Squire JA, Bayani J, Hide T, Henkelman RM, Cusimano MD, Dirks PB. Identification of human brain tumour initiating cells. *Nature* 2004; 432(7015):396-401; PMID:15549107; <http://dx.doi.org/10.1038/nature03128>
- Yuan X, Curtin J, Xiong Y, Liu G, Waschmann-Hogiu S, Farkas DL, Black KL, Yu JS. Isolation of cancer stem cells from adult glioblastoma multiforme. *Oncogene* 2004; 23(58):9392-9400; PMID:15558011; <http://dx.doi.org/10.1038/sj.onc.1208311>

8. Vauleon E, Avril T, Collet B, Mosser J, Quillien V. Overview of cellular immunotherapy for 18 patients with glioblastoma. *Clin. Dev. Immunol.* 2010; vol. 2010, Article ID 689171, 18 pages; PMID:20953324; <http://dx.doi.org/10.1155/2010/689171>
9. Chow KH, Gottschalk S. Cellular immunotherapy for high-grade glioma. *Immunotherapy* 2011; 3(3):423-34; PMID:21395383; <http://dx.doi.org/10.2217/imt.10.110>
10. Dutoit V, Herold-Mende C, Hilf N, Schoor O, Beckhove P, Bucher J, Dorsch K, Flohr S, Fritsche J, Lewandrowski P et al. Exploiting the glioblastoma peptidome to discover novel tumour-associated antigens for immunotherapy. *Brain* 2012; 135(Pt 4):1042-54; PMID:22418738; <http://dx.doi.org/10.1093/brain/awso42>
11. Gerber DE, Laterra J. Emerging monoclonal antibody therapies for malignant gliomas. *Expert Opin. Investig. Drugs.* 2007; 16(4):477-94; PMID:17371196; <http://dx.doi.org/10.1517/13543784.16.4.477>
12. Chung DS, Shin HJ, Hong YK. A new hope in immunotherapy for malignant gliomas: adoptive T cell transfer therapy. *J. Immunol. Res.* 2014; 2014:326545; PMID:25009822; <http://dx.doi.org/10.1155/2014/326545>
13. Lefranc MP, Rabbitts TH. A nomenclature to fit the organization of the human T-cell receptor gamma and delta genes. *Res. Immunol.* 1990; 141(7):615-8; PMID:2151348; [http://dx.doi.org/10.1016/0923-2494\(90\)90068-A](http://dx.doi.org/10.1016/0923-2494(90)90068-A)
14. Silva-Santos B, Serre K, Norell H. gammadelta T cells in cancer. *Nat. Rev. Immunol.* 2015; 15(11):683-91; PMID:26449179; <http://dx.doi.org/10.1038/nri3904>
15. Bonneville M, Scotet E. Human Vgamma9Vdelta2 T cells: promising new leads for immunotherapy of infections and tumors. *Curr. Opin. Immunol.* 2006; 18(5):539-46; PMID:16870417; <http://dx.doi.org/10.1016/j.coi.2006.07.002>
16. Yeh DC, Chen DR, Chao TY, Chen SC, Wang HC, Rau KM, Feng YH, Chang YC, Lee KD, Ou-Yang F et al. EORTC QLQ-BM22 quality of life evaluation and pain outcome in patients with bone metastases from breast cancer treated with zoledronic acid. *In vivo* 2014; 28(5):1001-4; PMID:25189922
17. Fournie JJ, Sicard H, Pouput M, Bezombes C, Blanc A, Romagné F, Ysebaert L, Laurent G. What lessons can be learned from gammadelta T cell-based cancer immunotherapy trials? *Cell. Mol. Immunol.* 2013; 10(1):35-41; PMID:23241899; <http://dx.doi.org/10.1038/cmi.2012.39>
18. Santolaria T, Robard M, Leger A, Catros V, Bonneville M, Scotet E. Repeated systemic administrations of both aminobisphosphonates and human Vgamma9Vdelta2 T cells efficiently control tumor development in vivo. *J. Immunol.* 2013; 191(4):1993-2000; PMID:23836057; <http://dx.doi.org/10.4049/jimmunol.1300255>
19. Nakazawa T, Nakamura M, Park YS, Motoyama Y, Hironaka Y, Nishimura F, Nakagawa I, Yamada S, Matsuda R, Tamura K et al. Cytotoxic human peripheral blood-derived gammadelta T cells kill glioblastoma cell lines: implications for cell-based immunotherapy for patients with glioblastoma. *J. Neurooncol.* 2014; 116(1):31-9; PMID:24062140
20. Cimini E, Piacentini P, Sacchi A, Gioia C, Leone S, Lauro GM, Martini F, Agrati C. Zoledronic acid enhances Vdelta2 T-lymphocyte antitumor response to human glioma cell lines. *Int. J. Immunopathol. Pharmacol.* 2011; 24(1):139-48; PMID:21496396
21. Das AV, James J, Zhao X, Rahnenfuhrer J, Ahmad I. Identification of c-Kit receptor as a regulator of adult neural stem cells in the mammalian eye: interactions with Notch signaling. *Dev. Biol.* 2004; 273(1):87-105; PMID:15302600; <http://dx.doi.org/10.1016/j.ydbio.2004.05.023>
22. Donnou S, Fisson S, Mahe D, Montoni A, Couez D. Identification of new CNS-resident macrophage subpopulation molecular markers for the discrimination with murine systemic macrophages. *J. Neuroimmunol.* 2005; 169(1-2):39-49; PMID:16169092; <http://dx.doi.org/10.1016/j.jneuroim.2005.07.016>
23. Harly C, Guillaume Y, Nedellec S, Peigné CM, Mönkkönen H, Mönkkönen J, Li J, Kuball J, Adams EJ, Netzer S et al. Key implication of CD277/butyrophilin-3 (BTN3A) in cellular stress sensing by a major human gammadelta T-cell subset. *Blood* 2012; 120(11):2269-79; PMID:22767497; <http://dx.doi.org/10.1182/blood-2012-05-430470>
24. Brocard E, Oizel K, Lalier L, Pecqueur C, Paris F, Vallette FM, Oliver L. Radiation-induced PGE2 sustains human glioma cells growth and survival through EGF signaling. *Oncotarget* 2015; 6(9):6840-9; PMID:25749386; <http://dx.doi.org/10.18632/oncotarget.3160>
25. Cho DY, Lin SZ, Yang WK, Lee HC, Hsu DM, Lin HL, Chen CC, Liu CL, Lee WY, Ho LH. Targeting cancer stem cells for treatment of glioblastoma multiforme. *Cell Transplant.* 2013; 22(4):731-9; PMID:23594862; <http://dx.doi.org/10.3727/096368912X655136>
26. Thon N, Damianoff K, Hegermann J, Grau S, Krebs B, Schnell O, Tonn JC, Goldbrunner R. Presence of pluripotent CD133+ cells correlates with malignancy of gliomas. *Mol. Cell. Neurosci.* 2010; 43(1):51-9; PMID:18761091; <http://dx.doi.org/10.1016/j.mcn.2008.07.022>
27. Silver DJ, Siebzehnrubl FA, Schildts MJ, Yachnis AT, Smith GM, Smith AA, Scheffler B, Reynolds BA, Silver J, Steindler DA. Chondroitin sulfate proteoglycans potently inhibit invasion and serve as a central organizer of the brain tumor microenvironment. *J Neurosci* 2013; 33(39):15603-17; PMID:24068827; <http://dx.doi.org/10.1523/JNEUROSCI.3004-12.2013>
28. Morita CT, Jin C, Sarikonda G, Wang H. Nonpeptide antigens, presentation mechanisms, and immunological memory of human Vgamma2Vdelta2 T cells: discriminating friend from foe through the recognition of prenyl pyrophosphate antigens. *Immunol. Reviews* 2007; 215:59-76; PMID:17291279; <http://dx.doi.org/10.1111/j.1600-065X.2006.00479.x>
29. Sandstrom A, Peigne CM, Leger A, Crooks JE, Konczak F, Gesnel MC, Breathnach R, Bonneville M, Scotet E, Adams EJ. The intracellular B30.2 domain of butyrophilin 3A1 binds phosphoantigens to mediate activation of human Vgamma9Vdelta2 T cells. *Immunity* 2014; 40(4):490-500; PMID:24703779; <http://dx.doi.org/10.1016/j.immuni.2014.03.003>
30. Pereboeva L, Harkins L, Wong S, Lamb LS. The safety of allogeneic innate lymphocyte therapy for glioma patients with prior cranial irradiation. *Cancer Immunol. Immunother.* 2015; 64(5):551-62; PMID:25676710; <http://dx.doi.org/10.1007/s00262-015-1662-z>
31. Lamb LS, Jr., Musk P, Ye Z, van Rhee F, Geier SS, Tong JJ, King KM, Henslee-Downey PJ. Human gammadelta(+) T lymphocytes have in vitro graft vs leukemia activity in the absence of an allogeneic response. *Bone Marrow Transplant.* 2001; 27(6):601-6; PMID:11319589; <http://dx.doi.org/10.1038/sj.bmt.1702830>
32. Bailey SL, Carpentier PA, McMahon EJ, Begolka WS, Miller SD. Innate and adaptive immune responses of the central nervous system. *Critical Rev. Immunol.* 2006; 26(2):149-88; PMID:16700651; <http://dx.doi.org/10.1615/CritRevImmunol.v26.i2.40>
33. Louveau A, Smirnov I, Keyes TJ, Eccles JD, Rouhani SJ, Peske JD, Derecki NC, Castle D, Mandell JW, Lee KS et al. Structural and functional features of central nervous system lymphatic vessels. *Nature* 2015; 523(7560):337-41; PMID:26030524; <http://dx.doi.org/10.1038/nature14432>
34. Jung G, Brandl M, Eisner W, Fraunberger P, Reifenberger G, Schlegel U, Wiestler OD, Reulen HJ, Wilmanns W. Local immunotherapy of glioma patients with a combination of 2 bispecific antibody fragments and resting autologous lymphocytes: evidence for in situ t-cell activation and therapeutic efficacy. *Int. J. Cancer* 2001; 91(2):225-30; PMID:11146449; [http://dx.doi.org/10.1002/1097-0215\(200002\)9999:9999%3c::AID-IJC1038%3e3.3.CO;2-7](http://dx.doi.org/10.1002/1097-0215(200002)9999:9999%3c::AID-IJC1038%3e3.3.CO;2-7)
35. Quattrocchi KB, Miller CH, Cush S, Bernard SA, Dull ST, Smith M, Gudeman S, Varia MA. Pilot study of local autologous tumor infiltrating lymphocytes for the treatment of recurrent malignant gliomas. *Neuro-oncol.* 1999; 45(2):141-57; PMID:10778730
36. Sloan AE, Dansey R, Zamorano L, Barger G, Hamm C, Diaz F, Baynes R, Wood G. Adoptive immunotherapy in patients with recurrent malignant glioma: preliminary results of using autologous whole-tumor vaccine plus granulocyte-macrophage colony-stimulating factor and adoptive transfer of anti-CD3-activated lymphocytes. *Neurosurg. Focus.* 2000; 9(6):e9; PMID:16817692; <http://dx.doi.org/10.3171/foc.2000.9.6.10>
37. Westphal M, Yla-Herttuala S, Martin J, Warnke P, Menei P, Eckland D, Kinley J, Kay R, Ram Z; ASPECT Study Group. Adenovirus-mediated gene therapy with sitimagene ceradenovec followed by intravenous ganciclovir for patients with operable high-grade glioma (ASPECT): a randomised, open-label, phase 3 trial. *Lancet Oncol*

- 2013; 14(9):823-33; PMID:23850491; [http://dx.doi.org/10.1016/S1470-2045\(13\)70274-2](http://dx.doi.org/10.1016/S1470-2045(13)70274-2)
38. Rogers MJ, Crockett JC, Coxon FP, Monkkonen J. Biochemical and molecular mechanisms of action of bisphosphonates. *Bone* 2011; 49(1):34-41; PMID:21111853; <http://dx.doi.org/10.1016/j.bone.2010.11.008>
39. Kobayashi H, Tanaka Y, Yagi J, Minato N, Tanabe K. Phase I/II study of adoptive transfer of gammadelta T cells in combination with zoledronic acid and IL-2 to patients with advanced renal cell carcinoma. *Cancer Immunol. Immunother.* 2011; 60(8):1075-84; PMID:21519826; <http://dx.doi.org/10.1007/s00262-011-1021-7>
40. Coleman RE. Risks and benefits of bisphosphonates. *Br. J. Cancer* 2008; 98(11):1736-40; PMID:18506174; <http://dx.doi.org/10.1038/sj.bjc.6604382>
41. Weiss HM, Pfaar U, Schweitzer A, Wiegand H, Skerjanec A, Schran H. Biodistribution and plasma protein binding of zoledronic acid. *Drug Metab. Dispos.* 2008; 36(10):2043-9; PMID:18625688
42. Kato Y, Tanaka Y, Tanaka H, Yamashita S, Minato N. Requirement of species-specific interactions for the activation of human gamma delta T cells by pamidronate. *J. Immunol.* 2003; 170(7):3608-13; PMID:12646624; <http://dx.doi.org/10.4049/jimmunol.170.7.3608>
43. Sabatino R, Antonelli A, Battistelli S, Schwendener R, Magnani M, Rossi L. Macrophage depletion by free bisphosphonates and zoledronate-loaded red blood cells. *PloS One* 2014; 9(6):e101260; PMID:24968029; <http://dx.doi.org/10.1371/journal.pone.0101260>
44. Rietkotter E, Menck K, Bleckmann A, Farhat K, Schaffrinski M, Schulz M, Hanisch UK, Binder C, Pukrop T. Zoledronic acid inhibits macrophage/microglia-assisted breast cancer cell invasion. *Oncotarget* 2013; 4(9):1449-60; PMID:24036536; <http://dx.doi.org/10.18632/oncotarget.1201>

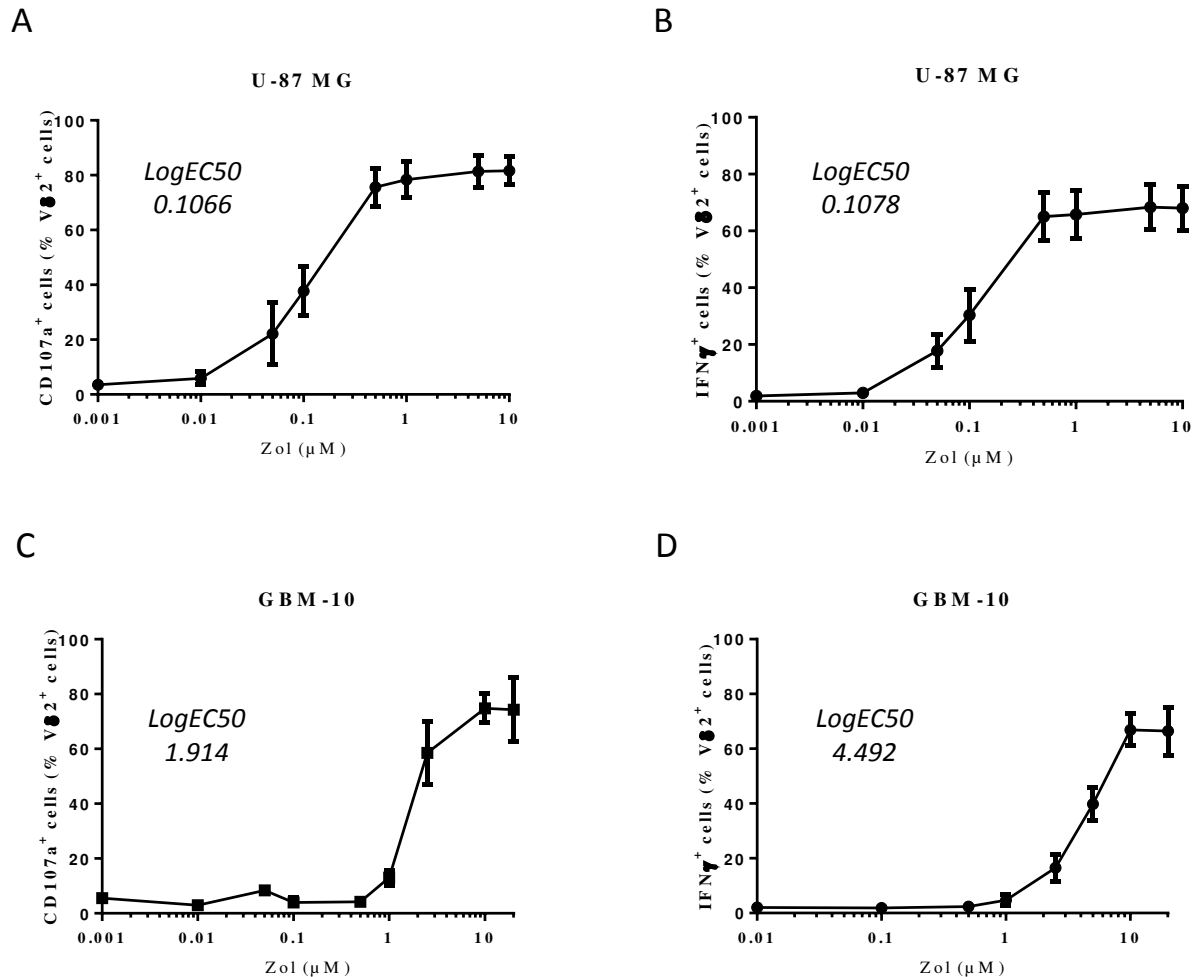
Jarry et al.

Supplemental Figure 1



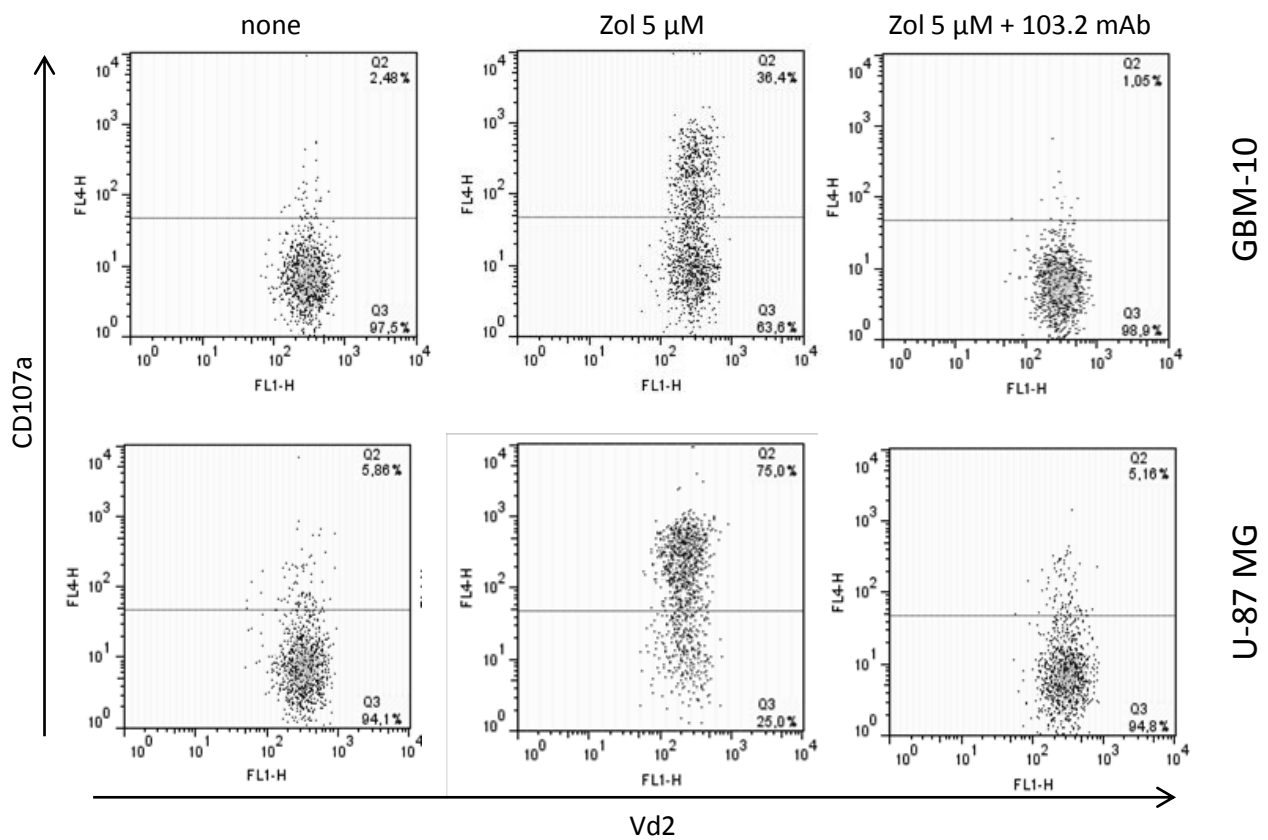
Supplemental Figure 1: Human $V\gamma 9V\delta 2$ T cells preparation purity.

Purity analysis of a representative human PBMC-gd T cell preparation. Three weeks after an initial amplification step (IL-2/PAg), lymphocytes were labeled with mixes of fluorochrome-labeled CD3, pangd or ab TCR and CD56 mAbs and next analyzed by flow cytometry. The percentage of positive cells is indicated in the quadrants.



Supplemental Figure 2: Zoledronate-sensitized GBM cells induce Vγ9Vδ2 T cells activation.

U-87MG (A-B) and GBM-10 primary cells (C-D) were pretreated overnight with different concentrations of zoledronate, washed and co-cultured for 4 h with Vγ9Vδ2 T cells (E/T ratio: 1/1). (A and C) Vγ9Vδ2 T cells were analyzed by flow cytometry for CD107a expression. (B and D) After co-culture, Vγ9Vδ2 T cells were incubated with FITC-labeled anti-human Vδ2 TCR mAb, permeabilized using the staining buffer (eBioscience, San Diego, CA) accordingly to the manufacturer's instructions, next incubated with PE-labeled anti-human IFN-g mAb (4S.B3; eBioscience) and finally analyzed by flow cytometry. Results are expressed as % positive cells among Vδ2⁺ cells (mean ± SEM, n=3).



Supplemental Figure 3: Antagonist anti-BTN3A/CD277 mAb inhibits the reactivity of human Vg9Vd2 T cells towards GBM tumor cells.

GBM cells from either primary patients established tumors (GBM-10) or cultured cell lines (U-87MG) were pretreated, or not, with 5 μ M of zoledronate, in the presence or the absence of the antagonist #103.2 mAb (10 mg/ml). Following extensive washes, treated GBM tumor cells were co-cultured for 4 h with Vg9Vd2 T cells (ratio 1/1). The upregulation of cell surface CD107a was measured by flow cytometry. Percentage values of TCRVd2⁺ CD107a⁺ T cells are indicated in the quadrants.

3 – Article 3 : Stereotactic Adoptive Transfer of Cytotoxic Immune Cells in Murine Models of Orthotopic Human Glioblastoma Multiforme Xenografts

Ulrich Jarry^{*1,2}, Noémie Joalland^{*1,2}, Cynthia Chauvin^{*1,2}, Béatrice Clemenceau^{1,2,3}, Claire Pecqueur^{1,2}, Emmanuel Scotet^{1,2}.

¹ INSERM, CNRS, Université d'Angers, Université de Nantes, CRCINA ; ² Immunotherapy, Graft, Oncology, LabEx IGO ; ³ Hopital de Nantes, Hotel Dieu.

* These authors contributed equally

Parmi les nouvelles stratégies immunothérapeutiques développées, le transfert adoptif d'effecteurs cytotoxiques permettrait d'éliminer les cellules tumorales invasives et chimio-radio-résistantes, impliquées dans la rechute rapide et fatale du GBM. Ainsi, une ou plusieurs administrations de cellules immunitaires réactives contre des cellules tumorales de GBM, dans le voisinage de la tumeur, représenterait une opportunité unique de délivrer des agents thérapeutiques efficaces et hautement concentrés au plus proche des cellules tumorales. Dans cet article, nous présentons un protocole, écrit et filmé, de préparation et d'administration stéréotaxique de LT humains chez des souris immunodéficientes porteuses d'une tumeur cérébrale humaine en orthotopique. Ce protocole est accompagné de résultats validant que les conditions de préparation et d'injection de ces effecteurs n'altèrent pas leur survie, leur capacité de prolifération et leur réactivité face aux cellules tumorales. Cette étude fournit des preuves de concept préclinique, complémentaires de celles présentées dans l'article précédent, pour la faisabilité et l'efficacité anti-tumorale de ces immunothérapies qui reposent sur des injections stéréotaxiques de LT humains en intracérébral, au plus proche de la tumeur.

Publié dans Journal of Visualized Experiments, 2018

Video Article

Stereotactic Adoptive Transfer of Cytotoxic Immune Cells in Murine Models of Orthotopic Human Glioblastoma Multiforme Xenografts

Ulrich Jarry^{*1,2}, Noémie Joalland^{*1,2}, Cynthia Chauvin^{*1,2}, Béatrice Clemenceau^{1,2,3}, Claire Pecqueur^{1,2}, Emmanuel Scotet^{1,2}¹INSERM, CNRS, Université d'Angers, Université de Nantes, CRCINA²Immunotherapy, Graft, Oncology, LabEx IGO³Hopital de Nantes, Hotel Dieu

*These authors contributed equally

Correspondence to: Emmanuel Scotet at Emmanuel.Scotet@inserm.frURL: <https://www.jove.com/video/57870>DOI: [doi:10.3791/57870](https://doi.org/10.3791/57870)

Keywords: Immunology and Infection, Issue 139, Cancer, glioblastoma, immunotherapy, adoptive transfer, stereotaxy, lymphocytes

Date Published: 9/1/2018

Citation: Jarry, U., Joalland, N., Chauvin, C., Clemenceau, B., Pecqueur, C., Scotet, E. Stereotactic Adoptive Transfer of Cytotoxic Immune Cells in Murine Models of Orthotopic Human Glioblastoma Multiforme Xenografts. *J. Vis. Exp.* (139), e57870, doi:10.3791/57870 (2018).

Abstract

Glioblastoma multiforme (GBM), the most frequent and aggressive primary brain cancer in adults, is generally associated with a poor prognosis, and scarce efficient therapies have been proposed over the last decade. Among the promising candidates for designing novel therapeutic strategies, cellular immunotherapies have been targeted to eliminate highly invasive and chemo-radioresistant tumor cells, likely involved in a rapid and fatal relapse of this cancer. Thus, administration(s) of allogeneic GBM-reactive immune cell effectors, such as human VY9Vδ2 T lymphocytes, in the vicinity of the tumor would represent a unique opportunity to deliver efficient and highly concentrated therapeutic agents directly into the site of brain malignancies. Here, we present a protocol for the preparation and the stereotaxic administration of allogeneic human lymphocytes in immunodeficient mice carrying orthotopic human primary brain tumors. This study provides a preclinical proof-of-concept for both the feasibility and the antitumor efficacy of these cellular immunotherapies that rely on stereotactic injections of allogeneic human lymphocytes within intracranial tumor beds.

Video Link

The video component of this article can be found at <https://www.jove.com/video/57870/>

Introduction

GBM (WHO grade IV astrocytoma), is the most frequent and aggressive primary brain cancer in adults. In spite of aggressive treatments that combine surgery and radio-chemotherapy, GBM remains associated with an extremely poor prognosis (median survival of 14.6 months and a 2-year-mortality > 73%)¹. This evidences that few efficient therapeutic advances have been validated over the last decade². Among candidates for the design of more effective therapeutic strategies^{3,4,5}, immunotherapies⁶ are currently explored to track and eliminate highly invasive and radio/chemo-resistant tumor cells, suspected for their key contribution to rapid and fatal tumor relapse⁷. Various potential immunological targets were identified and proposed for immunotherapies, involving natural or modified αβ or Yδ T lymphocytes such as GBM-specific tumor antigens or stress-induced molecules^{8,9,10}. The possibility to administrate selected GBM-reactive immune cell effectors represents a unique opportunity to deliver elevated amounts of effector lymphocytes directly into the site of residual malignancy. To support this strategy, we have recently shown that models based on immunodeficient mice carrying orthotopic primary human GBM xenografts faithfully recapitulate the development of brain tumors in GBM patients^{9,11}. Moreover, these models were used to demonstrate the strong antitumor efficiency of adoptively transferred allogeneic human VY9Vδ2 T lymphocytes.

This protocol describes the critical experimental steps for achieving stereotactic immunotherapies of brain tumors, such as GBM, based on the adoptive transfer of allogeneic T lymphocytes. The article shows: (i) the amplification of therapeutic allogeneic immune effector T lymphocytes, such as human VY9Vδ2 T lymphocytes; (ii) the preparation of these effector T lymphocytes for injection; (iii) the procedure for stereotactic administration within the brain, near the tumor. This article also provides insight into the behavior of these cellular effectors after stereotactic injection.

The therapeutic approach presented here is based on the injection of 20×10^6 effector cells *per* dose for each brain tumor-bearing immunodeficient mouse. An initial *in vitro* expansion step is required to produce large quantities of immune cells. Therefore, non-specific cell expansions are performed using phytohemagglutinin (PHA-L) and irradiated allogeneic feeder cells: peripheral-blood mononuclear cells (PBMCs) from healthy donors and Epstein Barr Virus (EBV)-transformed B-lymphoblastoid cell lines (BLCLs), derived from PBMCs by *in vitro* infection with EBV-containing culture supernatant from the Marmoset B95-8 cell line, in the presence of 1 μg/mL cyclosporin-A.

GBM-reactive effector immune cells are compared and selected from *in vitro* assays⁹. These effector cells are activated and amplified using standard protocols, according to their nature (e.g., human VY9Vδ2 T lymphocytes⁹ or human anti-herpes virus αβ T lymphocytes¹²) with a

minimum purity of > 80%, as routinely checked by cytometric analysis. The cell expansion procedure detailed below applies to various human lymphocyte subsets.

Protocol

The following procedure involving animal subjects was performed according to institutional guidelines (Agreement #00186.02; regional ethics committee of the Pays de la Loire [France]). Human PBMCs were isolated from the blood collected from informed healthy donors (Etablissement Français du Sang Nantes, France). All steps are performed under sterile conditions.

1. Non-specific Expansion of Cytotoxic Effector T Lymphocytes

1. Prepare and irradiate feeder cells at 35 Gy. For the stimulation of 2×10^5 - 4×10^5 effector cells, prepare 10×10^6 PBMCs and 1×10^6 BLCLs from three distinct, healthy donors.
2. Resuspend both feeder cells and effector cells in 15 mL of RPMI supplemented with 10% heat-inactivated FCS, 2 mM L-glutamine, penicillin (100 IU/mL), and streptomycin (0.1 μ g/mL) and 300 IU/mL recombinant IL-2.
3. Add PHA-L at a final concentration of 1 μ g/mL, carefully mix, and distribute 150 μ L of the cell suspension per well in 96-well U-bottomed plates.
4. Incubate at 37 °C and with 5% CO₂ in a humidified atmosphere.
5. Daily check the plate until large cell clumps form in the culture wells (~day 7).
6. Transfer the cells into a culture flask at 1×10^6 cells/mL in fresh culture medium.
7. Determine the total cell number by counting (2x a week) and maintain them at 1×10^6 cells/mL in fresh culture medium.
NOTE: Effector immune cells should be ready for the therapeutic administration at a resting state (usually 3 weeks after initial amplification stimulus). The purity and the reactivity of these effector cells should be checked prior to *in vivo* injections (e.g., with *in vitro* assays).

2. Pre-operative Effector Cells Preparation

1. After checking the effector cell count, collect the effector cells in a 50-mL tube by centrifugation (300 x g for 5 min).
NOTE: To compensate for any loss, prepare an excess of cells (e.g., 50×10^6).
2. Carefully remove the supernatant and resuspend the cells in 15 mL of sterile PBS and centrifuge for 5 min at 300 x g to perform the wash.
3. Carefully and completely remove the supernatant and then resuspend the cell pellet in 1 mL of sterile PBS.
4. Transfer the resuspended cells in a 1.5-mL microtube for centrifugation at 300 x g for 5 min.
5. Carefully and completely remove the supernatant by pipetting slowly.
6. Resuspend the cell pellet in 8 μ L of sterile PBS per mouse.
NOTE: This is a critical step.
7. Measure the volume of the cell suspension by using a micropipette. If necessary, add sterile PBS (20×10^6 cells in 15 μ L of PBS per dose) and mix carefully.
8. Check, by using a micropipette, that the final volume per mouse is between 15 and 20 μ L (imperatively < 20 μ L).
9. Keep the cells on ice until stereotactic injection.
NOTE: More than 3-h timepoints were not tested.

3. Stereotactic Injection

1. **Equipment set-up**
 1. Assemble and calibrate a small animal stereotactic frame according to the manufacturer's instructions to ensure the accuracy of intracranial injections (e.g., syringe size, desired volume, and rate of injection).
NOTE: A slow infusion rate is recommended (i.e., 2 - 3 μ L/min).
 2. Install the material under a microbial safety cabinet (MSC) to maintain the sterility of the instruments and to protect the mice from infections.
NOTE: Place "isothermal blocs" in a water bath at 37 °C. This system limits the hypothermia of mice during the surgery. Heating pads, which are necessary for post-procedural care, must be used during the continuous temperature monitoring.
2. **Pre-operative animal preparation**
 1. Anesthetize a mouse with an intraperitoneal injection of ketamine (10 mg/mL) and xylazine (0.1 mg/mL) at 10 μ L/g of body weight of the mouse.
 2. Perform a toe pinch test to ensure the complete anesthesia and analgesia of the animal.
NOTE: Any movement is an indication of non-deep analgesia and, if that occurs, a few more minutes are required before repeating the operation.
 3. Once the mouse is properly anesthetized, use scissors to remove the fur from the surgical site (between the two ears, up to the nose).
3. **Pre-operative cell preparation**
 1. Carefully resuspend the cells with a pipette (several times) prior to each injection to prevent any cell clumping.
 2. Carefully draw the required cell suspension volume (15 - 20 μ L) into the 22-G microsyringe to avoid the aspiration of bubbles.
NOTE: This cell-loading step into the microsyringe is important to minimize variances in injected volumes. Reload cells for each individual injection between procedures to prevent any cell clumping and to ensure an even number of effector cells administration in the cohort.
 3. Then, place the syringe into the adapted syringe pump.
4. **Procedural care**

1. Disinfect the surgical site with swabs soaked in povidone-iodine 5% solution at least 3x.
2. Place a lubricating ophthalmic ointment in the mouse's eyes to prevent any drying of the corneas.
3. Position the anesthetized mouse on the stereotactic frame, on a warm isothermal block covered with a sterile plastic wrap to maintain the mouse's temperature during surgery and limit the mortality.
NOTE: The mouse's nose and teeth should be appropriately positioned above the tooth bar, to ensure adequate respiratory flow during the procedure.
4. Once the mouse is positioned above the tooth bar, tighten the ear bars firmly under the mouse's ears to immobilize the head.
NOTE: Be careful to not damage the eardrums or to compromise the respiration.
5. Make a 1 - 2 cm midline sagittal skin incision with sterile scissors along the upper part of the cranium from anterior to posterior to expose the skull.
6. Identify the intersection of the sagittal and coronal sutures (Bregma) to serve as landmarks for stereotactic localization prior to the injection (shown in **Figure 1**).
7. Place the microsyringe above this point.
8. Move the microsyringe 2 mm right lateral and 0.5 mm anterior of the Bregma.
9. Using a microdrill, make a small hole in the skull with a sterile drill bit at predetermined coordinates. Be careful to remain superficial in order to avoid any traumatic injury of the brain.
NOTE: In this protocol, immune cells were injected within an established tumor (one week after tumor cell injection). The skin should be reopened (scar) and the injection is performed at the same coordinates used for the tumor cell implantation (the hole is generally still present up to 2 weeks after the injection). Coordinates were selected for injecting tumor and effector cells in the brain parenchyma^{13,14}.

5. Injection of immune effector cells

1. Carefully insert the microsyringe into the drilled hole and, moving slowly, forward the needle 3 mm down in the dura and then backward 0.5 mm to a final depth of 2.5 mm prior to injecting the effector cells.
2. Run the effector cell injection at 2 - 3 $\mu\text{L}/\text{min}$ and monitor the mice all along the injection time.
3. Once the injection is complete, withdraw the needle for only 1 mm and keep the microsyringe in place for one additional minute before slowly withdrawing completely the microsyringe, to prevent any leakage from the infusion site.
NOTE: Following the removal of the animal from the stereotactic device, immediately clean the injection equipment for upcoming experiments.

6. Post-operative care and follow-up of mouse

1. Remove the animal from the stereotactic frame and immediately apply povidone-iodine 5% solution on the incision site and close the skin with an appropriate surgical suture.
2. Apply 2% lidocaine gel directly on the wound and administer 0.15 $\mu\text{g}/\text{g}$ of buprenorphine by a subcutaneous injection for post-procedural analgesia.
3. Place back the anesthetized mouse to its cage above a heating pad set to 37 $^{\circ}\text{C}$ to maintain an appropriate mouse body temperature and to avoid any hypothermia.
NOTE: Separate housing is not necessary.
4. Monitor the mouse until it is fully recovered from anesthesia and transfer it to a housing room.
NOTE: To date, this protocol is well supported as few unforeseen complications have occurred (< 5% of injected mice).
5. Daily monitor the mice and euthanize them when any declining health signs are observed (e.g., hunched posture, reduced mobility, prostration, or significant body weight loss $\geq 15\%$).

Representative Results

This study describes the strategy of adoptive transfers of cellular immune effector cells within the brain of tumor-carrying mice, based on stereotactic injections performed directly within the tumor bed.

To minimize any risk of brain injury associated with a large injection volume, the effector cell suspension needs to be concentrated (20×10^6 cells in 15 - 20 μL of PBS). To check whether this cell concentration step might affect the viability of the effector cells, these cells were prepared according to the described protocol and loaded into the microsyringe. The effector cells were collected immediately, or 10 min after loading them into the microsyringe. The cells were stained with propidium iodide (PI), a fluorescent DNA intercalating agent that is not permeant to live cells and analyzed by flow cytometry at different timepoints (0, 24, and 72 hours). The results show that the preparation and the loading into the microsyringe do not significantly affect the viability of effector cells for at least 24 hours (**Figure 2A and 2B**). At 72 hours, a slight, but non-significant, increase of PI^{positive} cells was observed (14% compared to 11% for unloaded cells). In a similar way, the antitumor reactivity of effector cells that were prepared and maintained on ice for 3 hours was analyzed. Effector cells were cocultured with brain tumor cells for 4 hours in presence of an anti-CD107a mAb. The upregulation of the activation marker CD107a, similar to the value obtained in the control conditions, indicates that the reactivity of effector cells is not affected by the preparation and the loading into the microsyringe (**Figure 2C**).

To evaluate whether effector cells survive and move within the brain parenchyma following their intra-tumoral implantation, 20×10^6 effector cells were injected into the tumor site of mice carrying a brain tumor (GBM-1¹¹). One week later, the brains were collected, fixed, sectioned, and stained for hematoxylin, eosin, and safran coloration (HES) and anti-human CD3 mAb (IHC). HES coloration identified the structure of the brain tumors (**Figure 3, left panel**). The CD3 staining identified and localized the effector immune T lymphocytes (here, human VY9V δ 2 T cells) (**Figure 3, right panel**). Interestingly, effector T lymphocytes were detected around the tumor (**Figure 3, upper right panel**), in the tumor core (**Figure 3, middle right panel**), but also in the contralateral hemisphere (**Figure 3, bottom right panel**). Moreover, the function of human T lymphocytes isolated from the mouse brain 48 hours after their injection (4×10^6 $\alpha\beta$ T cells), which represent 2% of the brain cells, was analyzed. The results indicate that collected brain-injected effector allogeneic $\alpha\beta$ T cells expand and proliferate upon a non-specific PHA-feeder cells activation performed in the presence of IL-2 (**Figure 4**).

Together, these results show that effector T cells prepared and administrated under these procedures survive for hours in the brain and can patrol within the tumor and healthy brain tissues. These procedures have been used for assessing the antitumor efficiency of therapeutic stereotactic administrations of allogeneic human resting VY9Vδ2 T cells to control the development of human GBM brain tumors^{9,11}. These studies evidence that injections of allogeneic human effector T lymphocytes in the tumor bed significantly improve the survival of mice carrying brain tumors. Interestingly, surviving mice did not carry detectable tumor cells, thus indicating a complete tumor rejection.

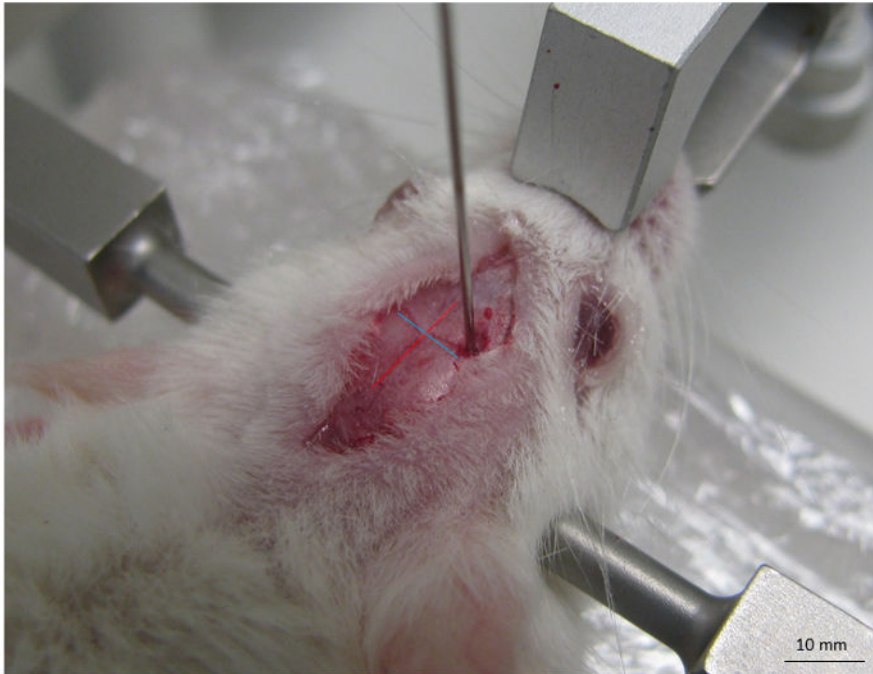


Figure 1: Picture of the main anatomical landmarks on the mouse skull. This includes sagittal (red line) and coronal (blue line) sutures and their intersection (Bregma) used to orient the site of injection. The scale bar is indicated. [Please click here to view a larger version of this figure.](#)

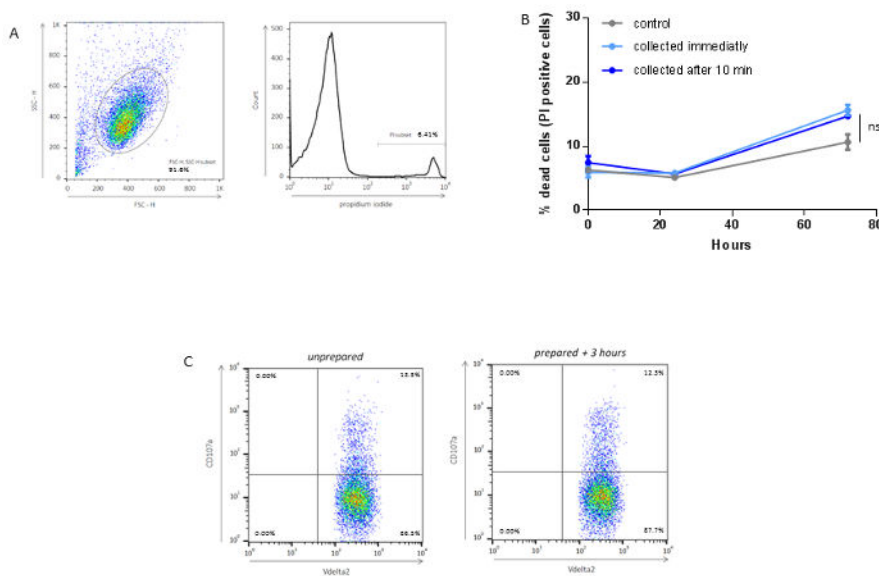


Figure 2: Survival and activation of prepared effector T lymphocytes. Effector cells (here, resting human peripheral VY9Vδ2 T cells) were amplified and prepared according to the described procedure. Staining of lymphocytes with propidium iodide (PI), a DNA intercalating fluorescent compound that is not permeant to live cells, and functional activation were performed. **(A)** This panel shows a representative plot of forward (FSC-H) versus side (SSC-H) scatter gating of effector lymphocytes (*left panel*). The histogram shows the PI staining of gated control lymphocytes (*right panel*). The percentage of PI^{positive} lymphocytes is indicated. **(B)** This panel shows the percentage of dead lymphocytes (PI^{positive}) collected immediately (light blue line) or after 10 min (dark blue line) in the microsyringe, measured at the indicated timepoints. As control, unloaded prepared cells were used (grey line). (*n* = 3; mean ± SD; ns = not significant.) **(C)** CD107a surface mobilization was measured by flow cytometry on either Vδ2^{positive} control cells (unprepared) or prepared lymphocytes maintained on ice (prepared + 3 h) following a coculture with target human primary brain tumor cells. The percentage of lymphocytes is indicated in each cytometric quadrant. [Please click here to view a larger version of this figure.](#)

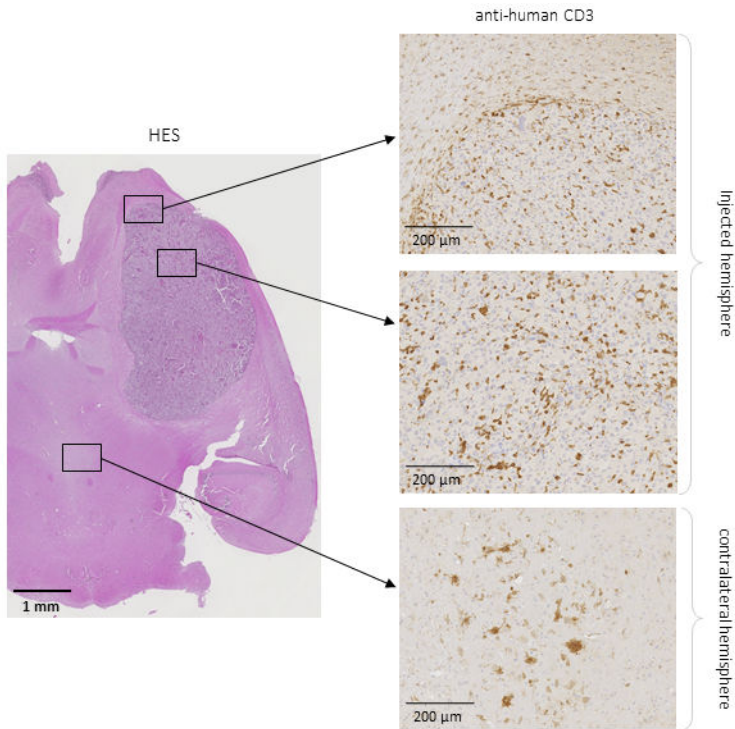


Figure 3: Detection and localization of effector T lymphocytes within the brain of tumor-bearing mice. One week after glioblastoma brain tumor implantation, effector immune cells (here, resting human peripheral VY9V62 T cells) were injected into the brains of mice. One week after the immunotherapeutic treatment, the brains were collected, fixed, and sectioned. Brain sections were colored for immunohistochemistry analysis (hematoxylin, eosin, and safran [HES] coloration) (*left panel*) or stained with anti-human CD3 antibody (*right panel*). The results shown are representative of three independent experiments. The scale bar is indicated.

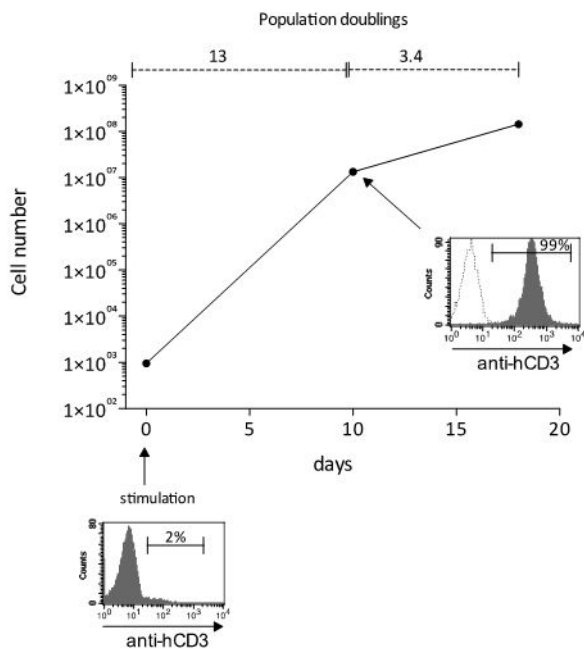


Figure 4: Activation of effector T lymphocytes collected from the brain of treated mice. Resting human T lymphocytes (here, 4×10^6 human $\alpha\beta$ T lymphocytes) were injected into the brains of NSG mice. After 48 hours, the brains were collected and dissociated. The percentage of human brain-infiltrating T lymphocytes was measured by flow cytometry using an anti-human CD3 antibody (*bottom panel*). The collected cells were seeded (10 cells/well) in 96-well U-bottomed plates and stimulated (PHA-feeder cells and IL-2) for 20 days (16 doubling cycles). Note, on day 10, 13.3×10^6 of human T lymphocytes were obtained (*right panel*).

Discussion

An adoptive transfer of selected native or engineered immune effector cells represents a promising approach to efficiently treat tumors, such as infiltrative brain cancers, taking care of limiting reactivities against non-transformed cells^{15,16,17,18}. However, the central nervous system, which comprises the brain, has a particular immune status, notably due to the existence of the blood-brain barrier and the lack of a classical lymphatic drainage system^{19,20}. These physiological features affect tissue trafficking and might compromise systemic injections of immune cells. To overcome these hindrances, intraparenchymal injections have been explored on the principle that antitumor cells are rather locally delivered, closely to the tumor site, as for microspheres that contain pharmacological compounds^{21,22}. On one hand, the limited dilution of lymphocytes within the organ might improve their antitumor efficiency, but it can also amplify deleterious mechanical or tumor adaptation effects, such as tissular compression, which is developing along brain tumor growth. This implies that this procedure requires small volumes of immunotherapeutic injections. This issue is even more critical in animal experimental models in which brain tumors cannot be surgically excised. This article describes a therapeutic approach for the preparation and the local delivery of brain tumor-specific cellular effectors, based on stereotactic injection(s) of allogeneic human T lymphocytes.

This study shows the preparation and the stereotaxic delivery of allogeneic human VY9Vδ2 T lymphocytes in immunodeficient NSG mice carrying human GBM xenografts. The first stage of this protocol describes a simple procedure for amplifying allogeneic T lymphocytes from PBMCs of healthy donors, using a standard nonspecific PHA-feeders-IL2 stimulation that produces large quantities of pure effector T lymphocytes, allowing their therapeutical utilization^{23,24}. The second stage of this article focuses on the preparation of resting T lymphocyte suspensions on the day of the stereotaxic administration. A particular focus was placed on this important step that requires a high cellular density that should not affect the viability and the function of the selected effector T lymphocytes. Finally, regarding *in vivo* experiments, the preparation of effector T lymphocytes and their injection within the tumor core is associated with their dissemination, not only within the tumor but also in the surrounding brain tissues, highlighting their particular ability to patrol and to track invasive tumor cells. Importantly, these preparation and injection methods retain the ability of these T lymphocytes to be activated within the brain upon a specific recognition of brain tumor cells. Altogether, these compelling characteristics ensure the ability of T lymphocytes to specifically and efficiently target and eliminate deep infiltrative brain tumor cells which are a hallmark of GBM²⁵. Of note, a special care has to be taken during the injection and the removal of the microsyringe to minimize any brain lesion or effector cell leaks.

In conclusion, this article describes an efficient procedure for delivering large amounts of allogeneic human anti-tumor lymphocytes, such as resting human VY9Vδ2T lymphocytes, within the vicinity of brain tumors. Importantly, this therapeutical procedure is not accompanied with adverse effects either on the transferred T lymphocytes (e.g., viability, reactivity) or on the brain tissues. Recent studies, based on murine orthotopic models of primary human GBM, have demonstrated that VY9Vδ2T lymphocytes efficiently target GBM cells, including tumor cells which have deeply infiltrated the brain parenchyma^{9,11}. These elements open opportunities for the development of novel adoptive T lymphocytes transfer procedures that could be applied in the first instance in mice carrying orthotopic brain tumors and, then, in clinical studies in GBM patients.

Disclosures

The authors have nothing to disclose.

Acknowledgements

The authors thank the staff of the University Hospital animal facility (UTE) of Nantes for animal husbandry and care, the cellular and tissular imaging core facility of Nantes University (MicroPICell) for imaging, and the Cytometry facility (Cytocell) from Nantes for their expert technical assistance. This work was funded by INSERM, CNRS, Université de Nantes, Institut National du Cancer (INCa#PLBio2014-155), Ligue Nationale contre le Cancer (AO InterRegional 2017), and the European consortium ERA-Net Transcan2 (Immunoglio). The team is funded by the Fondation pour la Recherche Medicale (DEQ20170839118). This work was realized in the context of the LabEX IGO and the IHU-Cesti programs, supported by the National Research Agency Investissements d'Avenir *via* the programs ANR-11-LABX-0016-01 and ANR-10-IBHU-005, respectively. The IHU-Cesti project is also supported by Nantes Metropole and the Pays de la Loire Region. The authors thank Chirine Rafia for providing help in correcting the manuscript.

References

1. Stupp, R., Roila, F. Malignant glioma: ESMO clinical recommendations for diagnosis, treatment and follow-up. *Annals of Oncology*. **20 Suppl 4**, 126-128 (2009).
2. Weller, M., Cloughesy, T., Perry, J. R., Wick, W. Standards of care for treatment of recurrent glioblastoma--are we there yet? *Neuro-Oncology*. **15** (1), 4-27 (2013).
3. Chen, S. H., Shine, H. D., Goodman, J. C., Grossman, R. G., Woo, S. L. Gene therapy for brain tumors: regression of experimental gliomas by adenovirus-mediated gene transfer *in vivo*. *Proceedings of the National Academy of Sciences of the United States of America*. **91** (8), 3054-3057 (1994).
4. Choi, P. J., Tubbs, R. S., Oskouian, R. J. Emerging Cellular Therapies for Glioblastoma Multiforme. *Cureus*. **10** (3), e2305 (2018).
5. Zhu, L. *et al.* Targeting and Therapy of Glioblastoma in a Mouse Model Using Exosomes Derived From Natural Killer Cells. *Frontiers in Immunology*. **9**, 824 (2018).
6. Chung, D. S., Shin, H. J., Hong, Y. K. A new hope in immunotherapy for malignant gliomas: adoptive T cell transfer therapy. *Journal of Immunology Research*. **2014**, 326545 (2014).

7. Vauleon, E., Avril, T., Collet, B., Mosser, J., Quillien, V. Overview of cellular immunotherapy for patients with glioblastoma. *Clinical and Developmental Immunology*. **2010** (2010).
8. Brown, C. E. *et al.* Regression of Glioblastoma after Chimeric Antigen Receptor T-Cell Therapy. *The New England Journal of Medicine*. **375** (26), 2561-2569 (2016).
9. Jarry, U. *et al.* Stereotaxic administrations of allogeneic human Vgamma9Vdelta2 T cells efficiently control the development of human glioblastoma brain tumors. *Oncoimmunology*. **5** (6), e1168554 (2016).
10. Dutoit, V. *et al.* Exploiting the glioblastoma peptidome to discover novel tumour-associated antigens for immunotherapy. *Brain*. **135** (Pt 4), 1042-1054 (2012).
11. Joalland, N. *et al.* IL-21 Increases the Reactivity of Allogeneic Human Vgamma9Vdelta2 T Cells Against Primary Glioblastoma Tumors. *Journal of Immunotherapy*. **41** (5), 224-231 (2018).
12. Clemenceau, B. *et al.* Effector memory alphabeta T lymphocytes can express FcgammaRIIIa and mediate antibody-dependent cellular cytotoxicity. *The Journal of Immunology*. **180** (8), 5327-5334 (2008).
13. Abdelwahab, M. G., Sankar, T., Preul, M. C., Scheck, A. C. Intracranial implantation with subsequent 3D *in vivo* bioluminescent imaging of murine gliomas. *Journal of Visualized Experiments*. (57), e3403 (2011).
14. Jarry, U. *et al.* Treg depletion followed by intracerebral CpG-ODN injection induce brain tumor rejection. *Journal of Neuroimmunology*. **267** (1-2), 35-42 (2014).
15. June, C. H., O'Connor, R. S., Kawalekar, O. U., Ghassemi, S., Milone, M. C. CAR T cell immunotherapy for human cancer. *Science*. **359** (6382), 1361-1365 (2018).
16. Baruch, E. N., Berg, A. L., Besser, M. J., Schachter, J., Markel, G. Adoptive T cell therapy: An overview of obstacles and opportunities. *Cancer*. **123** (S11), 2154-2162 (2017).
17. Bryant, N. L. *et al.* Characterization and immunotherapeutic potential of gammadelta T-cells in patients with glioblastoma. *Neuro-Oncology*. **11** (4), 357-367 (2009).
18. Pereboeva, L., Harkins, L., Wong, S., Lamb, L. S. The safety of allogeneic innate lymphocyte therapy for glioma patients with prior cranial irradiation. *Cancer Immunology, Immunotherapy*. **64** (5), 551-562 (2015).
19. Bailey, S. L., Carpentier, P. A., McMahon, E. J., Begolka, W. S., Miller, S. D. Innate and adaptive immune responses of the central nervous system. *Critical Reviews in Immunology*. **26** (2), 149-188 (2006).
20. Louveau, A. *et al.* Structural and functional features of central nervous system lymphatic vessels. *Nature*. **523** (7560), 337-341 (2015).
21. Menei, P. *et al.* Local and sustained delivery of 5-fluorouracil from biodegradable microspheres for the radiosensitization of glioblastoma: a pilot study. *Cancer*. **86** (2), 325-330 (1999).
22. Menei, P. *et al.* Stereotaxic implantation of 5-fluorouracil-releasing microspheres in malignant glioma. *Cancer*. **100** (2), 405-410 (2004).
23. Salot, S. *et al.* Large scale expansion of gamma 9 delta 2 T lymphocytes: Innacell gamma delta cell therapy product. *Journal of Immunological Methods*. **326** (1-2), 63-75 (2007).
24. Bennouna, J. *et al.* Phase-I study of Innacell gammadelta, an autologous cell-therapy product highly enriched in gamma9delta2 T lymphocytes, in combination with IL-2, in patients with metastatic renal cell carcinoma. *Cancer Immunology, Immunotherapy*. **57** (11), 1599-1609 (2008).
25. Singh, S. K. *et al.* Identification of human brain tumour initiating cells. *Nature*. **432** (7015), 396-401 (2004).

4 – Article 4 : IL-21 Increases the Reactivity of Allogeneic Human V γ 9V δ 2 T Cells Against Primary Glioblastoma Tumors

Noémie Joalland*†, Cynthia Chauvin*†, Lisa Oliver*†‡, François M. Vallette*†, Claire Pecqueur*†, Ulrich Jarry*†, and Emmanuel Scotet*†.

*CRCINA, INSERM, CNRS, Université d'Angers, Université de Nantes ; †LabEx IGO "Immunotherapy, Graft, Oncology"; ‡Hotel Dieu, Hôpital de Nantes, Nantes, France.

N.J. and C.C. contributed equally ; U.J. and E.S. are co-senior authors.

Dans l'article 2, ci-dessus, nous avons démontré l'efficacité anti-tumorale de la combinaison du Zolédronate aux LT V γ 9V δ 2 *in vivo*. Cependant, les effets indésirables d'une ou plusieurs injections de Zolédronate en intracérébral ne sont pas connus. Afin de s'affranchir du Zolédronate, tout en proposant une autre stratégie permettant d'augmenter l'efficacité thérapeutique du transfert adoptif de LT V γ 9V δ 2 allogéniques, nous avons choisi d'orienter cette étude sur l'amélioration de la cytotoxicité de ces effecteurs. Au cours de cette étude, nous avons donc analysé les effets d'un pré-conditionnement *ex vivo* par l'IL-21 des LT V γ 9V δ 2 avant un transfert adoptif dans un modèle murin de xénogreffe orthotopique de primocultures de GBM. En effet, il est connu que l'IL-21, une cytokine immunomodulatrice de la famille de l'IL-2, permet d'améliorer le potentiel cytotoxique des LT en augmentant leur niveau intracellulaire de granzyme. Nous avons tout d'abord mis en place un modèle murin préclinique basé sur l'implantation en orthotopique d'une primoculture de GBM et montré que ces cellules tumorales primaires étaient naturellement éliminées par les LT V γ 9V δ 2, principalement via la voie perforine/granzyme. Ensuite, nous avons démontré que l'effet du pré-conditionnement par l'IL-21, sur le niveau intracellulaire en granzyme B et sur la cytotoxicité des LT V γ 9V δ 2, était efficace dès 24 heures et se maintenait après plusieurs jours de sevrage. Enfin, nous avons mis en évidence l'efficacité thérapeutique du transfert adoptif de LT V γ 9V δ 2 humains allogéniques pré-conditionnés à l'IL-21, 24 heures avant injection, *ex vivo*, afin d'éviter tout effet indésirable lié à l'injection d'IL-21 au sein de la tumeur, dans notre modèle orthotopique de GBM. Ces résultats ouvrent la voie vers de nouvelles stratégies immunothérapeutiques par transfert adoptif d'effecteurs cytotoxiques chez les patients atteints de GBM.

Publié dans Journal of Immunotherapy, 2018

IL-21 Increases the Reactivity of Allogeneic Human V γ 9V δ 2 T Cells Against Primary Glioblastoma Tumors

Noémie Joalland,*† Cynthia Chauvin,*† Lisa Oliver,*†‡
François M. Vallette,*† Claire Pecqueur,*† Ulrich Jarry,*†
and Emmanuel Scotet*†

Summary: Glioblastoma multiforme (GBM) remains the most frequent and deadliest primary brain tumor in adults despite aggressive treatments, because of the persistence of infiltrative and resistant tumor cells. Nonalloreactive human V γ 9V δ 2 T lymphocytes, the major peripheral $\gamma\delta$ T-cell subset in adults, represent attractive effectors for designing immunotherapeutic strategies to track and eliminate brain tumor cells, with limited side effects. We analyzed the effects of ex vivo sensitizations of V γ 9V δ 2 T cells by IL-21, a modulating cytokine, on their cytolytic reactivity. We first showed that primary human GBM-1 cells were naturally eliminated by allogeneic V γ 9V δ 2 T lymphocytes, through a perforin/granzyme-mediated cytotoxicity. IL-21 increased both intracellular granzyme B levels and cytotoxicity of allogeneic human V γ 9V δ 2 T lymphocytes in vitro. Importantly, IL-21-enhanced cytotoxicity was rapid, which supports the development of sensitization(s) of $\gamma\delta$ T lymphocytes before adoptive transfer, a process that avoids any deleterious effect associated with direct administrations of IL-21. Finally, we showed, for the first time, that IL-21-sensitized allogeneic V γ 9V δ 2 T cells significantly eliminated GBM tumor cells that developed in the brain after orthotopic administrations in vivo. Altogether our observations pave the way for novel efficient stereotaxic immunotherapies in GBM patients by using IL-21-sensitized allogeneic human V γ 9V δ 2 T cells.

Key Words: $\gamma\delta$ T cells, immunotherapy, cytokines, cancer

(*J Immunother* 2018;00:000–000)

Glioblastoma multiforme (GBM), the most frequent human glioma, is highly aggressive and has a dismal prognosis (WHO grade IV; median survival of 9.4 mo and 2-y mortality > 86%).¹ Current treatment, based on surgery followed by radiotherapy and chemotherapy,² modestly improves the survival, but all patients rapidly die from tumor relapse. The efficacy of combined treatment is strongly hampered by the incompleteness of surgical excision and the toxicity of radiotherapy and chemotherapy.³ The highly proliferative and infiltrative nature of GBM cells, associated with cellular heterogeneity, as illustrated by the presence of

cancer stem cells (CSC), also strongly contributes to the therapeutic limitations.^{3–6} Cellular immunotherapies have been proposed to eradicate deep brain infiltrative tumor cells with minimal toxicities.⁷ Various cellular immunotherapies using different target T-cell effectors, such as $\alpha\beta$ or $\gamma\delta$ T lymphocytes, have been proposed to eradicate deep brain infiltrative tumor cells with minimal toxicities.^{7–10}

V γ 9V δ 2 T cells, found only in primates, represent the most frequent $\gamma\delta$ T lymphocyte subset in the peripheral blood of healthy adults (5%–10% of CD3⁺ lymphocytes) and carry a T-cell receptor (TCR) composed of V δ 2 chains, which are systematically paired to V γ 9 chains.^{11,12} Importantly, antigenic activation of V γ 9V δ 2 T cells is both species specific and contact dependent, but not restricted by major histocompatibility complex (MHC) molecules, thus excluding the emergence of any deleterious alloreactive response.¹³ V γ 9V δ 2 T-cell activation involves low-molecular-weight phosphorylated nonpeptidic molecules called phosphoantigens that are metabolites produced as intermediates of mevalonate microbial or mammalian pathways. Accordingly, cells either treated with aminobisphosphonates (NBP), which are pharmacologic inhibitors of the mevalonate pathway, or with a deregulated metabolism (eg, tumor cells) express higher amounts of phosphoantigens and activate V γ 9V δ 2 T cells. The specific antigenic activation of V γ 9V δ 2 T cells is tightly regulated by adhesion molecules and natural killer receptor axes, and it is controlled by butyrophilin BTN3A1 molecules, which are expressed by target cells.^{14–16} Numerous studies report that primate V γ 9V δ 2 T cells recognize a broad range of infected or transformed target cells from various tissular origins in vitro, including brain tumors. From a clinical standpoint, both passive and active immunotherapies targeting $\gamma\delta$ T cells in cancer patients have yielded promising clinical responses.¹⁷ In a recent study, we have shown both the feasibility and the antitumor efficacy of orthotopic administrations of allogeneic human V γ 9V δ 2 T cell in mice carrying orthotopic primary human GBM tumors.¹⁰ However, this effect required concomitant administration of NBP compounds and can induce potential deleterious effects on healthy brain tissue. In this study, we analyzed a promising alternative immunotherapeutic strategy enhancing natural responses toward GBM cells, following ex vivo sensitization of resting allogeneic human V γ 9V δ 2 T cells with IL-21, a strong modulatory cytokine.¹⁸

MATERIALS AND METHODS

Cells

Human mononuclear cells were isolated from healthy donor blood samples obtained from the Etablissement Français du Sang (EFS, Nantes, France) by Ficoll density centrifugation (Eurobio, Les Ullis, France). For specific expansions of V γ 9V δ 2 T cells, peripheral mononuclear cells were incubated with 3 μ M bromohydrin pyrophosphate,

Received for publication November 6, 2017; accepted March 8, 2018.
From the *CRCINA, INSERM, CNRS, Université d'Angers, Université de Nantes; †LabEx IGO "Immunotherapy, Graft, Oncology"; and ‡Hôtel Dieu, Hôpital de Nantes, Nantes, France.

N.J. and C.C. contributed equally.

U.J. and E.S. are co-senior authors.

Reprints: Emmanuel Scotet, INSERM UMR1232, Centre de Recherche en Cancérologie et Immunologie Nantes-Angers, IRS_UN, 8 quai Moncoussu, 44007 Nantes cedex 1, France (e-mail: emmanuel.scotet@inserm.fr).

Supplemental Digital Content is available for this article. Direct URL citations appear in the printed text and are provided in the HTML and PDF versions of this article on the journal's website, www.immunotherapy-journal.com.

Copyright © 2018 Wolters Kluwer Health, Inc. All rights reserved.

kindly provided by Innate Pharma (Marseille, France) in Roswell Park Memorial Institute supplemented with 10% heat-inactivated fetal calf serum, 2 mM L-glutamine, 10 mg/mL streptomycin, 100 IU/mL penicillin (Gibco, Carlsbad, CA), and 100 IU/mL recombinant human IL-2 (Chiron, Emeryville, CA). Cultures were supplemented with 300 IU/mL IL-2 at day 4, and the purity was measured by flow cytometry at week 3 (purity $\geq 95\%$). For rhuIL21 sensitization, resting IL-2-expanded human V γ 9V δ 2 T lymphocytes were incubated with 30 ng/mL of premium grade recombinant human IL-21 (Myltenyi Biotech, Bergisch-Gladbach, Germany). V γ 9V δ 2 T cells were washed in fresh Roswell Park Memorial Institute before experiments. U87-MG cell line (HTB-14; ATCC, Manassas, VA) was cultured in Dulbecco's modified eagle's medium (DMEM) medium (Gibco) supplemented with 10% heat-inactivated fetal calf serum, 2 mM L-glutamine, 10 mg/mL streptomycin, and 100 IU/mL penicillin. GBM-1 are human primary astrocytic cancer cells (GBM, grade IV, WHO 2016), derived from fresh tumor fragments (ie, biopsy and mechanical dissociation) collected from a GBM patient. GBM-1 primary culture was grown in defined medium containing DMEM/Ham-F12 (Gibco) supplemented with 2 mM L-glutamine, N2 and B27 supplements (Gibco), 2 mg/mL heparin (Sigma Aldrich, Saint Louis, MO), 20 ng/mL Epidermal Growth Factor (Peprotech, Rocky Hill, NJ), 25 ng/mL basic Fibroblast Growth Factor (Peprotech), 10 mg/mL streptomycin, and 100 IU/mL penicillin. For limiting dilution assays, cells were dissociated and seeded at an initial concentration of 2×10^3 cells/mL, from which serial dilutions were performed in a 96-well plate. Brain-derived cells were cultured for 2 weeks, after which the fraction of wells that did not contain neurospheres for each cell-plating density was calculated as described.¹⁹ Cells were cultured at 37°C in humidified atmosphere with 5% CO₂.

Flow Cytometry

For human GBM cell surface staining, primary cells were incubated with 10 μ g/mL of APC-labeled anti-human CD44 mAb (clone #G44-26; BD Biosciences, Franklin Lakes, NJ) or associated isotype controls. For intracellular staining, primary GBM cells were fixed with phosphate buffered saline (PBS)-paraformaldehyde (PFA) 4%, incubated with permeabilization buffer (Perm Buffer, eBiosciences, Life Tech, Courtaboeuf, France), and then stained with anti-human Nestin mAb (clone #10C2; Milipore, Billerica, MA). For V γ 9V δ 2 T cells intracellular staining, cells were fixed with PBS-PFA 4%, incubated with permeabilization buffer, and then stained with PE-labeled anti-human granzyme B (Gzmb) mAb (clone MHGB04; Invitrogen, Frederick, MD). Acquisition was performed using a FACSCalibur flow cytometer (BD Biosciences), and the events were analyzed using the FlowJo software (Treestar, Ashland, OR).

⁵¹Cr-Release Assays

Target cells were sensitized, or not, overnight with zoledronic acid (10 μ M; Sigma Aldrich) before incubation for 1 hour with ⁵¹Cr (2.77 μ Ci/ 1×10^6 cells), washed, and cocultured for 4 hours with allogeneic V γ 9V δ 2 T cells, at the indicated effector to target ratios. ⁵¹Cr release activity was measured in supernatants using a MicroBeta counter (Perkin Elmer, Waltham, MA). The percentage of tumor target cell lysis = (experimental release - spontaneous release) / (maximum release - spontaneous release) $\times 100$. Maximum and spontaneous release were determined by adding 1%

Triton X-100 or medium, respectively, to ⁵¹Cr-labeled target cells in the absence of T cells.

Immunodeficient Mice

This study was carried out in accordance with the recommendations of the French Regional Ethics Committee of the Pays de la Loire (Approvement #00186.02). Immunodeficient NOD.Cg-Prkdcscid Il2rgtm1Wjl/SzJ (NSG) mice were obtained from Charles River Laboratories (Wilmington, MA) and bred in the animal facility of the University of Nantes (UTE, SFR F. Bonamy) under SPF status. Mice aged 6–12 weeks were used. Human GBM cells were injected (1×10^4 cells resuspended in 2 μ L PBS) using a stereotaxic frame (Stoelting, Wood Dale, IL) at 2 mm on the right of the medial suture and 0.5 mm in front of the bregma, depth: 2.5 mm. For adoptive T-cell transfers, 2×10^7 allogeneic human V γ 9V δ 2 T cells were stereotaxically injected into the tumor bed at different time points after tumor cell implantation: on days 7 and 14 with 1- μ g zoledronate or alone on days 7, 14, and 21.

Immunohistochemistry

Brains were fixed with 4% PFA-PBS, embedded in paraffin wax, and serially sectioned. Sections were incubated with 2% bovine serum albumin and then with polyclonal rabbit anti-human CD3 Ab (Dako, Agilent Technologies, Santa Clara, CA) or rabbit anti-human MHC class I Ab (clone EPR1394Y; Abcam). Revelation was performed by using polymer histofine rabbit to mouse coupled to horse radish peroxidase (Microm Microtech France, Francheville, France) and a DAB detection system (Leica, Wetzlar, Germany). Slides were scanned using the NanoZoomer 2.0 HT (Hamamatsu Photonics K.K., Hamamatsu, Japan).

Statistical Analyses

Data are expressed as mean \pm SEM and were analyzed using GraphPad Prism 6.0 software (GraphPad Software Inc., San Diego, CA). Mann and Whitney ($*P < 0.05$; $**P < 0.005$; $***P < 0.0005$) or log-rank tests (see indicated *P*-value) were used to reveal significant differences. Relative Risk (RR) was calculated using the following formula: $RR = (\text{experimental event}/\text{total subjects})/(\text{control event}/\text{total subject})$, with experimental and control events representing the number of long-time surviving mice in each experimental group. RR value > 1 implies that the event is more likely to occur in the experimental group than in the control group.

RESULTS

Primary Human Glioblastoma Culture Cells for Analyzing the Reactivity of V γ 9V δ 2 T Cells

Owing to the species specificity of V γ 9V δ 2 T cells and the lack of natural counterparts in rodents, we designed an orthotopic model of human tumor xenograft in immunodeficient NSG mice. The objective of these initial experiments was to set up a reliable *in vivo* model that recapitulates human GBM tumor features. The following main requirements were chosen: tumor cell candidates should (i) grow to induce the death of orthotopically engrafted mice, (ii) form an infiltrative tumor, and (iii) naturally activate allogeneic human V γ 9V δ 2 T cells. Commercial human brain tumor cell lines, such as U87-MG, were characterized by a relative cellular homogeneity, triggering a compact and poorly invasive tumor mass *in vivo*.¹⁰ In contrast, primary human tumor cells, such as GBM-1 cells, established from fresh tumor

biopsies and grown in defined media, retained cellular heterogeneity, which was associated with invasive properties.²⁰ Following their orthotopic implantation, mouse brain IHC analysis, performed at days 7, 14, 28, and 45, indicated the rapid formation of highly infiltrative tumors (Fig. 1A). GBM-1 cell cultures, expressing stemness markers, as shown by cytometric analyses of CD44 and Nestin (Fig. 1B), were

characterized by the presence of ~25% of CSC, as determined by the limiting dilution assays (Fig. 1C). Our results show that, unlike U87-MG cells and the previously described GBM-10 cells,¹⁰ allogeneic human Vγ9Vδ2 T cells naturally kill primary GBM-1 cells in the absence of NBP (Fig. 1D). A recent study has reported that U87-MG cells with stemness features are more susceptible to natural killer (NK) cell

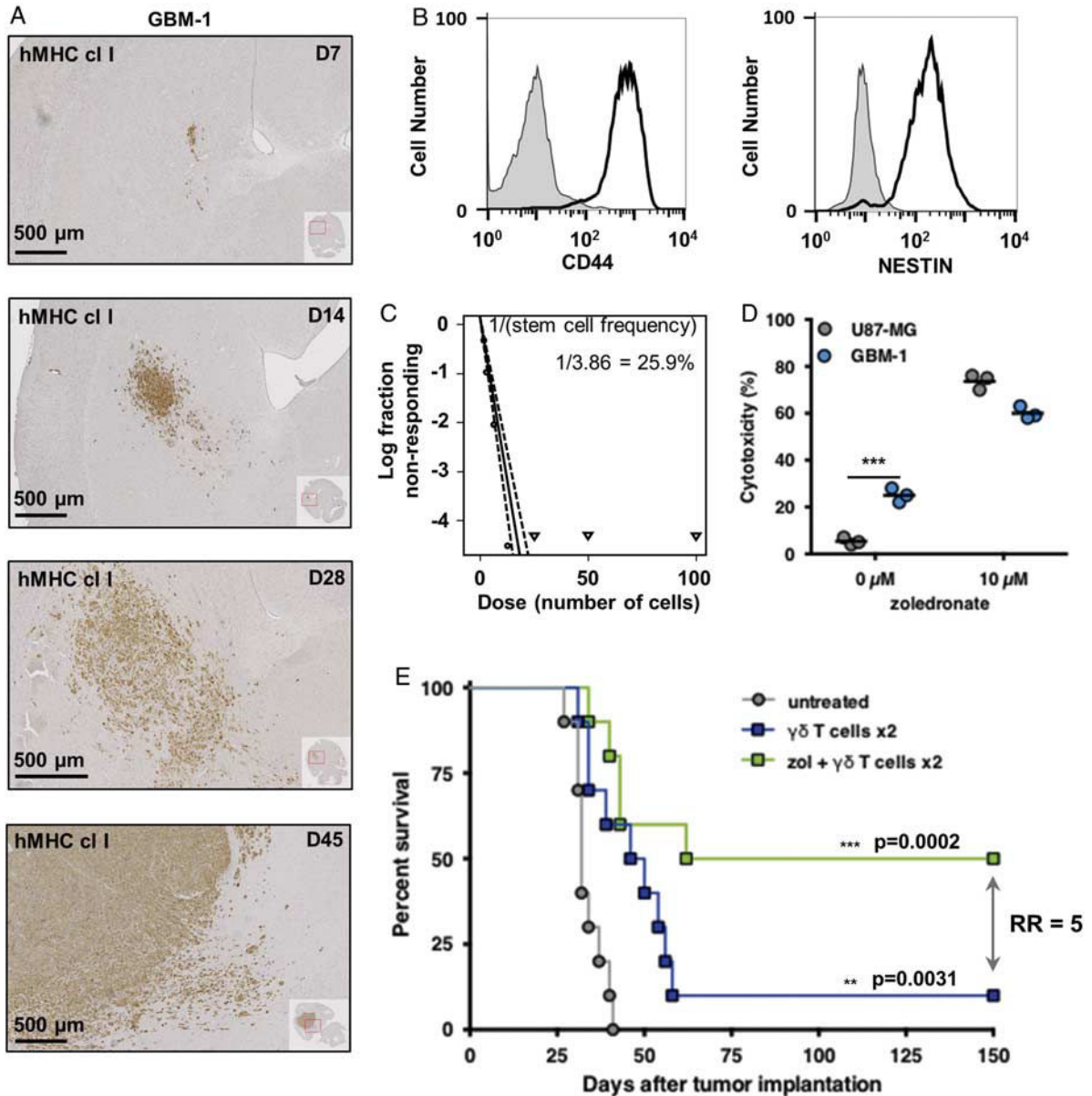


FIGURE 1. Primary human GBM-1 cells as tools for the establishment of orthotopic human GBM models. A, hMHC cl I expression was analyzed by immunohistochemistry on brain sections of NSG mice prepared at days (D) 7, 14, 28, and 45 after orthotopic implantation of GBM-1 cells. B, GBM-1 cells were analyzed by flow cytometry for CD44 and Nestin expression. Gray histograms correspond to staining obtained using isotype control antibody. C, GBM-1 cells were seeded with an initial concentration of 2×10^3 cells/mL in 96-well plates. After 15 days of culture, the fraction of wells that did not contain neurospheres was calculated for each cell-plating density condition. D, Human Vγ9Vδ2 T cells were cocultured for 4 hours with ⁵¹Cr-loaded U87-MG (gray) or GBM-1 (blue) cells after sensitization, or not, with 10 μM of zoledronic acid (n = 3; ***P < 0.001). E, Survival curves of GBM-1 tumor-bearing NSG mice untreated (gray) or treated at days 7 and 14 with only Vγ9Vδ2 T cells (Vγ9Vδ2 T cells x2, blue) or combined with zoledronic acid (zol+Vγ9Vδ2 T cells x2, green) (n = 10 mice). Statistical analyses are indicated; log-rank (**P < 0.01; ***P < 0.001) and relative risk tests were calculated to assess statistical significance of the survival differences among experimental groups. GBM indicates glioblastoma multiforme; hMHC cl I, human MHC class I.

cytotoxicity, because of an altered expression of NKG2D ligands.²¹ However, our results did not provide evidence of similar links between stemness of U87-MG cells, promoted by serum-free culture conditions, and the reactivity of V γ 9V δ 2 T lymphocytes (data not shown).

After stereotaxic engraftment, GBM-1 cells proliferated and formed a tumor that induced the death of mice (Fig. 1E). In line with our previously published observations,¹⁰ 2 successive combined local administrations of NBP and human allogeneic V γ 9V δ 2 T cells protected half of tumor-engrafted mice (RR = 5). Importantly, these experiments also showed that a significant fraction of mice was protected when human allogeneic V γ 9V δ 2 T cells were administered alone, in the absence of any NBP. Altogether, our results indicated that brain-invasive primary human GBM-1 cells, containing a significant fraction of CSC, could be further used for establishing invasive orthotopic GBM models, and for testing immunotherapeutic strategies that exclusively rely on administration(s) of allogeneic human V γ 9V δ 2 T cell effectors *in vivo*.

The Reactivity of V γ 9V δ 2 T Cells Toward GBM Cells is Boosted by IL-21 *in vitro*

We next aimed at establishing a process that enhances the natural reactivity of allogeneic human V γ 9V δ 2 T cells, almost exclusively using the perforin/granzyme pathway to kill human GBM tumor cells (Supplemental Fig. S1, Supplemental Digital Content 1, <http://links.lww.com/JIT/A503>). IL-21 is a strong modulating cytokine that was shown to increase both GzmB intracellular levels in immune

effectors,²² including human V γ 9V δ 2 T cells¹⁸ and, subsequently, their cytolytic activity. Resting peripheral blood lymphocytes (PBL)-amplified V γ 9V δ 2 T lymphocytes were briefly sensitized by rhuIL21 (24 h) before determining intracellular GzmB expression. As expected, rhuIL21 significantly increased GzmB levels within human V γ 9V δ 2 T cells (Fig. 2A), without affecting their viability (Supplemental Fig. S2, Supplemental Digital Content 1, <http://links.lww.com/JIT/A503>). These observations were extended to V γ 9V δ 2 T cells that originate from the blood from different human healthy donors ($n > 5$; Fig. 2B). The cytolytic activity of allogeneic human V γ 9V δ 2 T cells against GBM cells was measured in ⁵¹Cr-release cytolytic assays. As shown in Figure 2C, rhuIL21 sensitization increased V γ 9V δ 2 T-cell cytotoxic activity against GBM-1 cells, as compared with untreated V γ 9V δ 2 T cells (67% increase). It is interesting to note that rhuIL21 sensitization also increased V γ 9V δ 2 T-cell cytotoxicity against non-naturally recognized GBM cell lines such as U87-MG (Fig. 2C) and GBM-10 cells (data not shown). These results were confirmed in experiments that used increasing effector to GBM-1 target ratios (Fig. 2D). Together, these results indicated that rhuIL21 enhances the natural cytolytic activity of V γ 9V δ 2 T cells against GBM tumor cells *in vitro*, through an increase in GzmB, which represents a key V γ 9V δ 2 cytolytic player.

As various studies tend to suggest, for safety reasons, that IL-21 should not be directly administered *in vivo*,²³ kinetic parameters of efficiency of *ex vivo* sensitization of V γ 9V δ 2 T lymphocytes by this cytokine were determined next. First, allogeneic human PBL-V γ 9V δ 2 T lymphocytes

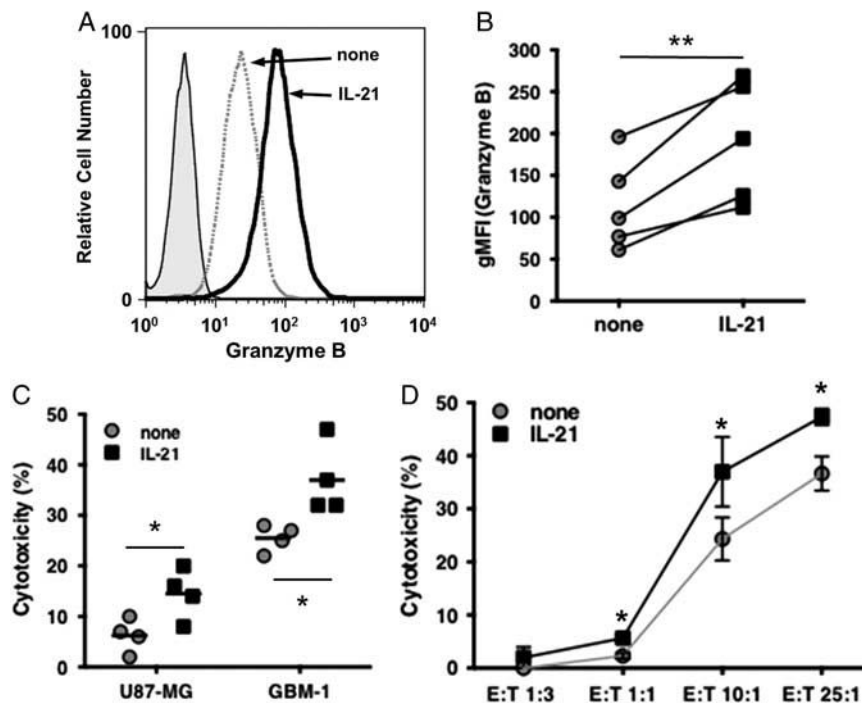


FIGURE 2. IL-21 increases both GzmB levels in V γ 9V δ 2 T cells and their cytotoxic activity against GBM cells. Human V γ 9V δ 2 T cells were sensitized, or not, with recombinant human IL-21 for 1 day. A, Representative flow cytometry histogram of intracellular GzmB expression in human V γ 9V δ 2 T cells (gray histograms indicate the staining with isotype control antibody). B, Compared GzmB expression (gMFI) of nontreated (none) and IL-21-sensitized V γ 9V δ 2 T cells from different PBL-donors ($n = 5$ donors; $**P < 0.01$). C, V γ 9V δ 2 T cells were cocultured for 4 h with ⁵¹Cr-loaded U87-MG and GBM-1 target cells at effector (E:T) ratio 10:1 ($n = 4$) or (D) with ⁵¹Cr-loaded GBM-1 cells at E:T ratios 1:3, 1:1, 10:1, and 25:1 ($n = 3$). Results are expressed as percentage of cytotoxicity ($*P < 0.05$). GBM indicates glioblastoma multiforme; GzmB, granzyme B.

were sensitized with rhuIL21 for 1, 3, 5, or 7 days, and intracellular GzmB expression was measured by flow cytometry. GzmB levels rapidly increased and remained at this level for at least 5 days (Fig. 3A). This enhanced expression of GzmB was accompanied by an increased tumor cytotoxicity that progressively diminished after 1 day of sensitization to reach a basal level at day 5 (Fig. 3B). In a second set of experiments, V γ 9V δ 2 T lymphocytes were sensitized with rhuIL21 (24 h) and then washed to determine how long T cells would remain sensitized after IL-21 withdrawal. It is interesting to note that the effect of IL-21 lasted at least for 24 hours, as assessed by measuring the GzmB level and the cytolytic activity of V γ 9V δ 2 T lymphocytes (Figs. 3C, D). IL-21-sensitized V γ 9V δ 2 T lymphocytes cultured in the absence of this cytokine progressively reduced both GzmB levels and cytotoxic activity to finally reach the initial levels after 7 days. Altogether, these results indicate that a short-term rhuIL21 treatment rapidly and significantly enhances the natural antitumor reactivity of human allogeneic V γ 9V δ 2 T cells through a long-lasting increase of intracellular GzmB levels.

IL-21 Enhances the Natural Activity of Human V γ 9V δ 2 T Cells Against Tumor Cells in vivo

Finally, we investigated whether, or not, rhuIL21 augmented the anti-GBM tumor reactivity of transferred allogeneic human V γ 9V δ 2 T cells in vivo. GBM-1 tumor-bearing

mice were treated with 3 cycles of stereotaxic administrations of allogeneic human V γ 9V δ 2 T cells (days 7, 14, and 21) that had been sensitized or not, with rhuIL21. Three days after the third stereotaxic administration of IL-21-sensitized V γ 9V δ 2 T cells at the tumor site, the brains were collected from the mice and immunohistochemical analyses were performed (anti-human CD3 ϵ mAb). Following transfer, IL-21-sensitized allogeneic human V γ 9V δ 2 T cells mainly colonized in the vicinity of the GBM tumor that developed in the brain (Fig. 4A, left). Of note, a small number of administrated V γ 9V δ 2 T cells were present in the second hemisphere, which was initially devoid of any tumor cells or T lymphocytes (Fig. 4A, right). Together, our data indicated that rhuIL21 sensitization does not affect the mobility of V γ 9V δ 2 T cells in vivo.

Although untreated mice rapidly died (mean survival = 27 d), 3 administrations of V γ 9V δ 2 T cells modestly, but significantly, improved the survival of treated mice (mean survival = 41 d) (Fig. 4B). Importantly, the mean survival of mice was increased from 41 days to 66 days when V γ 9V δ 2 T cells were sensitized with rhuIL21 before stereotaxic injection (RR = 4). Strikingly, under these experimental conditions, 3 mice survived > 150 days after GBM-1 cell implantation, indicating that this treatment eradicated GBM disease. Immunohistochemical analyses (anti-human MHC class I mAb) confirmed the total absence of tumor cells in the brains of surviving mice (Fig. 4B, right inserted panel). Altogether, our results indicated that rhuIL21 significantly enhances the

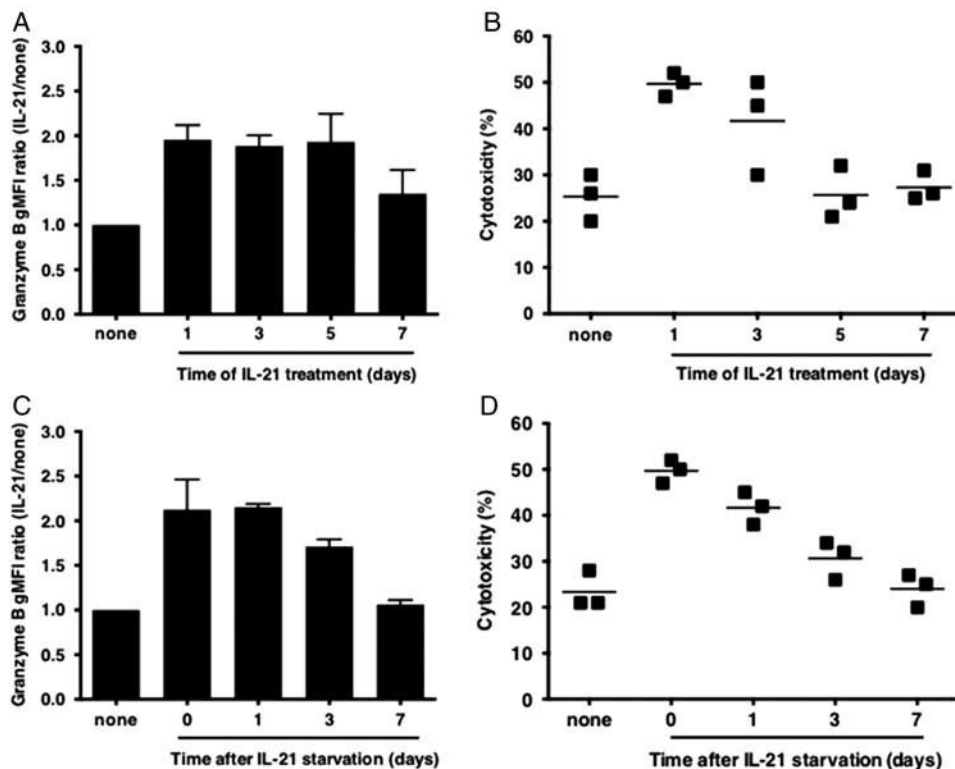


FIGURE 3. IL-21-increased granzyme B levels in V γ 9V δ 2 T cells and anti-GBM tumor cytolytic activity are long-lasting events. Human V γ 9V δ 2 T cells were sensitized, or not, with recombinant human IL-21 for either 1, 3, 5, 7 days (A, B) or 1 day (C, D). In this latter condition, washed $\gamma\delta$ T lymphocytes were next cultured for 1, 3, or 7 days in the absence of IL-21. Intracellular GzmB expression was measured in V γ 9V δ 2 T cells by flow cytometry. A and C, Results are expressed as a ratio of gMFI (gMFI of IL-21-sensitized cells/gMFI of control cells) (n = 3). B and D, V γ 9V δ 2 T cells were cocultured for 4 h with ^{51}Cr -loaded GBM-1 cells (E:T = 10:1). ^{51}Cr release was measured in culture supernatants. Results are expressed as percentage (%) of cytotoxicity (n = 3). GBM indicates glioblastoma multiforme.

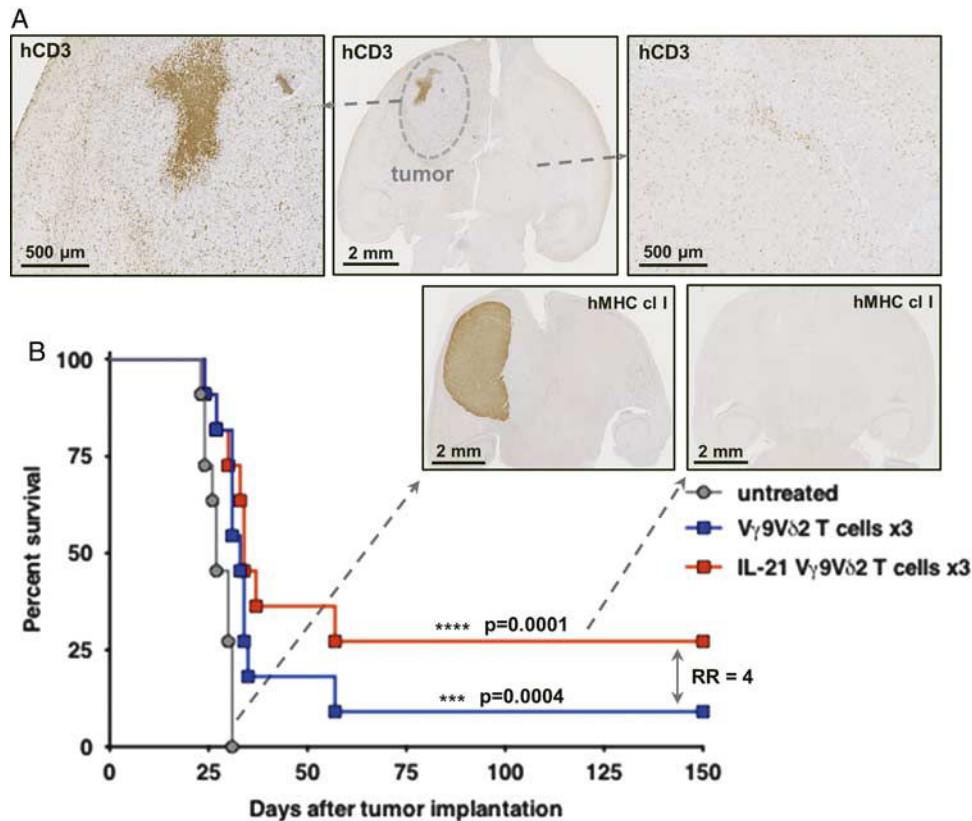


FIGURE 4. Adoptively transferred allogeneic human $V\gamma 9V\delta 2$ T cells sensitized with IL-21 efficiently eliminate orthotopic GBM-1 cells in vivo. A, Human CD3 ϵ (hCD3) expression was analyzed by immunohistochemistry on brain sections of NSG mice prepared 3 days after injection of IL-21-sensitized $V\gamma 9V\delta 2$ T cells in mice carrying orthotopic GBM-1 tumors. Dotted line delineates the GBM-1 tumor mass. B, Survival curves of GBM-1 brain tumor-bearing NSG mice untreated (gray lines, $n = 15$ mice) or successively treated at days 7, 14, and 21 with either allogeneic human $V\gamma 9V\delta 2$ T cells ($V\gamma 9V\delta 2$ T cells $\times 3$, blue line, $n = 15$ mice) or IL-21-sensitized $V\gamma 9V\delta 2$ T cells (IL-21 $V\gamma 9V\delta 2$ T cells $\times 3$, red line, $n = 11$ mice). Statistical analyses are indicated, log rank ($***P < 0.001$; $****P < 0.0001$) and relative risk tests were calculated to assess statistical significance of the survival differences among experimental groups. Right panels: hMHC class I expression was analyzed by immunohistochemistry on brain sections prepared from untreated mice and long-time surviving mice. GBM indicates glioblastoma multiforme; hMHC class I, human MHC class I.

natural cytotoxicity of stereotactically administered allogeneic human $V\gamma 9V\delta 2$ T cells toward invasive heterogeneous primary human GBM tumors.

DISCUSSION

Adoptive immunotherapies that rely on stereotactic transfer(s) of cellular immune effectors, such as allogeneic human $V\gamma 9V\delta 2$ T cells, represent novel promising approaches for eradicating aggressive, resistant, and brain-infiltrating GBM tumor cells, with limited side effects on healthy tissues.⁹ Following a previous proof-of-concept study that showed both the feasibility and antitumor efficacy of such strategies,¹⁰ our study first aimed at evaluating the spontaneous cytotoxicity of allogeneic human $V\gamma 9V\delta 2$ T lymphocytes against primary human GBM tumor cells in vivo, mainly involving the perforin/granzyme axis. Importantly, our data showed, for the first time that ex vivo sensitizations with IL-21 enhanced, through a massive and rapid but transient, GzmB increase in sensitized resting PBL-amplified $V\gamma 9V\delta 2$ T lymphocytes, their protective action against orthotopic GBM tumor cells in vivo.

Taking into account the initial characteristics and our previous observations, indicating that commercial human

U87-MG cells grow by forming noninfiltrative, compact and poorly physiological tumors in vivo,^{10,24} we focused our work on distinct primary human GBM cell cultures. These tumor cells, originating from GBM biopsies,²⁵ were phenotypically and functionally characterized to identify robust, reproducible, and physiologically relevant in vivo models. Among candidates, GBM-1 cells were selected, as they were also characterized by a cellular heterogeneity and the presence of CSCs, which might be involved in the rapid tumor recurrence and resistance to aggressive radiotherapy and chemotherapy.²⁶ GBM-1 are human primary astrocytic cancer cells (grade IV GBM), which are derived from fresh tumor fragments collected from a patient. These tumor cells are grown in a defined medium (DMEM/Ham-F12, L-glutamine, N2 and B27 supplements, heparin, Epidermal Growth Factor, and basic Fibroblast Growth Factor). These culture conditions were shown to help maintain the initial cellular heterogeneity and in particular the presence of cells with stem cell properties.²⁰ The stereotactic implantation of GBM-1 cells from primary cultures led to the death of mice, which was associated with a deep brain parenchyma tumor infiltration. Importantly, we observed that a significant fraction of xenografted mice survived upon single administrations of allogeneic human $V\gamma 9V\delta 2$ T cells, which

was in line with the results from in vitro cytotoxicity assays. Our results showed for the first time the direct and spontaneous eradication of primary GBM cells by allogeneic human V γ 9V δ 2 T lymphocytes. By showing that blockades of both the CD95-L and TRAIL axes slightly affected GBM cell cytotoxicity by V γ 9V δ 2 T cells, our analyses confirmed that the perforin/granzyme axis plays a major role in this tumor cell killing process.^{18,27} We previously showed the efficiency of GBM immunotherapies on the basis of combined administrations of allogeneic human V γ 9V δ 2 T cells and NBP.¹⁰ Under these experimental settings, the pharmacological NBP compounds, which have already been indicated for the treatment of calcemia and bone disorders,²⁸ would be directly injected into the brain tissues, as they are unable to cross over the blood-brain barrier.²⁹ However, their potential deleterious effects, as well as their pharmacodynamic parameters within the human brain, have not been studied, which hinders both ethically and scientifically any therapeutic use within the brain. Here, administrations of NBP could be efficiently bypassed with ex vivo IL-21 sensitizations of effector cells, at least in a subset of human GBM tumors.

We next aimed at defining strategies that modulate perforin/granzyme pathways and further enhance the spontaneous cytotoxicity of allogeneic human V γ 9V δ 2 T lymphocytes against GBM-1 cells. We demonstrated that IL-21, a strong regulatory cytokine,²² enhances the natural anti-GBM cytotoxicity displayed by human V γ 9V δ 2 effector T cells in vitro and in vivo. IL-21 is a cytokine that belongs to the IL-2 family and is mainly highly produced by T-helper lineages and some tumor cells, such as Hodgkin's lymphoma cells. It specifically binds to heterodimeric type I receptors that are expressed on the membrane of lymphocytes (eg, T, B, and NK), which leads to the activation of the janus kinases/signal transducers and activators of transcription pathway. This cytokine axis is implicated in various pathologic situations including allergies, autoimmunity, viral infections, and cancer.^{30,31} The most well-known direct effects of IL-21 are linked to its boosting action on cytotoxic immune effectors, such as T and NK cells, and proliferative actions on target cells. In the former case, IL-21 can increase the ability of T, B, and NK lymphocytes to kill target cells through upregulation of granzymes and perforin. In vitro, the cytotoxic activity increase of V γ 9V δ 2 T cells was correlated with a rapid augmentation of GzmB expression.¹⁸ The direct administration of IL-21 in tumor treatment in vivo remains debatable, as some studies have shown that it could favor the tumor growth and its migration in breast cancer³² and myeloma,³³ justifying why IL-21 should rather be considered for designing ex vivo sensitizations. Here, we show that IL-21 enhances both intracellular GzmB expression and cytolytic properties of resting allogeneic human-amplified V γ 9V δ 2 T cells toward primary GBM-1 tumor cells in vitro and in vivo. This effect could be detected within the first hours of sensitization and lasted for several days, even after cytokine starvation. It is interesting to note that the kinetics of GzmB and cytotoxicity upregulations did not strictly correlate, suggesting that GzmB is rapidly implied in V γ 9V δ 2 T-cell cytotoxicity but that the expression of inhibitory molecules (eg, ILT2, NKG2A), which could also be affected, would next dampen this process (ie, retro-control loop).^{18,34} On the basis of these observations that remained critical in the design of immunotherapeutic strategies, the antitumor activity of rhuIL21-sensitized V γ 9V δ 2 T cells was assessed in a GBM-1 brain tumor mice model. We demonstrated that injected IL-21-sensitized V γ 9V δ 2 T cells were detected both

in the vicinity of the tumor bed and in distant brain areas 3 days after their stereotaxic administration in vivo. This confirmed that ex vivo IL-21 sensitization alters neither the survival of V γ 9V δ 2 T cells nor their mobility once injected into the brain. Strikingly, this treatment greatly improved the survival of treated mice with a complete remission for almost 1/3 of them. These effects were observed using peripheral resting V γ 9V δ 2 T cells from various healthy donors. Whether or not this applies to other types of tumors from distinct patients remains to be established. Our results showed that IL-21 is a cytokine that enhances, through a rapid ex vivo sensitization step, the spontaneous anti-GBM cytolytic activity of resting amplified V γ 9V δ 2 T cells in vivo. The antigenic activation of V γ 9V δ 2 T cells, which is both T-cell receptor dependent and contact dependent, requires the expression of ubiquitous self-molecules such as butyrophilins¹⁵ but is not restricted by MHC molecules, thus excluding any deleterious alloreactive response.^{35,36} Therefore, the constitution of allogeneic V γ 9V δ 2 T-cell batches in therapeutic banks prepared from selected healthy donors and sensitized by boosting molecules, such as IL-21, represents promising therapeutic options for eradicating resistant and deep tissue infiltrative tumors such as GBM.

In conclusion, our study showed for the first time the significant antitumor effects of stereotaxic immunotherapies in vivo relying on local administrations of rhuIL21-sensitized allogeneic human V γ 9V δ 2 T cells for the treatment of highly infiltrating GBM tumors. In these settings, the potentially deleterious effects would be limited, if not excluded, because of the following reasons: (i) the lack of alloreactive responses mediated by allogeneic human V γ 9V δ 2 T cells, (ii) the rapid ex vivo cytokine-sensitization steps, and (iii) the absence of NBP administrations.

ACKNOWLEDGMENTS

The authors thank the staff of University Hospital animal facility of Nantes for animal husbandry and care, the cellular and tissular imaging core facility of Nantes university (MicroPICell) for imaging, and the Cytometry Facility Cytocell from Nantes for their expert technical assistance.

Conflicts of Interest/Financial Disclosures

Supported by INSERM, CNRS, Université de Nantes, Association pour la Recherche contre le Cancer (R10139NN), Institut National du Cancer (INCa, PLBio2013-201, PLBio2014-155), Agence Nationale de la Recherche (ANR, GDSTRESS), Ligue Nationale contre le Cancer (AO InterRegional 2012). This work was realized in the context of the LabEX IGO and the IHU-Cesti programs, supported by the National Research Agency Investissements d'Avenir via the programs ANR-11-LABX-0016-01 and ANR-10-IBHU-005, respectively. The IHU-Cesti project is also supported by Nantes Metropole and the Pays de la Loire Region. The authors did not receive support from National Institutes of Health (NIH); Wellcome Trust; Howard Hughes Medical Institute (HHMI).

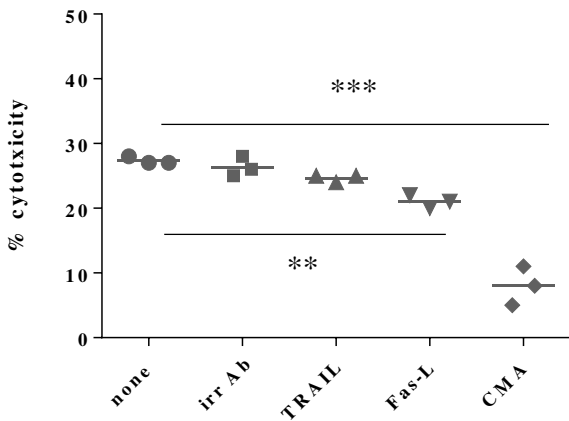
All authors have declared there are no financial conflicts of interest with regard to this work.

REFERENCES

1. Weller M, Cloughesy T, Perry JR, et al. Standards of care for treatment of recurrent glioblastoma—are we there yet? *Neuro-oncology*. 2013;15:4–27.

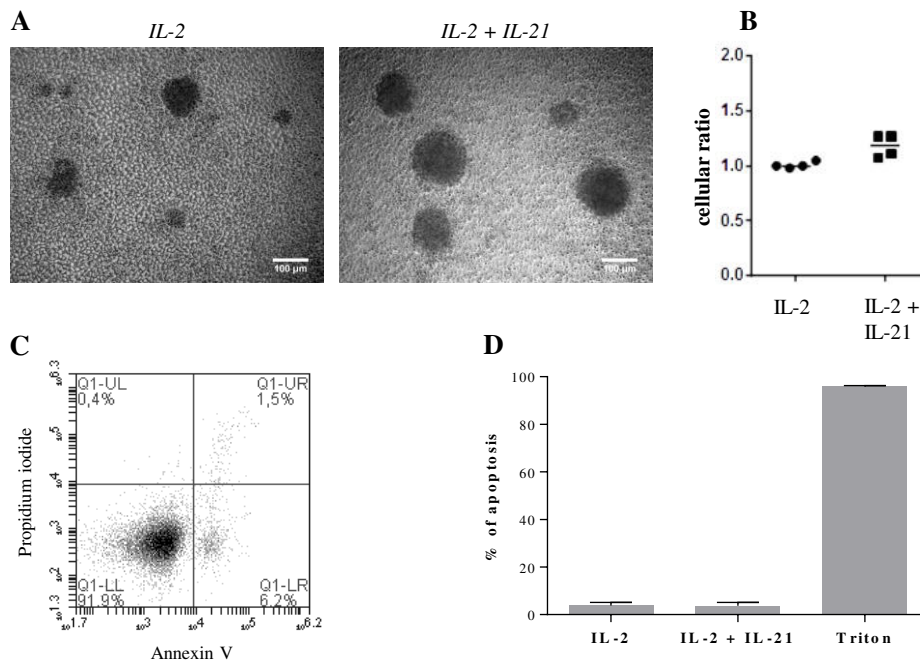
2. Stupp R, Roila F. Malignant glioma: ESMO clinical recommendations for diagnosis, treatment and follow-up. *Ann Oncol*. 2009;20(suppl 4):126–128.
3. Buckner JC, Brown PD, O'Neill BP, et al. Central nervous system tumors. *Mayo Clinic Proc*. 2007;82:1271–1286.
4. Yuan X, Curtin J, Xiong Y, et al. Isolation of cancer stem cells from adult glioblastoma multiforme. *Oncogene*. 2004;23:9392–9400.
5. Singh SK, Hawkins C, Clarke ID, et al. Identification of human brain tumour initiating cells. *Nature*. 2004;432:396–401.
6. Bao S, Wu Q, McLendon RE, et al. Glioma stem cells promote radioresistance by preferential activation of the DNA damage response. *Nature*. 2006;444:756–760.
7. Vauleon E, Avril T, Collet B, et al. Overview of cellular immunotherapy for patients with glioblastoma. *Clin Dev Immunol*. 2010;2010:1–18.
8. Dutoit V, Herold-Mende C, Hilf N, et al. Exploiting the glioblastoma peptidome to discover novel tumour-associated antigens for immunotherapy. *Brain*. 2012;135:1042–1054.
9. Bryant NL, Gillespie GY, Lopez RD, et al. Preclinical evaluation of ex vivo expanded/activated gammadelta T cells for immunotherapy of glioblastoma multiforme. *J Neurooncol*. 2011;101:179–188.
10. Jarry U, Chauvin C, Joalland N, et al. Stereotaxic administrations of allogeneic human Vgamma9Vdelta2 T cells efficiently control the development of human glioblastoma brain tumors. *Oncoimmunology*. 2016;5:e1168554.
11. Lefranc MP, Rabbitts TH. A nomenclature to fit the organization of the human T-cell receptor gamma and delta genes. *Res Immunol*. 1990;141:615–618.
12. Hayday AC. [gamma][delta] cells: a right time and a right place for a conserved third way of protection. *Ann Rev Immunol*. 2000;18:975–1026.
13. Chien YH, Meyer C, Bonneville M. gammadelta T cells: first line of defense and beyond. *Annu Rev Immunol*. 2014;32:121–155.
14. Harly C, Guillaume Y, Nedellec S, et al. Key implication of CD277/Butyrophilin-3 (BTN3A) in cellular stress sensing by a major human gammadelta T cell subset. *Blood*. 2012;120:2269–2279.
15. Harly C, Peigne CM, Scotet E. Molecules and Mechanisms Implicated in the Peculiar Antigenic Activation Process of Human Vgamma9Vdelta2 T Cells. *Front Immunol*. 2014;5:657.
16. Sandstrom A, Peigne CM, Leger A, et al. The intracellular B30.2 domain of butyrophilin 3A1 binds phosphoantigens to mediate activation of human Vgamma9Vdelta2 T cells. *Immunity*. 2014;40:490–500.
17. Fournie JJ, Sicard H, Poupot M, et al. What lessons can be learned from gammadelta T cell-based cancer immunotherapy trials? *Cell Mol Immunol*. 2013;10:35–41.
18. Thedrez A, Harly C, Morice A, et al. IL-21-mediated potentiation of antitumor cytolytic and proinflammatory responses of human V gamma 9V delta 2 T cells for adoptive immunotherapy. *J Immunol*. 2009;182:3423–3431.
19. Das AV, James J, Zhao X, et al. Identification of c-Kit receptor as a regulator of adult neural stem cells in the mammalian eye: interactions with Notch signaling. *Dev Biol*. 2004;273:87–105.
20. Oizel K, Chauvin C, Oliver L, et al. Efficient mitochondrial glutamine targeting prevails over glioblastoma metabolic plasticity. clinical cancer research: an official journal of the American Association for. *Cancer Res*. 2017;23:6292–6304.
21. Oh SJ, Yang JI, Kim O, et al. Human U87 glioblastoma cells with stemness features display enhanced sensitivity to natural killer cell cytotoxicity through altered expression of NKG2D ligand. *Cancer Cell Int*. 2017;17:22.
22. Leonard WJ, Wan CK. IL-21 signaling in immunity. *Fl000Research*. 2016;5:1–10.
23. Spolski R, Leonard WJ. Interleukin-21: a double-edged sword with therapeutic potential. *Nat Rev Drug Discov*. 2014;13:379–395.
24. Allen M, Bjerke M, Edlund H, et al. Origin of the U87MG glioma cell line: good news and bad news. *Sci Translational Med*. 2016;8:354re353.
25. Brocard E, Oizel K, Lalier L, et al. Radiation-induced PGE2 sustains human glioma cells growth and survival through EGF signaling. *Oncotarget*. 2015;6:6840–6849.
26. Cho DY, Lin SZ, Yang WK, et al. Targeting cancer stem cells for treatment of glioblastoma multiforme. *Cell Transplant*. 2013;22:731–739.
27. Barcia C Jr, Gomez A, Gallego-Sanchez JM, et al. Infiltrating CTLs in human glioblastoma establish immunological synapses with tumorigenic cells. *Am J Pathol*. 2009;175:786–798.
28. Coleman RE. Zoledronic acid ameliorates the effects of endocrine therapy on bone health in women with early-stage breast cancer. *Nat Clin Pract Endocrinol Metab*. 2009;5:72–73.
29. Weiss HM, Pfaar U, Schweitzer A, et al. Biodistribution and plasma protein binding of zoledronic acid. *Drug Metab Dispos*. 2008;36:2043–2049.
30. Spolski R, Leonard WJ. The Yin and Yang of interleukin-21 in allergy, autoimmunity and cancer. *Curr Opin Immunol*. 2008;20:295–301.
31. Spolski R, Leonard WJ. Interleukin-21: basic biology and implications for cancer and autoimmunity. *Ann Rev Immunol*. 2008;26:57–79.
32. Wang LN, Cui YX, Ruge F, et al. Interleukin 21 and its receptor play a role in proliferation, migration and invasion of breast cancer cells. *Cancer Genomics Proteomics*. 2015;12:211–221.
33. Brenne AT, Ro TB, Waage A, et al. Interleukin-21 is a growth and survival factor for human myeloma cells. *Blood*. 2002;99:3756–3762.
34. Skak K, Frederiksen KS, Lundsgaard D. Interleukin-21 activates human natural killer cells and modulates their surface receptor expression. *Immunology*. 2008;123:575–583.
35. Lamb LS Jr, Musk P, Ye Z, et al. Human gammadelta(+) T lymphocytes have in vitro graft vs leukemia activity in the absence of an allogeneic response. *Bone Marrow Transplant*. 2001;27:601–606.
36. Pereboeva L, Harkins L, Wong S, et al. The safety of allogeneic innate lymphocyte therapy for glioma patients with prior cranial irradiation. *Cancer Immunol Immunother*. 2015;64:551–562.

Supplemental Figure S1



Supplemental Figure S1. Allogeneic human V γ 9V δ 2 T lymphocytes preferentially lyse GBM-1 cells through perforin/granzymes pathways. V γ 9V δ 2 T lymphocytes were treated 2 h with concanamycin A (CMA, 50 nM, Sigma, C9705) or for 30 min with blocking mAbs directed against either CD95 ligand (Fas-L, 5 μ g/mL, BD Biosciences, NOK-1), TRAIL (TRAIL, 5 μ g/mL, BD Biosciences, RIK-1) or an isotype control mAb (irrAb, 5 μ g/mL, BioXCell, MOPC-21). V γ 9V δ 2 T cells were co-cultured, for 4 h with ⁵¹Cr-loaded GBM-1 target cells at effector to target ratio 10:1 (n=3). Results are expressed as percentage (%) of cytotoxicity (**p<0.01;***p<0.001).

Supplemental Figure S2



Supplemental Figure S2. IL-21 does not impact the survival of human V γ 9V δ 2 T cells *in vitro*. Resting IL-2-amplified human V γ 9V δ 2 T cells were incubated, or not, with recombinant IL-21 (30 ng/mL) for 24 hours. (A) Brightfield microscopy images of V γ 9V δ 2 T cells cultured 24 hours in either IL-2 medium (*left*) or IL-2 medium supplemented by human IL-21 (*right*). (B) Ratio (collected/seeded cells) of V γ 9V δ 2 T lymphocytes (n=4). (C) Representative AnnexinV/PI staining (Biolegend, Ref. #422201) of IL-21-treated human V γ 9V δ 2 T cells analyzed by flow cytometry. (D) Apoptosis rate values following AnnexinV/PI staining of V γ 9V δ 2 T cells cultured for 24 hours in the presence of either recombinant human IL-2 medium (n=4) or IL-2 medium supplemented by IL-21 (n=4). Positive control: Triton, incubation (10minutes) of cells with TritonX-100 lysing buffer (n=2). Results are expressed as percentage (%) of apoptosis.

5 – Article 5 : NKG2D pathway controls the natural reactivity of allogeneic V γ 9V δ 2 T lymphocytes against human mesenchymal glioblastoma cells

Cynthia Chauvin^{1,2,3#}, Noémie Joalland^{1,2,3#}, Ulrich Jarry^{1,2,3}, Laura Lafrance^{1,2,3}, Jeanne Perroteau^{1,2,3}, Catherine Willem^{1,2,6}, Christelle Retière^{1,2,6}, Catherine Gratas^{1,2,4}, Xavier Saulquin^{1,2,3}, François M. Vallette^{1,2,5}, Henri Vié^{1,2,3}, Emmanuel Scotet^{1,2,3§} and Claire Pecqueur^{1,2,3§}

¹ CRCINA - INSERM U1232, Nantes 44007 France ; ² Faculté de Médecine, Université de Nantes, Nantes 44007 France ; ³ LabEx IGO “Immunotherapy, Graft, Oncology”, Nantes 44007 France ; ⁴ Hotel Dieu, Hôpital de Nantes, Nantes 44007 France ; ⁵ Institut de Cancérologie de l’Ouest - René Gauducheau, St Herblain ; ⁶ Etablissement Français du Sang, Nantes, France.

#,§ Authors contributed equally to this work

Lors des études précédentes, nous avons analysé la réactivité et la cytotoxicité de LT V γ 9V δ 2 humains allogéniques contre des cellules primaires humaines de GBM et avons remarqué que la primoculture GBM-1 était naturellement reconnue et éliminée (Article 4) contrairement à la primoculture GBM-10 (Article 2). Dans cette étude, nous avons approfondi ce phénomène et mis en évidence que les primocultures appartenant au sous-type MES (mésenchymateux), telles que GBM-1, étaient naturellement mieux reconnues et éliminées que les autres primocultures dites CNP (classique, neural et prolifératif), telle que GBM-10. Grâce à la réalisation de tests de réactivité avec des LT V γ 9V δ 2 allogéniques générés à partir de différents donneurs, nous avons également mis en évidence une hétérogénéité de la reconnaissance des primocultures de GBM. Ainsi, nous avons cherché à comprendre pourquoi, à la fois, certaines primocultures de GBM étaient mieux reconnues que d’autres et pourquoi certaines populations de LT V γ 9V δ 2 étaient naturellement plus réactives que les autres. Grâce à une combinaison d’analyses transcriptomiques, phénotypiques et de tests fonctionnels, nous avons démontré à la fois que (i) les populations de LT V γ 9V δ 2 les plus réactives présentaient un niveau d’expression de NKG2D plus important, et (ii) que les primocultures MES expriment plus de molécules de stress, ligands de NKG2D, que les primocultures CNP. Pour finir, nous avons pu valider, *in vivo*, que les LT V γ 9V δ 2 hautement réactifs présentaient un meilleur potentiel thérapeutique aussi bien dans le modèle GBM-1 que dans le modèle GBM-10, en comparaison de LT V γ 9V δ 2 plus faiblement réactifs.

En préparation

NKG2D pathway controls the natural reactivity of allogeneic V γ 9V δ 2 T lymphocytes against human mesenchymal glioblastoma cells

Cynthia Chauvin^{1,2,3#}, Noémie Joalland^{1,2,3#}, Jeanne Perroteau^{1,2,3}, Ulrich Jarry^{1,2,3}, Laura Lafrance^{1,2,3}, Catherine Willem^{1,2,6}, Christelle Retière^{1,2,6}, Lisa Oliver^{1,4}, Catherine Gratas^{1,2,4}, Xavier Saulquin^{1,2,3}, François M. Vallette^{1,2,3,5}, Henri Vié^{1,2,3}, Emmanuel Scotet^{1,2,3§} and Claire Pecqueur^{1,2,3§}

¹ CRCINA - INSERM U1232, Nantes 44007 France

² Faculté de Médecine, Université de Nantes, Nantes 44007 France

³ LabEx IGO “Immunotherapy, Graft, Oncology”, Nantes 44007 France

⁴ Hotel Dieu, Hôpital de Nantes, Nantes 44007 France

⁵ Institut de Cancérologie de l’Ouest - René Gauducheau, St Herblain

⁶ Etablissement Français du Sang, Nantes, France

#,§ Authors contributed equally to this work

Running title: NKG2D-tuned reactivity of V γ 9V δ 2 T lymphocytes against mesenchymal glioblastoma cells

Key words: Human, glioblastoma multiforme, immunotherapy, V γ 9V δ 2 T lymphocytes, NKG2D

Corresponding authors:

- Claire Pecqueur, Centre de Recherche en Cancérologie et Immunologie Nantes-Angers, INSERM U1232, Université de Nantes, 8 quai Moncousu, 44007 Nantes, France; e-mail: claire.pecqueur@univ-nantes.fr; phone: (33)2 2808 0325; Fax: (33)2 2808 0204
- Emmanuel Scotet, Centre de Recherche en Cancérologie et Immunologie Nantes-Angers, INSERM U1232, Université de Nantes, 8 quai Moncousu, 44007 Nantes, France; e-mail: emmanuel.scotet@univ-nantes.fr; phone : (33)2 2808 0222 ; Fax: (33)2 2808 0204

Conflicts of Interest: The authors disclose no potential conflicts of interest

Abbreviations: GBM, glioblastoma multiforme; BrHPP, bromohydrin pyrophosphate; CSC, cancer stem cells; E/T, effector-to-target ratio; $\gamma\delta$ T cells, gamma delta T cells; IPP, isopentenyl pyrophosphate; NBP, aminobisphosphonates; PAg, phosphoantigens; MFI, mean fluorescence intensity; MICA/B, MHC class I polypeptide-related sequence A/B; NKG2D, natural killer group 2D; ULBP, UL16 binding protein

Acknowledgments

This work was supported by INSERM, CNRS, Université de Nantes, Association pour la Recherche contre le Cancer (#R10139NN), Institut National du Cancer (#V9V2THER, INCa#PLBio2013-201, #PLBio2014-155), Agence Nationale de la Recherche (ANR, #GDSTRESS), Ligue Nationale contre le Cancer (AO InterRegional 2012). This work was realized in the context of the LabEX IGO and the IHU-Cesti programs, supported by the National Research Agency Investissements d'Avenir via the programs ANR-11-LABX-0016-01 and ANR-10-IBHU-005, respectively. The IHU-Cesti project is also supported by Nantes Metropole and the Pays de la Loire Region. We thank the Cytocell platform, MicroPicell platform as well as the animal facility staff, in particular Sylvia Lambot (UTE, SFR). We would like to thank Pierre Autin, Lucie Lebreuilly and Fanny Geraldo for technical help.

Abstract

Glioblastoma multiform (GBM) is the most frequent and aggressive primary brain tumor in adults, with a dismal prognosis and few therapeutic advances made over the last decade. Cellular immunotherapies are currently being explored to eliminate highly invasive and chemo/radioresistant GBM cells likely involved in rapid disease relapse. Non-alloreactive allogeneic human V γ 9V δ 2 T lymphocytes are able to kill a wide range of human tumor cells, including GBM cells, and display effector functions, setting them up as promising cell effector candidates for efficient immunotherapies. Here, using human primary GBM cells, we evidence that GBM cells displaying a mesenchymal subtype signature are spontaneously and efficiently eliminated by allogeneic human V γ 9V δ 2 T lymphocytes. This natural reactivity process is mediated by $\gamma\delta$ TCR and tightly controlled by cellular stress-associated NKG2D pathway. This led to the identification of highly-reactive V γ 9V δ 2 T lymphocyte populations, independently of a TCR repertoire signature. Finally, we provide evidence of allogeneic V γ 9V δ 2 T lymphocyte immunotherapy efficacy in vivo, in absence of any prior tumor cell sensitization. By identifying key molecules and pathways implicated in the selective natural recognition of mesenchymal GBM cell subtypes, accounting for 30% of diagnosed cases, our results pave the way for targeted novel cellular immunotherapies.

Introduction

Glioblastoma (GBM) is the most frequent primary brain tumors in adult (incidence of 5 per 100 000). Current standard therapy, defined as Stupp's protocol, is composed by surgery followed by radiotherapy with concomitant and adjuvant chemotherapy (Stupp et al., 2005). Despite these aggressive treatments, the median survival of patients does not exceed 18 months, with less than 5% of patients alive at 5 years. This dismal prognosis includes deep invasive tumor growth, limiting surgery efficiency, as well as poor drug delivery across the Blood Brain Barrier and a high degree of GBM tumor heterogeneity. First, GBM display inter-tumor heterogeneity mostly characterized by distinct genetic alterations occurring in individual tumors and leading to various responses to identical patients. The genetic landscape of GBM has been performed through Genome Wide Association Studies (GWAS) allowing the identification of up to four molecular subtypes with relative prognosis or predictive significance (Phillips et al., 2006; Verhaak et al., 2010) with marked differences between the mesenchymal subtype (MES) and the 3 other ones (defined here as CNP, referring to Classical, Neural and Proneural subtypes). In general, CNP group is associated with a more favorable outcome in contrast to MES subtype associated with poor survival (Huse et al., 2011; Phillips et al., 2006; Zheng et al., 2012). Second, spatial heterogeneity within the same tumor, including active tumor zones as well as hypoxic and necrotic zones, is common in GBM. Importantly, hypoxic zones constitute cellular niches for cancer stem cells (CSC) with distinct phenotypic properties including transient quiescence, self-renewal and resistance to chemically and radiation-induced DNA damages. Thus, new strategies targeting highly resistant cancer cells, including mesenchymal GBM cells and CSC, may significantly improve patients outcomes.

Following their spectacular effects evidenced in various solid and circulating cancer indications, immunotherapies have also been proposed for treating GBM patients, including adoptive transfer of immune effector cells. Among them, V γ 9V δ 2 T lymphocytes, being mostly present in primates (5-10% of peripheral blood CD3⁺ cells in healthy adults), represent important players of natural host defenses against infection and malignancies (Silva-Santos et al., 2015). These transitional T lymphocytes are selectively activated by non-peptidic small molecules called phosphoantigens, such as isopentenyl pyrophosphate (IPP), in a TCR-dependent but MHC-independent manner. Accordingly, pharmacological aminobisphosphonate (NBP) compounds, such as zoledronate, inhibiting a key enzyme of the

mevalonate pathway that degrades phosphoantigens, upregulate the reactivity of V γ 9V δ 2 T lymphocytes. We identified a mandatory role played by CD277 butyrophilins which are type I glycoproteins from the B7 superfamily in this still unclear reactivity process. Besides TCR-dependent mechanism, cell recognition and subsequent V γ 9V δ 2 T cell activation also involved the engagement of Natural Killer (NK) receptors, such as the activating NKG2D (natural killer group 2, member D) receptor. This receptor recognizes molecular stress signatures that are barely expressed by normal cells while often upregulated by infected or transformed cells. Importantly, given the absence of MHC restriction, the injection of allogeneic V γ 9V δ 2 T lymphocytes within the surrounding cerebral parenchyma, following tumor resection would represent a unique opportunity to deliver elevated numbers of immune effectors, directly to the site of residual malignancy. Accordingly, we showed that concomitant stereotactic injection of allogeneic V γ 9V δ 2 T lymphocytes and zoledronate efficiently eliminate GBM growth *in vivo* (Jarry et al., 2016). We also observed recently that V γ 9V δ 2 T lymphocytes exhibit, through an unknown process, efficient and natural cytotoxicity against some primary human GBM cells (Joalland et al., 2018).

Here, we investigated the molecular mechanisms regulating this unexpected natural reactivity of allogeneic human V γ 9V δ 2 T lymphocytes toward GBM cells. Using human primary GBM cells deriving from patient that resume relevant features of human GBM, we demonstrated that allogeneic V γ 9V δ 2 T lymphocytes specifically and spontaneously recognized and killed mesenchymal GBM cells through both TCR and NKG2D engagement. This work next evidenced the existence of highly-reactive V γ 9V δ 2 T lymphocyte populations, independently of their TCR signature. Finally, we provided evidence of allogeneic V γ 9V δ 2 T lymphocyte immunotherapy efficacy *in vivo*, in absence of any prior sensitization.

Materials and Methods

Human primary GBM cultures

Human primary GBM cultures were derived after mechanical dissociation from high-grade glioma operated on 17 patients. All procedures involving human patients were performed in accordance with the ethical standards of the ethic national research committee and with the 1964 Helsinki declaration and its later amendments or comparable ethical standards. Informed consent was obtained from all individual participants included in this study. Primary GBM cells were cultured in define medium (DMEM/Ham F12 (Gibco, Cergy Pontoise, France), 2 mM L-glutamine (Gibco), N2- and B27-supplement (Gibco), 2 µg/ml heparin (Sigma Aldrich, Saint Louis, MO), 20 ng/ml EGF and 25 ng/ml bFGF (Peprotech, Rocky Hill, NJ), 100 IU/ml penicillin and 100 µg/ml streptomycin (Gibco)) at 37 °C in a humidified atmosphere with 5% CO₂. All the experiments were performed at early passages and cells were checked for mycoplasma contamination regularly.

Generation and expansion of allogeneic PBMC-derived human V γ 9V δ 2 T lymphocytes

Human peripheral-blood mononuclear cells (PBMCs) were isolated from blood of informed consent healthy adult volunteers recruited at the Etablissement Français du Sang (EFS, Nantes, France). For specific expansions of V γ 9V δ 2 T lymphocytes, PBMCs were incubated with 5 µM of zoledronic acid monohydrate (#82712, Sigma-Aldrich) or with 3 µM of BrHPP (bromohydin pyrophosphate), kindly provided by Innate Pharma (Marseille, France) in RPMI 1640 culture medium supplemented with 10 % heat inactivated FCS, 2 mM L-glutamine, 100 µg/ml streptomycin, 100 IU/ml penicillin (all from Gibco) and 100 IU/mL recombinant human IL-2 (rhIL-2) (Proleukin, Novartis, Bale, Suisse). After 4 days of culture, cells were supplemented with rhIL-2 (300 IU/mL). After 3 weeks, a non-specific expansion is performed using PHA-feeders: Leucoagglutinin PHA-L (#L4144, Sigma-Aldrich) and 35 Gy-irradiated allogeneic feeder cells mixing human PBMCs and Epstein-Barr Virus-transformed B-lymphoblastoid cell lines. V γ 9V δ 2 T lymphocytes were incubated in RPMI 1640 culture medium supplemented with 10 % heat inactivated FCS, 2 mM L-glutamine, 100 µg/ml streptomycin, 100 IU/ml penicillin (all from Gibco) and 300 IU/mL rhIL-2 (Novartis). Purity (> 85–95 %) of amplified V δ 2⁺ T lymphocyte populations was estimated at resting state (about 3 weeks) by flow cytometry.

Limiting dilution assays were used to clone polyclonal V γ 9V δ 2 T lymphocyte population, generated from PBMCs of healthy donors. Final cell dilutions ranged from 0.3 cell per well to 10 cells per well. At day 30, the fraction of wells free of T lymphocyte clones for each cell plating density was determined. These results were plotted against the number of cells plated per well. Growing cells from 0.3 cell per well dilution were transferred into larger wells. Clones were screened for V δ 2-TCR chain expression (purity > 99 %) and non-specifically expanded using PHA-feeders, as described above.

Transcriptomic analysis

Primary GBM cells were washed twice in PBS, then total RNA was isolated using the RNeasy MiniKit (Qiagen, Courtaboeuf, France) following the manufacturer's instructions with DNase I treatment. The quantity and quality of RNA were respectively evaluated using the NanoDrop® ND-1000 spectrophotometer (Thermo Fisher Scientific, Waltham, MA, USA) and the Agilent 2100 Bioanalyser (Agilent, Santa Clara, CA). RNA (1.5 μ g) was processed and hybridized to the Genechip Human Genome U133 Plus 2.0 Expression array (Affymetrix, CA), which contains over 54,000 probe sets analyzing the expression levels of over 47,000 transcripts and variants. This roughly corresponds to 29,500 distinct Unigene identifiers. The processing was done according to the recommendations of the manufacturer. The raw signals of each probes for all the arrays were normalized against a virtual median chip (median raw intensity per row) using a local weighted scattered plot smoother analysis. The data were filtered to remove probes with low intensity values by sample category in order to keep the signature of little class of sample. The hierarchical clustering used to detect groups of correlated genes supported by a statistical method (limma) to detect differential expression among biological conditions, was computed on median-gene-centered and log-transformed data using average linkage and uncentered correlation distances with the Cluster program (de Hoon MJL et al. Open source clustering software. *Bioinforma Oxf Engl.* 2004 Jun 12;20(9):1453–4). Functional annotations of gene clusters and differential expressed genes were performed using GoMiner software (Zeeberg et al. GoMiner: a resource for biological interpretation of genomic and proteomic data. *Genome Biol.* 2003;4(4):R28.) and the Gene Ontology database (Ashburner M et al. Gene ontology: tool for the unification of biology. The Gene Ontology Consortium. *Nat Genet.* 2000 May;25(1):25–9). Raw and normalized data have been deposited in the GEO database under accession number (GSE83626).

CD107a mobilization assay

GBM cells were cocultured with V γ 9V δ 2 T lymphocytes (1/1) in define culture medium containing 5 μ M monensin (Sigma-Aldrich) and APC-labelled anti-human CD107a mAb (clone H4A3 from BD Biosciences, Franklin lakes, NJ, USA and BioLegend, San Diego, CA, USA) for 4h at 37 °C in a humidified atmosphere with 5% CO₂. V γ 9V δ 2 T cells were then labeled with FITC-labeled anti-human V δ 2-TCR mAb (clone IMMU389; Beckman Coulter, Fullerton, CA) and analyzed by flow cytometry. Acquisition was performed using a FACSCalibur or an Accuri C6Plus flow cytometer (BD Biosciences) and the events were analyzed using the FlowJo software 10 (Treestar, Ashland, OR).

Cytotoxicity assays

Cytotoxic activity was assessed using a standard ⁵¹Cr release assay. Primary GBM cultures were labelled with ⁵¹Cr (75 μ Ci / 10⁶ cells) for 1h at 37°C, washed four times with define culture medium, plated at 3.10³ cells per well, and T cells were added at the indicated effector-to-target cell ratios in 96-well round-bottom plates. When indicated, tumor cells were pretreated overnight with zoledronate at 20 μ M. For blocking antibodies assays, cells were incubated (30 min, 37°C) prior to the coculture with mouse anti-human MICA/B mAb (clone 6D4; BioLegend) or mouse anti-human CD277/BTN3A1 mAb (clone 103.2; ImCheck Therapeutics, Marseille, France) for primary GBM cultures, and mouse anti-human NKG2D (clone 1D11; BioLegend) for V γ 9V δ 2 T cells. After 4 h co-culture at 37°C, ⁵¹Cr release activity was measured in supernatants using a scintillation counter (MicroBeta, Perkin Elmer, Courtaboeuf, France). Each test was performed in triplicate. Percentage of tumor target cell lysis=((experimental release - spontaneous release)/(maximum release - spontaneous release))*100. Maximum and spontaneous release were determined by adding 1 % Triton X-100 (Sigma) or medium respectively, to ⁵¹Cr-labeled tumor target cells in the absence of T cells.

Cell surface phenotyping

Primary GBM cell surface phenotype was determined by flow cytometry using the following mouse anti-human monoclonal antibodies (mAbs): anti-ULBP2,5,6-PE (clone 165903), anti-ULBP3-PE (clone 166510), anti-ULBP1-AF488 (clone 170818; R&D Systems, Minneapolis, MN, USA), anti-MICA/B-PE (clone 6D4; BD Biosciences, Le Pont de Claix, France) and associated isotype controls. To assess the whole NKG2D ligand expression, primary GBM cultures were incubated with FcR-blocking Reagent (Miltenyi Biotec), washed, labelled with 10 μ g/ml recombinant human NKG2D/CD134 Fc Chimera protein (R&D Systems) or isotype

control, incubated with 1 mg/ml Goat anti Human Biotin (EFS, Nantes, France) followed with Streptavidin-FITC staining (EFS, Nantes, France). V γ 9V δ 2 T cell surface phenotype was determined using anti-human NKG2D-PE (clone ID11; BD Biosciences), anti-NKG2A-PE (Z199; Beckman Coulter Immunotech, Marseille, France) or corresponding isotype-matched control mAbs. Data were collected using a FACSCalibur (BD Biosciences) and analyzed using Flowjo 7.6.1 and 8 software (TreeStar).

Video microscopy

Primary GBM cells were incubated in define medium overnight in Ibidi chamber slides (Martinsried, Germany) coated with fibronectin (Merck, Darmstadt, Germany). For intracellular Ca²⁺ measurements, V γ 9V δ 2 T cells were loaded with 1 μ M Fura-2/AM (Invitrogen, Carlsbad, CA) in Hanks' Balanced Salt Solution (HBSS, Gibco) supplemented with HEPES (Sigma). Recording was performed using a DMI 6000B microscope (Leica Microsystems, Wetzlar, Germany). Cells were illuminated every 10 s with a 300 W xenon lamp by using 340/10 nm and 380/10 nm excitation filters. Emission at 510 nm was captured using a Cool Snap HQ2 camera (Roper, Tucson, AZ, USA) and ratio measurements were performed with Metafluor software (Molecular Devices, Sunnyvale, CA, USA).

Stereotaxic implantation of human GBM and V γ 9V δ 2 T cells in mouse brain

NSG (*NOD.Cg-Prkdcscid Il2rgtm1Wjl/SzJ*) mice (Charles River Laboratories; Wilmington, MA), were bred in the animal facility of the University of Nantes (UTE, SFR F. Bonamy) under SPF status and used at 8–12 weeks of age, accordingly to institutional guidelines (Agreement # 00186.02; Regional ethics committee of the Pays de la Loire (France)). Primary GBM-1 or GBM-10 cultures (10^4 in 2 μ L PBS) were injected using a stereotactic frame (Stoelting, Wood Dale, IL) at 2 mm right lateral of the median suture and 0.5 mm anterior of the Bregma, depth: 2.5 mm. For adoptive V γ 9V δ 2 T cell transfer assays, 2×10^7 allogeneic human V γ 9V δ 2 T cells in 15-20 μ L sterile PBS were stereotaxically injected into the GBM tumor bed at 7, 14 and 21 days (3 injections) after tumor implantation.

Statistical analysis

Data are expressed as mean \pm SD/SEM and were analyzed using GraphPad Prism 6.0 software (GraphPad Software, Inc., San Diego, CA). The difference between groups was analyzed by Mann-Whitney or Kruskal-Wallis tests unless otherwise indicated (* $p < 0.05$, ** $p < 0.01$, *** $p < 0.001$).

Results

Selective natural cytotoxicity of V γ 9V δ 2 T lymphocytes toward primary mesenchymal GBM cultures

In order to define the mechanisms regulating the spontaneous reactivity of allogeneic V γ 9V δ 2 T lymphocytes against the GBM-1 cell line, as compared to GBM-10 (**Figure 1A**), we first extended this observation by analyzing their reactivity against a panel of various primary GBM cell cultures, dissociated from distinct patient tumors (n=17). Of note, these primary GBM cultures exhibited commonly observed genomic alterations such as amplification of *EGFR* and *PDGFR*, loss of *INK4a/ARF* locus or *PTEN* (**Supplemental Table 1**). The reactivity of V γ 9V δ 2 T lymphocytes against GBM cells, pretreated or not with zoledronate, was analyzed after a 4 hours-coculture (**Figure 1B and S1**). When primary GBM cells were sensitized with zoledronate, all V γ 9V δ 2 T lymphocytes strongly upregulated CD107a expression (**Supplemental Figure S1**). Importantly, 5 out of the 17 primary GBM cells spontaneously activated V γ 9V δ 2 T lymphocytes (**Figure 1B**). A supervised hierarchical transcriptomic analysis based on a previously published database (GEO GSE83626), identified the spontaneously recognized GBM cells as the mesenchymal subtype and non-naturally recognized ones as the CNP subtype, as shown in the volcano plot (**Figure 1C**). Accordingly, allogeneic V γ 9V δ 2 T lymphocytes reacted against mesenchymal GBM cells grouped according to this molecular signature, as compared to the other subtypes (**Figure 1D**). ⁵¹Cr-release assays were performed using a representative primary GBM cells from either mesenchymal or CNP subtypes, respectively GBM-1 and GBM-10 cells. As shown in **Figure 1E**, V γ 9V δ 2 T lymphocytes spontaneously killed only GBM-1 cells, but not GBM-10 cells, in a E/T-dependent manner. Altogether, these results evidenced that allogeneic human V γ 9V δ 2 T lymphocytes spontaneously recognize and eliminate mesenchymal human GBM cells, in the absence of any treatment.

V γ 9V δ 2 T lymphocytes display heterogeneous spontaneous reactivity against mesenchymal GBM cells

Besides this selective and spontaneous reactivity toward mesenchymal GBM cells, heterogeneous CD107a expression levels in activated T lymphocytes also suggested intrinsic activation abilities of V γ 9V δ 2 T lymphocytes. The activation against GBM-1 or GBM-10

cells of a broad panel of allogeneic human V γ 9V δ 2 T lymphocyte polyclonal lines (n=44), generated from different healthy donor blood samples, was next analyzed. Whereas a weak CD107a was detected in the majority of V γ 9V δ 2 T lymphocyte populations cocultured with GBM-10 cells, this expression was significantly higher upon coculture with GBM-1 cells (**Figure 2A**). Interestingly, this assays allowed the identification of highly reactive V γ 9V δ 2 T lymphocyte populations (CD107a>20%). Of note, the selective and spontaneous recognition of mesenchymal GBM cells was detected in both highly (L1 and L2) and poorly (L7 and L8) reactive V γ 9V δ 2 T cell lines (**Figure 2B**) and translated in the selective lysis of mesenchymal GBM tumor cells (**Figure 2C**). Zoledronate sensitization of GBM cells abolished these variations of reactivity (**Supplemental Figure S2**). The spontaneous cytotoxicity of L2, a highly reactive V γ 9V δ 2 T lymphocyte line, against mesenchymal GBM-1 cells (45%) reached cytotoxicity levels close to those observed following pretreatment with zoledronate (53%). Altogether, these results indicate that, besides their ability to selectively and spontaneously react against mesenchymal GBM cells, allogeneic human V γ 9V δ 2 T lymphocyte subsets display various functional reactivity levels toward tumor cells.

Specific V γ 9V δ 2 TCR-induced spontaneous reactivity is not driven by a specific TCR repertoire

V γ 9V δ 2 TCR engagement in the spontaneous, as well as in zoledronate-induced reactivity against mesenchymal GBM cells, was first clearly shown in ⁵¹Cr-release assays performed in the presence of BTN3A/CD277 blocking antibody (clone #103.2, **Figure 3A** and **Supplemental Figure S3**). To next investigate whether a specific TCR repertoire might be linked to this particular activation process, T lymphocyte clones were isolated from three highly reactive V γ 9V δ 2 T lymphocyte lines (L1, L2 and L3) from different healthy donors and next analyzed at a phenotypic (TCR repertoire) and functional (cytotoxicity) levels. Of note, only 25 clones sufficiently expanded among more than hundred clones that emerged in this process (**Supplemental Figure S4**). First, ⁵¹Cr release-assays were performed using mesenchymal GBM-1 cells to determine and compare the relative killing abilities of each V γ 9V δ 2 T lymphocyte clones (**Figure 3B**). Four T cell clones displayed a cytotoxic activity against GBM-1 cells higher than the polyclonal population whereas only two T lymphocyte clones were less reactive. To determine whereas such an elevated cytotoxic activity was associated with a specific TCR repertoire, V γ 9 and V δ 2 gene segments were sequenced. The majority of V γ 9V δ 2 T lymphocyte clones expressed a similar V γ 9 sequence (TRGV9*01;

TRG1P*01), with only two clones (L3-19 and L2-9) expressing different V γ 9 rearrangements (TRGV9*01; TRGJP1*01 and TRGV9*02 ;TRGJ1*02, respectively). As expected, more diversity was observed with the V δ 2 TCR repertoire since six signatures were detected. Of note, we were unable to completely determine the V δ 2 TCR repertoire for 1/3 of T lymphocyte clones (**Figure 3C**, group E). Nevertheless, this indicated that the V γ 9V δ 2 TCR repertoire was composed of, at least, four distinct clonotypes and that no specific V γ 9V δ 2 TCR signature was assigned to highly reactive T lymphocyte clones (**Figure 3D**). Altogether, these results show that selective spontaneous elimination of mesenchymal GBM cells involved TCR engagement, independently of a specific V γ 9V δ 2 TCR repertoire.

Spontaneous elimination of GBM cells by V γ 9V δ 2 T lymphocytes is regulated by NKG2D molecules

Besides TCR engagement, a variety of surface inhibitory or activating molecules are also involved in the fine-tuning of V γ 9V δ 2 T lymphocyte activation process. Videomicroscopy analysis of intracellular Ca²⁺ responses of activated V γ 9V δ 2 T lymphocytes showed that cell-to-cell contact with zoledronate-activated GBM cells triggered a rapid and sustained Ca²⁺ responses, characteristic of simultaneous engagement of TCR and tumor-associated costimulatory molecules (**Supplemental Figure S5**). Strikingly, in absence of zoledronate activation, this profile was higher with mesenchymal GBM-1 (**Figure 4A**). Surface phenotyping of selected activating (DNAM-1, NKG2C, NKG2D, NKp30, NKp44) and inhibitory (NKG2A, ILT2) receptors was performed in various V γ 9V δ 2 T lymphocyte lines. As shown in **Figure 4B**, an elevated expression of DNAM-1 (CD226) and NKG2D (*Natural Killer group 2D receptor*) was detected in all the analyzed lines. Importantly, a focus on NKG2D expression showed a significantly higher expression of this receptor in highly reactive V γ 9V δ 2 T lymphocyte lines (**Figure 4C**). The ability of V γ 9V δ 2 T lymphocytes to kill GBM-1 cells was significantly reduced in presence of the blocking NKG2D mAbs (**Figure 4D**) and the combination of NKG2D and BTN3 blocking mAbs totally abolished T lymphocyte cytotoxicity. Of note, when GBM cells were sensitized with zoledronate, no significant cytotoxicity inhibition was observed with the NKG2D blocking mAbs (**Supplemental Figure S6**). Together, these results show that NKG2D, which is highly expressed in GBM-reactive T lymphocytes, regulates the TCR-mediated spontaneous reactivity allogeneic V γ 9V δ 2 T lymphocytes.

Mesenchymal primary GBM cultures express high levels of NKG2D ligands

A bioinformatic PANTHER analysis ran on transcriptomic data showed that immune system process, immune response and response to stress represented 3 of the 6 most differentiated pathways between mesenchymal and CNP GBM cells (**Figure 5A**). The binding of Fc fragment recombinant human NKG2D showed that NKG2D ligands were expressed at a higher level by mesenchymal GBM cells, as compared to CNP cells (**Figure 5B**). Accordingly, RNA levels encoding for MICA/B (*MHC class I Chain related protein A and B*) and ULBP2 (*UL16 binding protein 2*) molecules, which described as NKG2D ligands, were significantly detected at a high level in mesenchymal GBM cultures as compared to CNP cultures (**Figure 5C**). No significant expression of ULBP 4, 5 and 6 molecules and no differences for other tumor cell ligands were observed at the mRNA level (*data not shown* and **Supplemental Figure S7**). The expression of ULBP2 and MICA/B was significantly increased at the surface of mesenchymal GBM cells (**Figure 5D**). These results show that mesenchymal GBM cells highly express several NKG2D ligands, as compared to their CNP counterparts, which might favor their recognition by immune effectors such as human V γ 9V δ 2 T lymphocytes.

Allogeneic V γ 9V δ 2 T lymphocytes control the development of mesenchymal GBM tumors in vivo

Finally, the ability of V γ 9V δ 2 T lymphocytes to spontaneously control the growth of mesenchymal GBM tumor cells *in vivo* was investigated in orthotopic mouse models. Human tumor cells, originating from either GBM-1 (mesenchymal) or GBM-10 (CNP), were orthotopically implanted into the cerebral subventricular zone of immunodeficient NSG mice. Tumor-bearing mice were next treated with 3 stereotactic injections of allogeneic human V γ 9V δ 2 T lymphocytes at days 7, 14 and 21 following tumor implantation (**Figure 6A**). Untreated GBM-1-tumor bearing mice displayed a median survival of 27 days whereas survival of GBM-10 tumor-bearing mice was longer (43.5 days) (**Figure 6B** and **Figure 6C**). Injections of poorly reactive V γ 9V δ 2 T lymphocytes in GBM-1 tumor-bearing mice slightly reduced tumor burden *in vivo*. Variable levels of responding mice could be distinguished after highly reactive V γ 9V δ 2 T lymphocyte administrations. Indeed, survival of 60% of the mice was similar to those injected with poorly reactive V γ 9V δ 2 T lymphocytes, whereas a more drastic effect was observed for the other 40% (highly reactive T lymphocytes conditions with

a mean survival = 32 days for poor responders vs 58 days for good responders) (**Figure 6B**). Among this latter group, 2 mice survived more than 150 days suggesting a complete elimination of tumor cells. Of note, a modestly increased median survival was also measured in GBM-10 group after injection of either poorly or highly reactive V γ 9V δ 2 T lymphocytes, with an higher effect with this latter T lymphocyte subset (**Figure 6C**).

Altogether these results showed that adoptive transfer of allogeneic V γ 9V δ 2 T lymphocytes significantly increased GBM-bearing mice lifespan, in particular when tumor displayed a mesenchymal signature.

Discussion

This study uncovers an unexpected natural reactivity, involving both TCR and costimulatory receptors NKG2D expressed by human V γ 9V δ 2 T lymphocytes against GBM cells displaying a mesenchymal molecular signature that represent 30% of primary diagnosed tumors, both *in vitro* and *in vivo*.

Human V γ 9V δ 2 T lymphocytes are antigenically activated, in a TCR-dependent manner, by phosphoantigens accumulated, probably through altered metabolic mevalonate pathway in transformed cells. It is proposed that non-peptidic phosphoantigens interact with recently highlighted molecules, like BTN3A1/CD277 butyrophilins, rather than being directly recognized by the TCR (Harly et al., 2012; Sandstrom et al., 2014). Human V γ 9V δ 2 T lymphocytes also detect additional stress-induced molecules, such as MICA/B and ULBP which are frequently upregulated in tumor cells, via a set of additional receptors such NKG2D. Our results show a natural recognition of mesenchymal GBM cells by V γ 9V δ 2 T lymphocytes, in absence of any prior sensitization. This study shows that this process involves both TCR and NKG2D costimulatory receptors based on the following complementary observations: (i) the fast and sustained intracellular Ca²⁺ flux profiles in activated T lymphocytes suggested a concomitant engagement of NKG2D-related receptors, together with TCR complexes (Nedellec et al., 2010) ; (ii) mesenchymal GBM cells display elevated expression levels of several NKG2D ligands, as compared to other subtypes; (iii) BTN3A/CD277 and NKG2D blocking mAbs reduce V γ 9V δ 2 T lymphocyte activation. Interestingly, mesenchymal GBM cell lysis was not inhibited by NKG2D blocking mAbs under elevated NBP concentrations suggesting that strong TCR-mediated signals overcome the role of costimulators for providing final threshold activation signals. This further evidences that antigenic activation of human V γ 9V δ 2 T lymphocytes is fine-tuned by a balance of TCR and inhibitory/stimulatory co-signals.

To decipher this, both peripheral human V δ 1⁺ and V δ 2⁺ T lymphocyte subsets displaying anti-tumoral properties were analyzed and only the latter one displayed a significant cytotoxicity against GBM cells (*data not shown*). In agreement with previous studies, TCR repertoire analysis of reactive-V γ 9V δ 2 T lymphocyte clones from distinct individuals provides clear evidence for rather conserved V γ 9 chain recombination associated to diverse V δ 2 chains (reviewed in Hoeres et al., 2018). Two major clonotypes have been identified but

there was no link between the cytolytic activity of clones towards GBM cells and their TCR composition. To illustrate this important point, some T lymphocyte clones exhibited a high reactivity but expressed a similar V γ 9V δ 2 TCR as compared to T lymphocyte clones displaying a barely detectable cytotoxicity. According to the results of previous studies, this indicated that mesenchymal GBM-directed reactivity is not tuned by a specific V γ 9V δ 2 TCR repertoire feature.

Phosphoantigens are usually generated through an altered metabolic mevalonate pathway. Tumor metabolism has been included as a hallmark of cancer with the tumor glycolytic avidity, also known as the Warburg effect, being the most prominent example (Hanahan and Weinberg, 2011). Changes in tumor metabolism go beyond glucose metabolism and also affect lipids and amino acids pathways. We have recently shown that GBM cells exhibited different oxidative metabolism depending on their molecular profile (Oizel et al., 2017). Whereas we did not observe differences in enzymatic expression of the mevalonate pathway (*data not shown*), we cannot exclude that mesenchymal GBM cells might produce different levels of phosphoantigens arising from IPP biosynthesis. The ability of V γ 9V δ 2 T lymphocytes to detect phosphoantigens has been studied *in vivo* using xenograft models of a wide variety of solid and haematological tumors, in particular after tumor cell sensitization using NBP such as zoledronate (review in Fisher et al., 2014). In addition to the anti-resorptive efficacy of zoledronate in prevention and treatment of bone destruction, an increasing number of studies reports its potential anti-tumor effects. However, in most of them, tumor cells are sensitized with either NBP, IL-2 or IL-21 prior or concomitantly to adoptive transfer of allogeneic V γ 9V δ 2 T cells (Joalland et al., 2018; Kabelitz et al., 2004; Santolaria et al., 2013; Zysk et al., 2017). Accordingly, zoledronate dramatically increased the efficiency of adoptive transfer of V γ 9V δ 2 T lymphocytes on GBM-10 tumor bearing mice (Jarry et al., 2016). However, the long-term use of zoledronate leading to jaw osteonecrosis, an increased risk of oesophageal cancer and bone fracture (review in Sellmeyer, 2010) combined with limitations of NBP administration since these compounds do not cross the blood-brain barrier, might limit the potential of these immunotherapeutic strategies. Importantly, allogeneic V γ 9V δ 2 T cells adoptive transfer do not require zoledronate tumor cell sensitization when GBM belongs to the mesenchymal subtype. This observation is of particular interest since these tumors are the most aggressive ones and present in most GBM relapse.

GBM is an archetype example of heterogeneous cancer with a strong histological, molecular and cellular heterogeneity both between patients and within the same individual tumor (Patel et al., 2012; Sottoriva et al., 2013). They are constituted by a mixture of stem cells (CSC, *Cancer Stem Cells*), with a preferential resistance to conventional therapies, as well as more differentiated cells. Several studies have implicated CSC in the poor response of GBM to treatment and tumor recurrence. GBM also exhibit 2 main molecular signatures, the mesenchymal one being associated with the worst patient prognosis. However, less is known about the correlation between CSC, molecular subtypes and immune responses. In our study, we used primary GBM cells directly isolated from human GBM tumor from different patients and cultured as spheres in order to take into account both the molecular and cellular heterogeneities (Oizel et al., 2017). Importantly, in contrast to GBM cell lines, these primary GBM cells trigger highly infiltrative tumor when orthotopically injected in the brain, similarly to what is observed in patients (Jarry et al., 2016; Joalland et al., 2018). Interestingly, by showing that mesenchymal GBM cells displayed a particular expression of NKG2D ligands, favoring their recognition by immune effectors, our results are in line with transcriptomic studies defining this subtype as “immunological reactive” through the enrichment of genes reflective of anti-tumor proinflammatory responses, including both adaptative and innate immunity as well as immune suppression (Doucette et al., 2013). Accordingly, a retrospective analysis of GBM patient receiving dendritic cell immunotherapy has shown that patients with mesenchymal signature had significantly extended survival compared to patients with proneural signatures or patients with mesenchymal GBM treated with various other therapies (Prins et al., 2011).

Altogether, our results reinforce molecular subtype identification as a fundamental basis for GBM patient stratification and highlight that mesenchymal GBM patients would be particularly eligible to immunotherapeutic strategies based on adoptive transfer of allogeneic human V γ 9V δ 2 T lymphocytes, independently of patient immune system.

References

- Doucette, T., Rao, G., Rao, A., Shen, L., Aldape, K., Wei, J., Dziurzynski, K., Gilbert, M., and Heimberger, A.B. (2013). Immune heterogeneity of glioblastoma subtypes: extrapolation from the cancer genome atlas. *Cancer Immunol. Res.* *1*, 112–122.
- Fisher, J.P., Heuvelink, J., Yan, M., Gustafsson, K., and Anderson, J. (2014). $\gamma\delta$ T cells for cancer immunotherapy: A systematic review of clinical trials. *Oncoimmunology* *3*, e27572.
- Hanahan, D., and Weinberg, R.A. (2011). Hallmarks of cancer: the next generation. *Cell* *144*, 646–674.
- Harly, C., Guillaume, Y., Nedellec, S., Peigné, C.-M., Mönkkönen, H., Mönkkönen, J., Li, J., Kuball, J., Adams, E.J., Netzer, S., et al. (2012). Key implication of CD277/butyrophilin-3 (BTN3A) in cellular stress sensing by a major human $\gamma\delta$ T-cell subset. *Blood* *120*, 2269–2279.
- Hoeres, T., Smetak, M., Pretscher, D., and Wilhelm, M. (2018). Improving the Efficiency of V γ 9V δ 2 T-Cell Immunotherapy in Cancer. *Front. Immunol.* *9*, 800.
- Huse, J.T., Phillips, H.S., and Brennan, C.W. (2011). Molecular subclassification of diffuse gliomas: seeing order in the chaos. *Glia* *59*, 1190–1199.
- Jarry, U., Chauvin, C., Joalland, N., Léger, A., Minault, S., Robard, M., Bonneville, M., Oliver, L., Vallette, F.M., Vié, H., et al. (2016). Stereotaxic administrations of allogeneic human V γ 9V δ 2 T cells efficiently control the development of human glioblastoma brain tumors. *Oncoimmunology* *5*, e1168554.
- Joalland, N., Chauvin, C., Oliver, L., Vallette, F.M., Pecqueur, C., Jarry, U., and Scotet, E. (2018). IL-21 Increases the Reactivity of Allogeneic Human V γ 9V δ 2 T Cells Against Primary Glioblastoma Tumors. *J. Immunother. Hagerstown Md 1997* *41*, 224–231.
- Kabelitz, D., Wesch, D., Pitters, E., and Zöller, M. (2004). Characterization of tumor reactivity of human V gamma 9V delta 2 gamma delta T cells in vitro and in SCID mice in vivo. *J. Immunol. Baltim. Md 1950* *173*, 6767–6776.
- Nedellec, S., Sabourin, C., Bonneville, M., and Scotet, E. (2010). NKG2D costimulates human V gamma 9V delta 2 T cell antitumor cytotoxicity through protein kinase C theta-dependent modulation of early TCR-induced calcium and transduction signals. *J. Immunol. Baltim. Md 1950* *185*, 55–63.
- Oizel, K., Chauvin, C., Oliver, L., Gratas, C., Geraldo, F., Jarry, U., Scotet, E., Rabe, M., Alves-Guerra, M.-C., Teusan, R., et al. (2017). Efficient Mitochondrial Glutamine Targeting Prevails Over Glioblastoma Metabolic Plasticity. *Clin. Cancer Res. Off. J. Am. Assoc. Cancer Res.* *23*, 6292–6304.
- Patel, M., Vogelbaum, M.A., Barnett, G.H., Jalali, R., and Ahluwalia, M.S. (2012). Molecular targeted therapy in recurrent glioblastoma: current challenges and future directions. *Expert Opin. Investig. Drugs* *21*, 1247–1266.
- Phillips, H.S., Kharbanda, S., Chen, R., Forrest, W.F., Soriano, R.H., Wu, T.D., Misra, A., Nigro, J.M., Colman, H., Soroceanu, L., et al. (2006). Molecular subclasses of high-grade glioma predict prognosis, delineate a pattern of disease progression, and resemble stages in neurogenesis. *Cancer Cell* *9*, 157–173.
- Prins, R.M., Soto, H., Konkankit, V., Odesa, S.K., Eskin, A., Yong, W.H., Nelson, S.F., and Liao, L.M. (2011). Gene expression profile correlates with T-cell infiltration and relative survival in glioblastoma patients vaccinated with dendritic cell immunotherapy. *Clin. Cancer Res. Off. J. Am. Assoc. Cancer Res.* *17*, 1603–1615.

- Sandstrom, A., Peigné, C.-M., Léger, A., Crooks, J.E., Konczak, F., Gesnel, M.-C., Breathnach, R., Bonneville, M., Scotet, E., and Adams, E.J. (2014). The intracellular B30.2 domain of butyrophilin 3A1 binds phosphoantigens to mediate activation of human V γ 9V δ 2 T cells. *Immunity* *40*, 490–500.
- Santolaria, T., Robard, M., Léger, A., Catros, V., Bonneville, M., and Scotet, E. (2013). Repeated systemic administrations of both aminobisphosphonates and human V γ 9V δ 2 T cells efficiently control tumor development in vivo. *J. Immunol. Baltim. Md 1950* *191*, 1993–2000.
- Sellmeyer, D.E. (2010). Atypical fractures as a potential complication of long-term bisphosphonate therapy. *JAMA* *304*, 1480–1484.
- Silva-Santos, B., Serre, K., and Norell, H. (2015). $\gamma\delta$ T cells in cancer. *Nat. Rev. Immunol.* *15*, 683–691.
- Sottoriva, A., Spiteri, I., Piccirillo, S.G.M., Touloumis, A., Collins, V.P., Marioni, J.C., Curtis, C., Watts, C., and Tavaré, S. (2013). Intratumor heterogeneity in human glioblastoma reflects cancer evolutionary dynamics. *Proc. Natl. Acad. Sci. U. S. A.* *110*, 4009–4014.
- Stupp, R., Mason, W.P., van den Bent, M.J., Weller, M., Fisher, B., Taphoorn, M.J.B., Belanger, K., Brandes, A.A., Marosi, C., Bogdahn, U., et al. (2005). Radiotherapy plus concomitant and adjuvant temozolomide for glioblastoma. *N. Engl. J. Med.* *352*, 987–996.
- Verhaak, R.G.W., Hoadley, K.A., Purdom, E., Wang, V., Qi, Y., Wilkerson, M.D., Miller, C.R., Ding, L., Golub, T., Mesirov, J.P., et al. (2010). Integrated genomic analysis identifies clinically relevant subtypes of glioblastoma characterized by abnormalities in PDGFRA, IDH1, EGFR, and NF1. *Cancer Cell* *17*, 98–110.
- Zheng, S., Chheda, M.G., and Verhaak, R.G.W. (2012). Studying a complex tumor: potential and pitfalls. *Cancer J. Sudbury Mass* *18*, 107–114.
- Zysk, A., DeNichilo, M.O., Panagopoulos, V., Zinonos, I., Liapis, V., Hay, S., Ingman, W., Ponomarev, V., Atkins, G., Findlay, D., et al. (2017). Adoptive transfer of ex vivo expanded V γ 9V δ 2 T cells in combination with zoledronic acid inhibits cancer growth and limits osteolysis in a murine model of osteolytic breast cancer. *Cancer Lett.* *386*, 141–150.

Figure 1

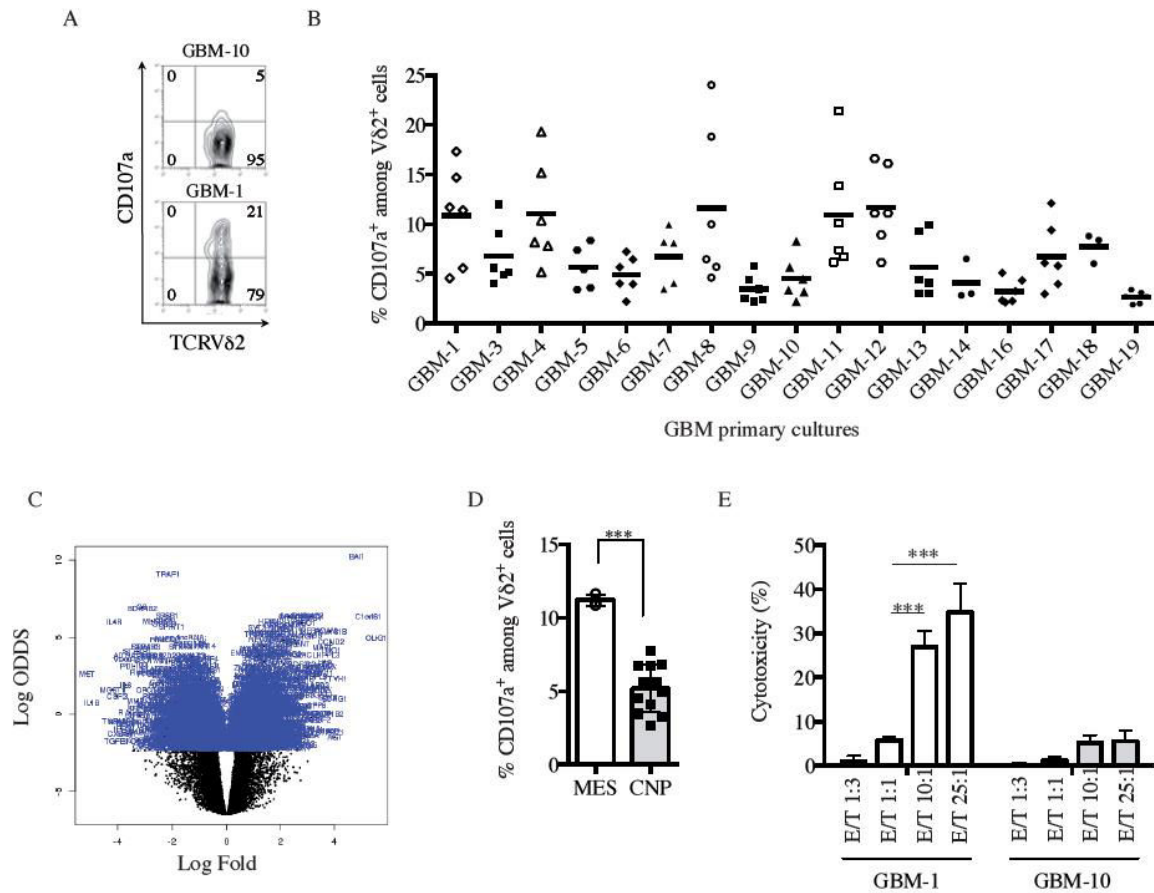


Figure 1. Selective natural cytotoxicity of V γ 9V δ 2 T lymphocytes toward mesenchymal GBM cells.

A. Representative flow cytometry analysis of CD107a cell surface protein expression of V γ 9V δ 2 T lymphocytes cocultured with primary GBM-1 or GBM-10 cells (E:T ratio 1:1). **B.** Frequency of CD107a positive cells among V γ 9V δ 2 T lymphocytes cocultured with 17 primary GBM cultures (E:T ratio 1:1). **C.** Volcano plot of CNP vs MES GBM cells showing the fold ratio and ODDS ratio. The blue spots represent the genes with significant differences between the 2 groups. **D.** Frequency of CD107a positive cells among V γ 9V δ 2 T lymphocytes depending on the molecular subtype of primary GBM cells. **E.** Cytotoxicity of V γ 9V δ 2 T lymphocytes against primary GBM cells using ^{51}Cr release assay. Results are expressed as % of cytotoxicity (mean \pm SD, n=2 in triplicates from 2 different V γ 9V δ 2 T cell lines, Sidak's multiple comparison test, ***p<0.001).

Figure 2

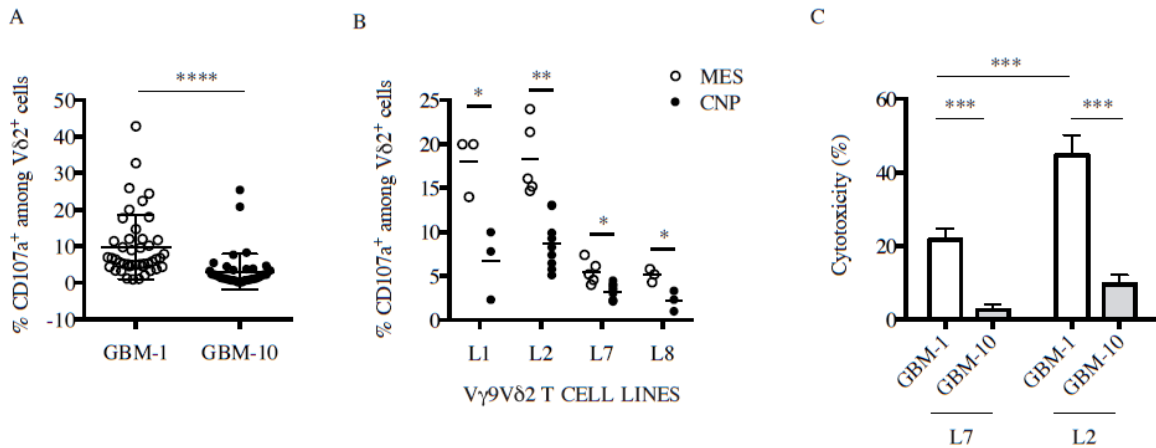


Figure 2. Heterogeneous reactivity of Vγ9Vδ2 T lymphocytes against mesenchymal GBM cells.

A. Frequency of CD107a positive cells among TCRVδ2⁺ lymphocytes (%). Each point corresponds to an individual allogeneic PBMC-derived Vγ9Vδ2 T lymphocyte lines (n=44, mean ± SD, Wilcoxon matched-pairs signed Rank test, ***p<0.001). **B.** CD107a expression in 4 representative Vγ9Vδ2 T lymphocyte lines after coculture with either mesenchymal (empty spot) or CNP (black spot) GBM cells (2-way ANOVA test, *p<0,05 and **p<0,01). **C.** Natural cytotoxicity of 2 representative Vγ9Vδ2 T lymphocyte lines (L2 and L7) against either mesenchymal GBM-1 or CNP GBM-10 cells in ⁵¹Cr-release assays (E:T ratio 10:1). Results are expressed as % of cytotoxicity (n=3 in triplicates, mean ± SD, 2-way ANOVA test, ***p<0.001).

Figure 3

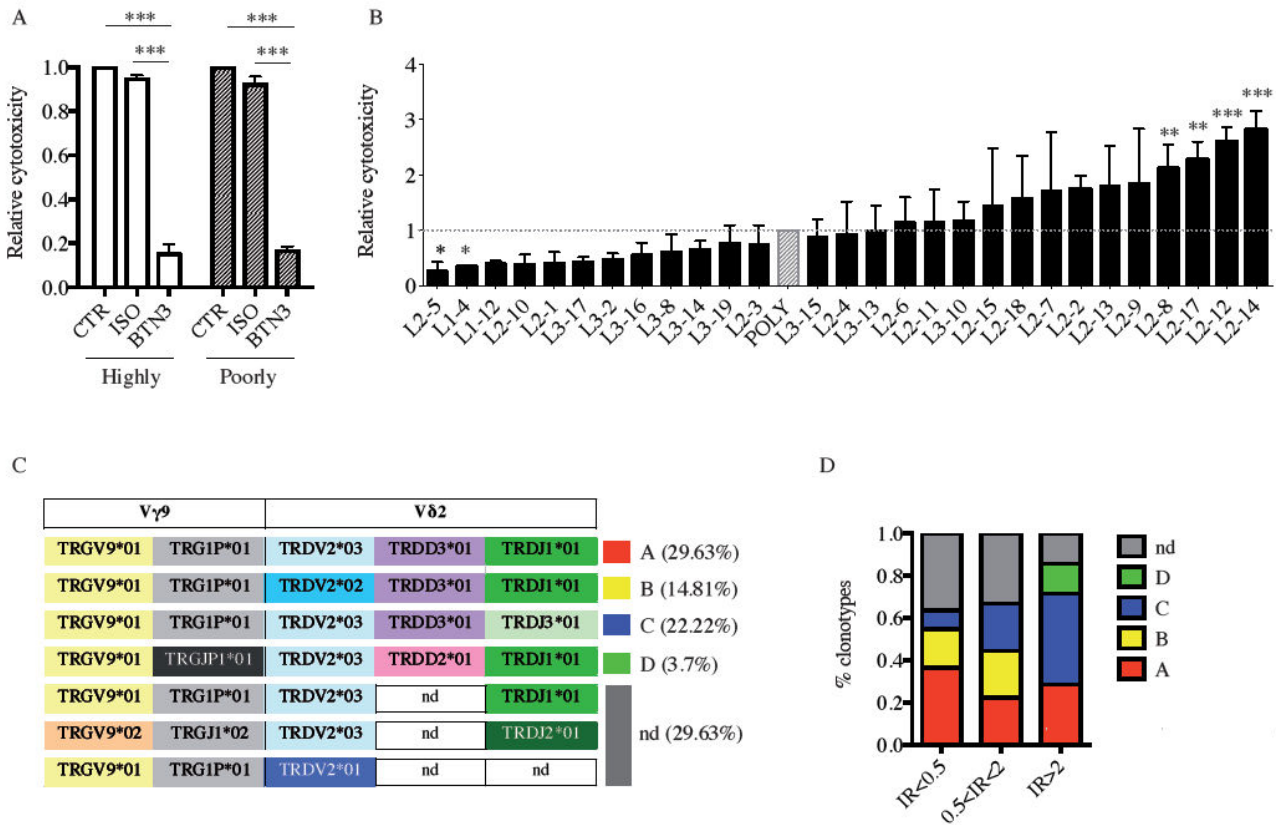


Figure 3. Spontaneous elimination of mesenchymal GBM cells through Vγ9Vδ2 TCR engagement independently of a particular TCR repertoire signature.

A. Natural cytotoxicity of Vγ9Vδ2 T lymphocytes in the presence of blocking mAb against BTN3A/CD277 (clone #103.2). ⁵¹Cr-release assays (E:T ratio 10:1) were performed using either highly or poorly reactive Vγ9Vδ2 T lymphocyte lines. Relative cytotoxicities of highly (n=3) and poorly (n=2) reactive T cells were normalized to cytotoxicity in absence of blocking antibody (mean ± SD; n≥2 in triplicates, Kruskal-Wallis test, ***p<0.001). **B.** Cytotoxicity of Vγ9Vδ2 T lymphocyte clones generated from 3 distinct highly reactive Vγ9Vδ2 T lymphocyte lines (L1, L2 and L3) against GBM-1 cells. Cytotoxicity was analyzed for each clone using ⁵¹Cr-release assays and normalized to respective polyclonal cytotoxicity (E:T ratio: 10:1). Results are expressed as relative cytotoxicity (n=3 in triplicates, mean ± SD). **C.** TCR repertoires of Vγ9Vδ2 T lymphocyte clonotypes. Vγ9 and Vδ2 TCR chain sequences are indicated with their respective frequencies among analyzed clonotypes. Undetermined gene segments are indicated as *nd*. **D.** Frequencies of TCR repertoire based on their respective reactivity profiles.

Figure 4

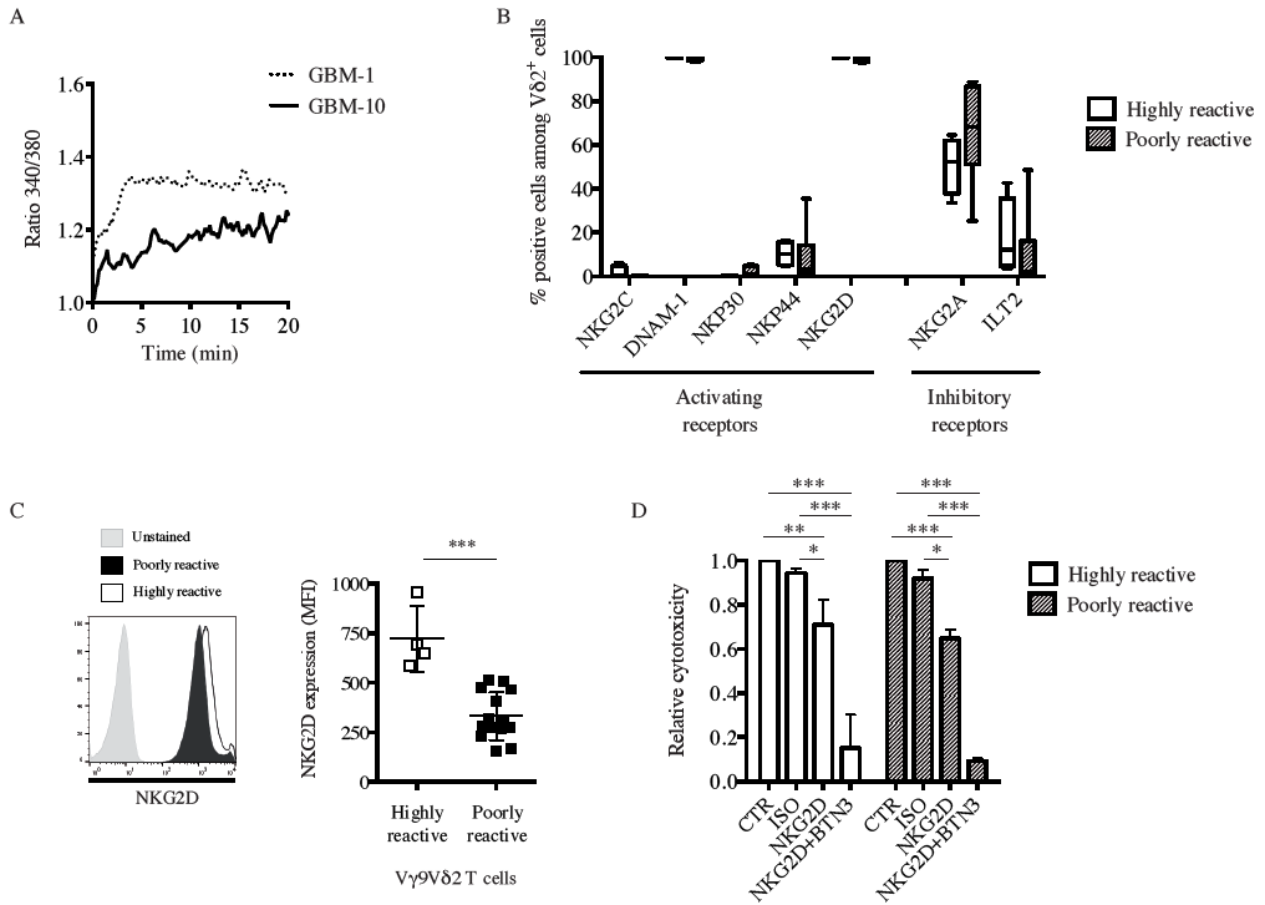


Figure 4. Spontaneous elimination of GBM cells by V γ 9V δ 2 T lymphocytes is tuned by NKG2D.

A. Intracellular Ca²⁺ levels monitored with the Fura-2/AM probe in V γ 9V δ 2 T lymphocytes after coculture with either GBM-1 or GBM-10 cells. **B.** Expression of activating and inhibiting NK receptor was analyzed using flow cytometry in highly (n=4) and poorly (n=14) V γ 9V δ 2 T lymphocyte lines. Results are expressed as % of positive cells. **C.** Highly (n=4) and poorly (n=14) V γ 9V δ 2 T lymphocyte lines were analyzed by flow cytometry for NKG2D receptor expression. Results are expressed as specific median fluorescence intensity (MFI) (MFI test - MFI isotype control) (mean \pm SD; Mann-Whitney test ***p<0.001). **D.** Relative cytotoxicity V γ 9V δ 2 T cell against GBM-1 cells (E:T ratio 10:1) in presence of NKG2D blocking antibody, alone or in combination with BTN3A/CD277 blocking antibody. Relative cytotoxicities of highly (n=3) and poorly (n=2) reactive T cells were normalized to cytotoxicity in absence of blocking antibody (mean \pm SD; n \geq 2 in triplicates, Kruskal-Wallis test, *p<0.05, **p<0.01, ***p<0.001).

Figure 5

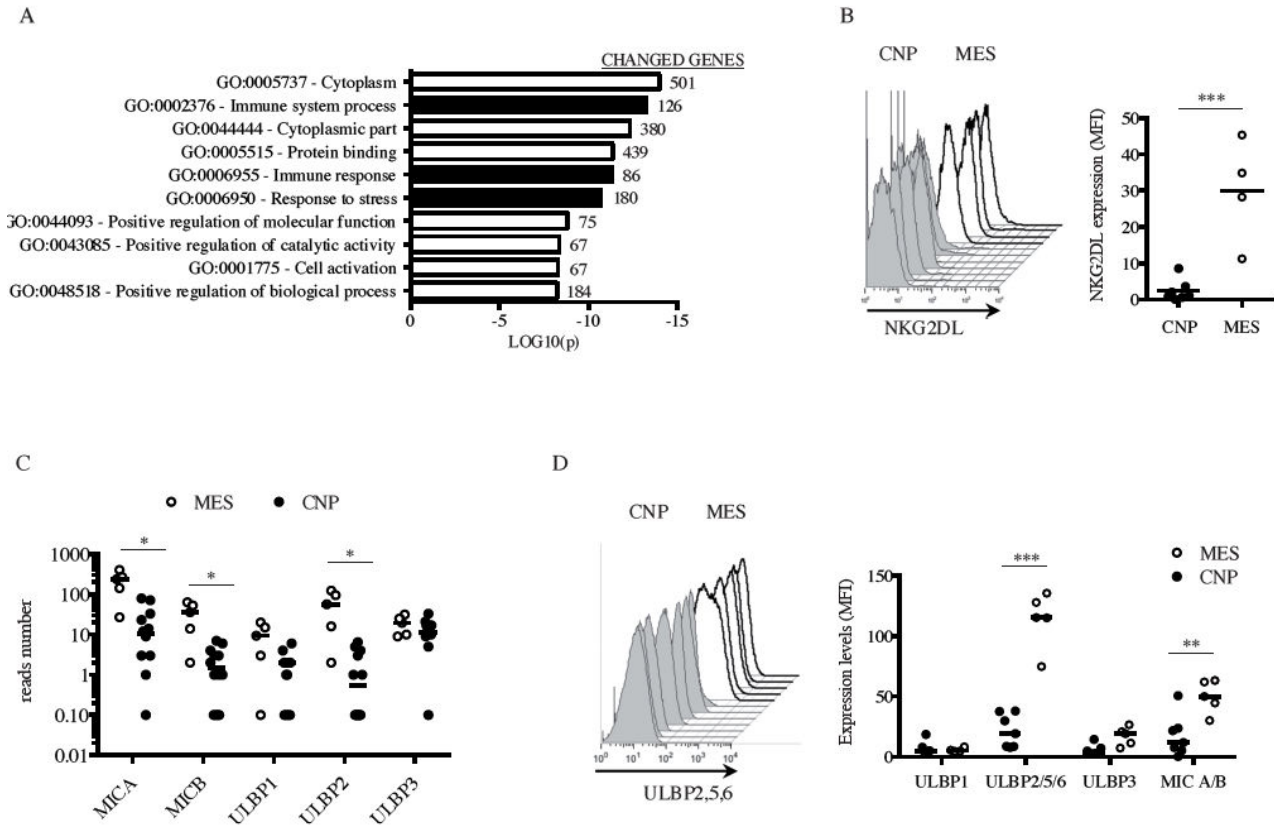


Figure 5. Mesenchymal primary GBM cell cultures highly express NKG2D ligands.

A. Up-regulated pathways in MES primary GBM cultures compared to CNP. Clusters obtained after transcriptomic analysis (DNA microarrays) followed by functional annotations of differentially expressed genes (GO: Gene Ontology) with indicated number of changed genes. **B.** Tumor cell surface phenotyping performed by flow cytometry with a recombinant human NKG2D-Ig fusion protein to assess whole NKG2D ligands expression. *Left panel:* grey and white histograms correspond respectively to CNP and MES GBM cultures. *Right panel:* Results are expressed as specific median fluorescence intensity (MFI) (mean \pm SD; Mann-Whitney test, *** p <0.001). **C.** Transcriptomic expression analysis of known V γ 9V δ 2 T cell ligands in mesenchymal (n=5) and CNP primary cells (n=12). **D.** Tumor cell surface phenotyping performed by flow cytometry using specific antibodies against ULBP 1, ULBP 2/5/6, ULBP 3 and MIC A/B expression. Histograms correspond to, respectively, CNP and MES GBM cultures as in (B). Results are expressed as specific median fluorescence intensity (MFI) (mean \pm SD; 2-way ANOVA test, ** p <0.01 and *** p <0.001).

Figure 6

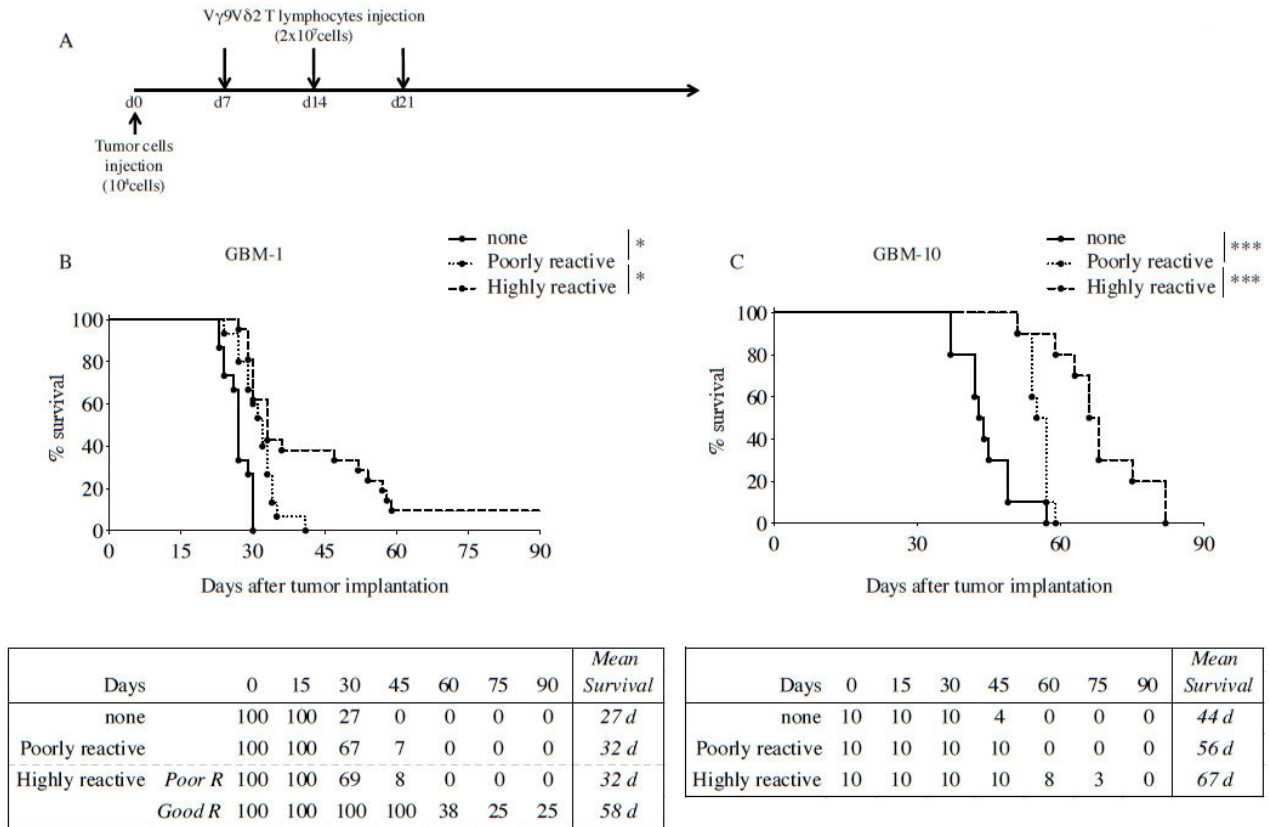


Figure 6. Allogeneic human V γ 9V δ 2 T lymphocytes efficiently eliminate primary GBM cells *in vivo*.

A. Illustration of the experimental protocol. Allogeneic human V γ 9V δ 2 T lymphocyte were injected at the tumor site at day 7, 14 and 21 after tumor cell implantation. **B-C.** Survival curves of GBM-1 (B) and GBM-10 (C) tumor-bearing mice treated with poorly or highly reactive V γ 9V δ 2 T lymphocyte. The relative number of subjects at risk for each group as well as the median survival is indicated in the table (bottom panel) (n=15 mice per group for GBM-1 and n=10 per group for CNP1; Log-rank Test, *p<0,05 and ***p<0.001).

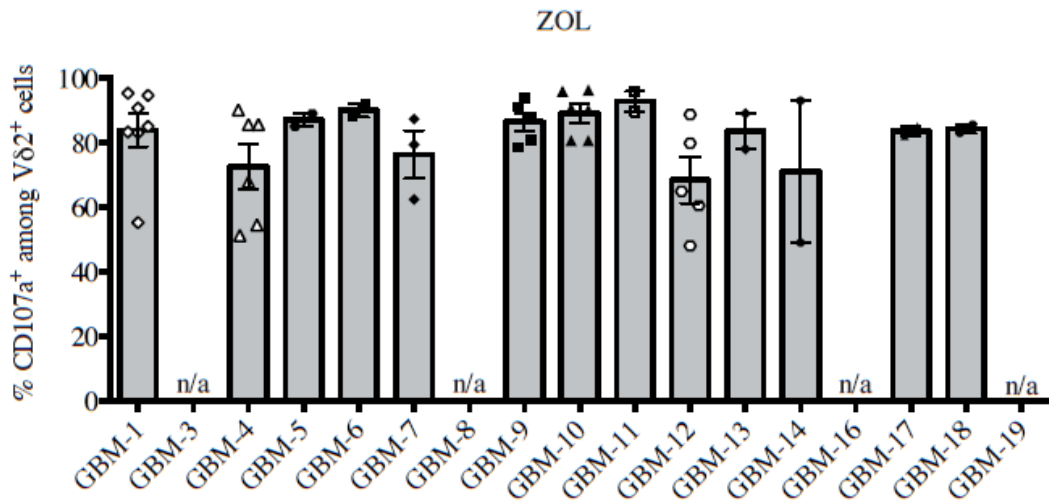
Supplemental Table 1

	MESENCHYMAL					CLASSIC, NEURAL, PRONEURAL (CNP)												
	GBM-1	GBM-4	GBM-8	GBM-11	GBM-12	GBM-3	GBM-5	GBM-6	GBM-7	GBM-9	GBM-10	GBM-13	GBM-14	GBM-16	GBM-17	GBM-18	GBM-19	
TP53	present	present	present	present	present	present	present	present	present	present	present	present	present	present	present	present	present	present
EGFR	normal	normal	normal	normal	normal	normal	normal	normal	normal	amplified	amplified	normal						
PDGFR	normal	normal	normal	normal	normal	normal	normal	normal	amplified	amplified	amplified	amplified	normal	normal	normal	normal	normal	normal
PTEN	normal	normal	normal	normal	normal	normal	normal	normal	normal	normal	normal	normal	normal	loss	normal	normal	normal	normal
INK4a/ARF	loss	loss	present	present	loss	loss	present	loss	present									
IDH1	wild-type	wild-type	wild-type	wild-type	wild-type	wild-type	wild-type	wild-type	wild-type	wild-type	wild-type	wild-type	wild-type	wild-type	wild-type	wild-type	wild-type	wild-type
MGMT	absent	absent	absent	expressed	absent	expressed	absent	absent	absent	absent	absent	expressed	absent	absent	absent	absent	expressed	absent

Supplemental Table 1. Genomic information of primary GBM cultures.

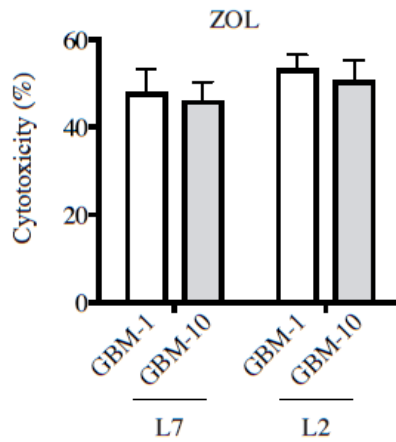
Primary cultures were classified based on their molecular signature: M stands for mesenchymal and CNP for Classical, Neural and Proneural.

Supplemental Figure 1



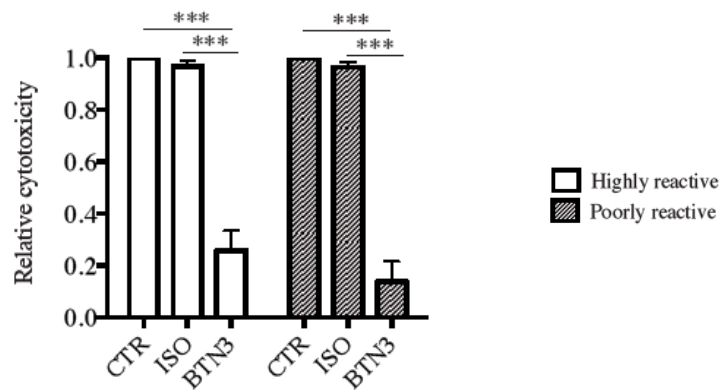
Supplemental Figure 1. Zoledronate induced-reactivity of Vγ9Vδ2 T cells against primary GBM cultures. Frequency of CD107a positive cells among Vγ9Vδ2 T lymphocytes cocultured 4h with 17 primary GBM cultures after overnight zoledronate sensitization (E:T ratio 1:1).

Supplemental Figure 2



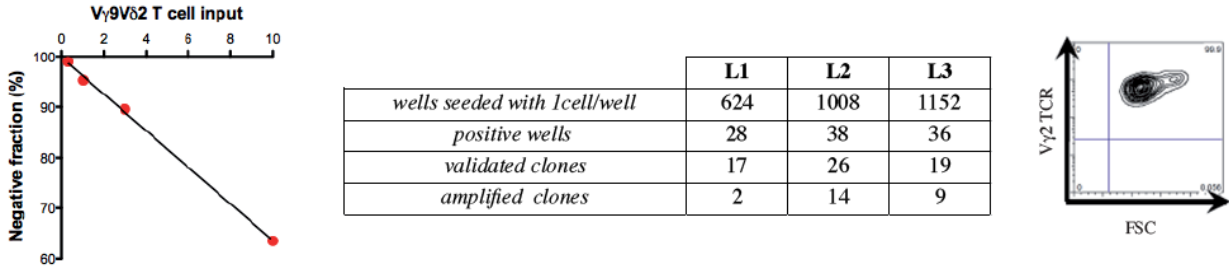
Supplemental Figure 2. Zoledronate induced-cytotoxicity of V γ 9V δ 2 T cells against primary GBM cultures. Cytotoxicity of V γ 9V δ 2 T lymphocytes against primary GBM cells, after overnight zoledronate sensitization, using ^{51}Cr release assay (E:T ratio 10:1 ; mean \pm SD ; n = 3 in triplicates).

Supplemental Figure 3



Supplemental Figure 3. Zoledronate induced-cytotoxicity of V γ 9V δ 2 T lymphocytes in the presence of blocking mAb against BTN3A/CD277. ^{51}Cr -release assays (E:T ratio: 10:1) were performed using either highly (*white*) or poorly (*grey*) reactive V γ 9V δ 2 T lymphocyte lines and GBM cells incubated with blocking antibody against BTN3A/CD277 (clone #103.2). Relative cytotoxicities of highly (n=3) and poorly (n=2) reactive T cells were normalized to cytotoxicity in absence of blocking antibody (mean \pm SD; n \geq 2 in triplicates, Kruskal-Wallis test, ***p<0.001).

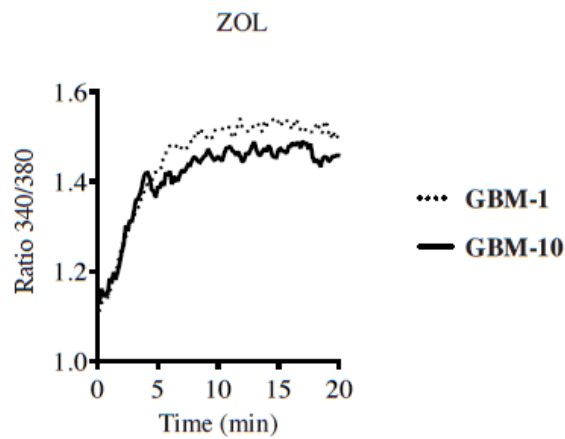
Supplemental Figure 4



Supplemental Figure 4. Generation of Vγ9Vδ2 T clones

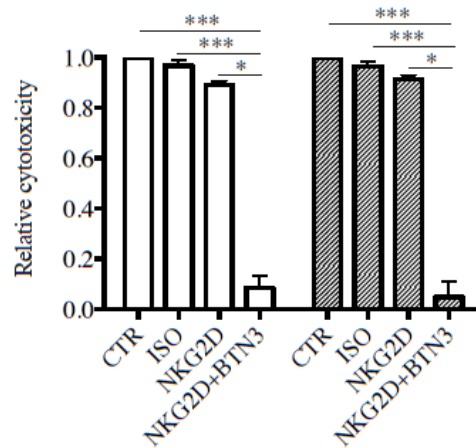
Three highly reactive Vγ9Vδ2 T cell lines (L1, L2 and L3) were subcloned using dilution assay (*left panel*) or FACS sorter. Ninety two clones emerged from 2784 individual seeded wells but only 25 clones amplified sufficiently for subsequent analyses (*Table*). Representative flow cytometry analysis for T cell clones purity (*right panel*).

Supplemental Figure 5



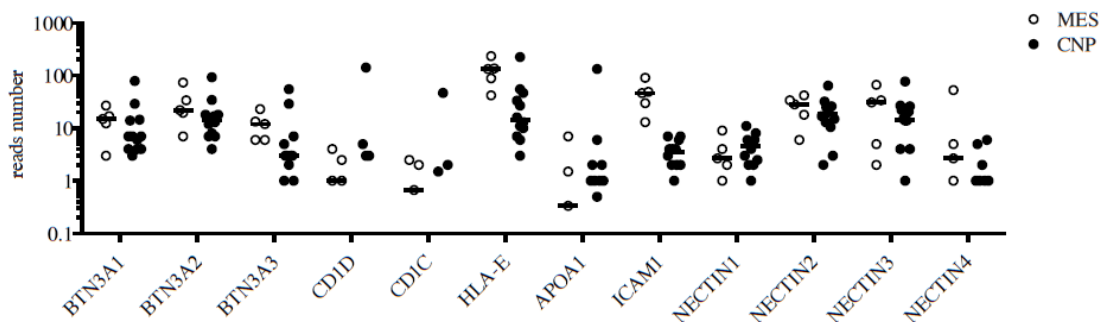
Supplemental Figure 5. Ca²⁺ activation profil of Vγ9Vδ2 T cells against zoledronate sensitized GBM primary cultures. Intracellular Ca²⁺ levels monitored with Fura-2/AM probe in Vγ9Vδ2 T lymphocytes during coculture with either GBM-1 or GBM-10 cells previously sensitized overnight with zoledronate.

Supplemental Figure 6



Supplemental Figure 6. Zoledronate induced-cytotoxicity of V γ 9V δ 2 T lymphocytes in the presence of blocking mAb against NKG2D. Relative cytotoxicity of V γ 9V δ 2 T cell against zoledronate sensitized GBM-1 cells (E:T ratio 10:1) in presence of NKG2D blocking antibody (clone #1D11) and BTN3A/CD277 blocking antibody (clone #103.2). Relative cytotoxicities of highly (n=3) and poorly (n=2) reactive T cells were normalized to cytotoxicity in absence of blocking antibody (mean \pm SD; n \geq 2 in triplicates, Kruskal-Wallis test, *p<0,05, **p<0,001 and ***p<0.001).

Supplemental Figure 7



Supplemental Figure 7. Transcriptomic expression of V γ 9V δ 2 T cell ligands in GBM primary cultures. Transcriptomic expression analysis of known $\gamma\delta$ TCR and NKG2D ligands in mesenchymal/MES (n=5) and CNP primary cells (n=12).

6 – Etude de la toxicité du Zolédronate sur des cellules cérébrales

Au cours de ces différentes études, nous avons étudié le potentiel thérapeutique de plusieurs protocoles d'immunothérapies basés sur le transfert adoptif de LT V γ 9V δ 2 humains allogéniques. Le protocole conduisant à la meilleure efficacité thérapeutique combine l'injection des LT V γ 9V δ 2 et de Zolédronate en intracérébral. Bien que le Zolédronate soit déjà utilisé en clinique dans le traitement des métastases osseuses (Dhillon and Lyseng-Williamson, 2008), il n'a jamais été testé de l'injecter en intracérébral pour le traitement du GBM. Les effets secondaires potentiels sur le tissu sain sont donc inconnus. Seules les cellules capables de pinocytose vont capter le Zolédronate et pourraient être reconnues et détruites par les LT V γ 9V δ 2. Parmi les cellules du SNC, ce sont donc les astrocytes et les cellules de la microglie les plus susceptibles de provoquer des effets secondaires liés à l'injection de Zolédronate en intracérébral.

Afin de pouvoir confirmer cela, nous avons sensibilisé des astrocytes primaires (ScienCell Research Laboratories, Carlsbad, CA) avec une dose de Zolédronate permettant la reconnaissance maximale des cellules tumorales de GBM (10 μ M), avant de réaliser un test de cytotoxicité au ^{51}Cr (chrome 51) (Figure 38A). La sensibilisation au Zolédronate conduit à une élimination des astrocytes tout comme pour les cellules tumorales de la lignée U-87MG. Cependant, il est important de prendre en compte que les astrocytes utilisés ici sont des cellules achetées, qui après dissociation à partir de cortex cérébral humain ont été placées en culture dans un milieu contenant du SVF et des facteurs de croissance. De ce fait, ces astrocytes sont maintenus en prolifération, dans un milieu qui n'est pas physiologique, ce qui doit très certainement modifier leur phénotype. Notamment du fait de la division cellulaire, qui entraîne des besoins en cholestérol, leur métabolisme n'est plus représentatif de celui des cellules cérébrales d'un adulte sain, qui sont des cellules différenciées et qui restent dans un stade quiescent.

De plus, les astrocytes ne représentent qu'un type cellulaire parmi tous ceux qui composent le SNC. Afin d'être le plus représentatif de la physiologie cérébrale humaine il faudrait pourvoir étudier tous les types de cellules cérébrales dans le contexte le plus physiologique possible.

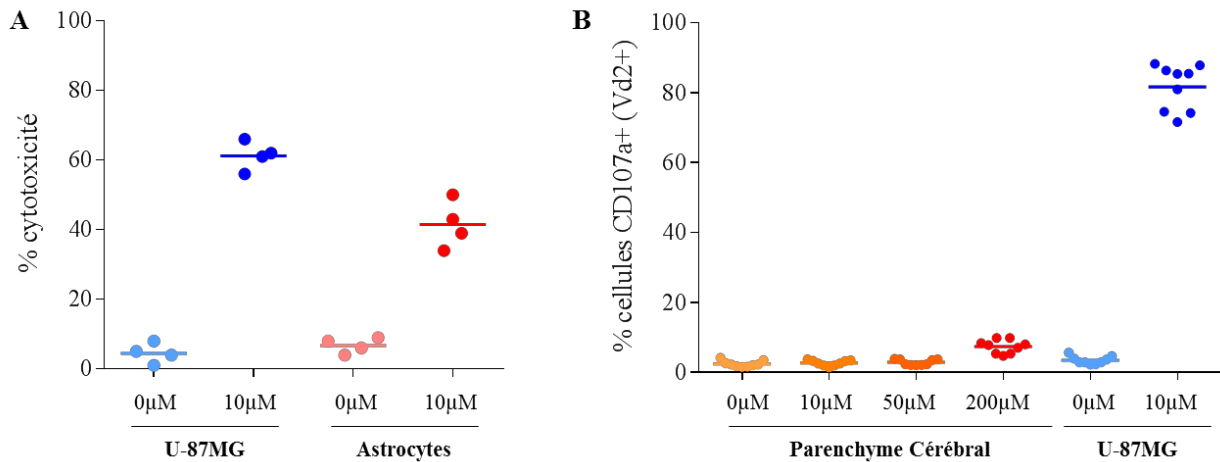


Figure 38 : Reconnaissance de cellules cérébrales sensibilisées au Zolédronate par les LT V γ 9V δ 2. (A) Test de cytotoxicité au ^{51}Cr sur des astrocytes humains achetés (ScienCell) ou des cellules tumorales de la lignée U-87MG. Après sensibilisation au Zolédronate sur la nuit, les cellules cibles sont chargées au ^{51}Cr puis une coculture avec des LT V γ 9V δ 2 est réalisée à un ratio E:T de 10:1 (n=4 en triplicats). Les résultats sont exprimés en % de cellules lysées. (B) Test de réactivité au CD107a face à des cellules tumorales de la lignée U-87MG ou face à des cellules cérébrales issues de la dissociation de fragments de parenchyme cérébral. Après sensibilisation au Zolédronate sur la nuit, les cibles sont cocultivées avec des LT V γ 9V δ 2 à un ratio E:T de 1:1 (n=9 avec trois donneurs de LT V γ 9V δ 2). Les résultats sont exprimés en % de cellules activées (CD107a $^{+}$).

Bien qu'il soit très difficile de se procurer un fragment de parenchyme cérébral chez un adulte sain, nous avons eu la chance de récupérer des échantillons de tissu cérébral en bon état au moment de l'autopsie de patients du Dr David LAPLAUD, neurologue au CHU Hotel Dieu de Nantes. Le premier échantillon que nous avons récupéré provient d'un homme atteint de sclérose en plaque et a été divisé en deux fragments en fonction de la zone de prélèvement : un fragment correspondant à de la substance blanche et l'autre au cortex temporal. Pour le second échantillon, qui provient d'une patiente également atteinte de sclérose en plaque mais décédée d'une pneumonie, un seul fragment de parenchyme cérébral a été récupéré. Dans tous les cas, il s'agit de zones cérébrales non lésées par la maladie neurodégénérative atteignant les patients.

Après récupération, les échantillons ont été dissociés à l'aide du kit de dissociation Adult Brain Dissociation Kit de chez Miltenyi. Que les cellules aient été utilisées immédiatement ou congelées avant utilisation, elles étaient placées dans du milieu défini, sans SVF, et n'ont pas été maintenues en culture plus que le temps des expérimentations.

Dans un premier temps, nous avons souhaité réaliser des tests de cytotoxicité, comme pour les astrocytes achetés, cependant ces échantillons étant très fragiles, les cellules ne survivaient pas au chargement au ^{51}Cr . Nous avons donc choisi de réaliser des tests de réactivité au CD107a.

De façon intéressante, à une dose de Zolédronate suffisante pour induire une forte reconnaissance de la lignée cellulaire U-87MG, aucune réactivité des LT V γ 9V δ 2 n'est observée (Figure 38B). Il faut augmenter la dose de Zolédronate de 20 fois pour voir apparaître une faible réactivité des LT V γ 9V δ 2, qui reste inférieure à 10 % de cellules CD107a $^{+}$. Ces résultats très encourageants nous permettent d'envisager plus sereinement la possibilité d'injecter du Zolédronate en intracérébral en association au transfert adoptif de LT V γ 9V δ 2 humains allogéniques.

7 - Conclusion

Ce projet est inclus dans le programme de financement LabEx IGO (laboratoire d'excellence en immunology in graft and oncology) et fait l'objet d'une collaboration entre l'équipe 1 et l'équipe 9 du CRCINA (centre de recherche en cancérologie et immunologie Nantes Angers) autour de l'immunothérapie par transfert adoptif comme nouvelle stratégie thérapeutique pour le traitement des patients atteints de GBM. Ce projet nous a permis de mettre en place plusieurs modèles de GBM, représentatifs de la pathologie humaine, basés sur la xénogreffe en orthotopique de primocultures issues de patients atteints de GBM.

Cette collaboration nous a permis d'implanter en orthotopique chez des souris NSG une dizaine de primocultures de GBM, caractérisées en fonction de leur sous-type moléculaire et de leur métabolisme (Oizel et al., 2017). De façon intéressante, la majorité des primocultures implantées ont une croissance lente et n'induisent pas de signe clinique. Néanmoins, des analyses par IHC réalisées sur les cerveaux de souris 6 mois après implantation des primocultures ont montré, contre toute attente, que des cellules tumorales envahissent le parenchyme cérébral jusque dans l'hémisphère controlatéral (résultats non montrés). Bien que l'infiltration hétérogène observée chez ces animaux soit similaire à celle visible chez les patients, la durée de croissance tumorale et l'absence de signes cliniques détectables ne nous permettaient pas d'utiliser la plupart de ces modèles pour la réalisation d'études précliniques. Cependant, deux modèles, plus rapides tout en étant représentatifs de la pathologie humaine ont pu être utilisés. Le premier est basé sur l'utilisation de la primoculture GBM-10, appartenant au sous-type CNP (Article 2), alors que le second repose sur l'implantation de la primoculture GBM-1, caractérisée pour être du sous-type MES (Article 4). Il est également intéressant de noter que la croissance des cellules tumorales GBM-1 est plus rapide *in vivo*, ce qui est cohérent avec le fait que le sous-type MES est connu pour être le plus agressif chez les patients (Phillips et al., 2006; Verhaak et al., 2010).

L'utilisation de ces deux modèles nous a permis de comparer la réactivité *in vitro* et *in vivo* des LT V γ 9V δ 2, en fonction du sous-type moléculaire (Article 5). Ainsi, le transfert adoptif de LT V γ 9V δ 2 humains allogéniques en intracérébral permet une élimination naturelle des cellules primaires de GBM, du sous-type MES et CNP. Une différence de reconnaissance des sous-types de GBM, lié à l'expression de ligand de stress, notamment ligands de NKG2D, a également été mise en évidence.

En effet, les cellules tumorales appartenant au sous-type MES sont mieux reconnues et éliminées par les LT V γ 9V δ 2. De façon intéressante, ces différences de reconnaissance naturelle peuvent être exploitées au cours de protocoles d'immunothérapies.

C'est le chemin qu'a suivi l'équipe de Lawrence LAMB. Ils ont récemment démontré que le TMZ, la chimiothérapie de référence dans le traitement du GBM, conduisait à une augmentation de l'expression des ligands de NKG2D par les cellules tumorales de GBM et à une augmentation de la cytotoxicité par les LT V γ 9V δ 2 (Chitadze et al., 2016). Ils ont également mis au point un protocole permettant de générer, au grade GMP, des LT V γ 9V δ 2 résistants au TMZ afin de pouvoir combiner de façon efficace la chimiothérapie et l'immunothérapie (Lamb et al., 2013). Ces résultats vont leur permettre de démarrer prochainement un essai clinique de phase I/II.

De façon générale, l'efficacité thérapeutique du transfert adoptif cellulaire peut être augmentée soit par l'amélioration du potentiel cytotoxique des effecteurs, soit par une augmentation de la reconnaissance des cellules cibles. Dans le cas du GBM, nous avons testé les deux stratégies. D'un côté, l'IL-21, utilisée en pré-conditionnement, permet d'augmenter la cytotoxicité des LT V γ 9V δ 2 *in vitro* et *in vivo* afin d'obtenir une meilleure efficacité thérapeutique, tout en évitant l'injection d'IL-21 dans le microenvironnement tumoral (Article 4). Néanmoins, comme évoqué dans la Partie I, lors de l'injection des LT aux patients dans le cadre du transfert adoptif, l'injection est faite immédiatement après décongélation des LT, il faut donc que le pré-conditionnement à l'IL-21 ait eu lieu avant la congélation et que son efficacité sur l'augmentation en granzyme B soit maintenue après la décongélation. Malheureusement, que les LT V γ 9V δ 2 soit pré-conditionnés ou non à l'IL-21 avant la congélation, leur cytotoxicité est plus faible en sortie de décongélation (résultats non montrés).

Par ailleurs, l'augmentation de la reconnaissance des cellules de GBM est très efficacement obtenue aussi bien *in vitro* qu'*in vivo* grâce au Zolédronate (Article 2). De façon intéressante, nous avons pu montrer, *in vitro* et *in vivo*, que le Zolédronate était efficace pour sensibiliser aussi bien les cellules tumorales de GBM issues de lignées que de primocultures, quel que soit leur sous-type moléculaire. De plus, une amélioration de la survie a été observée dans les trois modèles précliniques utilisés (Articles 2 et 4) après injection intracérébrale concomitante de Zolédronate et de LT V γ 9V δ 2. Une élimination complète de la tumeur a même été obtenue chez un nombre important d'animaux, et validée par IHC.

Tous ces résultats sont très encourageants et ouvrent des perspectives de transfert vers la clinique. Dans un premier temps, une seule de ces stratégies peut être proposée et la plus efficace est celle combinant l'injection intracérébrale de LT V γ 9V δ 2 humains allogéniques et de Zolédronate. Différents essais cliniques ont déjà validé l'injection d'effecteurs immunitaires cytotoxiques en intracérébral, chez des patients atteints de GBM, sans démontrer de toxicité importante liée à ces injections ou à la réponse immunitaire anti-tumorale associée (Brown et al., 2016; O'Rourke et al., 2017).

L'obstacle principal de cette stratégie est donc la potentielle toxicité liée au Zolédronate. Les expériences réalisées sur les fragments de SNC dissociés sont plutôt en faveur d'une très faible voire d'une absence de toxicité contre les cellules saines, surtout pour de faibles doses de Zolédronate. Néanmoins, de nombreux facteurs sont négligés dans cette analyse et sont à prendre en compte, tels que la biodistribution du Zolédronate en intracérébral, la présence de myéline autour des neurones qui pourrait jouer un rôle protecteur pour ces cellules, ou encore les différences de pharmacocinétique/pharmacodynamique liées à la zone d'injection et au drainage par le LCR.

L'injection de cellules tumorales en orthotopique et les collaborations liées au projet Labex IGO, m'ont permis de travailler avec plusieurs personnes de l'équipe 9 et de l'équipe 14 du CRCINA. Ces collaborations ont pour point commun l'amélioration des modèles murins que nous avons mis en place. Notamment, l'étude des mécanismes de résistance à la chimiothérapie (Rabe et al., Annexes pages 268 à 307) et à la radiothérapie (Degorre et al., Annexes pages 308 à 333). Mais également autour des différences de métabolisme entre les différents sous-types moléculaires de GBM, qui représentent une cible thérapeutique intéressante pour le développement de nouvelles stratégies (Oizel et al., 2017) (Oizel et al., Annexes pages 249 à 267). Ces projets nous poussent à vouloir améliorer les modèles que nous avons mis en place, en incluant le traitement standard des patients, et plus précisément le protocole de Stupp. C'est pourquoi nous sommes actuellement en train de mettre en place un protocole dit « Stupp-like » basé sur l'injection intrapéritonéale de TMZ et sur l'irradiation locale et fractionnée, par rayons X, de la tumeur.

C. DISCUSSION

I – Pertinence des modèles murins précliniques

Le choix d'un bon modèle murin est primordial à l'étude de la compréhension d'une pathologie. Ces modèles peuvent également aider à la prédiction d'une réponse thérapeutique et à anticiper les effets secondaires liés à de nouvelles stratégies.

Dans le cas des LT V γ 9V δ 2, il n'est pas possible de travailler dans des modèles murins syngéniques car il n'existe pas d'équivalent de cette population lymphocytaire chez la souris (Kazen and Adams, 2011; Sturm et al., 1992). Des souris immunodéprimées sont donc utilisées, afin de mettre en place des modèles murins humanisés, car elles supportent les greffes de cellules humaines, aussi bien tumorales qu'immunitaires. D'emblée cela pose la question de l'impact du microenvironnement tumoral, sur la réaction immunitaire anti-tumorale, qui ne sera pas physiopathologique du fait de l'absence d'un système immunitaire complet et fonctionnel. Reconstituer un système immunitaire humain chez la souris est possible grâce à l'injection systémique de PBMC chez des souris irradiées (Morton et al., 2016). Néanmoins, la présence de LT dans le greffon conduit à une forte réaction xénogénique contre l'hôte, limitant la relevance et la durée d'utilisation de ces animaux. De plus, la gestion et la reproductibilité de ce type de modèle reste compliqués à ce jour.

La forme d'humanisation la plus simple, reste l'injection de cellules tumorales chez ces souris immunodéprimées. En cancérologie, beaucoup d'études sont réalisées dans des modèles murins basés sur l'injection sous-cutanée de cellules tumorales de lignée cellulaire. Ce type de protocole présente de nombreux avantages. Les cellules tumorales issues de lignées sont des cellules robustes qui peuvent être modifiées génétiquement selon les intérêts du projet, et il est possible d'en obtenir et d'en injecter de grandes quantités. De plus, l'injection en sous-cutané tout comme le suivi de la croissance tumorale qui s'en suit, par mesure physique du volume tumoral, sont des gestes faciles à réaliser. Cela permet de façon simple et rapide d'obtenir des résultats et de fournir des preuves de concept pour de nouvelles stratégies thérapeutiques (Santolaria et al., 2013). Cependant ces modèles sont rarement représentatifs de la pathologie humaine, du fait du nombre de cellules important généralement implantées qui rend le développement tumoral rapide, et de la localisation tissulaire qui n'est pas orthotopique et ne reproduit pas les symptômes et/ou les complications liés aux organes atteints (Perrin, 2014; Wege, 2018).

Afin de rendre un modèle murin le plus représentatif de la pathologie humaine, il faut, dans un premier temps, injecter les cellules tumorales en orthotopique et de préférence en faibles quantités afin de pouvoir mimer au mieux les premières phases de développement de la maladie puis sa dissémination naturelle en fonction de l'organe d'origine.

Dans un second temps, il est intéressant de caractériser au maximum la tumeur qui se développe en multipliant les techniques telles que l'imagerie, l'histologie ou l'analyse du phénotype cellulaire et moléculaire des cellules tumorales. C'est ce que nous avons tenté de faire avec nos modèles de GBM et de CEO (Articles 1, 2 et 4). Après une injection orthotopique des cellules tumorales, leur dissémination dans le tissu sain (SNC ou abdomen) a été particulièrement suivie car elle représente une des principales causes de récurrence chez les patients.

Un outil indiscutable pour rendre un modèle murin représentatif de la pathologie humaine est l'utilisation d'échantillons issus de patients. Deux stratégies sont actuellement utilisées : soit l'injection de cellules tumorales dissociées et mises en culture ; soit l'implantation de fragments de tumeur ou PDX (patient derived xenograft). Ces deux techniques présentent des avantages et des inconvénients.

Dans le cas de cellules tumorales primaires dissociées et mises en culture, toutes ces étapes de préparation peuvent affecter leur phénotype et peuvent favoriser la croissance de certains variants tumoraux rendant l'échantillon peu homogène, alors que l'utilisation d'un fragment assure l'intégrité tissulaire et l'hétérogénéité cellulaire (Jung et al., 2018). Cependant, l'implantation de PDX issus d'une tumeur humaine est rarement possible en orthotopique du fait de la taille de la souris et/ou de la difficulté chirurgicale que cela implique (ex. GBM en intracérébrale). De plus, si un fragment de PDX prend et croît *in vivo*, cela implique de devoir le rediviser à partir d'une certaine taille afin de reimplanter à nouveau de petits fragments qui peuvent donc ne plus être représentatifs de toute la tumeur. De plus, petit à petit le microenvironnement humain disparaît pour être remplacé par un stroma murin, diminuant encore la pertinence de ce type de modèle (Jung et al., 2018). De ce fait, l'utilisation de cellules en culture est plus simple et permet une injection des cellules tumorales en petite quantité et précisément au site de départ du développement de la maladie. L'amélioration des protocoles de culture cellulaire nous permettant de conserver au mieux l'hétérogénéité de l'échantillon.

C'est pourquoi nous avons choisi cette stratégie pour nos modèles. Bien que la croissance de primocultures de CEO *in vivo* n'ait pas été concluante, l'implantation des cellules tumorales issues de lignées cellulaires en orthotopique nous a permis de reproduire de façon similaire la dissémination tumorale observée chez les patientes (Article 1). A l'inverse, dans le cas du GBM, c'est l'utilisation de primocultures en orthotopique qui conduit à une infiltration des cellules tumorales mimant celle observée chez les patients, les cellules tumorales issues de lignées cellulaires forment au contraire une masse tumorale très dense (Articles 2 et 4). Les cellules tumorales infiltrantes représentant le challenge thérapeutique et notre cible pour la mise en place de nouveaux protocoles d'immunothérapies par transfert adoptif de LT V γ 9V δ 2, nos modèles murins doivent présenter cette caractéristique.

Quelle que soit l'efficacité thérapeutique d'une nouvelle stratégie obtenue dans un modèle préclinique, il est très peu probable qu'elle puisse être testée chez des patients en absence de traitement standard. Par ailleurs, ces traitements font partie intégrante de l'évolution de la maladie, notamment via l'apparition de cellules tumorales résistantes (ex. chimio- ou radio-résistantes), qui sont une cible thérapeutique d'intérêt. Ainsi, une fois que l'on possède un modèle murin représentatif du développement tumoral humain, l'idéal est d'y ajouter le traitement standard des patients, notamment afin d'anticiper d'éventuelles interférences ou bénéfices de ces combinaisons.

De façon intéressante, l'impact du traitement standard peut être bénéfique et renforcer l'efficacité de l'immunothérapie, comme l'ont montré L. LAMB et ses collaborateurs (Chitadze et al., 2016). Dans le cas du GBM, la chimiothérapie standard (TMZ) permet une meilleure reconnaissance des cellules tumorales via l'augmentation de l'expression de ligands de stress. A l'inverse, le traitement de référence peut interférer de façon négative avec l'immunothérapie. C'est ce que nous avons démontré dans l'Article 1, où le traitement des cellules tumorales de CEO par du Paclitaxel induit une forte diminution de la réactivité des LT V γ 9V δ 2 via la diminution du niveau d'expression de molécules d'adhésion. Dans tous les cas, prendre en compte le traitement standard des patients augmente la pertinence des modèles murins, la prédictibilité de la réponse thérapeutique et peut nous permettre de trouver LA bonne fenêtre thérapeutique permettant d'envisager un essai clinique.

Le choix du modèle préclinique est primordial mais les modalités d'injection du traitement sont également très importantes. Chez l'Homme, l'administration des traitements se fait principalement par voie orale ou par voie systémique. Cependant, ces voies d'administration, bien que simples et peu contraignantes pour les patients, sont généralement la source de forte toxicité sur les tissus sains. De plus en plus d'études ont ainsi prouvé le bénéfice d'agir localement afin de diminuer la toxicité systémique tout en augmentant les doses thérapeutiques. Cette généralité est applicable au transfert adoptif de LT V γ 9V δ 2, et l'injection en local permet également d'injecter les effecteurs cellulaires au plus proche des cellules cibles (Pauza et al., 2018; Yuasa et al., 2009). Il est tout de même nécessaire de s'assurer que les LT pourront survivre et se déplacer après une injection péri-tumorale car selon la localisation de la tumeur, il ne s'agit pas forcément d'un tissu où les LT sont naturellement présent (ex. SNC). Ainsi, nous avons pu valider dans nos modèles murins de GBM et d'EOC, qu'après une injection intracérébrale ou intrapéritonéale, les LT V γ 9V δ 2 sont capables de survivre, patrouiller et éliminer des cellules tumorales disséminées, conduisant à une réponse thérapeutique (Articles 1, 2, 3, 4). De plus, il est intéressant de noter que l'injection d'IL-2 *in vivo* n'a pas été nécessaire, ce qui représente un intérêt non négligeable du fait de la forte toxicité qu'elle peut induire chez les patients (ex. tempête cytokinique) (Dhupkar and Gordon, 2017).

II – Faisabilité d’une banque de LT V γ 9V δ 2 humains allogéniques

Forts de tous les arguments en faveur de l’utilisation de LT V γ 9V δ 2 humains allogéniques en immunothérapie anti-tumorale, beaucoup d’essais précliniques ont été réalisés prouvant l’efficacité thérapeutique de cette stratégie et encourageant le passage vers la clinique.

De nombreux essais cliniques basés sur l’utilisation des LT V γ 9V δ 2 humains ont déjà été réalisés, soit par injection de molécules activatrices (PAG ou ABP) chez les patients, soit par transfert adoptif de LT V γ 9V δ 2 autologues après amplification *ex vivo* (Hoeres et al., 2018). De façon générale, beaucoup d’essais cliniques reposant sur le transfert adoptif cellulaire sont actuellement en cours, mais, dans le cas des LT V γ 9V δ 2, il s’agit exclusivement de transferts autologues. En effet, le plus gros obstacle au transfert cellulaire allogénique est justement le risque de GVHD, notamment contre les cellules saines de l’hôte, phénomène bien connu et souvent problématique dans les situations de greffes d’organes, du fait de l’incompatibilité du CMH entre le donneur et le receveur.

Dans le cas des LT V γ 9V δ 2, le risque de GVHD n’est pas un frein, car leur reconnaissance des cellules cibles n’est pas restreinte au CMH et que les mécanismes régissant cette reconnaissance les rendent capables de discriminer les cellules normales des cellules stressées bien qu’elles produisent toutes des PAG et expriment toutes BTN3 (Boutin and Scotet, 2018; Chien et al., 2014; Harly et al., 2014). Par contre, le risque de rejet de l’hôte contre le greffon n’est pas négligeable. En effet, bien que les patients atteints de cancer et traités par chimiothérapie soient généralement immunodéprimés, il ne faut pas exclure la possibilité d’une réaction des LT du patient contre les LT V γ 9V δ 2 allogéniques injectés. Ainsi, dans le cadre de la création d’une banque cellulaire allogénique, il peut être intéressant de sélectionner plusieurs donneurs sains possédant les haplotypes du CMH les plus courants et ensuite de traiter les patients avec le greffon le plus adapté pour limiter le risque de rejet tout en augmentant les chances de survie des LT V γ 9V δ 2 allogéniques administrés.

De la même façon il est possible de sélectionner des donneurs sains suivant des critères de pureté ou du nombre de divisions possible des LT V γ 9V δ 2 obtenues après amplification spécifique (Résultats Partie 1) (Ryan et al., 2016) ; pour l’expression de corécepteurs d’intérêt tels que le FcR, qui permet d’augmenter l’efficacité thérapeutique des LT V γ 9V δ 2 quand ils sont associés à un anticorps (Gertner-Dardenne et al., 2009; Hoeres et al., 2018) ; ou tels que les NKR qui peuvent conduire à une augmentation de la réactivité et de la cytotoxicité des LT V γ 9V δ 2 (Article 4) (Hoeres et al., 2018).

Cela renforce l'intérêt de pouvoir réaliser de multiples amplifications sur les LT V γ 9V δ 2 d'un même donneur afin de pouvoir produire de très grandes quantités de cellules.

Avant de pouvoir traiter des patients, il est donc indispensable de pouvoir mettre en place cette banque cellulaire. Malheureusement, toutes les techniques mises en place dans les laboratoires pour amplifier des cellules ne sont pas forcément applicables pour une production cellulaire au grade GMP. Dans le cas des LT V γ 9V δ 2, bien qu'une telle banque n'ait encore jamais été mise en place, plusieurs techniques sont à notre disposition et sont applicables de façon concrète. Dans un premier temps, de nombreuses études ont validé l'amplification spécifique des LT V γ 9V δ 2 *ex vivo* grâce à l'utilisation de PAg de synthèse (ex. BrHPP, Phosphostim) (Bennouna et al., 2008). Il est donc tout à fait envisageable d'utiliser un de ces protocoles sur des PBMC de donneurs sains plutôt que sur des PBMC de patients, avec de meilleures chances de réussite.

Dans ces essais cliniques, les LT V γ 9V δ 2 des patients leurs étaient alors réinjectés mais dans le cadre de la création d'une banque cellulaire allogénique, afin de pouvoir traiter tous les patients, la quantité de cellules nécessaire est beaucoup plus importante. Comme évoqué précédemment (Conclusion Partie I), la stimulation non spécifique par PHA-feeders est la plus efficace pour induire un nombre de division important, sans altérer ni la pureté ni les fonctions effectrices des LT V γ 9V δ 2 (Résultats Partie 1-3). De nombreux essais cliniques ont recours à des procédés d'amplification non spécifiques pour produire de grandes quantités d'effecteurs cytotoxiques, notamment à une version grade GMP de la stimulation PHA-feeders (Labarriere et al., 2013; Vivien et al., 2018).

Tous ces outils nous permettent d'envisager la mise en place de banques cellulaires de LT V γ 9V δ 2 allogéniques en suivant le protocole hypothétique présenté dans la Figure 39. Après récupération, des PBMC de donneurs sains pourraient être amplifiés de façon spécifique grâce au BrHPP. Il pourrait également être envisagé de modifier ce protocole, en remplaçant le BrHPP par un ABP produit au grade GMP, tel que le Zolédronate (Zometa, Novartis). A l'issue de cette première étape d'amplification spécifique et au vu de nos résultats (Partie 1-3), 2 ou 3 stimulations non spécifiques par PHA-feeders pourraient être réalisées afin de produire de très grandes quantités de cellules (plusieurs centaines de milliards) sans épuiser les effecteurs qui n'en seraient qu'à la moitié de leur potentiel de division. Une fois congelées, les cellules pouvaient être utilisées pour traiter des patients selon les besoins de chacun.

Bien que tout ce processus de mise en place d'une banque cellulaire de LT $V\gamma 9V\delta 2$ allogéniques représente de gros besoins en infrastructure, en personnel, en consommables et donc financier, la constitution de telles banques présente également de beaucoup d'avantages. En effet, de cette façon ce traitement, qui est générique, est toujours disponible et en très grande quantité. Il est donc possible de soigner un patient dès qu'il en a besoin, sans avoir à attendre plusieurs semaines pour la personnalisation et l'amplification cellulaire, délai pendant lequel la maladie continue de progresser.

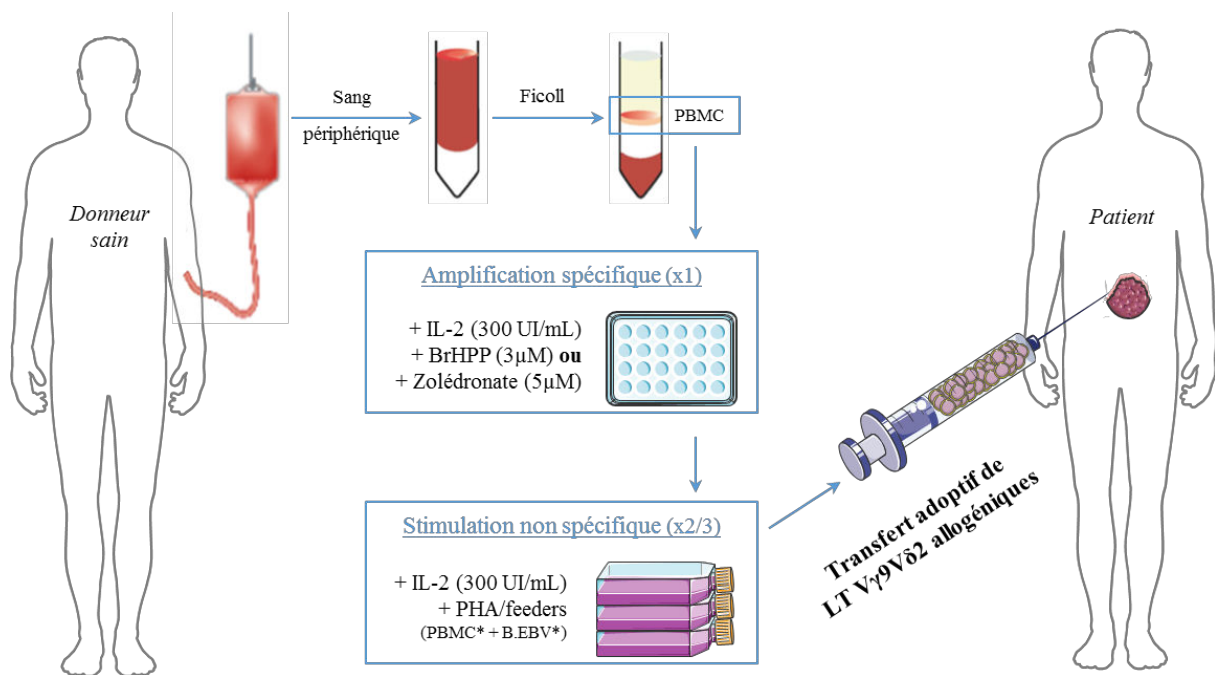


Figure 39 : Protocole hypothétique de production d'une banque de LT $V\gamma 9V\delta 2$ allogéniques au grade GMP.

Après récupération du sang de donneur(s) sain(s), les PBMC sont isolés et amplifiés de façon spécifique, grâce à un PAg de synthèse (ex. BrHPP) ou un ABP (ex. Zolédronate), en présence d'IL-2. Une fois revenue au repos (environ 3 semaines) et après vérification de la pureté en LT $V\gamma 9V\delta 2$ de la population récupérée, celle-ci peut être stimulée plusieurs fois de façon non spécifique (PHA/feeders/IL-2). Les LT $V\gamma 9V\delta 2$ sont ensuite congelés pour être conservés jusqu'à ce que des patients atteints de cancer ait besoin du traitement.

Le bilan des avantages et des inconvénients a fini par pencher en faveur du bénéfice potentiel puisqu'une équipe de l'Université de Jinan (Guangzhou, Chine) est actuellement en train de réaliser un essai clinique qui repose sur le transfert adoptif de LT $V\gamma 9V\delta 2$ humains allogéniques chez des patients atteints de tumeurs solides à des stades très avancés.

Au cours de la conférence internationale sur les LT $\gamma\delta$ de cette année (Bordeaux, 7-10 Juin 2018), le Dr Zhinan Yin nous a confié les résultats préliminaires de cette étude. De façon intéressante, il nous a confirmé l'absence de toxicité et de réaction allogénique liée à une ou plusieurs injections systémiques de LT V γ 9V δ 2 allogéniques. Ils ont même eu la possibilité de réaliser 3 injections de LT V γ 9V δ 2 venant de trois donneurs sains différents chez le même patient, sans observer d'effets secondaires importants. D'un point de vue thérapeutique, une amélioration de la qualité de vie et une stabilisation de la maladie ont pu être observées chez plusieurs patients. L'étude étant actuellement en cours, un peu de patience est encore nécessaire pour faire le bilan sur la survie des patients et conclure de façon définitive sur la sécurité et le bénéfice de l'injection de LT V γ 9V δ 2 allogéniques chez des patients atteints de cancer.

III – Utilisation concomitante du Zolédronate

Parmi tous les protocoles d'immunothérapies que nous avons testés, les plus efficaces sont ceux qui combinent l'utilisation du Zolédronate au transfert adoptif de LT V γ 9V δ 2 humains allogéniques. Bien que l'effet pharmacologique des ABP ne soit pas restreint à la sensibilisation des cellules à la reconnaissance par les LT V γ 9V δ 2, cet aspect est contact- et espèce-dépendant (Kato et al., 2003, 2006). Malheureusement, nous travaillons dans des modèles murins humanisés du fait de l'absence d'équivalent des LT V γ 9V δ 2 chez la souris, il est donc impossible d'anticiper une éventuelle réactivité *in vivo* des effecteurs contre des cellules saines du fait de la sensibilisation au Zolédronate.

Afin de répondre à cette problématique, nous avons envisagé de travailler chez le primate et plus précisément chez le babouin, qui possède des LT V γ 9V δ 2 activables par les PAg. En effet, grâce à une collaboration avec le Laboratoire des Grands Animaux de Nantes, nous avons la possibilité de réaliser des injections de LT V γ 9V δ 2 et de Zolédronate en intracérébral chez des babouins en fin d'expérimentation pour des projets de transplantation. Nous avons donc collecté du sang de babouin et réalisé des amplifications spécifiques sur les PBMC, soit avec du BrHPP soit avec du Zolédronate. Malheureusement, nous n'avons pas réussi à obtenir de populations pures à plus de 40 % en LT V γ 9V δ 2 et du fait du peu d'animaux disponibles, les injections intracérébrales n'ont pu être réalisées.

Néanmoins, nous avons pu effectuer des tests de réactivité *in vitro*, sur des cellules cérébrales de babouin récupérées par dissociation à partir d'un fragment de parenchyme. Tout comme pour les tests de réactivité réalisés sur cellules cérébrales humaines, les LT V γ 9V δ 2 réagissent peu ou pas (< 10 % de cellules CD107a positives) contre les cellules cérébrales de babouin sensibilisées au Zolédronate (résultats non montrés). Du fait de la difficulté de l'utilisation des primates non-humains en expérimentation animale, ce type de modèle ne nous a pas permis de conclure davantage sur la toxicité liée à l'association du Zolédronate aux LT V γ 9V δ 2 humains allogéniques sur des tissus sains tels que les cellules cérébrales. De façon intéressante, il a récemment été mis en évidence l'existence de LT V γ 9V δ 2 activés par des PAg chez d'autres espèces que les primates, notamment chez l'alpaga, qui peut représenter un modèle alternatif intéressant (Karunakaran et al., 2014).

Le Zolédronate étant largement utilisé dans les pathologies présentant une augmentation de la résorption osseuse et/ou une hypercalcémie, les effets secondaires propres au Zolédronate sont donc déjà connus. Les patients recevant du Zolédronate, par injection intraveineuse, présentent principalement un état grippal, d'intensité faible à modérée, qui disparaît généralement au bout de 2 à 3 semaines. De plus, chez 5 à 10 % des patients, une ostéonécrose de la mâchoire peut survenir et nécessite des contrôles dentaires réguliers ainsi qu'une hygiène bucco-dentaire adaptée.

En cas d'injections répétées, pendant un laps de temps important (> 1 injection par semaine pendant plusieurs mois), les fonctions rénales devront également être surveillées avec attention (De Luca et al., 2011; Wellington and Goa, 2003). Ces effets indésirables et le suivi qui en découle est déjà pris en compte chez les patients atteints de métastases osseuses et traités par injection intraveineuse de Zolédronate (Dhillon and Lyseng-Williamson, 2008; Green and Lipton, 2010). Il pourrait donc être envisageable au cours d'un essai clinique, de compléter le traitement de ces patients par des injections de LT V γ 9V δ 2 allogéniques.

Cette stratégie a fait l'objet d'une collaboration avec l'équipe de F. REDINI (Laboratoire de Physiopathologie de la Résorption Osseuse, Inserm U1238, Nantes) autour de l'ostéosarcome, la tumeur osseuse primaire la plus fréquente chez les jeunes adultes (Biteau et al., 2016). Après avoir mis en place un modèle murin préclinique basé sur l'implantation en orthotopique (paratibiale) de cellules tumorales issues de la lignée cellulaire KHOS, nous avons mesuré l'efficacité thérapeutique d'injection systémique de Zolédronate et de LT V γ 9V δ 2 allogénique *in vivo*. Malheureusement, l'efficacité thérapeutique obtenue était limitée (ralentissement de la croissance tumorale, sans amélioration significative de la survie des animaux ; résultats non montrés). De plus, l'essai clinique de phase III visant à valider l'utilisation du Zolédronate dans le traitement de l'ostéosarcome n'a pas été concluant (Piperno-Neumann et al., 2016).

Dans le cas du GBM et du CEO, ces tumeurs se développent dans des cavités naturellement protégées par une barrière cellulaire, respectivement la BHE (barrière hématoencéphalique) et le péritoine. Il faudrait donc des doses et une biodistribution suffisante du Zolédronate pour atteindre des doses suffisantes à la sensibilisation des cellules tumorales de façon localisée. Or chez l'Homme, des études de pharmacocinétiques ont mis en évidence qu'après une injection systémique, le temps de demi-vie du Zolédronate n'est que de 15 minutes (De Luca et al., 2011).

La majorité du Zolédronate étant éliminée rapidement par filtration rénale. Par contre le Zolédronate fixé à l'os peut ensuite être relargué à long terme (jusqu'à 10 ans) mais à des concentrations extrêmement faibles.

De plus, une étude de biodistribution menée chez le chien a mis en évidence que le Zolédronate ne pouvait pas passer la BHE (Weiss et al., 2008), résultats que nous avons confirmés sur nos souris NSG (résultats non montrés). Cependant, il est connu dans le cas du GBM, que le développement de la tumeur est associé à la formation anarchique de vaisseaux qui compromettent l'intégrité de la BHE. Il serait donc intéressant de vérifier ces données dans ce contexte physiopathologique. La chirurgie et les traitements standards (chimio- et radiothérapie) représentent également des facteurs non négligeables, qui peuvent altérer aussi bien la BHE que le péritoine.

Dans tous les cas, les effets secondaires liés à l'injection systémique de Zolédronate ne pourront être évités et bien qu'ils puissent être anticipés et gérés au cas par cas, ils ne sont pas négligeables. Ce qui renforce l'intérêt de travailler en local. L'effet sur les cellules saines ne peut pas être ignoré et peu de données sont actuellement disponibles mais l'utilisation de faibles doses en local permettrait tout de même d'atteindre des doses thérapeutiques. Dans le cas du CEO, l'essai actuellement mené par Yuki Abe et Hideo Matsui au Japon, basé sur l'injection intrapéritonéale de Zolédronate et de LT V γ 9V δ 2 humains autologues, dans le traitement de l'ascite de CEO, nous apportera des réponses pour ce qui est de la toxicité péritonéale.

Par contre dans le cas du GBM, aucun essai actuellement en cours ou passé ne nous donne d'informations à ce sujet. Seules les données que nous avons récoltées, soit une absence de réactivité de LT V γ 9V δ 2 humains allogéniques face à des cellules cérébrales dissociées à partir de fragments de parenchyme de cerveau humain et sensibilisées au Zolédronate (Résultats Partie 3-6), nous permettent d'espérer une très faible toxicité contre les cellules saines en cas d'injections concomitantes de Zolédronate et de LT V γ 9V δ 2 humains allogéniques.

Bien que ce type de protocoles ne soit pas encore couramment utilisé, il suscite de plus en plus d'intérêt. En effet, réaliser un traitement localement permet d'augmenter les doses utilisées sans pour autant augmenter la toxicité à distance. Cependant, la toxicité locale représente un frein majeur car le tissu sain environnant peut-être indispensable et qu'il est parfois difficile d'anticiper ces effets secondaires.

IV – Conclusion personnelle

Cette expérience intense de 3 ans qu'est la thèse n'a pas seulement été l'occasion d'améliorer mon esprit scientifique et d'affiner mon sens critique, ça a également été l'occasion de m'inclure dans la vie du laboratoire et de développer des compétences non scientifiques représentant un intérêt personnel.

Tout d'abord, chaque encadrement de stagiaires, sur des périodes plus ou moins longues, a été une expérience très enrichissante autant d'un point de vue pédagogique qu'humain. C'est également une responsabilité importante de former un jeune scientifique et de tenter de lui fournir toutes les cartes pour qu'il puisse évoluer aussi bien sur le plan technique que théorique.

Au cours de ma thèse, j'ai également eu la chance d'être formée à l'expérimentation animale. Cet aspect de la recherche appliquée représente un intérêt particulier à mes yeux car c'est un domaine de compétence qui nécessite rigueur, précision, éthique et respect envers les animaux mais qui est également l'occasion de partager avec de nombreuses personnes quel que soit leur domaine d'expertise (scientifiques, animaliers ou vétérinaires). Ainsi, l'expérimentation animale correspond à une part très importante de mon travail de thèse autant par le temps de formation qui a été nécessaire afin que je maîtrise toutes les techniques, notamment chirurgicales, indispensable à la mise en place de nos modèles murins précliniques mais également par l'investissement que m'a demandé la formation complète d'une technicienne et la gestion de l'élevage de souris NSG mise en place par l'équipe.

En effet, la majorité des collaborations auxquelles j'ai participé ont tourné autour des modèles murins. Ces collaborations vont du simple partage des animaux (Equipes 8 et 13 du CRCINA) à la conception et à la réalisation des expériences (Equipes 9 et 14 du CRCINA). L'une des collaborations les plus fructueuse est celle que nous entretenons autour des modèles de GBM et qui m'a permis de travailler sur d'autres stratégies thérapeutiques, telles que l'utilisation d'anticorps thérapeutiques ou d'inhibiteurs métaboliques.

Un des objectifs de mon travail de thèse a été de mettre en place des modèles murins précliniques les plus représentatifs possibles de la pathologie humaine. Les modèles de GBM et de CEO présentés ici, bien qu'ils puissent encore être améliorés, sont basés sur l'implantation des cellules tumorales en orthotopique et sont caractérisés par une importante dissémination tumorale, une des principales causes de récidives chez les patients et notre cible thérapeutique.

Les différents protocoles préclinique d'immunothérapies réalisés dans ces modèles murins nous ont amené à travailler avec des cliniciens, qui nous ont apporté leurs précieux conseils, aussi bien autour du CEO (Jean-Marc CLASSE, Nantes ; Véronique CATROS et Vincent LAVOUE, Rennes) que du GBM (Philippe MENEI, Anne CLAVREUL, Angers).

Le potentiel thérapeutique des LT V γ 9V δ 2 est loin d'être inconnu et fait déjà l'objet de nombreuses études précliniques et d'essais cliniques. J'espère donc que ce travail de thèse renforcera les arguments déjà à notre disposition au sujet de :

- la pertinence d'utiliser des modèles murins les plus représentatifs de la pathologie humaine ou au moins mimants au mieux notre challenge thérapeutique,
- la mise en place de banques de LT V γ 9V δ 2 allogéniques afin de fournir aux patients, à tout instant, un traitement générique efficace et présentant de faibles risques d'effets indésirables,
- la réalisation des injections de manière localisée, au plus proche de la tumeur, quand cela est possible, afin de la cibler et de l'éliminer au mieux.

La création d'une banque cellulaire représente le premier pas à réaliser avant d'espérer pouvoir mettre en place un essai clinique basé sur l'injection de LT V γ 9V δ 2 allogéniques en France. Il se trouve que tous les outils pour cela sont disponibles sur Nantes. Non seulement l'amplification spécifique au grade GMP de LT V γ 9V δ 2 a déjà été validée (Salot et al., 2007) mais certains membres de notre équipe possèdent également une expertise importante dans le domaine de l'amplification d'effecteurs cellulaires au grade GMP (Vivien et al., 2018). Seul le besoin financier freine actuellement ce projet. J'espère donc avoir prochainement la chance de relever un tel défi et de participer à la réalisation d'un projet aussi excitant.

D. BIBLIOGRAPHIE

- Abe, Y., Muto, M., Nieda, M., Nakagawa, Y., Nicol, A., Kaneko, T., Goto, S., Yokokawa, K., and Suzuki, K. (2009). Clinical and immunological evaluation of zoledronate-activated Vgamma9gammadelta T-cell-based immunotherapy for patients with multiple myeloma. *Exp. Hematol.* *37*, 956–968.
- Agrati, C., Cimini, E., Sacchi, A., Bordoni, V., Gioia, C., Casetti, R., Turchi, F., Tripodi, M., and Martini, F. (2009). Activated V gamma 9V delta 2 T cells trigger granulocyte functions via MCP-2 release. *J. Immunol. Baltim. Md 1950* *182*, 522–529.
- Allison, T.J., Winter, C.C., Fournié, J.J., Bonneville, M., and Garboczi, D.N. (2001). Structure of a human gammadelta T-cell antigen receptor. *Nature* *411*, 820–824.
- Amobi, A., Qian, F., Lugade, A.A., and Odunsi, K. (2017). Tryptophan Catabolism and Cancer Immunotherapy Targeting IDO Mediated Immune Suppression. *Adv. Exp. Med. Biol.* *1036*, 129–144.
- Angelini, D.F., Borsellino, G., Poupot, M., Diamantini, A., Poupot, R., Bernardi, G., Poccia, F., Fournié, J.-J., and Battistini, L. (2004). FcgammaRIII discriminates between 2 subsets of Vgamma9Vdelta2 effector cells with different responses and activation pathways. *Blood* *104*, 1801–1807.
- Aoki, Y., Takakuwa, K., Kodama, S., Tanaka, K., Takahashi, M., Tokunaga, A., and Takahashi, T. (1991). Use of adoptive transfer of tumor-infiltrating lymphocytes alone or in combination with cisplatin-containing chemotherapy in patients with epithelial ovarian cancer. *Cancer Res.* *51*, 1934–1939.
- Arnett, H.A., and Viney, J.L. (2014). Immune modulation by butyrophilins. *Nat. Rev. Immunol.* *14*, 559–569.
- Band, H., Hochstenbach, F., Parker, C.M., McLean, J., Krangel, M.S., and Brenner, M.B. (1989). Expression of human T cell receptor-gamma delta structural forms. *J. Immunol. Baltim. Md 1950* *142*, 3627–3633.
- Bank, I., Book, M., Huszar, M., Baram, Y., Schnirer, I., and Brenner, H. (1993). V delta 2+ gamma delta T lymphocytes are cytotoxic to the MCF 7 breast carcinoma cell line and can be detected among the T cells that infiltrate breast tumors. *Clin. Immunol. Immunopathol.* *67*, 17–24.
- Bansal, R.R., Mackay, C.R., Moser, B., and Eberl, M. (2012). IL-21 enhances the potential of human $\gamma\delta$ T cells to provide B-cell help. *Eur. J. Immunol.* *42*, 110–119.
- Barjon, C., Michaud, H.-A., Fages, A., Dejoux, C., Zampieri, A., They, L., Gennetier, A., Sanchez, F., Gros, L., Eliaou, J.-F., et al. (2017). IL-21 promotes the development of a CD73-positive V γ 9V δ 2 T cell regulatory population. *Oncoimmunology* *7*, e1379642.
- Bennouna, J., Bompas, E., Neidhardt, E.M., Rolland, F., Philip, I., Galéa, C., Salot, S., Saiagh, S., Audrain, M., Rimbart, M., et al. (2008). Phase-I study of Innacell gammadelta, an autologous cell-therapy product highly enriched in gamma9delta2 T lymphocytes, in combination with IL-2, in patients with metastatic renal cell carcinoma. *Cancer Immunol. Immunother.* *CII* *57*, 1599–1609.
- Bennouna, J., Levy, V., Sicard, H., Senellart, H., Audrain, M., Hirt, S., Rolland, F., Bruzzoni-Giovanelli, H., Rimbart, M., Galéa, C., et al. (2010). Phase I study of bromohydrin pyrophosphate (BrHPP, IPH 1101), a Vgamma9Vdelta2 T lymphocyte agonist in patients with solid tumors. *Cancer Immunol. Immunother.* *CII* *59*, 1521–1530.
- Benyamine, A., Le Roy, A., Mamessier, E., Gertner-Dardenne, J., Castanier, C., Orlanducci, F., Pouyet, L., Goubard, A., Collette, Y., Vey, N., et al. (2016). BTN3A molecules considerably improve V γ 9V δ 2 T cells-based immunotherapy in acute myeloid leukemia. *Oncoimmunology* *5*, e1146843.

- Bhoola, S., and Hoskins, W.J. (2006). Diagnosis and management of epithelial ovarian cancer. *Obstet. Gynecol.* *107*, 1399–1410.
- Biteau, K., Guiho, R., Chatelais, M., Taurelle, J., Chesneau, J., Corradini, N., Heymann, D., and Redini, F. (2016). L-MTP-PE and zoledronic acid combination in osteosarcoma: preclinical evidence of positive therapeutic combination for clinical transfer. *Am. J. Cancer Res.* *6*, 677–689.
- du Bois, A., Reuss, A., Pujade-Lauraine, E., Harter, P., Ray-Coquard, I., and Pfisterer, J. (2009). Role of surgical outcome as prognostic factor in advanced epithelial ovarian cancer: a combined exploratory analysis of 3 prospectively randomized phase 3 multicenter trials: by the Arbeitsgemeinschaft Gynaekologische Onkologie Studiengruppe Ovarialkarzinom (AGO-OVAR) and the Groupe d'Investigateurs Nationaux Pour les Etudes des Cancers de l'Ovaire (GINECO). *Cancer* *115*, 1234–1244.
- Bonneville, M., and Scotet, E. (2006). Human Vgamma9Vdelta2 T cells: promising new leads for immunotherapy of infections and tumors. *Curr. Opin. Immunol.* *18*, 539–546.
- Bonneville, M., O'Brien, R.L., and Born, W.K. (2010). Gammadelta T cell effector functions: a blend of innate programming and acquired plasticity. *Nat. Rev. Immunol.* *10*, 467–478.
- Borst, J., Wicherink, A., Van Dongen, J.J., De Vries, E., Comans-Bitter, W.M., Wassenaar, F., and Van Den Elsen, P. (1989). Non-random expression of T cell receptor gamma and delta variable gene segments in functional T lymphocyte clones from human peripheral blood. *Eur. J. Immunol.* *19*, 1559–1568.
- Boutin, L., and Scotet, E. (2018). Towards Deciphering the Hidden Mechanisms That Contribute to the Antigenic Activation Process of Human Vγ9Vδ2 T Cells. *Front. Immunol.* *9*, 828.
- Brandes, M., Willimann, K., Lang, A.B., Nam, K.-H., Jin, C., Brenner, M.B., Morita, C.T., and Moser, B. (2003). Flexible migration program regulates gamma delta T-cell involvement in humoral immunity. *Blood* *102*, 3693–3701.
- Brandes, M., Willimann, K., and Moser, B. (2005). Professional antigen-presentation function by human gammadelta T Cells. *Science* *309*, 264–268.
- Brandes, M., Willimann, K., Bioley, G., Lévy, N., Eberl, M., Luo, M., Tampé, R., Lévy, F., Romero, P., and Moser, B. (2009). Cross-presenting human gammadelta T cells induce robust CD8+ alphabeta T cell responses. *Proc. Natl. Acad. Sci. U. S. A.* *106*, 2307–2312.
- Brenner, M.B., McLean, J., Dialynas, D.P., Strominger, J.L., Smith, J.A., Owen, F.L., Seidman, J.G., Ip, S., Rosen, F., and Krangel, M.S. (1986). Identification of a putative second T-cell receptor. *Nature* *322*, 145–149.
- Bröker, M. (2016). Potential protective immunogenicity of tetanus toxoid, diphtheria toxoid and Cross Reacting Material 197 (CRM197) when used as carrier proteins in glycoconjugates. *Hum. Vaccines Immunother.* *12*, 664–667.
- Brown, C.E., Alizadeh, D., Starr, R., Weng, L., Wagner, J.R., Naranjo, A., Ostberg, J.R., Blanchard, M.S., Kilpatrick, J., Simpson, J., et al. (2016). Regression of Glioblastoma after Chimeric Antigen Receptor T-Cell Therapy. *N. Engl. J. Med.* *375*, 2561–2569.
- de Bruin, R.C.G., Veluchamy, J.P., Loughheed, S.M., Schneiders, F.L., Lopez-Lastra, S., Lameris, R., Stam, A.G., Sebestyen, Z., Kuball, J., Molthoff, C.F.M., et al. (2017). A bispecific nanobody approach to leverage the potent and widely applicable tumor cytolytic capacity of Vγ9Vδ2-T cells. *Oncoimmunology* *7*, e1375641.

- Bukowski, J.F., Morita, C.T., and Brenner, M.B. (1999). Human gamma delta T cells recognize alkylamines derived from microbes, edible plants, and tea: implications for innate immunity. *Immunity* *11*, 57–65.
- van der Burg, S.H., Arens, R., Ossendorp, F., van Hall, T., and Melief, C.J.M. (2016). Vaccines for established cancer: overcoming the challenges posed by immune evasion. *Nat. Rev. Cancer* *16*, 219–233.
- Burton, A.L., Roach, B.A., Mays, M.P., Chen, A.F., Ginter, B.A.R., Vierling, A.M., Scoggins, C.R., Martin, R.C.G., Stromberg, A.J., Hagendoorn, L., et al. (2011). Prognostic significance of tumor infiltrating lymphocytes in melanoma. *Am. Surg.* *77*, 188–192.
- Buss, N.A.P.S., Henderson, S.J., McFarlane, M., Shenton, J.M., and de Haan, L. (2012). Monoclonal antibody therapeutics: history and future. *Curr. Opin. Pharmacol.* *12*, 615–622.
- Butterfield, L.H. (2015). Cancer vaccines. *BMJ* *350*, h988.
- Caccamo, N., Battistini, L., Bonneville, M., Poccia, F., Fournié, J.J., Meraviglia, S., Borsellino, G., Kroczek, R.A., La Mendola, C., Scotet, E., et al. (2006). CXCR5 identifies a subset of Vgamma9Vdelta2 T cells which secrete IL-4 and IL-10 and help B cells for antibody production. *J. Immunol. Baltim. Md 1950* *177*, 5290–5295.
- Caccamo, N., La Mendola, C., Orlando, V., Meraviglia, S., Todaro, M., Stassi, G., Sireci, G., Fournié, J.J., and Dieli, F. (2011). Differentiation, phenotype, and function of interleukin-17-producing human Vγ9Vδ2 T cells. *Blood* *118*, 129–138.
- Calinescu, A.-A., Kamran, N., Baker, G., Mineharu, Y., Lowenstein, P.R., and Castro, M.G. (2015). Overview of current immunotherapeutic strategies for glioma. *Immunotherapy* *7*, 1073–1104.
- Capietto, A.-H., Martinet, L., and Fournié, J.-J. (2011). Stimulated γδ T cells increase the in vivo efficacy of trastuzumab in HER-2+ breast cancer. *J. Immunol. Baltim. Md 1950* *187*, 1031–1038.
- Casetti, R., Agrati, C., Wallace, M., Sacchi, A., Martini, F., Martino, A., Rinaldi, A., and Malkovsky, M. (2009). Cutting edge: TGF-beta1 and IL-15 Induce FOXP3+ gammadelta regulatory T cells in the presence of antigen stimulation. *J. Immunol. Baltim. Md 1950* *183*, 3574–3577.
- Casorati, G., De Libero, G., Lanzavecchia, A., and Migone, N. (1989). Molecular analysis of human gamma/delta+ clones from thymus and peripheral blood. *J. Exp. Med.* *170*, 1521–1535.
- Castella, B., Kopecka, J., Sciancalepore, P., Mandili, G., Foglietta, M., Mitro, N., Caruso, D., Novelli, F., Riganti, C., and Massaia, M. (2017). The ATP-binding cassette transporter A1 regulates phosphoantigen release and Vγ9Vδ2 T cell activation by dendritic cells. *Nat. Commun.* *8*, 15663.
- Castiglione, F., Taddei, A., Buccoliero, A.M., Garbini, F., Gheri, C.F., Freschi, G., Bechi, P., Rossi Degl'Innocenti, D., and Taddei, G.L. (2008). TNM staging and T-cell receptor gamma expression in colon adenocarcinoma. Correlation with disease progression? *Tumori* *94*, 384–388.
- Chambers, C.A., Kuhns, M.S., Egen, J.G., and Allison, J.P. (2001). CTLA-4-mediated inhibition in regulation of T cell responses: mechanisms and manipulation in tumor immunotherapy. *Annu. Rev. Immunol.* *19*, 565–594.
- Chen, H.-C., Joalland, N., Bridgeman, J.S., Alchami, F.S., Jarry, U., Khan, M.W.A., Piggott, L., Shanneik, Y., Li, J., Herold, M.J., et al. (2017). Synergistic targeting of breast cancer stem-like cells by human γδ T cells and CD8+ T cells. *Immunol. Cell Biol.* *95*, 620–629.

- Chien, Y., and Konigshofer, Y. (2007). Antigen recognition by gammadelta T cells. *Immunol. Rev.* *215*, 46–58.
- Chien, Y., Meyer, C., and Bonneville, M. (2014). $\gamma\delta$ T cells: first line of defense and beyond. *Annu. Rev. Immunol.* *32*, 121–155.
- Chitadze, G., Lettau, M., Luecke, S., Wang, T., Janssen, O., Fürst, D., Mytilineos, J., Wesch, D., Oberg, H.-H., Held-Feindt, J., et al. (2016). NKG2D- and T-cell receptor-dependent lysis of malignant glioma cell lines by human $\gamma\delta$ T cells: Modulation by temozolomide and A disintegrin and metalloproteases 10 and 17 inhibitors. *Oncoimmunology* *5*, e1093276.
- Colombo, N., Conte, P.F., Pignata, S., Raspagliesi, F., and Scambia, G. (2016). Bevacizumab in ovarian cancer: Focus on clinical data and future perspectives. *Crit. Rev. Oncol. Hematol.* *97*, 335–348.
- Colombo, P.-E., Fabbro, M., Theillet, C., Bibeau, F., Rouanet, P., and Ray-Coquard, I. (2014). Sensitivity and resistance to treatment in the primary management of epithelial ovarian cancer. *Crit. Rev. Oncol. Hematol.* *89*, 207–216.
- Constant, P., Davodeau, F., Peyrat, M.A., Poquet, Y., Puzo, G., Bonneville, M., and Fournié, J.J. (1994). Stimulation of human gamma delta T cells by nonpeptidic mycobacterial ligands. *Science* *264*, 267–270.
- Conti, L., Casetti, R., Cardone, M., Varano, B., Martino, A., Belardelli, F., Poccia, F., and Gessani, S. (2005). Reciprocal activating interaction between dendritic cells and pamidronate-stimulated gammadelta T cells: role of CD86 and inflammatory cytokines. *J. Immunol. Baltim. Md 1950* *174*, 252–260.
- Coppens, I. (2013). Targeting lipid biosynthesis and salvage in apicomplexan parasites for improved chemotherapies. *Nat. Rev. Microbiol.* *11*, 823–835.
- Cordova, A., Toia, F., La Mendola, C., Orlando, V., Meraviglia, S., Rinaldi, G., Todaro, M., Cicero, G., Zichichi, L., Donni, P.L., et al. (2012). Characterization of human $\gamma\delta$ T lymphocytes infiltrating primary malignant melanomas. *PloS One* *7*, e49878.
- Corvaisier, M., Moreau-Aubry, A., Diez, E., Bennouna, J., Mosnier, J.-F., Scotet, E., Bonneville, M., and Jotereau, F. (2005). V gamma 9V delta 2 T cell response to colon carcinoma cells. *J. Immunol. Baltim. Md 1950* *175*, 5481–5488.
- Curtis, S.A., Cohen, J.V., and Kluger, H.M. (2016). Evolving Immunotherapy Approaches for Renal Cell Carcinoma. *Curr. Oncol. Rep.* *18*, 57.
- Das, H., Wang, L., Kamath, A., and Bukowski, J.F. (2001a). Vgamma2Vdelta2 T-cell receptor-mediated recognition of aminobisphosphonates. *Blood* *98*, 1616–1618.
- Das, H., Groh, V., Kuijl, C., Sugita, M., Morita, C.T., Spies, T., and Bukowski, J.F. (2001b). MICA engagement by human Vgamma2Vdelta2 T cells enhances their antigen-dependent effector function. *Immunity* *15*, 83–93.
- Davey, M.S., Lin, C.-Y., Roberts, G.W., Heuston, S., Brown, A.C., Chess, J.A., Toleman, M.A., Gahan, C.G.M., Hill, C., Parish, T., et al. (2011). Human neutrophil clearance of bacterial pathogens triggers anti-microbial $\gamma\delta$ T cell responses in early infection. *PLoS Pathog.* *7*, e1002040.
- Davey, M.S., Willcox, C.R., Hunter, S., Kasatskaya, S.A., Remmerswaal, E.B.M., Salim, M., Mohammed, F., Bemelman, F.J., Chudakov, D.M., Oo, Y.H., et al. (2018). The human V δ 2+ T-cell compartment comprises distinct innate-like V γ 9+ and adaptive V γ 9- subsets. *Nat. Commun.* *9*, 1760.

- De Luca, A., Lamura, L., Gallo, M., Daniele, G., D'Alessio, A., Giordano, P., Maiello, M.R., Pergameno, M., Perrone, F., and Normanno, N. (2011). Pharmacokinetic evaluation of zoledronic acid. *Expert Opin. Drug Metab. Toxicol.* 7, 911–918.
- Deauvieau, F., Ollion, V., Doffin, A.-C., Achard, C., Fonteneau, J.-F., Verronese, E., Durand, I., Ghittoni, R., Marvel, J., Dezutter-Dambuyant, C., et al. (2015). Human natural killer cells promote cross-presentation of tumor cell-derived antigens by dendritic cells. *Int. J. Cancer* 136, 1085–1094.
- Déchanet, J., Merville, P., Bergé, F., Bone-Mane, G., Taupin, J.L., Michel, P., Joly, P., Bonneville, M., Potaux, L., and Moreau, J.F. (1999). Major expansion of gammadelta T lymphocytes following cytomegalovirus infection in kidney allograft recipients. *J. Infect. Dis.* 179, 1–8.
- Devilder, M.-C., Maillet, S., Bouyge-Moreau, I., Donnadieu, E., Bonneville, M., and Scotet, E. (2006). Potentiation of antigen-stimulated V gamma 9V delta 2 T cell cytokine production by immature dendritic cells (DC) and reciprocal effect on DC maturation. *J. Immunol. Baltim. Md 1950* 176, 1386–1393.
- Devilder, M.-C., Allain, S., Dousset, C., Bonneville, M., and Scotet, E. (2009). Early triggering of exclusive IFN-gamma responses of human Vgamma9Vdelta2 T cells by TLR-activated myeloid and plasmacytoid dendritic cells. *J. Immunol. Baltim. Md 1950* 183, 3625–3633.
- Dhillon, S., and Lyseng-Williamson, K.A. (2008). Zoledronic acid: a review of its use in the management of bone metastases of malignancy. *Drugs* 68, 507–534.
- Dhupkar, P., and Gordon, N. (2017). Interleukin-2: Old and New Approaches to Enhance Immune-Therapeutic Efficacy. *Adv. Exp. Med. Biol.* 995, 33–51.
- Dieli, F., Troye-Blomberg, M., Ivanyi, J., Fournié, J.J., Krensky, A.M., Bonneville, M., Peyrat, M.A., Caccamo, N., Sireci, G., and Salerno, A. (2001). Granulysin-dependent killing of intracellular and extracellular *Mycobacterium tuberculosis* by Vgamma9/Vdelta2 T lymphocytes. *J. Infect. Dis.* 184, 1082–1085.
- Dieli, F., Gebbia, N., Poccia, F., Caccamo, N., Montesano, C., Fulfaro, F., Arcara, C., Valerio, M.R., Meraviglia, S., Di Sano, C., et al. (2003). Induction of gammadelta T-lymphocyte effector functions by bisphosphonate zoledronic acid in cancer patients in vivo. *Blood* 102, 2310–2311.
- Dieli, F., Vermijlen, D., Fulfaro, F., Caccamo, N., Meraviglia, S., Cicero, G., Roberts, A., Buccheri, S., D'Asaro, M., Gebbia, N., et al. (2007). Targeting human {gamma}delta T cells with zoledronate and interleukin-2 for immunotherapy of hormone-refractory prostate cancer. *Cancer Res.* 67, 7450–7457.
- Dimova, T., Brouwer, M., Gosselin, F., Tassignon, J., Leo, O., Donner, C., Marchant, A., and Vermijlen, D. (2015). Effector Vγ9Vδ2 T cells dominate the human fetal γδ T-cell repertoire. *Proc. Natl. Acad. Sci. U. S. A.* 112, E556-565.
- Dranoff, G. (2004). Cytokines in cancer pathogenesis and cancer therapy. *Nat. Rev. Cancer* 4, 11–22.
- van Driel, W.J., Koole, S.N., and Sonke, G.S. (2018). Hyperthermic Intraperitoneal Chemotherapy in Ovarian Cancer. *N. Engl. J. Med.* 378, 1363–1364.
- Dudley, E.C., Girardi, M., Owen, M.J., and Hayday, A.C. (1995). Alpha beta and gamma delta T cells can share a late common precursor. *Curr. Biol. CB* 5, 659–669.
- Dunn, G.P., Bruce, A.T., Ikeda, H., Old, L.J., and Schreiber, R.D. (2002). Cancer immunoediting: from immunosurveillance to tumor escape. *Nat. Immunol.* 3, 991–998.

- Dunn, G.P., Old, L.J., and Schreiber, R.D. (2004). The three Es of cancer immunoediting. *Annu. Rev. Immunol.* 22, 329–360.
- Dunne, M.R., Mangan, B.A., Madrigal-Estebas, L., and Doherty, D.G. (2010). Preferential Th1 cytokine profile of phosphoantigen-stimulated human V γ 9V δ 2 T cells. *Mediators Inflamm.* 2010, 704941.
- Eberl, M., Roberts, G.W., Meuter, S., Williams, J.D., Topley, N., and Moser, B. (2009). A rapid crosstalk of human gammadelta T cells and monocytes drives the acute inflammation in bacterial infections. *PLoS Pathog.* 5, e1000308.
- Ehl, S., Schwarz, K., Enders, A., Duffner, U., Pannicke, U., Kühr, J., Mascart, F., Schmitt-Graeff, A., Niemeyer, C., and Fisch, P. (2005). A variant of SCID with specific immune responses and predominance of gamma delta T cells. *J. Clin. Invest.* 115, 3140–3148.
- Elit, L., Oliver, T.K., Covens, A., Kwon, J., Fung, M.F.-K., Hirte, H.W., and Oza, A.M. (2007). Intraperitoneal chemotherapy in the first-line treatment of women with stage III epithelial ovarian cancer: a systematic review with metaanalyses. *Cancer* 109, 692–702.
- Espinosa, E., Belmont, C., Pont, F., Luciani, B., Poupot, R., Romagné, F., Brailly, H., Bonneville, M., and Fournié, J.J. (2001). Chemical synthesis and biological activity of bromohydrin pyrophosphate, a potent stimulator of human gamma delta T cells. *J. Biol. Chem.* 276, 18337–18344.
- Falk, A.T., Barrière, J., François, E., and Follana, P. (2015). Bevacizumab: A dose review. *Crit. Rev. Oncol. Hematol.* 94, 311–322.
- Ferrarini, M., Heltai, S., Pupa, S.M., Mernard, S., and Zocchi, R. (1996). Killing of laminin receptor-positive human lung cancers by tumor infiltrating lymphocytes bearing gammadelta(+) t-cell receptors. *J. Natl. Cancer Inst.* 88, 436–441.
- Fiore, F., Castella, B., Nuschak, B., Bertieri, R., Mariani, S., Bruno, B., Pantaleoni, F., Foglietta, M., Boccadoro, M., and Massaia, M. (2007). Enhanced ability of dendritic cells to stimulate innate and adaptive immunity on short-term incubation with zoledronic acid. *Blood* 110, 921–927.
- Fountzilias, C., Patel, S., and Mahalingam, D. (2017). Review: Oncolytic virotherapy, updates and future directions. *Oncotarget* 8, 102617–102639.
- Fournié, J.-J., Sicard, H., Poupot, M., Bezombes, C., Blanc, A., Romagné, F., Ysebaert, L., and Laurent, G. (2013). What lessons can be learned from $\gamma\delta$ T cell-based cancer immunotherapy trials? *Cell. Mol. Immunol.* 10, 35–41.
- Freeman, G.J., Long, A.J., Iwai, Y., Bourque, K., Chernova, T., Nishimura, H., Fitz, L.J., Malenkovich, N., Okazaki, T., Byrne, M.C., et al. (2000). Engagement of the PD-1 immunoinhibitory receptor by a novel B7 family member leads to negative regulation of lymphocyte activation. *J. Exp. Med.* 192, 1027–1034.
- Fujita, K., Ikarashi, H., Takakuwa, K., Kodama, S., Tokunaga, A., Takahashi, T., and Tanaka, K. (1995). Prolonged disease-free period in patients with advanced epithelial ovarian cancer after adoptive transfer of tumor-infiltrating lymphocytes. *Clin. Cancer Res. Off. J. Am. Assoc. Cancer Res.* 1, 501–507.
- García, V.E., Sieling, P.A., Gong, J., Barnes, P.F., Uyemura, K., Tanaka, Y., Bloom, B.R., Morita, C.T., and Modlin, R.L. (1997). Single-cell cytokine analysis of gamma delta T cell responses to nonpeptide mycobacterial antigens. *J. Immunol. Baltim. Md 1950* 159, 1328–1335.
- Gentles, A.J., Newman, A.M., Liu, C.L., Bratman, S.V., Feng, W., Kim, D., Nair, V.S., Xu, Y., Khuong, A., Hoang, C.D., et al. (2015). The prognostic landscape of genes and infiltrating immune cells across human cancers. *Nat. Med.* 21, 938–945.

- Gertner-Dardenne, J., Bonnafous, C., Bezombes, C., Capietto, A.-H., Scaglione, V., Ingoure, S., Cendron, D., Gross, E., Lepage, J.-F., Quillet-Mary, A., et al. (2009). Bromohydrin pyrophosphate enhances antibody-dependent cell-mediated cytotoxicity induced by therapeutic antibodies. *Blood* *113*, 4875–4884.
- Gober, H.-J., Kistowska, M., Angman, L., Jenö, P., Mori, L., and De Libero, G. (2003). Human T cell receptor gammadelta cells recognize endogenous mevalonate metabolites in tumor cells. *J. Exp. Med.* *197*, 163–168.
- Gouy, S., Ferron, G., Glehen, O., Bayar, A., Marchal, F., Pomel, C., Quenet, F., Bereder, J.M., Le Deley, M.C., and Morice, P. (2016). Results of a multicenter phase I dose-finding trial of hyperthermic intraperitoneal cisplatin after neoadjuvant chemotherapy and complete cytoreductive surgery and followed by maintenance bevacizumab in initially unresectable ovarian cancer. *Gynecol. Oncol.* *142*, 237–242.
- Green, J., and Lipton, A. (2010). Anticancer properties of zoledronic acid. *Cancer Invest.* *28*, 944–957.
- Gross, G., Waks, T., and Eshhar, Z. (1989). Expression of immunoglobulin-T-cell receptor chimeric molecules as functional receptors with antibody-type specificity. *Proc. Natl. Acad. Sci. U. S. A.* *86*, 10024–10028.
- Gu, S., Nawrocka, W., and Adams, E.J. (2014). Sensing of Pyrophosphate Metabolites by V γ 9V δ 2 T Cells. *Front. Immunol.* *5*, 688.
- Gu, S., Sachleben, J.R., Boughter, C.T., Nawrocka, W.I., Borowska, M.T., Tarrasch, J.T., Skiniotis, G., Roux, B., and Adams, E.J. (2017). Phosphoantigen-induced conformational change of butyrophilin 3A1 (BTN3A1) and its implication on V γ 9V δ 2 T cell activation. *Proc. Natl. Acad. Sci. U. S. A.* *114*, E7311–E7320.
- Gustafsson, K., Junevik, K., Werlenius, O., Holmgren, S., Karlsson-Parra, A., and Andersson, P.-O. (2011). Tumour-loaded α -type 1-polarized dendritic cells from patients with chronic lymphocytic leukaemia produce a superior NK-, NKT- and CD8+ T cell-attracting chemokine profile. *Scand. J. Immunol.* *74*, 318–326.
- Harly, C., Guillaume, Y., Nedellec, S., Peigné, C.-M., Mönkkönen, H., Mönkkönen, J., Li, J., Kuball, J., Adams, E.J., Netzer, S., et al. (2012). Key implication of CD277/butyrophilin-3 (BTN3A) in cellular stress sensing by a major human $\gamma\delta$ T-cell subset. *Blood* *120*, 2269–2279.
- Harly, C., Peigné, C.-M., and Scotet, E. (2014). Molecules and Mechanisms Implicated in the Peculiar Antigenic Activation Process of Human V γ 9V δ 2 T Cells. *Front. Immunol.* *5*, 657.
- Hashida, Y., Taniguchi, A., Yawata, T., Hosokawa, S., Murakami, M., Hiroi, M., Ueba, T., and Daibata, M. (2015). Prevalence of human cytomegalovirus, polyomaviruses, and oncogenic viruses in glioblastoma among Japanese subjects. *Infect. Agent. Cancer* *10*, 3.
- Hayday, A.C. (2009). Gammadelta T cells and the lymphoid stress-surveillance response. *Immunity* *31*, 184–196.
- Hebbeler, A.M., Cairo, C., Cummings, J.S., and Pauza, C.D. (2007). Individual V γ 2-J γ 1.2+ T cells respond to both isopentenyl pyrophosphate and Daudi cell stimulation: generating tumor effectors with low molecular weight phosphoantigens. *Cancer Immunol. Immunother.* *CII* *56*, 819–829.
- Hodi, F.S., O'Day, S.J., McDermott, D.F., Weber, R.W., Sosman, J.A., Haanen, J.B., Gonzalez, R., Robert, C., Schadendorf, D., Hassel, J.C., et al. (2010). Improved survival with ipilimumab in patients with metastatic melanoma. *N. Engl. J. Med.* *363*, 711–723.

- Hoeres, T., Smetak, M., Pretscher, D., and Wilhelm, M. (2018). Improving the Efficiency of V γ 9V δ 2 T-Cell Immunotherapy in Cancer. *Front. Immunol.* *9*, 800.
- Hu, J.C.C., Coffin, R.S., Davis, C.J., Graham, N.J., Groves, N., Guest, P.J., Harrington, K.J., James, N.D., Love, C.A., McNeish, I., et al. (2006). A phase I study of OncoVEXGM-CSF, a second-generation oncolytic herpes simplex virus expressing granulocyte macrophage colony-stimulating factor. *Clin. Cancer Res. Off. J. Am. Assoc. Cancer Res.* *12*, 6737–6747.
- Ismaili, J., Orlislagers, V., Poupot, R., Fournié, J.-J., and Goldman, M. (2002). Human gamma delta T cells induce dendritic cell maturation. *Clin. Immunol. Orlando Fla* *103*, 296–302.
- Jaaback, K., Johnson, N., and Lawrie, T.A. (2016). Intraperitoneal chemotherapy for the initial management of primary epithelial ovarian cancer. *Cochrane Database Syst. Rev.* CD005340.
- Jarry, U., Chauvin, C., Joalland, N., Léger, A., Minault, S., Robard, M., Bonneville, M., Oliver, L., Vallette, F.M., Vié, H., et al. (2016). Stereotaxic administrations of allogeneic human V γ 9V δ 2 T cells efficiently control the development of human glioblastoma brain tumors. *Oncoimmunology* *5*, e1168554.
- Jarry, U., Joalland, N., Chauvin, C., Clemenceau, B., Pecqueur, C., and Scotet, E. (2018). Stereotactic Adoptive Transfer of Cytotoxic Immune Cells in Murine Models of Orthotopic Human Glioblastoma Multiforme Xenografts. *J. Vis. Exp. JoVE*.
- Joalland, N., Chauvin, C., Oliver, L., Vallette, F.M., Pecqueur, C., Jarry, U., and Scotet, E. (2018). IL-21 Increases the Reactivity of Allogeneic Human V γ 9V δ 2 T Cells Against Primary Glioblastoma Tumors. *J. Immunother. Hagerstown Md 1997* *41*, 224–231.
- Johnson, L.A., Morgan, R.A., Dudley, M.E., Cassard, L., Yang, J.C., Hughes, M.S., Kammula, U.S., Royal, R.E., Sherry, R.M., Wunderlich, J.R., et al. (2009). Gene therapy with human and mouse T-cell receptors mediates cancer regression and targets normal tissues expressing cognate antigen. *Blood* *114*, 535–546.
- Jouen-Beades, F., Paris, E., Dieulois, C., Lemeland, J.F., Barre-Dezelus, V., Marret, S., Humbert, G., Leroy, J., and Tron, F. (1997). In vivo and in vitro activation and expansion of gammadelta T cells during *Listeria monocytogenes* infection in humans. *Infect. Immun.* *65*, 4267–4272.
- Jung, J., Seol, H.S., and Chang, S. (2018). The Generation and Application of Patient-Derived Xenograft Model for Cancer Research. *Cancer Res. Treat. Off. J. Korean Cancer Assoc.* *50*, 1–10.
- Juszczak, A., Gupta, A., Karavitaki, N., Middleton, M.R., and Grossman, A.B. (2012). Ipilimumab: a novel immunomodulating therapy causing autoimmune hypophysitis: a case report and review. *Eur. J. Endocrinol.* *167*, 1–5.
- Kabelitz, D., Wesch, D., Pitters, E., and Zöller, M. (2004). Characterization of tumor reactivity of human V gamma 9V delta 2 gamma delta T cells in vitro and in SCID mice in vivo. *J. Immunol. Baltim. Md 1950* *173*, 6767–6776.
- Kaiko, G.E., Horvat, J.C., Beagley, K.W., and Hansbro, P.M. (2008). Immunological decision-making: how does the immune system decide to mount a helper T-cell response? *Immunology* *123*, 326–338.
- Kalaitidou, M., Kueberuwa, G., Schütt, A., and Gilham, D.E. (2015). CAR T-cell therapy: toxicity and the relevance of preclinical models. *Immunotherapy* *7*, 487–497.
- Kamath, A.B., Wang, L., Das, H., Li, L., Reinhold, V.N., and Bukowski, J.F. (2003). Antigens in tea-beverage prime human Vgamma 2Vdelta 2 T cells in vitro and in vivo for memory and nonmemory antibacterial cytokine responses. *Proc. Natl. Acad. Sci. U. S. A.* *100*, 6009–6014.

- Karunakaran, M.M., Göbel, T.W., Starick, L., Walter, L., and Herrmann, T. (2014). V γ 9 and V δ 2 T cell antigen receptor genes and butyrophilin 3 (BTN3) emerged with placental mammals and are concomitantly preserved in selected species like alpaca (*Vicugna pacos*). *Immunogenetics* 66, 243–254.
- Kato, Y., Tanaka, Y., Tanaka, H., Yamashita, S., and Minato, N. (2003). Requirement of species-specific interactions for the activation of human gamma delta T cells by pamidronate. *J. Immunol. Baltim. Md 1950* 170, 3608–3613.
- Kato, Y., Tanaka, Y., Hayashi, M., Okawa, K., and Minato, N. (2006). Involvement of CD166 in the activation of human gamma delta T cells by tumor cells sensitized with nonpeptide antigens. *J. Immunol. Baltim. Md 1950* 177, 877–884.
- Kazen, A.R., and Adams, E.J. (2011). Evolution of the V, D, and J gene segments used in the primate gammadelta T-cell receptor reveals a dichotomy of conservation and diversity. *Proc. Natl. Acad. Sci. U. S. A.* 108, E332-340.
- Keir, M.E., Butte, M.J., Freeman, G.J., and Sharpe, A.H. (2008). PD-1 and its ligands in tolerance and immunity. *Annu. Rev. Immunol.* 26, 677–704.
- Khan, M.W.A., Eberl, M., and Moser, B. (2014). Potential Use of $\gamma\delta$ T Cell-Based Vaccines in Cancer Immunotherapy. *Front. Immunol.* 5, 512.
- Kobayashi, H., Tanaka, Y., Yagi, J., Toma, H., and Uchiyama, T. (2001). Gamma/delta T cells provide innate immunity against renal cell carcinoma. *Cancer Immunol. Immunother. CII* 50, 115–124.
- Kobayashi, H., Tanaka, Y., Yagi, J., Osaka, Y., Nakazawa, H., Uchiyama, T., Minato, N., and Toma, H. (2007). Safety profile and anti-tumor effects of adoptive immunotherapy using gamma-delta T cells against advanced renal cell carcinoma: a pilot study. *Cancer Immunol. Immunother. CII* 56, 469–476.
- Kobayashi, H., Tanaka, Y., Shimmura, H., Minato, N., and Tanabe, K. (2010). Complete remission of lung metastasis following adoptive immunotherapy using activated autologous gammadelta T-cells in a patient with renal cell carcinoma. *Anticancer Res.* 30, 575–579.
- Kobayashi, H., Tanaka, Y., Yagi, J., Minato, N., and Tanabe, K. (2011). Phase I/II study of adoptive transfer of $\gamma\delta$ T cells in combination with zoledronic acid and IL-2 to patients with advanced renal cell carcinoma. *Cancer Immunol. Immunother. CII* 60, 1075–1084.
- Kochenderfer, J.N., Wilson, W.H., Janik, J.E., Dudley, M.E., Stetler-Stevenson, M., Feldman, S.A., Maric, I., Raffeld, M., Nathan, D.-A.N., Lanier, B.J., et al. (2010). Eradication of B-lineage cells and regression of lymphoma in a patient treated with autologous T cells genetically engineered to recognize CD19. *Blood* 116, 4099–4102.
- Krangel, M.S., Yssel, H., Brocklehurst, C., and Spits, H. (1990). A distinct wave of human T cell receptor gamma/delta lymphocytes in the early fetal thymus: evidence for controlled gene rearrangement and cytokine production. *J. Exp. Med.* 172, 847–859.
- Krishnan, V., Berek, J.S., and Dorigo, O. (2017). Immunotherapy in ovarian cancer. *Curr. Probl. Cancer* 41, 48–63.
- Kühl, A.A., Pawlowski, N.N., Grollich, K., Blessenohl, M., Westermann, J., Zeitz, M., Loddenkemper, C., and Hoffmann, J.C. (2009). Human peripheral gammadelta T cells possess regulatory potential. *Immunology* 128, 580–588.
- Kunzmann, V., Bauer, E., and Wilhelm, M. (1999). Gamma/delta T-cell stimulation by pamidronate. *N. Engl. J. Med.* 340, 737–738.

- Kunzmann, V., Bauer, E., Feurle, J., Weissinger, F., Tony, H.P., and Wilhelm, M. (2000). Stimulation of gammadelta T cells by aminobisphosphonates and induction of antiplasma cell activity in multiple myeloma. *Blood* 96, 384–392.
- Kunzmann, V., Kretzschmar, E., Herrmann, T., and Wilhelm, M. (2004). Polyinosinic-polycytidylic acid-mediated stimulation of human gammadelta T cells via CD11c dendritic cell-derived type I interferons. *Immunology* 112, 369–377.
- Kurman, R.J., and Shih, I.-M. (2016). The Dualistic Model of Ovarian Carcinogenesis: Revisited, Revised, and Expanded. *Am. J. Pathol.* 186, 733–747.
- Labarriere, N., Fortun, A., Bellec, A., Khammari, A., Dreno, B., Saïagh, S., and Lang, F. (2013). A full GMP process to select and amplify epitope-specific T lymphocytes for adoptive immunotherapy of metastatic melanoma. *Clin. Dev. Immunol.* 2013, 932318.
- Lafont, V., Liautard, J., Liautard, J.P., and Favero, J. (2001). Production of TNF-alpha by human V gamma 9V delta 2 T cells via engagement of Fc gamma RIIIA, the low affinity type 3 receptor for the Fc portion of IgG, expressed upon TCR activation by nonpeptidic antigen. *J. Immunol. Baltim. Md 1950* 166, 7190–7199.
- Lafont, V., Sanchez, F., Laprevotte, E., Michaud, H.-A., Gros, L., Eliaou, J.-F., and Bonnefoy, N. (2014). Plasticity of $\gamma\delta$ T Cells: Impact on the Anti-Tumor Response. *Front. Immunol.* 5, 622.
- Lamb, L.S., Bowersock, J., Dasgupta, A., Gillespie, G.Y., Su, Y., Johnson, A., and Spencer, H.T. (2013). Engineered drug resistant $\gamma\delta$ T cells kill glioblastoma cell lines during a chemotherapy challenge: a strategy for combining chemo- and immunotherapy. *PloS One* 8, e51805.
- Lang, F., Peyrat, M.A., Constant, P., Davodeau, F., David-Ameline, J., Poquet, Y., Vié, H., Fournié, J.J., and Bonneville, M. (1995). Early activation of human V gamma 9V delta 2 T cell broad cytotoxicity and TNF production by nonpeptidic mycobacterial ligands. *J. Immunol. Baltim. Md 1950* 154, 5986–5994.
- Lang, J.M., Kaikobad, M.R., Wallace, M., Staab, M.J., Horvath, D.L., Wilding, G., Liu, G., Eickhoff, J.C., McNeel, D.G., and Malkovsky, M. (2011). Pilot trial of interleukin-2 and zoledronic acid to augment $\gamma\delta$ T cells as treatment for patients with refractory renal cell carcinoma. *Cancer Immunol. Immunother. CII* 60, 1447–1460.
- Lavoué, V., Cabillic, F., Toutirais, O., Thedrez, A., Dessarthe, B., de La Pintièrre, C.T., Daniel, P., Foucher, F., Bauville, E., Henno, S., et al. (2012). Sensitization of ovarian carcinoma cells with zoledronate restores the cytotoxic capacity of V γ 9V δ 2 T cells impaired by the prostaglandin E2 immunosuppressive factor: implications for immunotherapy. *Int. J. Cancer* 131, E449-462.
- Leget, G.A., and Czuczman, M.S. (1998). Use of rituximab, the new FDA-approved antibody. *Curr. Opin. Oncol.* 10, 548–551.
- Lesport, E., Baudhuin, J., Sousa, S., LeMaout, J., Zamborlini, A., Rouas-Freiss, N., Carosella, E.D., and Favier, B. (2011). Inhibition of human gamma delta [corrected] T-cell antitumoral activity through HLA-G: implications for immunotherapy of cancer. *Cell. Mol. Life Sci. CMLS* 68, 3385–3399.
- Li, X., Kang, N., Zhang, X., Dong, X., Wei, W., Cui, L., Ba, D., and He, W. (2011). Generation of human regulatory gammadelta T cells by TCRgammadelta stimulation in the presence of TGF-beta and their involvement in the pathogenesis of systemic lupus erythematosus. *J. Immunol. Baltim. Md 1950* 186, 6693–6700.

- Li, X., Lu, P., Li, B., Zhang, W., Yang, R., Chu, Y., and Luo, K. (2017). Interleukin 2 and interleukin 10 function synergistically to promote CD8+ T cell cytotoxicity, which is suppressed by regulatory T cells in breast cancer. *Int. J. Biochem. Cell Biol.* *87*, 1–7.
- Liu, Z., Guo, B.L., Gehrs, B.C., Nan, L., and Lopez, R.D. (2005). Ex vivo expanded human V γ 9V δ 2+ γ δ -T cells mediate innate antitumor activity against human prostate cancer cells in vitro. *J. Urol.* *173*, 1552–1556.
- Lo Presti, E., Dieli, F., and Meraviglia, S. (2014). Tumor-Infiltrating $\gamma\delta$ T Lymphocytes: Pathogenic Role, Clinical Significance, and Differential Programming in the Tumor Microenvironment. *Front. Immunol.* *5*, 607.
- Lo Presti, E., Caccamo, N., Orlando, V., Dieli, F., and Meraviglia, S. (2016). Activation and selective IL-17 response of human V γ 9V δ 2 T lymphocytes by TLR-activated plasmacytoid dendritic cells. *Oncotarget* *7*, 60896–60905.
- Louis, D.N., Ohgaki, H., Wiestler, O.D., Cavenee, W.K., Burger, P.C., Jouvet, A., Scheithauer, B.W., and Kleihues, P. (2007). The 2007 WHO classification of tumours of the central nervous system. *Acta Neuropathol. (Berl.)* *114*, 97–109.
- Louis, D.N., Perry, A., Reifenberger, G., von Deimling, A., Figarella-Branger, D., Cavenee, W.K., Ohgaki, H., Wiestler, O.D., Kleihues, P., and Ellison, D.W. (2016). The 2016 World Health Organization Classification of Tumors of the Central Nervous System: a summary. *Acta Neuropathol. (Berl.)* *131*, 803–820.
- Ma, C., Zhang, Q., Ye, J., Wang, F., Zhang, Y., Wevers, E., Schwartz, T., Hunborg, P., Varvares, M.A., Hoft, D.F., et al. (2012). Tumor-infiltrating $\gamma\delta$ T lymphocytes predict clinical outcome in human breast cancer. *J. Immunol. Baltim. Md 1950* *189*, 5029–5036.
- Mantovani, A., Cassatella, M.A., Costantini, C., and Jaillon, S. (2011). Neutrophils in the activation and regulation of innate and adaptive immunity. *Nat. Rev. Immunol.* *11*, 519–531.
- Marcu-Malina, V., Heijhuurs, S., van Buuren, M., Hartkamp, L., Strand, S., Sebestyen, Z., Scholten, K., Martens, A., and Kuball, J. (2011). Redirecting $\alpha\beta$ T cells against cancer cells by transfer of a broadly tumor-reactive $\gamma\delta$ T-cell receptor. *Blood* *118*, 50–59.
- Margolin, K. (2016). The Promise of Molecularly Targeted and Immunotherapy for Advanced Melanoma. *Curr. Treat. Options Oncol.* *17*, 48.
- Matulonis, U.A., Sood, A.K., Fallowfield, L., Howitt, B.E., Sehouli, J., and Karlan, B.Y. (2016). Ovarian cancer. *Nat. Rev. Dis. Primer* *2*, 16061.
- Maymon, R., Bar-Shira Maymon, B., Holzinger, M., Tartakovsky, B., and Leibovici, J. (1994). Augmentative effects of intracellular chemotherapy penetration combined with hyperthermia in human ovarian cancer cells lines. *Gynecol. Oncol.* *55*, 265–270.
- McCarron, M., Osborne, Y., Story, C.J., Dempsey, J.L., Turner, D.R., and Morley, A.A. (1987). Effect of age on lymphocyte proliferation. *Mech. Ageing Dev.* *41*, 211–218.
- McVay, L.D., and Carding, S.R. (1996). Extrathymic origin of human gamma delta T cells during fetal development. *J. Immunol. Baltim. Md 1950* *157*, 2873–2882.
- Meraviglia, S., Eberl, M., Vermijlen, D., Todaro, M., Buccheri, S., Cicero, G., La Mendola, C., Guggino, G., D'Asaro, M., Orlando, V., et al. (2010). In vivo manipulation of V γ 9V δ 2 T cells with zoledronate and low-dose interleukin-2 for immunotherapy of advanced breast cancer patients. *Clin. Exp. Immunol.* *161*, 290–297.

- Meuter, S., Eberl, M., and Moser, B. (2010). Prolonged antigen survival and cytosolic export in cross-presenting human gammadelta T cells. *Proc. Natl. Acad. Sci. U. S. A.* *107*, 8730–8735.
- Mócsai, A. (2013). Diverse novel functions of neutrophils in immunity, inflammation, and beyond. *J. Exp. Med.* *210*, 1283–1299.
- Morgan, R.A., Dudley, M.E., Wunderlich, J.R., Hughes, M.S., Yang, J.C., Sherry, R.M., Royal, R.E., Topalian, S.L., Kammula, U.S., Restifo, N.P., et al. (2006). Cancer regression in patients after transfer of genetically engineered lymphocytes. *Science* *314*, 126–129.
- Morita, C.T., Verma, S., Aparicio, P., Martinez, C., Spits, H., and Brenner, M.B. (1991). Functionally distinct subsets of human gamma/delta T cells. *Eur. J. Immunol.* *21*, 2999–3007.
- Morita, C.T., Beckman, E.M., Bukowski, J.F., Tanaka, Y., Band, H., Bloom, B.R., Golan, D.E., and Brenner, M.B. (1995). Direct presentation of nonpeptide prenyl pyrophosphate antigens to human gamma delta T cells. *Immunity* *3*, 495–507.
- Morita, C.T., Jin, C., Sarikonda, G., and Wang, H. (2007). Nonpeptide antigens, presentation mechanisms, and immunological memory of human Vgamma2Vdelta2 T cells: discriminating friend from foe through the recognition of prenyl pyrophosphate antigens. *Immunol. Rev.* *215*, 59–76.
- Morton, J.J., Bird, G., Refaeli, Y., and Jimeno, A. (2016). Humanized Mouse Xenograft Models: Narrowing the Tumor-Microenvironment Gap. *Cancer Res.* *76*, 6153–6158.
- Muldoon, L.L., Soussain, C., Jahnke, K., Johanson, C., Siegal, T., Smith, Q.R., Hall, W.A., Hynynen, K., Senter, P.D., Peereboom, D.M., et al. (2007). Chemotherapy delivery issues in central nervous system malignancy: a reality check. *J. Clin. Oncol. Off. J. Am. Soc. Clin. Oncol.* *25*, 2295–2305.
- Müller, I., Munder, M., Kropf, P., and Hänsch, G.M. (2009). Polymorphonuclear neutrophils and T lymphocytes: strange bedfellows or brothers in arms? *Trends Immunol.* *30*, 522–530.
- Nakajima, J., Murakawa, T., Fukami, T., Goto, S., Kaneko, T., Yoshida, Y., Takamoto, S., and Kakimi, K. (2010). A phase I study of adoptive immunotherapy for recurrent non-small-cell lung cancer patients with autologous gammadelta T cells. *Eur. J. Cardio-Thorac. Surg. Off. J. Eur. Assoc. Cardio-Thorac. Surg.* *37*, 1191–1197.
- Nedellec, S., Bonneville, M., and Scotet, E. (2010). Human Vgamma9Vdelta2 T cells: from signals to functions. *Semin. Immunol.* *22*, 199–206.
- Neelapu, S.S., Tummala, S., Kebriaei, P., Wierda, W., Gutierrez, C., Locke, F.L., Komanduri, K.V., Lin, Y., Jain, N., Daver, N., et al. (2018). Chimeric antigen receptor T-cell therapy - assessment and management of toxicities. *Nat. Rev. Clin. Oncol.* *15*, 47–62.
- Nicol, A.J., Tokuyama, H., Mattarollo, S.R., Hagi, T., Suzuki, K., Yokokawa, K., and Nieda, M. (2011). Clinical evaluation of autologous gamma delta T cell-based immunotherapy for metastatic solid tumours. *Br. J. Cancer* *105*, 778–786.
- Noguchi, A., Kaneko, T., Kamigaki, T., Fujimoto, K., Ozawa, M., Saito, M., Ariyoshi, N., and Goto, S. (2011). Zoledronate-activated Vγ9γδ T cell-based immunotherapy is feasible and restores the impairment of γδ T cells in patients with solid tumors. *Cytotherapy* *13*, 92–97.
- Oizel, K., Chauvin, C., Oliver, L., Gratas, C., Geraldo, F., Jarry, U., Scotet, E., Rabe, M., Alves-Guerra, M.-C., Teusan, R., et al. (2017). Efficient Mitochondrial Glutamine Targeting Prevails Over Glioblastoma Metabolic Plasticity. *Clin. Cancer Res. Off. J. Am. Assoc. Cancer Res.* *23*, 6292–6304.

- O'Rourke, D.M., Nasrallah, M.P., Desai, A., Melenhorst, J.J., Mansfield, K., Morrissette, J.J.D., Martinez-Lage, M., Brem, S., Maloney, E., Shen, A., et al. (2017). A single dose of peripherally infused EGFRvIII-directed CAR T cells mediates antigen loss and induces adaptive resistance in patients with recurrent glioblastoma. *Sci. Transl. Med.* *9*.
- Ostrom, Q.T., Gittleman, H., Liao, P., Vecchione-Koval, T., Wolinsky, Y., Kruchko, C., and Barnholtz-Sloan, J.S. (2017). CBTRUS Statistical Report: Primary brain and other central nervous system tumors diagnosed in the United States in 2010-2014. *Neuro-Oncol.* *19*, v1–v88.
- Pardoll, D.M. (2012). The blockade of immune checkpoints in cancer immunotherapy. *Nat. Rev. Cancer* *12*, 252–264.
- Parker, C.M., Groh, V., Band, H., Porcelli, S.A., Morita, C., Fabbi, M., Glass, D., Strominger, J.L., and Brenner, M.B. (1990). Evidence for extrathymic changes in the T cell receptor gamma/delta repertoire. *J. Exp. Med.* *171*, 1597–1612.
- Patin, E.C., Soulard, D., Fleury, S., Hassane, M., Dombrowicz, D., Faveeuw, C., Trottein, F., and Paget, C. (2018). Type I IFN Receptor Signaling Controls IL7-Dependent Accumulation and Activity of Protumoral IL17A-Producing $\gamma\delta$ T Cells in Breast Cancer. *Cancer Res.* *78*, 195–204.
- Pauza, C.D., and Cairo, C. (2015). Evolution and function of the TCR Vgamma9 chain repertoire: It's good to be public. *Cell. Immunol.* *296*, 22–30.
- Pauza, C.D., Liou, M.-L., Lahusen, T., Xiao, L., Lapidus, R.G., Cairo, C., and Li, H. (2018). Gamma Delta T Cell Therapy for Cancer: It Is Good to be Local. *Front. Immunol.* *9*, 1305.
- Pawelec, G., Barnett, Y., Mariani, E., and Solana, R. (2002). Human CD4+ T cell clone longevity in tissue culture: lack of influence of donor age or cell origin. *Exp. Gerontol.* *37*, 265–269.
- Pereira, P., and Boucontet, L. (2004). Rates of recombination and chain pair biases greatly influence the primary gammadelta TCR repertoire in the thymus of adult mice. *J. Immunol. Baltim. Md 1950* *173*, 3261–3270.
- Perrin, S. (2014). Preclinical research: Make mouse studies work. *Nature* *507*, 423–425.
- Pfeffer, K., Schoel, B., Plesnila, N., Lipford, G.B., Kromer, S., Deusch, K., and Wagner, H. (1992). A lectin-binding, protease-resistant mycobacterial ligand specifically activates V gamma 9+ human gamma delta T cells. *J. Immunol. Baltim. Md 1950* *148*, 575–583.
- Phillips, H.S., Kharbanda, S., Chen, R., Forrest, W.F., Soriano, R.H., Wu, T.D., Misra, A., Nigro, J.M., Colman, H., Soroceanu, L., et al. (2006). Molecular subclasses of high-grade glioma predict prognosis, delineate a pattern of disease progression, and resemble stages in neurogenesis. *Cancer Cell* *9*, 157–173.
- Pierpont, T.M., Limper, C.B., and Richards, K.L. (2018). Past, Present, and Future of Rituximab-The World's First Oncology Monoclonal Antibody Therapy. *Front. Oncol.* *8*, 163.
- Piperno-Neumann, S., Le Deley, M.-C., Rédini, F., Pacquement, H., Marec-Bérard, P., Petit, P., Brisse, H., Lervat, C., Gentet, J.-C., Entz-Werlé, N., et al. (2016). Zoledronate in combination with chemotherapy and surgery to treat osteosarcoma (OS2006): a randomised, multicentre, open-label, phase 3 trial. *Lancet Oncol.* *17*, 1070–1080.
- Poccia, F., Cipriani, B., Vendetti, S., Colizzi, V., Poquet, Y., Battistini, L., López-Botet, M., Fournié, J.J., and Gougeon, M.L. (1997). CD94/NKG2 inhibitory receptor complex modulates both anti-viral and anti-tumoral responses of polyclonal phosphoantigen-reactive V gamma 9V delta 2 T lymphocytes. *J. Immunol. Baltim. Md 1950* *159*, 6009–6017.

- Poccia, F., Agrati, C., Martini, F., Capobianchi, M.R., Wallace, M., and Malkovsky, M. (2005). Antiviral reactivities of gammadelta T cells. *Microbes Infect.* 7, 518–528.
- Pont, F., Familiades, J., Déjean, S., Fruchon, S., Cendron, D., Poupot, M., Poupot, R., L'faqihi-Olive, F., Prade, N., Ycart, B., et al. (2012). The gene expression profile of phosphoantigen-specific human $\gamma\delta$ T lymphocytes is a blend of $\alpha\beta$ T-cell and NK-cell signatures. *Eur. J. Immunol.* 42, 228–240.
- Pradeu, T., and Vivier, E. (2016). The discontinuity theory of immunity. *Sci. Immunol.* 1.
- Prat, J., and FIGO Committee on Gynecologic Oncology (2015). Abridged republication of FIGO's staging classification for cancer of the ovary, fallopian tube, and peritoneum. *Cancer* 121, 3452–3454.
- Qin, G., Mao, H., Zheng, J., Sia, S.F., Liu, Y., Chan, P.-L., Lam, K.-T., Peiris, J.S.M., Lau, Y.-L., and Tu, W. (2009). Phosphoantigen-expanded human gammadelta T cells display potent cytotoxicity against monocyte-derived macrophages infected with human and avian influenza viruses. *J. Infect. Dis.* 200, 858–865.
- Raulet, D.H., and Guerra, N. (2009). Oncogenic stress sensed by the immune system: role of natural killer cell receptors. *Nat. Rev. Immunol.* 9, 568–580.
- Reni, M., Mazza, E., Zanon, S., Gatta, G., and Vecht, C.J. (2017). Central nervous system gliomas. *Crit. Rev. Oncol. Hematol.* 113, 213–234.
- Rhodes, D.A., Chen, H.-C., Price, A.J., Keeble, A.H., Davey, M.S., James, L.C., Eberl, M., and Trowsdale, J. (2015). Activation of human $\gamma\delta$ T cells by cytosolic interactions of BTN3A1 with soluble phosphoantigens and the cytoskeletal adaptor periplakin. *J. Immunol. Baltim. Md* 1950 194, 2390–2398.
- Riaño, F., Karunakaran, M.M., Starick, L., Li, J., Scholz, C.J., Kunzmann, V., Olive, D., Amslinger, S., and Herrmann, T. (2014). V γ 9V δ 2 TCR-activation by phosphorylated antigens requires butyrophilin 3 A1 (BTN3A1) and additional genes on human chromosome 6. *Eur. J. Immunol.* 44, 2571–2576.
- Riganti, C., Massaia, M., Davey, M.S., and Eberl, M. (2012). Human $\gamma\delta$ T-cell responses in infection and immunotherapy: common mechanisms, common mediators? *Eur. J. Immunol.* 42, 1668–1676.
- Rizvi, N.A., Mazières, J., Planchard, D., Stinchcombe, T.E., Dy, G.K., Antonia, S.J., Horn, L., Lena, H., Minenza, E., Menecier, B., et al. (2015). Activity and safety of nivolumab, an anti-PD-1 immune checkpoint inhibitor, for patients with advanced, refractory squamous non-small-cell lung cancer (CheckMate 063): a phase 2, single-arm trial. *Lancet Oncol.* 16, 257–265.
- Rochman, Y., Spolski, R., and Leonard, W.J. (2009). New insights into the regulation of T cells by gamma(c) family cytokines. *Nat. Rev. Immunol.* 9, 480–490.
- Rock, E.P., Sibbald, P.R., Davis, M.M., and Chien, Y.H. (1994). CDR3 length in antigen-specific immune receptors. *J. Exp. Med.* 179, 323–328.
- Rosenberg, S.A., and Restifo, N.P. (2015). Adoptive cell transfer as personalized immunotherapy for human cancer. *Science* 348, 62–68.
- Rosenberg, S.A., Packard, B.S., Aebersold, P.M., Solomon, D., Topalian, S.L., Toy, S.T., Simon, P., Lotze, M.T., Yang, J.C., and Seipp, C.A. (1988). Use of tumor-infiltrating lymphocytes and interleukin-2 in the immunotherapy of patients with metastatic melanoma. A preliminary report. *N. Engl. J. Med.* 319, 1676–1680.

- Ryan, P.L., Sumaria, N., Holland, C.J., Bradford, C.M., Izotova, N., Grandjean, C.L., Jawad, A.S., Bergmeier, L.A., and Pennington, D.J. (2016). Heterogeneous yet stable V δ 2(+) T-cell profiles define distinct cytotoxic effector potentials in healthy human individuals. *Proc. Natl. Acad. Sci. U. S. A.* *113*, 14378–14383.
- Saito, H., Kranz, D.M., Takagaki, Y., Hayday, A.C., Eisen, H.N., and Tonegawa, S. (1984). Complete primary structure of a heterodimeric T-cell receptor deduced from cDNA sequences. *Nature* *309*, 757–762.
- Sallusto, F., and Lanzavecchia, A. (1994). Efficient presentation of soluble antigen by cultured human dendritic cells is maintained by granulocyte/macrophage colony-stimulating factor plus interleukin 4 and downregulated by tumor necrosis factor alpha. *J. Exp. Med.* *179*, 1109–1118.
- Salot, S., Laplace, C., Saïagh, S., Bercegeay, S., Tenaud, I., Cassidanius, A., Romagne, F., Dreno, B., and Tiollier, J. (2007). Large scale expansion of gamma 9 delta 2 T lymphocytes: Innacell gamma delta cell therapy product. *J. Immunol. Methods* *326*, 63–75.
- Sanders, J.M., Ghosh, S., Chan, J.M.W., Meints, G., Wang, H., Raker, A.M., Song, Y., Colantino, A., Burzynska, A., Kafarski, P., et al. (2004). Quantitative structure-activity relationships for gammadelta T cell activation by bisphosphonates. *J. Med. Chem.* *47*, 375–384.
- Santolaria, T., Robard, M., Léger, A., Catros, V., Bonneville, M., and Scotet, E. (2013). Repeated systemic administrations of both aminobisphosphonates and human V γ 9V δ 2 T cells efficiently control tumor development in vivo. *J. Immunol. Baltim. Md 1950* *191*, 1993–2000.
- Sato, E., Olson, S.H., Ahn, J., Bundy, B., Nishikawa, H., Qian, F., Jungbluth, A.A., Frosina, D., Gnjjatic, S., Ambrosone, C., et al. (2005). Intraepithelial CD8+ tumor-infiltrating lymphocytes and a high CD8+/regulatory T cell ratio are associated with favorable prognosis in ovarian cancer. *Proc. Natl. Acad. Sci. U. S. A.* *102*, 18538–18543.
- Scapini, P., and Cassatella, M.A. (2014). Social networking of human neutrophils within the immune system. *Blood* *124*, 710–719.
- Scheper, W., Sebestyen, Z., and Kuball, J. (2014). Cancer Immunotherapy Using $\gamma\delta$ T Cells: Dealing with Diversity. *Front. Immunol.* *5*, 601.
- Schiller, J.T., and Müller, M. (2015). Next generation prophylactic human papillomavirus vaccines. *Lancet Oncol.* *16*, e217-225.
- Schreiber, R.D., Old, L.J., and Smyth, M.J. (2011). Cancer immunoediting: integrating immunity's roles in cancer suppression and promotion. *Science* *331*, 1565–1570.
- Schucht, P., Beck, J., Abu-Isa, J., Anderegg, L., Murek, M., Seidel, K., Stieglitz, L., and Raabe, A. (2012). Gross total resection rates in contemporary glioblastoma surgery: results of an institutional protocol combining 5-aminolevulinic acid intraoperative fluorescence imaging and brain mapping. *Neurosurgery* *71*, 927-935; discussion 935-936.
- Scotet, E., Martinez, L.O., Grant, E., Barbaras, R., Jenö, P., Guiraud, M., Monsarrat, B., Saulquin, X., Maillat, S., Estève, J.-P., et al. (2005). Tumor recognition following Vgamma9Vdelta2 T cell receptor interactions with a surface F1-ATPase-related structure and apolipoprotein A-I. *Immunity* *22*, 71–80.
- Sebestyen, Z., Scheper, W., Vyborova, A., Gu, S., Rychnavska, Z., Schiffler, M., Cleven, A., Chéneau, C., van Noorden, M., Peigné, C.-M., et al. (2016). RhoB Mediates Phosphoantigen Recognition by V γ 9V δ 2 T Cell Receptor. *Cell Rep.* *15*, 1973–1985.

- Shankaran, V., Ikeda, H., Bruce, A.T., White, J.M., Swanson, P.E., Old, L.J., and Schreiber, R.D. (2001). IFN γ and lymphocytes prevent primary tumour development and shape tumour immunogenicity. *Nature* *410*, 1107–1111.
- Siegel, R.L., Miller, K.D., and Jemal, A. (2016). Cancer statistics, 2016. *CA. Cancer J. Clin.* *66*, 7–30.
- Silva-Santos, B., Serre, K., and Norell, H. (2015). $\gamma\delta$ T cells in cancer. *Nat. Rev. Immunol.* *15*, 683–691.
- Spencer, C.T., Abate, G., Sakala, I.G., Xia, M., Truscott, S.M., Eickhoff, C.S., Linn, R., Blazevic, A., Metkar, S.S., Peng, G., et al. (2013). Granzyme A produced by $\gamma(9)\delta(2)$ T cells induces human macrophages to inhibit growth of an intracellular pathogen. *PLoS Pathog.* *9*, e1003119.
- Straetemans, T., Kierkels, G.J.J., Doorn, R., Jansen, K., Heijhuurs, S., Dos Santos, J.M., van Muyden, A.D.D., Vie, H., Clemenceau, B., Raymakers, R., et al. (2018). GMP-Grade Manufacturing of T Cells Engineered to Express a Defined $\gamma\delta$ TCR. *Front. Immunol.* *9*, 1062.
- Stupp, R., Mason, W.P., van den Bent, M.J., Weller, M., Fisher, B., Taphoorn, M.J.B., Belanger, K., Brandes, A.A., Marosi, C., Bogdahn, U., et al. (2005). Radiotherapy plus concomitant and adjuvant temozolomide for glioblastoma. *N. Engl. J. Med.* *352*, 987–996.
- Sturm, E., Braakman, E., Fisch, P., Vreugdenhil, R.J., Sondel, P., and Bolhuis, R.L. (1990). Human V gamma 9-V delta 2 T cell receptor-gamma delta lymphocytes show specificity to Daudi Burkitt's lymphoma cells. *J. Immunol. Baltim. Md 1950* *145*, 3202–3208.
- Sturm, E., Bontrop, R.E., Vreugdenhil, R.J., Otting, N., and Bolhuis, R.L. (1992). T-cell receptor gamma/delta: comparison of gene configurations and function between humans and chimpanzees. *Immunogenetics* *36*, 294–301.
- Su, Z., Graybill, W.S., and Zhu, Y. (2013). Detection and monitoring of ovarian cancer. *Clin. Chim. Acta Int. J. Clin. Chem.* *415*, 341–345.
- Sugarbaker, P.H. (1995). Peritonectomy procedures. *Ann. Surg.* *221*, 29–42.
- Taal, W., Oosterkamp, H.M., Walenkamp, A.M.E., Dubbink, H.J., Beerepoot, L.V., Hanse, M.C.J., Buter, J., Honkoop, A.H., Boerman, D., de Vos, F.Y.F., et al. (2014). Single-agent bevacizumab or lomustine versus a combination of bevacizumab plus lomustine in patients with recurrent glioblastoma (BELOB trial): a randomised controlled phase 2 trial. *Lancet Oncol.* *15*, 943–953.
- Tanaka, Y., Morita, C.T., Tanaka, Y., Nieves, E., Brenner, M.B., and Bloom, B.R. (1995). Natural and synthetic non-peptide antigens recognized by human gamma delta T cells. *Nature* *375*, 155–158.
- Tangye, S.G., Ma, C.S., Brink, R., and Deenick, E.K. (2013). The good, the bad and the ugly - TFH cells in human health and disease. *Nat. Rev. Immunol.* *13*, 412–426.
- Thedre, A., Sabourin, C., Gertner, J., Devilder, M.-C., Allain-Maillet, S., Fournié, J.-J., Scotet, E., and Bonneville, M. (2007). Self/non-self discrimination by human gammadelta T cells: simple solutions for a complex issue? *Immunol. Rev.* *215*, 123–135.
- Thedre, A., Harly, C., Morice, A., Salot, S., Bonneville, M., and Scotet, E. (2009). IL-21-mediated potentiation of antitumor cytolytic and proinflammatory responses of human V gamma 9V delta 2 T cells for adoptive immunotherapy. *J. Immunol. Baltim. Md 1950* *182*, 3423–3431.
- Thompson, K., and Rogers, M.J. (2004). Statins prevent bisphosphonate-induced gamma,delta-T-cell proliferation and activation in vitro. *J. Bone Miner. Res. Off. J. Am. Soc. Bone Miner. Res.* *19*, 278–288.

- Thompson, K., Rojas-Navea, J., and Rogers, M.J. (2006). Alkylamines cause Vgamma9Vdelta2 T-cell activation and proliferation by inhibiting the mevalonate pathway. *Blood* *107*, 651–654.
- Thurnher, M., Nussbaumer, O., and Gruenbacher, G. (2012). Novel aspects of mevalonate pathway inhibitors as antitumor agents. *Clin. Cancer Res. Off. J. Am. Assoc. Cancer Res.* *18*, 3524–3531.
- Tivnan, A., Heilinger, T., Lavelle, E.C., and Prehn, J.H.M. (2017). Advances in immunotherapy for the treatment of glioblastoma. *J. Neurooncol.* *131*, 1–9.
- Todaro, M., Orlando, V., Cicero, G., Caccamo, N., Meraviglia, S., Stassi, G., and Dieli, F. (2013). Chemotherapy sensitizes colon cancer initiating cells to Vγ9Vδ2 T cell-mediated cytotoxicity. *PLoS One* *8*, e65145.
- Tokuyama, H., Hagi, T., Mattarollo, S.R., Morley, J., Wang, Q., So, H.-F., Fai-So, H., Moriyasu, F., Nieda, M., and Nicol, A.J. (2008). V gamma 9 V delta 2 T cell cytotoxicity against tumor cells is enhanced by monoclonal antibody drugs--rituximab and trastuzumab. *Int. J. Cancer* *122*, 2526–2534.
- Torre, L.A., Trabert, B., DeSantis, C.E., Miller, K.D., Samimi, G., Runowicz, C.D., Gaudet, M.M., Jemal, A., and Siegel, R.L. (2018). Ovarian cancer statistics, 2018. *CA. Cancer J. Clin.*
- Tribel, F., Lefranc, M.P., and Hercend, T. (1988). Further evidence for a sequentially ordered activation of T cell rearranging gamma genes during T lymphocyte differentiation. *Eur. J. Immunol.* *18*, 789–794.
- Trichet, V., Benezech, C., Dousset, C., Gesnel, M.-C., Bonneville, M., and Breathnach, R. (2006). Complex interplay of activating and inhibitory signals received by Vgamma9Vdelta2 T cells revealed by target cell beta2-microglobulin knockdown. *J. Immunol. Baltim. Md 1950* *177*, 6129–6136.
- Uldrich, A.P., Le Nours, J., Pellicci, D.G., Gherardin, N.A., McPherson, K.G., Lim, R.T., Patel, O., Beddoe, T., Gras, S., Rossjohn, J., et al. (2013). CD1d-lipid antigen recognition by the γδ TCR. *Nat. Immunol.* *14*, 1137–1145.
- Vantourout, P., and Hayday, A. (2013). Six-of-the-best: unique contributions of γδ T cells to immunology. *Nat. Rev. Immunol.* *13*, 88–100.
- Vavassori, S., Kumar, A., Wan, G.S., Ramanjaneyulu, G.S., Cavallari, M., El Daker, S., Beddoe, T., Theodossis, A., Williams, N.K., Gostick, E., et al. (2013). Butyrophilin 3A1 binds phosphorylated antigens and stimulates human γδ T cells. *Nat. Immunol.* *14*, 908–916.
- Velcheti, V., and Schalper, K. (2016). Basic Overview of Current Immunotherapy Approaches in Cancer. *Am. Soc. Clin. Oncol. Educ. Book Am. Soc. Clin. Oncol. Meet.* *35*, 298–308.
- Verhaak, R.G.W., Hoadley, K.A., Purdom, E., Wang, V., Qi, Y., Wilkerson, M.D., Miller, C.R., Ding, L., Golub, T., Mesirov, J.P., et al. (2010). Integrated genomic analysis identifies clinically relevant subtypes of glioblastoma characterized by abnormalities in PDGFRA, IDH1, EGFR, and NF1. *Cancer Cell* *17*, 98–110.
- Vermijlen, D., Ellis, P., Langford, C., Klein, A., Engel, R., Willimann, K., Jomaa, H., Hayday, A.C., and Eberl, M. (2007). Distinct cytokine-driven responses of activated blood gammadelta T cells: insights into unconventional T cell pleiotropy. *J. Immunol. Baltim. Md 1950* *178*, 4304–4314.
- Vermijlen, D., Gatti, D., Kouzeli, A., Rus, T., and Eberl, M. (2018). γδ T cell responses: How many ligands will it take till we know? *Semin. Cell Dev. Biol.*
- Viey, E., Fromont, G., Escudier, B., Morel, Y., Da Rocha, S., Chouaib, S., and Caignard, A. (2005). Phosphostim-activated gamma delta T cells kill autologous metastatic renal cell carcinoma. *J. Immunol. Baltim. Md 1950* *174*, 1338–1347.

- Vinuesa, C.G., Tangye, S.G., Moser, B., and Mackay, C.R. (2005). Follicular B helper T cells in antibody responses and autoimmunity. *Nat. Rev. Immunol.* 5, 853–865.
- Vivien, R., Saïagh, S., Lemarre, P., Chabaud, V., Jesson, B., Godon, C., Jarry, U., Guillaume, T., Chevallier, P., Vié, H., et al. (2018). The doubling potential of T lymphocytes allows clinical-grade production of a bank of genetically modified monoclonal T-cell populations. *Cytotherapy* 20, 436–452.
- Wada, I., Matsushita, H., Noji, S., Mori, K., Yamashita, H., Nomura, S., Shimizu, N., Seto, Y., and Kakimi, K. (2014). Intraperitoneal injection of in vitro expanded V γ 9V δ 2 T cells together with zoledronate for the treatment of malignant ascites due to gastric cancer. *Cancer Med.* 3, 362–375.
- Walczak, H., and Krammer, P.H. (2000). The CD95 (APO-1/Fas) and the TRAIL (APO-2L) apoptosis systems. *Exp. Cell Res.* 256, 58–66.
- Wang, P., and Malkovsky, M. (2000). Different roles of the CD2 and LFA-1 T-cell co-receptors for regulating cytotoxic, proliferative, and cytokine responses of human V gamma 9/V delta 2 T cells. *Mol. Med. Camb. Mass* 6, 196–207.
- Wege, A.K. (2018). Humanized Mouse Models for the Preclinical Assessment of Cancer Immunotherapy. *BioDrugs Clin. Immunother. Biopharm. Gene Ther.* 32, 245–266.
- Weiss, H.M., Pfaar, U., Schweitzer, A., Wiegand, H., Skerjanec, A., and Schran, H. (2008). Biodistribution and plasma protein binding of zoledronic acid. *Drug Metab. Dispos. Biol. Fate Chem.* 36, 2043–2049.
- Wellington, K., and Goa, K.L. (2003). Zoledronic acid: a review of its use in the management of bone metastases and hypercalcaemia of malignancy. *Drugs* 63, 417–437.
- Werter, I.M., Schneiders, F.L., Scotet, E., Verheul, H.M.W., de Gruijl, T.D., and van der Vliet, H.J. (2014). V γ 9V δ 2-T cells as antigen presenting cells for iNKT cell based cancer immunotherapy. *Oncoimmunology* 3, e955343.
- Wesch, D., Glatzel, A., and Kabelitz, D. (2001). Differentiation of resting human peripheral blood gamma delta T cells toward Th1- or Th2-phenotype. *Cell. Immunol.* 212, 110–117.
- Wesch, D., Peters, C., Oberg, H.-H., Pietschmann, K., and Kabelitz, D. (2011). Modulation of $\gamma\delta$ T cell responses by TLR ligands. *Cell. Mol. Life Sci. CMLS* 68, 2357–2370.
- Wesch, D., Peters, C., and Siegers, G.M. (2014). Human gamma delta T regulatory cells in cancer: fact or fiction? *Front. Immunol.* 5, 598.
- Wiemer, D.F., and Wiemer, A.J. (2014). Opportunities and challenges in development of phosphoantigens as V γ 9V δ 2 T cell agonists. *Biochem. Pharmacol.* 89, 301–312.
- Wilhelm, M., Kunzmann, V., Eckstein, S., Reimer, P., Weissinger, F., Ruediger, T., and Tony, H.-P. (2003). Gammadelta T cells for immune therapy of patients with lymphoid malignancies. *Blood* 102, 200–206.
- Wilhelm, M., Smetak, M., Schaefer-Eckart, K., Kimmel, B., Birkmann, J., Einsele, H., and Kunzmann, V. (2014). Successful adoptive transfer and in vivo expansion of haploidentical $\gamma\delta$ T cells. *J. Transl. Med.* 12, 45.
- Wu, P., Wu, D., Ni, C., Ye, J., Chen, W., Hu, G., Wang, Z., Wang, C., Zhang, Z., Xia, W., et al. (2014). $\gamma\delta$ T17 cells promote the accumulation and expansion of myeloid-derived suppressor cells in human colorectal cancer. *Immunity* 40, 785–800.

Wu, Y., Wu, W., Wong, W.M., Ward, E., Thrasher, A.J., Goldblatt, D., Osman, M., Digard, P., Canaday, D.H., and Gustafsson, K. (2009). Human gamma delta T cells: a lymphoid lineage cell capable of professional phagocytosis. *J. Immunol. Baltim. Md 1950* 183, 5622–5629.

Xu, B., Pizarro, J.C., Holmes, M.A., McBeth, C., Groh, V., Spies, T., and Strong, R.K. (2011). Crystal structure of a gammadelta T-cell receptor specific for the human MHC class I homolog MICA. *Proc. Natl. Acad. Sci. U. S. A.* 108, 2414–2419.

Yi, Y., He, H.-W., Wang, J.-X., Cai, X.-Y., Li, Y.-W., Zhou, J., Cheng, Y.-F., Jin, J.-J., Fan, J., and Qiu, S.-J. (2013). The functional impairment of HCC-infiltrating $\gamma\delta$ T cells, partially mediated by regulatory T cells in a TGF β - and IL-10-dependent manner. *J. Hepatol.* 58, 977–983.

Yuasa, T., Sato, K., Ashihara, E., Takeuchi, M., Maita, S., Tsuchiya, N., Habuchi, T., Maekawa, T., and Kimura, S. (2009). Intravesical administration of gammadelta T cells successfully prevents the growth of bladder cancer in the murine model. *Cancer Immunol. Immunother. CII* 58, 493–502.

Zhao, Y., Niu, C., and Cui, J. (2018). Gamma-delta ($\gamma\delta$) T cells: friend or foe in cancer development? *J. Transl. Med.* 16, 3.

Zheng, B.J., Chan, K.W., Im, S., Chua, D., Sham, J.S., Tin, P.C., He, Z.M., and Ng, M.H. (2001). Anti-tumor effects of human peripheral gammadelta T cells in a mouse tumor model. *Int. J. Cancer* 92, 421–425.

Zimmer, L., Goldinger, S.M., Hofmann, L., Loquai, C., Ugurel, S., Thomas, I., Schmidgen, M.I., Gutzmer, R., Utikal, J.S., Göppner, D., et al. (2016). Neurological, respiratory, musculoskeletal, cardiac and ocular side-effects of anti-PD-1 therapy. *Eur. J. Cancer Oxf. Engl.* 1990 60, 210–225.

Zou, C., Zhao, P., Xiao, Z., Han, X., Fu, F., and Fu, L. (2017). $\gamma\delta$ T cells in cancer immunotherapy. *Oncotarget* 8, 8900–8909.

Site Internet :

D'après <http://www.drmulier.com/2%20fr%20pat%20info%20ovarium.html>

E. ANNEXES

Listes des publications

2016 : Ulrich Jarry, Cynthia Chauvin, Noémie Joalland, Alexandra Léger, Sandrine Minault, Myriam Robard, Marc Bonneville, Lisa Oliver, François M. Vallette, Henri Vié, Claire Pecqueur & Emmanuel Scotet, **Stereotaxic administrations of allogeneic human V γ 9V δ 2 T cells efficiently control the development of human glioblastoma brain tumors**, Oncoimmunology, DOI : 10.1080/2162402X.2016.1168554

2017 : Hung-Chang Chen, Noémie Joalland, John S Bridgeman, Fouad S Alchami, Ulrich Jarry, Mohd Wajid A Khan, Luke Piggott, Yasmin Shanneik, Jianqiang Li, Marco J Herold, Thomas Herrmann, David A Price, Awen M Gallimore, Richard W Clarkson, Emmanuel Scotet, Bernhard Moser & Matthias Eberl, **Synergistic targeting of breast cancer stem-like cells by human $\gamma\delta$ T cells and CD8+ T cells**, Immunology and Cell Biology, DOI : 10.1038/icb.2017.21.

2018 : Noémie Joalland, Cynthia Chauvin, Lisa Oliver, François M. Vallette, Claire Pecqueur, Ulrich Jarry, & Emmanuel Scotet, **IL-21 Increases the Reactivity of Allogeneic Human V γ 9V δ 2 T Cells Against Primary Glioblastoma Tumors**, Journal of Immunotherapy, DOI : 10.1097/CJI.0000000000000225.

2018 : Ulrich Jarry, Noémie Joalland (co-first author), Cynthia Chauvin, Béatrice Clemenceau, Claire Pecqueur & Emmanuel Scotet, **Stereotactic Adoptive Transfer of Cytotoxic Immune Cells in Murine Models of Orthotopic Human Glioblastoma Multifforme Xenografts**, Journal Of Visualized Experiments, DOI : 10.3791/57870.

Soumis : Kristell Oizel, Chendong Yang, Ophelie Renoult, Quyen N. Do, Noémie Joalland, Xiaofei Gao, Bookyung Ko, François Vallette, Woo-Ping Ge, Ralph J Deberardinis, Claire Pecqueur, **Glutamine uptake and utilization of human mesenchymal Glioblastoma in orthotopic mouse model.**

Soumis : Marion Rabé, Solenne Dumont, Arturo Álvarez-Arenas Alcamí, Hicham Janati, Juan Belmonte-Beitia, Gabriel F. Calvo, Christelle Thibault-Charpentier, Quentin Séry, Cynthia Chauvin, Noémie Joalland, Floriane Briand, Emmanuel Scotet, Claire Pecqueur, Jean Clairambault, Lisa Oliver, Arulraj Nadaradjane, Victor Perez-Garcia, Pierre François Cartron, Catherine Gratas, François M. Vallette, **A transient population precedes and supports the acquisition of temozolomide resistance in human glioblastoma.**

Soumis : Noémie Joalland, Laura Lafrance, Thibault Oullier, Séverine Marionneau-Lambot, Delphine Loussouarn, Ulrich Jarry & Emmanuel Scotet, **Combined chemotherapy and allogeneic human V γ 9V δ 2 T lymphocyte-immunotherapies efficiently control the development of human epithelial ovarian cancer cells *in vivo*.**

En préparation : Cynthia Chauvin, Noémie Joalland (co-first author), Ulrich Jarry, Laura Lafrance, Jeanne Perroteau, Catherine Willem, Christelle Retière, Catherine Gratas, Xavier Saulquin, François M. Vallette, Henri Vié, Emmanuel Scotet & Claire Pecqueur, **Allogeneic human V γ 9V δ 2 T cells naturally recognize and eliminate mesenchymal primary glioblastoma cells through NKG2D and BTN3 pathways.**

En préparation : Charlotte Degorre, Ophélie Renoult, Charbel Touma, Manon Pietri, Noémie Joalland, Natacha Galopin, Catherine Gratas, François Vallette, Claire Pecqueur and François Paris, **Senescent endothelial cells increase the bellicosity of GBM cells surviving from radiation therapy through secretion of CXCL5/8.**

Article 6 : Synergistic targeting of breast cancer stem-like cells by human $\gamma\delta$ T cells and CD8⁺ T cells

Hung-Chang Chen^{1,10}, Noémie Joalland^{2,3}, John S Bridgeman^{1,11}, Fouad S Alchami⁴, Ulrich Jarry^{2,3}, Mohd Wajid A Khan¹, Luke Piggott^{1,5}, Yasmin Shanneik¹, Jianqiang Li⁶, Marco J Herold^{6,7}, Thomas Herrmann⁶, David A Price^{1,8}, Awen M Gallimore^{1,8}, Richard W Clarkson^{5,9}, Emmanuel Scotet^{2,3}, Bernhard Moser^{1,8} and Matthias Eberl^{1,8}

¹Division of Infection and Immunity, School of Medicine, Cardiff University, Cardiff, UK ; ²INSERM, Unité Mixte de Recherche 892, Centre de Recherche en Cancérologie Nantes Angers, Institut de Recherche en Santé de l'Université de Nantes, Nantes, France ; ³Centre National de la Recherche Scientifique (CNRS), Unité Mixte de Recherche 6299, Nantes, France ; ⁴Cardiff and Vale University Health Board, University Hospital of Wales, Cardiff, UK ; ⁵School of Biosciences, Cardiff University, Cardiff, UK ; ⁶Institute for Virology and Immunobiology, Julius-Maximilians-Universität Würzburg, Würzburg, Germany ; ⁷Walter and Eliza Hall Institute of Medical Research, Parkville, Victoria, Australia ; ⁸Systems Immunity Research Institute, Cardiff University, Cardiff, UK and ⁹European Cancer Stem Cell Research Institute, Cardiff University, Cardiff, UK.

¹⁰Current address: Cancer Research UK Cambridge Institute, University of Cambridge, Li Ka Shing Centre, Cambridge CB20RE, UK. ¹¹Current address: Cellular Therapeutics Ltd, Manchester M139XX, UK.

La résistance aux thérapies standard inhérente aux cellules souches cancéreuses (CSC) présentes au sein des tumeurs malignes est largement impliquée dans l'inefficacité des traitements actuels. Dans cette étude, nous avons mis en place un modèle expérimental nous permettant d'évaluer une nouvelle stratégie d'immunothérapie ciblant ces CSC et reposant sur l'interaction entre les LT V γ 9V δ 2 et des LT CD8⁺ spécifique d'un antigène tumoral. Ce modèle repose sur l'utilisation de deux types cellulaires, CSC et non-CSC, dérivant de cellules tumorales humaines de cancer mammaire. Ainsi, une lignée stable de CSC a été établie et caractérisée pour : (i) l'expression des marqueurs CD44^{hi} CD24^{lo} GD2⁺, (ii) sa capacité à former des mammosphères dans des conditions de culture non-adhérentes et (iii) son potentiel tumorigène, d'auto-renouveau et de différenciation dans un modèle murin de xénogreffe. Bien que ces CSC ne soient pas naturellement reconnues par des LT V γ 9V δ 2, une sensibilisation au Zolédronate permet de lever cette résistance. De plus, les LT V γ 9V δ 2 induisent, par leur sécrétion d'IFN- γ , une augmentation de l'expression des molécules du CMH de classe I, ce qui facilite la reconnaissance et l'élimination de ces CSC par des LT $\alpha\beta$ CD8⁺ spécifique de l'antigène pp65 du CMV. Nos résultats mettent en avant un synergisme entre des LT restreints ou non-restreints aux molécules du CMH pour l'éradication des CSC du cancer du sein.

Publié dans Immunology and Cell Biology, 2017

ORIGINAL ARTICLE

Synergistic targeting of breast cancer stem-like cells by human $\gamma\delta$ T cells and CD8⁺ T cells

Hung-Chang Chen^{1,10}, Noémie Joalland^{2,3}, John S Bridgeman^{1,11}, Fouad S Alchami⁴, Ulrich Jarry^{2,3}, Mohd Wajid A Khan¹, Luke Piggott^{1,5}, Yasmin Shanneik¹, Jianqiang Li⁶, Marco J Herold^{6,7}, Thomas Herrmann⁶, David A Price^{1,8}, Awen M Gallimore^{1,8}, Richard W Clarkson^{5,9}, Emmanuel Scotet^{2,3}, Bernhard Moser^{1,8} and Matthias Eberl^{1,8}

The inherent resistance of cancer stem cells (CSCs) to existing therapies has largely hampered the development of effective treatments for advanced malignancy. To help develop novel immunotherapy approaches that efficiently target CSCs, an experimental model allowing reliable distinction of CSCs and non-CSCs was set up to study their interaction with non-MHC-restricted $\gamma\delta$ T cells and antigen-specific CD8⁺ T cells. Stable lines with characteristics of breast CSC-like cells were generated from *ras*-transformed human mammary epithelial (HMLER) cells as confirmed by their CD44^{hi} CD24^{lo} GD2⁺ phenotype, their mesenchymal morphology in culture and their capacity to form mammospheres under non-adherent conditions, as well as their potent tumorigenicity, self-renewal and differentiation in xenografted mice. The resistance of CSC-like cells to $\gamma\delta$ T cells could be overcome by inhibition of farnesyl pyrophosphate synthase (FPPS) through pretreatment with zoledronate or with FPPS-targeting short hairpin RNA. $\gamma\delta$ T cells induced upregulation of MHC class I and CD54/ICAM-1 on CSC-like cells and thereby increased the susceptibility to antigen-specific killing by CD8⁺ T cells. Alternatively, $\gamma\delta$ T-cell responses could be specifically directed against CSC-like cells using the humanised anti-GD2 monoclonal antibody hu14.18K322A. Our findings identify a powerful synergism between MHC-restricted and non-MHC-restricted T cells in the eradication of cancer cells including breast CSCs. Our research suggests that novel immunotherapies may benefit from a two-pronged approach combining $\gamma\delta$ T-cell and CD8⁺ T-cell targeting strategies that triggers effective innate-like and tumour-specific adaptive responses.

Immunology and Cell Biology (2017) 95, 620–629; doi:10.1038/icb.2017.21

Cancer stem cells (CSCs) are the principal cause of disease recurrence, distant metastasis, and eventually morbidity and mortality in patients with different malignancies, including breast cancer.¹ The inherent resistance of CSCs to existing therapies has largely hampered the development of effective treatments for patients with advanced disease, and there is a paucity of studies aiming at directly targeting the CSC pool.² While CSCs are very rare cells and challenging to work with, in particular in humans, progress has been made by linking the cellular epithelial-to-mesenchymal transition (EMT) programme to the generation of CSC-like cells, especially in breast cancer.³ In this respect, immortalised human mammary epithelial cells undergoing EMT acquire CSC properties, as judged by their CD44^{hi} CD24^{lo} phenotype, their ability to form mammospheres and their tumour initiation potential.^{3–5}

Immunotherapy offers novel and potentially effective routes to treating cancer, and progress has been made with regard to

adoptively transferring expanded or genetically engineered T cells back into patients.^{6,7} However, the safety and efficacy of CD8⁺ T-cell-based therapies depend on whether the corresponding target antigens are exclusively expressed by tumour cells and not by healthy tissues, and whether they are recognised by the T-cell receptor (TCR) with sufficient affinity. Most importantly, the MHC restriction of tumour-specific epitopes limits the potential benefit of cytotoxic CD8⁺ T cells to patients with appropriate MHC haplotypes.⁸ Alternative immunotherapies are therefore being sought that exploit non-MHC-restricted, ‘unconventional’ T cells that recognise stress-induced changes in transformed cells.^{9–12} In this context, human V γ 9/V δ 2 T cells have been shown to kill CSC-like tumour initiating cells derived from colon cancer,¹³ ovarian cancer¹⁴ and neuroblastoma,¹⁵ especially upon sensitisation of tumour cells by aminobisphosphonates such as zoledronate.

¹Division of Infection and Immunity, School of Medicine, Cardiff University, Cardiff, UK; ²INSERM, Unité Mixte de Recherche 892, Centre de Recherche en Cancérologie Nantes Angers, Institut de Recherche en Santé de l’Université de Nantes, Nantes, France; ³Centre National de la Recherche Scientifique (CNRS), Unité Mixte de Recherche 6299, Nantes, France; ⁴Cardiff and Vale University Health Board, University Hospital of Wales, Cardiff, UK; ⁵School of Biosciences, Cardiff University, Cardiff, UK; ⁶Institute for Virology and Immunobiology, Julius-Maximilians-Universität Würzburg, Würzburg, Germany; ⁷Walter and Eliza Hall Institute of Medical Research, Parkville, Victoria, Australia; ⁸Systems Immunity Research Institute, Cardiff University, Cardiff, UK and ⁹European Cancer Stem Cell Research Institute, Cardiff University, Cardiff, UK

¹⁰Current address: Cancer Research UK Cambridge Institute, University of Cambridge, Li Ka Shing Centre, Cambridge CB2 0RE, UK.

¹¹Current address: Cellular Therapeutics Ltd, Manchester M13 9XX, UK.

Correspondence: Dr M Eberl, Division of Infection and Immunity, School of Medicine, Cardiff University, Henry Wellcome Building, Heath Park, Cardiff CF14 4XN, UK.
E-mail: eberlm@cf.ac.uk

Received 26 February 2017; revised 17 March 2017; accepted 24 March 2017; accepted article preview online 30 March 2017; advance online publication, 9 May 2017

To establish novel immunotherapy approaches that efficiently target CSCs, we here utilised transformed cell lines with CSC-like properties as experimental model for primary breast CSCs, and well-characterised T-cell epitopes as surrogates for yet-to-be-discovered CSC-associated antigens. We demonstrate that the CSC-like cells established in this study are relatively resistant to killing both by antigen-specific CD8⁺ T cell and by V γ 9/V δ 2 T cells. However, the resistance of CSC-like cells to $\gamma\delta$ T cells could readily be overcome by inhibition of farnesyl pyrophosphate synthase (FPPS) through pretreatment with zoledronate or with FPPS-targeting short hairpin RNA,¹⁶ or by opsonisation with the GD2-specific monoclonal antibody hu14.18K322A.¹⁷ Most importantly, $\gamma\delta$ T cells induced upregulation of MHC class I and CD54 on CSC-like cells via secretion of interferon gamma (IFN- γ), and thereby increased the susceptibility to antigen-specific killing by CD8⁺ T cells.

RESULTS

Phenotypical characterisation of HMLER-derived CSC-like cells

We first sought to establish a well-defined cellular model that allows a reliable distinction of CSC-like cells and non-CSCs based on phenotypical, morphological and functional criteria. Immortalised human mammary epithelial cells transformed by overexpression of human telomerase reverse transcriptase, SV40 large T antigen and oncogenic *ras* (referred to as HMLER cells)¹⁸ showed a predominant CD44^{lo} CD24^{hi} phenotype under adherent culture conditions, yet contained a distinct and stable population of CD44^{hi} CD24^{lo} cells that comprised 0.4–2% of all cells (Figure 1a).³ This minor population of putative CSC-like cells could be enriched to >20% of the total population in primary mammosphere cultures, and to >70% in secondary mammosphere cultures (Figures 1a and b), due to drastically reduced survival of CD44^{lo} CD24^{hi} non-CSCs (Figure 1c). At the same time, only CD44^{hi} CD24^{lo} CSC-like cells divided under non-adherent conditions as evidenced by dilution of membrane dyes (Figure 1d). As expected,^{4,19} antibodies against the ganglioside GD2 stained a proportion of CSC-like cells but not non-CSCs (Figure 1e).

Next, we sorted CD44^{hi} CD24^{lo} CSC-like cells and CD44^{lo} CD24^{hi} non-CSCs from parental HMLER cells to purities >99.5% (Supplementary Figure S1). In complete medium, both cell lines maintained their characteristic phenotype over a period of up to 32 days in adherent culture (Figure 1f, Supplementary Figure S1). Morphologically, non-CSCs displayed an epithelial growth pattern, whereas CSC-like cells had a mesenchymal appearance (Figure 1f), in accordance with the proposed acquisition of CSC properties by cells undergoing EMT.³ CSC-like cells stained positively for the mesenchymal markers vimentin and (albeit less prominently) fibronectin extra domain A, whereas only a minor fraction of epithelial-like non-CSCs expressed these markers (Figure 1g). Moreover, CSC-like cells showed no expression of cytokeratin-14 (CK-14) as epithelial marker for the basal/myoepithelial lineage and only intermediate levels of the luminal lineage marker CK-18, as opposed to non-CSCs (Figure 1g). In summary, the phenotype and morphology of CD44^{lo} CD24^{hi} non-CSCs was consistent with epithelial characteristics, while CD44^{hi} CD24^{lo} CSC-like cells showed signs of an incomplete EMT with predominantly mesenchymal characteristics.

Functional characterisation of HMLER-derived CSC-like cells

In support of their CSC-like phenotype, CD44^{hi} CD24^{lo} cells had a far greater potential to self-renew and form mammospheres than their non-CSC counterparts that formed only very small aggregates (Figure 2a). Moreover, only CSC-like cells but not non-CSCs survived and proliferated under such anchorage-independent culture

conditions (Figure 2b). This functional difference was particularly apparent in secondary mammosphere cultures, after dissociation and re-seeding of primary aggregates (Figures 2a and b). The distinct mammosphere-forming abilities of sorted CSC-like cells and non-CSCs replicated both quantitatively and qualitatively the characteristics of the CD44^{hi} CD24^{lo} and CD44^{lo} CD24^{hi} subpopulations, respectively, within the parental HMLER line.

We next determined the tumour take and tumour growth rates of sorted CSC-like cells and non-CSCs in a xenograft model using immunodeficient NOD *scid* gamma (NSG) mice. To this end, we transduced CSC-like cells and non-CSCs with lentiviral vectors that conferred co-expression of the red fluorescent protein tdTomato to allow non-invasive tumour imaging, and of influenza virus matrix protein M1 (FluM1) as surrogate tumour-specific antigen (Supplementary Figure S2). Lentivirally transduced CSC-like cells and non-CSCs were indistinguishable from the corresponding parental cell lines with respect to phenotype, morphology and long-term stability in culture (data not shown). Upon injection into NSG mice, CD44^{hi} CD24^{lo} CSC-like cells showed a striking potential to form tumours in 100% of treated animals, at numbers as low as 1×10^3 CSC-like cells per mouse, as evidenced by *in vivo* imaging of tdTomato fluorescence as well as caliper measurements of palpable tumours (Figure 2c, Supplementary Figure S3). In contrast, CD44^{lo} CD24^{hi} non-CSCs exhibited very poor tumorigenicity with only 1/6 mice developing a sizeable tumour, with much slower growth rate, after receiving 2×10^6 non-CSCs. Fluorescence imaging revealed tumour cells in the lung and draining lymph nodes, but not in non-draining nodes, spleen or liver, of several mice receiving CSC-like cells. No metastasis was observed in mice injected with non-CSCs (Figure 2c).

Finally, we examined the plasticity and differentiation of CSC-like and non-CSCs. In adherent cultures with mammosphere medium, CD44^{hi} CD24^{lo} CSC-like cells expanded and gave rise to CD44^{lo} CD24^{hi} cells with epithelial-like morphology, whereas CD44^{lo} CD24^{hi} non-CSCs failed to survive under such culture conditions (Figure 1f). Tumours derived from CSC-like cells exhibited a capacity to differentiate (Figure 2d), especially after prolonged periods of tumour development (Supplementary Tables S1 and S2). In contrast, tumours derived from non-CSCs showed no signs of differentiation or enrichment of contaminant CSC-like cells (Figure 2d). Histologically, 7/11 tumours arising from CSC-like cells were intimately associated with native mouse mammary ducts, cuffing the vessels with areas of necrosis distal to the vessels. The majority of such tumours showed at least moderate levels of epithelioid differentiation as confirmed by their expression of pan-cytokeratin (AE1/AE3) (Figure 2e); lung metastases showed predominant epithelioid differentiation with no residual features of CSC-like cells (data not shown). However, tumours derived from CSC-like cells uniformly stained for vimentin (Figure 2e), indicative of an only partial reverse EMT process during tumour development *in vivo*. No adenocarcinoma differentiation was identified morphologically, as judged by the absence of carcinoma embryonic antigen expression (Supplementary Table S2).

In summary, HMLER-derived CD44^{hi} CD24^{lo} cells could be maintained stably in culture and manipulated by lentiviral transduction, while displaying phenotypical, morphological and functional features *in vitro* and *in vivo* that are typically associated with breast CSCs. We conclude that such CSC-like cells may represent a powerful experimental model system for the targeting of CSCs, especially CSC subpopulations with EMT-like characteristics, by human immune cells.

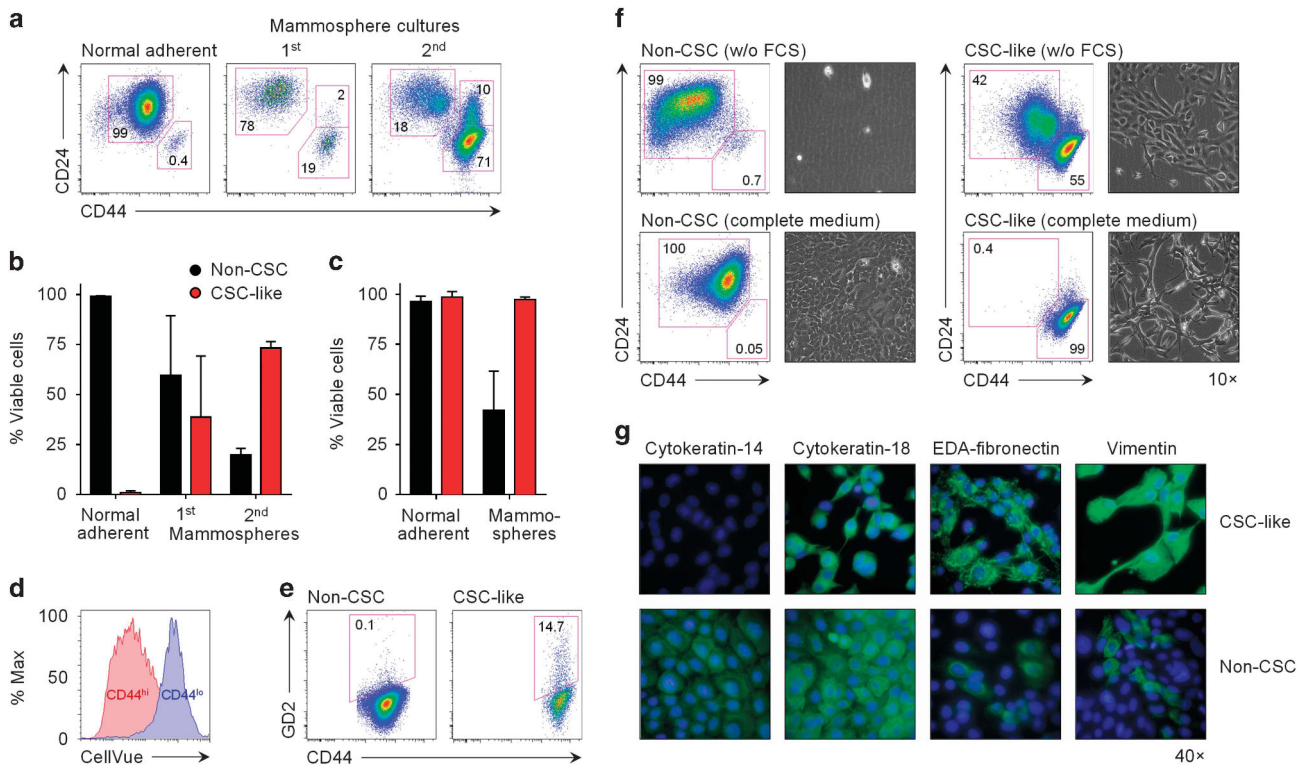


Figure 1 Phenotypical characterisation of HMLER-derived non-CSC and CSC-like cells. (a, b) Enrichment of CSC-like HMLER cells under mammosphere-forming conditions. HMLER cells from normal adherent cultures or from primary or secondary mammosphere cultures were examined for the proportion of CD44^{hi} CD24^{lo} (CSC-like) cells and CD44^{lo} CD24^{hi} (non-CSC) cells. Gates were set sequentially on intact, single and live cells. Representative fluorescence-activated cell sorting (FACS) plots are shown in (a), means \pm s.d. from three independent cultures in (b). (c) Differential viability of CSC-like cells and non-CSCs depending on the culture conditions, as assessed by live/dead staining of HMLER cells and gating on intact and single cells. Data shown are means \pm s.d. from four independent experiments. (d) Proliferation of CD44^{hi} cells but not of CD44^{lo} cells in mammosphere cultures of HMLER cells, as assessed by dilution of CellVue labelling (representative of two independent experiments). (e) GD2 expression by HMLER cells in normal adherent cultures, gated on CD44^{hi} CD24^{lo} CSC-like cells and CD44^{lo} CD24^{hi} non-CSCs within the parental cell line. FACS plots shown are representative of three independent experiments. (f) Stability of CSC-like cells and non-CSCs depending on the culture conditions. FACS-sorted CD44^{hi} CD24^{lo} and CD44^{lo} CD24^{hi} cells were cultured for 14 days in serum-free or complete medium, and examined by flow cytometry and light microscopy. Images shown are representative of two independent experiments. (g) Expression of epithelial (cytokeratin-14, cytokeratin-18) and mesenchymal markers (EDA-fibronectin, vimentin) by sorted CSC-like cells and non-CSCs seeded on cover-slip chamber slides and labelled with purified antibodies. AF488-conjugated secondary antibodies were used to visualise stained cells by fluorescence microscopy. Representative images shown were collected from two independent experiments. FCS, foetal calf serum.

MHC-restricted killing of CSC-like cells by antigen-specific CD8⁺ T cells

CSCs are intrinsically resistant to radiation and chemotherapy, and exploit a number of immune evasion strategies.^{2,20} To address the recognition of HMLER-derived CSC-like cells and non-CSCs by human T cells, we utilised well-characterised peptides that served as surrogate antigens, namely the immunodominant epitopes of FluM1, p58-66 (GILGFVFTL), and of the human cytomegalovirus (CMV) lower matrix phosphoprotein UL83/pp65, p495-503 (NLVPMVATV). Tumour cells pulsed with FluM1 p58-66 peptides were readily targeted by FluM1-specific CD8⁺ T cells, but not by pp65-specific CD8⁺ T cells as control (Supplementary Figure S4). Similarly, tumour cells pulsed with CMV pp65 p495-503 peptides were only lysed by pp65-specific CD8⁺ T cells but not by FluM1-specific CD8⁺ T cells, demonstrating the specificity of the experimental system. Of note, while epitope-specific CD8⁺ T cells were able to kill both CSC-like cells and non-CSCs when pulsed with the cognate peptides, CSC-like cells were significantly more resistant to killing (Supplementary Figure S4).

Next, we translated these observations to lentivirally transduced target cells that expressed endogenous FluM1. As expected, FluM1⁺ CSC-like cells and FluM1⁺ non-CSCs were both killed by FluM1-specific CD8⁺ T cells. However, CSC-like cells were killed less

efficiently than their non-CSC counterparts (Figure 3a). Many tumour cells evade the immune system by downmodulating MHC molecules and other proteins involved in antigen presentation and target cell recognition.²⁰ Indeed, HMLER-derived CSC-like cells expressed lower levels of MHC class I and of CD54 (ICAM-1) on the cell surface than non-CSCs (Figure 3b), thereby possibly explaining their relative resistance to CD8⁺ T-cell-mediated killing. Recombinant IFN- γ readily stimulated upregulation of MHC class I and CD54 expression on CSC-like cells (Figure 3c), which in turn led to a significantly improved susceptibility to CD8⁺ T-cell-mediated cytotoxicity (Figure 3d). A similar sensitisation to CD8⁺ T-cell-mediated killing by IFN- γ was observed for non-CSCs (data not shown). These findings demonstrate that IFN- γ effectively sensitises CSC-like cells to killing by tumour antigen-specific T cells.

Non-MHC-restricted killing of CSCs by innate-like $\gamma\delta$ T cells

The dependence of effective tumour cell killing on exogenously provided IFN- γ prompted investigations into the role of $\gamma\delta$ T cells, which represent a major and early source of pro-inflammatory cytokines upon activation *in vitro* and *in vivo*.^{21,22} Human $\gamma\delta$ T cells are increasingly appreciated as promising effectors for novel immunotherapy strategies, not the least due to their ability to

recognise stress-induced changes in a wide range of transformed cells, including breast cancer cells, in a non-MHC-restricted manner.^{11,12} Here, both HMLER-derived CSC-like cells and non-CSCs showed a striking resistance to expanded V γ 9/V δ 2 T cells. However,

pretreatment of either population with zoledronate resulted in effective activation of co-cultured V γ 9/V δ 2 T cells as judged by targeted cytotoxicity (Figure 4a), as well as mobilisation of CD107a and secretion of IFN- γ (Figure 4b). A similar sensitisation could be

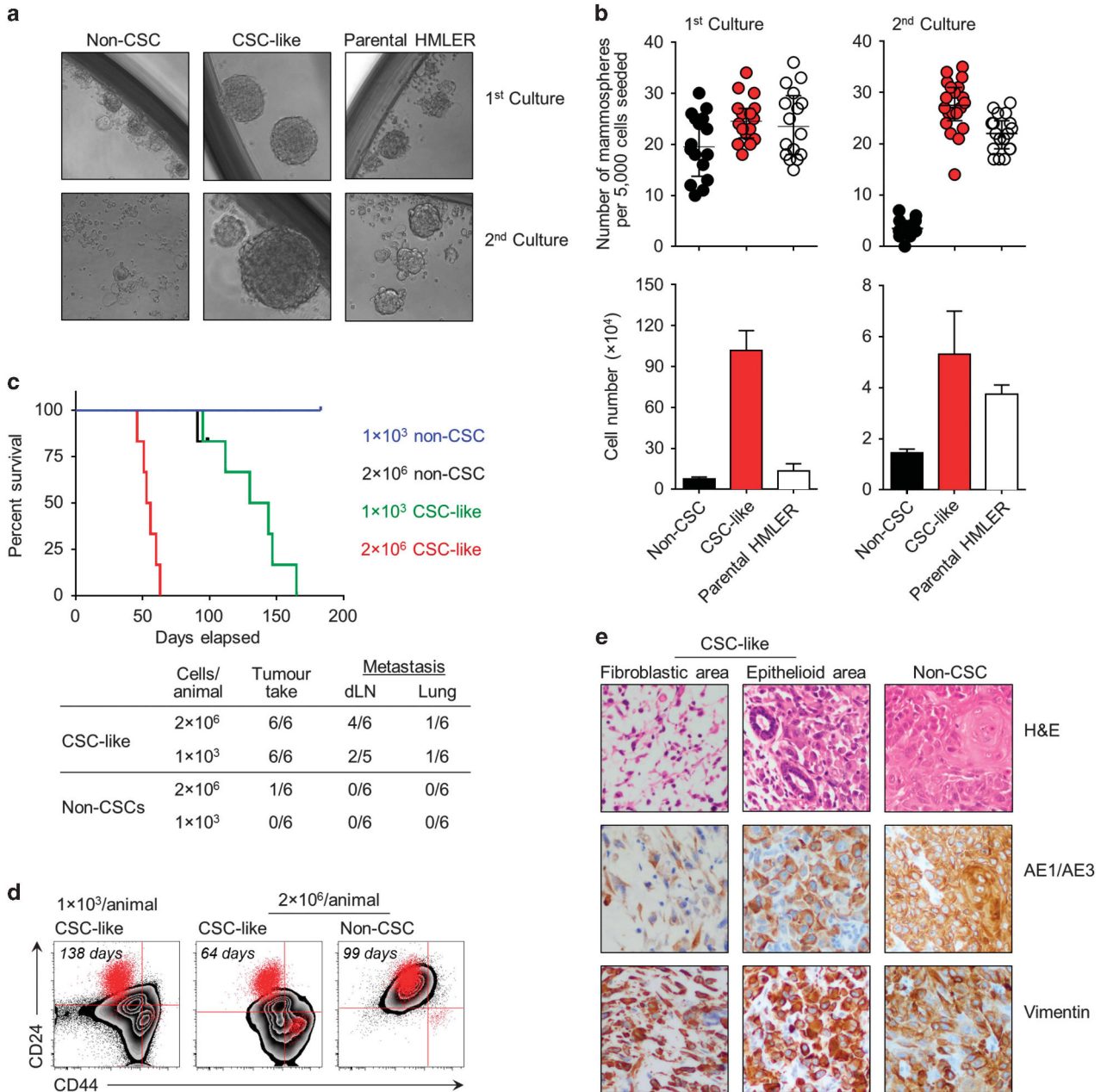


Figure 2 Functional characterisation of HMLER-derived non-CSC and CSC-like cells. (a, b) Self-renewal under non-adherent conditions. Sorted CSC-like cells and non-CSCs were seeded in ultralow-attachment 96-well plates at a density of 5000 cells per well and cultured in mammosphere medium for 7 days. (a) Representative pictures of three independent experiments ($\times 10$ magnification). (b) Mammosphere counts and total cell numbers. Each data point represents an independent culture well, error bars depict the median \pm interquartile range. Data were analysed using one-way ANOVA; asterisks indicate significant differences. (c) Tumour take in NSG mice ($n=6$ per group). Mice receiving high doses of CSCs or non-CSCs (2×10^6 cells per animal) were monitored for up to 98 days, and mice receiving low doses (1×10^3 cells per animal) for up to 180 days after injection. End points were determined as no further increase in tdTomato signal over 2 weeks; disease was defined as presence of a palpable tumour with the longest diameter reaching 1 cm. Disease-free survival curves were plotted using the Kaplan–Meier method. The table shows tumour take rate and occurrence of metastasis to lung and draining lymph nodes (dLNs). (d) Phenotypical analysis of dissociated tumours derived from injection of FluoM1-transduced non-CSCs and CSC-like cells at high and low doses. Tumours were collected when their sizes reached 1000 mm^3 at the time points indicated. CD44 and CD24 expression of each tumour is shown as zebra plots, with parental HMLER cells as red dots serving as internal reference. FACS plots shown are representative of $n=6$ (left), $n=6$ (middle) and $n=1$ (right) tumours, respectively. (e) Histological analysis of collected tumours, shown as H&E staining (top row), and expression of pan-cytokeratin AE1/AE3 (middle row) and vimentin (bottom row). Images are representative sections of $n=11$ CSC-like and $n=1$ non-CSC derived tumours ($\times 400$ magnification). ANOVA, analysis of variance.

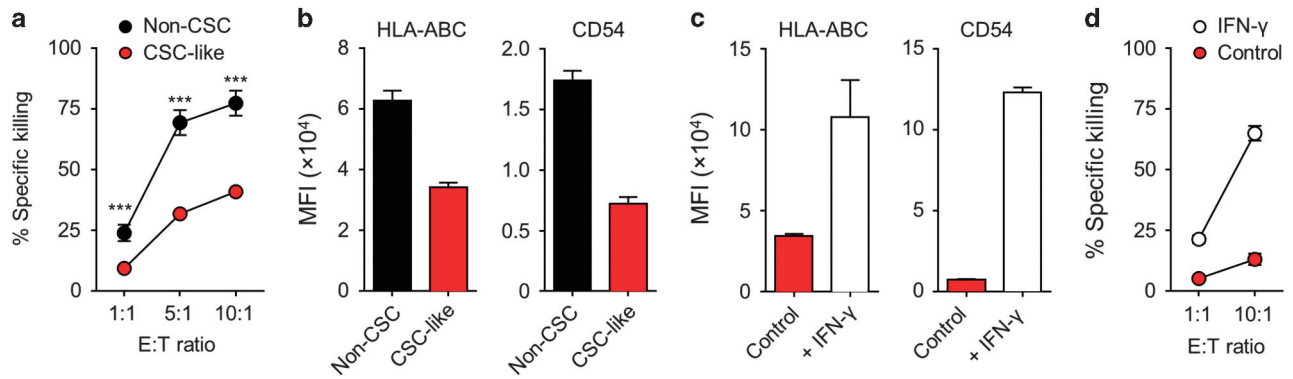


Figure 3 IFN- γ -dependent sensitisation of CSC-like cells to antigen-specific CD8⁺ T cells. (a) FluM1-transduced CSC-like cells and non-CSCs were mixed in equal numbers, and used as targets for killing by FluM1-specific CD8⁺ T cells at different effector:target (E:T) ratios. Specific killing of CellVue and PKH67-labelled target cells was assessed by live/dead staining and analysed by flow cytometry. Data shown are from a triplicate experiment representative of two independent experiments. Significance of differences was calculated by two-way ANOVA. (b) MHC class I (HLA-ABC) and CD54 expression levels on the cell surface of non-CSCs and CSC-like cells as determined by flow cytometry. Bar diagrams show means+s.d. from three independent experiments. MFI, mean fluorescence intensity. (c) MHC class I and CD54 expression levels on CSC-like cells after overnight sensitisation with 100 U ml⁻¹ recombinant human IFN- γ as determined by flow cytometry. Results shown are means+s.d. from three independent experiments. (d) Sensitisation of FluM1-transduced CSC-like cells to CD8⁺ T-cell-mediated cytotoxicity after overnight sensitisation with 100 U ml⁻¹ IFN- γ . Treated and untreated CSC-like cells were mixed in equal numbers, and used as targets for killing by FluM1-specific CD8⁺ T cells at different E:T ratios. Specific killing of CellVue and PKH67-labelled target cells was assessed by live/dead staining and analysed by flow cytometry. Data shown are representative of two experiments performed in triplicate.

achieved via short hairpin RNA-induced knockdown of FPPS, the enzyme inhibited by zoledronate (Supplementary Figure S5).¹⁶ Confirming the recognition via the TCR, degranulation of V γ 9/V δ 2 T cells and secretion of IFN- γ in response to zoledronate treated CSC-like cells and non-CSCs could readily be blocked by neutralising antibodies against TCR-V γ 9 and butyrophilin 3A (BTN3A/CD277),²³ but not by antibodies against NKG2D (Figure 4c and data not shown).

Besides recognition via the TCR and NKG2D, V γ 9/V δ 2 T cells have also been shown to target tumour cells including breast cancer cells upon engagement of CD16 (Fc γ RIII).^{24–26} In line with the expression of GD2 by CSC-like cells, we observed a relatively modest but detectable enhancement of V γ 9/V δ 2 T-cell responses toward CSC-like cells pretreated with the humanised anti-GD2 antibody hu14.18K322A (Figure 4d). Taken together, these experiments demonstrate that CSC-like cells can be sensitised to recognition by human $\gamma\delta$ T cells upon inhibition of FPPS via zoledronate treatment or using short hairpin RNAs, and through the use of CSC-specific opsonising antibodies.

Synergistic targeting of CSC-like cells by V γ 9/V δ 2 T cells and cytotoxic CD8⁺ T cells

Having shown that CSC-like cells can be sensitised to killing by either human $\alpha\beta$ T cells and $\gamma\delta$ T cells, we addressed the potential synergy of combining the antigen-specific nature of cytotoxic CD8⁺ T cells and the innate killer function of V γ 9/V δ 2 T cells. In line with the general perception that IFN- γ increases tumour immunogenicity,²⁷ and with our own observation that recombinant IFN- γ had a striking effect on CSC-like cells (Figure 3), we saw an upregulation of MHC class I and CD54 expression on CSC-like cells upon exposure to supernatants of activated $\gamma\delta$ T cells (Figure 5a). By using blocking antibodies, we identified IFN- γ as the main factor in these supernatants (Figure 5b), demonstrating that activated $\gamma\delta$ T cells readily boost the potential of CSC-like cells to present antigens to CD8⁺ T cells. A similar $\gamma\delta$ T-cell-induced upregulation of MHC class I and CD54 expression was seen with non-CSCs and parental HMLER cells, as well as with a panel of luminal-like and basal-like breast cancer cell lines (MCF-7, SKBR3 and MDA-MD-231) (data not shown), implying that $\gamma\delta$ T-cell-derived

cytokines generally enhance the susceptibility of breast cancer cells of different origins to be targeted by CD8⁺ T cells.

In support, overnight pretreatment of both FluM1-expressing CSC-like cells and non-CSCs with $\gamma\delta$ T-cell-conditioned medium significantly enhanced their susceptibility to killing by FluM1-specific CD8⁺ T cells as compared to untreated controls (Figure 5c). Similarly, $\gamma\delta$ T-cell supernatants enhanced the cytotoxic response of FluM1 or CMV pp65-specific CD8⁺ T cells to CSC-like cells and non-CSCs pulsed with the corresponding peptides (data not shown). Blocking with anti-IFN- γ neutralising antibodies diminished the effect of $\gamma\delta$ T-cell supernatants on enhancing the cytotoxicity of CD8⁺ T cells toward both CSC-like cells and non-CSCs (Figure 5d).

This $\gamma\delta$ T-cell-mediated sensitisation of tumour cells to CD8⁺ T-cell killing was particularly striking when observed in real time using video microscopy, revealing an increased and more persistent calcium flux in CD8⁺ T cells in response to sensitised CSC-like cells (Figure 5e) that resulted in substantial target killing (Figure 5f; Supplementary Movies S1–S3). These findings thus identified non-MHC-restricted $\gamma\delta$ T cells as potent adjuvant facilitating subsequent antigen-specific CD8⁺ T-cell immunity against tumour cells, including breast CSC-like cells, through their secretion of IFN- γ .

DISCUSSION

We identified a powerful synergism between $\gamma\delta$ T cell and CD8⁺ T cells in the eradication of tumour cells, including CSC-like cells, suggesting that novel immunotherapies may benefit from a combination of MHC-restricted and non-MHC-restricted approaches. To be able to demonstrate this, we established a stable HMLER-derived cell line with a mesenchymal appearance and a CD44^{hi} CD24^{lo} GD2⁺ phenotype with high expression levels of extra domain A-fibronectin and vimentin. These CSC-like cells readily formed mammospheres under non-adherent conditions, induced subcutaneous tumours in the mammary fat pad of NSG mice at numbers as low as 1 × 10³ cells per animal, and had the potential to metastasise to the lung and undergo epithelioid differentiation *in vivo*. We conclude that the present study provides a useful experimental model to study CSC-like cells and non-CSCs derived from the same parental material under identical

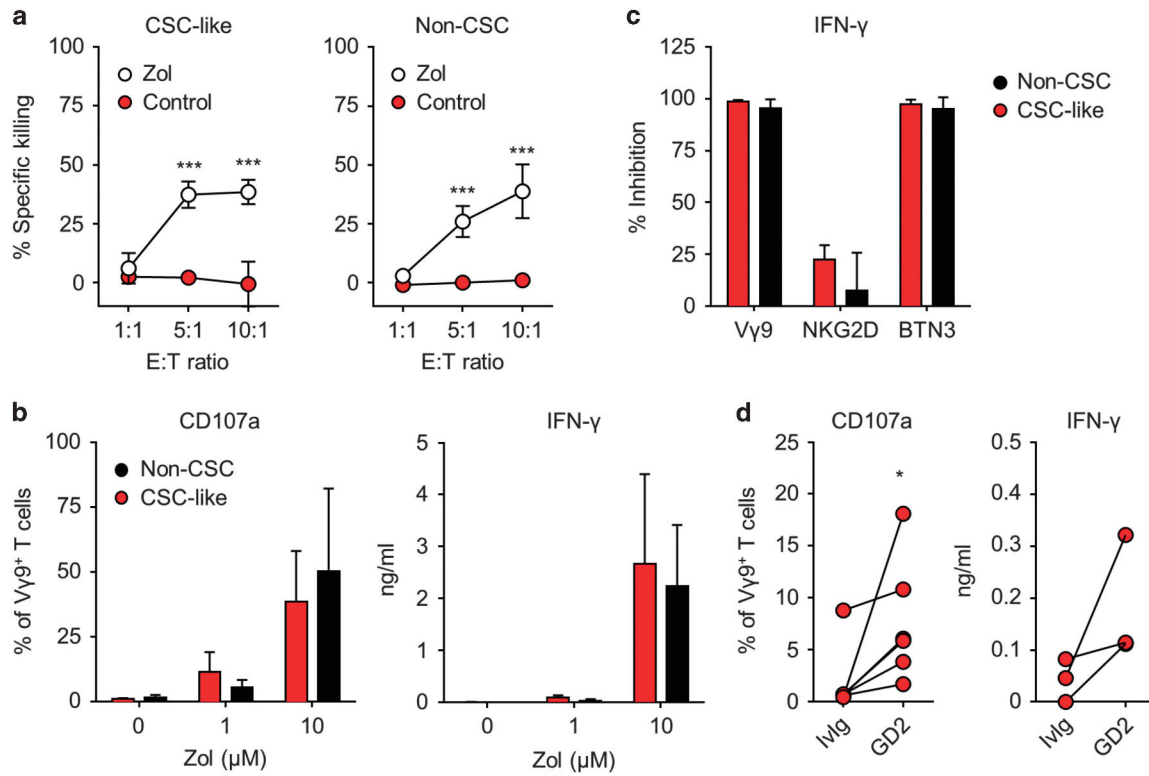


Figure 4 Sensitisation of CSC-like cells to $\gamma\delta$ T cells using zoledronate or opsonising antibodies. (a) CSC-like cells (left) and non-CSCs (right) treated overnight with $10\ \mu\text{M}$ zoledronate were mixed in equal numbers with untreated CSC-like cells and non-CSCs, respectively, and used as targets for killing by expanded V γ 9/V δ 2 T cells at different effector:target (E:T) ratios. Specific killing of CellVue and PKH26-labelled target cells was assessed by live/dead staining and analysed by flow cytometry. Data shown are from two independent experiments with $\gamma\delta$ T cells from three healthy individuals each; differences were assessed by two-way ANOVA. (b) $\gamma\delta$ T-cell degranulation (left) and IFN- γ secretion (right) in response to CSC-like cells and non-CSCs treated overnight with zoledronate. CD107a mobilisation was measured by flow cytometry in $\gamma\delta$ T cells after 5 h of co-culture with target cells in the presence of GolgiSTOP and anti-CD107a; IFN- γ levels were determined after 24 h by ELISA ($n=4$). (c) Effect of neutralising antibodies on IFN- γ secretion by $\gamma\delta$ T cells in response to CSC-like cells and non-CSCs treated overnight with zoledronate. Data shown are relative inhibition by each blocking antibody as compared with the corresponding isotype controls. Anti-V γ 9 and anti-NKG2D were added directly to target/ $\gamma\delta$ T-cell co-cultures. For the blocking of BTN3, target cells were incubated with anti-BTN3 for 1 h and then washed before co-culture with $\gamma\delta$ T cells. Data shown are means \pm s.d. from four independent experiments. (d) Specific sensitisation of CSC-like cells to $\gamma\delta$ T cells by opsonising antibodies. CSC-like cells were co-cultured with expanded $\gamma\delta$ T cells in the presence of $10\ \mu\text{g ml}^{-1}$ humanised anti-GD2 monoclonal antibodies or $10\ \mu\text{g ml}^{-1}$ human intravenous immunoglobulin (Ivlg) as control. Data show $\gamma\delta$ T-cell degranulation (left; $n=6$) and IFN- γ secretion (right; $n=3$) in response to opsonised and control CSC-like cells; differences were assessed by Wilcoxon matched-pairs signed-rank tests.

culture conditions, for a direct comparison of their susceptibility not only to killing by immune cells, but also to chemotherapies and radiation. The stability of HMLER-derived CSC-like and non-CSCs in culture conveniently overcomes the limitations of approaches that depend on long-term sphere cultures, which may change the nature of both CSCs and non-CSCs with respect to differentiation and dedifferentiation. These advantages notwithstanding, the fact that HMLER cells are transformed mammary epithelial cells and not derived from primary breast tumours poses certain limitations, and future work will seek to provide further relevance by sensitising primary CSCs.

Adoptive transfer studies have shown promising potential in patients with different types of tumours, most notably in melanoma.^{6–8} Currently, such studies are conducted with tumour-infiltrating lymphocytes, chimeric antigen receptors or TCR-engineered T cells. However, all three approaches have relatively limited applicability.^{28,29} Most importantly, many tumours evade the immune system by downmodulating surface expression of MHC molecules and/or adhesion molecules, especially within the CSC pool.^{30–33} In agreement, the breast CSC-like cells in the present study expressed relatively low levels of MHC class I and CD54. The poor

susceptibility of CSC-like cells to killing by antigen-specific CD8⁺ T cells could be overcome by pretreatment with $\gamma\delta$ T-cell conditioned media, demonstrating that $\gamma\delta$ T cells are capable of delivering pro-inflammatory cytokines including IFN- γ and rendering poorly immunogenic tumours visible for the immune system. These findings are in accordance with earlier reports showing that IFN- γ rescues MHC class I expression on CSCs of different origins,^{31,32} and offer hope for efficient targeting of CSCs by adoptively transferred tumour-infiltrating lymphocytes and engineered T cells. However, this study was conducted using well-characterised viral epitopes as surrogate antigens for which high affinity TCRs are available, thereby allowing studies into efficient killing of transduced CSC-like cells by antigen-specific CD8⁺ T cells.³⁴ Follow-up experiments therefore need to replicate these findings using relevant tumour-associated antigens, such as aldehyde dehydrogenase 1A1 (ALDH1A1), which was identified as a novel CSC-specific tumour antigen for cytotoxic CD8⁺ T cells in squamous cell carcinoma of head and neck.^{35,36}

The resistance of breast CSC-like cells to $\gamma\delta$ T cells could be overcome upon pretreatment with zoledronate, resulting in increased cytotoxicity of $\gamma\delta$ T cells. Zoledronate is widely used to prevent excessive bone resorption and skeletal fractures in patients with

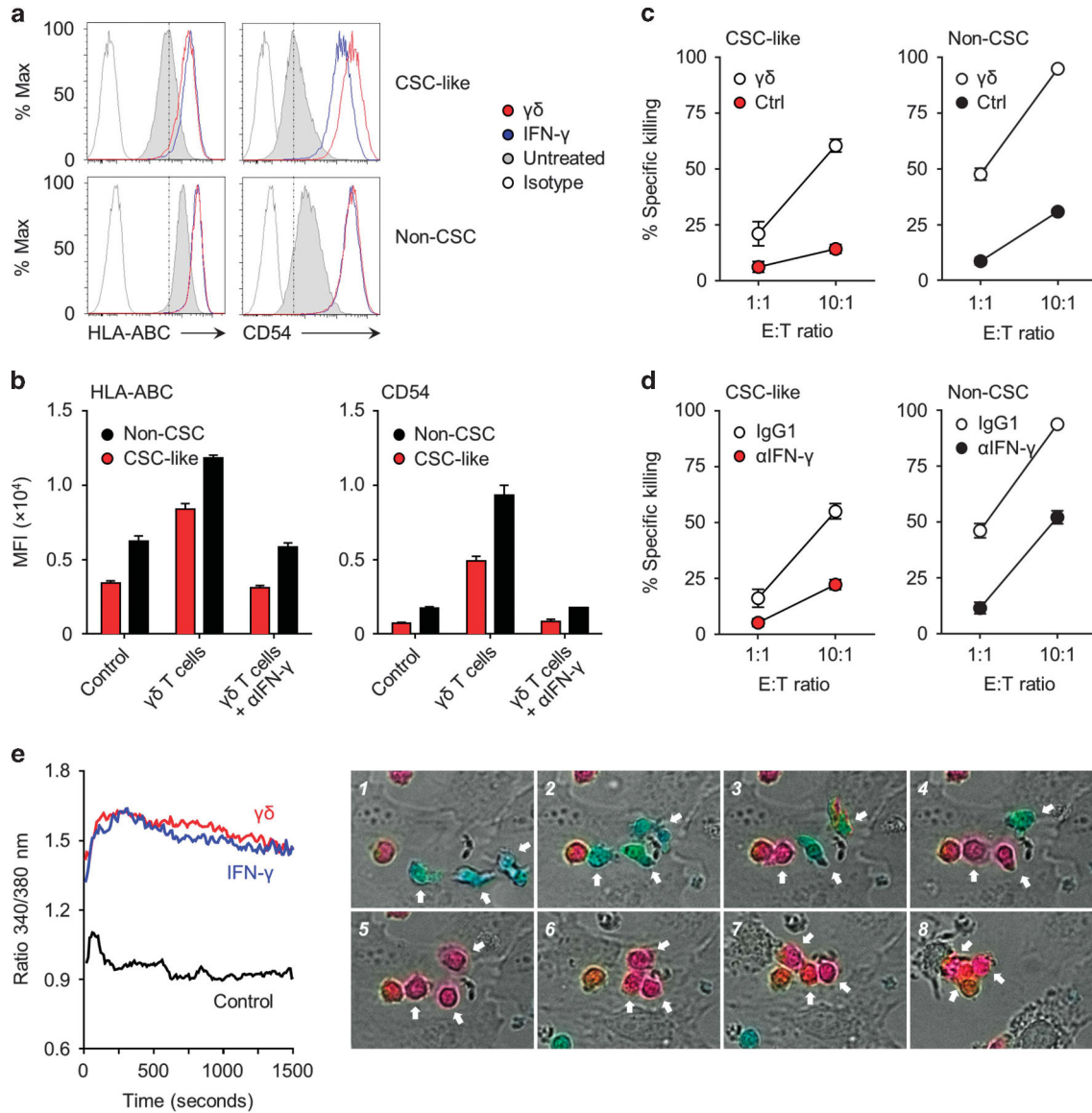


Figure 5 Sensitisation of CSC-like cells and non-CSCs to cytotoxic CD8⁺ T cells by V γ 9/V δ 2 T cells. (a) Upregulation of MHC class I (HLA-ABC) and CD54 expression on sorted CSC-like cells and non-CSCs by $\gamma\delta$ T cells. Target cells were treated overnight with 1:10 (*w/v*) $\gamma\delta$ T-cell conditioned medium or with 100 U ml⁻¹ recombinant human IFN- γ , and analysed by flow cytometry. Histograms shown are representative for two independent experiments. (b) Sorted CSC-like cells and non-CSCs were treated overnight with $\gamma\delta$ T-cell conditioned medium in the absence or presence of IFN- γ neutralising antibodies or mouse IgG1 isotype controls, and analysed for their expression of MHC class I (left) and CD54 (right) by flow cytometry. Data shown are representative of two independent experiments using supernatants of expanded $\gamma\delta$ T cells from three healthy individuals; differences were assessed by two-way ANOVA. (c) Sensitisation of FluM1-transduced CSC-like cells and non-CSCs to CD8⁺ T-cell-mediated cytotoxicity after overnight treatment with 1:10 (*w/v*) $\gamma\delta$ T-cell conditioned medium. Treated and untreated target cells were mixed in equal numbers, and used as targets for killing by FluM1-specific CD8⁺ T cells at different E:T ratios. Specific killing of CellVue and PKH67-labelled target cells was assessed by live/dead staining and analysed by flow cytometry. Data shown are representative of two independent experiments using supernatants of expanded $\gamma\delta$ T cells from three donors. (d) Sensitisation of FluM1-transduced CSC-like cells and non-CSCs to CD8⁺ T-cell-mediated cytotoxicity after overnight sensitisation with 1:10 (*w/v*) $\gamma\delta$ T-cell conditioned medium in the presence of IFN- γ neutralising antibodies or matched isotype controls (IgG1). Treated and untreated target cells were mixed as before, and specific killing was assessed by flow cytometry. Data shown are representative of two independent experiments using supernatants of expanded $\gamma\delta$ T cells from three donors. (e) Intracellular Ca²⁺ levels as monitored by video microscopy for the indicated acquisition time starting from the moment when Fura-2 AM loaded FluM1-specific CD8⁺ T cells entered in the focal plane. Graphs represent the kinetics of intracellular Ca²⁺ levels, depicted as 340:380 nm ratio; values correspond to the mean emission measured among all T cells present in the field of four independent experiments. Photos are representative pictures of the kinetics of intracellular Ca²⁺ levels and tumour cell killing, using FluM1-transduced CSC-like cells pretreated with $\gamma\delta$ T-cell conditioned medium as targets.

multiple myeloma, bone metastases and osteoporosis. In addition to its direct effect on the bone, recent meta-analyses provided compelling evidence for a clinical benefit of zoledronate on the development of bone metastases and breast cancer mortality in post-menopausal women or those receiving ovarian suppression therapy.³⁷ The

underlying mechanisms are unclear, but may stem at least in part from the activity of zoledronate on V γ 9/V δ 2 T cells.^{38,39} Studies directly aimed at activating V γ 9/V δ 2 T cells in preclinical models and in diverse cancer patient groups have in fact shown promising results, showing that targeting V γ 9/V δ 2 T cells *in vivo* is feasible and

safe.^{10–12,40,41} In addition to sensitisation with zoledronate, anti-GD2 antibodies selectively directed V γ 9/V δ 2 T-cell responses against CSC-like cells but not non-CSCs, demonstrating that specific opsonisation represents an alternative approach to sensitise resistant tumour cells to targeted cytotoxicity. Similar strategies have been employed for treating neuroblastoma by natural killer cells,^{17,42} and for facilitating cross-presentation of tumour antigens by V γ 9/V δ 2 T cells to CD8⁺ T cells.⁴³ The relatively weak efficacy of anti-GD2 antibodies may have been due to the variable and often low expression of CD16 on the expanded V γ 9/V δ 2 T cells used in those assays. Besides GD2, further markers with a potential to target V γ 9/V δ 2 T cells specifically against breast CSCs include the human epidermal growth factor receptor 2 (HER2).⁴⁴ Indeed, the HER2-specific monoclonal antibody trastuzumab was recently shown to opsonise human breast cancer xenografts and enhance the ability of $\gamma\delta$ T cells to control tumour progression.²⁶ The availability of approved drugs and biologics to enhance the TCR-mediated and antibody-dependent cytotoxicity of $\gamma\delta$ T cells therefore allows a rapid translation of the present findings in the clinic.

Taken together, we have identified a powerful synergism between MHC-restricted and non-MHC-restricted T cells in the targeting of breast CSC-like cells. Our research provides proof of principle that novel immunotherapies may benefit significantly from combining targeted strategies that trigger effective innate and adaptive responses.⁴⁵ In addition to their cytotoxic effector functions against malignant cells and their ability to boost adaptive $\alpha\beta$ T-cell responses by modulating the immunogenicity of transformed cells, human V γ 9/V δ 2 T cells also possess a unique ability to act as professional antigen-presenting cells, including the capacity to cross-present exogenous antigens to CD8⁺ T cells.^{43,46–48} These observations lend further credence for the potential of a combined immunotherapy approach where patients receiving autologous tumour-infiltrating lymphocytes or engineered T cells may benefit from a co-administration of *ex vivo* expanded $\gamma\delta$ T cells or by concomitant treatment with safe and effective $\gamma\delta$ T-cell stimuli such as zoledronate. Such therapy regimes that boost the efficacy of adoptive CD8⁺ T-cell transfer can now be tested in preclinical models and in patients.

METHODS

Tumour cells

HMLER cells were kindly provided by Dr Robert Weinberg (Whitehead Institute for Biomedical Research, Cambridge, MA, USA) and cultured in DMEM:F12 (1:1) medium (Invitrogen, Paisley, UK) supplemented with 10% foetal calf serum, 10 ng ml⁻¹ recombinant human epidermal growth factor (Peprotech, London, UK), 10 μ g ml⁻¹ insulin (Sigma-Aldrich, Dorset, UK), 0.5 μ g ml⁻¹ hydrocortisone (Sigma-Aldrich), 1 μ g ml⁻¹ puromycin (Sigma-Aldrich) and 50 μ g ml⁻¹ penicillin/streptomycin (Invitrogen).^{3,18} CD44^{hi} CD24^{lo} CSC-like and CD44^{lo} CD24^{hi} non-CSC-like HMLER cells were sorted to >99.5% purity using a BD FACSAria II and maintained in culture in complete DMEM:F12 medium. The human breast cancer cell lines MDA-MB-231, MCF-7, SKBR3 and BT-474 were cultured using RPMI-1640 medium supplemented with 10% foetal calf serum, 2 mM L-glutamine, 50 μ g ml⁻¹ penicillin/streptomycin and 100 μ M non-essential amino acids (Invitrogen). Mammospheres were grown in ultralow-attachment plates (Corning, Schiphol, Netherlands), using serum-free MEBM medium (Lonza, Slough, UK) supplemented with B27 (Invitrogen), 20 ng ml⁻¹ epidermal growth factor (Peprotech), 5 μ g ml⁻¹ insulin, 0.1 μ M β -mercaptoethanol and 1 μ g ml⁻¹ hydrocortisone (all from Sigma-Aldrich).⁴⁹

T cells

Human T cells were cultured in RPMI-1640 medium supplemented with 10% foetal calf serum, 2 mM L-glutamine, 1% sodium pyruvate and 50 μ g ml⁻¹ penicillin/streptomycin. V γ 9/V δ 2 T cells were expanded from peripheral blood

mononuclear cells of healthy donors with 1 μ M zoledronate (Zometa; Novartis, Basel, Switzerland) and 100 U ml⁻¹ IL-2 (Proleukin; Novartis) for 14 days, and further enriched to purities >98% CD3⁺ V γ 9⁺ by negative selection using a modified human $\gamma\delta$ T-cell isolation kit that depletes B cells, $\alpha\beta$ T cells, NK cells, dendritic cells, stem cells, granulocytes and monocytes (Stem Cell Technologies, Cambridge, UK). Resulting V γ 9/V δ 2 T-cell populations were predominantly CD45RA⁻ CD27⁻ effector/memory cells, with <15% CD45RA⁻ CD27⁺ central memory cells and <5% CD45RA⁺ CD27⁻ terminally differentiated cells; CD16 expression on expanded V γ 9/V δ 2 T cells varied from 6 to 74% CD16⁺ (data not shown). $\gamma\delta$ T-cell conditioned medium was generated by culturing purified V γ 9/V δ 2 T cells overnight in the presence of 10 nM HMB-PP (kindly provided by Dr Hassan Jomaa, Justus-Liebig University Giessen, Germany). FluM1-specific and CMV pp65-specific CD8⁺ T cells were expanded from peripheral blood mononuclear cells of HLA-A2⁺ donors to >99% tetramer positivity using the immunodominant peptides of influenza matrix protein, FluM1 p58-66 (GILGFVFTL) and of CMV lower matrix phosphoprotein, UL83/pp65 p495-503 (NLVPMVATV), respectively, at a concentration of 0.1 μ M in the presence of 100 U ml⁻¹ IL-2 and 20 ng ml⁻¹ IL-15 (Miltenyi, Bisley, UK).^{47,48}

Generation of FluM1⁺ tdTomato⁺ target cells

The cDNA of FluM1 of influenza strain A/Puerto Rico/8/34 (H1N1) was cloned from pMA_MPT_matrix_protein (kindly provided by Dr Mai Ping Tan, Cardiff University) between the *Sall* and *Xma*I cloning sites of the lentiviral transfer vector pELNSxv (kindly provided by Dr James Riley, University of Pennsylvania, PA, USA). PCR reactions were carried out using the Phusion High-Fidelity PCR kit (New England Biolabs, Hitchin, UK) and customised primers; forward, 5'-GAATCCCGGCCCTAGGATGAGCCTGCTGACCAGAGGT-3'; reverse, 5'-GAGGTTGATTGTCGACTCACTTGAACCGCTGCATCT-3' (Eurofins, Wolverhampton, UK). For the production of lentiviral particles containing pELNSxv-tdTomato-T2A-FluM1 vectors, HEK 293 T cells were transiently transfected with lentiviral packaging, envelop and transfer plasmids by CaCl₂ precipitation. Lentiviral particles were collected and purified for transfection of CSC-like cells and non-CSCs in the presence of 4 μ g ml⁻¹ polybrene (Sigma-Aldrich). Lentivirally transduced cells were identified based on their expression of tdTomato, and sorted to >98% purity using a BD FACSAria II.

Constitutive and inducible knockdown of FPPS

Constitutive FPPS knockdown cells were generated as described.¹⁶ The inducible vector FUTG(INSR), which contains a knockdown construct for rat insulin receptor,⁵⁰ served as negative control for the inducible FPPS knockdown vector SR22 for the target sequence V2HS_228248 (Thermo Scientific, Open Biosystems, Huntsville, AL, USA).¹⁶ Specific oligos were annealed and subsequently ligated into the *Bbs*I and *Xho*I sites of pH1tet-flex; 5'-TCCACCAGCAGTGTTCTTGCAATATTTCAAGAGAATATTGCAAGAACTGCTGGTTTTTTC-3' (forward) and 5'-TCGAGAAAAACCAGCAGTGTCTTTCGAATATTCTCTTGAATATTGCAAGAACAACACTGCTGGT-3' (reverse). The H1tet-shRNA22 cassette was cloned into the *Pac*I site of the lentiviral vector FH1tUTG⁵⁰ using specific primers; 5'-CGTGTATTAATTAACCATGGATTTCGAACGCTGAC-3' (forward) and 5'-CGATCTTAATTAACAGGCTAGCTAGGACGCG-3' (reverse). All retroviral or lentiviral constructs were transduced into the respective target cells by transient transfection of HEK 293 T cells using CaCl₂ precipitation. After 24 h, 10 nM sodium butyrate was added, and virus containing supernatants were collected on the following day and added to target cells in the presence of polybrene.

Flow cytometry

Cells were acquired on an eight-colour FACSCanto II (BD Biosciences, Oxford, UK) and analysed with FlowJo (TreeStar, Ashland, OR, USA). Single cells of interest were gated based on their appearance in side and forward scatter area/height, exclusion of live/dead staining (fixable Aqua; Invitrogen) and surface staining. The following monoclonal antibodies (mAbs) were used for surface labelling: anti-CD3 (UCHT1), CD8 (HIT8a and SK1), CD16 (3G8), CD24 (ML5), CD44 (G44-26), GD2 (14.G2a) from BD Biosciences; anti-TCR-V γ 9 (Immu360) from Beckman Coulter, High Wycombe, UK; and anti-HLA-ABC (w6/32) from Biogen, London, UK; together with appropriate isotype

controls. Intracellular cytokines were detected using anti-IFN- γ mAbs (B27, BD Biosciences). Surface mobilisation of CD107a was detected by adding anti-CD107a (H4A3; BD Biosciences) mAbs and GolgiStop (BD Biosciences) to cultures for 5 h prior to flow cytometric analysis.

Functional T-cell assays

CD107a mobilisation, expression of activation markers and cytokine production were assessed by flow cytometry-based assays as described previously for the activation of $\gamma\delta$ T cells and CD8⁺ T cells.⁴⁸ $\gamma\delta$ T cells and CD8⁺ T cells treated with PMA and ionomycin were used as positive control in functional assays. For the sensitisation, CSC-like cells and non-CSCs were treated overnight with 10 μ M zoledronate (Zometa; Novartis), washed and used as targets in co-culture with effector T cells at specified effector:target (E:T) ratio. Cytotoxicity assays were conducted in co-cultures of two distinct target cell populations to assess preferential killing of specific targets.^{48,49} In brief, two different target cell populations were labelled separately with different lipophilic dyes (PKH26, PKH67 or CellVue; all from Sigma-Aldrich), and mixed at 1:1 ratio for subsequent co-culture with effector T cells at different E:T ratios. After 4 h at 37 °C, cultures were collected, stained using the Live/dead fixable Aqua dead cell stain kit (Invitrogen) and acquired on a BD FACSCanto II. The analysis was performed by serial gating on single cells (FSC-A/FSC-H) and distinctively stained targets (for example, CellVue⁺ PKH67⁻ or CellVue⁻ PKH67⁺), and the proportion of dead cells was determined for each target population. In these functional assays, the neutralising antibodies anti-TCR-V γ 9 (Immu360; Beckman Coulter), anti-BTN3A (103.2; Dr Daniel Olive, Institut Paoli Calmettes, Marseille, France), anti-NKG2D (1D11; Biologend) and anti-IFN- γ (B27; Biologend) were used at 10 μ g ml⁻¹. To test the role of opsonising antibodies, tumour cells were pretreated with anti-GD2 (hu14.18K322A; Dr Fariba Navid, St Jude Children's Research Hospital, Memphis, TN, USA) for 30 min at 10 μ g ml⁻¹. Levels of secreted IFN- γ in culture supernatants were determined by ELISA (Biologend, eBioscience, Cheshire, UK), using a Dynex MRX II reader.

Animal studies

All procedures were performed in accordance with the Animals (Scientific Procedures) Act 1986 and approved by the UK Home Office under project license 30/2891. Surgery was performed under isoflurane anaesthesia, and every effort was made to minimise suffering. Female NSG mice were purchased from Charles River Laboratories at 5–7 weeks of age and housed in specific pathogen-free conditions. For xenograft transplantations, the indicated numbers of tumour cells (ranging from 1×10^3 to 2×10^6 per mouse) were resuspended in a mixture of DMEM/F12 medium with Matrigel (Corning) at 1:1 ratio and injected s.c. in NSG mice near the mammary fat pad. Tumour growth was monitored twice a week by external measurement of xenografts using a Vernier caliper and by fluorescence imaging (Kodak FX-PRO, Rochester, NY, USA). Mice were culled before tumours reached 1.5 cm in diameter. For flow cytometric analyses or cell sorting, tumours were excised, chopped into pieces using scalpel blades and mashed with a syringe plunger. The resulting cell suspension was passed through 70 μ m nylon cell strainers (BD Falcon) and stained with indicated panel of mAbs. Tumours, tumour-draining inguinal lymph nodes and the contralateral non-draining lymph nodes as well as livers, lungs, brains and spleens were collected for fluorescence imaging, and subsequently fixed in neutral buffered formalin and embedded in paraffin.

Histology and immunohistochemistry

Four micrometre sections were cut from paraffin-embedded blocks of tumours and organs, and mounted on slides. Dewaxed and hydrated sections were stained in Harris haematoxylin solution (Thermo Scientific) and blued with Scott's tap water substitute (Sigma-Aldrich). Sections were then stained in eosin solution (Sigma-Aldrich), dehydrated and mounted in DPX (VWR International, Lutterworth, UK). For immunohistochemical analyses, freshly cut tissue sections were stained by primary antibodies against carcinoma embryonic antigen (II-7), vimentin (V9) and cytokeratin (AE1-AE3), using Dako Autostainer Link 48 on an automated staining platform and the Dako EnVision FLEX detection kit (Dako, Ely, UK). Slides were counterstained with haematoxylin before dehydration and mounting in DPX (VWR International).

Digital microscopy

Photographs of live cultures were taken using a Leica DM IRBE inverted microscope (Leica Microsystems, Milton Keynes, UK) with a Hamamatsu ORCA-ER camera supported with OpenLab 3.1.7 (Improvision, Conventry, UK), or using a LumaScope 500 inverted microscope (Etaluma, Labtech, Uckfield, UK). For confocal immunofluorescence microscopy, CSC-like cells and non-CSCs were grown in Nunc Lab-Tek cover-slip chamber slides to subconfluency and fixed with acetone/methanol for staining with a series of primary mAbs against α -SMA (1A4), N-cadherin (8C11), cytokeratin-14 (LL001), CK-18 (RGE53), extra domain A-fibronectin (IST-9) and vimentin (V9) (all from Santa Cruz Biotechnology, Heidelberg, Germany), together with appropriate isotype controls, followed by AF488-conjugated secondary antibodies with counterstaining for cell nucleus by DAPI. Prepared slides were imaged and analysed using a Zeiss AxioVert fluorescence microscope (Zeiss, Cambridge, UK). Images were processed with Photoshop 6.0 (Adobe, San Jose, CA, USA). For video microscopy, target cells were incubated overnight in Ibidi chamber slides (Martinsried, Germany) coated with fibronectin (Millipore). For intracellular Ca²⁺ measurements, CD8⁺ T cells were loaded with 1 μ M Fura-2/AM (Invitrogen) and analysed using a DMI 6000B microscope (Leica Microsystems). Cells were illuminated every 10 s with a 300 W xenon lamp by using 340/10 nm and 380/10 nm excitation filters. Emission at 510 nm was captured using a Cool Snap HQ2 camera (Roper, Tucson, AZ, USA) with Metafluor software (Molecular Devices, Sunnyvale, CA, USA). Ratio measurements were performed with Imaris 8.1 imaging software (Oxford Instruments, Abingdon, UK).

Statistics

Data were analysed using two-tailed Student's *t*-tests for normally distributed data and Mann-Whitney tests for non-parametric data (GraphPad Prism 6.0, La Jolla, CA, USA). Paired data were analysed using Wilcoxon matched-pairs signed-rank tests. Differences between groups were analysed using one-way analysis of variance with Bonferroni's post tests; two-way analysis of variance was used when comparing groups with independent variables. Differences were considered significant as indicated in the figures: **P* < 0.05; ***P* < 0.01; ****P* < 0.001.

CONFLICT OF INTEREST

The authors declare no conflict of interest.

ACKNOWLEDGEMENTS

We would like to thank Robert Weinberg for providing HLMER cells; James Riley and Mai Ping Tan for plasmids; Andrew Thomas for recombinant FluM1 protein and HLA-A2 tetramers; Fariba Navid for hu14.18K322A antibodies; Daniel Olive for BTN3A blocking antibodies; Hassan Jomaa for synthetic HMB-PP; Nooshin Tabatabaei-Zavareh for custom-made $\gamma\delta$ T-cell isolation kits; Catherine Naseryan, Kelly Miners and Kristin Ladell for cell sorting; Aled Clayton for help with confocal microscopy; Tamsin Dockree, Chia-Te Liao and Lisa Starick for help with lentiviral constructs; Emily Colbeck, Emma Jones and Anwen Williams for help with histology; Garry Dolton, Ellyn Hughes and Emma Kempshall for help with animal studies; and the Cellular and Tissular Imaging Core Facility of Nantes University (MicroPICell) and Lola Boutin for help with video microscopy and calcium experiments. This research was supported by the Wales Cancer Research Centre and the Cardiff CR-UK Centre Development Fund; Cancer Research UK grants C28524/A9497, C42921/A13823 and C16731/A21200; Institut National de la Santé et de la Recherche Médicale (INSERM); Centre National de la Recherche Scientifique (CNRS); Université de Nantes; Institut National du Cancer (INCa PLBIO 2014-155) and Investissements d'Avenir (Agence Nationale de la Recherche-Programme Laboratoires d'Excellence Immunotherapy Graft Oncology; #ANR-11-LABX-0016-01); Wilhelm Sander-Stiftung grant 2013.907.1; Tenovus PhD Studentships to H-CC and LP; a Government Scholarship for Study Abroad from the Taiwanese Ministry of Education (H-CC); an Erasmus+ Traineeship (YS); and a Cardiff Incoming Visiting Fellowship (TH). DAP is supported by a Wellcome Trust Senior Investigator Award (100326/Z/12/Z).

- 1 Hanahan D, Weinberg RA. Hallmarks of cancer: the next generation. *Cell* 2011; **144**: 646–674.
- 2 Smalley M, Piggott L, Clarkson R. Breast cancer stem cells: obstacles to therapy. *Cancer Lett* 2013; **338**: 57–62.
- 3 Mani SA, Guo W, Liao MJ, Eaton EN, Ayyanan A, Zhou AY *et al*. The epithelial-mesenchymal transition generates cells with properties of stem cells. *Cell* 2008; **133**: 704–715.
- 4 Battula VL, Shi Y, Evans KW, Wang RY, Spaeth EL, Jacamo RO *et al*. Ganglioside GD2 identifies breast cancer stem cells and promotes tumorigenesis. *J Clin Invest* 2012; **122**: 2066–2078.
- 5 Hollier BG, Tinnirello AA, Werden SJ, Evans KW, Taube JH, Sarkar TR *et al*. FOXO2 expression links epithelial-mesenchymal transition and stem cell properties in breast cancer. *Cancer Res* 2013; **73**: 1981–1992.
- 6 June CH, Blazar BR, Riley JL. Engineering lymphocyte subsets: tools, trials and tribulations. *Nat Rev Immunol* 2009; **9**: 704–716.
- 7 Restifo NP, Dudley ME, Rosenberg SA. Adoptive immunotherapy for cancer: harnessing the T cell response. *Nat Rev Immunol* 2012; **12**: 269–281.
- 8 Rosenberg SA, Restifo NP. Adoptive cell transfer as personalized immunotherapy for human cancer. *Science* 2015; **348**: 62–68.
- 9 Riganti C, Massaia M, Davey MS, Eberl M. Human $\gamma\delta$ T-cell responses in infection and immunotherapy: common mechanisms, common mediators? *Eur J Immunol* 2012; **42**: 1668–1676.
- 10 Fournié JJ, Sicard H, Poupot M, Bezombes C, Blanc A, Romagné F *et al*. What lessons can be learned from $\gamma\delta$ T cell-based cancer immunotherapy trials? *Cell Mol Immunol* 2013; **10**: 35–41.
- 11 Fisher JP, Heuvelinkx J, Yan M, Gustafsson K, Anderson J. $\gamma\delta$ T cells for cancer immunotherapy: a systematic review of clinical trials. *Oncoimmunology* 2014; **3**: e27572.
- 12 Silva-Santos B, Serre K, Norell H. $\gamma\delta$ T cells in cancer. *Nat Rev Immunol* 2015; **15**: 683–691.
- 13 Todaro M, D'Asaro M, Caccamo N, Iovino F, Francipane MG, Meraviglia S *et al*. Efficient killing of human colon cancer stem cells by gammadelta T lymphocytes. *J Immunol* 2009; **182**: 7287–7296.
- 14 Lai D, Wang F, Chen Y, Wang C, Liu S, Lu B *et al*. Human ovarian cancer stem-like cells can be efficiently killed by $\gamma\delta$ T lymphocytes. *Cancer Immunol Immunother* 2012; **61**: 979–989.
- 15 Nishio N, Fujita M, Tanaka Y, Maki H, Zhang R, Hirose T *et al*. Zoledronate sensitizes neuroblastoma-derived tumor-initiating cells to cytotoxicity mediated by human $\gamma\delta$ T cells. *J Immunother* 2012; **35**: 598–606.
- 16 Li J, Herold MJ, Kimmel B, Muller I, Rincon-Orozco B, Kunzmann V *et al*. Reduced expression of the mevalonate pathway enzyme farnesyl pyrophosphate synthase unveils recognition of tumor cells by V γ 9V δ 2 T cells. *J Immunol* 2009; **182**: 8118–8124.
- 17 Navid F, Sondel PM, Barfield R, Shulkin BL, Kaufman RA, Allay JA *et al*. Phase I trial of a novel anti-GD2 monoclonal antibody, Hu14.18K322A, designed to decrease toxicity in children with refractory or recurrent neuroblastoma. *J Clin Oncol* 2014; **32**: 1445–1452.
- 18 Elenbaas B, Spirio L, Koerner F, Fleming MD, Zimonjic DB, Donaher JL *et al*. Human breast cancer cells generated by oncogenic transformation of primary mammary epithelial cells. *Genes Dev* 2001; **15**: 50–65.
- 19 Liang YJ, Ding Y, Levery SB, Lobaton M, Handa K, Hakomori SI. Differential expression profiles of glycosphingolipids in human breast cancer stem cells vs. cancer non-stem cells. *Proc Natl Acad Sci USA* 2013; **110**: 4968–4973.
- 20 Schatton T, Frank MH. Antitumor immunity and cancer stem cells. *Ann N Y Acad Sci* 2009; **1176**: 154–169.
- 21 Gao Y, Yang W, Pan M, Scully E, Girardi M, Augenlicht LH *et al*. $\gamma\delta$ T cells provide an early source of interferon gamma in tumor immunity. *J Exp Med* 2003; **198**: 433–442.
- 22 Welton JL, Morgan MP, Martí S, Stone MD, Moser B, Sewell AK *et al*. Monocytes and $\gamma\delta$ T cells control the acute-phase response to intravenous zoledronate: insights from a phase IV safety trial. *J Bone Miner Res* 2013; **28**: 464–471.
- 23 Rhodes DA, Chen HC, Price AJ, Keeble AH, Davey MS, James LC *et al*. Activation of human $\gamma\delta$ T cells by cytosolic interactions of BTN3A1 with soluble phosphoantigens and the cytoskeletal adaptor periplakin. *J Immunol* 2015; **194**: 2390–2398.
- 24 Lafont V, Liautard J, Liautard JP, Favero J. Production of TNF- α by human V γ 9V δ 2 T cells via engagement of Fc γ RIIIA, the low affinity type 3 receptor for the Fc portion of IgG, expressed upon TCR activation by nonpeptidic antigen. *J Immunol* 2001; **166**: 7190–7199.
- 25 Gertner-Dardenne J, Bonnafous C, Bezombes C, Capietto AH, Scaglione V, Ingoure S *et al*. Bromohydrin pyrophosphate enhances antibody-dependent cell-mediated cytotoxicity induced by therapeutic antibodies. *Blood* 2009; **113**: 4875–4884.
- 26 Capietto AH, Martinet L, Fournié JJ. Stimulated $\gamma\delta$ T cells increase the in vivo efficacy of trastuzumab in HER-2+ breast cancer. *J Immunol* 2011; **187**: 1031–1038.
- 27 Vesely MD, Kershaw MH, Schreiber RD, Smyth MJ. Natural innate and adaptive immunity to cancer. *Annu Rev Immunol* 2011; **29**: 235–271.
- 28 Yang JC, Rosenberg SA. Adoptive T-cell therapy for cancer. *Adv Immunol* 2016; **130**: 279–294.
- 29 June CH, Riddell SR, Schumacher TN. Adoptive cellular therapy: a race to the finish line. *Sci Transl Med* 2015; **7**: 280ps7.
- 30 Schatton T, Schutte U, Frank NY, Zhan Q, Hoerning A, Robles SC *et al*. Modulation of T-cell activation by malignant melanoma initiating cells. *Cancer Res* 2010; **70**: 697–708.
- 31 Di Tomaso T, Mazzoleni S, Wang E, Sovena G, Clavenna D, Franzin A *et al*. Immunobiological characterization of cancer stem cells isolated from glioblastoma patients. *Clin Cancer Res* 2010; **16**: 800–813.
- 32 Chen HC, Chou AS, Liu YC, Hsieh CH, Kang CC, Pang ST *et al*. Induction of metastatic cancer stem cells from the NK/LAK-resistant floating, but not adherent, subset of the UP-LN1 carcinoma cell line by IFN- γ . *Lab Invest* 2011; **91**: 1502–1513.
- 33 Tallero R, Todaro M, Di Franco S, Maccalli C, Garofalo C, Sottile R *et al*. Human NK cells selective targeting of colon cancer-initiating cells: a role for natural cytotoxicity receptors and MHC class I molecules. *J Immunol* 2013; **190**: 2381–2390.
- 34 Brown CE, Starr R, Martinez C, Aguilar B, D'Apuzzo M, Todorov I *et al*. Recognition and killing of brain tumor stem-like initiating cells by CD8+ cytolytic T cells. *Cancer Res* 2009; **69**: 8886–8893.
- 35 Liao T, Kaufmann AM, Qian X, Sangvatanakul V, Chen C, Kube T *et al*. Susceptibility to cytotoxic T cell lysis of cancer stem cells derived from cervical and head and neck tumor cell lines. *J Cancer Res Clin Oncol* 2013; **139**: 159–170.
- 36 Visus C, Wang Y, Lozano-Leon A, Ferris RL, Silver S, Szczepanski MJ *et al*. Targeting ALDH(bright) human carcinoma-initiating cells with ALDH1A1-specific CD8+ T cells. *Clin Cancer Res* 2011; **17**: 6174–6184.
- 37 Hadji P, Coleman RE, Wilson C, Powles TJ, Clézardin P, Aapro M *et al*. Adjuvant bisphosphonates in early breast cancer: consensus guidance for clinical practice from a European Panel. *Ann Oncol* 2016; **27**: 379–390.
- 38 Kunzmann V, Wilhelm M. Adjuvant zoledronic acid for breast cancer: mechanism of action? *Lancet Oncol* 2011; **12**: 991–992.
- 39 Welton JL, Martí S, Mahdi MH, Boobier C, Barrett-Lee PJ, Eberl M. $\gamma\delta$ T cells predict outcome in zoledronate-treated breast cancer patients. *Oncologist* 2013; **18**: e22–e23.
- 40 Chen HC, Dieli F, Eberl M. An unconventional TRAIL to cancer therapy. *Eur J Immunol* 2013; **43**: 3159–3162.
- 41 Jarry U, Chauvin C, Joalland N, Léger A, Minault S, Robard M *et al*. Stereotaxic administrations of allogeneic human V γ 9V δ 2 T cells efficiently control the development of human glioblastoma brain tumors. *Oncoimmunology* 2016; **5**: e1168554.
- 42 Ahmed M, Hu J, Cheung NK. Structure based refinement of a humanized monoclonal antibody that targets tumor antigen disialoganglioside GD2. *Front Immunol* 2014; **5**: 372.
- 43 Himoudi N, Morgenstern DA, Yan M, Vernay B, Saraiva L, Wu Y *et al*. Human $\gamma\delta$ T lymphocytes are licensed for professional antigen presentation by interaction with opsonized target cells. *J Immunol* 2012; **188**: 1708–1716.
- 44 Korkaya H, Wicha MS. HER2 and breast cancer stem cells: more than meets the eye. *Cancer Res* 2013; **73**: 3489–3493.
- 45 Moynihan KD, Opel CF, Szeto GL, Tzeng A, Zhu EF, Engreitz JM *et al*. Eradication of large established tumors in mice by combination immunotherapy that engages innate and adaptive immune responses. *Nat Med* 2016; **22**: 1402–1410.
- 46 Brandes M, Willmann K, Bioley G, Levy N, Eberl M, Luo M *et al*. Cross-presenting human $\gamma\delta$ T cells induce robust CD8+ $\alpha\beta$ T cell responses. *Proc Natl Acad Sci USA* 2009; **106**: 2307–2312.
- 47 Meuter S, Eberl M, Moser B. Prolonged antigen survival and cytosolic export in cross-presenting human $\gamma\delta$ T cells. *Proc Natl Acad Sci USA* 2010; **107**: 8730–8735.
- 48 Khan MW, Curbishley SM, Chen HC, Thomas AD, Pircher H, Mavilio D *et al*. Expanded human blood-derived $\gamma\delta$ T cells display potent antigen-presentation functions. *Front Immunol* 2014; **5**: 344.
- 49 Piggott L, Omidvar N, Martí Perez S, French R, Eberl M, Clarkson RW. Suppression of apoptosis inhibitor c-FLIP selectively eliminates breast cancer stem cell activity in response to the anti-cancer agent, TRAIL. *Breast Cancer Res* 2011; **13**: R88.
- 50 Herold MJ, van den Brandt J, Seibler J, Reichardt HM. Inducible and reversible gene silencing by stable integration of an shRNA-encoding lentivirus in transgenic rats. *Proc Natl Acad Sci USA* 2008; **105**: 18507–18512.



This work is licensed under a Creative Commons Attribution 4.0 International License. The images or other third party material in this article are included in the article's Creative Commons license, unless indicated otherwise in the credit line; if the material is not included under the Creative Commons license, users will need to obtain permission from the license holder to reproduce the material. To view a copy of this license, visit <http://creativecommons.org/licenses/by/4.0/>

© The Author(s) 2017

**Synergistic targeting of breast cancer stem-like cells by
human $\gamma\delta$ T cells and CD8⁺ T cells**

Hung-Chang Chen^{1,*}, Noémie Joalland^{2,3}, John S. Bridgeman^{1,‡}, Fouad S. Alchami⁴, Ulrich Jarry^{2,3}, Mohd Wajid A. Khan¹, Luke Piggott^{1,5}, Yasmin Shanneik¹, Jianqiang Li⁶, Marco J. Herold^{6,7}, Thomas Herrmann⁶, David A. Price^{1,8}, Awen M. Gallimore^{1,8}, Richard W. Clarkson^{5,9}, Emmanuel Scotet^{2,3}, Bernhard Moser^{1,8}, and Matthias Eberl^{1,8}

SUPPLEMENTARY MATERIAL

Table S1. Basic histological examination of tumours derived from CSC-like cells or non-CSCs in NSG mice

Cell type and dose (cells/mouse)	Mouse no.	Mouse mammary tissue	Degree of differentiation	Possible squamous differentiation	Inter-cellular bridges	Necrosis	Apoptosis	Days that tumour size reached 1 cm diameter
10 ³ CSC-like cells per mouse	1	N	Poor	Y	0	None	0	112
	2	Y	Poor	N	0	Moderate	1	95
	3	Y	Poor	N	0	None	0	195
	4	Y	Poor	N	0	None	0	147
	5*	-	-	-	-	-	-	130
	6	N	Poor	N	0	Mild	0 [#]	144
2×10 ⁶ CSC-like cells per mouse	1	Y	Poor	N	0	None	0	51
	2	N	Poor	N	0	Extensive	1	53
	3	Y	Poor	N	0	Moderate	1	63
	4	Y	Poor	Y	Possible	Mild	0	46
	5	Y	Poor	N	0	None	0	60
	6	N	Poor	N	0	None	0	56
2×10 ⁶ non-CSCs per mouse	1	N	Well	Y	Present	None	0	91

*Tumour collected from this mouse was only analyzed by flow cytometry and was not included in histological examinations.

[#]Apoptosis noticed in infiltrated neutrophils.

Table S1. Basic histological examination of tumours derived from CSC-like cells or non-CSCs in NSG mice (continued)

Cell type and dose (cells/mouse)	Mouse no.	Cytoplasmic vacuoles	Multi-nucleate giant cells	Bizarre nuclei	Large nucleus	Intra-nuclear inclusion	Separate vascular proliferation	Inter-cellular bridges	Neutrophil infiltration	
10 ³ CSC-like cells per mouse	1	1	0	0	1	0	0	0	1	
	2	1	1	1	1	1	1	0	3	
	3	1	1	1	1	1	0	0	2	
	4	0	0	0	0	1	1	0	2	
	5*	–	–	–	–	–	–	–	–	
	6	1	1	1	1	1	1	1	0	2
2×10 ⁶ CSC-like cells per mouse	1	0	1	1	1	0	0	0	1	
	2	0	1	1	1	0	0	0	1	
	3	0	1	1	1	0	0	0	1	
	4	1	0	0	0	1	0	0	Possible	1
	5	0	0	0	0	0	0	0	0	
	6	0	0	0	0	1	0	0	0	0
2×10 ⁶ non-CSCs per mouse	1	0	0	0	0	0	0	Present	0	

*Tumour collected from this mouse was only analyzed by flow cytometry and was not included in histological examinations.

Table S2. Epithelial differentiation of tumours derived from CSC-like cells and non-CSCs in NSG mice

Cell type and dose (cells/mouse)	Mouse no.	% CD44 ^{hi} CD24 ^{lo} cells	% CD44 ^{lo} CD24 ^{hi} cells	% Tumour tissue with epithelioid appearance	Mitosis rate [#] of epithelial-like component	Mitosis rate [#] of mesenchymal-like component	AE1/AE3 IHC score [§]	% AE1/AE3 ⁺ stain of whole tissue	Vimentin IHC score	% Vimentin ⁺ stain of whole tissue
10 ³ CSC-like cells per mouse	1	40.4	7.98	25	44	120	1	25	3	75
	2	54.2	8.8	80	57	21	2	80	3	20
	3	0.847	15.6	85	42	33	1	5	3	95
	4	2.11	56.3	10	N/A	22	1	5	3	95
	5*	26	64.2	–	–	–	–	–	–	–
	6	0.54	19.9	100	113	N/A	2	75	3	25
2×10 ⁶ CSC-like cells per mouse	1	56.6	4.18	100	68	N/A	1	10	3	90
	2	9.6	28.3	100	21	N/A	2	20	3	80
	3	46.3	9.24	100	70	N/A	1	5	3	95
	4	15.3	15.4	100	59	N/A	0	0	3	100
	5	30.9	23.8	1	N/A	39	0	0	3	100
	6	20	18.4	50	35	35	1	20	3	80
2×10 ⁶ non-CSCs per mouse	1	0.024	96.4	100	20	N/A	3	100	1	0

*Tumour collected from this mouse was only analyzed by flow cytometry and was not included in histological examinations.

[#]Mitotic rate: mitosis per 10 high power fields (0.5 mm in diameter) in the epithelioid or mesenchymal component; N/A is applied if the area is smaller than 0.5 mm in diameter.

[§]IHC score: strength of the staining for indicated marker

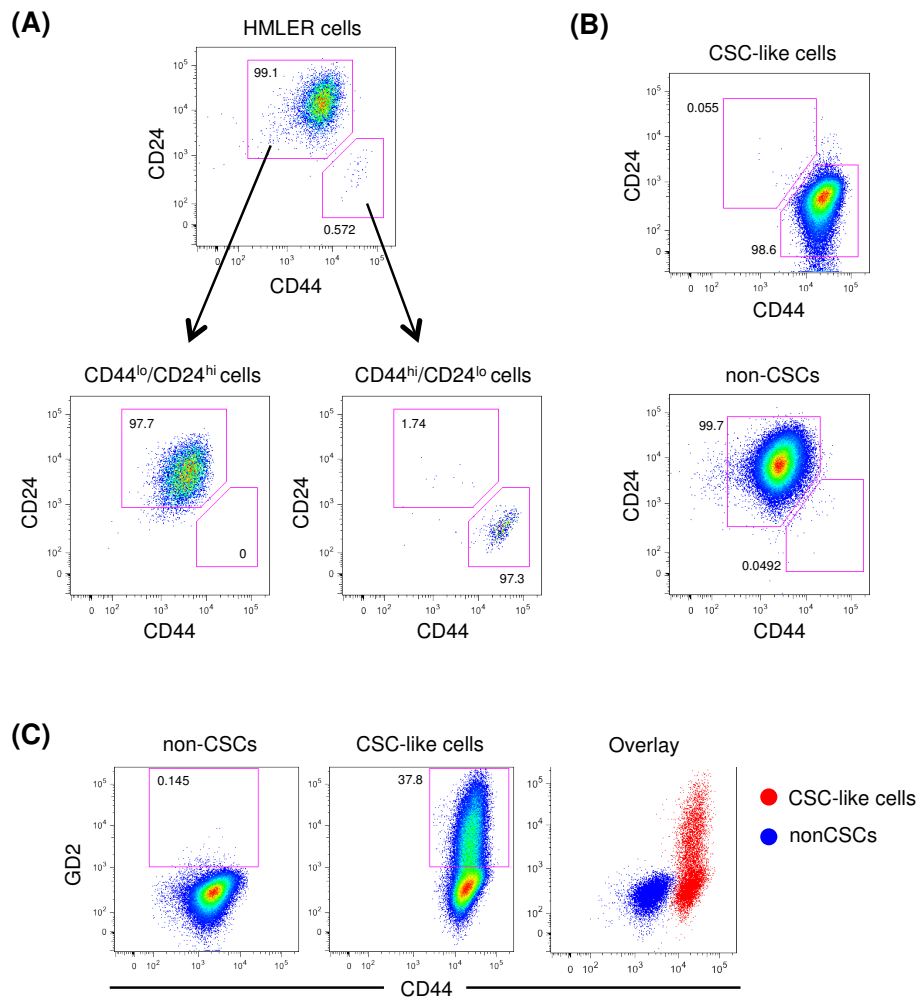


Figure S1. Isolation of CD44^{hi} CD24^{lo} CSC-like cells and CD44^{lo} CD24^{hi} non-CSCs from the parental HMLER cell line. (A) HMLER cells were labelled with anti-CD44 and anti-CD24 mAbs and sorted to purities >99% using a BD FACS Aria cell sorter. (B) CD44/CD24 expression profiles of the sorted cell populations after the sort and (B) after 32 days of culture under normal adherent culture conditions. (C) GD2 expression of CSC-like cells and non-CSCs maintained in normal adherent culture as assessed by flow cytometry.

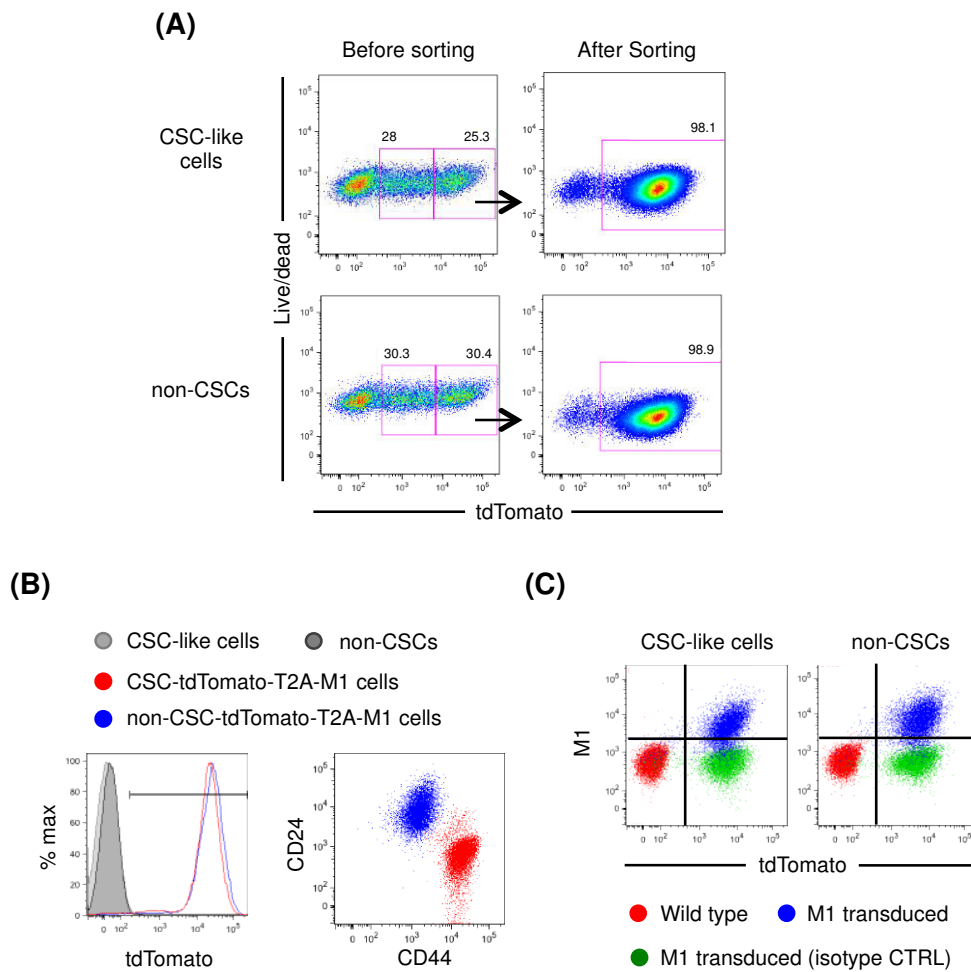


Figure S2. Generation of $CD44^{hi} CD24^{lo}$ CSC-like cells and $CD44^{lo} CD24^{hi}$ non-CSCs co-expressing tdTomato and FluM1. (A) CSC-like cells and non-CSCs were transduced with lentiviral particles delivering a bicistronic tdTomato-T2A-M1 gene cassette. Successfully transduced tdTomato^{hi} cells were sorted to purities >99% using a BD FACS Aria cell sorter. (B) tdTomato expression and CD44/CD24 phenotype of transduced CSC-like cells and non-CSCs as assessed by flow cytometry. (C) Intracellular expression of FluM1 by transduced CSC-like cells and non-CSCs as assessed by flow cytometry.

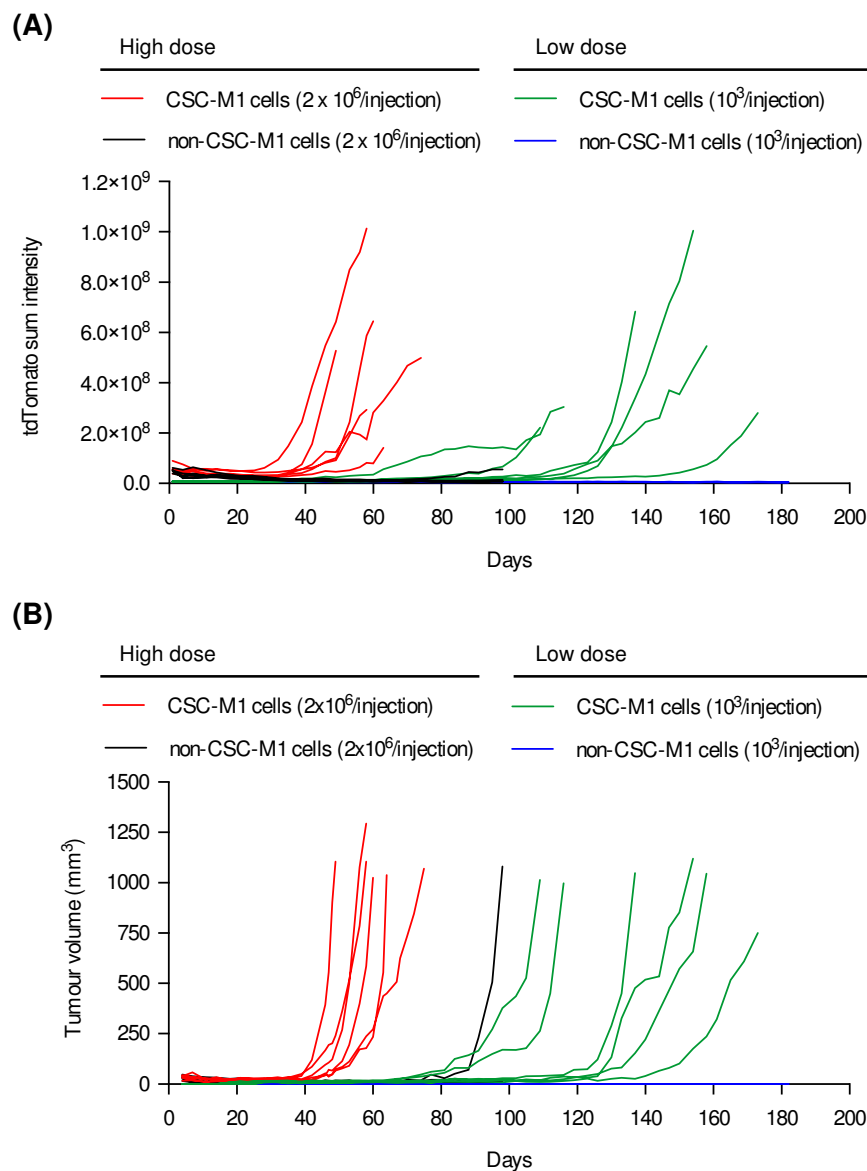


Figure S3. Development of tumours derived from CSC-like cells and non-CSCs co-expressing tdTomato and FlucM1. CSC-like cells or non-CSCs were xenotransplanted with matrigel into the mammary fat pad of NSG mice at two different doses; at a high dose of 2×10^6 cells/mouse and at a low dose of 1×10^3 cells/mouse ($n=6$ per group). Tumour development and growth were monitored **(A)** by live imaging of tdTomato using the Kodak Fx-Pro system and **(B)** by caliper measurements.

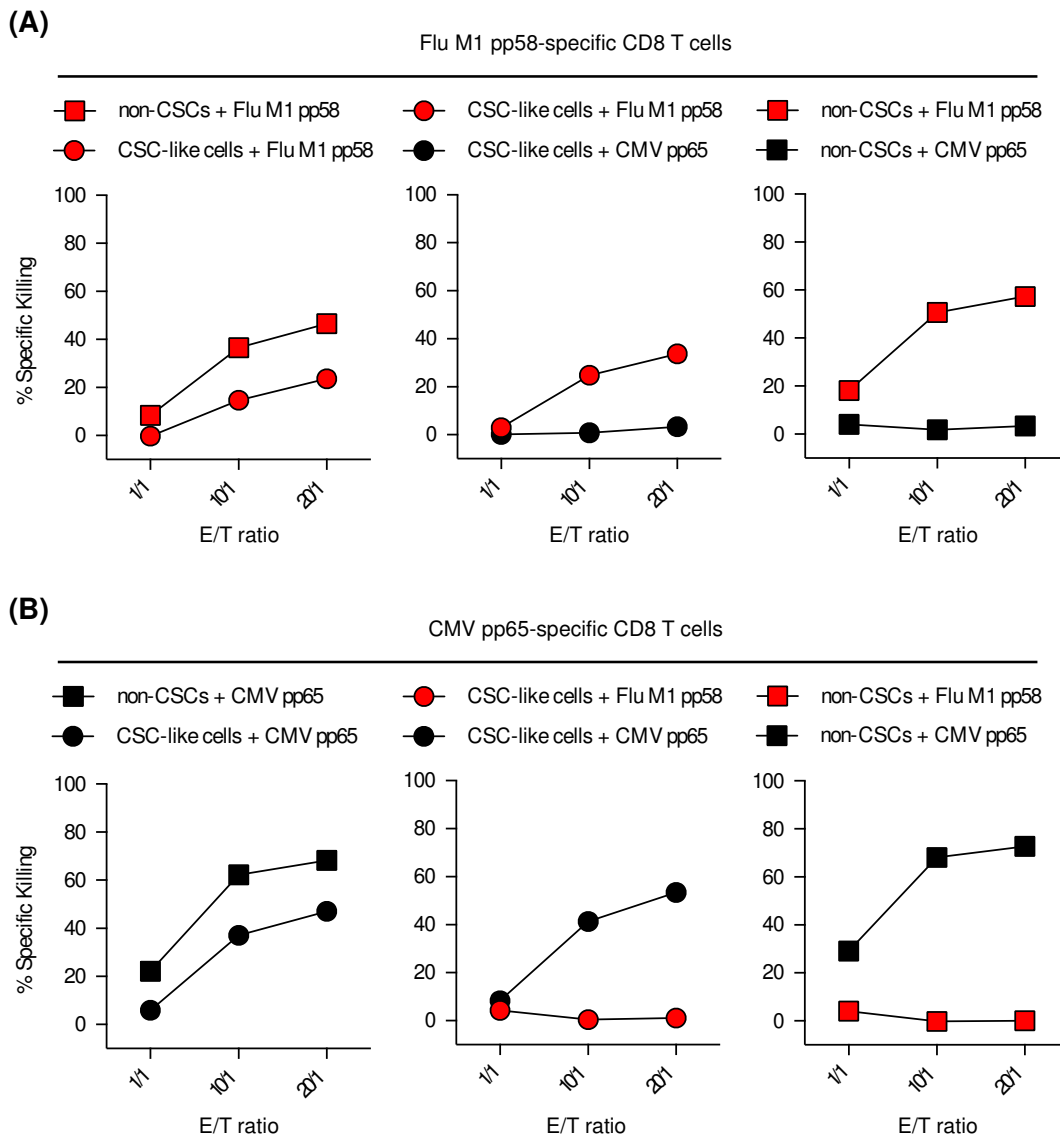


Figure S4. Increased resistance of CSC-like cells to MHC-restricted cytotoxic CD8⁺ T cells. CSC-like cells and non-CSCs were pulsed with FluM1 p58-66 peptides or CMV pp65 p495-503 peptides, labelled with CellVue or PKH26, and mixed in equal numbers to generate the different combinations as shown in the figure. These combinations were then used as targets for killing by (A) FluM1 specific CD8⁺ T cells, or (B) CMV pp65-specific CD8⁺ T cells, at different effector:target (E:T) ratios. Specific killing of CellVue and PKH26-labelled target cells was assessed by live/dead staining and analysed by flow cytometry. Data shown are representative of two independent experiments performed in duplicate.

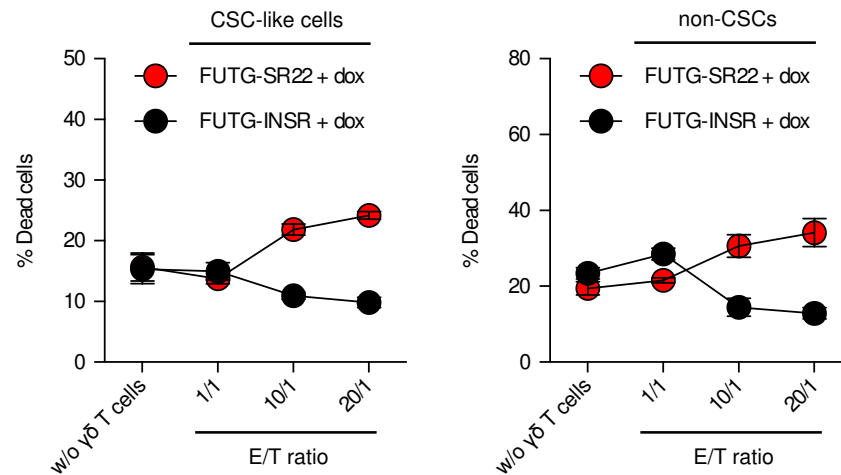


Figure S5. Sensitisation of CSC-like cells and non-CSCs to $\gamma\delta$ T cell-mediated killing by FPPS knockdown. CSC-like cells and non-CSCs transduced with FUTG-INSR control vector or FUTG-SR22 vector were pre-treated overnight with 0.1 $\mu\text{g}/\text{ml}$ doxycycline to induce expression of shRNA targeting FPPS in cells with FUTG-SR22 expression. After overnight treatment, CSC-like cells and non-CSCs transduced with FUTG-INSR or FUTG-SR22 vector were mixed in equal numbers and used as targets for $\gamma\delta$ T cell-mediated killing, at different effector:target (E:T) ratios. Specific killing of CellVue and PKH26-labelled target cells was assessed by live/dead staining and analysed by flow cytometry. Data shown are from one experiment performed in duplicate.

Movie S1. Killing of CSC-like cells by antigen-specific CD8⁺ T cells. FluM1-specific CD8⁺ T cells were loaded with Fura2 and added to FluM1-transduced target cells. The video shows the kinetics of intracellular Ca²⁺ levels and tumour cell killing by CD8⁺ T cells, and is representative of four experiments performed. Cells were illuminated every 10 seconds, videos were recorded with a time lapse of 12 images per second.

Movie S2. Sensitisation of CSC-like cells to killing by antigen-specific CD8⁺ T cells using IFN- γ . FluM1-specific CD8⁺ T cells were loaded with Fura2 and added to FluM1-transduced target cells that had been pre-treated with 100 U/ml IFN- γ for 24 hours. The video shows the kinetics of intracellular Ca²⁺ levels and tumour cell killing by CD8⁺ T cells, and is representative of four experiments performed. Cells were illuminated every 10 seconds, videos were recorded with a time lapse of 12 images per second.

Movie S3. Sensitisation of CSC-like cells to killing by antigen-specific CD8⁺ T cells using V γ 9/V δ 2 T cells. FluM1-specific CD8⁺ T cells were loaded with Fura2 and added to FluM1-transduced target cells that had been pre-treated with $\gamma\delta$ T cell conditioned medium for 24 hours. The video shows the kinetics of intracellular Ca²⁺ levels and tumour cell killing by CD8⁺ T cells, and is representative of four experiments performed using $\gamma\delta$ T cells from three different donors. Cells were illuminated every 10 seconds, videos were recorded with a time lapse of 12 images per second.

Article 7 : Glutamine uptake and utilization of human mesenchymal Glioblastoma in orthotopic mouse model

Kristell Oizel¹, Chendong Yang¹, Ophelie Renoult⁵, Quyen N. Do², Noemie Joalland^{5,6}, Xiaofei Gao¹, Bookyung Ko¹, François Vallette⁵, Woo-Ping Ge^{1,3}, Ralph J Deberardinis¹, Claire Pecqueur^{5,6}

¹ Children's Research Institute, UT Southwestern Medical Center, Dallas, TX 75390, United States ; ² Department of Radiology, UT Southwestern Medical Center, 5323 Harry Hines Blvd, Dallas, TX 75390-9061, United States ; ³ Department of Pediatrics, Neuroscience, Neurology & Neurotherapeutics, University of Texas Southwestern Medical Center, Dallas, TX 75390, United States ; ⁴ Advanced Imaging Research Center, UT Southwestern Medical Center, 5323 Harry Hines Blvd., Dallas, TX, 75390-8568, United States ; ⁵ CRCINA, INSERM, CNRS, Université de Nantes, France ; ⁶ Labex Immunotherapy Graft Oncology

Le glioblastome multiforme (GBM) est connu pour sa forte hétérogénéité cellulaire et moléculaire. Il a également été mis en évidence *in vitro* que le métabolisme de la glutamine permettait de discriminer le sous-type mésenchymateux (MES) des autres sous-types moléculaires de GBM sur des primocultures dérivant d'échantillons de patients. Afin d'étudier le métabolisme glutaminergique *in vivo*, nous avons utilisé des modèles murins de xéno greffe orthotopique. Les tumeurs se développant suite à l'implantation de primocultures de GBM présentant des profils moléculaires différents ont été analysées par spectrométrie de masse afin d'évaluer l'enrichissement en ¹³C (carbone 13) suite à l'injection de ¹³C-glutamine *in vivo*. Nos résultats confirment que les primocultures de sous-type MES captent et utilisent davantage la glutamine que les autres sous-type de GBM *in vivo*. De plus, la glutamine-synthase et la transglutaminase-2 sont exprimées en accord avec le profil métabolique des primocultures de GBM. Ainsi, le métabolisme de la glutamine représente une cible thérapeutique d'intérêt pour le traitement des patients atteints de GBM du sous-type MES.

Soumis

Glutamine uptake and utilization of human mesenchymal Glioblastoma in orthotopic mouse model

Kristell Oizel¹, Chendong Yang¹, Ophelie Renoult⁵, Quyen N. Do², Noemie Joalland^{5,6}, Xiaofei Gao¹, Bookyung Ko¹, François Vallette⁵, Woo-Ping Ge^{1,3}, Ralph J Deberardinis¹, Claire Pecqueur^{5,6, #}

¹ Children's Research Institute, UT Southwestern Medical Center, Dallas, TX 75390, United States

² Department of Radiology, UT Southwestern Medical Center, 5323 Harry Hines Blvd, Dallas, TX 75390-9061, United States

³ Department of Pediatrics, Neuroscience, Neurology & Neurotherapeutics, University of Texas Southwestern Medical Center, Dallas, TX 75390, United States

⁴ Advanced Imaging Research Center, UT Southwestern Medical Center, 5323 Harry Hines Blvd., Dallas, TX, 75390-8568, United States

⁵ CRCINA, INSERM, CNRS, Université de Nantes, France

⁶ Labex Immunotherapy Graft Oncology

corresponding author : Claire Pecqueur, CRCINA, INSERM, University, de Nantes, France, 8 quai Moncoussu BP 70721, 44007 Nantes, France. Phone: 332 0228 080325; Fax: 332 0228 080204; E-mail:claire.pecqueur@univ-nantes.fr;

Abstract

Background : Glioblastoma (GBM) are highly heterogeneous on the cellular and molecular basis. It has been proposed that glutamine metabolism *in vitro* discriminates GBM molecular subtypes of primary cells established from human tumors. **Methods** : To study glutamine metabolism *in vivo*, we used a human orthotopic mouse model for GBM. Tumors evolving from the implanted primary GBM cells expressing different molecular signatures were analyzed using mass spectrometry for their metabolites pools and enrichment in carbon 13 (¹³C) after ¹³C-glutamine infusion. **Results** : Our results showed that mesenchymal GBM tumors displayed increased glutamine uptake and utilization compared to both control brain tissue and other GBM subtypes. Furthermore, both glutamine synthase and transglutaminase-2 were expressed accordingly to GBM metabolic phenotypes. **Conclusion** : Thus, our results show enhanced glutamine metabolism *in vivo* of human mesenchymal GBM subtype.

Introduction

With an incidence of 5 per 100000, Glioblastoma (GBM), grade IV glioma, is the most frequent primary brain tumor in adults. Its prognosis is dismal, with a 5-year survival under 5%, and a mean survival of 15 months despite aggressive treatment. These treatments include surgery followed by concomitant radio- and chemotherapy with temozolomide. Unfortunately, no significant improvement in the therapy has been made since 2009 with the inclusion of temozolomide as a radiosensitizer in the clinical protocol (1). Many factors could explain failure of current therapies. Besides being highly infiltrative, essentially eliminating the possibility of complete resection, GBM display a very heterogeneous profile on a cellular and molecular basis leading to different patient responses to identical treatment (2). In the past 10 years, 4 molecular subtypes (mesenchymal, classical, neural and proneural) have been established based on genetic and molecular alterations as well as patient's prognosis (3,4). However, a recent study with extensive gene expression profiling both at the whole tumor level and individual tumor cells highlights 2 main tumor-intrinsic transcriptional subtypes, the mesenchymal and the non-mesenchymal (defined in our study as CNP) (5) .

From the cellular heterogeneity point of view, the presence of cancer stem cells (CSC) inside the tumor could play a role in the resistance through their low proliferative profile and their enhanced DNA repair machinery (6). Furthermore, CSC generate cellular heterogeneity by installing a differentiation hierarchy leading to various distinct cell types present within the tumor (7). Unfortunately, the efficacy of CSC targeting has been difficult to study due to the limited characterization of CSC markers. Several markers, such as CD133, CD44, CD166, CD24, and ALDH1 activity, have proven useful for prospective isolation of CSCs in multiple solid tumors (8). However, CSC marker expression is not uniform between tumor types. For instance, while CD133 has been used as a marker to identify CSCs in GBM, it is not expressed by CSCs belonging to the mesenchymal subtype (9).

We have recently shown that human primary cultures derived from GBM patient after surgery capture both the molecular and the cellular heterogeneity, and as such are powerful tools for investigating tumor biology. Using these cells, we showed that, *in vitro*, the molecular signature mirrors a metabolic signature. In particular, while the CNP subtype strongly relied on glucose, survival and proliferation of the mesenchymal GBM subtype was strongly dependent on

glutamine. However, the importance of glutamine dependence *in vivo* for GBM is controversial. First, it has been clearly shown that the microenvironment can modulate the metabolism of cancer cells (10). Second, it has been demonstrated that, using an orthotopic murine model of GBM deriving from 3 different primary human GBM, tumor cells used glucose rather than glutamine *in vivo* to produce energy and to provide an anaplerotic flux for the TCA cycle (11). Cells derived from these tumors did not require glutamine to sustain viability and proliferation when cultured *ex vivo*.

Thus, glutamine dependence is not a universal feature of human-derived GBM cells and tumors. Here, using an orthotopic murine model of GBM deriving from either mesenchymal or CNP GBM subtypes, we provide evidence of enhanced glutamine uptake and utilization in the mesenchymal GBM subtype.

Materials and Methods

Unless stated otherwise, all cell culture material was obtained from Life Technologies (Cergy Pontoise, France) and chemicals were from Sigma-Aldrich (St. Louis, MO, USA).

Human GBM tumor cells

Primary GBM cultures were derived after mechanical dissociation from high-grade glioma operated on 4 patients. All procedures involving human participants were in accordance with the ethical standards of the ethic national research committee and with the 1964 Helsinki declaration and its later amendments or comparable ethical standards. Informed consent was obtained from all individual participants included in this study. Primary GBM cells were cultured in defined medium (DMEM/HAM-F12, 2 mM L-glutamine, N2 and B27 supplement, 2 μ g/ml heparin, 20 ng/ml EGF and 25 ng/ml bFGF, 100 U/ml penicillin and 100 μ g/ml streptomycin). All the experiments with primary GBM cells were performed at early passages. Cells were checked for mycoplasma regularly.

Western blots and immunohistochemistry

Fifty micrograms of cell lysates were used for western blots analysis (12). Primary antibodies were used according to the manufacturer's recommendations and secondary antibodies coupled to HRP were used. For immunochemistry, paraffin-embedded specimens were fixed in 4% PFA and then processed as previously described in (13). Primary antibody was a rabbit anti-human MHC class I (clone EPR1394Y; Abcam).

Seahorse analysis

Mitochondrial oxygen consumption (OCR) and extracellular acidification rate (ECAR) were measured in non-buffered medium supplemented with glucose (5 mmol/L), pyruvate (1 mmol/L), and glutamine (2 mmol/L) using an XF24 Analyzer (Seahorse Bioscience). Specific mitochondrial respiration fueled with either glucose (Δ OCR_{GLC}) or glutamine (Δ OCR_{GLN}) was determined as previously described (9) by the difference of the mean of the 3 values of OCR in the absence of substrate and the mean of the 4 values of OCR after injection of the substrate. Glucose was injected to a final concentration of 10 mmol/L and glutamine 2 mmol/L.

Orthotopic injections of human primary GBM cells in NSG mice

All animal experiments were carried out in accordance with protocols approved by the Institutional Animal Care and Use Committee at University of Texas Southwestern Medical Center, and to French institutional guidelines (Agreement # 00186.02; Regional ethics committee of the Pays de la Loire, France). For global metabolites enrichment, orthotopic injections of 10^4 human GBM cells were performed using a stereotactic frame (Stoelting) at 2 mm on the right of the medial suture and 0.5 mm in front of the bregma, depth: 2.5 mm. Animals were observed daily and euthanized when characteristic symptoms occurred, such as reduced mobility and significant weight loss. For ^{13}C enrichment infusions, 10^4 tumor cells in suspension were transplanted in mouse brains at the same coordinates via a glass micropipette (WIRETROL, DRUMMOND[®]) with a 50 μm tip generated by a Micropipette Puller (P-97, Sutter Instrument Co.). Tumor growth was regularly monitored using a 1T Desktop magnetic resonance scanner (M2 Compact, Aspect Imaging, Shoham, Israel) and a mouse head coil when characteristic symptoms started to occur such as weight loss. The general T1-weighted and T2-weighted imaging was performed with a spin echo (TR/TE = 326/13ms) and a fast spin echo (TR/TE = 2500/80ms) sequence respectively (prone position). When the diameter of the tumor reached 3mm, mice were infused with $^{13}\text{C}_5$ glutamine (99% enrichment; Cambridge Isotope Laboratories, Andover, MA) through the jugular vein. A bolus of 187 mg/kg of labeled glutamine diluted in 0.2mL saline was first injected within 1min, then 5 mg/kg/min was perfused during 5 h. Blood was collected before $^{13}\text{C}_5$ glutamine perfusion then at different time points until the end of the perfusion and the plasma was used to determine the enrichment in $^{13}\text{C}_5$ glutamine. At the end of the perfusion, mice were decapitated and brain and liver tissue were collected. Brain tumor and contralateral tissues were rapidly dissected under a microscope, weighed, transferred in 1mL of 80% methanol solution and stored at -80°C before further analysis.

Metabolite extraction and measurement of ^{13}C fractional enrichments in tissue and cells samples

Snap-frozen tissues or cell samples were homogenized in ice-cold methanol. Metabolites extraction for LC-MS/MS analysis were prepared as previously described (14). Peaks were normalized against the total ion count. For ^{13}C enrichments, homogenates were subjected to three rapid freeze-thaw cycles by transferring them from liquid nitrogen to a 37°C water bath. Samples were centrifuged at 13000g at 4°C for 15min and the supernatant transferred to a screw-topped glass tube with 50nM of sodium-2-oxobutyrate then completely evaporated at

42°C under blown air. Evaporated samples were re-suspended in 30uL pyridine containing methoxyamine (10mg/mL). After 10 min at 70°C, 70uL of MTBSTFA reagent was added and heated at 70°C for 1h. GC-MS was performed using an Agilent 6890N Gas Chromatograph coupled to an Agilent 5973 Mass Selective Detector (Agilent Technologies, Santa Clara, CA). One microliter of each standard or sample was injected and analyzed in scan mode.

Measurement of ¹³C Fractional Enrichments in blood

Blood samples were processed to measure ¹³C₅ enrichment in glutamine by gas chromatography-mass spectrometry (GC-MS), as previously described (11). A three-point standard curve was prepared by mixing unenriched glutamine with ¹³C₅ glutamine such that 0%, 50%, or 100% of glutamine was ¹³C labeled. GC-MS was performed using an Agilent 6890N Gas Chromatograph coupled to an Agilent 5973 Mass Selective Detector (Agilent Technologies, Santa Clara, CA). One microliter of each standard or sample was injected and analyzed in scan mode. Fragment ions of *m/z* 258 (unenriched) and 263 (enriched) ¹³C₅ glutamine were quantified for both standard and experimental samples. Linear regression was used to calculate the enrichment of each plasma sample.

Statistical Analysis

Data were analyzed and statistical analyses were performed using GraphPad Prism 6.00 (GraphPad Software, San Diego, CA, USA). Data points are expressed as mean ± SD unless otherwise indicated. For statistical analyses, results are compared to CTR group unless stated otherwise. * *p*<0.05, ** *p*<0.01, *** *p*<0.001. Hierarchical clustering was realized using XLSTAT software.

Results

Metabolic and molecular signatures of human GBM primary cultures in vitro

Tumor samples from 4 different patients were dissociated and cultured in defined media in order to maintain their original molecular and cellular heterogeneity. As shown in Figure 1A, unsupervised hierarchical transcriptomic analysis clearly identified 2 out of 4 primary cultures as mesenchymal (M1, M2) while the other 2 belong to the CNP subtype (CNP1, CNP2). These primary cultures exhibited genomic alterations commonly observed in human GBM (Figure 1B). These included amplification of *EGFR* and *PDGFR*. All primary cultures had loss of *INK4a/ARF* and expressed *PTEN*. We next examined expression of several enzymes involved either in glycolysis or glutamine metabolism (Figure 1C). For most enzymes, we did not observe any difference in their expression. However, transglutaminase 2 (TGM2) was exclusively expressed in mesenchymal GBM cells while glutamine synthase (GS) expression was restricted to CNP cells. Analysis performed using the Seahorse technology, measuring respectively the mitochondrial respiration (OCR) and glycolysis through extracellular acidification (ECAR), did not show difference in global metabolism between mesenchymal and CNP cells (Figure 1D). However, a finer analysis of the substrates fueling mitochondrial respiration clearly distinguished the 2 subtypes (Figure 1E and 1F). All primary cells used glucose to sustain their oxidative metabolism, but CNP cells demonstrated enhanced glucose oxidation compared to mesenchymal cells. Furthermore, mesenchymal cells are also able to use glutamine to sustain oxidative phosphorylation in contrast to CNP cells. Altogether, our results clearly discriminate mesenchymal and CNP cultures *in vitro*.

Human orthotopic tumors (HOT) are enriched for intermediates of glucose metabolism

To investigate tumor metabolism *in vivo*, 2 human primary tumor cells (M1 and CNP1) were implanted into the striatum of one hemisphere (see details in methods) of NOD-SCID gamma mice (NSG) (Figure 2A). After 3 to 5 months, the mice presented symptoms as the result of an expanding tumor mass. Brains were then collected, split between the tumor and the contralateral hemispheres (defined here as the CTR) (Figure 2A) and immediately frozen for metabolic studies. Histological analysis using anti-MHC-I antibodies demonstrated that most of the tumor mass resided within one hemisphere (Figure 2B). We then used liquid chromatography–tandem mass spectrometry (LC-MS/MS) to determine the relative quantities of 105 metabolites extracted from each specimen. This analysis revealed a number of metabolites enriched in the tumor-containing hemispheres relative to the contralateral hemisphere (Figure 2C).

In particular, glycolytic products and intermediates, such as glucose, glucose 6-phosphate (G6P) and lactate, were significantly enriched in tumor with no significant differences between subtypes (Figure 2 D-F). Ribose 5P, an intermediate of the pentose phosphate pathway, was also significantly more abundant in tumors compared to CTR brain (Figure 2G).

Glutamine and Glutamine-derived metabolites from HOT and control brain

We next examined closely relative enrichment of glutamine and glutamine-derived metabolites from each specimen. Interestingly, our results showed higher glutamine abundance in M1 tumors but not in CNP1 tumors (Figure 3A). Glutamate, which can be derived from glutamine through the activity of glutaminase, was more abundant in M1 tumors compared to either CTR brain or CNP1 tumors (Figure 3B). Ammonia (NH_4^+) is the byproduct of both glutaminase and glutamate dehydrogenase (GDH), the latter converting glutamate to α -ketoglutarate, entry point into the tricarboxylic cycle (TCA) where it will be converted into succinate and malate. Interestingly, mesenchymal HOT displayed higher levels of succinate, malate and ammonia (Figure 3C-E). Finally, glutathione is a tripeptide of glutamate, cysteine and glycine and its formation is highly dependent on glutamine in some cells. Again, glutathione was more abundant in M1 tumors compared to CTR brain or CNP1 tumors (Figure 3F). Altogether our results showed that mesenchymal HOT were enriched in glutamine and glutamine-derived metabolites compared to either CTR brain or CNP tumor.

Metabolism of ^{13}C -Glutamine in HOT-bearing mice

To further explore glutamine metabolism *in vivo*, 2 human primary tumor cells from each subtype were implanted into the striatum of NSG mice (Figure 4A). Tumor mass expansion was followed over time using MRI. When the tumor reached 3mm, the mice were infused with $[\text{U-}^{13}\text{C}]$ glutamine as a bolus over 1 min followed by a continuous 5-h infusion. A time-course was performed to establish maximal ^{13}C -glutamine enrichment in the plasma of the HOT-bearing mice. For all infused mice, 40% or more of the plasma glutamine was labeled after 60 min and this level was maintained for the duration of the infusion (Figure 4B). At the end of the infusion, mice were sacrificed and both the liver and the brain were rapidly removed. The tumor and the contralateral healthy tissue were isolated. Analysis of metabolites extracted from the liver at 300 min showed in most mice a 20% enrichment of ^{13}C -glutamine (Figure 4C). Finally, labeled glutamine and glutamine-derived metabolites extracted from CTR hemispheres were analyzed. On average, an enrichment of ^{13}C -Glutamine of $3.6 \pm 0.5\%$ was measured in

CTR tissues without any noticeable differences between HOT molecular signatures (Figure 4D). To assess metabolism of glutamine in the brain, ^{13}C -enrichment was examined in glutamate and several TCA cycle intermediates, and then normalized to the level of labeled glutamine in the tissue. Relative ^{13}C labeling on all carbons in glutamate (m+5), fumarate (m+4) and malate (m+4) reached 20 to 40%. Levels of the m+4 isotopologue of citrate (^{13}C -labeled in four carbons) were higher than levels of m+5 isotopologue of citrate (respectively 31 ± 14 vs 9 ± 6), the later being an indicator of reductive carboxylation. Again, no significant differences were observed in metabolites enrichment from CTR hemispheres of HOT-bearing mice from different subtypes.

We next examined ^{13}C -labeled metabolites from tumors in all mice. Although absolute levels of ^{13}C -labeled glutamine were low, we measured on average a 4-fold enrichment of ^{13}C -glutamine in tumors compared to CTR tissues (mean \pm sem of all tumors: $+4.1\pm 0.6\%$) (Figure 5A). Furthermore, these levels were significantly higher in tumors from mice-bearing mesenchymal HOT compared to mice-bearing CNP HOT (respectively 5.7 ± 0.8 vs 2.1 ± 0.3 , $p=0.0025$). We then examined labeling in metabolites potentially derived from ^{13}C -glutamine. In CNP tumors, ^{13}C -glutamine was metabolized to glutamate, fumarate, malate and citrate in a similar manner to CTR brain (Figure 5B). In contrast, most mesenchymal tumors displayed an increased in m+5 glutamate compared to its level in CTR tissue or CNP tumors. Labeling of downstream metabolites was not significantly different between these two molecular subtypes or between the tumor and CTR tissues. Altogether, our results provide evidence for increased glutamine uptake and conversion to glutamate in mesenchymal GBM tumors compared to CNP tumors and CTR brain.

Discussion

Given the energy-generating and biosynthetic roles that glutamine plays in growing cells, inhibition of glutaminolysis might have the potential to effectively target cancer cells. We analyzed nutrient metabolism in a biologically accurate mouse model of GBM that takes into account their molecular signatures. Our data show that mesenchymal GBM cells exhibited increased glutamine uptake and utilization compared to other GBM molecular subtypes. In fact, the comparison of both the metabolite pools and ^{13}C metabolism demonstrated that first all GBM display important glycolytic substrates pools in agreement with a glycolytic metabolism, and second a significant accumulation of glutamine and glutamine-derived metabolites is observed in mesenchymal tumors. Significant glutamine uptake and metabolism have not been reported in similar *in vivo* metabolic studies (11). This apparent contradiction might be explained by the lack of mesenchymal primary GBM cells in those studies. However, our results are in agreement with our recent publication establishing *in vitro* that metabolic substrates dependency reflects molecular subtypes (9).

Glutamine homeostasis is controlled by GS and GLS, two enzymes catalyzing opposite reactions. GS catalyzes the condensation of glutamate and ammonia to form glutamine whereas GLS, which exists as at least 2 isoforms, hydrolyses glutamine to glutamate and ammonia. Tardito et al. (15) recently showed a causal link between GS expression and glutamine independence. In line with this observation, we report here that expression of GS is restricted to CNP GBM cells, which have been shown to be glutamine-independent for their growth and survival (9). In contrast, mesenchymal GBM cells do not express GS, at least in presence of glutamine, and rely on glutamine for their proliferation. Knowing that several subtypes coexist within the same tumor (16), GS expression may accord with specific molecular subtypes localization within the tumor and relative glutamine enrichment of the microenvironment. Furthermore, one can suggest existence of a dialogue between glutamine synthesis and utilization where GS expressing cells supply glutamine to GS negative ones.

Glutamine is used for both energy generation and as a source of carbon and nitrogen for biomass accumulation. Indeed, following the conversion of glutamine to glutamate by GLS, glutamate is subsequently converted either to α -ketoglutarate through an ammonia-releasing process or to other amino acids by several non-ammonia-producing transaminases. Glutamine can also serve

as an alternative carbon source to fuel fatty acids synthesis through reductive carboxylation of α -ketoglutarate to produce citrate. Finally, glutamine is a precursor of glutathione in particular by being responsible directly and indirectly of 2 out of 3 amino acid components of glutathione, glutamate and glycine. Our data suggest that the increased glutamine utilization and conversion to glutamate in mesenchymal GBM cells may not be associated with any differences in glutamine's contributions to the TCA cycle. In this regard, it is interesting to consider that glutamine's major role in these tumors is to supply glutathione synthesis. This could be important given the larger glutathione pool in mesenchymal tumors. These results are at odds with our previous hypothesis, based on *in vitro* experiments, suggesting that in mesenchymal GBM cells, glutamine was mostly used as an energy-generating substrate (9).

These discrepancy between our *in vitro* and *in vivo* data may reflect an adaptation to culture condition or a loss of microenvironmental constraints which have been shown to shape metabolic abilities (10). In fact, these results may reflect the extended metabolic abilities and plasticities of tumor cells depending on their microenvironment.

Recent advances in molecular biology have highlighted the molecular and genetic heterogeneities of GBM. Understanding the impact of these signatures on tumor development and its role in treatment resistance is primordial to design efficient therapies. For instance, the O⁶-methylguanine-DNA methyltransferase (MGMT) promoter methylation status is an important prognostic factor in the treatment of glioblastoma (17). Bevacizumab, a humanized monoclonal antibody against VEGF, has recently been included in several clinical trials and seems to improve prognosis of recurrent GBM (18,19). During the past decade, targeting cancer metabolism has emerged as a promising strategy for the development of selective antineoplastic agents. The potential to develop personalized metabolically targeted cancer therapies assumes that some tumors have metabolic preferences and vulnerabilities that distinguish them from normal tissue. Whereas additional metabolic investigations of glutamine metabolism are definitively needed *in vivo*, ¹³C metabolism analysis in H₂O₂-bearing mice combined with increased survival of mice-bearing mesenchymal GBM tumors when glutamine metabolism is inhibited (9) point out glutamine metabolism as a potential metabolic marker and thus therapeutic target of mesenchymal GBM tumors. This could be important given that mesenchymal GBM are the most resistant to therapy and radiation promotes a molecular shift from CNP to mesenchymal (20).

Declaration

All procedures involving human participants were in accordance with the ethical standards of the ethic national research committee and with the 1964 Helsinki declaration and its later amendments or comparable ethical standards. Informed consent was obtained from all individual participants included in this study. This manuscript is not concurrently submitted elsewhere, and all authors are aware of and fully agree with its contents and declare no conflicts of interest.

Conceptualization, C.P. and R.J.B. ; Methodology, KO, C.Y, N. J. ; Investigation, K.O., O.R., C.Y., C.P., Resources, C.P., F.M.V., Writing-Original Draft, C.P.; Writing-Review&Editing, all authors ; Funding acquisition, C.P., R.J.B., WP.G.

Acknowledgments

We thank the metabolic platform Mikaël Croyal and Audrey Aguesse from the Mass Spectrometry platform of Nantes University for expert technical assistance. We would like to thank Kevin Andre for technical help and F. Paris and Robert E. Lenkinski for scientific discussion. Kristell Oizel was funded by ARC foundation. This work was supported by N.C.I. (R35 CA220449) to R.J.B, Exploratory/Development Grant from NINDS (R21NS099950) to W.-P.G., "Ligue contre le cancer" and Region Pays de la Loire to C.P.. This work was realized in the context of the LabEX IGO program (ANR-11-LABX-0016-01).

References

1. Stupp R, Hegi ME, Mason WP, van den Bent MJ, Taphoorn MJB, Janzer RC, et al. Effects of radiotherapy with concomitant and adjuvant temozolomide versus radiotherapy alone on survival in glioblastoma in a randomised phase III study: 5-year analysis of the EORTC-NCIC trial. *Lancet Oncol.* 2009 May;10(5):459–66.
2. Olar A, Aldape KD. Using the molecular classification of glioblastoma to inform personalized treatment. *J Pathol.* 2014 Jan;232(2):165–77.
3. Phillips HS, Kharbanda S, Chen R, Forrest WF, Soriano RH, Wu TD, et al. Molecular subclasses of high-grade glioma predict prognosis, delineate a pattern of disease progression, and resemble stages in neurogenesis. *Cancer Cell.* 2006 Mar;9(3):157–73.
4. Verhaak RGW, Hoadley KA, Purdom E, Wang V, Qi Y, Wilkerson MD, et al. Integrated genomic analysis identifies clinically relevant subtypes of glioblastoma characterized by abnormalities in PDGFRA, IDH1, EGFR, and NF1. *Cancer Cell.* 2010 Jan 19;17(1):98–110.
5. Wang Q, Hu B, Hu X, Kim H, Squatrito M, Scarpace L, et al. Tumor evolution of glioma intrinsic gene expression subtype associates with immunological changes in the microenvironment. *Cancer Cell.* 2017 Jul 10;32(1):42–56.e6.
6. Pecqueur C, Oliver L, Oizel K, Lalier L, Vallette FM. Targeting Metabolism to Induce Cell Death in Cancer Cells and Cancer Stem Cells. *Int J Cell Biol.* 2013;2013:1–13.
7. Clevers H. The cancer stem cell: premises, promises and challenges. *Nat Med.* 2011 Mar;17(3):313–9.
8. Medema JP. Cancer stem cells: the challenges ahead. *Nat Cell Biol.* 2013 Apr;15(4):338–44.
9. Oizel K, Chauvin C, Oliver L, Gratas C, Geraldo F, Jarry U, et al. Efficient Mitochondrial Glutamine Targeting Prevails Over Glioblastoma Metabolic Plasticity. *Clin Cancer Res Off J Am Assoc Cancer Res.* 2017 Oct 15;23(20):6292–304.
10. Reina-Campos M, Moscat J, Diaz-Meco M. Metabolism shapes the tumor microenvironment. *Curr Opin Cell Biol.* 2017;48:47–53.
11. Marin-Valencia I, Yang C, Mashimo T, Cho S, Baek H, Yang X-L, et al. Analysis of tumor metabolism reveals mitochondrial glucose oxidation in genetically diverse human glioblastomas in the mouse brain in vivo. *Cell Metab.* 2012 Jun 6;15(6):827–37.
12. Oizel K, Gratas C, Nadaradjane A, Oliver L, Vallette FM, Pecqueur C. D-2-Hydroxyglutarate does not mimic all the IDH mutation effects, in particular the reduced etoposide-triggered apoptosis mediated by an alteration in mitochondrial NADH. *Cell Death Dis.* 2015 Mar 26;6:e1704.
13. Jarry U, Chauvin C, Joalland N, Léger A, Minault S, Robard M, et al. Stereotaxic administrations of allogeneic human V γ 9V δ 2 T cells efficiently control the development of human glioblastoma brain tumors. *Oncoimmunology.* 2016 Jun;5(6):e1168554.

14. Yuan M, Breitkopf SB, Yang X, Asara JM. A positive/negative ion-switching, targeted mass spectrometry-based metabolomics platform for bodily fluids, cells, and fresh and fixed tissue. *Nat Protoc.* 2012 Apr 12;7(5):872–81.
15. Tardito S, Oudin A, Ahmed SU, Fack F, Keunen O, Zheng L, et al. Glutamine synthetase activity fuels nucleotide biosynthesis and supports growth of glutamine-restricted glioblastoma. *Nat Cell Biol.* 2015 Dec;17(12):1556–68.
16. Sottoriva A, Spiteri I, Piccirillo SGM, Touloumis A, Collins VP, Marioni JC, et al. Intratumor heterogeneity in human glioblastoma reflects cancer evolutionary dynamics. *Proc Natl Acad Sci U S A.* 2013 Mar 5;110(10):4009–14.
17. Hegi ME, Liu L, Herman JG, Stupp R, Wick W, Weller M, et al. Correlation of O6-methylguanine methyltransferase (MGMT) promoter methylation with clinical outcomes in glioblastoma and clinical strategies to modulate MGMT activity. *J Clin Oncol Off J Am Soc Clin Oncol.* 2008 Sep 1;26(25):4189–99.
18. Lai A, Tran A, Nghiemphu PL, Pope WB, Solis OE, Selch M, et al. Phase II study of bevacizumab plus temozolomide during and after radiation therapy for patients with newly diagnosed glioblastoma multiforme. *J Clin Oncol Off J Am Soc Clin Oncol.* 2011 Jan 10;29(2):142–8.
19. Friedman HS, Prados MD, Wen PY, Mikkelsen T, Schiff D, Abrey LE, et al. Bevacizumab alone and in combination with irinotecan in recurrent glioblastoma. *J Clin Oncol Off J Am Soc Clin Oncol.* 2009 Oct 1;27(28):4733–40.
20. Halliday J, Helmy K, Pattwell SS, Pitter KL, LaPlant Q, Ozawa T, et al. In vivo radiation response of proneural glioma characterized by protective p53 transcriptional program and proneural-mesenchymal shift. *Proc Natl Acad Sci U S A.* 2014 Apr 8;111(14):5248–53.

Figure 1

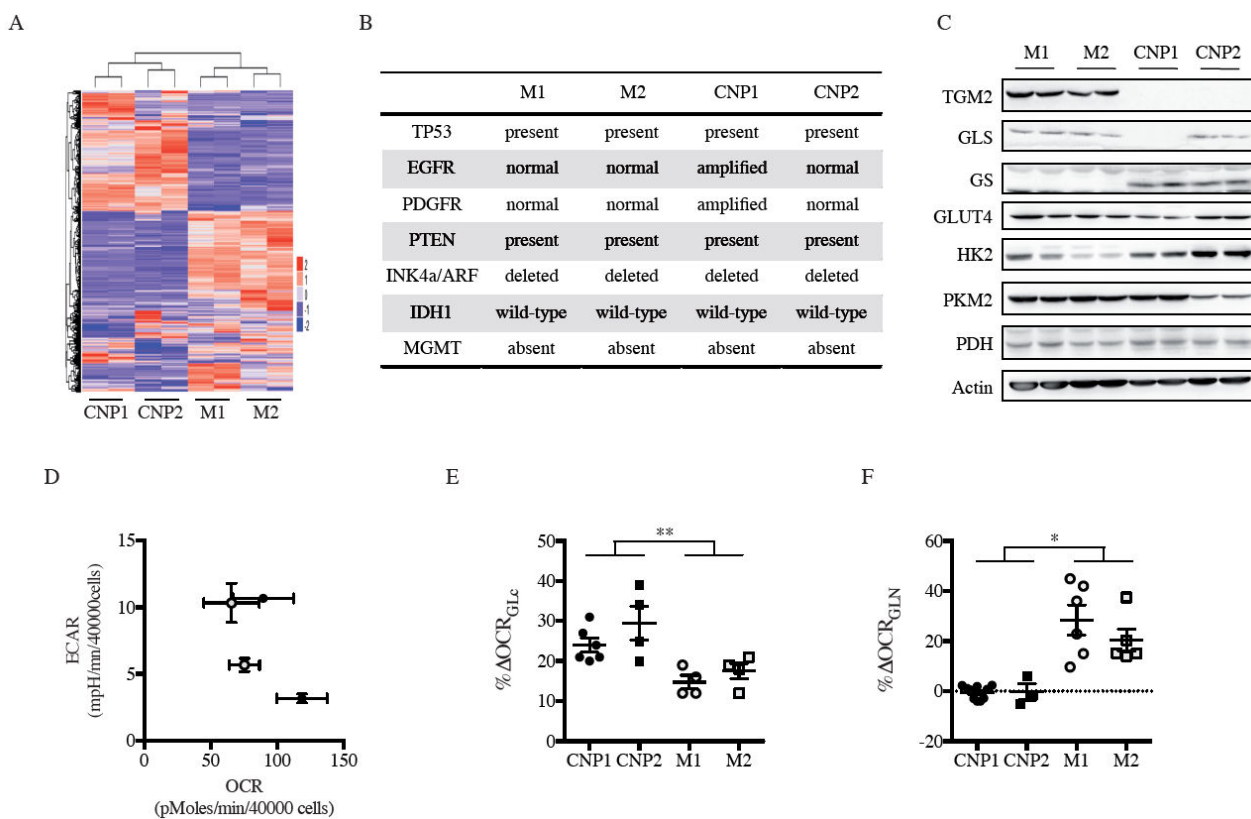


Figure 1 - Human primary cultures classification

A. Heat map of unsupervised hierarchical classification. B. Genomic data. C. Protein abundance of glycolytic and glutaminolytic enzymes : Transglutaminase 2 (TGM2), Glutaminase (GLS), Glutamine synthase (GS), Glucose transporter 4 (GLUT4), Hexokinase 2 (HK2), Isoform M2 of Pyruvate Kinase (PKM2), Pyruvate dehydrogenase (PDH). D. Global metabolism using the Seahorse technology. E-F. Mitochondrial respiration based on glutamine ($\Delta\text{OCR}_{\text{GLN}}$)(E) and glucose ($\Delta\text{OCR}_{\text{GLC}}$)(F). Results are presented as mean \pm sem, n=5. * p<0.05; ** p<0.01.

Figure 2

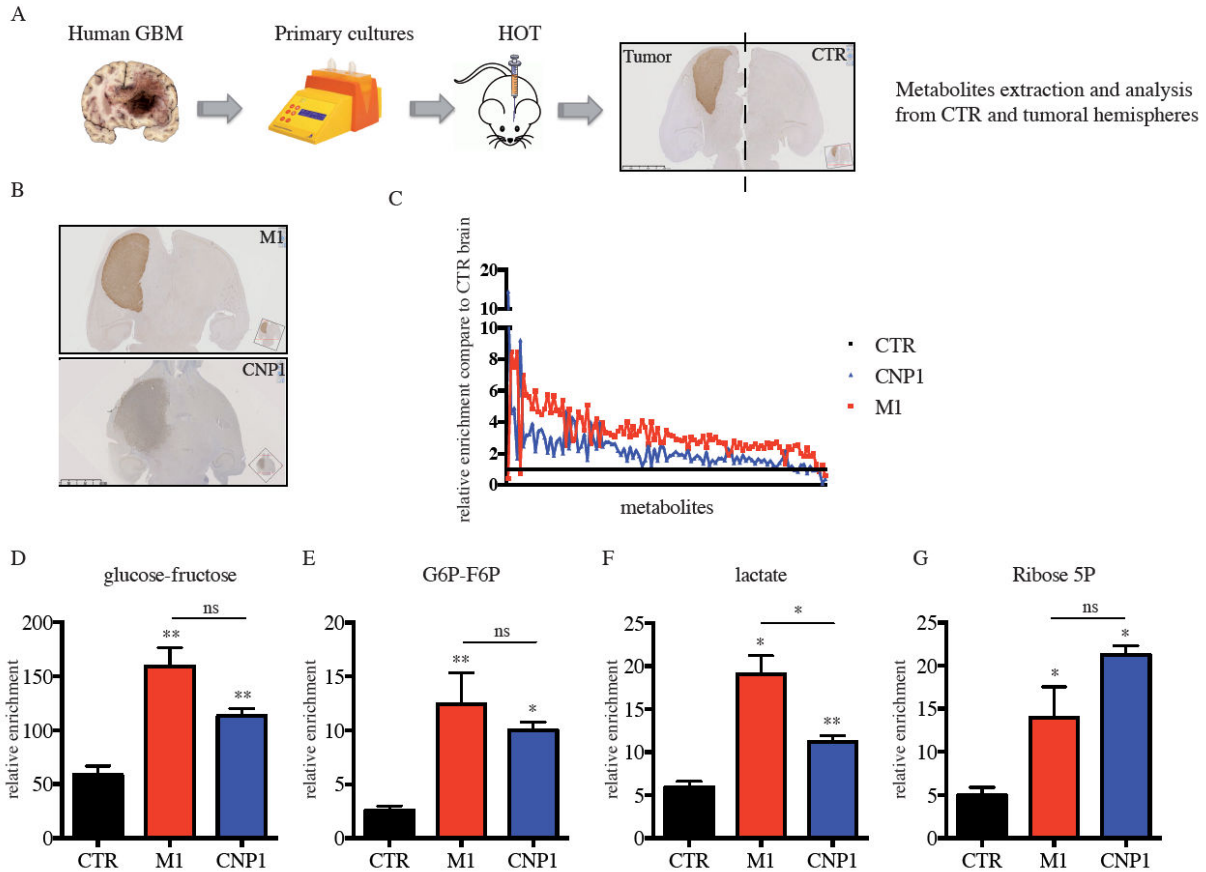


Figure 2 - Metabolic profile in human orthotopic tumors (HOT) and control brain

A. Illustration of the experimental protocol. B. IHC analysis of representative mouse HOTA derived from parental primary cultures (CNP1, M1) stained with MHC-I antibody. C. Relative abundance of 105 metabolites using LCMS analysis. Results are presented as the mean of 3 samples. D-G Abundance in mesenchymal HOTA M1 (n=3), in CNP1 HOTA (n=3) and surrounding brain (n=3) of Glucose-Fructose (D), Glucose 6-phosphate and Fructose 6-phosphate (E), lactate (F) and Ribose 5-phosphate (G). Results are presented as mean±sem. Results are compared to CTR unless stated otherwise. * p<0.05; ** p<0.01.

Figure 3

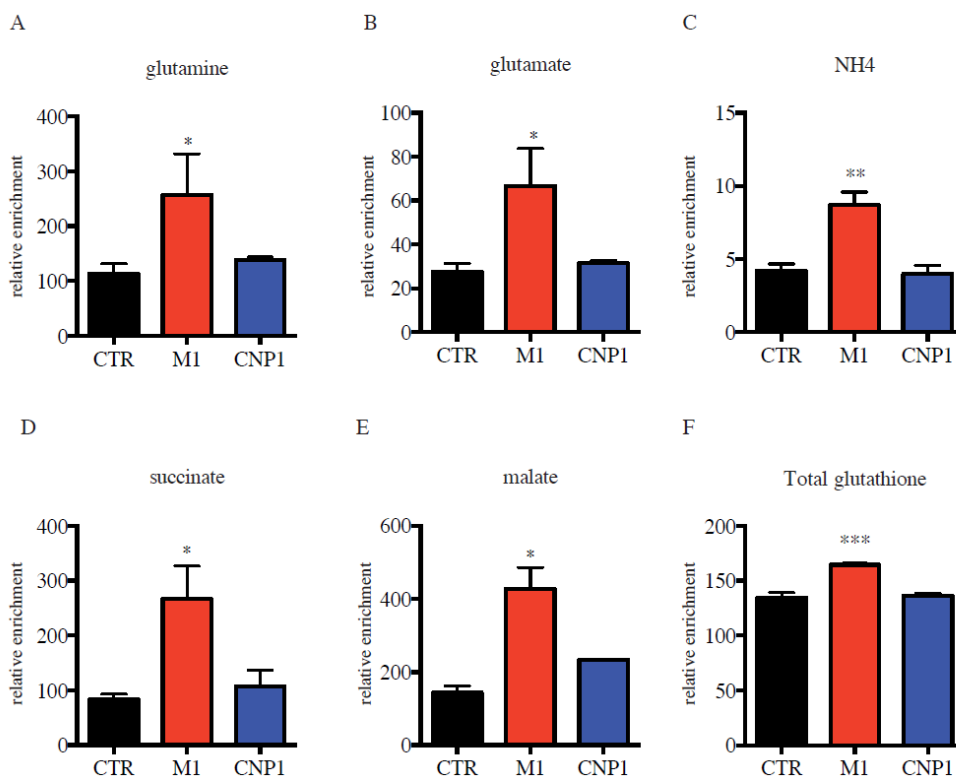


Figure 3 - Glutamine and Glutamine-derived metabolites from HOT and control brain

A-F Abundance of Glutamine (A), Glutamate (B), Ammonia (C), Succinate (D), Malate (E), Total glutathione (F). Results are presented as mean \pm sem, n=3, * p<0.05; ** p<0.01; *** p<0.001.

Figure 4

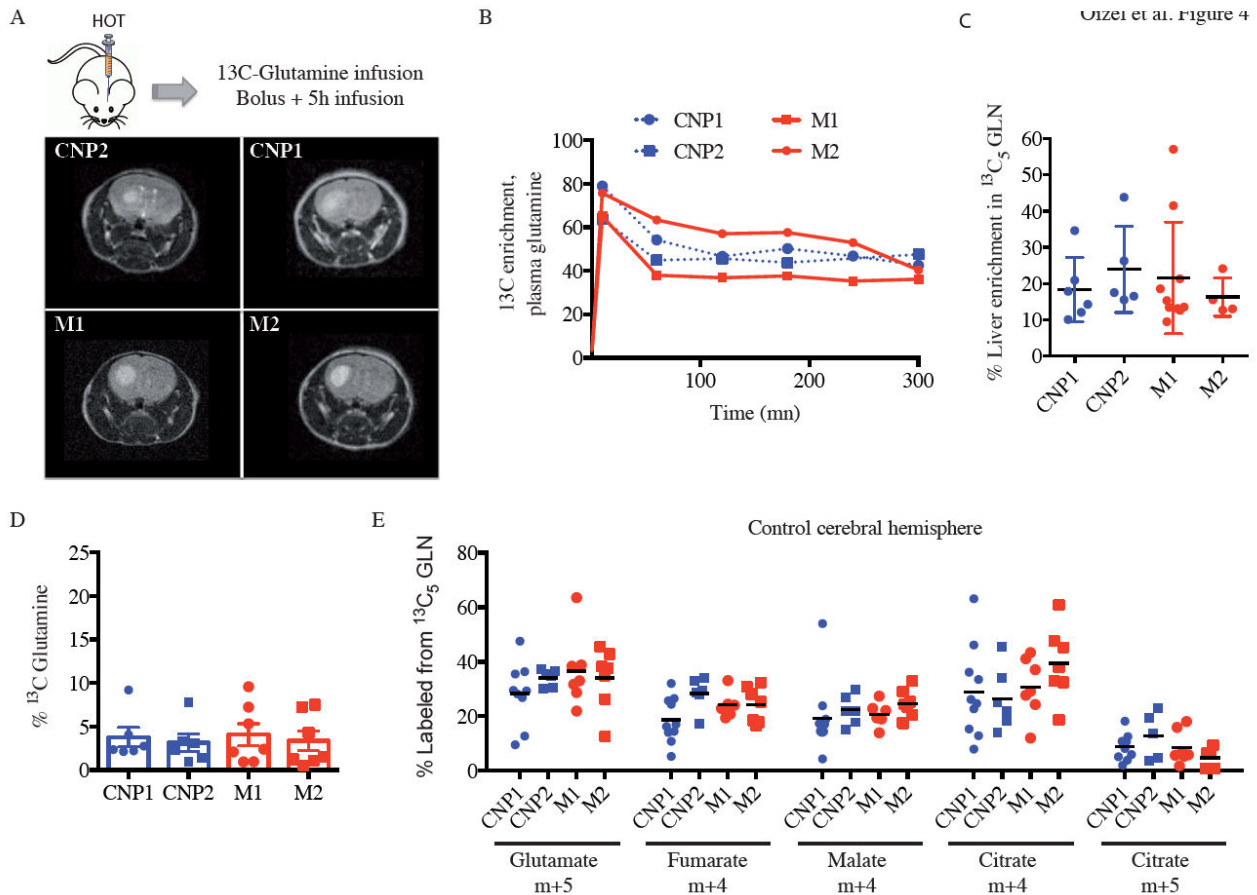


Figure 4 - ^{13}C -Glutamine infusions in HOT-bearing mice

A. MRI of representative mouse HOT derived from each parental primary cultures (CNP1, CNP2, M1, M2). B. HOT-bearing mice derived from each parental primary cultures (CNP1, CNP2, M1, M2) were infused with $^{13}\text{C}_5$ -Glutamine for the indicated times. The time course shows representative ^{13}C glutamine enrichment in plasma (%). All mice received a bolus of $^{13}\text{C}_5$ -Glutamine over 1 min followed by a continuous $^{13}\text{C}_5$ -Glutamine infusion. C-D. Enrichment in ^{13}C -glutamine (%) from HOT-bearing mice derived from each parental primary cultures (CNP1, CNP2, M1, M2) after 300 minutes in liver (C) and control cerebral hemisphere (D). E. Relative enrichment of labeled Glutamate, Fumarate, Malate and Citrate from ^{13}C -glutamine in control cerebral hemisphere from HOT-bearing mice derived from each parental primary cultures (CNP1, CNP2, M1, M2).

Figure 5

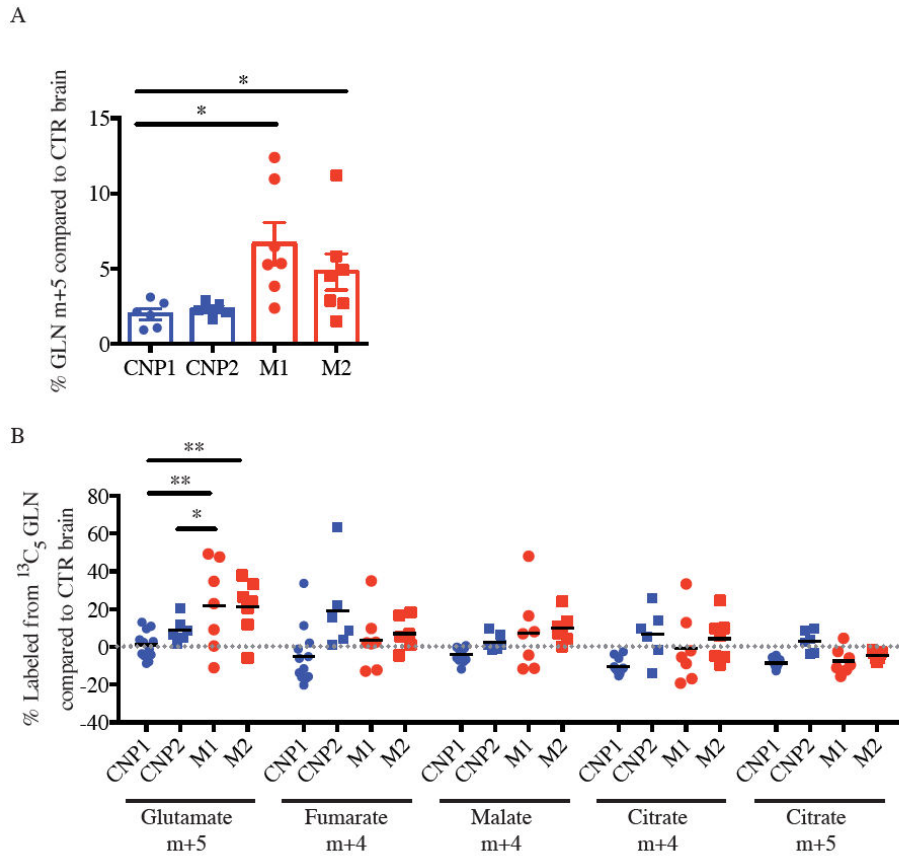


Figure 5 - Uptake and metabolism of ¹³C-Glutamine in HOT compared to control brain

A. Relative enrichment of ¹³C-Glutamine (%) from mouse HOT derived from each parental primary cultures (CNP1, CNP2, M1, M2). B. Relative enrichment of labeled Glutamate, Fumarate, Malate and Citrate from ¹³C-glutamine from HOT-bearing mice derived from each parental primary cultures (CNP1, CNP2, M1, M2). * p<0.05; ** p<0.01.

Article 8 : A transient population precedes and supports the acquisition of temozolomide resistance in human glioblastoma.

Marion Rabé^{1,2}, Solenne Dumont^{1,2,3}, Arturo Álvarez-Arenas Alcamí⁴, Hicham Janati⁵, Juan Belmonte-Beitia⁴, Gabriel F. Calvo⁴, Christelle Thibault-Charpentier⁶, Quentin Séry^{1,2,7}, Cynthia Chauvin^{1,2}, Noémie Joalland^{1,2}, Floriane Briand^{1,2}, Emmanuel Scotet^{1,2}, Claire Pecqueur^{1,2}, Jean Clairambault⁵, Lisa Oliver^{1,2,8}, Arulraj Nadaradjane^{1,2,7}, Victor Perez-Garcia⁴, Pierre François Cartron^{1,2,7}, Catherine Gratas^{1,2,8*}, François M. Vallette^{1,2,7*}.

1. CRCINA, INSERM, Nantes, France ; 2. Université de Nantes, Nantes, F-44007, France ; 3. GenoBiRD, SFR François Bonamy, Université de Nantes, France ; 4. Department of Mathematics and MÔLAB-Mathematical Oncology Laboratory. University of Castilla-la Mancha, Ciudad Real, Spain ; 5. Inria, Mamba team and Sorbonne Université, Paris 6, UPMC, Laboratoire Jacques-Louis Lions, Paris, France ; 6. IGBMC - CNRS UMR 7104 - Inserm U 1258, Université de Strasbourg, Illkirch, F- 67404 France ; 7. Institut de Cancérologie de l'Ouest, LaBCT, St Herblain, F-44805, France ; 8. CHU Nantes, Nantes, F-44093, France

La résistance aux thérapies standard des cellules tumorales de glioblastome multiforme (GBM) affecte l'efficacité de ces traitements et conduit inévitablement à une rechute via des mécanismes encore mal décrit. Dans cette étude, nous avons combiné des analyses mathématiques et transcriptomique afin d'étudier la résistance de la lignée cellulaire de GBM U251 cultivée en présence de Temozolomide (TMZ), la chimiothérapie de référence pour le traitement des patients atteints de GBM. Nous avons mis en évidence que les cellules U251 devenaient résistantes au TMZ en induisant l'expression de la O-méthylguanine-DNA méthyltransferase (MGMT), une protéine de réparation de l'ADN. Cependant, cette expression n'est pas immédiate, le TMZ induit d'abord un état transitoire pendant lequel les cellules U251 adoptent une morphologie et expriment des gènes spécifiques. Des drogues épigénétiques, telles que les inhibiteurs de l'histone désacetylase, cible spécifiquement les cellules tumorales dans cet état transitoire et empêche le développement de la résistance au TMZ. Cette étude met en avant que non seulement cet état transitoire est indispensable à l'apparition de la résistance à la chimiothérapie mais également qu'il représente une cible thérapeutique d'intérêt pour le traitement des patients atteints de GBM.

Soumis

A transient population precedes and supports the acquisition of temozolomide resistance in human glioblastoma.

Marion Rabé^{1,2}, Solenne Dumont^{1,2,3}, Arturo Álvarez-Arenas Alcamí⁴, Hicham Janati⁵, Juan Belmonte-Beitia⁴, Gabriel F. Calvo⁴, Christelle Thibault-Charpentier⁶, Quentin Séry^{1,2,7}, Cynthia Chauvin^{1,2}, Noémie Joalland^{1,2}, Floriane Briand^{1,2}, Emmanuel Scotet^{1,2}, Claire Pecqueur^{1,2}, Jean Clairambault⁵, Lisa Oliver^{1,2,8}, Arulraj Nadaradjane^{1,2,7}, Victor Perez-Garcia⁴, Pierre François Cartron^{1,2,7}, Catherine Gratas^{1,2,8*}, François M. Vallette^{1,2,7*}.

1. CRCINA, INSERM, Nantes, France

2. Université de Nantes, Nantes, F-44007, France

3. GenoBiRD, SFR François Bonamy, Université de Nantes, France

4. Department of Mathematics and MÔLAB-Mathematical Oncology Laboratory. University of Castilla-la Mancha, Ciudad Real, Spain

5. Inria, Mamba team and Sorbonne Université, Paris 6, UPMC, Laboratoire Jacques-Louis Lions, Paris, France.

6. IGBMC - CNRS UMR 7104 - Inserm U 1258, Université de Strasbourg, Illkirch, F- 67404 France.

7. Institut de Cancérologie de l'Ouest, LaBCT, St Herblain, F-44805, France

8. CHU Nantes, Nantes, F-44093, France

***corresponding authors:** François M. Vallette (francois.vallette@inserm.fr); Catherine Gratas (catherine.gratas@univ-nantes.fr)

Running title: acquisition of TMZ resistance in glioblastoma

Key words: glioblastoma, persister, temozolomide, resistance, HDAC

Financial support: This work was supported by INSERM, Ligue Contre le Cancer Grand Ouest and the “ERRATA” programme from the Région Pays de la Loire. AAAA was supported by a fellowship from UCLM [2015/4062]. This work was realized in the context of the LabEX IGO program supported by the National Research Agency via the investment of the future program ANR-11-LABX-0016-0.

Abstract

Drug resistance affects the therapeutic efficacy in cancers and leads to tumour recurrence through ill-defined mechanisms. Here, we use both mathematical and a combination of transcriptomic and single cell analyses, to study drug resistance in the human glioma cell line, U251, cultured in the presence of Temozolomide, the chemotherapy standard of care for patients with glioblastoma. We found that U251 cells become resistant to TMZ along with the induction expression of the DNA repair protein O6-methylguanine-DNA methyl-transferase. However, prior to MGMT expression, TMZ induced a transient state wherein cells adopted a distinct morphology and expressed a specific set of genes. Epigenetics drugs, in particular histone desacetylase inhibitors, were shown to specifically target this population and prevent the appearance of resistant cells to temozolomide. Our results show that this transient population is essential for the development of resistant cancer cells and could constitute a therapeutic target in glioblastoma.

Significance: These findings show that the acquisition of temozolomide resistance implicates a transient cell population which is a potential new therapeutic target in glioblastoma.

Introduction

Cancer resistance to treatment is a main cause for therapeutic failures. The evolution of tumour cells under therapy can be viewed as a Darwinian process with replacement of sensitive by resistant clones (1). This model is supported by the contention that tumours are composed of a large number of clones and that treatment could change the normal course of cancer evolution as dominant clones at diagnosis could be replaced by others, previously present within the entire cell population, because of therapy selective pressure (2,3). Alternatively, the cancer stem cell hypothesis postulates a hierarchical organisation of tumours, in which only a proportion of cells are tumorigenic and exhibit intrinsic resistance to most treatments (4). Both models can account for tumour resistance and heterogeneity. A large number of studies comparing original tumours with their recurrences suggests that these models are not mutually exclusive and indeed co-exist in many cases. However, in both cases, the cancer cells plasticity appears to be an important component of tumour progression under treatment (5). Specific mutations are major drivers in many cancers and thus are considered to be the cornerstone of tumour resistance (6). However, specific inhibitors targeting these mutations have almost always shown only short-term success and did not prevent the development of resistant cancer cells. This is probably linked to the fact that differential drug responses can be observed between clones genetically and epigenetically related indicating that resistance can occur at late stages of tumorigenesis as demonstrated recently (7).

Recently, the notion of persisters/tolerant cells which were first observed in micro-organisms (8) resistance to treatment have been reported in some tumours (9-11). These cells represent an intermediate state which has been described in the case of lung cancer and melanoma cell lines exposed to Tyrosine Kinase Inhibitors (TKI) in which resistance is preceded by a tolerant state supported by a distinct population within cancer cells (9-11).

Glioblastoma (GBM) are the major and deadliest form of brain cancers in adult. Temozolomide (TMZ) is the standard of care for chemotherapy in patients with GBM. The resistance to this drug in GBM is modulated by DNA repair systems and in particular the O6-methylguanine-DNA methyltransferase (MGMT) (12,13). The expression of MGMT is silenced by promoter methylation in approximately half of GBM tumors, and clinical studies have shown that elevated MGMT protein levels or lack of MGMT promoter methylation is associated with TMZ resistance in GBM (14,15).

However, invariably GBM recur even after aggressive TMZ/ irradiation regimen and recurrent tumors are highly resistant to treatments and often express MGMT when the original tumour did not (16). It is nonetheless admitted that resistance can occur through multiple pathways that might occur independently or simultaneously (16,17).

In this work we have studied, via *in vitro*, *in vivo* and *in silico*, the occurrence of resistance to TMZ in a glioma cell line from a sensitive state to a fully resistant one by a combination of phenotypic, metabolic, RNA sequencing, and single cell analyses. We identified an intermediate cellular population crucial in the acquisition of resistance to the drug.

Materials and Methods

Reagents. Temozolomide (TMZ) was from Interchim (Montluçon, France), all other drugs were from Sigma (Saint Louis, MO, USA) unless otherwise noted. All cell culture products were obtained from Life Technologies (Carlsbad, CA).

Cell culture. Cell lines were cultured as previously described (18). U251 cell line authentication was certified by Eurofins Genomics (Ebersberg, Germany) and RNA sequencing confirmed its identity. All cell lines were mycoplasma-free.

Cytotoxicity assay and cell counts. MTT assays were performed as described (18). Viable cell counts were performed using the Countess II (Invitrogen, CA, USA). Data are presented as percentage of viable cells after treatment compared to untreated cells.

Clonogenic assay. U251 cells, pretreated or not with 50 μ M TMZ at indicated times, were trypsinized and seeded at appropriate densities in 6 well dishes. At least two dilutions of cells were used for each TMZ treatment time. Cultures were incubated for 1 to 2 weeks for colony formation. Then cells were stained with 0,5% crystal violet and colonies were counted using ImageJ (NIH, USA). Colony forming efficiency of TMZ treated cells was calculated as: [(number of clones/number of plated cells)/(number of wells * Plated Efficiency for untreated U251S cells)](19).

Gene knockdown using si-RNA. To inhibit CHI3L1, KLK5, HBEGF, and FAT2 expression, ONTARGETplus – SMARTpool Human siRNA (Dharmacon, CO) were transfected at final concentration of 15nM in U251 cells with Lipofectamine RNAi Max (Life technologies, CA) according to the recommended protocol. siRNA Scramble (Scr) (sc-37007, Santa-Cruz, TX) was used as negative control. Cells were reverse transfected when they were plated (day-1). A second classical transfection was done at day 4. Cells were treated with TMZ 50 μ M at day 0 and day 3, and harvested at day 7.

Quantitative RT-PCR. RNA preparation and qPCR were performed as described (18,20) except that First Strand cDNA Synthesis Kit was used for the reverse transcription (Thermo Scientific, MA) and quantitative real-time PCR (qPCR) assays were performed using the Perfecta™ SYBR® Green FastMix™, Low ROX™ (Quanta BioSciences, CA) and the real-time thermal cycler qTower (Analytik Jena AG, Germany). Primers sequences are given in Supplemental Table 1. The housekeeping genes RPLPO, TATA and HGPRT, were amplified and used for normalization.

RNA-Seq. Library construction (n=4 for each time point) was performed from 500ng of total RNA with SureSelect Strand-Specific RNA Library Prep for Illumina Multiplexed kit according to Agilent_PrepLib_G9691-90010_juillet2015_vD protocol (Agilent, CA, USA). Purifications were carried out with NucleoMag NGS Clean-up and Size Select (Macherey-Nagel, Düren, Germany). Paired-end sequencing (2x100 cycles) was carried out in four lanes on HiSeq® 2500 system (Illumina). Curated reads (Supplemental Methods) were finally aligned against human hg19 reference genome with Tophat 2.0.10 (21), counted with HTseq-count from HTSeq-0.5.4p5 (22) and differential analysis was performed with DESeq2 (23).

Variant detection. The analysis was performed with GATK (v 3.6.0) HaplotypeCaller from alignment files using hg19 reference genome. Variants were annotated and their predicted effects on known genes were calculated with SnpEff 4.3. Variants are then filtered out based on some criteria: less than 3 replicates of D0 with the variant; DP > 10 in at least one replicate. Only variants with high putative impact were kept (Supplementary Info.2) (24,25).

Single-cell qRT-PCR. Expression of 88 genes (Supplemental Table 2) was measured in single cells using the C1 Single-Cell Auto Prep System coupled with the real-time PCR reader BiomarkHD (Fluidigm, CA, USA). Single cells from untreated and from cells treated with 50µM TMZ for 4,9,12 and 16 days, were captured, in Single-Cell PreAmp IFC 10-17µM (U251S and U251R), and 17-25µM (U251TR), according to manufacturer's protocol. Pre-amplified cDNAs were then loaded into 96.96 Dynamic Array microfluidic chips and qPCR were performed following the manufacturer instructions. Results were analyzed using the Singular Analysis Toolset Software provided by Fluidigm.

Western blot analysis. Proteins were extracted from adherent cells and separated as previously described (26). Primary antibodies were as following: MGMT clone MT3.1(#NB 100-692 Novus,MO, USA) and anti-actin (clone C4, MAB1501 Millipore). Peroxydase-conjugated secondary antibodies (Jackson Immunoresearch Laboratories, PA) were detected using the ECL detection system (Amersham Biosciences, NJ, USA).

DNA extraction and bisulfitation. DNA was extracted using the Nucleospin tissue kit (Macherey-Nagel, Düren, Germany) according to the manufacturer's instructions. DNA (500 ng) was bisulfited using the EZ DNA Methylation Gold kit (Zymo Research, CA, USA) and semiquantitative methyl-specific PCR was performed as previously described (27).

Metabolic studies. Mitochondrial oxygen consumption (OCR) and extracellular acidification rate (ECAR), reflect of glycolysis, were measured in non-buffered medium supplemented with glucose (5 mmol/L), pyruvate (1 mmol/L), and glutamine (2 mmol/L) using an XF24 Analyzer (Agilent, CA, USA).

Orthotopic injections of human glioma cell lines in NSG mice. Orthotopic injections of cells (104 in 2 μ l PBS), were performed as previously described (28). U251S, U251TR-D9 (cells treated *in vitro* for 9 days at 50 μ M TMZ) and U251R were injected on the same day. Animals were observed daily and euthanized when characteristic symptoms occurred, such as reduced mobility and significant weight loss. Tumors were snap-frozen or fixed in PFA. Sections (2 μ m) were used for immunohistological staining (28). Slides were scanned using nanoZoomer 2.0 HT (Hamamatsu Photonics K.K., Japan)

DNA extraction and qMSRE. A QIAcube automate and QIAmp DNA Mini QiaCube kit (Qiagen, France) were used to isolate DNA. *MGMT* promoter methylation was quantified using OneStep qMethyl Kits (Zymo Research/Ozyme, France). Typically, 100 ng of genomic DNA were digested with 40U of enzymes at 37°C for 2h in 50 μ L of reaction. Control samples were treated in the same way but without the addition of the enzyme. 5 μ L of digestion mixture were used for qPCR. The QuantiFast SYBR Green PCR Kit and Rotor-Gene Q (Qiagen, France) were used to perform the qPCR.

Protein analysis by ELISA. Proteins extracts were obtained by using RIPA Lysis and Extraction Buffer (Thermo Scientific, France) in accordance with the manufacturer's instructions. ELISAs were performed according to the manufacturer's instructions (MyBiosource, MBS2022854, USA).

Statistical analysis. All results are presented as mean \pm SD. Statistical analyses were done using GraphPad Prism 6 with difference considered statistically significant at $p < 0.05$.

For more information, see Supplementary Methods

Data availability: data will be available on NCBI trace Archive. Submission number: SUB4187245

Results

Timeline of the acquisition of resistance to Temozolomide by the U251 glioma cell line.

To elucidate the mechanism(s) underlying resistance to TMZ, we used a human glioma cell line (U251) as a model of clonal evolution upon treatment with TMZ. U251 cells were treated every 3 days for up to 3 weeks with 50 μ M TMZ, a dose relevant to the clinical situation (26). A maximum of cell death was observed after 3 days of TMZ exposure as described previously (26) and cell cycle arrest (G2/M blockade) was observed between Day3 (D3) and D9 before cells resumed cell cycle (Supplementary Fig.S1). Morphologically, U251 cells, upon the TMZ treatment, exhibited a reproducible pattern of adaptation to the drug as in a first phase, the surviving cells exhibited a flattened cell body with few cellular extensions (D6 to 9) and in a second phase cells started to grow as colonies (D9 to D12) before a third phase (i.e. after D12) when cells recolonized the dish (Fig. 1a). The resistance to TMZ, measured by cell viability, was observed at D16 (Fig 1b). We called U251S (S for sensitive), the untreated cells and U251R (R for resistant) cells treated with 50 μ M TMZ for 16 days. As shown in Fig.1b, the two cell lines, as expected, exhibited different sensitivities to TMZ. To establish a pattern of acquisition of resistance, we treated U251 for 3 or 6 days with TMZ but left them untreated until D16 (U251R3 and U251R6 respectively). Quite remarkably, their resistance to TMZ was intermediate to that observed in U251S and U251R. Of note U251R left untreated for 3 months (U251R wash out, U251R/WO) remained resistant to TMZ although to a lesser degree (Fig.1b). These results suggest that TMZ resistance follow a gradual pattern and can only be partially reversed by washing out TMZ. Thus, the response to TMZ appeared to be different from that described to TKI response where resistance traits appeared to be completely reversible after drug washout (29-31).

We also analyzed the clonogenic survival of the U251 cells during the course of TMZ treatment. Cells treated for 3 (D3) and 6 days (D6) with TMZ present a very low colony forming efficiency while U251R (D16) exhibited limited clonogenicity compared to U251S (Fig. 1c). Mitochondrial oxidative phosphorylation has recently been linked to treatment resistance in several cancers (32,33). We thus analyzed the mitochondrial metabolism during the TMZ treatment using the Seahorse technology as previously described (34). U251S and U251R have a comparable higher metabolism than the intermediate cells (i.e. U251 at D9 after TMZ treatment) in which oxidative phosphorylation was predominant over glycolysis (Fig.1d).

Since cells from D3 to D12 with TMZ show specific properties and we called them U251TR for U251 transient state. To evaluate and compare the tumorigenic properties of U251S, U251TR and U251R as well as the possible influence of the microenvironment, we implanted these cells in an orthotopic NSG mice model (28). We found that U251S and U251R grew at a similar rate while the U251TR grew much more slowly with a 50% longer survival rate (Fig.1e). The gross morphological aspects of the tumours derived from these cells did not show any significant differences in terms of cell density and diffusion (Fig.1f).

Acquisition of resistance to Temozolomide by the U251 glioma cell line is accompanied by the expression of MGMT.

The expression of MGMT has been associated with resistance to TMZ in GBM (13,35) and in particular in U251(26). We analyzed by both RT-qPCR and Western blots its expression during the time course of U251 exposed to TMZ. MGMT was not present at day 0 (neither at mRNA nor at protein levels) but MGMT RNA was significantly detected after 9-day exposure to TMZ and MGMT expression was increased continuously afterwards (Fig.2a). At the protein level, the expression of MGMT was unambiguously detected only at D16 (Fig.2b). We analyzed MGMT expression in U251R/WO after 1.5 and 3 months and we found that MGMT level was unaffected before 3 months of wash out (data not shown). These results suggest that the expression of MGMT is associated with the resistance of U251 to TMZ. MGMT transcription is controlled by promoter methylation which silences the gene expression in GBM (14,15,27). We compared the expression of MGMT with promoter methylation status, obtained as previously described in clinical studies (14,27), in seven independently obtained U251R. As shown in Fig.2c, although the level of MGMT expression was different between the cell lines, we observed no major differences between U251R and U251S in the promoter methylation. Different methylated CpG regions, inside and outside the promoter region, influenced MGMT expression (36,37) and significant changes in MGMT methylation status occurred during the evolution of GBM i.e. primary tumour and its recurrence (38). Thus, we ask if the *de novo* expression of MGMT was associated with a more complex change in the MGMT gene methylation pattern using methyl-sensitive restriction endonucleases (MSRE) PCR and ELISA specific quantification of MGMT (Nadaradjane et al., in preparation) to determine methylated regions in the MGMT gene (Fig.2d).

We found in U251R a specific demethylation of MGMT gene (CpG2) (Fig.2e). This demethylation is associated with the expression of MGMT as quantified by ELISA (Fig.2f). We also performed a similar study on a small cohort of GBM patients for whom both primary and recurrent tumours were available. We found that 4/7 patients overexpressed MGMT in recurrent tumours when compared to the primary tumours and that this overexpression was associated with a demethylation of CpG2 while CpG1 status was not affected (Fig.2g). Similar to U251, the expression of MGMT protein was correlated with the methylation of CpG2 sites (Fig.2h). Our results showed that resistance to TMZ in U251 was mainly associated to the re-expression of MGMT due to a modification of non-classical MGMT methylation gene region.

Mathematical modelisation of the TMZ resistance in U251.

The resistant population obtained after D16 could be due to the selection of a preexisting clone or to an acquired program by some of the U251 cells. To quantify the relevance of these two paradigms, we developed two different mathematical models corresponding to the two frameworks based on proliferation properties of the U251 cells (Supplementary Info.1) with the expression of MGMT as the read out for resistance. In the clonal selection model, a subpopulation with high levels of resistance is supposed to pre-exist in the original population (Fig3a). The selection induced by TMZ would result in an important decrease in the sensitive population, while the resistant cells will grow unaffected by TMZ to becoming the dominant clones. This process can be modeled with a system of two differential equations in combination with the standard least squares method to estimate the kinetic parameters, obtaining fits to the experimental data (Supplementary Info.1). In the first model, a large number of possible combinations for the initial fraction of resistant cells and the proliferation rate was found that could fit the experimental data (Fig.3b), indicating that the initial proportion of resistant cells, i.e. U251R, could vary from 0.02% to 6.97% of the starting population, i.e. U251S (Supplementary Info. 1). However, when looking at the normalized MGMT expression of the total population, the model predictions based on a purely clonal selection interpretation could not explain all the observed results. One parameter (α) to account for the MGMT expression ratio of resistant cells with respect to the basal values of sensitive cells was used (Supplementary Info.1). At early stages (first six days), the MGMT expression kinetics agrees well with the experimental results (insets in Fig.3c).

In contrast, at longer times (days 12-16), it was not possible to fit well the large variability observed in the MGMT expression (Fig.3c), thus indicating that a purely selection mechanism was not adequate. Within the adaptive model, cells evolve from a sensitive to a resistant phenotype through acquisition of a new gene expression array triggered by the drug. Based on previous observations (30), this mechanism is not direct, and cells go through a transient state, during which they do not proliferate and do not undergo apoptosis. Thus, in addition to the sensitive and resistant populations, an intermediate population, similar to the “TR” population, was considered in the mathematical model (Fig.3d). Our model incorporated the age-structure displayed by this emergent “TR” population (Supplementary Info.1). Just as it occurred with the clonal selection model, different parameter combinations were able to explain the cell number data (Fig.3e), now assuming a zero initial resistant population. When looking at the MGMT expression, within the purely adaptive hypothesis, it was possible to find values and different parameter combinations that could explain the variability during all the experimental time points (Fig.3f).

RNA sequencing analyses of U251 during the acquisition of resistance to TMZ.

The characteristic features of the U251TR (D4 to D12) suggested a profound change in gene expression upon exposure to TMZ. Fig.4a shows that U251S and U251R are not significantly different regarding the pathways implicated in proliferation and DNA repair (i.e. activation of ATR). We performed RNA sequencing of U251 cell lines at D0, D4, D9, D12, and D16 after TMZ exposure. Fig.4b shows PCA (principal component analysis) and HCA (hierarchical clustering analysis) of the normalized RNA sequencing data. The PCA revealed three separate stages corresponding to sensitive cells from D0, cells in transient state from D4 to D12 and resistant cells D16 but showed a proximity between samples from day 4, 9 and 12 (i.e. U251TR) and another one between U251S and U251R. The PCA axes gave thus an interesting insight regarding the group of genes they are strongly correlated with and Fig.4b shows the categories of pathways positively and negatively correlated with these axes. The correlation of each gene with both axes were computed with correlations higher than 0.6 (in module) analysed using over-representation tests of pathways. Thus, PCA and heatmaps indicated that U251S and U251R exhibited high levels of similarity while U251TR cells were clustering in a spatially restricted group (Fig.4b).

Resistance to apoptosis, presence of cancer stem cells and epithelial to mesenchymal-like transition (EMT) have been associated to treatment resistance in many cancers. We examined key genes implicated in apoptosis, stemness and EMT (Figs.4c-e) in the different populations at different times. We found no differences between U251s, U251TR and U251R except for the expression of p21 in U251TR (which could be related to cell cycle arrest) and fibronectin in U251R (which could be related to cell migration/invasion). We also analyzed the amount of mutations following the TMZ treatment and as shown in Fig.4f, the mutation rates increased significantly from D0 to D4 and become stabilized thereafter. Of note, we did not identify any specific pathways with high mutation rates induced by the treatments.

As the main transcriptomic differences were seen in the TR group we focused our analysis on this group. We used the STRING interactive network program to analyze pathways overrepresented in U251TR and we found two major high-level molecular interaction networks centered on histone and integrin/collagen pathways (Fig.4g).

The U251 transient population induced by TMZ is characterized by a “4 genes” signature.

RNA sequencing allowed us to identify the overexpression of many genes following TMZ treatment however we focused on the period D4-D12 which represent the TR stage. First, we selected 3 genes over expressed during this period (i.e. after cell death peak and before MGMT expression) (i.e. KLK5, CHI3L1, FAT2,) with no connection or relationship associated with TMZ resistance but with suspected role in some cancers (Fig.5a).. We also used as marker of this stage, HB-EGF, gene already shown as overexpressed in U251S shortly after TMZ treatment (18). The transient expression of these genes over the course of TMZ resistance acquisition was confirmed by Q-PCR (Fig.5b-e). From these results, we conclude that U251TR could be characterized with this 4 genes signature. We treated three other glioma cell lines with different MGMT status (U87, LN18 and A172) with TMZ at various concentrations and analyzed the expression of the 4 genes signature. As shown in Fig.5f, these genes were also expressed although with different intensity and time course upon TMZ treatment. To establish the function of the 4 genes signature, we selectively inhibit genes expression by RNA interference using siRNA specifically designed for each gene (see materials and methods).

We treated U251 for 7 days with gene specific siRNA and control scrambled RNA in the presence or the absence of TMZ. As shown in Figure 5g, the specific inhibition of the CHI3L1, FAT2 and KLK5 had an important effect on cell survival (Fig.5g -left) but no impact on the TMZ-induced cell death (Fig.5g right). On the other hand, the down expression of HB-EGF had no effect on U251 survival and TMZ response (Fig.5g). These results suggested that these genes had an influence on U251 survival *per se*.

Single cell analyses show that transient population U251TR is not uniform.

Next, we ask whether the U251TR population was composed of clones expressing one or several of the 4 genes determined above using a single cell approach. We used for this purpose the Fluidigm C1 technology followed by HD Biomark quantitative PCR analyses (see materials and methods). We defined 84 sets of primers to analyze representative genes of different cellular function including apoptosis, stemness along with the 4 genes signature (Supplementary Table S2). Single cell studies were performed at D0, D4, D9, D12 and D16 after TMZ treatment. After unsupervised analysis, PCA representation allowed a clear distinction between U251S, U251TR and U251R (Fig.6a). Violin plot representation of the evolution of gene expression after TMZ treatment (Fig.6b) indicated that the distribution of most genes is unimodal along the TMZ treatment while some genes appear to evolve from unimodal to a bimodal distribution from U251S to U252TR and return to the unimodal stage in U251R (i.e. Bcl-2, USP9X, EGFR, TGF alpha, ADAM10, ADAM17 and ANPG). Quite interestingly, most of these genes are associated to cell survival and/or are implicated in TMZ resistance. Next, we studied the expression cell by cell of the 4 genes signature and of MGMT. The expression of MGMT appeared at D9 and was distributed first in few cells to become expressed in many cells after Day 12. On the other hand, the 4 genes expression was distributed randomly among the cells at D4 to D9 and seems to be co-expressed with MGMT in some cells (Fig. 6c, Supplementary Fig.S2). These results show that there are no cells expressing MGMT at D0 and that the number of cells expressing MGMT increased with time after treatment. Of note, not all cells express MGMT plus our 4 genes signature, suggesting that TR state is unlikely to correspond to a single clone.

Epigenetic targeting of U251TR prevents the rise of U251S in vitro and in vivo.

Since U251TR seemed to preferentially use mitochondrial oxidative-ATP-synthesis (Fig.1d), we explored the effect of Metformin (Met), a NADH dehydrogenase (complex I) inhibitor of mitochondrial respiration, in U251S, U251TR and U251R. We found no significant effect of 4mM metformin on the viability of U251S or U251TR as a single agent or in combination with TMZ while a small but significant effect of metformin on U251R was observed (Fig.7a). The re-expression of the MGMT could represent a change in the global epigenetic status of the U251 (36,37). Thus, we tested the DNMT inhibitor 5-azacytidine to analyze the effect of inhibition of DNA methylation in the U251 subpopulation. Fig.7b shows that 5-azacytidine affected moderately the viability of both U251R and U251TR but not that of U251S. As for the inhibition of histone desacetylation Trichostatin A (TSA) had no significant effect on U251S but affected the U251R and even more U251TR (Fig.7c) in agreement with histone modifications observed in Fig.4g. We thus designed a treatment in which the U251TR population was generated by a single TMZ treatment for 72h and then treated with TSA in combination with TMZ (Fig. 7d). As shown in Fig.7e, the sequence efficiently eradicated U251TR and prevented the onset of U251R *in vitro*. The *in vivo* implantation of U251S, U251TR or U251R cells treated or not with TSA indicated that this regimen was efficient to reduce the growth of U251TR while it did not affect that of U251S and U251R (Fig.7f).

Discussion

Drug resistance can be viewed under a Darwinian perspective with first line treatments as a major “ecological” driver for the tumour through selection pressure (6,7). Recently, a small population of cancer cells, referred to as “persisters” or “drug tolerant”, has been identified in some cancers as being in a specific cellular state (slow cycling, low cell death, epigenetic alterations, dysregulation of specific pathway...) that allows them to survive drug treatment and to give rise of resistant and highly proliferative cancer cells (5,30,39) These studies have been conducted mainly in melanoma or lung cancer derived cell lines treated with tyrosine kinase inhibitors (10,11,39,40). Several therapeutic targets have been identified in these cells offering promising treatments to prevent resistance/relapse in these cancers. For example, in GBM, Liau et al. showed that Dasatinib induced a rapid and reversible state in cancer stem cells that was epigenetically regulated and associated with the expression of neurodevelopmental and quiescent signatures (41). However, persisters have not been identified in cancer cell lines treated with cytotoxic treatments currently used in cancer therapies.

We have used a glioma cell line, as a model to explore the acquisition of resistance to TMZ, the current chemotherapy in glioblastoma (GBM). We found that resistance is accompanied by the re-expression of a DNA repair enzyme, the MGMT, which is epigenetically silenced in nearly half of the GBM patients. Deep sequencing of control and TMZ-treated U251 cell lines allowed us to identify new genes implicated in their survival that are transiently overexpressed after TMZ addition. Analysis of the expression reveals that, both qualitatively and quantitatively, the level of genomic heterogeneity appeared to be reduced in treated cells during a transient period (i.e. D4 to D12) before increasing at D16. A Principal component analysis based on RNA seq data revealed that sensitive cells (i.e. Day 0) form a cluster that is closer to resistant cells (i.e. day 16) than to the transient resistance state (TR) (Fig. 4b). From this study we determined a 4 genes signature which appears to define this state (Fig. 5). We performed, in control and TMZ-treated cells, single cell analysis of the expression of 88 genes including the 4-genes signature and others implicated in cell death program and survival mechanisms, (Fig. 6). This study showed that, using our 4 genes signature, the transient state was not due to a subpopulation of cells but rather to uniform distribution of the TR characters along surviving cells. Analysis of the pathways overexpressed in U251TR cells revealed that histones could undergo important modifications. Targeting of histone acetylation by TSA, an HDAC inhibitor, indeed proved to efficiently eradicate these cells and thus to prevent the appearance of highly resistant and proliferative cells both *in vitro* and *in vivo* (Fig. 7).

Our results, coupling phenotypic analyses on cell death and proliferation rates to RNA seq techniques, suggest that the cell line upon TMZ undergo an initial rapid selection process. This step constitutes a “bottleneck” during which the cells rely on a few survival mechanisms and have a reduced heterogeneity. Next, the cells are expanding to become “fit and resistant” through many different mechanisms rendering these cells difficult to target. This hypothesis fits partially with the “drug tolerant population” recently observed and described by several groups (9-11) upon selection by TKI. However, few marked differences can be pointed out: our results are in favor of the acquisition of MGMT expression by a specific epigenetic process during TMZ rather than selection of pre-existing clone. The expression is not reversible when selective pressure by TMZ is removed, in contrast with other tumors, such as in non-small-cell lung carcinoma cells (11) where reversibility to a former sensitive state has been observed. The U251TR population observed between D4 and D9 is not a uniform one as the 4 genes used as its signature are not equally distributed along the cells. This result suggests that these genes are expressed in particular cells that might cooperate together to create a transient state.

Our study suggests several new directions in the treatment of glioblastoma: using TMZ to induce a TR population and then apply epigenetic drugs to target this population and prevent the appearance of resistant clones.

Acknowledgments: This work was supported by grants by INSERM (Plan Cancer HTE), the Région Pays de la Loire (programme ERRATA) and the Ligue Contre le Cancer Grand Ouest. MR was supported by a doctoral training grant from the ED Biosanté (UBL) and AAAA was supported by a fellowship from UCLM [2015/4062]. This work was realized in the contexts of the LabEX IGO (ANR-11-LABX-0016-0) and of the SIRIC ILIAD Nantes-Angers (INCa-DGOS). We thank the sequencing facility of GenoBird-Biogenouest for expert technical assistance. We also thanks Dr. F. Paris for fruitful comments.

Authors contributions: MR, CG, QS, FB, CP and LO performed and analyzed the biological data obtained with cell cultures. SD, AAAA, JBB, GFC, HJ, JC, VPG performed and analyzed the bioinformatics and mathematical studies. AN, PFC designed and performed the MGMT methylation studies. CC, NJ, ES performed and designed the in vivo experiments. CTC supervised the single cell C1/HD experiments. FMV designed and supervised the experiments with CG, analyzed the data and wrote the manuscript with the contribution of all the authors.

References

1. Merlo LM, Pepper JW, Reid BJ, Maley CC. Cancer as an evolutionary and ecological process. *Nat Rev Cancer* 2006;6:924-35
2. Wang J, Cazzato E, Ladewig E, Frattini V, Rosenbloom DI, Zairis S, *et al.* Clonal evolution of glioblastoma under therapy. *Nat Genet* 2016;48:768-76
3. Yates LR, Campbell PJ. Evolution of the cancer genome. *Nat Rev Genet* 2012;13:795-806
4. Lamprecht S, Schmidt EM, Blaj C, Hermeking H, Jung A, Kirchner T, *et al.* Multicolor lineage tracing reveals clonal architecture and dynamics in colon cancer. *Nat Commun* 2017;8:1406
5. Hammerlindl H, Schaidler H. Tumor cell-intrinsic phenotypic plasticity facilitates adaptive cellular reprogramming driving acquired drug resistance. *J Cell Commun Signal* 2018;12:133-41
6. Gatenby RA, Brown J. Mutations, evolution and the central role of a self-defined fitness function in the initiation and progression of cancer. *Biochim Biophys Acta* 2017;1867:162-6
7. Roerink SF, Sasaki N, Lee-Six H, Young MD, Alexandrov LB, Behjati S, *et al.* Intra-tumour diversification in colorectal cancer at the single-cell level. *Nature* 2018;556:457-62
8. Balaban NQ, Merrin J, Chait R, Kowalik L, Leibler S. Bacterial persistence as a phenotypic switch. *Science* 2004;305:1622-5
9. Al Emran A, Marzese DM, Menon DR, Stark MS, Torrano J, Hammerlindl H, *et al.* Distinct histone modifications denote early stress-induced drug tolerance in cancer. *Oncotarget* 2018;9:8206-22
10. Hata AN, Niederst MJ, Archibald HL, Gomez-Caraballo M, Siddiqui FM, Mulvey HE, *et al.* Tumor cells can follow distinct evolutionary paths to become resistant to epidermal growth factor receptor inhibition. *Nat Med* 2016;22:262-9
11. Ramirez M, Rajaram S, Steininger RJ, Osipchuk D, Roth MA, Morinishi LS, *et al.* Diverse drugresistance mechanisms can emerge from drug-tolerant cancer persister cells. *Nat Commun* 2016;7:10690
12. Stupp R, van den Bent MJ, Hegi ME. Optimal role of temozolomide in the treatment of malignant gliomas. *Curr Neurol Neurosci Rep* 2005;5:198-206
13. Hegi ME, Diserens AC, Gorlia T, Hamou MF, de Tribolet N, Weller M, *et al.* MGMT gene silencing and benefit from temozolomide in glioblastoma. *N Engl J Med* 2005;352:997-1003
14. Esteller M, Garcia-Foncillas J, Andion E, Goodman SN, Hidalgo OF, Vanaclocha V, *et al.* Inactivation of the DNA-repair gene MGMT and the clinical response of gliomas to alkylating agents. *N Engl J Med* 2000;343:1350-4
15. Hegi ME, Liu L, Herman JG, Stupp R, Wick W, Weller M, *et al.* Correlation of O6-methylguanine methyltransferase (MGMT) promoter methylation with clinical outcomes in glioblastoma and clinical strategies to modulate MGMT activity. *J Clin Oncol* 2008;26:4189-99
16. Wiewrodt D, Nagel G, Dreimuller N, Hundesberger T, Pernecky A, Kaina B. MGMT in primary and recurrent human glioblastomas after radiation and chemotherapy and comparison with p53 status and clinical outcome. *Int J Cancer* 2008;122:1391-9

17. Bobola MS, Tseng SH, Blank A, Berger MS, Silber JR. Role of O6-methylguanine-DNA methyltransferase in resistance of human brain tumor cell lines to the clinically relevant methylating agents temozolomide and streptozotocin. *Clin Cancer Res* 1996;2:735-41
18. Sery Q, Rabe M, Oliver L, Vallette FM, Gratas C. HB-EGF is associated with DNA damage and Mcl-1 turnover in human glioma cell lines treated by Temozolomide. *Biochem Biophys Res Commun* 2017;493:1377-83
19. Munshi A, Hobbs M, Meyn RE. Clonogenic cell survival assay. *Methods Mol Med* 2005;110:21-8
20. Tripodi D, Quemener S, Renaudin K, Ferron C, Malard O, Guisle-Marsollier I, *et al.* Gene expression profiling in sinonasal adenocarcinoma. *BMC Med Genomics* 2009;2:65
21. Kim D, Pertea G, Trapnell C, Pimentel H, Kelley R, Salzberg SL. TopHat2: accurate alignment of transcriptomes in the presence of insertions, deletions and gene fusions. *Genome Biol* 2013;14:R36
22. Anders S, Pyl PT, Huber W. HTSeq--a Python framework to work with high-throughput sequencing data. *Bioinformatics* 2015;31:166-9
23. Love MI, Huber W, Anders S. Moderated estimation of fold change and dispersion for RNA-seq data with DESeq2. *Genome Biol* 2014;15:550
24. McKenna A, Hanna M, Banks E, Sivachenko A, Cibulskis K, Kernytsky A, *et al.* The Genome Analysis Toolkit: a MapReduce framework for analyzing next-generation DNA sequencing data. *Genome Res* 2010;20:1297-303
25. Cingolani P, Platts A, Wang le L, Coon M, Nguyen T, Wang L, *et al.* A program for annotating and predicting the effects of single nucleotide polymorphisms, SnpEff: SNPs in the genome of *Drosophila melanogaster* strain w1118; iso-2; iso-3. *Fly (Austin)* 2012;6:80-92
26. Gratas C, Sery Q, Rabe M, Oliver L, Vallette FM. Bak and Mcl-1 are essential for Temozolomide induced cell death in human glioma. *Oncotarget* 2014;5:2428-35
27. Karayan-Tapon L, Quillien V, Guilhot J, Wager M, Fromont G, Saikali S, *et al.* Prognostic value of O6-methylguanine-DNA methyltransferase status in glioblastoma patients, assessed by five different methods. *J Neurooncol* 2010;97:311-22
28. Jarry U, Chauvin C, Joalland N, Leger A, Minault S, Robard M, *et al.* Stereotaxic administrations of allogeneic human Vgamma9Vdelta2 T cells efficiently control the development of human glioblastoma brain tumors. *Oncoimmunology* 2016;5:e1168554
29. Roesch A, Vultur A, Bogeski I, Wang H, Zimmermann KM, Speicher D, *et al.* Overcoming intrinsic multidrug resistance in melanoma by blocking the mitochondrial respiratory chain of slow-cycling JARID1B(high) cells. *Cancer Cell* 2013;23:811-25
30. Sharma SV, Lee DY, Li B, Quinlan MP, Takahashi F, Maheswaran S, *et al.* A chromatin-mediated reversible drug-tolerant state in cancer cell subpopulations. *Cell* 2010;141:69-80
31. Roesch A, Fukunaga-Kalabis M, Schmidt EC, Zabierowski SE, Brafford PA, Vultur A, *et al.* A temporarily distinct subpopulation of slow-cycling melanoma cells is required for continuous tumor growth. *Cell* 2010;141:583-94
32. Pecqueur C, Oliver L, Oizel K, Lalier L, Vallette FM. Targeting metabolism to induce cell death in cancer cells and cancer stem cells. *Int J Cell Biol* 2013;2013:805975

33. Bosc C, Selak MA, Sarry JE. Resistance Is Futile: Targeting Mitochondrial Energetics and Metabolism to Overcome Drug Resistance in Cancer Treatment. *Cell Metab* 2017;26:705-7
34. Oizel K, Chauvin C, Oliver L, Gratas C, Geraldo F, Jarry U, *et al.* Efficient Mitochondrial Glutamine Targeting Prevails Over Glioblastoma Metabolic Plasticity. *Clin Cancer Res* 2017;23:6292-304
35. Weller M, Stupp R, Reifenberger G, Brandes AA, van den Bent MJ, Wick W, *et al.* MGMT promoter methylation in malignant gliomas: ready for personalized medicine? *Nat Rev Neurol* 2010;6:39- 51
36. Bhakat KK, Mitra S. CpG methylation-dependent repression of the human O6-methylguanine-DNA methyltransferase gene linked to chromatin structure alteration. *Carcinogenesis* 2003;24:1337-45
37. Watts GS, Pieper RO, Costello JF, Peng YM, Dalton WS, Futscher BW. Methylation of discrete regions of the O6-methylguanine DNA methyltransferase (MGMT) CpG island is associated with heterochromatinization of the MGMT transcription start site and silencing of the gene. *Mol Cell Biol* 1997;17:5612-9
38. Brandes AA, Franceschi E, Tosoni A, Bartolini S, Bacci A, Agati R, *et al.* O(6)-methylguanine DNAmethyltransferase methylation status can change between first surgery for newly diagnosed glioblastoma and second surgery for recurrence: clinical implications. *Neuro Oncol* 2010;12:283- 8
39. Terai H, Kitajima S, Potter DS, Matsui Y, Quiceno LG, Chen T, *et al.* ER Stress Signaling Promotes the Survival of Cancer "Persister Cells" Tolerant to EGFR Tyrosine Kinase Inhibitors. *Cancer Res* 2018;78:1044-57
40. Chisholm RH, Lorenzi T, Lorz A, Larsen AK, de Almeida LN, Escargueil A, *et al.* Emergence of drug tolerance in cancer cell populations: an evolutionary outcome of selection, nongenetic instability, and stress-induced adaptation. *Cancer Res* 2015;75:930-9
41. Liao BB, Sievers C, Donohue LK, Gillespie SM, Flavahan WA, Miller TE, *et al.* Adaptive Chromatin Remodeling Drives Glioblastoma Stem Cell Plasticity and Drug Tolerance. *Cell Stem Cell* 2017;20:233-46 e7

Figure 1

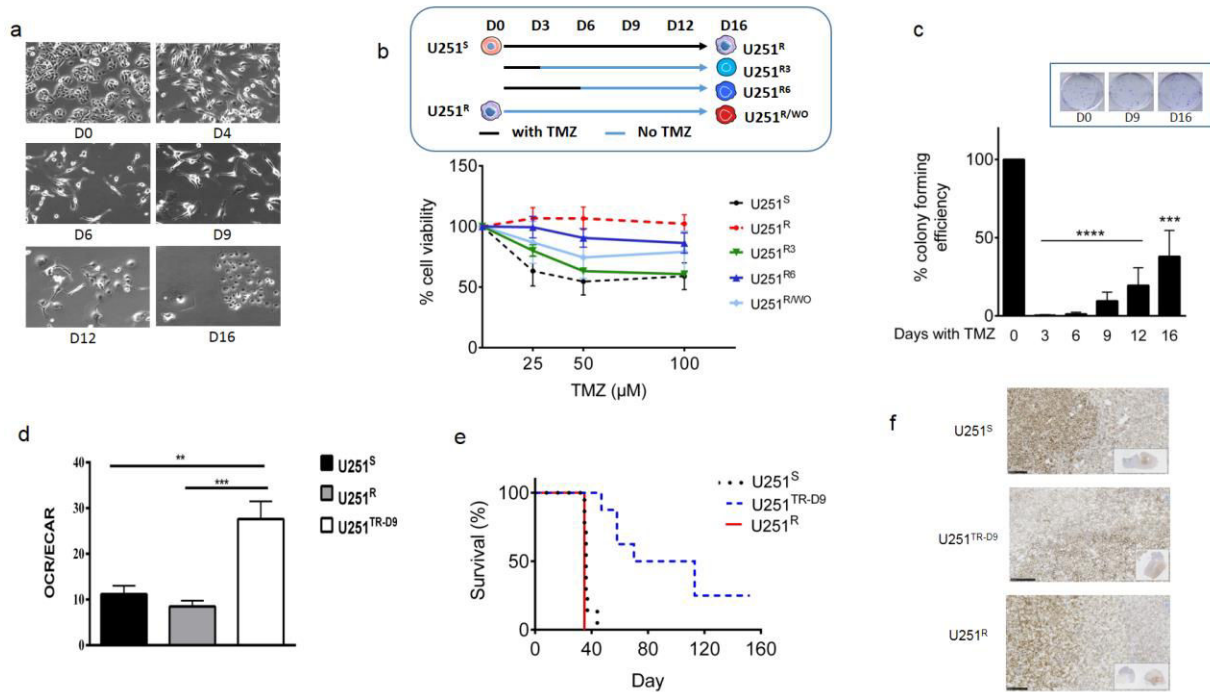


Figure 1 | U251 cells follow a reproducible and distinctive pathway after TMZ treatment.

(a). Morphological aspect (light microscopy, x 32) of U251 treated with 50 μ M TMZ every 3 days from day 0 (D0) to day 16 (D16). (b). (top): Experimental design of TMZ treatment before determination of cell viability by MTT. U251R: U251 cells were treated at 50 μ M TMZ every 3 days for 16 days; U251R3, U251R6: U251 cells were treated respectively 3 and 6 days with 50 μ M TMZ and collected at day 16; U251R/WO: U251 were treated with TMZ for 16 days and then left untreated for 12 weeks. (Bottom) Cell viability assayed at D16 by MTT, after 72h exposure to TMZ at 25, 50, 100 μ M. (c). Colony forming efficiency of U251 during the time course of treatment: U251 cells were exposed to TMZ 50 μ M for 0,3,6,9,12,or 16 days and cells were then respectively plated at 100, 30000, 15000, 2000, 500 and 300 cells per well. (n=3). (d). Oxygen consumption rate (OCR) and extracellular acidification rate (ECAR) ratio of U251S, U251TR-D9 (cells collected after 9 days of TMZ treatment), and U251R measured by Seahorse Technology. (e). Kaplan-Meier survival curves from mice injected orthotopically with U251S, U251R and U251TR-D9 cells. U251TR-D9 were cells obtained after 9 days exposure to TMZ 50 μ M. N=7 for U251S, N=3 for U251R and N=8 for U251TR-D9. (f). Representative immuno-histochemistry of one tumor of each group. Sections were stained with human MHC class I antibody.

Figure 2

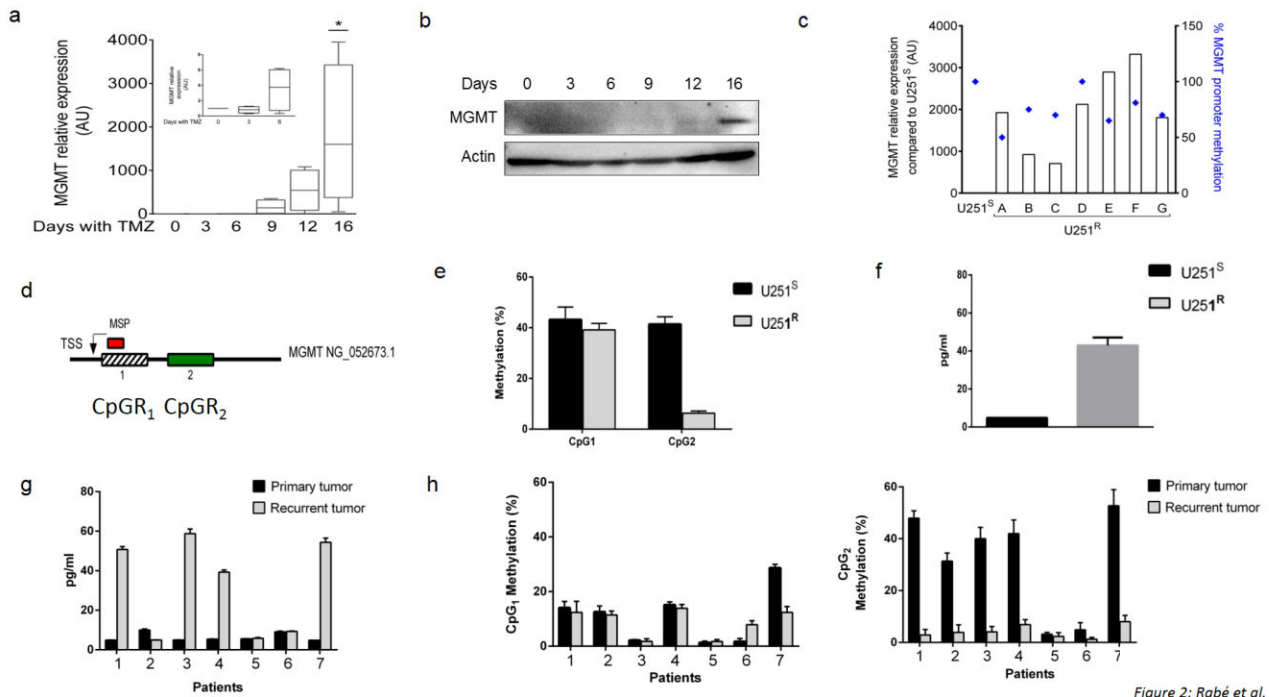


Figure 2: Rabé et al.

Figure 2 | MGMT status along the time course of acquisition of resistance

(a). MGMT relative expression, measured by qPCR, in U251 during the time course of resistance acquisition (n=4). Inset: detail analysis of the first 6 days. (b). Representative western blot for MGMT protein expression. Actin was used as loading control. (c). MGMT promoter methylation (qMSP-PCR) and MGMT RNA expression in U251S and U251R (n=7) (d). Schematic representation of MGMT promoter region CpG1 and CpG2 studied by MRSE, TSS: transcription start site; MSP: sequence amplified by qMSP-PCR (e). Analysis of CpG1 and CpG2 in U251S and U251R (f). MGMT protein expression in U251S and U251R (g). MGMT protein expression in 7 GBM tumours (primary and recurrent).(h). Analysis of CpG1 and CpG2 methylation in the 7 primary and recurrent tumours.

Figure 3

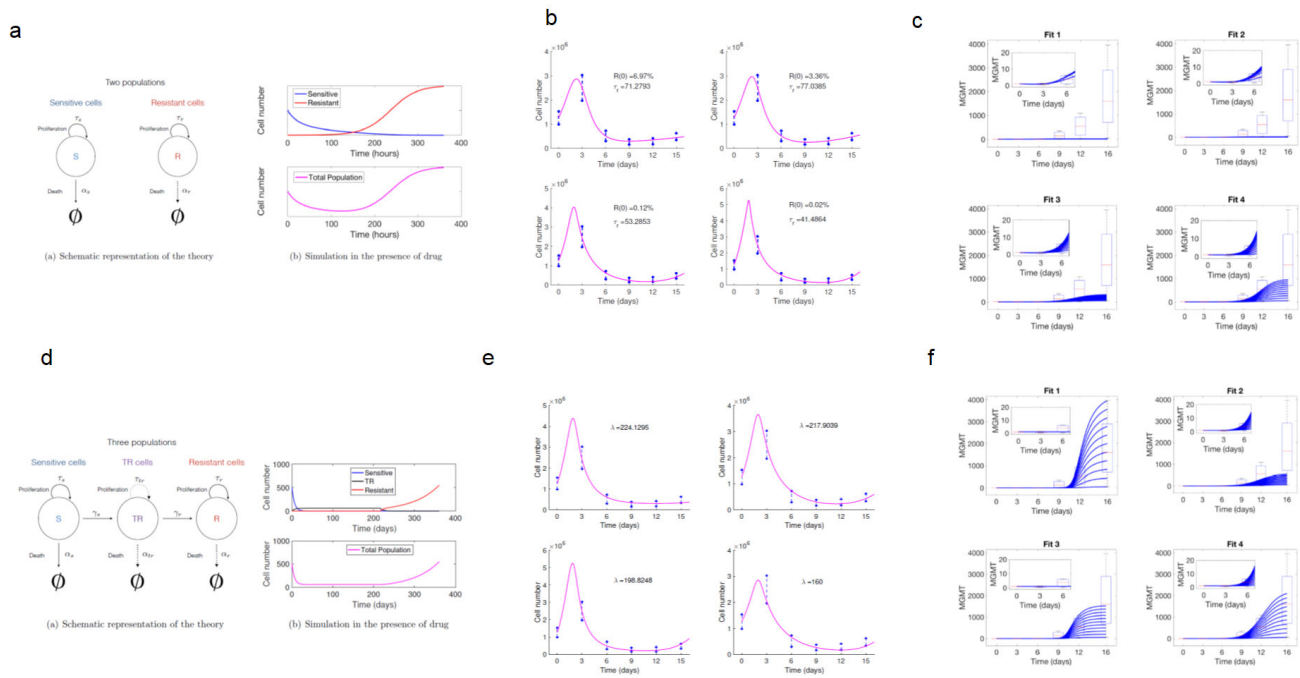


Figure 3 | Mathematic model of resistance acquisition

(a) Scheme and basic dynamics of the clonal selection framework: (left) Schematic representation of the theory; (right) mathematical simulation of cell proliferation in the presence of TMZ (see Supplementary Info 2) (b). Data fittings according to the clonal selection interpretation. (c). MGMT variability within the clonal selection mode according to the 4 fits in (b). (d). Scheme and basic dynamics of the acquired resistance model: (left) Schematic representation of the theory; (right) mathematical simulation of cell proliferation in the presence of TMZ (see Supplementary Info 2). (e). Data fittings according to the acquired resistance / transient population model. (f). MGMT Variability within the clonal selection mode according to the 4 fits in (d).

Figure 4

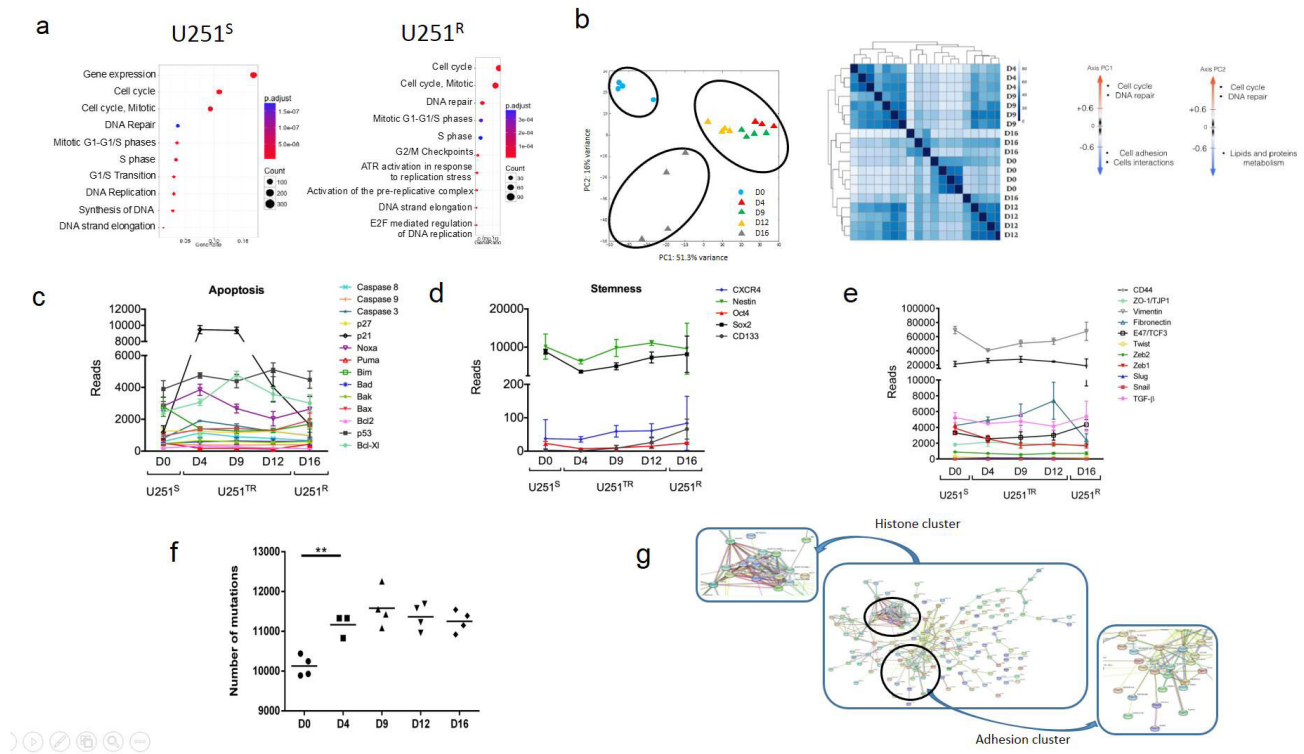


Figure 4 | RNaseq analysis

(a). Over representation tests; first 15 categories of pathways highlighted during TMZ treatment of U251. left: U251S. Right: U251R. Gene Ratio: proportion of mapped genes to each pathway. Count: number of genes. (b).(left) Principal Component Assay (PCA) and heatmap resulting from the transcriptome analysis of U251 after 0,4,9,12,16 days with 50µM TMZ treatment. PCA axes interpretation in terms of correlated pathways. (Right) Groups of genes highly correlated are tested using Reactome pathways database. (c-e).Number of reads during acquisition of resistance for genes belonging to the apoptosis (c), stemness (d), and epithelial to mesenchymal transition families (e). (f). Mutation burden as a function of days of TMZ treatment expressed as number of mutations in U251 compared to normal human genome. (g).Functional proteins association networks (STRING analysis) of genes overexpressed during the transient state (D4, D9 and D12) (fold change >log2).

Figure 5

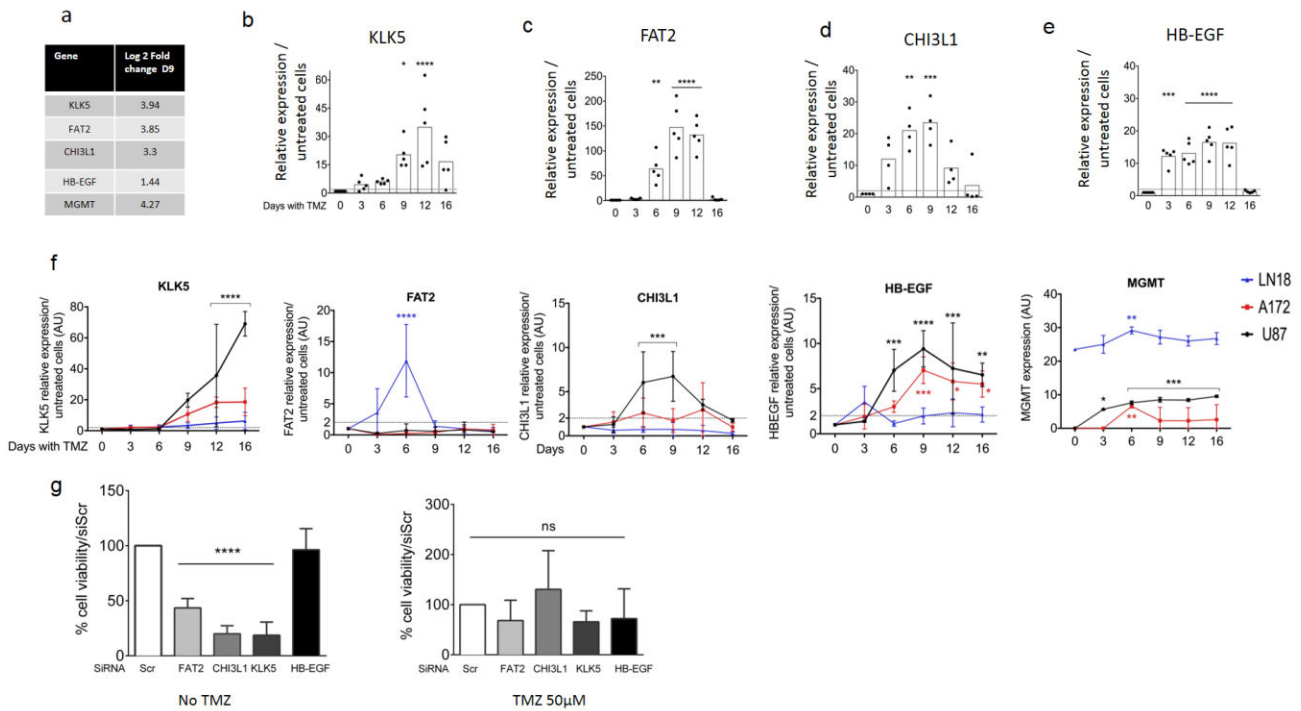


Figure 5 | Genes signature

(a). Relative expression of the 4 genes signature (KLK5, FAT2, CHI3L1, HBEGF) obtained from the RNAseq analysis: in the tolerant U251TR-D9 cells (b-e). Time course of the expression of KLK5, FAT2, CHI3L1 and HBEGF by RT-qPCR during acquisition of resistance of U251 cells treated with 50 μ M TMZ, n= 5 (f). Q-PCR analyses of the expression of KLK5, CHI3L1, FAT2, HBEGF and MGMT in A172, U87, LN18 human glioma cell lines treated respectively by 50, 250 and 350 μ M TMZ over 16 days (g). Knock down of molecular signature genes with siRNA directed against the respective genes in U251 cells non treated (left) and in U251 cells treated with TMZ 50 μ M for 6 days (right). Cells were collected and counted on day 7.

Figure 6

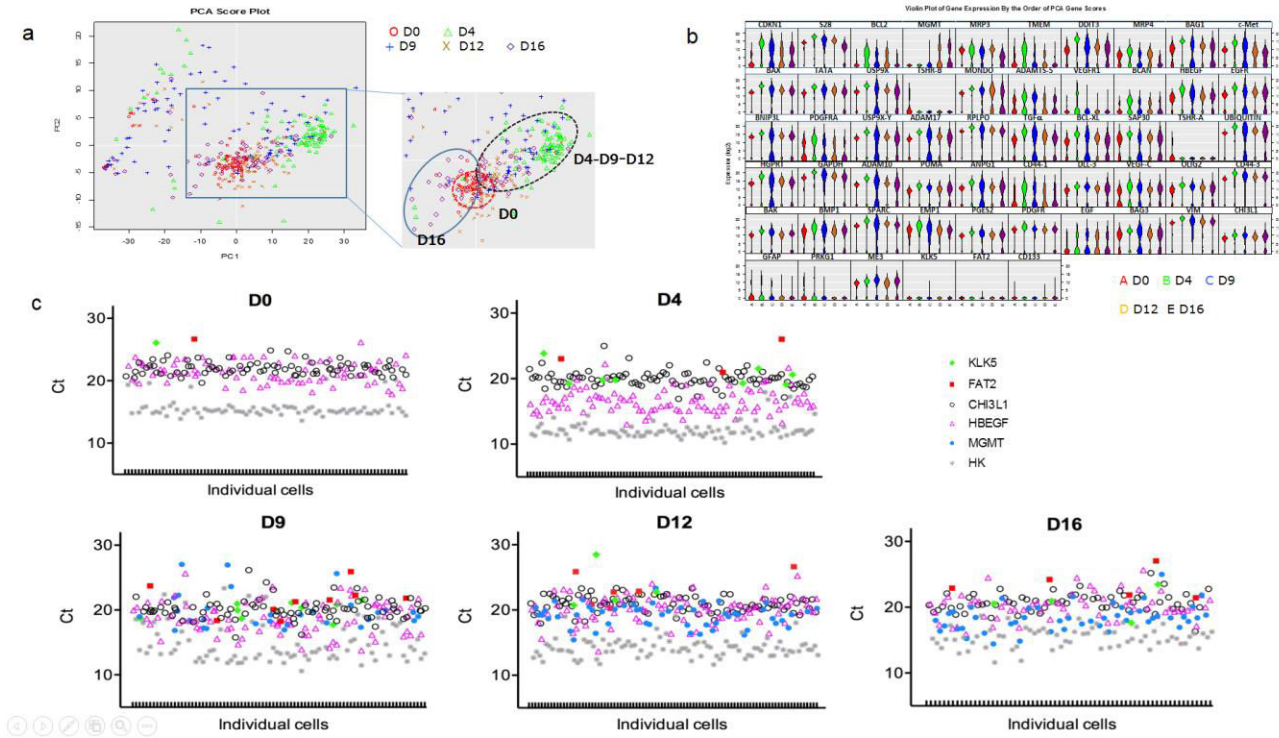


Figure 6| Single cell analyses

(a). PCA resulting from single cell analysis of U251, and U251 treated for 4,9,12, and 16 days at 50 μM TMZ. (b). Violin plot of gene expression used in the C1/HD experiments. A=Day 0, B= Day 4; C= Day 9; D= Day 12 and E=Day 16. Y axis represent (Threshold-Ct), meaning that the expression level is correlated to the y value.(c). Expression of the molecular signature genes in single cell during the time course of the acquisition of resistance. All graphs are representative of one single cells analysis out of 3.

Figure 7

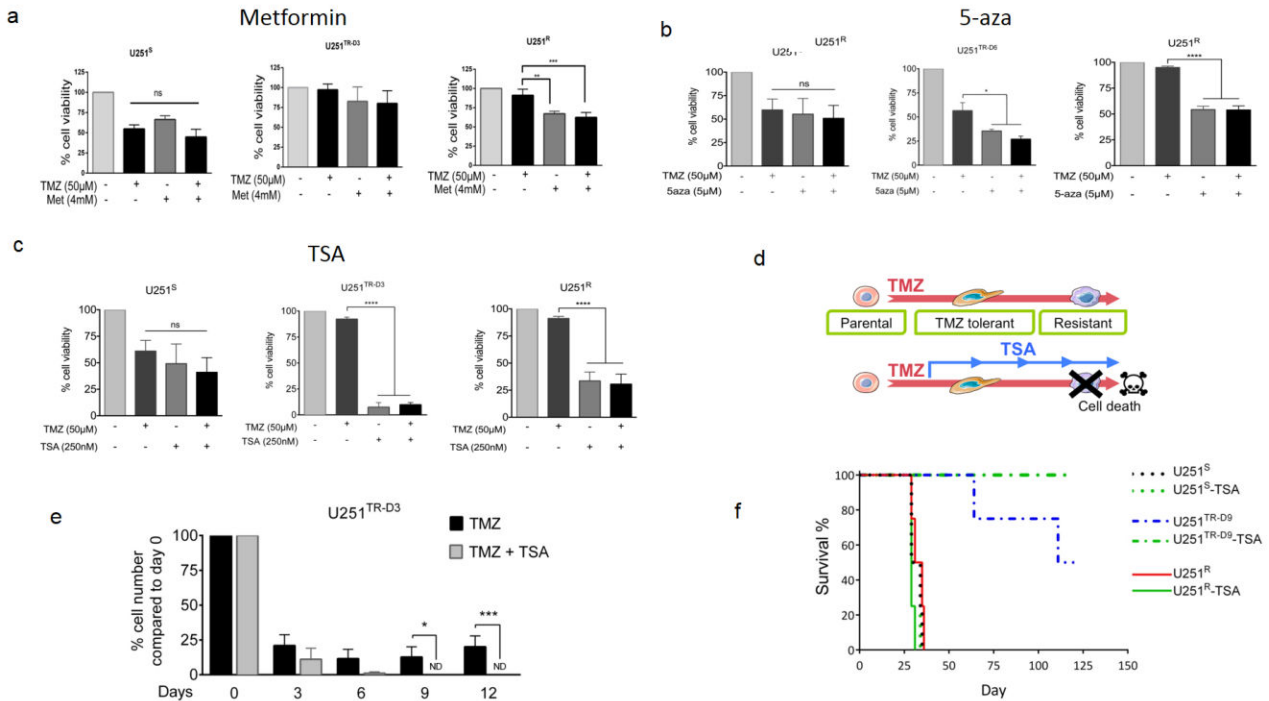
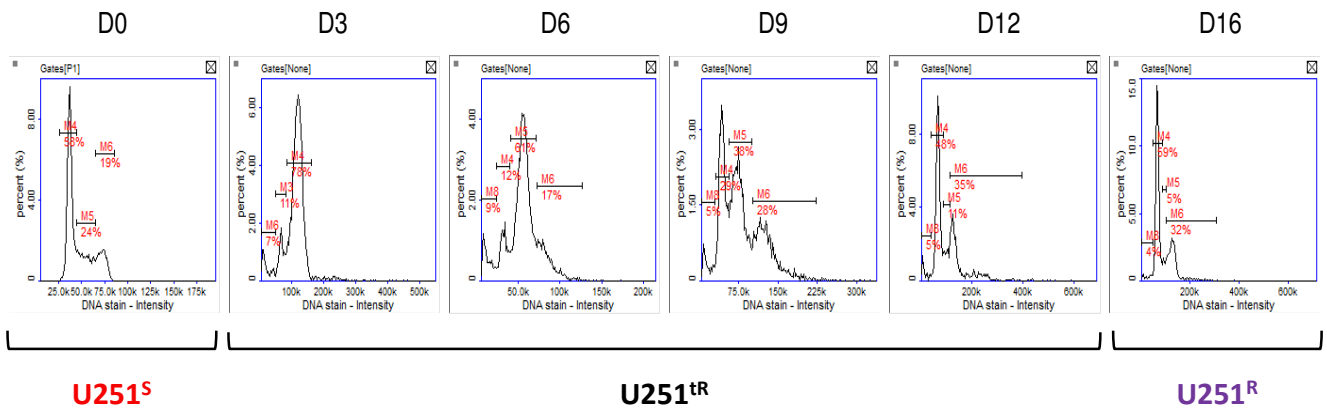


Figure 7| Drug sensitivities of the different U251 populations.

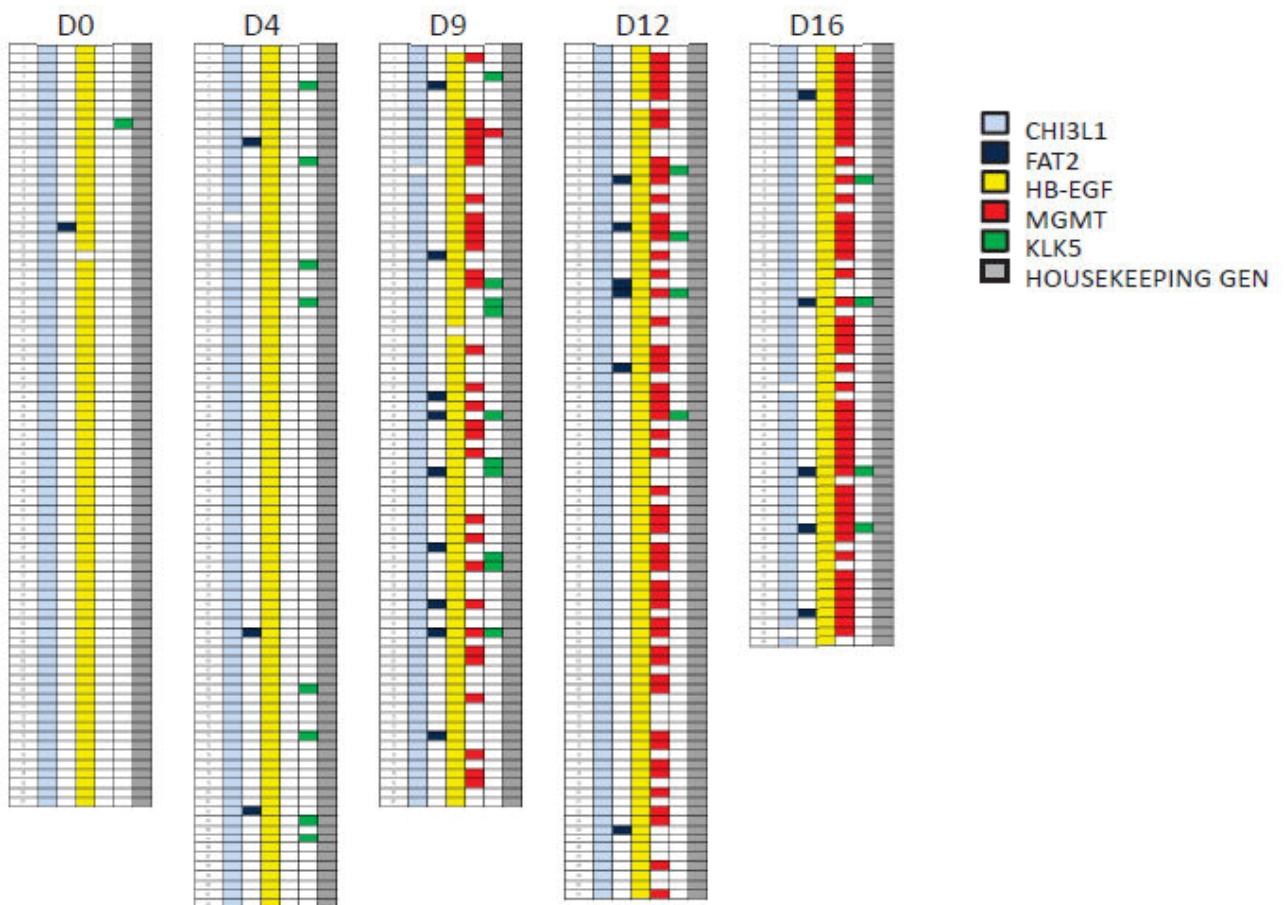
Cell viability evaluated by MTT after 72h exposure to different drugs combinations in U251S, U251TR-D3 and U251R: (a). 4mM Metformin, an inhibitor of mitochondrial respiration, (b). 5µM of 5-aza, a DNA demethylation agent (c). 250 nM TSA, an histone deacetylase inhibitor (HDAC). Data are expressed as % of viable cells compared to non-treated cells (d). Schematic representation of a therapeutic strategy to prevent emergence of resistant cells (e). Long term effect of 250nM TSA on U251TR-D3. Cells were counted every 3 days during a 50µM TMZ treatment combined with 250nM TSA. (f) . Kaplan-Meier survival curves from mice injected orthotopically with U251S, U251R and U251 TR-D9 cells treated or not with TSA 250 nM (n=4 for each group).

Rabe et al.

Supplementary Figure 1



Supplementary Figure 2



Rabe et al.

Supplementary Table S1 : Primers Sequences

Primer name	Sequence
S28 (S)	TTTTGGAGTCAGAGCGAG
S28 (AS)	CTGTGACAGACCATTCCC
RPLPO (S)	GATTACACCTTCCCCTTGCT
RPLPO (AS)	TAGTCAAAGAGACCAAATCCCA
TATA (S)	CAAGAGTGAAGAACAGTCCAG
TATA (AS)	ACAAGGCCTTCTAACCTTATAGG
HGPRT (S)	GAAGAGCTATTGTAATGACCAG
HGPRT (AS)	GCCAGTGTCAATTATATCTTCC
HB-EGF (S)	GAGAGTCACTTTATCCTCCA
HB-EGF (AS)	GTCCTTGTATTTCCGAAGAC
MGMT (S)	CTGAATGCCTATTTCCACCA
MGMT (AS)	TGCTGGTAAGAAATCACTTCTC
CHI3L1 (S)	TGTCGGAGGATGGAACCTTGG
CHI3L1 (AS)	GCCTTCATTTCTTGATTAGGGT
KLK5 (S)	CGTCTCCTCTCATTGTCCCT
KLK5 (AS)	TGGTGCATCTATCTGTCTCGG
FAT2 (S)	CATGAAGATGTGGACCTGTG
FAT2 (AS)	TGGACTTTGACATTGAGAAGAC

Supplementary Figure 2 : List of genes used in the single cell experiment

ADAM10	KRT13	CHI3L1	RPS4Y1	DKK1	BCL2	BAG3	MONDO
ANKRD1	ADAMTS 5	CCND2	DDX3Y	S28	TSHR-B	CRHR1	c-Met
GMR8	ADCY2	FAT2	FAT2	EFEMP	ADAM17	MGMT	EGF
ME3	CD137	SAP30	PRKG1	SPARC	PRKG1	USP9X	HGF-1
RPLPO	GAPDH	UBIQUITIN	HGPRT	TMEM	KLK5	CDKN1A	ANPG1
BAX	BAK	MCL1	HBEGF	CD137	VEGFC	SKG3	BAG1
PUMA	BNIP3L	BCL-XL	PDGFRA	USP9X-Y	IEX-1	EFEMP-1	HER4
CD133	VIM	CADH	EMP1	FAT2	MRP3	MRP4	TSHR-A
VEGFR1	MGMT	LEMD1	DDIT3	CD44-1	CD44-3	BCAN	KLK5
PDGFR	OLIG2	DLL3	GFAP	MEDAG	SCN9A	BMPER	CHI3L1
PGES2	TATA	COX2	IGF	BMPER	TGF α	EGFR	KRT13

Primer sequences will be available on demand

Supplementary Methods

RNA seq. Fragments size of libraries was controlled on D1000 ScreenTape with 2200 TapeStation system (Agilent Technologies). Libraries with P5-P7 adaptors were specifically quantified on LightCycler® 480 Instrument II (Roche Life Science) and normalized with DNA Standards (1-6) (# KK4903, KAPABIOSYSTEMS - CliniSciences). 12 pM of each library was pooled and prepared according to Denaturing and diluting libraries protocol for the HiSeq and GAIIx, part#15050107 v02 (Illumina) for cluster generation on cBot™ system. After sequencing, demultiplexing and quality control with fastQC_0.11.2 (<http://www.bioinformatics.babraham.ac.uk/projects/fastqc/>), Illumina adapter were trimmed with Cutadapt-1.2.1 (1) and reads with Phred quality score below 30 were filtered with prinseq-lite- 0.20.3 (2,3).

siRNA from Dharmacon, GE Healthcare: CHI3L1: # L-012568-01, KLK5: L-005916-00, HBEGF: L-019624, and FAT2: L-011270-00.

Cell cycle analyses. Determination of G0/G1, S and G2/M cell cycle phases were obtained in U251 cells during TMZ treatment every 3 days and up to 16 days were done with the NucleoCounter® NC-250™ system (Chemometec, Denmark) according to the protocol for cell cycle analysis in fixed cells. Briefly, cells were harvested and fixed in 70% ethanol. After further wash, cells were stained with Solution 3 (Chemometec, 1µg/ml DAPI, 0.1% triton X-100 in PBS) and quantified for their DNA content.

Orthotopic injections of human glioma cell lines in NSG mice. NSG (NOD.Cg-Prkdcscid Il2rgtm1Wjl/SzJ) mice (Charles River Laboratories, France) were bred in the animal facility of the University of Nantes (UTE, SFR F.Bonamy) under SPF status and used at age of 6 to 12 weeks, according to institutional guidelines (Agreement # 00186.02; Regional ethics committee of the Pays de la Loire, France). Orthotopic injections of cells (10⁴ in 2 µl PBS), were performed using a stereotactic frame (Stoelting) at 2 mm on the right of the medial suture and 0.5 mm in front of the bregma, depth: 2.5 mm. U251S, U251TR-D9 (treatment *in vitro* for 9 days at 50µM TMZ) and U251R were injected on the same day. Animals were observed daily and euthanized when characteristic symptoms occurred, such as reduced mobility and significant weight loss. Tumors were fixed in PFA Some tumors were analyzed and sections (2µm) were used for histological staining by hematoxylin-eosine, and a rabbit anti-human anti-MHC class I Ab (clone EPR1394Y; Abgent). Slides were scanned using nanoZoomer 2.0 HT (Hamamatsu Photonics K.K., Hamamatsu, Japan).

Tumor samples. Tumors were collected from the “Réseau des tumorothèques du Canceropole Grand-Ouest/réseau Gliome”, the “Base clinico-biologique des Glioblastomes (n°BRIF: BB-0033-00093), CHU Angers, France" and the Biological Resource Center of University hospital of Angers and used according to French laws and recommendations of the French National Ethics Committee. All subjects signed a specific informed consent form approved by an Ethics Committee, the French State Department for National Education, Higher Education and Research and the CNIL.

1. Martin M. Cutadapt removes adapter sequences from high-throughput sequencing reads. *EMBnetJournal* 2011;17:10-3
2. Schmieder R, Edwards R. Quality control and preprocessing of metagenomic datasets. *Bioinformatics* 2011;27:863-4
3. Schmieder R, Edwards R. Fast identification and removal of sequence contamination from genomic and metagenomic datasets. *PLoS One* 2011;6:e17288

Supplementary Information 1 : Mathematical models

Experimental results:

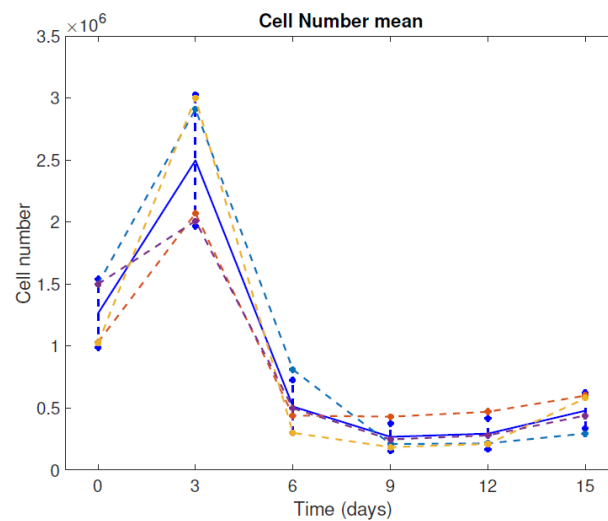


Figure SI2.1: Evolution of U251 cell numbers sampled at days 3; 6; 9; 12 and 15. The solid blue line and the vertical error bars correspond to the mean and standard deviation of four replica experiments.

This behaviour suggests that TMZ does not exhibit an immediate effect on cancer cells. To better understand the underlying processes, we looked at information in the existing literature and found the following information:

- In References [1]-[3] experiments with the same cell line, U251, were carried out in the absence of drugs. From the measured results for cell growth, we can "estimate" the doubling time τ_s of these cells. The obtained values were $\tau_s = 34.35$; 28.86 and 34.75 hours, respectively. Therefore, the doubling time used in the *in silico* simulations should be within those values.
- In Ref. [4] changes in survival of U251 cells were measured with a concentration of $150 \mu\text{M}$ of TMZ. No significant changes in cell survival were observed during the first 24 h. See Ref. [4] Figure 1.
- In another work (Ref. [5]), cell survival was measured after 48h in the same cell line with different concentrations of TMZ. In the experiments with $50 \mu\text{M}$, which correspond to the same concentration employed in the present study, there was almost no significant difference in cell survival during the first two days. See Ref. [5] Figure 2.A.

Therefore, very similar results during the initial course of TMZ administration on U251 cells have been previously obtained and support our experimental findings. Thus, in our mathematical model we make a first hypothesis: TMZ does not display an immediate effect on U251 cell survival for a concentration of $50 \mu\text{M}$. The time delay required to observe a significant TMZ-induced cell death is around two days. We further assume that this change from no response to total response is progressive. Hence, a drug response function will be defined and will be present as a product factor in all those processes where TMZ is involved. This function depends on time, and goes from 0, corresponding to no effect, to 1, implying a total effect. The profile of this function is depicted in Figure SI2.2.

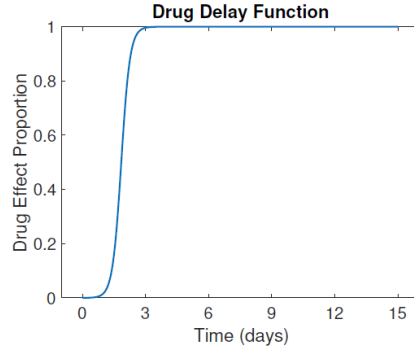


Figure SI2.2: Effect of TMZ on U251 cells during drug administration, starting at time $t = 0$.

Mathematical analyses:

Here we wished to address the following questions. Is the final resistant population due to a Darwinian-type selection of a resistant clone already present from the beginning? Or, else, does a resistant population emerge as a consequence of a Lamarckian-type of evolution leading to phenotypic variation from which the non-genetic inheritance of an acquired adaptive trait can be transmitted to the offspring? These two questions reflect two possible hypotheses. To identify which is more plausible, we develop two different mathematical models according to the two premises.

1.1 Clonal Selection Model

The idea behind this hypothesis is the existence of a subpopulation with high levels of resistance. The presence of the drug will result in an important decrease of the sensitive population, while the resistance cells will continue to grow eventually becoming the dominant clone (see figure 3a).

From a mathematical point of view, such dynamics can be easily described with a system of two ordinary differential equations. Assuming a logistic growth, the equations can be written as:

$$\frac{dS}{dt} = \frac{S}{\tau_s} \left(1 - \frac{S+R}{K} \right) - DE(t)\alpha_s S, \quad (1a)$$

$$\frac{dR}{dt} = \frac{R}{\tau_r} \left(1 - \frac{S+R}{K} \right) - DE(t)\alpha_r R, \quad (1b)$$

$$S(0) \neq 0, \quad (1c)$$

$$R(0) \neq 0, \quad (1d)$$

where $DE(t)$ is the drug effect function mentioned before. With these equations and using a least squares method to estimate the parameter values, it is possible to fit the experimental data. However, due to the number of parameters to be evaluated there are several combinations that could explain the experimental results. In Figure 3B we present four possible fits, with their corresponding parameters presented in Table 1.

Parameter	Description	Fit 1	Fit 2	Fit 3	Fit 4
τ_s	Sensitive cells doubling time (h)	35.640	38.585	26.643	21.366
τ_r	Resistant cells doubling time (h)	71.279	77.039	53.285	41.486
K	Saturation parameter (cells)	10^7	10^7	10^7	10^7
α_s	Sensitive death rate, $50\mu\text{m}$ TMZ (h^{-1})	0.058	0.050	0.052	0.060
α_r	Resistant death rate, $50\mu\text{m}$ TMZ (h^{-1})	0.010	0.006	0.001	0.001
$\frac{S(0)}{S(0)+R(0)}$	Initial proportion of sensitive cells (%)	93.03	96.64	99.88	99.98
$\frac{R(0)}{S(0)+R(0)}$	Initial proportion of resistant cells (%)	6.97	3.36	0.12	0.02
drug delay	Parameter of the function $DE(t)$ (h)	63.081	59.805	47.316	45.472
a	Parameter of the function $DE(t)$	0.035	0.0485	0.124	0.5

Table SI2.1: Estimated parameter values within the clonal selection interpretation. Parameter K was fixed before the analysis.

1.2 Acquired Genetic Expression

Within the realm of the Lamarckian-type evolution, we can think of the emergence of resistant cells not due to a pre-existing clone but as a consequence of genetic noise amplified by the presence of the drug. In this framework we hypothesize that cells can evolve from a sensitive phenotype towards a resistant one, so cells which were initially sensitive can acquire partial or total resistance to the administered drug. This mechanism is not direct, and cells need to go through a transient state, in which they remain non-proliferative but significantly reduce their apoptosis induced by the drug. Therefore, in addition to the sensitive and resistant populations, we incorporate another population, called "transitory resistant" (TR). The basic scheme is shown in Figure 3d. To represent this new dynamic, we put forward an gstructured model, including a new variable, the age a (time) of transition from TR to resistant cells. Since sensitive and resistant cells do not depend on this variable, it is not necessary to include it in both populations. Our system can be written as:

$$\frac{dS}{dt} = \frac{S}{\tau_s} \left(1 - \frac{S + TR + R}{K} \right) - DE(t)\alpha_s S - DE(t)\gamma_s S, \quad (2a)$$

$$\frac{\partial TR(a, t)}{\partial t} = -\frac{\partial}{\partial a}(v(a)TR(a, t)) - DE(t)\gamma_r F(a)TR(a, t) + \gamma_s S(t)\mathbb{1}_{(a=0)}, \quad (2b)$$

$$\frac{dR}{dt} = \frac{R}{\tau_r} \left(1 - \frac{S + TR + R}{K} \right) - \alpha_r R + \int_0^{a_{max}} \gamma_r F(a)TR(a, t) da \quad (2c)$$

$$S(0) \neq 0, TR(0) = 0, R(0) = 0. \quad (2d)$$

In these equations, $F(a)$ denotes a distribution function. Figure SI2.3 illustrates an example of this function.

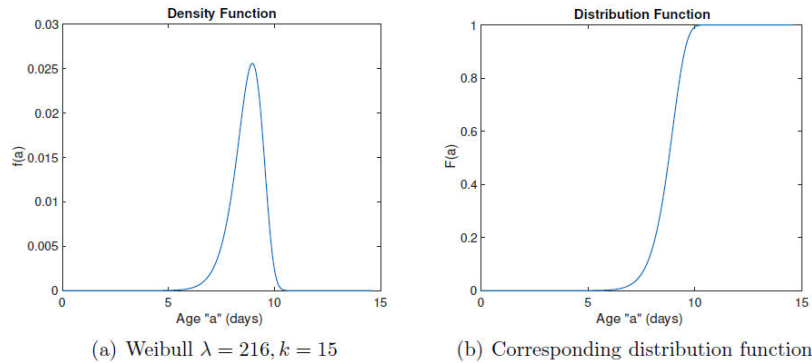


Figure SI2.3: Functions used in this simulations

As in the clonal selection model, there are several combinations of parameters that explain the measured cell number at different times. In Figure 3d, four examples of possible combinations are shown, with the corresponding parameters collected in Table SI2.2. An important feature of these simulations is that, initially, only sensitive cells are present in the cell cultures.

Parameter	Description	Fit 1	Fit 2	Fit 3	Fit 4
τ_s	Sensitive cells proliferation time (h)	23.46	29.45	19.07	40
τ_r	Resistant cells proliferation time (h)	46.92	56.54	23.86	44
K	Saturation parameter (cells)	10^7	10^7	10^7	10^7
α_s	Sensitive death rate, $50\mu\text{m}$ TMZ (h^{-1})	0.06	0.047	0.07	0.038
α_r	Resistant death rate, $50\mu\text{m}$ TMZ (h^{-1})	0.01	0.0016	0.02	0.001
γ_s	Transition rate from S to TR (h^{-1})	0.0017	0.0002	0.0011	0.00018
γ_r	Transition rate from TR to R (h^{-1})	0.0075	0.01	0.0089	0.002
λ	Parameter from the Weibull distribution	224.13	217.90	198.82	160
k	Parameter from the Weibull distribution	14.98	0.75	15.01	0.75
$\frac{S(0)}{S(0)+DTP(0)+R(0)}$	Initial proportion of sensitive cells (%)	100	100	100	100
drug delay	Parameter of the function $DE(t)$	44 h	44 h	44 h	44 h
a	Parameter of the function $DE(t)$	0.1	0.1	0.1	0.1

Table SI2.2: Estimated parameter values for the acquired genetic expression model.

2. MGMT expression

In this section, we analyze the MGMT expression of the total population, which is a biomarker of resistance. During the first six days there is almost no change in MGMT expression, with an important increase occurring from day 9. Changes in population's MGMT expression are shown in Figure 2a, where the dynamics of 4 different experiments are plotted, and represented with the corresponding boxplots.

2.1 Clonal Selection Hypothesis

Cancer cells have basal values of the protein MGMT, and its overexpression is related with a resistant phenotype. Within the clonal selection hypothesis, the normalized MGMT expression of the total population can be easily modelled by means of the following equation:

$$MGMT(t) = \frac{m_1 S(t) + m_2 R(t)}{S(t) + R(t)}, \quad m_1 < m_2, \quad (3)$$

where m_1 and m_2 are weight parameters. To analyze how MGMT expression in cancer cells is changing with the treatment, our obtained results are compared with untreated cells, i.e., with the MGMT expression at day 0. Therefore, the relative MGMT expression is given by:

$$[MGMT]_{\text{Rel}}(t) = \frac{MGMT(t)}{MGMT(0)} = \frac{\frac{m_1 S(t) + m_2 R(t)}{S(t) + R(t)}}{\frac{m_1 S(0) + m_2 R(0)}{S(0) + R(0)}} = \frac{S(t) + \alpha R(t)}{S(0) + \alpha R(0)}, \quad \text{with } \alpha = \frac{m_2}{m_1}. \quad (4)$$

Note that due to the employed normalization, there is only one parameter, α , which stands for the MGMT expression ratio of resistant cells with respect to the basal values of sensitive cells (Table SI2.3). We wish to set forth two relevant questions. Can the MGMT changes observed in the experiments be explained with this theory? Is the final variability in agreement with the observations?

In Figure 3c we show how different values of fits provide dissimilar MGMT curves. In Fit 3 and Fit 4 plots, with a low initial percentage of resistant cells (0.12 and 0.02% respectively), the clonal selection interpretation could explain some of the observed experimental results. However, even though the variability is well captured during the first six days; this mathematical model is not able to explain the high variability from day 9 to 16, as all the MGMT curves are well below the median.

Fit	R(0)	α min	α max
1	6.97 %	22.79	1000
2	3.36 %	13.02	248.12
3	0.12%	53.98	516.12
4	0.02 %	51.10	1215.7

Table SI2.3: estimated parameter value for the clonal model

2.2 Acquired Resistance Hypothesis

Within the acquired resistance hypothesis, and assuming TR cells are changing their MGMT expression from the basal value m_1 to the resistant level m_2 according to their age, MGMT expression can be expressed as follows:

$$MGMT(t) = \frac{m_1 S(t) + m_2 R(t) + \int_{a_{\min}}^{a_{\max}} TR(a, t) M(a, m_1, m_2, \lambda, k) da}{S(t) + R(t) + \int_{a_{\min}}^{a_{\max}} TR(a, t) da}, \quad m_1 < m_2. \quad (5)$$

where,

$$M(a, m_1, m_2, \lambda, k) = \frac{m_2 - m_1}{2} (1 + \tanh(k(a - \lambda))) + m_1. \quad (6)$$

is a function ranging from m_1 to m_2 , depending on the parameter λ and k . The relative expression would depend also on the same parameter, α

$$[MGMT]_{\text{Rel}}(t) = \frac{\frac{S(t) + \alpha R(t) + \int_{a_{\min}}^{a_{\max}} TR(a, t) M(a, \alpha, \lambda, k) da}{S(t) + R(t) + \int_{a_{\min}}^{a_{\max}} TR(a, t) da}}{\frac{S(0) + \alpha R(0) + \int_{a_{\min}}^{a_{\max}} TR(a, 0) M(a, \alpha, \lambda, k) da}{S(0) + R(0) + \int_{a_{\min}}^{a_{\max}} TR(a, 0) da}}, \quad \alpha = \frac{m_2}{m_1}. \quad (7)$$

As in this hypothesis there are only sensitive cells at the beginning, $R(0)=0$ and $TR(a,0)=0 \forall a > 0$, eq. (7) becomes

$$[MGMT]_{\text{Rel}}(t) = \frac{S(t) + \alpha R(t) + \int_{a_{\min}}^{a_{\max}} TR(a, t) M(a, \alpha, \lambda, k) da}{S(t) + R(t) + \int_{a_{\min}}^{a_{\max}} TR(a, t) da}, \quad \alpha = \frac{m_2}{m_1}. \quad (8)$$

where,

$$M(a, \alpha, \lambda, k) = \frac{\alpha - 1}{2} (1 + \tanh(k(a - \lambda))) + 1. \quad (9)$$

It is reasonable to think that cells are changing from TR to resistant cells as fast as they are changing their MGMT expression from $m1$ to $m2$. Therefore, for each fit, those values are the same as those shown in Table 2. As mentioned before, there are many parameter values that could explain the cell number curves. Each combination of the different parameters provides dissimilar MGMT curves, where the parameters λ and k are very important in this analysis (Table SI2.4). To gain insight of the meaning of these parameters, in Figure SI2.4, the influence of both parameters is analyzed. The value of λ marks the time at which cells have acquired half of the total MGMT, and the value of k provides information about how fast is the process of resistance acquisition; the larger the value of k , the faster the process becomes.

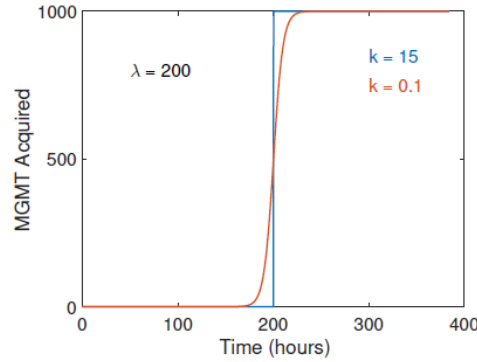


Figure SI2.4: example of the effect of λ and k in the function

Figure 3C shows the different behaviours of the different fits, with their corresponding α min and α max values shown in Table SI2.4. We analyze the corresponding figures: There is almost no variability during the first 9 days in fits 1 and 3 plots. After that, and depending on the value of α , fit is possible to get high variability at day 16. With this theory and the present model, when k is around 0.75 it is possible to get a large variability during the first 9 days. In the fourth fit, different values of α provide high variability during all the experimental days, as observed in the experiments. Let's notice that with this theory, as only sensitive cells are present at the beginning, and only resistant cells at the end (or almost only), the final value of MGMT is close to α .

$$RE_MGMT(t_f) \simeq \frac{\alpha R(t_f)}{\frac{R(t_f)}{S(0)}} \simeq \alpha \quad (10)$$

Fit	λ	k	α min	α max
1	224.13	14.98	52.32	4183
2	217.90	0.75	51.78	564
3	198.82	15.01	49.82	1532
4	160	0.75	52.10	2213

Table SI2.4: estimated parameter for the acquired resistance model

3. Conclusions

After making a number of hypothesis about the delay in the effect of TMZ on U251 cells, we have seen that both theories are able to explain the behaviour of the cell number dynamics. In both of them, there are several possible combinations for the parameters. The predictions of the mathematical models, representing each of the theoretical frameworks, for the cell number behaviour can be very similar and, thus, when fitting the current experimental results, it is not possible to decide with certainty which of the two interpretations, clonal selection versus acquired resistance, yields the best explanation. Now, if the MGMT expression of the population is followed over time then, after making the corresponding hypotheses, we saw how the MGMT expression changed according to the two different interpretations. In both of them, there was only one new parameter, ρ representing the MGMT expression ratio of resistant cells with respect to the sensitive ones. Within the clonal selection framework, it was possible to find values of ρ that could explain some of the observed experimental results, those with the lower final values of MGMT. However, for all the explored parameter combinations it was no possible to find any ρ that could explain the high variability at day 16. Presumably, had the follow-up of the cell populations being extended further in time, the agreement would have worsened rather than improved. In contrast, within the acquired resistance hypothesis, it was possible to find values of ρ and different parameter combinations that could explain the variability during all the experimental time points. Therefore, although one cannot completely discard the clonal selection hypothesis when looking only at the cell number dynamics, we may conclude that if both the cell number curves and the MGMT expression results are considered, then the hypothesis that there is a transient state from sensitive to resistant cells appears to provide a better underlying explanation of the experimental results. It should be pointed out that it is not possible to rule out that a combination of the two interpretations may actually take place simultaneously. Since they are not mutually exclusive, it could thus occur that both a small initial population of resistant cells is present and also that sensitive cells may traverse an intermediate TR state before becoming fully resistant.

4. References

- [1] Austin M. Guo, Ju Sheng, Gloria M. Scicli, Ali S. Arbab, Norman L. Lehman, Paul A. Edwards, John R. Falck, Richard J. Roman and A. Guillermo Scicli. Expression of CYP4A1 in U251 Human Glioma Cell Induces Hyperproliferative Phenotype in Vitro and Rapidly Growing Tumors in Vivo *Journal of Pharmacology and Experimental Therapeutics* October 1, 2008, 327 (1) 10-19.
- [2] Liu, X., Li, G., Su, Z., Jiang, Z., Chen, L., Wang, J. ... Liu, Z. (2013). Poly(amido amine) is an ideal carrier of miR-7 for enhancing gene silencing effects on the EGFR pathway in U251 glioma cells. *Oncology Reports*, 29, 1387-1394.
- [3] Wang, F., Sun, J., Zhu, Y., Liu, N., Wu, Y., & Yu, F. (2014). MicroRNA-181 inhibits glioma cell proliferation by targeting cyclin B1. *Molecular Medicine Reports*, 10, 2160-2164.
- [4] Murphy, AC., Weyhenmeyer B, Schmid J, et al. Activation of executioner caspases is a predictor of progression-free survival in glioblastoma patients: a systems medicine approach. *Cell Death Disease*.2013; 4(5):e629.
- [5] Cheng Y, Sk UH, Zhang Y, et al. Rational Incorporation of Selenium into Temozolomide Elicits Superior Antitumor Activity Associated with Both Apoptotic and Autophagic Cell Death. Wu GS, ed. *PLoS ONE*. 2012;7(4): e35104.

Supplementary Information 2 : List of putative impacts taken into account for variants filtering with SnpEff:

chromosome_number_variation
exon_loss_variant
frameshift_variant
stop_gained
stop_lost
start_lost
splice_acceptor_variant
splice_donor_variant
rare_amino_acid_variant
missense_variant
disruptive_inframe_insertion
conservative_inframe_insertion
disruptive_inframe_deletion
conservative_inframe_deletion
5_prime_UTR_truncation+exon_loss_variant
3_prime_UTR_truncation+exon_loss
splice_branch_variant
splice_region_variant
stop_retained_variant
initiator_codon_variant

Article 9 : Senescent endothelial cells increase the bellicosity of GBM cells surviving from radiation therapy through secretion of CXCL5/8.

Charlotte Degorre¹, Ophélie Renoult¹, Charbel Touma¹, Manon Pietri^{1,2}, Noémie Joalland^{1,4}, Natacha Galopin¹, Catherine Gratas^{1,3}, François Vallette^{1,2,4}, Claire Pecqueur^{1,4§} and François Paris^{1,2 §}

¹CRCINA, INSERM, CNRS, Université de Nantes, Nantes, France, ²Institut de Cancérologie de l'Ouest, Saint-Herblain, France, ³Centre Hospitalier-Universitaire de Nantes, Nantes, France, ⁴LabEx IGO "Immunotherapy, Graft, Oncology", Nantes, France.

Malgré un traitement agressif, les patients atteints de glioblastome multiforme (GBM) rechute rapidement dans la zone péri-tumorale, autour de la zone d'exérèse chirurgicale. La tumeur récidivante est généralement résistante à une nouvelle radiothérapie, du fait de la radiorésistance intrinsèque des cellules tumorales infiltrantes et de l'altération du microenvironnement péri-tumoral irradié. Par exemple, la sénescence des cellules endothéliales, après irradiation, conduit à la libération des chimiokines pro-inflammatoires. Dans cette étude, nous avons évalué l'influence de ces cellules endothéliales sénescents sur le comportement de cellules tumorales de GBM survivantes après une exposition aux rayonnements ionisants. L'observation du phénotype des cellules tumorales irradiées par microscopie fournit une preuve directe que le sécrétome des cellules endothéliales sénescents diminue la prolifération et la radiosensibilité des cellules GBM, tout en augmentant les anomalies mitotiques et l'instabilité génomique. L'analyse de ce sécrétome démontre l'implication des chimiokines CXCL5 et CXCL8, qui imitent les effets du sécrétome des cellules sénescents sur les cellules tumorales de GBM. L'injection orthotopique, dans un modèle murin de xénogreffe, de cellules de GBM survivantes à une irradiation ou prétraitées par du sécrétome de cellules endothéliales sénescents ou par CXCL5/8 démontre une augmentation de l'agressivité et de la létalité de ces cellules. Ces données mettent en avant le rôle crucial des cellules endothéliales sénescents dans l'agressivité des cellules GBM qui survivent à la radiothérapie.

En préparation

Senescent endothelial cells increase the bellicosity of GBM cells surviving from radiation therapy through secretion of CXCL5/8

Charlotte Degorre¹, Ophélie Renoult¹, Charbel Touma¹, Manon Pietri^{1,2}, Noemie Joalland¹, Natacha Galopin¹, Catherine Gratas^{1,3}, François Vallette^{1,2,4}, Claire Pecqueur^{1,4} § & François Paris^{1,2} §

Authors affiliation: ¹CRCINA, INSERM, CNRS, Université de Nantes, Nantes, France, ²Institut de Cancérologie de l'Ouest, Saint-Herblain, France, ³Centre Hospitalier-Universitaire de Nantes, Nantes, France, ⁴LabEx IGO “Immunotherapy, Graft, Oncology”, Nantes, France.

§ Corresponding authors:

- François Paris, Centre de Recherche en Cancérologie et Immunologie Nantes-Angers, INSERM U1232, Université de Nantes, 8 quai Moncoussu, 44007 Nantes, France; e-mail: francois.paris@inserm.fr; phone: (33) 228080302; Fax: (33) 228080204
- Claire Pecqueur, Centre de Recherche en Cancérologie et Immunologie Nantes-Angers, INSERM U1232, Université de Nantes, 8 quai Moncoussu, 44007 Nantes, France; e-mail: claire.pecqueur@univ-nantes.fr; phone: (33)2 2808 0325; Fax: (33)2 2808 0204

Authors contribution: CD, CP, FP designed research, FV provided primary human samples; CD, OR, CT, MP, NJ, NG, CG performed research, CD, CP, FP analyzed data, CD, CP, FP manuscript writing

Keywords: endothelium, senescence, genomic instability, radiation resistance,

Acknowledgements: We thank the microscopy platform MicroPICell, the cytometry core facility Cytocell for technical help and genomic platform (ERRATA project). We also thank La ligue contre le cancer.

The authors declare no conflict of interest

Abstract

Despite an aggressive combined treatment, glioblastoma (GBM) tumor are rapidly relapsing in the irradiated peritumoral area around the site of the surgical site. The recurrent tumor is resistant to new radiotherapy, which is commonly explained by the intrinsic radioresistance of infiltrating tumor cells, disregarding the plasticity alteration of irradiated peritumoral microenvironment. In fact, senescence of microvascular endothelial cells relarguing proinflammatory chemokines has been noticed in culture but also in GBM biopsies after irradiation. In this present, manuscript, we are suggesting that senescent endothelial cells are alleviating the behavior and the aggressiveness of surviving GBM cells after exposure to ionizing radiation. Those data demonstrate a crucial role of senescent endothelial cells through the secretion of CXCL5/8 cells in the bellicosity of GBM cells surviving from radiation therapy. We clearly demonstrate using long-term time lapse microscopy that secretome from senescent endothelial cells is lowering the proliferation and death of irradiated GBM cells, but also increasing mitotic abnormalities, genomic instability considered by micronuclei generation and cellular aneuploidy. Functional characterization of the secretome demonstrates the involvement of the chemokines CXCL5 and CXCL8, which are mimicking effects of the whole secretome of senescent cells on irradiated GBM cells. Inhibition of those chemokines or of CXCR2, their shared receptor, in GBM cells reduced the induction of micronuclei and the aneuploidy. Orthotopic injection in mouse brain of irradiation-surviving GBM cells pretreated either by SASP or CXCL5/8 showed an increase of aggressiveness and lethality as compared to those treated with medium from non-senescent endothelial cells.

Introduction

Radiation therapy by inducing irreversible DNA damage and thereafter death of cancer cells, is one of the most common curative anti-cancer treatments, allowing, in some cases, a complete regression of the tumor. Unfortunately, its efficacy against aggressive tumors like glioblastoma is challenged by the intrinsic tumor resistance of infiltrating cellular clones, such as a subpopulation of cancer stem cells. The highly infiltrative features of these tumors requires large field radiotherapy covering up to a third of the whole brain, leading to significant irradiation of the surrounding healthy tissue. Despite these aggressive treatments, median survival of GBM patients does not exceed 18 months and most patients experienced tumor recurrence at the original tumor location within the year of primary treatment. Those tumor relapse acquired a gain of aggressiveness and resistance to genotoxic treatment. Indeed, they are usually insensitive to a second run of radiation therapy. The resistance may also be mediated by the ability of radiation to induce DNA damage. If left un- or mis-repaired, DNA breaks leads to genomic instability in which genetic alterations range from nucleotide changes to chromosomal translocations and aneuploidy. This genomic instability may lead to mitotic catastrophe and cell death, but also to emergence of novel radio-resistant subpopulations of tumor cells.

In the purpose to kill the whole population of tumor cells and avoid tumor relapse, new therapeutic approaches are developed targeting not only clonogenic tumor cells, but also non-transformed cells from the stroma (Moding, Cancer J, 2016). Because of its ubiquity and its vital function in normal and tumoral tissues, vascular network is one of the stimulating stroma's targets. Microvasculature lined by a single inner layer of endothelial cells supported by pericytes is delivering nutrients and oxygen to tissues while removing metabolic wastes. Abundant evidences highlight that endothelial cells dysfunctions induced by radiation impact tumor responses. High doses of ionizing radiation induce endothelial cells apoptosis within the tumor, subsequently sensitizing cancer cells to radiation allowing tumor regression (Garcia-Barros, Paris et al. 2003). Endothelial cell apoptosis is triggered by the rapid generation of ceramide, a pro-apoptotic sphingolipid, upon the hydrolysis of sphingomyelin by acid sphingomyelinase (aSMase) (Niaudet et al., Cellular Signaling, 2017). The genetic disruption of the *asmase* gene in mice prevents endothelial cells apoptosis and the radiation-induced tumor regression (Garcia-Barros, Paris et al. 2003). High doses of radiation also induce a well-known tumor bed effect characterized by an impaired neovascularization with

reduced blood perfusion and low oxygen tension (Rofstadt EK, Cancer Res 2005). This hypoxic microenvironment triggers an extended latency period and a low growth rate in tumor, but also enhances radiation resistance as compared to the same tumor budding in a more oxygenated bed.

Besides its acute effects, radiation exposure of endothelial cells may lead to long-term dysfunctions including adhesion and aggregation of platelets, development of platelet-fibrin thrombi and ultimately cellular senescence. Senescence is a premature aging process characterized by the inability of the cell to cycle, the up-regulation of senescence-associated β -galactosidase (SA β -gal) staining, the maintenance of a Senescence-Associated Secretory Phenotype (SASP) and the persistence of DNA lesion. Senescent endothelial cells perturb the normal tissue homeostasis by enhancing ischemia or fibrosis through increase of hypoxia and inflammation. We recently better deciphered the radio-induced senescence in quiescent primary microvascular endothelial cells and showed the induction of 2 different mechanisms implying either cytoplasmic p53 activation, initiated by long lasting DNA damage and ATM phosphorylation, or the induction of superoxide stress, triggered in part by a dysfunctional complex II of the mitochondrial respiratory chain (Lafargue 2017).

Induction of tumor cell senescence by radio- or chemo-therapy is now a well-accepted strategy to participate to the tumor control (Yang, Nature 2017) by limiting the number of tumor cell able to divide. However, the chronic maintenance of a secretory phenotype (senescent associated secretory phenotype or SASP) also interferes in the dialog between senescent cells and the other cells within the tumor. This secretome includes inflammatory cytokines, chemokines, proteases and growth factors. Whereas some factors fuel beneficial effects limiting tumor progression, other factors may have deleterious tumorigenic properties, for example by stimulating cell proliferation, neoangiogenesis or Epithelial-Mesenchymal transition (EMT) (DeMaria, 2016). Normal stromal fibroblasts also enter senescence after DNA-damaging treatment. These senescent cells and their SASP can promote tumor cell proliferation and invasion. For example, secreted matrix metalloprotease 3 (MMP-3) is disrupting alveolar and branching morphogenesis, inducing a functional differentiation of non-malignant breast epithelial cells and finally stimulating epithelial cell proliferation leading to carcinogenesis (Krtolica et al., 2001) (Parrinello et al., 2005).

Senescent endothelial cells have been detected in 20 Gy-irradiated brains of nude mice and in the tumor vicinity of post-mortem biopsies of recurrent glioblastoma from patients treated with surgery and 60 Gy radiotherapy (Borovski et al., 2013) (De Pascalis et al., 2018). However, whether endothelial cell senescence modulates biological response to radiation therapy remains unclear. In the present manuscript, we are assessing how senescent endothelial cells mitigate GBM response to ionizing radiation. We demonstrated that CXCL5 and CXCL8 chemokines secreted by senescent endothelial cells are enhancing radiation-induced genomic instability, aneuploidy and aggressiveness of tumor recurrence proving that the modification of tumor microenvironment plasticity by irradiation directly impacts the bellicosity of GBM cells surviving from radiation therapy.

Results

SASP enhances tumor genomic instability in response to radiation

In order to analyze SASP effects on GBM cell response to radiation, irradiated U251 tumor cells were stalked by videomicroscopy after pretreatment with conditioned medium from non-irradiated (CM) or 15 Gy-induced senescent (SASP) endothelial cells. As compared to CM, SASP treatment significantly decreased the proliferation of unirradiated U251 cells. This inhibition was dramatically emphasized by the combination of 5 Gy-irradiation and SASP (Figure 1A and supplementary data S1). Furthermore, we observed the occurrence of abnormal divisions corresponding to cells that either divided in more than two cells or are unable to finish their mitosis because of chromosomal bridge. Indeed, whereas the number of abnormal divisions in non-irradiated and irradiated cells treated in CM was around 2% at all time points, it increased to 10% when cells were irradiated in SASP (Fig 1B). Because abnormal divisions lead to genome misdistribution and polyploidy, we counted the number of polynucleated cells 72 hours after 5 Gy and found 2-times more polynucleated cells when cells were pretreated by SASP as compared to CM (Fig. 1C).

To further evaluate GBM cell response to radiation in presence of senescent endothelial cell, U251 clonogenic cell assays were performed at different radiation doses (0-15Gy) in presence of SASP or CM. Plating efficiency was not altered by SASP since the number of colonies in absence of irradiation was similar in both conditions (Fig 1D). Interestingly, SASP increased the number of U251 colonies only after exposure to high dose of radiation (Fig. 1D and 1E). The radioprotective properties of SASP was confirmed using primary cultures of GBM cells directly isolated from human tumors, since the number of colonies was higher in presence of SASP compared to CM after radiation in a dose-dependent manner up to 10 Gy (Fig. 1F).

Because of its relation to abnormal division and genomic instability, micronuclei (MN), corresponding to extranuclear organelles containing DNA, were evaluated in 5 Gy-irradiated U251 pretreated with CM or SASP. As expected, significant number of MN was only observed in irradiated U251 cells (Figure 2A and 2B). Furthermore, SASP triggered a faster and stronger production of MN as compared to CM. These micronuclei mostly sequestered damaged DNA regardless of the culture conditions, as shown by γ H2AX staining (Figure 2C). Interestingly, the frequency of cells displaying various numbers of MN 72 hours after 5Gy

was significantly different between the 2 conditions. In fact, 50% of the irradiated cells displayed no MN after CM treatment vs. 35% after SASP (Figure 2D). On the other hand, 22% of irradiated cells with SASP showed 3 MN or more as compared to 11% after CM. These observations were confirmed in various primary GBM cells where the number of MN per cell was significantly increased when cells were irradiated in presence of the SASP (Figure 2E). To determine whether SASP-induced MN formation is limited to tumor cells or also occurs in normal cells, the endothelial cell line HUVEC was cultured in presence of either CM or the SASP, and irradiated at 5 Gy. Again, the SASP increased MN production in response to 5Gy-irradiation (Supplementary data S2). Altogether, these results showed that the SASP promotes MN formation in response to radiation.

Identification of key cytokines from the SASP

RNAseq analysis was performed on radio-induced senescent endothelial cells in order to identify the key SASP factors involved in GBM cell genomic instability. The comparison of transcriptional profiling between non-irradiated and senescent endothelial cells identified 242 genes differentially expressed, with a majority of them being up-regulated (Figure 3A). Bioinformatics analysis using gene annotation analysis showed an enrichment of proteins involved in several binding processes, in particular receptor binding (Supplementary data S3). This latter category included 13 potentially secreted factors such as chemokines, cytokines and growth factors (Figure 3B). To validate these results, RTqPCR (Figure 3C) and ELISA (Figure 3D) were performed focusing on the 2 most up-regulated proteins, LIF and CXCL5, as well as 2 well-known interleukins secreted by endothelial cells, CXCL8 and IL-33. Surprisingly, if RTqPCR confirmed the transcriptional upregulation of those chemokines, a strong discrepancy were observed by ELISA at the secretion level. IL-33 was detectable neither in the CM nor in the SASP. LIF was present without difference of concentration in both CM and the SASP. Remarkably, when a low concentration of CXCL8 and CXCL5 were detected in CM (0.87 ± 0.4 and 0 respectively), their amounts were significantly increased in SASP (2.6 ± 0.6 and 25 ± 6 respectively).

CXCL8 and CXCL5 modulated radiation-induced genomic instability and colonegenic survival through binding to the shared receptor CXCR2

To determine whether these 2 chemokines secreted by senescent endothelial cells were impacting radiation responses of GBM cells, blocking antibodies against CXCL8 and CXCL5

respectively were added to CM or SASP prior to tumor cell irradiation. Blocking either CXCL8 or CXCL5 significantly reduced micronuclei production when U251 cells were irradiated in presence of the SASP whereas it did not affect significantly micronuclei formation when cells were irradiated in CM (Figure 4A). Of note, the combination of both blocking antibodies did not displayed additional effect on micronuclei formation compared to each individual blocking antibody. To confirm these results, CXCL8 (1ng/ml), CXCL5 (50pg/ml) or a combination of both were added to the cell media 24 hours prior to irradiation. Each chemokine increased micronuclei production in response to 5 Gy (Figure 4B). Moreover, addition of both CXCL8 and CXCL5 triggered the same amount of micronuclei after irradiation compared to SASP itself. Similar experiments using CM supplemented with both CXCL8 and CXCL5 were realized to analyze polynucleated cell frequencies and radioresistance. Again, the combination of both chemokines increased the number of polynucleated cells (Figure 4C) as well as the number of U251 colonies (Figure 4D) after irradiation. CXCL8 chemokine binds to CXCR1 and CXCR2. Interestingly, CXCR2 is also a receptor for CXCL5. U251 cells did not express CXCR1 in contrast to CXCR2 that was slightly but significantly expressed (Figure 5A). Various primary GBM cell models also expressed CXCR2 receptor (Figure 5B). To investigate whereas CXCL8 and CXCL5 trigger genomic instability through binding to their common receptor, CXCR2 antagonist (SB332235 (SB)) or a CXCR2 blocking antibody (MAB331 (MAB)) was added to SASP before U251 irradiation. Both pharmacological and immunological approaches to block CXCR2 activation were able to reduce micronuclei formation (Figure 5C) and polynucleated cells frequency (Figure 5D) while no effect was observed when it was added to CM. Altogether, these results show that the binding of CXCL8 and CXCL5 to CXCR2 fully recapitulates the SASP-induced phenotypes.

SASP triggers the phosphorylation of CHK1, NPM and ERK through CXCL8 and CXCL5

To better investigate the molecular mechanisms triggering SASP-induced genomic instability, the activation of DNA damage response and stress pathways were analyzed by western blot in irradiated U251. As expected, phosphorylation of DDR proteins, including DNA-PK, ATM, ATR, NPM, CHK1, CHK2 were enhanced after irradiation (Figure 6 and Supplementary data S4). Studied stress pathways (AKT, P38 MAPK) were constitutively activated without radiation (data not shown). The SASP pretreatment did not alter the phosphorylation level for

most of those proteins. Only, the phosphorylated forms of NPM, CHK1 and ERK1/2 were significantly increased when U251 cells were irradiated in presence of the SASP (Figure 6A). Importantly, individual inhibition of the activation of those proteins significantly reduced radio-induced MN formation (Figure 6B) and polynucleated cell frequency (Figure 6C) triggered by addition of CXCL8 and CXCL5 in the CM.

CXCL8 and CXCL5 present in SASP increases U251 cells bellicosity in vivo

To investigate whether this genomic instability is associated to tumor aggressiveness *in vivo*, U251 cells clones surviving from irradiation after pretreatment by either CM or SASP (respectively called RCM and RSASP), then injected orthotopically into the cerebral subventricular zone of NSG mice. As shown in Figure 7A, mice bearing RCM tumors survived longer than the ones bearing RSASP tumors (median survival: 58 days for RCM vs 42 days for RSASP; $p=0.0028$; Figure 7E). Similar experiments were repeated with U251 clones surviving from radiation after treatment with CM containing CXCL8 and CXCL5 chemokines (called R_{CM}CXCL). Interestingly, the survival of the mice population transplanted with R_{CM}CXCL was reduced and similar to the one of RSASP (median survival 40.5 days) (Figure 7B). Finally, we assessed the opposite experiment by collecting radio-resistant U251 clones pretreated with SASP and CXCR2 inhibitors, using either the blocking antibody or the antagonist (respectively called R_{SASP}MAB and R_{SASP}SB). If the survival of the population of mice transplanted with R_{SASP}SB were moderately modulated, the one of R_{SASP}MAB was strongly enhanced and the mice were surviving as well as those with RMC (median survival 49 days for R_{SASP}MAB and 57.5 days for R_{SASP}SB) (Figure 7C and 7D). Altogether, these results showed that tumor cells arising in a senescent environment are more bellicuous than the ones cultured in regular CM. Importantly, presence of both CXCL8 and CXCL5, the 2 chemokines triggering genomic instabilities, was sufficient to recapitulate this aggressiveness *in vivo*.

Discussion

Our previous studies highlighted how early apoptosis in microvascular endothelial cells are enhancing tumor regression after exposure to high-dose of ionizing radiation (Garcia-Barros et al., Science 2001). In the present study, we now established that long-term endothelial senescent is driven an aggressive phenotype to relapse GBM cells after radiotherapy through the secretion of CXCL5 and CXCL8 leading to enhancement of genomic instability.

The recurrence of tumor after first-line therapy represents a major issue in oncology. In fact, it is well-accepted that tumor cells inside a cancerous mass may respond differently to the therapy. This heterogeneity will select the survival of resistant tumor cells when the most sensitive will be killed. Furthermore, genotoxic treatment against cancer will also induce gene mutation leading to chromosome rearrangement and development of cancer clones with a gain of resistance. In the present manuscript, we described that the modification of peritumoral microenvironment plasticity by radiation therapy also enhances the aggressiveness of tumor relapse. The irradiation of the peritumoral area after surgery is commonly provided for infiltrating tumors, such as GBM or mammary carcinoma to kill the remaining tumor cells. We prove that the irradiation of this peritumoral area will induce the chronic senescence of non-transformed endothelial cells which is enhancing GBM tumor cell instability through a paracrine response.

Because of the inability of tumor cell to divide and to migrate, senescence is emerging as a therapeutic strategy to repress the overall tumor growth after radiation therapy (Sabin RJ et al. Genome integ. 2011). However, its detrimental effects including tumor promotion, relapse and metastasis, must be considered (Coppé et al., 2006; Parrinello et al., 2005; Krtolica et al., 2001). Senescence-Associated Secretory Phenotype (SASP) is associated with the release of numerous cytokines, chemokines, growth factors and proteases. Whereas some SASP factors are known to fuel the deleterious effects of senescent cells, other factors may have beneficial effects. Consistent with its complex composition, the SASP can have various effects from stimulating cell proliferation to cell differentiation or EMT stimulation. Tumor cell senescence induced by ionizing radiation may also modify microenvironment homeostasis by enhancing angiogenesis or inflammation-induced immune response or cell surface heparin proteoglycan syndecan 1 (SDC1) expression in malignant breast stromal fibroblasts (Liakou

et al Aging, 2016). The over-expression of SDC1 in those fibroblast are, in return, creating a favorable setting for human mammary carcinoma cell proliferation via FGF2 activation. Our results on endothelial cell senescence driven GBM aggressiveness and recurrence confirm how senescence of tumor microenvironment cellular compound is deleterious on the behavior of the tumor exposed ionizing radiation.

Long-term time lapse microscopy provides a direct evidence that the SASP from endothelial cells is lowering the proliferation and radiosensitivity of GBM cells, but also increasing their genomic instability distinguishable by mitotic abnormalities and induction of aneuploidy and micronuclei. Characterization of the SASP demonstrates the involvement of the chemokines CXCL5 and CXCL8 that are mimicking the effects on irradiated GBM induced by the whole secretome of senescent cells. Inhibition of those chemokines or of CXCR2, their shared receptor, in GBM cells reduced the induction of micronuclei and aneuploidy. Finally, orthotopic injection in mouse brain of irradiation-surviving GBM cells pretreated either by SASP or by a combination of CXCL8 and CXCL5 showed an increase of aggressiveness and lethality as compared to those treated with medium from non-senescent endothelial cells, or in presence of CXCR2 inhibition. Those data clearly demonstrate a crucial role of senescent endothelial cells through the secretion of CXCL5/8 cytokines in the bellicosity of GBM cells surviving from radiation therapy.

Material and methods:

Cell culture

Culture of Primary Human Lung Microvascular Endothelial Cell (HMVEC-L) was performed as described previously (Lafargue et al., 2017). Briefly, HMVEC cells were cultured in EBM medium. At confluence, HMVEC cells were irradiated at 15Gy and maintained for 28 days. Conditioned media was collected during 28 days of culture every 7days, centrifuged 5min at 3000rpm and directly frozen on nitrogen.

Human glioblastoma cell lines, U251 MG, were cultured in DMEM supplemented with 10% fetal bovine serum, 1% Penicillin/Streptomycin and 2mM Glutamine. Primary GBM cultures were obtained from high grade glioma patients, mechanically dissociated and cultured in defined medium as previously described in (Oizel et al., 2017). For micronuclei study, only primary adherent GBM cultures were used.

Tumor cells were seeded and cultured in appropriate medium for at least 2hours before being treated overnight with conditioned media (volume to volume), EBM containing either 1ng/ml IL-8 (Preprotech, Rocky hill, USA) and/or 50pg/ml CXCL5 (Preprotech, Rocky hill, USA), or conditioned media containing 0.5µg/ml of blocking antibodies against IL-8 and/or 0.2µg/ml of blocking antibodies against CXCL5 (respectively 18672 and 9802; Abcam, Cambridge, UK), or 250ng/ml of blocking antibody against CXCR2, MAB331 (MB) (R&D, Minneapolis, USA), or 1nM of CXCR2 antagonist, SB332235 (SB) (TOCRIS Bioscience, Bristol, UK), or 20µM of ERK1/2 inhibitor (FR180204; Bioscience, Bristol, UK), or 0.1µM of CHK1 inhibitor (Rabusertib (LY2603618); Selleckchem, Houston, USA). When indicated, tumor cells were irradiated 16 hours after addition of conditioned media.

Resistant cells were obtained after seeding U251 cells at very low density in either CM, SASP, CM supplemented with both CXCL8 and CXCL5 or SASP supplemented with either CXCR2 blocking antibody (MAB) or CXCR2 antagonist (SB). Cells were irradiated at 15 Gy and resistant clones were amplified for 3 to 5 weeks before orthotopic injections in mice (respectively RCM, RSASP and R_{CM}CXCL, R_{SASP}MAB and R_{SASP}SB).

Genomic instability

Tumor cells were seeded, treated with conditioned media overnight and irradiated at 5Gy. Seventy-two hours after irradiation, cells were fixed in 4% paraformaldehyde and stained with Hoechst (FP-BB1340 Interchim, Montlucon, France) 30min at 37°C. Ten pictures per well were captured using Zeiss microscope 60X oil, (Zeiss, Oberkochen, Allemagne) and then analyzed using Image J Software (>100 cells per condition). Micronuclei were identified by distinct staining of Hoechst in structures outside of the nucleus and manually counted for each field. Polynucleated cells were manually counted for each field.

Clonogenic assay

Tumor cells were plated in 6-well plates accordingly to their respective plating efficiency (PE) and radiation doses. Cells were treated with conditioned media overnight and then exposed to increasing doses of X-rays (0, 2, 5, 10 and 15Gy). When colonies are formed, cells were washed with PBS, stained with a solution of crystal violet (229288 from sigma-aldrich, St. Quentin Fallavier, France). Plating efficiency (PE) and survival fraction (SF) and Relative Survival Fraction (RSF) were calculated using the following formula:

$PE = \text{number of colony} / \text{number of plating cells}$

$SF = \text{number of colony} / (\text{number of plating cells} * PE)$

$RSF = SF(SASP) / SF(CM)$

Time-lapse assay

Time lapse movies were performed on tumor cells plated in 12-well plates (10000 cells/well) stained overnight with 0,5µM of SiR-DNA (SC007, Spirochrome Switzerland). Cells were irradiated (XRAD225Cx preclinical irradiator, Precision X-Ray Inc, CT, USA) at 5Gy and maintained in conditioned media for 5days. Each film was composed of a sequence of pictures taken every 10minutes using a Nikon microscope (ECLIPSE Ti-E, Japan). Four fields per well were recorded. The number of cells, micronuclei and abnormal divisions were quantified on each film every 6 or 12hours.

ELISA assay

LIF, IL-33, CXCL8 (R&D system, Minneapolis, USA).and CXCL5 (Invitrogen, Villebon-sur-Yvette, France) dosages were performed by ELISA on HMVEC-L conditioned media according to the manufacturer instruction.

RTqPCR

RNA was extracted using Nucleospin RNA/Protein kit (Macherey Nagel, Düren, Germany) according to the manufacturer instruction. DNase treatment was included in the protocol. The quantity and quality of RNA were evaluated using the NanoDrop® (Ozyme, Saint Quentin Yvelines, France). Primers sequences are given in Table below. The housekeeping genes were HGPRT, TATA and GAPDH.

Genes	Primer sequences for/reverse
IL-33	GGTCCAGAAATATACTAGAGCAC / GACTCATAGTAACTCAGTAACACC
LIF	AGTGCCAATGCCCTCTTTATTCTC / CCAAGGTACACGACTATGCGG
CXCL5	ATCTGCAAGTGTTGCGCA / TCCTTGTTTCCACCGTCCA
IL-8	GACATACTCCAAACCTTTCCA / AACTTCTCCACAACCCTCTG
GAPDH	GAAGGTGAAGGTCGGAGTC / GAAGATGGTGATGGGATTTC
HGPRT	GAAGAGCTATTGTAATGACCAG / GCCAGTGTCAATTATATCTTCC
TATA	CAAGAGTGAAGAACAGTCCAG / ACAAGGCCTTCTAACCTTATAGG

Flow cytometry

To assess expression of CXCR1 and CXCR2 on membrane surface, tumour cells were collected, washed once with cold PBS and incubated using antibodies against CXCR1, CXCR2 or corresponding isotype in PBS BSA 0,1% (respectively 551080 and 555933 BD Pharmingen, Le pont de Claix, France). Fluorescence staining was measured with FACSCalibur flow cytometer (BD bioscience, Paris, France). Each measurement was conducted on 10000 events on CellQuest software (BD bioscience, Paris, France) and analyzed using FlowJo Software (FlowJo LLC, USA). Results are presented as Geomean of fluorescence.

RNAseq analysis

After demultiplexing and quality control with fastQC_0.11.2 (<http://www.bioinformatics.babraham.ac.uk/projects/fastqc/>), illumina adapter was trimmed with cutadapt-1.2.15 and reads with Phred quality score below 30 were filtered with prinseq-lite-0.20.36.

Reads were aligned against human hg19 reference genome with tophat2.0.107, reads count was realised with htseq-count from HTSeq-0.5.4p58 and differential analysis with DESeq29.

Western blot

Twenty micrograms of proteins were separated by SDS-PAGE and transferred to PVDF Immobilon-P membranes (Millipore). Milk 5% saturated membranes were hybridized overnight at 4°C with a primary antibody, and with a HRP-coupled secondary antibody. Proteins of interest were revealed by Clarity Western Blot ECL substrate (Biorad). Primary antibodies used in Western Blot were directed against phospho- Thr202/Tyr204 Erk1/2, phospho-Thr199 NPM, phospho-Ser345 CHK1 (respectively 4370, 3541, 2348; Cell Signaling) and actin (05-636, MAB1501; Millipore). Densitometry analyses of the proteins were performed from Fusion Capt FX7 (Vilber).

Immunocytochemistry

Tumor cells were seeded at 10000cells/well on glass coverslips coated with 1% gelatin in appropriate medium for at least 2hours before being treated overnight with conditioned media (volume to volume). Cells were irradiated at 5Gy 16hours after addition of conditioned media. Cells were gently washed with cold PBS, fixed in 4% paraformaldehyde for 10minutes, permeabilized in 0,1% Triton X-100 for 10minutes and blocked in PBS-5% serum goat for 30minutes. Cells were incubated with the primary antibody 1/200 γ H2AX (9718, Cell Signaling) overnight at 4°C and the secondary antibody 1/200 anti-IgG-Alexa568 (A11036, Invitrogen) during one hour at room temperature. Coverslips were mounted in slides with Prolong Gold with DAPI (P39635, molecular Probes from Life technology, Saint Aubin, France). Slides were observed on laser confocal microscope (model FV1000, Olympus or Nikon-A1) and images were processed using Image J.

Orthotopic injections of U251 human tumor cells in NSG mice.

This study was carried out in accordance with the recommendations of the French Regional Ethics Committee of the Pays de la Loire (Approvement #00186.02). Immunodeficient NOD.Cg-PrkdscidII2rgtm1Wjl/SzJ (NSG) mice, aged 8–12 weeks, were obtained from Charles River Laboratories (Wilmington, MA) and bred in the animal facility of the University of Nantes (UTE, SFR F. Bonamy) under SPF status. Orthotopic injections of resistant U251 cells (10^4 in 2 μ l PBS), respectively RCM, RSASP and RCXCL8/5, were performed in the subventricular zone of brain (2 mm on the right of the medial suture and 0.5 mm in front of the bregma, depth: 2.5 mm) using a stereotaxic frame (Stoelting, Wood Dale, IL). Animals were observed daily and euthanized when characteristic symptoms occurred, such as reduced mobility and significant weight loss.

Statistical analysis

Experiments were repeated at least 3 times. Data are presented as mean \pm SEM or SD as indicated in the figures. Statistical analyses were carried out using Prism5 (Version 5.0c, GraphPad, USA) software. $P < 0.05$ was considered statistically significant.

References

- Bent, E.H., Gilbert, L.A., and Hemann, M.T. (2016). A senescence secretory switch mediated by PI3K/AKT/mTOR activation controls chemoprotective endothelial secretory responses. *Genes Dev.* *30*, 1811–1821.
- Borovski, T., Verhoeff, J.J.C., Cate, R. ten, Cameron, K., de Vries, N.A., van Tellingen, O., Richel, D.J., van Furth, W.R., Medema, J.P., and Sprick, M.R. (2009). Tumor microvasculature supports proliferation and expansion of glioma-propagating cells. *Int. J. Cancer* *125*, 1222–1230.
- Borovski, T., Beke, P., van Tellingen, O., Rodermond, H.M., Verhoeff, J.J., Lascano, V., Daalhuisen, J.B., Medema, J.P., and Sprick, M.R. (2013). Therapy-resistant tumor microvascular endothelial cells contribute to treatment failure in glioblastoma multiforme. *Oncogene* *32*, 1539–1548.
- Calabrese C, Poppleton H, Kocak M, L.Hogg T, Fuller C, Hamner B, Young Oh E, M. Waleed Gaber, Finklestein D, Allen M, et al. (2007). A Perivascular Niche for Brain Tumor Stem Cells. *Cancer Cell* *11*, 69–82.
- Coppé, J.-P., Kauser, K., Campisi, J., and Beauséjour, C.M. (2006). Secretion of vascular endothelial growth factor by primary human fibroblasts at senescence. *J. Biol. Chem.* *281*, 29568–29574.
- Jamal, M., Rath, B.H., Williams, E.S., Camphausen, K., and Tofilon, P.J. (2010). Microenvironmental regulation of glioblastoma radioresponse. *Clin. Cancer Res.* *16*, 6049–6059.
- Krtolica, A., Parrinello, S., Lockett, S., Desprez, P.Y., and Campisi, J. (2001). Senescent fibroblasts promote epithelial cell growth and tumorigenesis: a link between cancer and aging. *Proc. Natl. Acad. Sci. U.S.A.* *98*, 12072–12077.
- Lafargue, A., Degorre, C., Corre, I., Alves-Guerra, M.-C., Gaugler, M.-H., Vallette, F., Pecqueur, C., and Paris, F. (2017). Ionizing radiation induces long-term senescence in endothelial cells through mitochondrial respiratory complex II dysfunction and superoxide generation. *Free Radic. Biol. Med.* *108*, 750–759.
- Parrinello, S., Coppe, J.-P., Krtolica, A., and Campisi, J. (2005). Stromal-epithelial interactions in aging and cancer: senescent fibroblasts alter epithelial cell differentiation. *J. Cell. Sci.* *118*, 485–496.
- Stupp, R., Mason, W.P., van den Bent, M.J., Weller, M., Fisher, B., Taphoorn, M.J.B., Belanger, K., Brandes, A.A., Marosi, C., Bogdahn, U., et al. (2005). Radiotherapy plus concomitant and adjuvant temozolomide for glioblastoma. *N. Engl. J. Med.* *352*, 987–996.
- Xue, W., Zender, L., Miething, C., Dickins, R.A., Hernando, E., Krizhanovsky, V., Cordon-Cardo, C., and Lowe, S.W. (2007). Senescence and tumour clearance is triggered by p53 restoration in murine liver carcinomas. *Nature* *445*, 656–660.
- (2007). A Perivascular Niche for Brain Tumor Stem Cells. *Cancer Cell* *11*, 69–82.

Figure 1

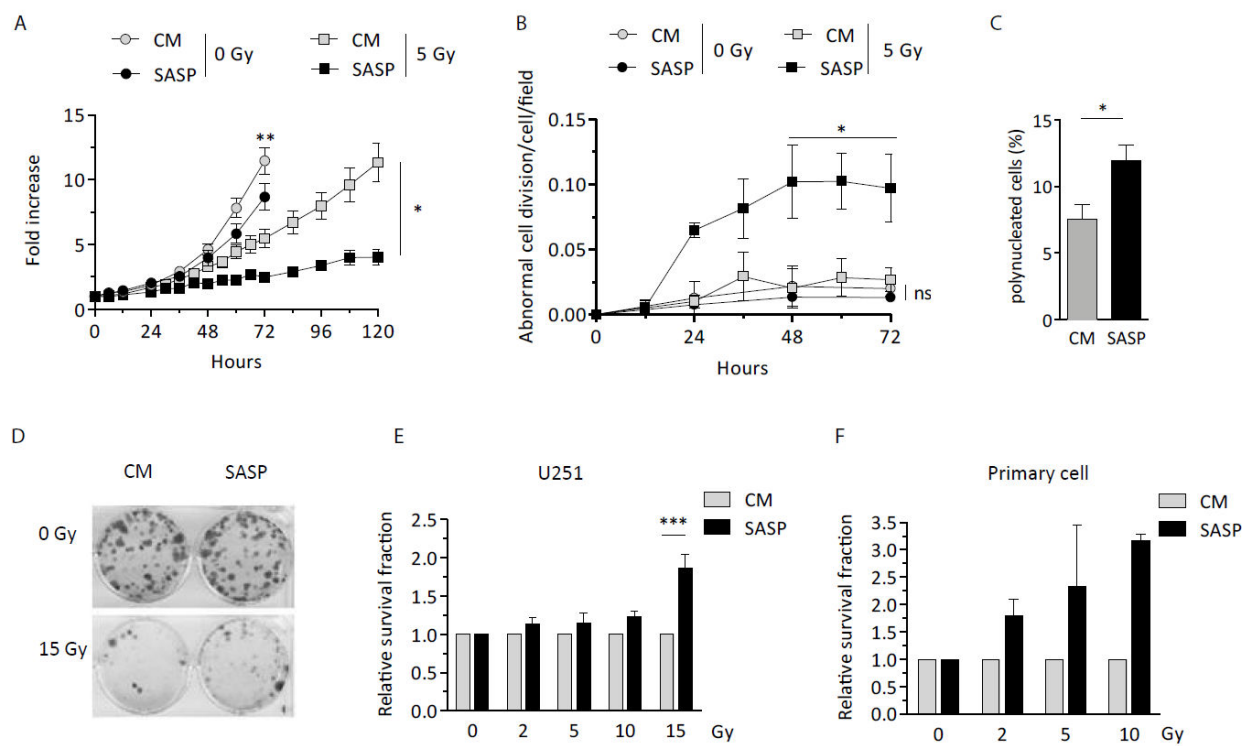


Figure 1: SASP enhances resistance and genomic instabilities after radiation.

A. Proliferation of U251 cells in CM (grey) and SASP (black) in response to radiation using videomicroscopy analysis. Results are presented as the number of cells per field normalized to the initial number of cells (mean±sem, n≥3, Two-Way Anova; *p<0.05; ** p<0.01). **B.** Abnormal divisions U251 cells in CM (grey) and SASP (black) in response to radiation using videomicroscopy analysis. Results are presented as the relative frequency of abnormal cell division per field normalized to sham (CM and no irradiation) (mean±sem, n≥3, Two-Way Anova; *p<0.05; ** p<0.01). **C.** Frequency of polynucleated U251 cells in CM (grey) and SASP (black) in response to radiation. Cells were counted 72 hours after 5Gy-irradiation (mean±sem, n=6, t-test; *p<0.05). **D.** Clonogenic assay of U251 cells in CM or SASP in response to 15Gy-irradiation. **E.** Survival fraction of U251 cells in CM or SASP in response to increased doses of irradiation (0 to 15 Gy). Results are presented as the relative survival fraction as compared to sham (mean±sem, n≥3, Two-Way Anova *** p<0.001). **F.** Survival fraction of primary GBM cells in CM or SASP in response to irradiation (0, 2, 5 and 10 Gy). Results are presented as the relative survival fraction as compared to sham (mean±sem, n=2).

Figure 2

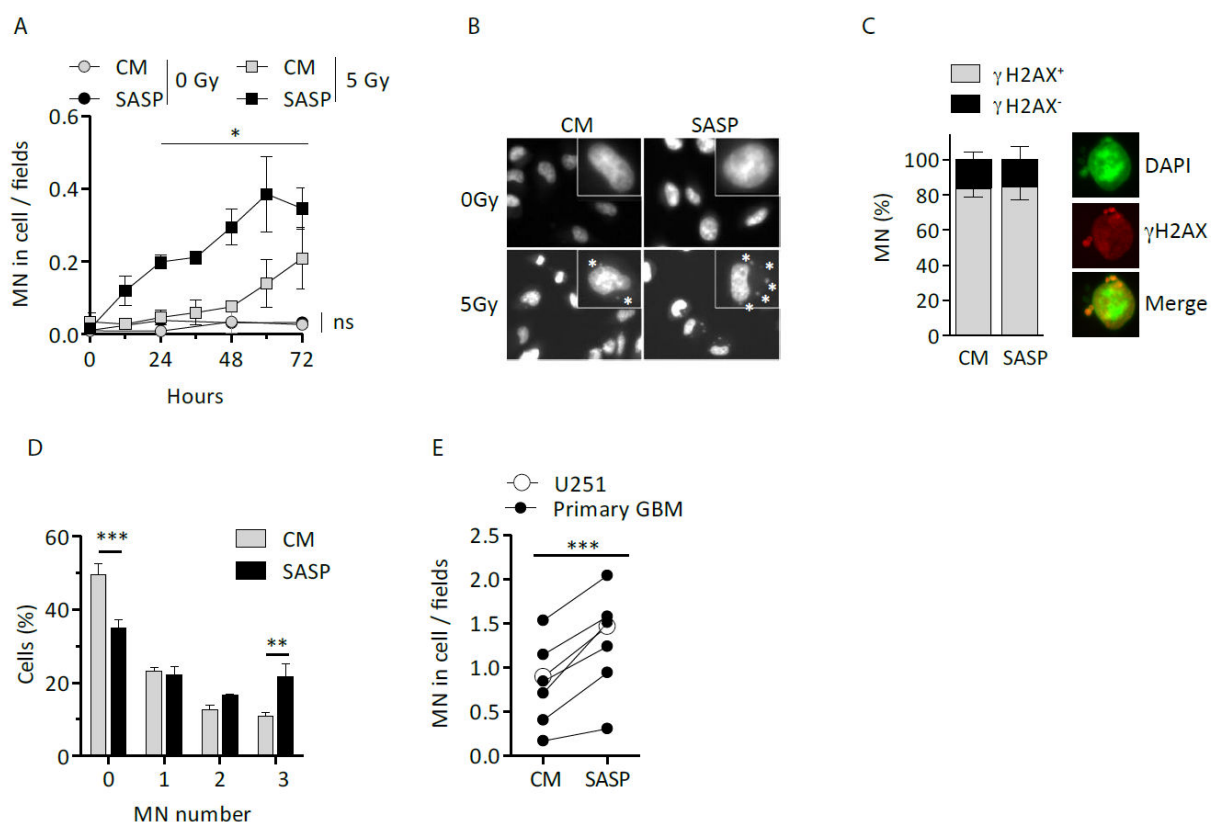


Figure 2: SASP enhances micronuclei formation in tumor cells

A. Micronuclei production in U251 cells in CM (grey) and SASP (black) in response to 5Gy-radiation using videomicroscopy analysis. Results are presented as the mean of micronuclei (MN) in cells per field (mean±sem, n=3, 2-Way Anova; *p<0.05). **B.** Representative pictures of MN-containing cells in CM and SASP 72hours after 5Gy-irradiation. **C.** Frequency of γ -H2AX positive MN in CM and SASP in response to radiation. MN were analyzed for DAPI and γ -H2AX staining 72 hours after 5Gy-irradiation. (mean±sem, n=3, 2-way ANOVA; *p<0.05). Representative pictures of immunofluorescence staining are presented on the right panel. **D.** Production of micronuclei in U251 cells in CM or SASP 72hours following 5Gy-irradiation (mean±sem, n=3, 2-Way Anova; ** p<0.01; *** p<0.001). **E.** Production of micronuclei in primary cells in CM or SASP 72hours following 5Gy-irradiation. Mean production of micronuclei in U251 cells is indicated (white spot) (mean±sem, n=3, 2-Way Anova; *** p<0.001).

Figure 3

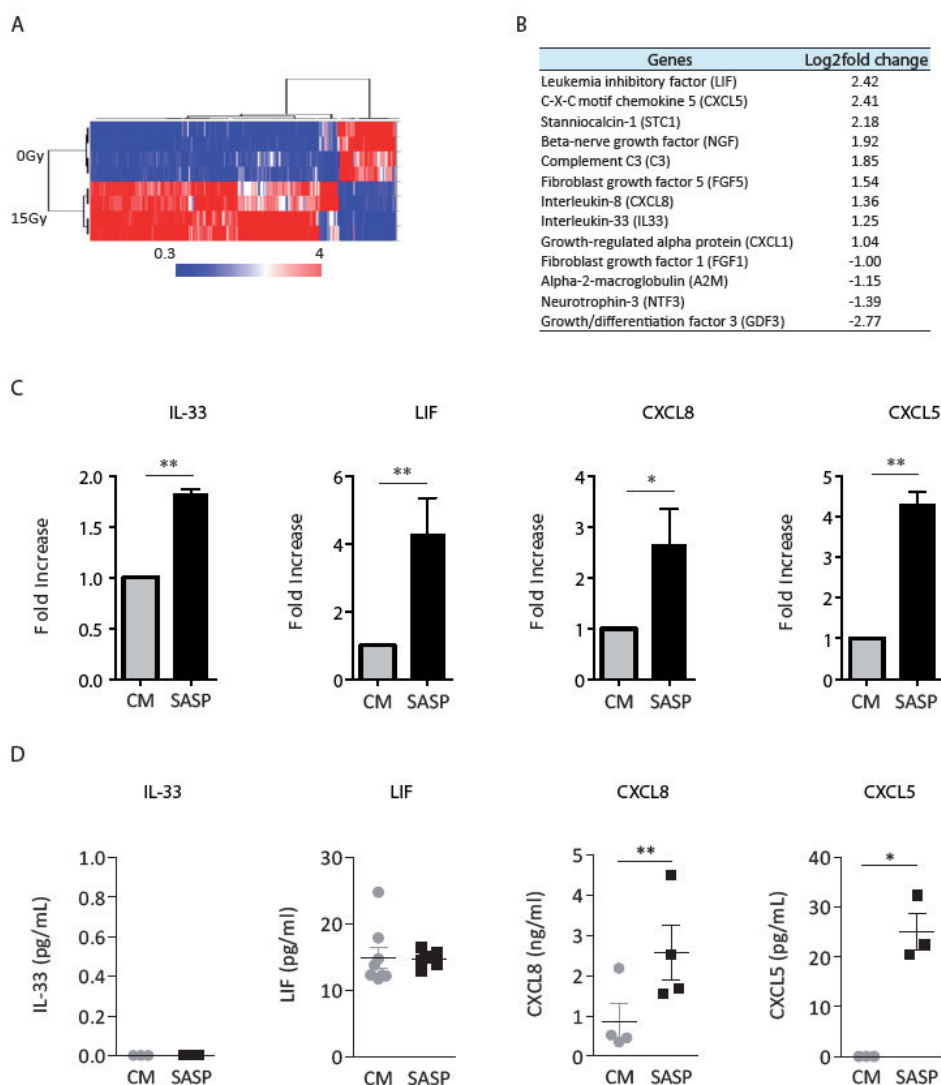


Figure 3: Identification of key cytokines from the SASP

A. Hierarchical clustering of the 242 genes differentially expressed in endothelial cells 21 days after 0Gy or 15Gy. The expression values are normalized using the mean of all samples and presented as a heat map (XLstat analysis). **B.** PANTHER gene list belonging to the “Receptor Binding” category and corresponding log2 fold change compared to non-irradiated endothelial cells. **C.** Relative level of RNA coding IL-33, LIF, CXCL8 and CXCL5 in U251 cells 72 hours after 5Gy irradiation in SASP. Relative RNA level is expressed as compared as U251 cells in CM 72 hours after 5Gy irradiation (mean±sem, n≥3, t-test; * p<0.05, **p<0.01). **D.** ELISA assay of IL-33, LIF, CXCL8 and CXCL5 in CM and SASP 72 hours after 5Gy irradiation. (mean±sem, n≥3, t-test; *p<0.05).

Figure 4

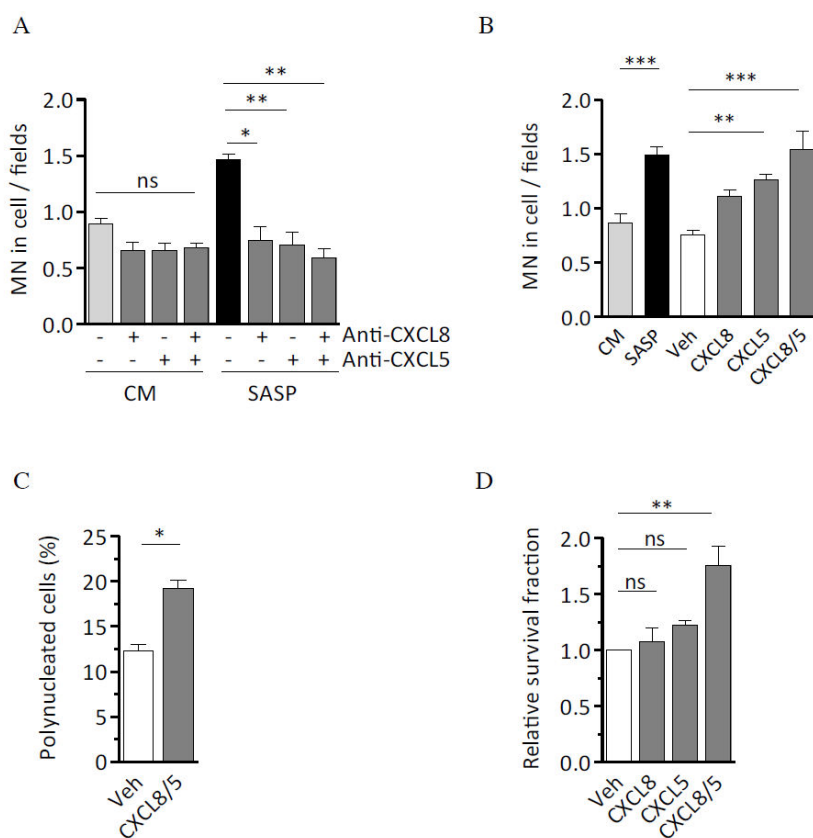


Figure 4: Combination of CXCL8 and CXCL5 fully recapitulates SASP-induced genomic instability and radio-resistance.

A. Production of micronuclei in cells in CM or SASP supplemented with blocking antibody against CXCL8 and/or CXCL5, respectively at 0.5 μ g/mL and/or 0.2 μ g/mL. (mean \pm sem, n \geq 3, one-Way Anova; *p<0.05; ** p<0.01). **B.** Production of micronuclei in cells treated with vehicle, CXCL8 (1ng/mL) and CXCL5 (50pg/mL), alone or in combination, 72hours following 5Gy-irradiation (mean \pm sem, n \geq 3, one-Way Anova; *p<0.05, *** p<0.001). **C.** Frequency of polynucleated cells in U251 cells 72 hours after 5Gy-irradiation in CM supplemented with vehicle or a combination of CXCL8/CXCL5 (respectively 1ng/mL and 50pg/mL). (mean \pm sem, n=33, one-Way Anova; *p<0.05). **D.** Survival fraction of U251 cells following 15Gy-irradiation in presence of vehicle, CXCL8 (1ng/mL), CXCL5 (50 pg/mL), alone or in combination. Results are presented as the relative survival fraction as compared to vehicle. (mean \pm sem, n=4, one-Way Anova; **p<0.01).

Figure 5

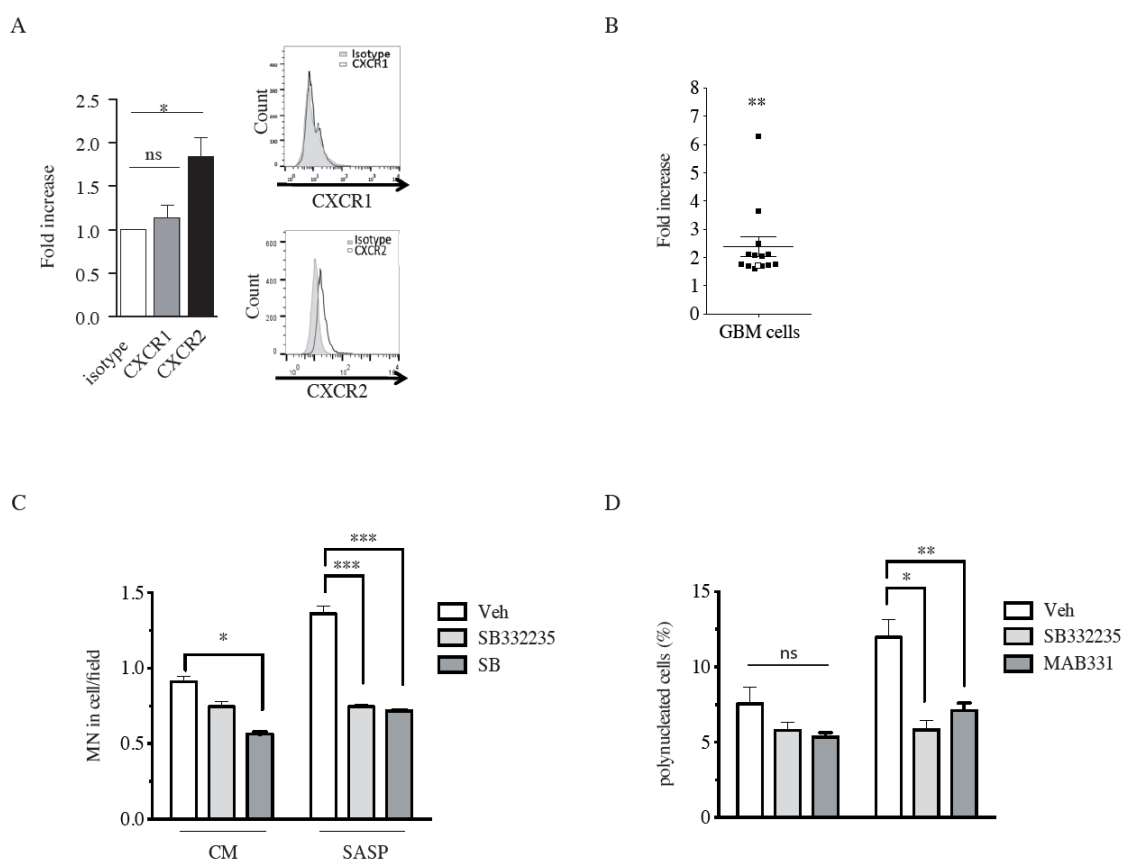


Figure 5: CXCL8 and CXCL5 trigger genomic instabilities through binding to CXCR2.

A. CXCR1 and CXCR2 expression in U251 cells by FACS analysis. *Left panel*, Results are presented as the relative fluorescence (geomean) compared to isotype; *Right panel*, representative FACS histograms. (mean±sem, n≥3, t-test; *p<0.05). **B.** CXCR2 expression in GBM primary cells by FACS analysis. Results are presented as in (A). Mean CXCR2 expression in U251 cells is indicated as a white square on the graph (mean±sem, n≥3, t-test; **p<0.01). **C.** Production of MN 72 hours after 5Gy-irradiation in U251 cells in CM or SASP supplemented with 250ng/ml of blocking antibody against CXCR2 (MAB), or 1nM of CXCR2 antagonist (SB). (mean±sem, n≥3, One Way Anova; *p<0.05). **D.** Frequency of polynucleated cells 72hours after 5Gy-irradiation of U251 cells in CM or SASP supplemented with 250ng/ml of CXCR2 blocking antibody (MAB) or 1nM of CXCR2 antagonist (SB). (mean±sem, n≥3, One Way Anova; *p<0.05, ** p<0.01).

Figure 6

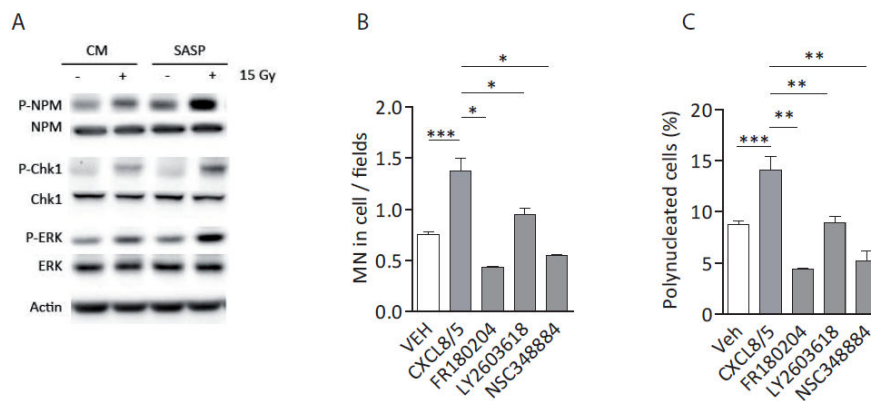


Figure 6 : SASP triggers the phosphorylation of CHK1, NPM and ERK through CXCL8 and CXCL5.

A. Total and phosphorylated forms of NPM, CHK1 and ERK proteins evaluated by Western blot 24 hours after 15Gy-irradiation in CM or SASP (n=4, representative blots). **B.** Production of micronuclei in U251 cells 72 hours in response to 5Gy-irradiation after inhibition of ERK1/2, CHK1 and NPM. Inhibitors, respectively an ATP-competitive inhibitor of ERK1/2 (FR 180204, 20µM), a CHK1 inhibitor (LY2603618) or a NPM inhibitor (NSC348884), were added in U251 cell media supplemented with both CXCL8 (1ng/ml) and CXCL5 (50pg/ml). (mean±sem, n≥3, One-Way Anova; *p<0.05, *** p<0.001). **C.** Frequency of polynucleated cells in U251 cells 72 hours after 5Gy-irradiation after inhibition of ERK1/2, Chk1 and NPM as in (B). (mean±sem, n≥3, One-Way Anova; **p<0.01, *** p<0.001).

Figure 7

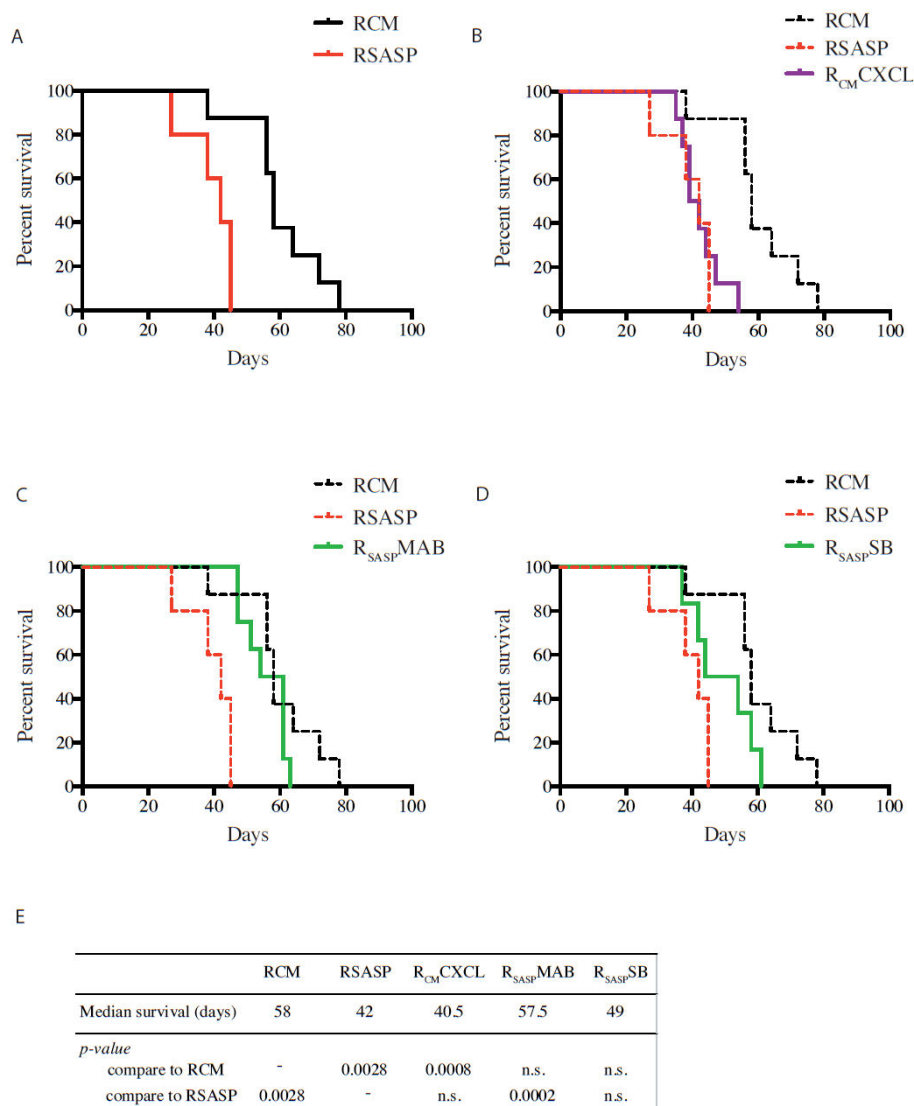
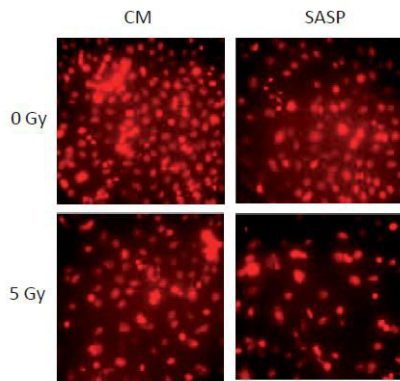


Figure 7 SASP increases resistant U251 bellicosity in an orthotopic GBM murine model

A. Mean survival of tumor-bearing mice after orthotopic injections of radioresistant U251 cells. Radioresistant U251 cells were obtained from surviving clones 3 weeks after 15Gy-irradiation in presence of either CM or SASP (respectively called RCM (n=8) and RSASP(n=6)). **B.** Mean survival of tumor-bearing mice after orthotopic injections of radioresistant U251 cells obtained in presence of CM supplemented with CXCL8 and CXCL5 (R_{CM}CXCL) (n=8). **C.** Mean survival of tumor-bearing mice after orthotopic injections of radioresistant U251 cells obtained in presence of SASP supplemented with CXCR2 blocking antibody (n=8). **D.** Mean survival of tumor-bearing mice after orthotopic injections of radioresistant U251 cells obtained in presence of SASP supplemented with CXCR2 antagonist (R_{SASP}SB) (n=6). **E.** Median survival of tumor-bearing mice after orthotopic injection of radioresistant U251 cells. Log-rank p-values are indicated as compare to mice survival injected with either RCM radioresistant cells or RSASP radioresistant cells.

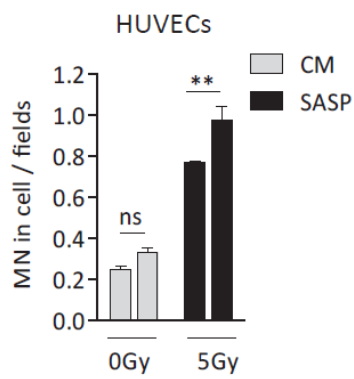
Degorre et al.

Supplemental Figures



Supplemental Figure 1

Time lapse analysis after 5Gy-irradiation of U251 cells cultured in CM or SASP. Cells were stained with the SirDNA probe. Representative pictures were taken 72 hours after irradiation.

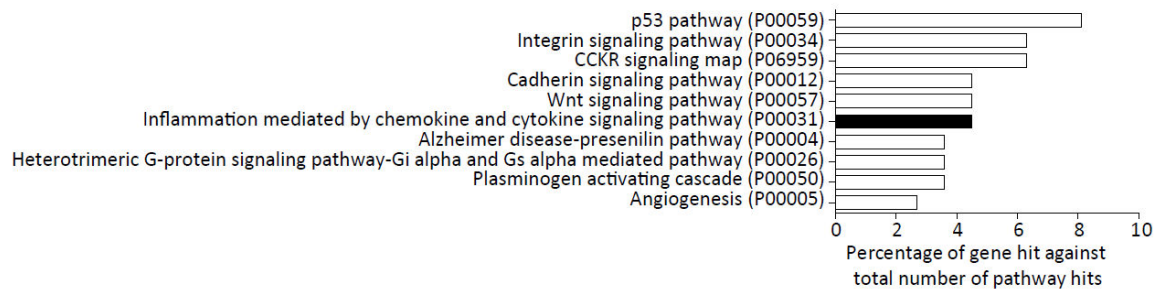


Supplemental Figure 2

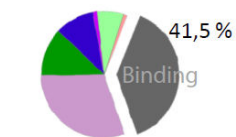
Production of micronuclei in HUVEC in CM or SASP 72 hours following 5Gy irradiation (mean±sem, n=3, 2-Way Anova, ** p<0,01).

Degorre et al.

Supplemental Figures

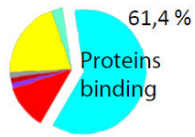


Molecular functions



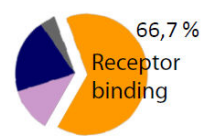
- Antioxydant
- Catalytic
- Receptor
- Signal transducer
- Structural molecule
- Transporter

Binding



- Calcium ion
- Ca-dependent lipid
- Chromatin
- Lipid
- Nucleic acid
- Nucleotide

Protein binding



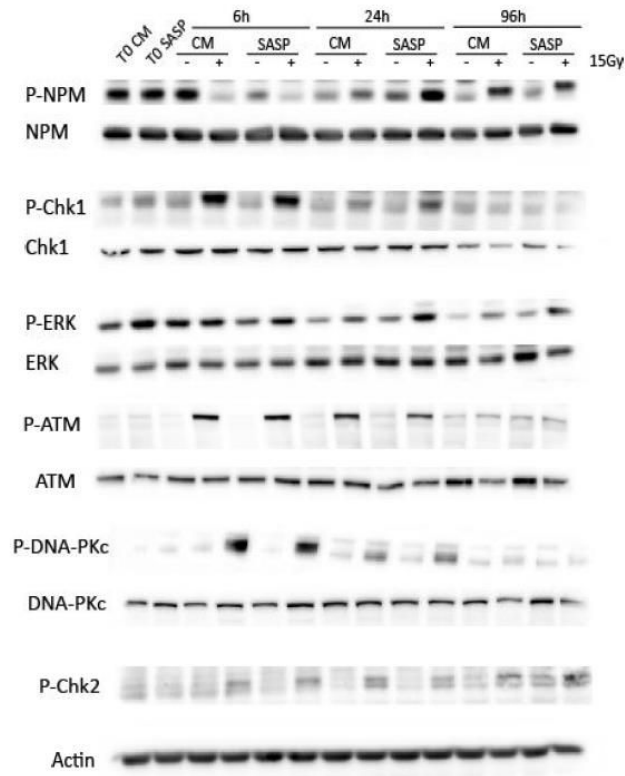
- Calmodulin
- Cytoskeletal protein
- Transcription factor

Supplemental Figure 3

Transcriptomic analyses of the 10 most up-regulated pathways using PANTHER analysis. Top panel : Functional annotations of differentially expressed pathways are indicated (GO : Gene Ontology). Bottom panel : Transcriptomic analyses using PANTHER software for molecular functions focusing on genes involved in protein binding. Results are presented as pie charts.

Degorre et al.

Supplemental Figures



Supplemental Figure 4

Western blot analysis of total and phosphorylated forms of NPM, Chk1, ATM, DNA-PK, CHK2 and ERK proteins after 15Gy irradiation in CM or SASP at indicated timepoints. Actin was used as loading control (n=4, representative blots).

Listes des communications

16 et 17 juin 2016 – 10^{ème} Journées du Cancéropôle Grand Ouest (Les Sables d'Olonne).

Présentation d'un poster intitulé : Evaluation of human V γ 9V δ 2 T cells reactivity in an orthotopic epithelial ovarian cancer model. N. Joalland, U. Jarry et E. Scotet.

22 novembre 2016 – Les Folles Souris Nantaises (Nantes).

Communication orale intitulée : Evaluation du potentiel thérapeutique des LT V γ 9V δ 2 en immunothérapie anti-tumorale dans des modèles murins. N. Joalland, U. Jarry et E. Scotet.

28 au 30 novembre 2016 – Congrès de la Société Française d'Immunologie (Paris).

Présentation d'un poster intitulé : *in vitro* and *in vivo* reactivity of human V γ 9V δ 2 T cells against epithelial ovarian cancer cells : Impact of chemotherapeutic agents. N. Joalland, U. Jarry et E. Scotet.

15 et 16 décembre 2016 – Journées Scientifique de l'Ecole Doctorale Biologie Santé (Nantes).

Présentation d'un poster intitulé : *in vitro* and *in vivo* reactivity of human V γ 9V δ 2 T cells against epithelial ovarian cancer cells : Impact of chemotherapeutic agents. N. Joalland, U. Jarry et E. Scotet.

Lauréate du 3^{ème} prix poster.

9 et 10 février 2017 – Journées Scientifiques Immunothérapies du Cancéropôle Grand Ouest (Pornic).

Communication orale intitulée : Impact de la chimiothérapie sur la réactivité des LT V γ 9V δ 2 dans un modèle de cancer épithélial de l'ovaire. N. Joalland, L. Lafrance, U. Jarry et E. Scotet.

6 et 7 avril 2017 – 5^{ème} Journées Scientifiques du Groupe Coopératif GINOVA (Nantes).

Communication orale intitulée : LT V γ 9V δ 2 humains et modèles murins humanisés de cancer de l'ovaire. N. Joalland, L. Lafrance, U. Jarry et E. Scotet.

27 et 28 avril 2017 – Journées Intra-Labex IGO (Immunology in Graft and Oncology)
(Nantes).

Communication orale intitulée : Human V γ 9V δ 2 T cells spontaneously eliminate particular subsets of primary glioblastoma tumor cells. C. Chauvin, N. Joalland, U. Jarry, C. Pecqueur et E. Scotet.

1 et 2 juin 2017 – 22^{ème} congrès NAT « Immunotherapies in transplantation & cancer »
(Nantes).

Communication orale intitulée : IL-21 increases the cytotoxicity of V γ 9V δ 2 T cells against primary glioblastoma tumors. N. Joalland, C. Chauvin, C. Pecqueur, U. Jarry et E. Scotet.

et

Présentation d'un poster intitulé : *in vitro* and *in vivo* reactivity of human V γ 9V δ 2 T cells against epithelial ovarian cancer cells : Impact of chemotherapeutic agents. N. Joalland, L. Lafrance, U. Jarry et E. Scotet.

29 et 30 juin 2017 – 11^{ème} Journées du Cancéropôle Grand Ouest (Vannes).

Présentation d'un poster intitulé : *in vitro* and *in vivo* reactivity of human V γ 9V δ 2 T cells against epithelial ovarian cancer cells : Impact of chemotherapeutic agents. N. Joalland, L. Lafrance, U. Jarry et E. Scotet. *Lauréate du 2^{ème} prix Poster.*

7 au 10 juin 2018 – Gamma Delta Conference 2018 (Bordeaux).

Communication orale intitulée : Chemotherapies combined with allogeneic human V γ 9V δ 2 T cells for the elimination of epithelial ovarian cancer. N. Joalland, L. Lafrance, U. Jarry et E. Scotet.

et

Présentation d'un poster intitulé : Allogeneic human V γ 9V δ 2 T cells naturally recognize defined subsets of primary glioblastoma tumor cells *in vitro* and *in vivo*. N. Joalland, C. Chauvin, L. Lafrance, U. Jarry, C. Pecqueur et E. Scotet

Titre : Immunothérapie anti-tumorale par transfert adoptif de LT V γ 9V δ 2 :

Utilisation préclinique de LT V γ 9V δ 2 humains allogéniques en immunothérapie anti-tumorale dans des modèles murins de xénogreffes orthotopiques

Mots clés : Cancer ; Immunothérapie ; Transfert Adoptif ; LT V γ 9V δ 2 ; Zolédronate ; Modèles murins ; Cancer épithélial de l’ovaire ; Glioblastome multiforme.

Résumé : Le cancer est une pathologie caractérisée par la prolifération anarchique de cellules tumorales. Malgré de nombreuses avancées technologiques en terme de dépistage, d’imagerie médicale, de chirurgie et de traitements, le cancer représente encore un challenge thérapeutique. Depuis quelques années, le développement d’immunothérapies, telles que le transfert adoptif cellulaire, fait l’objet de nombreuses études. Les Lymphocytes T V γ 9V δ 2 (LT V γ 9V δ 2) font partie des effecteurs immunitaires candidats du fait de leurs nombreuses fonctions effectrices et de leur non-alloréactivité. En effet, la reconnaissance de leurs cibles n’est pas restreinte au complexe majeur d’histocompatibilité, il est donc possible de créer une banque cellulaire de LT V γ 9V δ 2 allogéniques qui pourront être administrés aux patients sans risque de réaction allogénique contre l’hôte. De plus, cette reconnaissance peut être induite grâce à des molécules pharmacologiques telles que le zolédronate. L’objectif de cette thèse a donc été d’évaluer l’efficacité thérapeutique de LT V γ 9V δ 2 humains allogéniques dans des modèles murins précliniques de xénogreffes orthotopiques. Deux modèles ont été mis en place : (i) un modèle de cancer épithélial de l’ovaire incluant le traitement standard des patientes par chirurgie et chimiothérapie, suivie d’une rechute avec carcinose péritonéale ; (ii) un modèle de glioblastome multiforme basé sur l’implantation intracrânienne de cellules tumorales primaires. Ainsi, le bénéfice thérapeutique du transfert adoptif de LT V γ 9V δ 2 humains allogéniques, associés ou non au zolédronate, a pu être démontré dans plusieurs modèles précliniques, ouvrant la voie vers un transfert en clinique.

Title: Anti-tumor immunotherapy by adoptive transfer of V γ 9V δ 2 T lymphocytes

Preclinical use of allogeneic human V γ 9V δ 2 T lymphocytes for anti-tumor immunotherapy in mouse models of orthotopic xenografts »

Keywords: Cancer; Immunotherapy; Adoptive Transfer; V γ 9V δ 2 T lymphocytes; Zoledronate; Murine Models; Epithelial Ovarian Cancer; Glioblastoma multiforme.

Abstract: Cancer is a pathology characterized by uncontrolled proliferation of tumor cells. Despite many technological advances in terms of screening, medical imaging, surgery and treatments, cancer is still a therapeutic challenge. In recent years, development of immunotherapies, such as adoptive cell transfer, has been the aim of many studies. V γ 9V δ 2 T lymphocytes are interesting immune effectors because of their numerous effector functions and their non-alloreactivity. In fact, their targets recognition is not restricted to the major histocompatibility complex, so it is possible to create allogeneic V γ 9V δ 2 T cell banks that could be used to treat patients without risk of allogeneic reaction against the host. Moreover, this recognition can be induced by pharmacological molecules such as zoledronate. The aim of this thesis was to evaluate the therapeutic efficacy of allogeneic human V γ 9V δ 2 T lymphocytes in preclinical mouse models of orthotopic xenografts. Two models have been developed: (i) a model of epithelial ovarian cancer including standard treatment of patients by surgery and chemotherapy, followed by relapse with peritoneal carcinosis ; (ii) a model of glioblastoma multiforme based on intracranial injection of primary tumor cells. Thus, the therapeutic efficacy of adoptive transfer of allogeneic human V γ 9V δ 2 T lymphocytes, whether or not associated with zoledronate, has been demonstrated in several preclinical models, paving the way for clinical transfer.